THE THERMAL PERFORMANCE AND LIFE CYCLE ASSESSMENT OF A GREEN ROOF IN PITTSBURGH, PENNSYLVANIA

by

Lisa M. Kosareo

B.S., University of Pittsburgh, 2002

Submitted to the Graduate Faculty of

School of Engineering in partial fulfillment

of the requirements for the degree of

Master of Science

University of Pittsburgh

2007

UNIVERSITY OF PITTSBURGH

SCHOOL OF ENGINEERING

This thesis was presented

by

Lisa M. Kosareo

It was defended on

July 16, 2007

and approved by

Dr. Ronald D. Neufeld, Professor, Department of Civil and Environmental Engineering

Dr. David A. Dzombak, Professor, Department of Civil and Environmental Engineering

Carnegie Mellon University

Thesis Advisor: Dr. Robert J. Ries, Assistant Professor, Department of Civil and Environmental Engineering

THE THERMAL PERFORMANCE AND LIFE CYCLE ASSESSMENT OF A GREEN ROOF IN PITTSBURGH, PENNSYLVANIA

Lisa M. Kosareo, M.S.

University of Pittsburgh, 2007

A green roof, a roof with a vegetative cover, is one passive technique that can be used to address environmental issues in an urban setting. Research has shown that green roofs can be used to mitigate numerous urban problems such as storm water runoff and the urban heat island effect. Green roofs can also increase the life span of roofing materials. By adding additional layers to the roof, the performance of a rooftop can be greatly enhanced.

A 12,300 square foot extensive green roof was constructed at a commercial site in Pittsburgh. A conventional gravel ballasted roof covers the remainder of the building. The green roof consists of a drainage layer, 5.5 inch thick layer of soil substrate, and vegetation. Using the conventional roof as a control, a monitoring system measured performance parameters of temperature, net radiation, relative humidity, wind speed, and wind direction.

The data results clearly show the effect the respective roof coverings have on the roof membranes. The gravel ballast covering the membrane on the control roof cannot protect the membrane from ambient conditions or radiation. The green roof works effectively during the summer and fall, when the high ambient temperature is greater than 65°F and high incident solar radiation is greater than 400 $W*m^{-2}$ net. For example, on August 25, 2006 the ambient high was 90°F, the low 70°F. The control roof membrane reached an afternoon high temperature of 130°F and a low temperature of 65°F. Meanwhile, on that same day at the green roof membrane

high temperature was 86°F and 73°F at night. While the green roof outperformed the conventional roof during the summer and fall, during the winter they perform equally.

An Environmental Life Cycle Assessment was also used to determine the effect of roof type on the overall environment. A conventional, extensive green, and intensive green roof were modeled. The extensive green roof impact was roughly 50% less than the control roof in a variety of environmental damage categories. The intensive green roof actually varied with each damage category, from 10% to 44%. Still, green roofs were the environmental preferable choice.

TABLE OF CONTENTS

LIST OF TABLES

LIST OF FIGURES

ACKNOWLEDGEMENTS

The author would like to thank her advisor, Dr. Robert Ries for his support and guidance throughout her graduate career. She would also like to thank the members of her thesis committee, Dr. Ronald Neufeld and Dr. David Dzombak for their encouragement and assistance. Special gratitude is extended to her colleagues in the Department of Civil and Environmental Engineering for the invaluable support provided throughout the project. Most of all, the author is thankful for the love and support she has always received from her family, especially her husband Brandon Chavel, her parents, Daniel and Anna Kosareo, and her brothers Nicholas and Michael Kosareo.

1.0 INTRODUCTION

A green roof, a roof with a vegetative cover, is one passive technique that can be used to address environmental issues in an urban setting. While not an entirely new concept, green roofs have gained popularity in recent years. Research has shown that green roofs can be used to mitigate problems associated with storm water runoff, the urban heat island effect, wildlife habitat, and air and water quality. Green roofs can also increase the life span of roofing materials. By adding additional layers to the roof, such as drainage, soil, and vegetation layers, the performance of a rooftop can be greatly enhanced.

Several green roofs can be found in the area of Pittsburgh, Pennsylvania. While they may not be commonly recognized as green roofs, city parks that cover underground parking garages were some of the first “green roofs” that were built in the city. In the cases of Mellon Square (Osmundson, 1999) and the Soldiers and Sailor Memorial, the green roof is at street level, allowing for public use of the green space, while still providing parking to the surrounding area. Recently, the number of green roofs in the Pittsburgh area has increased, due to the work of The Pittsburgh Green Building Alliance (GBA) and Three Rivers Wet Weather (3RWW). These two organizations have increase awareness of green roofs and other sustainable construction methods. Through a grant from the U.S. Environmental Protection Agency (EPA), 3RWW has been able to fund the construction and study of three new green roofs. The focus of 3RWW is to quantify the environmental benefits of green roofs in the Pittsburgh area, particularly the effect roof type has on water runoff. 3RWW has endorsed the study of the three new green roofs through local universities, the University of Pittsburgh and Carnegie Mellon University. The research at both universities has examined the effects roof type has on the environment by comparing the newly constructed green roofs to a conventional roof at the same site. The goal of this research is to develop a manual to be used within the city when constructing a green roof.

The focus of this thesis is one of the green roofs funded by 3RWW. This roof has a more conventional setting; it covers a large one-storey grocery store. The project is part of the renovation and expansion of the Shadyside Giant Eagle supermarket. The 60,000 square foot addition makes use of a conventional, gravel ballasted, or weighted, roof and a 12,000 square foot green roof. This layout allowed researchers to monitor a green and conventional roof at the same site to compare performance. This project was designed to address the possible environmental benefits of green roof installation.

1.1 OBJECTIVES

This research consists of three major tasks:

1. Develop a Monitoring System specific to the Giant Eagle site. This monitoring system will be used to measure and evaluate roof performance. The instrumentation at the site monitors surface temperature, ambient temperature, precipitation, growing media moisture content, relative humidity, solar radiation, wind direction and speed, stormwater retention, stormwater runoff, and runoff quality. The objective of the qualitative sampling is to assess the long and short

term changes in the roof environment as a consequence of the addition of a vegetative area.

2. Use the monitoring system data to quantify the performance of both roof types at the Giant Eagle site. This thesis will center on the thermal performance of both roofs, focusing on the effect roof type has on the thermal stress of the roof membrane. It will also examine the possible effects roof type broader issues of environmental concern, such as the urban heat island effect.
3. A Life Cycle Impact Assessment model will be created to determine the environmental impact roof type has in the global environment. The model examines both roof types utilized at the Giant Eagle location, as well as an additional fictitious green roof for comparison. The model considers all aspects of the roof life cycle, from creation or materials to disposal of the roof layer.

This research is organized by chapter. Chapter 2 discusses the history and background of green roofs world wide. It describes the components or layers that are built up to form a roof, and the supplementary layers needed to construct a green roof. This chapter also reports the specific environmental issues researchers hope green roofs can help mitigate. The benefits of green roofs are thought to be many, and Chapter 2 describes each benefit and how green roofs provide these benefits. Chapter 3 is an extensive literature review that identifies previous experimental and analytical research related to green roofs. Chapter 4 outlines the monitoring set up used to observe the Giant Eagle site. Chapter 5 presents the data and analysis of the collected from the monitoring system over a 6 month period from July 2006 to January 2007.

Chapter 6 covers the Life Cycle Assessment model and results. Finally, Chapter 7 summarizes the findings and conclusions of this thesis.

2.0 HISTORY, DESCRIPTION, COMPONANTS, AND BENEFITS OF GREEN ROOFS

This chapter will present the basic information on green history, structure, and maintenance. It will also provide information on the generally recognized benefits of green roofs. This section will discuss the differences between conventional roofs and green roofs. Since the primary goal of this research is related to the thermal performance and life cycle assessment of green roofs, this background section will provide the information needed to understand how green roofs differ from conventional construction methods and how they might affect the surrounding environment.

Foremost, it is important to note the difference between green roofs and green buildings. Green roofs refer to a roof top garden or vegetation sustained on a roof alone. Green buildings are buildings designed in such a way as to reduce the impact made on human health and the environment. (USGBC, 2007) The goal is often to design these buildings to lessen the land, energy, water, or materials needed to construct, operate, and maintain the building. A green roof can be a part of a green building, but one can exist without the other. The U.S. Green Building Council (USGBC) is a non profit organization that integrates concepts in sustainability in the built environment and industry. The USGBC developed the Leadership in Energy and Environmental Design, or LEED®, Green Building Rating System™ as a nation wide consensus for designating and quantifying the performance of sustainable buildings. (USGBC, 2007) Green roofs are one of the many tools or techniques that can contribute to a LEED certification.

Not for profit organizations, like “Green Roofs for Healthy Cities,” are trying to increase awareness of the economic, environmental, and social benefits green roofs provide throughout North America. (Greenroof, 2007) These organizations in addition to professionals in architecture, construction, horticulture, landscaping, urban planners, environmental management, ecology, and conservations are all involved in promoting and studying green roofs and the green roof industry. (Dunnett and Kingsbury, 4) It is these individuals and groups that are driving the research and support of green roofs in North America today.

2.1 HISTORY OF GREEN ROOFS

The idea of using soil and vegetation to protect the outer building materials of a structure is not a new concept. Documentation of roof top gardens, or green roofs, has gone back as far as biblical times and the Tower of Babylon. (Osmundson, 1999) Early American settlers utilized sod to protect their homes in the early 1800’s. The 1868 World Exhibition in Paris, France featured a planted concrete structured “nature roof” that was the first of several similar projects in western Europe at the time. During the early 1900’s notable architects such as Frank Lloyd Wright and Walter Gropius experimented with green roofs on restaurants. (Dunnett and Kingsbury, 9) Roof top gardens have long been used to increase the aesthetic value of a building since the age of modern architecture. Underground parking garages often have a green roof or small urban park on the top most layer visible to the public. Apartment complexes in dense urban neighborhoods use green roofs to attract renters with additional green space. (Dunnett and Kingsbury, 10)

In addition to aesthetic enhancement, green roofs have enhanced the life span of roofing materials. The drainage, growing medium, and vegetation layers protect the waterproofing membrane. A department store in Great Britain, Derry and Tom's installed an intensive green roof to the top layer of its store in 1938 and has not had to replace the waterproofing membrane as of 1999. (Osmundson, 1999) While additional maintenance is required to keep the roof in good condition, the cost of maintenance is significantly less than the cost of replacing the roofing membrane every 10-15 years due to normal wear and tear. History has shown that people enjoy and use green roofs for aesthetic and cost-oriented reasons for many years.

However, the environmental benefits of green roofs have only recently been considered. In the later half of the twentieth century brought the technology and materials needed to build large flat roofs that could support the added weight of roof top vegetation. The movement to green urban areas by adding vegetation to the large flat space available in most cities on roofs started in Germany in the 1980's. (Dunnett and Kingsbury, 10) Here, innovators used green roofs to improve the perception of a city and region. Stuttgart is an example of one such city. Its industrial history and location in a valley led to high levels of air pollution. To improve the city's image green roofs were used to "green" the once industrial town. It was hoped that the plants would improve the air quality of the city. (Toronto, 2007) Researchers found that green roofs provided many environmental benefits beyond aesthetics and air pollution. The increased vegetation in the area reduced the urban heat island. Stormwater run-off was reduced. Buildings were kept cooler in the summer. Germany quickly became the center of the green roof movement and others quickly followed. Other European countries started to develop their own green roof research programs. Green roofs spread to North America and Asia. Green roofs are even being adapted to tropical areas, where the warm climate is expected to benefit of additional green space even more that northern countries. (Osmundson, 1999) This passive mode of environmental improvement is quickly spreading the globe and gaining interest world wide.

2.2 COMPONENTS OF CONVENTIONAL AND GREEN ROOFS

A green roof is a roof that is partially or completely covered with vegetation and growing medium and placed over a waterproofing membrane. Additional layers in between the waterproofing membrane and growing medium layer may also exist, including root barrier and drainage layers. (Wikipedia, 2006) Green roofs can be flat or sloped, above ground, or at ground level. Green roofs come in three varieties, intensive, extensive, and modular. Intensive green roofs are often considered more traditional roof gardens that range from 6 inches to 4 feet of growing material in which large plants, conventional lawns, and even small shrubs and trees grow. An intensive roof needs to be carefully planned and designed, since it will add a significant load to the roof of the building. Generally, intensive green roofs require intensive maintenance. Corresponding to the intensive green roof is the extensive green roof. This type of green roof has only 2-6 inches of growing medium, which means only small plants called sedum, with shallow root systems, and mosses can be supported. Extensive green roofs are designed to be virtually self sustaining and require very little maintenance. (Wikipedia, 2006) The growing medium in extensive green roofs is often man-made growing medium. called substrate, which is light in weight and allows for easy drainage of the soil layer. Extensive green roofs can be retro-fitted to existing building easily because of their light weight and low maintenance. However, extensive green roof vegetation is generally not designed for pedestrians or recreation. Modular green roofs are trays of vegetation in a growing medium that are grown offsite, and then placed on a roof to create coverage. The trays come in thicknesses that vary in growing medium depth from 3-12 inches. Modular green roofs are similar to extensive green roofs in that they are lightweight, self sustaining, and cannot support pedestrians or recreational use. (Toronto, 2007)

2.2.1 Conventional Roof Components

Throughout this thesis, the layers of a built-up conventional roof will often be referred to as the conventional or control roof. A conventional roof is made up of several layers of materials that protect the interior of the building from exposure to rain, snow, wind, and sun. Typically these layers from the bottom (interior) to the top (exterior) are: structural support, roof deck, insulation, underlayment, and waterproofing membrane. The structural support is typically made up of joists that support the outer layers of roofing material. They must be able to support some live load so that maintenance personal can access the roof when needed. (Dunnett and Kingsbury, 61) The roof deck is placed on the structural support. The roof deck is a flat planar layer that the other roof materials are laid on. The roof deck can be any material but is usually a corrugated steel deck in commercial buildings. Insulation is placed on the roof deck. The insulation layer works to keep the interior climate stable by reducing the transfer of heat in and out of a building. Insulation is commonly made from fiberglass, but other more sustainable materials can be found. The insulation is covered with a composite board or underlayment of some type to protect the insulation when the waterproofing membrane is assembled. The waterproofing membrane is a plastic-asphalt combination that, as the name suggests, water-proofs the building. The waterproofing membrane or roofing membrane is constantly exposed to elements that can damage it. Rain, wind, sun, and cold cause the roof membrane to erode and shrink and expand, creating a considerable amount of wear and tear. It is the exposure to the elements that limits the life span of the waterproofing membrane. The average life span of a conventional roof membrane is 15 years. (Roofscapes, 2005)

2.2.2 Green Roof Components

The greening of roof space, or the creation of green roofs, means the addition of additional layers to the roof structure. (Dunnett and Kingsbury, 57) The bottom layers of the roof from structural supports to the waterproofing membrane are the same for both green and conventional roofs. However, green roofs are most commonly made up from a drainage layer, root protection, growing medium, and vegetation built up on top of the roof membrane. The drainage layer encourages the flow of water so that stormwater run off is properly carried away from the building and minimizes the occurrence of standing water, which deteriorates the roof. The root protection is needed to keep the plant roots from the vegetation from penetrating the drainage layer and roof membrane. The growing medium is soil or a man-made soil called substrate to provide a place for the vegetation to grow. The growing medium thickness varies depending on green roof type (extensive or intensive) and the type of vegetation that will be supported. The soil medium is designed to promote regular drainage and provide the plants roots ample space to grow in. Finally vegetation is planted in the growing medium layer. The vegetation layer is made up of the plants and any air space in between or around the plants. Vegetation varies by roof type. Vegetation is selected based on the amount of maintenance the building owner can provide, and the load the roof can support. Drought resistant plants require minimal irrigation and care and are a popular choice for extensive green roofs. The vegetation should reflect the type of plants naturally found in the area of the building. (Roofscapes, 2005) A sample green roof cross-section is shown in Figure 1.

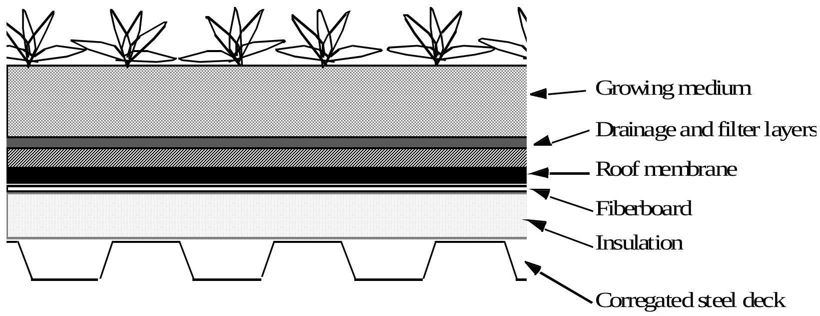

Figure 1. Typical Green Roof Cross-Section

2.3 ENVIRONMENTAL ISSUES IN URBAN AREAS

Green roofs provide numerous benefits; environmental, economic, and aesthetic. To best understand the benefits green roofs provide, two serious problems that plague the urban environment must be discussed. These issues are the urban heat island effect and stormwater management. Both issues have great impacts on the quality of health and environment on people, plants, and wildlife in urban areas.

2.3.1 Urban Heat Island Effect

The Urban Heat Island Effect refers to the fact that urban air and surface temperatures can be up to 10º F warmer than the surrounding rural areas as described by the United States Environmental Protection Agency (U.S. EPA) (Dunnett and Kingsbury, 51). Figure 2 shows the

Urban Heat Island Profile as it ranges from rural, open settings to dense urban settings. Heat Islands form as cities replace natural land cover with asphalt and concrete infrastructure. This development displaces trees and vegetation minimizing the natural cooling effect shading and evapotranspiration; the combined effect of transpiration, the movement through a plant from its roots to the release of vapor from leaves, and the evaporation of water from soil and plant leaves. Tall building and narrow streets can constrict the flow of air in urban centers. (U.S.EPA, 2006) The increased amount of concrete and asphalt in cities also prevent cities from cooling as much as rural areas at night, when radiation from the sun does not contribute to raising temperatures. During the daylight hours man made structures of asphalt and concrete absorb incoming solar radiation. These materials store the radiated energy during the day then, at night, release the stored energy back into the atmosphere. This repetitive cycle leads to an increase in surface and air temperatures.

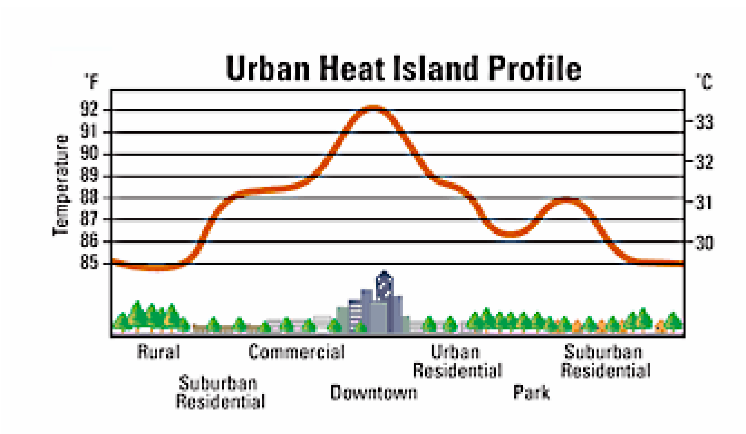

Figure 2. Urban Heat Island (Source: U.S. Environmental Protection Agency)

Heat Islands can occur at any time. They are year-round phenomena, however their negative impacts are felt strongly in summer months as opposed to winter months. They occur both night and day. In fact the inability for cities to cool in the evening results in the largest urban-rural temperature differences to occur three to five hours after sunset. (U.S. EPA, 2006) Heat islands have numerous negative effects on a city, including increased air conditioning demand, heat-related public health risks and reduced thermal comfort. More importantly the need for air conditioning drives energy demands and results in air pollution and greenhouse gas emissions from the increased output from power plants, which could contribute to global warming. (U.S. EPA, 2006) Constricted air flow in the urban environment can also lead to increased humidity and polluted air, increasing risk of asthma and other respiratory problems. (Dunnett and Kingsbury, 51)

2.3.2 Water Management

Another environmental issue that impacts cities seriously is storm water management. This underground and often ignored issue becomes vitally important when a storm event hits an urban area. Two problems combine to make each storm event and environmental jumble for most cities. First, the increased asphalt, concrete, and other impervious surfaces in the city prevents any storm water absorption, meaning all rainfall that lands on an impervious urban surface becomes surface run-off and must be diverted through a storm water drainage system to drain away. In a rural environment the storm water would be absorbed by the soil, where a portion would be used by the plant life supported by the soil, and the rest would go back into the water table. (Dunnett and Kingsbury, 43) Due to the lack of green space in cities, 75% of the rainfall that lands on an urban surface becomes surface run-off and enters the storm water management system. (Dunnett and Kingsbury 43) Superfluous surface run-off is harmful because it picks up pollutants on city surfaces and transports them to receiving body of water. Surface water pollutants include particulates, oil and other synthetic hydrocarbons, heavy metals, road salt, pesticides, and animal waste. (Dunnett and Kingsbury 45) Surface run-off greatly deteriorates the quality of local rivers and the neighboring environment.

The second problem that cities face is inadequate wastewater systems. Some systems combine waste and stormwater. Other systems have waste and stormwater pipe networks, but in a storm event, storm water can infiltrate the wastewater sewage system through cracked pipes and infiltration. This overloads the wastewater treatment facility and as a result, hundreds of sites of untreated wastewater are released into the receiving body of water, before being treated. This raw sewage release can effect manholes, roadways, and basements of houses. (3 Rivers Wet Weather, 2006) For example a storm event of as little as $1/10^{th}$ of an inch of rainfall can result in a raw sewage overflow, in the city of Pittsburgh, Pennsylvania. (3RWW, 2006) As a result from raw sewage overflows, river advisories are put into place 50% (70 days) of the recreational boating season (May through September in the Pittsburgh area) when bacteria and viruses in the waterway place humans at a health risk. This phenomena is often referred to as combined sewer overflow, or CSO. CSO simply means that the area impacted has no or a limited stormwater drainage system in place. When a heavy rainfall event occurs, the access runoff must be channeled through the sewer system. This event flushes pollutants into the receiving body of water before the pollutants can be removed by a sewage treatment plant. (Bass and Baskaran, 2001) For the urban area of Pittsburgh, Pennsylvania, three rivers, the Allegheny, Monongahela, and Ohio, provide 90% of the drinking water for the region. (3 RWW, 2006) As a result, government agencies like the U.S. Environmental Protection Agency and the Pennsylvania Department of Environmental Protection along with corresponding local organizations are looking for ways to repair and upgrade the sewer system in existing cities, while controlling surface run off for new developments as well. For additional information about this serious issue, see Bliss, 2007.

2.4 BENEFITS OF GREEN ROOFS

Green roofs offer a variety of benefits, environmental, economic, and aesthetic. These benefits have been documented in the North American region since the mid 1990's. (Dunnett and Kingsbury, 23) The benefits of green roofs are sometimes scaled. In some instances the benefits can be enjoyed by a single building with immediate results. Unfortunately, this is not always the case. More commonly, the ability of green roofs to combat urban economic and environmental issues takes time and large quantities of roof space. (Dunnett and Kingsbury, 23) This section will document the many possible benefits of green roofs, regardless or time, space or cost restrictions.

2.4.1 Environmental Benefits of Green Roofs

For years, green roofs have been monitored and compared to conventional roofing systems. The literature review in the next chapter shows that green roofs are monitored in several areas; solar reflectance, heat flux, temperature profile, rainfall, microclimate (relative humidity and wind speed and direction), soil moisture, and surface run-off quantity and quality. By monitoring these environmental aspects, researchers paint a picture of how well green roofs perform, compared to conventional roofs. Researchers are trying to capture the impact green roofs have on broader environmental issues, such as Urban Heat Island Effect and storm water run-off quality, with these indicators. The following describes different ways a green roof can benefit the private and public environment.

2.4.1.1 Thermal Protection

Green roofs play an important role in managing the energy needs of a building. Initially, it was thought that the greatest benefit green roofs provided buildings was as additional insulation. However, research has shown this is only a small part of what green roofs can provide (Roofscapes, 2006). Green roofs shade the underlying building. This benefit applies primarily to the summer season, when energy is needed to cool the building. The foliage absorbs radiant energy from the sun, and prevents that energy from reaching the roof surface. Green roofs also reduce heat transfer through advection. Advection occurs when air movement causes thermal transfer. The higher the velocity of air movement, the greater the thermal transfer. This phenomenon is often referred to wind chill during the winter months. However, advection can occur during the summer months as well, having warm air continuously introduced to the building. (Roofscapes, 2006)

The greatest property of green roofs is generally believed to be the thermal mass effect. (Roofscapes, 2006) Green roofs can absorb and store large amounts of energy, especially when wet. The effect of the thermal mass helps create a buffer against daily fluctuations in temperatures. This buffer helps to keep the temperature of the roof at a constant moderate temperature, reducing temperature extremes in the roof and prolonging the life of the roof membrane. This also helps to reduce the overall heat transfer through a building, making heating and cooling the building more energy efficient. This does not mean that green roofs can replace the need for insulation in a building. In fact, it has been shown that buildings perform best when both elements are utilized. (Del Barrio, 1997)

Some benefits of green roofs are seasonal. Evapotranspiration is an important property of green roofs, but only occurs during the warm months when the vegetation is in leaf. Evapotranspiration is water loss through the combined effect of transpiration of plants in their natural biological process and evaporation of water in the soil or growing medium that supports those plants. (U.S.EPA, 2006) The rate of evapotranspiration is dependent on two things. The first is the wind velocity, constant air movement encourages evaporation and transpiration by bringing fresh, dry air to the area. The other factor is relative humidity. The processes of evaporation and transpiration are encouraged by dry air. (Liu, 2002) Therefore, the effect of evapotranspiration is greatest on days when the humidity is low and air movement is high and lowest on days when the humidity is high and the air is still.

Green roofs are also effective in reducing the urban heat island effect. Each component of the green roof has a role in this effect. Foliage absorbs radiant energy and uses it a fuel for photosynthesis. This foliage also shades the area beneath it. The soil medium placed over the roof is also a thermal mass, which keeps the roof membrane from absorbing radiant energy during the day, but also holds that energy at night. Green roofs also moderate extreme temperatures on the roof from peak sunlight to cold nights, reducing the amount of energy needed to control the internal temperature of the building and reducing energy consumption. Green roofs provide more benefits than white or light roofs. White roofs do not absorb as much radiant energy as conventional black roofs; however they reflect that energy back into space, or into neighboring buildings. (Roofscapes, 2006)

Green roofs provide some benefit as simple insulators when the growing medium is dry. It is important to note that green roofs are not good insulators and the real thermal benefit of green roofs comes from their ability to act as heat capacitors, absorbing and releasing energy, and to act as latent heat managers. (Roofscapes, 2006) The "R" value of the growing medium layer depends on the formulation of the growing media. Fine-grained material provides the best protection. (Roofscapes, 2006) However, when the roof is moist, the "R" value is reduced. On the other hand, when frozen, the green roof still provides insulation since the air trapped in the growing medium continues to provide cover. Finding an appropriate "R" value for green roofs is hard to do, because of the variability of insulation. To include a green roof in a building envelope analysis, an effective "R" value can be used. The effective "R" value is determined through back calculations and computer simulation.

2.4.1.2 Water Management

The fate of rain or snow in an urban environment is much different then the fate of precipitation in a forested or rural area. Up to 75% of rainfall on cities or towns is lost as surface run-off, compared to roughly 5% for forested areas. (Dunnett and Kingsbury, 43) As noted before, surface run-off leads to problems related to combined sewer overflow. CSO overloads sewage systems and pollutes receiving bodies of water. However, green roofs can change this. Green roofs can manipulate water run-off in a number of ways. Firstly, the soil substrate and vegetation its supports can trap and store, or retain precipitation. By trapping the water before it becomes surface run-off, green roofs provide areas where water can evaporate back into the atmosphere, reducing the amount of water that becomes run-off. (Dunnett and Kingsbury, 47)

Green roofs can also increase the time in which a rain fall event becomes run-off. During a heavy storm event, rainfall can quickly become run-off as soon as it comes in contact with an impermeable surface and flows into the storm sewer system. Research has shown that rainfall that falls onto conventional roofs quickly enters the storm water system mimicking the storm event, and tapers off quickly. Green roofs have been shown to delay the flow of water into the storm water system, as well as elongating the time it takes for run-off to reach the storm sewer. (Dunnett and Kingsbury, 47) More information on this important benefit of green roofs and related research can be found in (Bliss, 2007).

2.4.1.3 Other Environmental Benefits

A variety of other environmental benefits are possible with the utilization of green roofs. Green roofs can serve as wildlife habitats especially in areas where these habitats have been lost to development. Many green roofs feature plant types native to the location of the roof. They can also be used as stepping stones linking green space on a building to a near by park or garden. (Dunnett and Kingsbury, 41) Green roofs can increase the ecological value of a building by creating a place for birds and invertebrates to live. (Dunnett and Kingsbury, 40)

2.4.2 Economic Benefits of Green Roofs

One of the most significant economic benefits of green roofs comes from their thermal protection. While this seems to overlap with the environmental benefit of green roofs, the thermal protection provided by green roofs can easily translate into cost savings for the building owner. For a private owner, the most noticeable benefit comes in reduced HVAC costs. (Dunnett and Kingsbury, 33) The benefits vary based on climate type and roof type, which is why monitoring green roofs is so important. Some studies have shown a 90% reduction is solar gain in plant shaded areas. (Dunnett and Kingsbury, 34) In temperate areas, the greatest economic benefit for building owners comes in reduced air conditioning cost in the summer months. It has been found that green roofs keep buildings 3-4º Celsius (5-7º Fahrenheit) cooler when the outdoor ambient temperature is roughly 25-30º Celsius (77-86º Fahrenheit). (Dunnett and Kingsbury, 33) Several properties of green roofs contribute to their thermal performance, from direct shading to evaporative cooling to thermal mass. (Liu, 2003) Through out summer months, green roofs reduce the heat gain in the building below, creating energy cost savings for the owner.

Another economic benefit of green roofs is the increase in roof life cycle. A common misperception is that green roofs pool water on the waterproofing membrane causing leaks and requiring roof replacement more often. In fact the opposite is true. (Dunnett and Kingsbury, 29) Typical roof membranes are constantly exposed to damaging elements like solar radiation and rain. In fact, green roofs actually protect the roof membrane by shielding it from damaging elements and solar radiation. (Liu and Baskaran, 2003) A conventional exposed roof membrane absorbs solar radiation throughout the day, causing the surface temperature to rise. At night, the roof membrane reradiates the stored energy and drops in temperature. The diurnal temperature fluctuations create thermal stresses damaging the membrane. (Dunnett and Kingsbury, 30) A green roof, depending on vegetation selection, can reduce these diurnal temperature fluctuations greatly. (Dunnett and Kingsbury, 30) This protection generates a longer life span for the waterproofing membrane.

While prolonging the life span for some roof materials, green roofs do have a higher initial cost than conventional roofs. This is because of the additional materials needed to build up the layers of the green roof. Many researchers are trying to show that while the initial costs are higher, the life cycle costs of a green roof compared to the life cycle cost of a conventional roof is lower. Green roofs modify roof behavior in many ways; insulating the building from temperature extremes, shading the roof materials, reducing the impact of solar radiation and weather elements, and increasing the R-value of the building. (Wong et al., 2003b) This translates to reduced cooling costs for the interior of the building, prolonged membrane life, and decreased maintenance costs. Green roofs offer other economic benefits like increased property values and marketability. One interesting study closely compared the economic value for a conventional flat roof, an extensive green roof, an intensive green roof with shrubs, and an intensive green roof with trees. The model created found that the initial installation costs for each roof was $49.35, $89.86, $178.93, and $197.16 per square meter respectively. However, when the study took into account the entire 40 year life cycle of the roof, including energy expenses and material maintenance, the results differed greatly. When the three green roof types were compared to the conventional roof, the extensive green roof showed an increase in costs of 8.5%, however, the intensive green roof using shrubs showed an decrease in costs of 22.4% and the green roof with trees showed a decrease in costs of 42.6%. (Wong at el., 2003b) Depending on type and vegetation selection, green roofs can provide a great economic benefit.

2.4.3 Aesthetic Benefits of Green Roofs

Green roofs can also give a number of amenity and aesthetic benefits to a community. Urban areas can develop additional green space by utilizing the flat areas on roof tops. One of the advantages to having recreation space on a roof top is security. Since access is limited, green roofs can offer a safe activity space for building tenants or occupants. (Dunnett and Kingsbury, 24) Roof gardens can be used for socializing, light walks, pet recreation, clothes drying and even barbecuing. With proper planning, roof tops can be converted to small golf courses or even playing fields, the possibilities are endless. Green roofs offer building owners and renters a higher quality living or working space.

Instead of recreational uses, green roofs can be used for food production. Some urban areas have difficulty with transporting fresh local food to supermarkets and shops. Green roofs can be used to provide local citizens access to fresher herbs, fruits and vegetables. Most herbs grow well in the shallow well drained soil of an extensive green roof. With the proper structural support, intensive green roofs could be used to grow and harvest fruit and vegetables. (Dunnett and Kingsbury, 26) The best example of utilizing roof space in this way is the Fairmount hotel in Vancouver, Canada. The 2098 sq. ft. roof garden has an 18 inch soil depth. The garden provides all the herbs the hotel uses in its restaurant at a great quality and lowered cost. (Dunnett and Kingsbury, 26)

Finally, green roofs have an aesthetic value as well. In many urban areas, building windows only give views of unattractive asphalt or bituminous roof tops. This is especially true for building surrounding industrial or commercial sites. Even when roof tops are inaccessible but clearly viewed; a green roof garden can still be beneficial. The therapeutic effects of exposure to plants and nature include stress reduction, lowered blood pressure, relief of muscle tension, and increased positive feeling. (Dunnett and Kingsbury, 29) These therapeutic effects are not restricted to apartment dwellers. Office workers, hospital patients, and school students are also benefited. Green roofs provide a variety of environmental, economic, and aesthetic advantages. (Dunnett and Kingsbury, 29)

3.0 LITERATURE REVIEW

3.1.1 Introduction

A literature review was conducted to determine the existing research on the thermal performance and life cycle of green roofs. The literature review is divided into two sections. The first section covers papers focusing on the thermal performance and energy efficiency of buildings with green roofs and verifying the monitoring systems of green roofs. The second section focuses on the life cycle cost and environmental impact of green roofs. Both sections include discussion of instrument set up if available. From this literature review, the standard for green roof analysis was determined for use throughout this thesis.

3.1.2 Thermal Performance of Green Roofs- Instrumentation and Results

"Energy Efficiency and Environmental Benefits of Rooftop Gardens," by K.K.Y. Liu, describes an experimental study performed by Liu and her associates at a National Research Council site in Ottawa, Canada. (Liu, 2002) An 800 square foot low slope roof was divided into two equal areas by a parapet wall. A generic extensive green roof was installed on one side of the wall, while the other half had a conventional roofing assembly. This roof was monitored for both stormwater performance and thermal performance, but this literature review will focus on the thermal performance of the roof. Both sides of the roof were equipped to monitor the temperature profile within the roofing system, heat flow across the system, solar reflectance of the roof surface, soil moisture content, and the microclimate created by the roof plants. Local meteorological data was collected with a weather station located on the parapet wall which measured temperature, relative humidity, rainfall, and solar radiation. Additional weather station data was collected at a site 150 feet from the site. While monitoring at this site is ongoing, the results presented in this paper cover one calendar year of study.

In terms of thermal performance, the research found that the rooftop garden did keep the roofing membrane cool in the summer months through shading, insulating, and evaporative cooling. On an average sunny summer day with an ambient temperature of 95 degrees Fahrenheit (°F), the reference or conventional roof absorbed solar radiation and its temperature reached 158°F, while the membrane underneath the extensive green roof remained relatively constant at 77°F. The study found that the exposed conventional membrane absorbed heat during the day and re-released it at night. The author thought this diurnal temperature fluctuation created thermal stresses on the roof membrane which could affect its long-term performance. The case study continued to measure roof thermal performance in the fall, winter, and spring seasons. While the green roof did provide some protection from temperature fluctuations in the winter, the amount was reduced by the accumulation of snow. The rooftop garden significantly moderated the daily temperature fluctuations in the spring and summer months. The median daily membrane temperature fluctuations were 83 degrees for the reference roof and 22 degrees for the extensive green roof.

In terms of energy efficiency, the green roof did reduce the energy demand of the building. Heat flow through the roof membrane creates energy demand for space conditioning.

Solar radiation and snow coverage also affected the energy demand of the building. In the winter months the roof garden acted as an insulation layer providing moderate energy demand reduction until the soil layer froze. With snow pack, the two roofs performed similarly. The greatest thermal benefit of the green roof came in the spring and summer months, where the shading and evapotranspirative properties of the green roof reduced the energy demand for the corresponding part of the building by 75% compared to the energy needs of the part of the building corresponding to the reference roof.

In another paper by Liu and Bas Baskaran, "Thermal Performance of Green Roofs through Field Evaluation," the authors discuss the temperature profile and temperature fluctuation results found at the same experimental site in depth. (Liu and Baskaran, 2003) The maximum temperature of the waterproofing membrane for both the reference and green roof was compared to the ambient air temperature over a 660 day period. While the air temperature exceeded 30º Celsius (C), or 86ºF, on only 10% of the 660 day period, the reference roof membrane was above 30ºC over 50% of the 660 days, and the green roof membrane went above 30º C only 3% of the 660 days. The reference roof membrane endured large temperature changes each day and varied greatly as the seasons changed. It is also important to note that the reference roof is light gray in color; a darker roof membrane exposed to the elements would achieve even greater temperature extremes. While long-term durability data from the study is not available yet, the author predicts that this temperature change and exposure to UV radiation may accelerate the membrane age, while a green roof would extend the life of a roof membrane.

A report on the complete study of the previous two papers can be found in "Evaluating Rooftop and Vertical Gardens as an Adaptation Strategy for Urban Areas." (Bass and Baskaran, 2001). This report discusses in detail the methodology and reasoning behind the green roof research for the National Research Council of Canada. While much of the thermal data gathered in the study is discussed in the previous papers, this paper documents the daily ambient (above surface) and membrane temperature fluctuations for nearly an entire year. From November 22, 2000 to September 30, 2001 the maximum and minimum daily temperature is graphed. At the reference roof the maximum and minimum temperatures vary little during the winter and by up to 40°C during the summer months. The green roof membrane temperature fluctuations show little variation throughout the year. Also, the temperature of the membrane underneath the green roof does not vary as greatly between the winter and summer maximums. This shows the reduced thermal stress the green roof membrane is exposed to. The heat flow through the roof was also monitored. While the reference roof gained heat during the day and lost that heat at night, the green roof remained very stable. This trend was found during both the summer and winter seasons. The study found that the green roof consistently out performed the control roof in thermal management.

"Green Roof Test Plot; 2003 End of Year Project Summary Report" prepared by MWH Americas Inc. for the City of Chicago Department of Environment, covers an experimental program to compare the temperature and runoff characteristics of green roofs to those of conventional roof systems. (Green Roof Test Plot, 2004) Several 6ft by 6ft by 3.5ft structures were built and outfitted with data logging instrumentation. Six unique green roof products were tested along with three conventional roof products, stone, black tar, and white reflective paint. Ambient weather conditions for the test site were monitored for air temperature, rainfall, wind speed and direction, and relative humidity. The data was recorded every 5 minutes with a data logger. For temperature, each structure was monitored at three or four locations. Temperature probes were used to monitor several locations within the horizon of the structure; the surface temperature, the soil temperature (for the green roofs only), the membrane temperature, and the interior temperature of the shed. The probe measuring surface temperature was outfitted with a radiation shield to maintain accurate measurements, and was placed four inches above the roofing surface. The sensor measuring soil temperature was buried in the soil medium. The membrane temperature was taken just below the impermeable membrane and sealed with foam insulation. The interior temperature was taken in the shed eight inches from the ceiling. These temperature measurements were taken every 15 minutes and recorded using a data logger. While undergoing continuous monitoring, data from one week in July 2003 was used in this report. The data showed that the black tar roof reached the hottest daytime temperature peaks and the lowest nighttime temperatures. The white roof and stone ballasted roof did not hit the extremes the black tar roof did during the day, and both were cooler in the night. The green roofs had the lowest maximum daytime temperatures the highest daily minimums, and thus the smallest temperature fluctuations. The green roof surfaces were consistently 5-10° C cooler than the conventional roofs in the daytime. The data also showed a time lag between the green roofs and the conventional roof types. The green roofs reached their daily maximum afternoon temperatures 1.5-3.0 hours after the other roofs. At night, the green roofs were also slower to reradiate the heat they stored during the day. This could be because the additional layers needed to make the green roofs act as insulators that slow down the absorption and re-radiation process.

Green roofs have also been studies in tropical climates. In “Investigation of Thermal Benefits of Rooftop Garden in the Tropical Environment” a green roof was studied in a tropical and urban area of Singapore. (Wong et al., 2003a) The research looked to identify the reduction of surface temperatures caused by different plants, the reduction in heat gain caused by the plants, and the variation of ambient variables caused by the plants. The paper also focused on the monitoring system designed for the study. Field measurements at the site in Singapore included ambient air, relative humidity, wind velocity, solar radiation and the temperature profiles for the site. Thermocouples were used to capture surface temperature measurements at hard surfaces (pavers), the soil surface, on the surface underneath the vegetation, in the soil layer, and the temperature at the roof membrane. The temperature profile also included 3 points above the hard surface portion of the roof 300, 600 and 1000mm from the surface respectively, and at 3 points above the green roof vegetation 300, 600, and 1000mm above the surface respectively. Interior air temperatures were taken at 2 points in rooms directly below the roof. The air temperature sensors were covered with white wooden shelters that protected the sensors from direct sunshine and rainwater but encouraged natural ventilation. The study found that the green roof plants reduced the roof surface temperature and heat transfer into the rooms below. The hard surfaces reached a maximum temperature of 57º C in the afternoon when solar radiation was 1400 W/m^2. The temperature taken at the hard surface varied 30º C through out the day. The bare soil however, reached a maximum afternoon temperature of 42º C and only varied 20º throughout the day. This is likely because if the affect the evaporation of moisture in the soil had on the soil surface. The temperature of the surface underneath a plant was dependent on the leaf area index (LAI) of the plant. The highest temperature recorded underneath a plant was 36º, although temperatures as low as 26.5º were found. The variation in surface temperature throughout the day also reduced to 3ºC.

The heat flux through out several roof types was also calculated. The U-values[1] for different roof surfaces were obtained and total heat gain/m² over a day was calculated. The bare hard surface was found to have the most heat gain during the day and inverse heat flux at night. While dependent on plant type, surface areas underneath the plants maintain inverse heat flux through out the day and night. However, the plants did not have a heat saving effect or insulative effect at night. Areas under the plants performed only slightly better than bare soil at night. The author believes that this might mean that the soil layer provides some added insulation but the real benefits of green roofs come in the shading effect of the plants. The above surface thermocouples also made a profile of the hard surface and vegetation affects on ambient air temperature and the Urban Heat Island. While during the day, temperatures nearer the surface increased about the same amount for both the hard surfaces and vegetated surfaces, at night the vegetated surfaces had a larger drop in temperature. The greatest difference in temperature between hard and vegetated surfaces was 4.2º C measured at 300mm height at 1800 hours. No significant difference in relative humidity was found at 1m above the surfaces.

A continuation of this study is documented in "Study of Thermal Performance of Extensive Rooftop Greenery Systems in the Tropical Climate." (Wong et al., 2007) In this case study, temperature measurements were taken before and after a building was outfitted with four different extensive green roof systems. The first phase of measurement was carried out for 22

---

[1] U and R values are used to describe the ability of a building material to resist heat transmission. The R-value is the resistance of material to heat flow. The units of the R-value are hour*ft^2*°F/Btu. The higher the R-value, the more the material resists the flow of heat. The U-value is the inverse of the R-value, or the amount of heat a material can transfer. The units of the U-value are Btu/hour*ft^2*°F. The lower the U-value, the better insulating quality the material has. (Heerwagen, 2004)

days between May 19th and June 9th 2003. After the extensive green roofs were installed, a second phase of measurement was conducted for 18 days between February 14th and March 3rd 2004. The tropical location of the study site means that weather is relatively constant year-round. The two periods in the paper were selected because the weather was similar in temperature and rainfall for both study periods. The building used in this study is a multi-storey parking garage. Thermocouple wire was used to measure the surface temperature at eight points on the top of the parking structure. The monitoring plan was designed to measure two surface points for each section of the future green roof. In addition to the surface temperature, ambient air, relative humidity, and reflected radiation were also recorded at a single site for each future extensive green roof area. Relative humidity and ambient air temperature were measured 30cm and 120cm above the surface. Reflected radiation was measured 80cm above the roof surface. Lastly, a single weather station on site was used to measure ambient air temperature, relative humidity, solar radiation, wind speed, wind direction, and rainfall. A two day period from both the before and the after sessions were selected for discussion in the paper.

Generally, the study found that the after session had lower air temperatures, higher relative humidity, and lower wind velocity. The surface temperatures demonstrate the thermal performance of the measured object. The temperature fluctuation of the roof top during the after session was significantly reduced compared to the before session. While the roof membrane had improved thermal performance, the substrate surface of the extensive green roofs did not show any reduction in temperature. The authors found that the color and low thermal capacity of the thin substrate resulted in high surface temperatures. A prolonged drought and limited vegetation may have also affected the results.

Heat flux was also monitored throughout the study period. Generally, the before session had minimal heat flux at night and maximum heat flux during the day. The after session had the opposite result. It was found that during the before session the roof showed a significant amount of heat gained during the day, and little or no heat lost at night. During the after session, the roof showed reduced heat gain during the day. The roof also lost heat at night after green roof insulation. The author contributed this affect to the wet drainage system now on the roof reducing the heat transfer of the roof system.

The ambient air temperature, or air temperature above the roof actually tended to be warmer over the vegetative surfaces as opposed to the concrete surface in the before session. The high surface temperature of the substrate was the likely cause of this effect. Unfortunately, the cooling ability of the vegetation on the extensive green roofs was minimal. The after session did experience lower ambient temperatures at night, with reductions in temperature up to 3.5°C. The two different elevations (30 and 120 cm) above the surface were slightly different. The temperature tended to be warmer at the lower elevation and cooler at the higher elevation. Unfortunately, the low cover in vegetation and dry substrate blurred the effect of the green roof on ambient temperature.

Interestingly, the greatest success in this case study was in monitoring the reflected radiation. The reflected radiation was much lower in the after scenario. Unfortunately, a number of factors could contribute to this phenomenon. The extensive green roof reflects radiation less directly and diffuses it, while the smooth concrete surface did not have that effect. Regrettably, the high substrate temperature could increase long wave radiation, a factor the instruments could not measure. None the less, one monitoring point decreased the peak reflected radiation more than 50%. The darker color of the substrate absorbed more radiation than the concrete surface.

The other data points showed a reduction in reflected radiation by 30%. Overall, the newly installed green roofs had a greater thermal performance than the concrete roof top, but the effect was skewed by the poor vegetation cover and drought.

3.1.3 Thermal Performance of Green Roofs- Mathematical Models

The “Analysis of the Green Roof Thermal Properties and Investigation of its Energy Performance” conducted an investigation in two phases. (Niachou et al., 2001) In the first phase extensive air and surface temperatures were measured inside and outside the building. In the second phase the thermal properties and energy savings of the green roof were examined using a mathematical approach. Both insulated and non-insulated roof types were included in the study. The case study took place in Athens, Greece. In the instrumentation of the green roof several instruments were used to detect temperature and humidity changes on two roof surfaces, green and flat. An infrared camera measured surface temperatures. An infrared thermometer was used to measure temperature of interior and exterior surfaces. A thermometer-psychrometer measured the indoor and outdoor air temperature and the relative humidity. Temperature sensors were used to record indoor air temperatures for the study of thermal comfort conditions. Measurements were taken at a 30 minute interval for a 1.5 month period from June 30th to August 17th in 2000.

A number of surfaces were monitored for temperature. They include insulated buildings with and without vegetated roofs, and non-insulated building with and without vegetated roofs. Temperature ranged based on location on the roof for the insulated buildings. Large thick vegetation kept the surface temperature between 25º- 29ºC. Sparse vegetation or bare soil areas had surface temperatures ranging from 36º- 40ºC. However, a similar temperature range was found on the hard roof insulated building were similar. White shaded surfaces had temperatures of 27ºC and white un-shaded areas rose in temperature to 40ºC. A significant difference in surface temperature was found on the non-insulated buildings where the green roof held temperatures between 28º- 40ºC, while the conventional roof surface temperature reached 42º-48ºC. For buildings with no insulation, green roofs greatly improved the thermal performance of the building.

Part of this study focused on the indoor air temperature and comfort levels. Studies were performed throughout periods of air conditioning use and with no air conditioning. The green roof kept the indoor areas cooler (in the summer months) and also decreased the temperature width- or the difference between the maximum and minimum daily temperatures. Throughout the 1.5 month measurement period, 2325 measurements were taken, with 5% of the measurements exceeding 30ºC for the green roof and 18% of the measurements exceeding 30ºC for the roof with no vegetation or soil. Of those measurements, 3% of the non-green roof measurements exceeded 32ºC. No measurement under the green roof exceeded 32ºC.

Finally, a mathematical model of the thermal performance and energy savings was created. The model looked at buildings with various degrees of roof insulation, with and without additional green roof layers. A computer model was used to estimate the mass and heat transfer in the interior of the building. Different scenarios were run to include the affects of night ventilation to varying degrees. The results showed that non-insulated roofs with no green roof had the greatest amount of heat transfer. Well insulated roofs performed the same regardless of whether a green roof was present or not. Green roofs provide the biggest benefit to buildings with low or no insulation. However, green roofs provided significant energy saving to all roof insulation types, especially when night ventilation was included in the model. The total energy consumption savings for the building models was 7% for the non-insulated roofs and 2% for the well insulated roofs.

Another mathematical model to predict green roof thermal performance was published in "The Contribution of a Planted Roof to the Thermal Protection of Buildings in Greece." (Eumorfopoulou and Aravantinos, 1998) It was found that while the green roof contributed to the thermal protection of the building, it could not replace the thermal insulation layer. Heat transfer of a green roof differs from that of a bare roof as the external climatic factors; solar radiation, external temperature, relative humidity, and wind, are all slowed down or reduced as they pass through the foliage layer of the roof. A significant part of the solar radiation is absorbed by the foliage and used for their biological functions, photosynthesis, respiration, transpiration, and evaporation. Thermal loads throughout the year also play a role in the thermal performance model. In the summer, the roof takes the greatest thermal load, 2 times greater than the south wall and 1.5 times greater than the east and west walls. However, in the winter, the walls receive the greater thermal load, with the roof only receiving 1/3 or the southern wall's load and 2/3 of the load from the east and west walls. A value of thermal transmittance, U, was calculated for a number of different roof types with varying amounts of thermal insulation, green roof layers, and vegetation densities. The resulting U value helped to model when green roofs are most applicable in the built environment. In fact a roof with high vegetation but no thermal insulation performed at the same level as a thermally insulated bare roof.

A common conclusion among authors is that green roofs do not act as a cooling device as much as a protective and insulating device, reducing the heat flux through the roof. In "Analysis of the Green Roofs Cooling Potential in Buildings" green roof design parameters, leaf area index, soil density, thickness, and moisture content, are used to depict the cooling potential of green roofs (Del Barrio, 1998). The outdoor conditions affecting the mathematical equations are solar radiation flux, air temperature, relative humidity, and wind speed and direction. Heat and mass fluxes are assumed to be vertical to simplify the equations. A significant portion of the mathematical model variables are dependent on the moisture content of the growing medium, and the temperature. Another portion of the model addresses the vegetation canopy. The thermal state of the canopy is dependent on incoming solar radiation, reflective radiation, convective heat transfer, evapotranspiration, evaporation of water in the soil medium, and convective heat transfer. By modeling these factors the author found that LAI (leaf area index) played a significant role in the equations as the role of the canopy as a shadowing device was strong. The soil thickness, density, and moisture content determined its thermal diffusivity. Evapotranspiration also affected the heat flux of the roof due to the hydrothermal state of the canopy. No study was done to compare the thermal performance of the roof during the winter months.

One paper addressed the issue of including green roof simulation models in building energy simulations. The paper, “Summer Period Analysis of the Performance of a Planted Roof as a Passive Cooling Technique” takes another mathematical approach to evaluating green roofs. (Theodosiou, 2003) This study was verified by a parametric study of an existing construction site in the Mediterranean area that evaluated the main planted roof characteristics that affect the performance of a planted roof as a passive cooling technique. Unfortunately, passive cooling techniques tend to be overlooked since they cannot be accurately included in the building simulation model. In Greece the goal is to study green roofs for long-term performance so validation can occur. (Del Barrio, 1998) The mathematical part of the model is solved with a

Gauss-Seidel method. Temperature measurements were taken at 21 nodes throughout a roof cross-section. Steady U values for the growing medium were not used due to the variation of insulative quality based on time and water content. The author used Suncode P.C. to model the case study building and added an additional module, a thermal zone above the waterproofing membrane, to model the green roof. This method allowed the programmer to model a building with a green roof using a typical building energy modeling program, and created a thermal zone above the conventional roof that affected the building's internal temperature. The study was validated by comparing the measured and calculated temperatures for the 4 node points over a 20 day summer period when the building was not in use. During this period, ventilation, internal temperature, humidity, AC function, and internal gains were controlled and monitored. The climatic file used as input consisted of data measured on the top of the building roof by a weather station. A sensitivity analysis was performed on green roof characteristics including foliage height, foliage density, soil layer thickness, type of soil medium, insulation thickness, relative humidity, and wind speed. The results showed that:

- Foliage Height: Short foliage limited the shading provided, cancelling out the affect of transpiration. A shorter foliage layer also adversely affected the ability of the layer to cool the layers surrounding it. High foliage height was more successful in keeping the building cool even in days of excessive heat
- Foliage Density: This was dependent on LAI (leaf area index). Hot dry days were optimal for the plants and their biological process (transpiration) were successful in keeping the roof cool. However the plants did keep the roof cool based more on their affect on the soil layer, keeping it shaded, transpiration, and less connection with the ambient air.

- Soil Layer Thickness: Values from 0.05-0.5m were chosen for evaluation. The greatest effect the soil layer thickness had on the model came from thermal inertia, where the lag and reduced variation in thermal flux was apparent. The thicker the soil layer, the longer it was able to maintain a lower temperature.
- Roof Type: When different roof types we utilized, soil thickness, foliage height and drainage layer height increased simultaneously. The combination of these factors drastically changed the thermal flux. The thicker the layers, the better the thermal performance of the roof.
- Insulation Thickness: This controls the thermal connection of the interior of the building to the ambient air temperatures. Higher insulation levels reduce heat flux and neglect the cooling ability of the green roof on the interior.
- Climate Conditions: Relative humidity and to a lesser extent, wind speed, have a significant impact on the cooling ability of the green roof. Dry windy days encourage the evapotranspiration process, while stagnant humid days slow the process.

The possible positive impact of green roofs on the Urban Heat Island is very important. "Measurement of Thermal Environment in Kyoto City and its Prediction by CFD Simulation" uses a computational fluid dynamic (CFD) model to evaluate the real thermal environment of an urban area. (Takahashi et al., 2004) This code could then be used to investigate the effect of additional green spaces (green roofs and parks) on the urban heat island and the thermal environment at street level. Intensive measurement of urban environment was performed including air temperature, surface temperature of building walls and city streets, solar radiation, long-wave radiation, sensible heat flux, and latent heat flux. The model and verifying measurements should that the urban city center had a distinct air temperature difference when compared to a university campus with ample green space. It was found that increasing green space could have a significant positive impact on the urban heat island.

3.1.4 Life Cycle Cost Assessment of Green Roofs

A common misperception of green roofs is that while they are environmentally beneficial, the initial costs make them unfavorable. It is not always the case. “Life Cycle Cost Analysis of Rooftop Gardens in Singapore” highlights the economic benefits of green roofs that can offset the initial costs and compares the initial cost of green roofs compare to a traditional flat roof. (Wong et al., 2003b) To quote Manfred Koehler, a leading German green roof expert, “ green surfaces are less expensive than tiled roofs in the long run because they last longer’”. (Wong et al., 2003b) However, in countries where use of green roofs is not widespread, models and life cycle analysis must be performed to determine if such a statement is true in all areas of the world. Unfortunately, the greatest economic benefit of green roofs, the increase of roof membrane life, takes years to establish. Until enough time passes to ensure roof membrane longevity, initial costs will inhibit the construction of green roofs. Some researchers have found that green roof initial costs can be three to six times higher than traditional roof costs. Still, the economic benefits of green roofs have been documented. These benefits include reduced temperature extremes, shading, and higher insulation value resulting in reduced energy costs during the life of the green roof. By protecting the roof membrane from weather and temperature extremes, the maintenance and replacement cost of the membrane can be reduced.

Finally, green roofs can be economical by increasing the property value and marketability of a building, increasing the production of workers with a view of the roof garden, and harvesting rainwater for domestic needs. Green roofs provide numerous benefits to the building and community surrounding it.

In the life cycle cost analysis three roof types were examined, conventional, extensive green and intensive green. The model included information about the structural costs, initial costs, life cycle costs, and life cycle energy costs of each roof over a specified period. The structural costs of each roof increased with weight of the system, where the traditional roof weighed the least and the intensive roof weighed the most. The initial costs also varied with roof type, the traditional roof with the lowest cost and the intensive with the largest cost. The life cycle costs included the initial costs, as well as maintenance and replacement costs. The intensive roof was costlier than the traditional roof, due to the regular maintenance, however, the extensive green roof did provide some cost savings from the reduced maintenance. Lastly, the energy costs were included in the model. Since the green roof options increase the insulative value of the building, they provide significant cost savings over the life cycle of the roof. The results of the study find that including the energy costs into the model equates the cost of the extensive green roof to that of the traditional roof. This includes all costs from start-up to replacement. The extensive green roof is an economically and environmentally friendly choice.

Finally, in "Comparative Life Cycle Assessment of Standard and Green Roofs" life cycle assessment is used to evaluate the benefits, primarily from reduced energy consumption, resulting from the addition of a green roof to an eight storey residential building in Madrid, Spain. (Saiz et al, 2006) The study examined the LCA over a 50 year life span of the building. The study evaluates the life cycle environmental impacts of the multi-storey building with a conventional flat roof, reflective white roof, and an extensive green roof. The study also performed a sensitivity analysis considering the environmental impacts of roof type on potential energy savings resulting from a reduced urban heat island, if green roofs were prevalent throughout the city.

The conventional roof in this study was a flat roof protected by porous concrete tiles, a type common in Madrid. The roof tiles consist of a rigid porous 4 cm concrete layer and a 4 cm extruded polystyrene layer set on a PVC membrane adhered to the structural roof deck. The alternative roof types in the model were a reflective white roof and an extensive green roof. The reflective white roof had the same composition as the conventional roof tiles, with a reflective white paint coating on the external surface. The extensive green roof also utilized the roof tile base of the conventional roof type. However, a glass fiber filter layer, 9 cm of soil substrate and vegetation were placed on top of the roof tiles.

The energy performance of the building was simulated using Environmental Systems Performance – research (ESP-r) software. Natural gas is used to heat the building, while electricity is used for space cooling. The thermal performance of the building was evaluated for the climate of Madrid, with average summer temperatures of 19.4°C (66.9°F) and average winter temperatures of 9.7°C (49.5°F). The model was validated through the analysis of the summer peak temperatures and heat fluxes. Energy consumption model of the building resulted in only a 1% reduction in energy demand for the year by using a green roof rather than the conventional roof.

Simapro software was used to model the LCA of the building in three stages, material production and transportation, building operation, and building maintenance. The LCA results showed that the conventional roof building had the largest negative impact on the environment.

More than 50% of this impact came from the use phase of the building. The most significant contribution to these results came from the use of electricity as an energy source. The use of natural gas for heating was the second largest contributor. The materials phase of the building contributed about 20% to the environmental impact. However, only 1% of these materials were needed to construct the conventional roof.

The addition of a green roof made some impact on the models created in this study. First, the green roof reduced the annual energy consumption 1.2%, primarily by reducing the summer cooling load 6%. By substituting a green roof for the common flat roof, the environmental impact was reduced by 1-5.3%, depending on the impact category. A majority of this reduction in environmental impact came from the reduction in energy needs, in the use phase of the building. There is also a modest change in the materials phase of the building, since the green roof extended the life span of the roof membrane. Overall, the addition of the green roof did prove to be environmentally beneficial. The green roof covered on 16% of the building surface, and still significantly reduced its cooling load. As a result, the green roof's greatest impact was in environmental stressors most impacted by electricity use. The white roof obtained 65% of the green roof's cooling reduction, but did not increase the life span of the roofing materials. To end with, the sensitivity analysis assumed that if green roofs were installed over 50% of the city and 3% were saturated; a 1° drop in temperature would be obtained. These numbers were obtained from a report by the city of Toronto. The study found that is those statistics were applied to Madrid the city's cooling load would be reduced 33%. Overall the study found that green roofs may be beneficial in reducing the urban heat island in Madrid.

4.0 SITE DESCRIPTION AND PROTOCOL FOR TEMPERATURE, RELATIVE HUMIDITY, SOLAR RADIATION, HEAT FLUX AND WIND MEASUREMENTS

4.1 INTRODUCTION

The objective of this research is to look for a way to reduce the urban heat island effect (UHI), lengthen the life cycle of the roof membrane, reduce the runoff volume, and improve stormwater runoff quality from a dense urban site with a vegetated roof system on a retail store. This research was funded by a grant from the U.S. Environmental Protection Agency to the non-profit organization Three Rivers Wet Weather (3RWW) which uses the grant to create demonstration projects to develop new and innovated ways of addressing the combined sewer overflow (CSO) problem in Allegheny County. This research will compare the thermal and water quantity and quality measurements taken at two different roof types, an extensive green roof, and a conventional rock-ballasted roof. This thesis focuses solely on the temperature and thermal performance measurements and how they compare to the urban heat island and roof membrane life cycle.

The green roof project is part of the renovation and expansion of the Shadyside Giant Eagle supermarket. Prior to expansion, the site consisted of approximately 20 single and multi-family residential units and 2 commercial properties. These properties were comprised of 11 attached row houses, 1 3-storey eight unit apartment building, a vacant single story commercial garage, and a vacant Eckerd Pharmacy. The site totaled 3 acres in size. The vacant structures were demolished and in March 2004 excavation began for a new 2-storey underground parking garage and retail store expansion. A 5-storey apartment complex with 78 residential units was constructed above and behind the Giant Eagle store and parking garage. The extensive green roof was installed on about 12,300 sq. ft. of the supermarket roof, as a temperature and storm water management apparatus and visual amenity for the apartment occupants.

This project was designed to address the possible benefits of green roof installation, such as reducing the urban heat island effect (UHI) and combined sewer overflow (CSO) events that afflict Allegheny County. The instrumentation at the site will monitor surface temperature, ambient temperature, precipitation, growing media moisture content, relative humidity, solar radiation, wind direction and speed, stormwater retention, stormwater runoff, and runoff quality. The objective of the qualitative sampling was to assess the long and short term changes in the roof environment as a consequence of the addition of a vegetative area. This chapter will describe the layout, instrumentation, and set-up utilized to monitor the temperature, thermal performance, and water management of the Giant Eagle Roof site.

4.2 SITE DESCRIPTION

Figure 3 shows the general layout of the Giant Eagle supermarket addition. The location of the green roof at the Giant Eagle site is the green rectangle in the center of the figure. The expanded grocery store extends to the top of the figure. The apartment complex is shown towards the bottom. Several locations at this site are being monitored for a variety of environmental factors, such as thermal transmittance and water run-off quantity and quality. Four locations on roof of the entire addition were designated as temperature measurement locations. Two were located on the green roof, while two were located over the conventional roof to act as a control scenario. These locations were named A, B, C, and D. Locations A and B are the measuring sites over the green roof and locations C and D measure the control roof. These locations are marked on Figure 3. Soil Moisture sensors were positioned at locations A and B. Solar radiation, heat flux, and relative humidity were each measured at two temperature locations, A and C. Wind speed and direction was measured only at location C. Finally, a rain gauge was located on the control roof, between temperature locations C and D.

In addition to the temperature and weather measurements, water quantity and quality was also monitored. One roof drain from both the green and control roofs were separated from the rest of the roof drainage system. These two drains drain similar 4000 square foot drainage areas of the conventional rock-ballasted roof and green roof. The drainage from these two is directed street level to an area next to the parking lot and garage for the supermarket. Here, the flow is directed into 2 flumes, one for each the green roof and control roof drainage, measured with ultrasonic sensors to determine the amount of flow. A small portion of the flow is siphoned off and collected in small bottles that are collected and taken to the Environmental Lab at the University of Pittsburgh for laboratory experiments to determine the quality of the water. The flow is then directed into the main storm water drainage system.

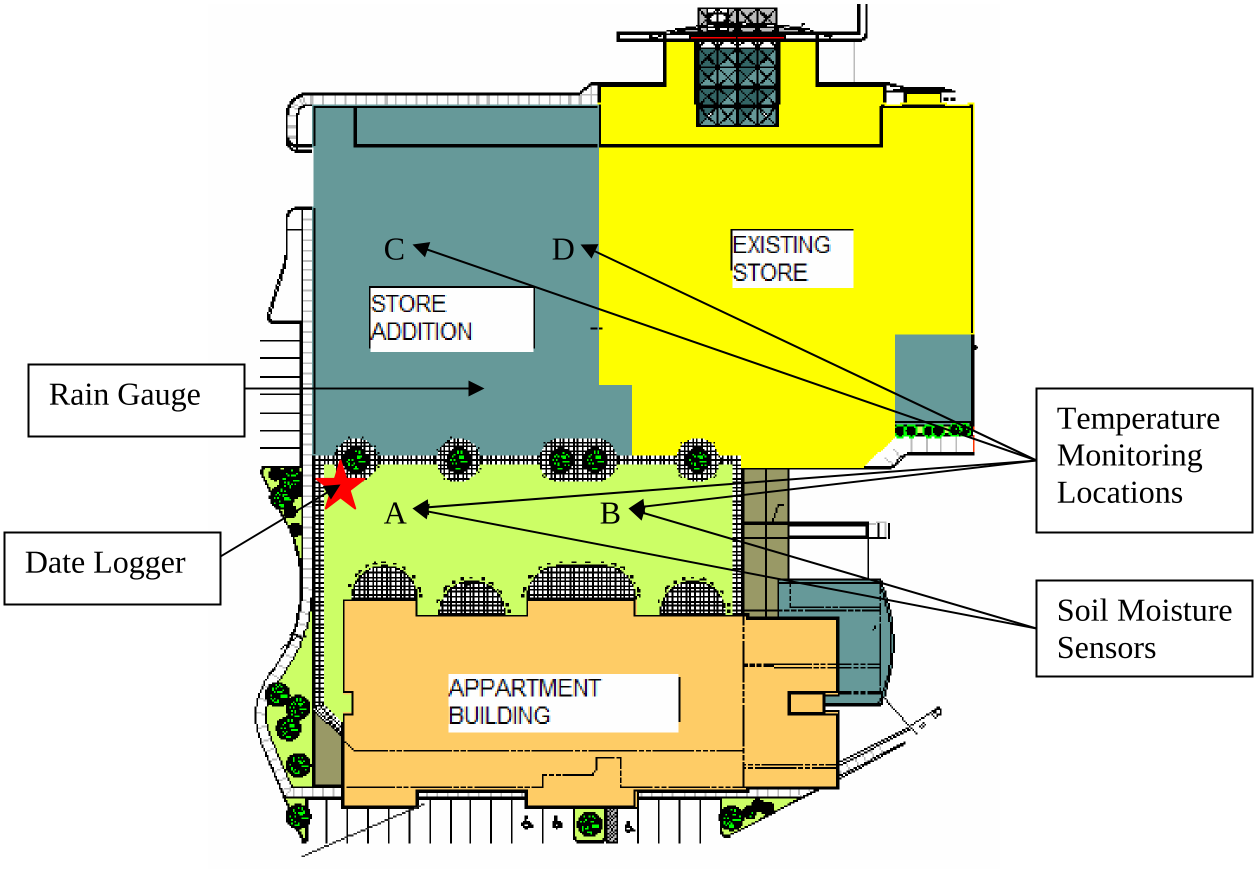

Figure 3. Giant Eagle Supermarket Addition Plan View

4.3 MONITORING SITE LOCATIONS

As discussed earlier, four monitoring stations were placed on the overall Giant Eagle addition site. Two will be placed on the green roof, while the other two are placed over the conventional roof. The sites over the green roof will be named A and B, over the conventional roof they will be called C and D. The general location of these sites is shown in Figure 3. The location of each site was chosen so that the influence of one site on the other attributable to the environment and wind should be minimal. The four sites over the roof area were placed away from the drainage areas of the roof so the measurements remain accurate. A is 40 feet from left edge of the building and 48 feet from the north facing wall of the apartment structure. B is 40 feet from the right edge of the building and 48 feet from the north facing wall of the structure. The conventional roof stations, C and D, are 92 feet directly north from the corresponding green roof measurement sites.

Some precautions were taken over the green roof portion of the project. Variables such as plant placement were considered when finalizing the location of the monitoring stations. Constant shade may adversely skew the measurements. The layout of the entire supermarket and apartment complex site must also be considered when placing the instruments and measuring stations. The five-storey apartment building structure is at the south end of the site. The green roof is situated just north of this structure. This means that the green roof will be shaded from direct sunlight by the apartment building at certain times during the day. Unfortunately the location of the green roof relative to the apartment building was non-negotiable. Consideration must be taken when analyzing the results from this experiment. Finally, wind current will have some effect on all temperature measurements. All four measurement stations were positioned a minimum of 100 feet from all vents and mechanical equipment to keep the influence minimal. Proper precautions with each instrument should minimize adverse influence in the measurements.

4.4 INSTRUMENTATION

This section describes the specific instruments used to monitor the two types of roofs at the Giant Eagle location. The following weather and temperature measurements are needed to determine how green roofs perform differently from conventional roofs.

4.4.1 Relative Humidity

Two monitoring locations, A and C, have a HMP 45C Temperature and Relative Humidity Probes. This probe monitors the relative humidity near the surface level. It was placed 24”above the roof surface in a radiation shield. For location both locations A and C, the RH probe will simultaneously measure relative humidity and ambient temperature, eliminating the need for multiple pieces of equipment in the same location.

The relative humidity measurement is an important parameter of the green roof. Relative humidity affects the rate at which the vegetation transpires. Generally, the less humid it is, the more the plants transpire. The more the plants transpire the greater the cooling effect for the green roof. The purpose of monitoring the relative humidity on the roof is to determine if humidity is an indicator for green roof performance. The sensor will be placed in the vegetation layer to monitor the microclimate at that layer.

As noted, each probe will be housed in a radiation shield. They require the DC042 12-plate Gill Radiation Shield and Adaptor. For each instrument there will be a lead length, or the length between the instrument and the data logger. Ideally, the HMP 45C allows for 6 feet of lead length, but this can be adjusted for longer lengths. The approximate error for lead length is

0.56°C for temperature and 0.56% for relative humidity per 100 feet of lead length. Maintenance for the RH probe is minimal. The radiation shield and sensor are checked for contaminants and debris monthly. If needed, the sensor can be rinsed with distilled water to remove debris. Finally, the RH sensor must be recalibrated by Campbell Scientific annually. A picture of the RH sensor in a radiation shield at the site location is shown in Figure 4.

Figure 4. Relative Humidity Sensor in Radiation Shield

4.4.2 Roof, Growing Media, and Plant Level Air Temperatures

All temperature measurements are situated at monitoring stations A, B, C and D. All four stations are designed so the temperature measurements are symmetrical at all four locations, with additional measurements taken in the additional layers necessary for the green roof. The temperature measurements were taken with a combination of thermocouple wire, HMP 45C Relative Humidity and Temperature Probes, and Model 107AT Temperature Probes. These sensors will provide a temperature profile vertically throughout the green and conventional roof structures. The thermocouples will be used to measure temperature throughout the roof structural system; below the corrugated steel deck, above the steel deck, above the insulation, and below the waterproofing membrane; on the surface; and at 7, 15, 30, 60, and 100 cm above the roof surface. The thermocouples exposed to the outside environment will need to be shielded from solar radiation. A simple, aluminum foil-covered, open-air wooden structure, or shelter, protect each above surface monitoring point. Additional soil temperature measurements will be obtained with the temperature probes. These model 107 temperature probes are buried 3” into the soil substrate on the green roof. The ambient air temperature is monitored by the RH probes, a dual function probe, which is protected in a radiation shield. The temperature profile created is described in Table 1: Temperature Measurement Locations.

Table 1. Temperature Measurement Locations

Horizon ID	Temperature Measurement Location
Overall Ambient	Taken by RH Probe 12” above surface at locations A and C only.
Ambient 1m	Attached to pole 1 meter above roof surface.
Ambient 60cm	Attached to pole 60 cm above roof surface.
Ambient 30cm	Attached to pole 30 cm above roof surface.
Ambient 15 cm	Attached to pole 15 cm above roof surface (above vegetation).
Ambient 7cm	Attached to pole 7 cm above roof surface (just above vegetation)
Surface	Placed on Roof or Soil Surface
Soil	**Buried in planting medium at ½ depth (green roof only).**
Filter Membrane	Just above the filter membrane, sealed in insulation (green roof only).
Drainage Layer	Below Drainage Layer (green roof only).
Waterproofing Membrane	Just below the impermeable membrane, sealed in insulation (both green and conventional roof).
Support Panel	Just below support panel.
Insulation	At the bottom of the insulation layer.
Roof Deck	Just below the roof decking.

Black denotes Thermocouple used.
Bold denotes 107 Temperature Probe used.
Underline denotes RH sensor used.

The temperature profile created by these measurements will provide data on the thermal performance of both roofs. The temperatures taken at the different locations within the roof itself will provide data to determine the insulation properties thermal transmittance of each structural layer, as well as the layers of the green roof. (Eumorfopoulou, 1998 and Niachou, 2001) They will also be vital in documenting and modeling the heat flux through the roof structures. (Del Barrio, 1998) The temperature readings above the roof surface measure the temperature differential between the roof surface and the air above it. (Wong et al, 2003a) The structural assembly temperature measurement locations are based on those depicted in the Ottawa campus experiment (Liu, 2003).

In addition to the temperature monitoring sites below, on, and above the roof surface, two supplementary sensors will provide an additional measurement. These supplementary measurements from the relative humidity sensors provide the ambient temperature for the site. Since the sensor is protected by a radiation shield, it should provide an accurate ambient temperature, not influenced by radiating or reflected heat from the surrounding building or from the sun.

The 107 Temperature Probes can have lead lengths up to 1000 feet. Precautions must be taken in electronically "noisy" environments. AC power lines can effect the measurements. A 60 MHz rejection should be used if the probe is in an electronically noisy environment. Maintenance for the temperature probes is minimal. The radiation shield should be checked monthly for debris. Calibration should not be needed after the instruments are set up. Thermocouple wire was purchased from Omega. A sample of the above surface thermocouple at the Giant Eagle site, without the radiation shields, is found is Figure 5.

Figure 5. Thermocouple Wire Attached to Tripod

4.4.3 Incident Solar Radiation and Long-wave Radiation

One site over both the conventional and green roof (at locations A and C) each will house a Net Radiometer, or high-output thermopile sensor, which measures all incoming and outgoing radiation. The sensors are mounted on a tripod roughly 40cm above the roof or vegetation surface. (Wong et al, 2003a) The sensor head was aligned so that it points south. The sensor has a wind shield pre-installed to minimize the effect convective cooling on the sensor.

Incident and long-wave radiation measurements are very important to this project. The measurement of incident solar radiation is needed to determine the amount of energy being received from the sun. This is important to determine the energy balance of the roof. (Del Barrio, 1998) The long-wave radiation then shows the amount of energy the roof or vegetation is reflecting. The instrument output represents the algebraic sum of short and long wave radiation is out-putted by the instrument. Both incident and long-wave radiation was used in the mathematical model created by Del Barrio in analyzing the cooling potential of green roofed buildings.

The Net Radiometer is a sensitive instrument. It is sensitive to the convective cooling effect wind has on the sensor area. This can be adjusted with a correction factor given by the manufacturer. The desiccant needs to be inspected monthly to make sure the gel is blue and white in color. If it turns pink, the gel needs to be replaced. This can occur commonly in wet weather. Condensation on the wind shield can eliminate the long-wave radiation reading. An RV2 ventilator is recommended by the vendor to prevent condensation. The windshields should be inspected often, cleaned as needed with distilled water, and replaced on a regular schedule (every 3-6 months). Finally, birds can pose a threat to the Radiometer. A series of wire ties were used to keep birds from standing on the long arm of the sensor. The net radiometer is depicted in Figure 6.

Figure 6. Net Radiometer

4.4.4 Heat Flux

A Thin-Film Heat Flux Sensor was used to measure the effective heat flow between the structure and the outside. Two sensors were used. One was placed in the conventional zone at location C and one in the green roof zone at location A. The sensors were placed in between the insulation and outer membrane of the roof.

The HFS Series heat flux sensor is effective for convection, conduction, and radiation heat transfer uses. The temperature range for the instrument is -200 to 150°C. Readout is accomplished by connecting a sensor to any direct reading dc microvoltmeter or recorder. The data is given in BTU/Ft^{2}Hr or W/m^2. The normal lead wires are 3.1 meters in length. The product is available through Omega. The Heat Flux sensor is illustrated in Figure 7.

Figure 7. Heat Flux Sensor

4.4.5 Wind Speed and Direction

Wind Speed and direction is another important measurement that needs to be made on site. A Young Wind Sentry Anemometer will be used. The Sentry Anemometer will need to be placed upwind of eddy causing obstructions. The Sentry anemometer will be used to measure the wind speed of the microclimate around the green and control roof. A single instrument will be placed in the center of the four monitoring points to get a general wind speed for the site.

Wind speed is used as another factor in modeling the productivity of the plants of the green roof. Generally, as wind speed increases, so does the ability of the plants to transpire, creating a greater cooling effect. The wind sentry set is shown in Figure 8.

Figure 8. Wind Sentry Set

4.4.6 Data Collection

A National Instruments Fieldpoint Datalogging System was used to operate the roof instruments and collect data for the project. The Fieldpoint System is made up of modular units which read a variety of inputs. For this project, a power supply (PS-4 module), a network module (FP-2000), six thermocouple modules (FP-TC-120), a counter module (FP-CTR-502), two digital output module (FP-DO-401), and two analog input modules (AI-100) were used to communicate, power, and record data from all the different weather, temperature, and water sensing equipment. The thermocouple modules are designed to read voltage from a thermocouple module and directly convert the reading to degrees Fahrenheit. Programming language was needed for the other instruments. The network module holds an Ethernet port that allows the Fieldpoint system to communicate with computers both directly connected or over the internet. A Digital Subscriber Line (DSL) connection was used to transfer data from the Fieldpoint System to a computer on the University of Pittsburgh campus. The Fieldpoint System is protected in a six foot long weather proof box on the Giant Eagle roof. The Fieldpoint unit is shown is Figure 9.

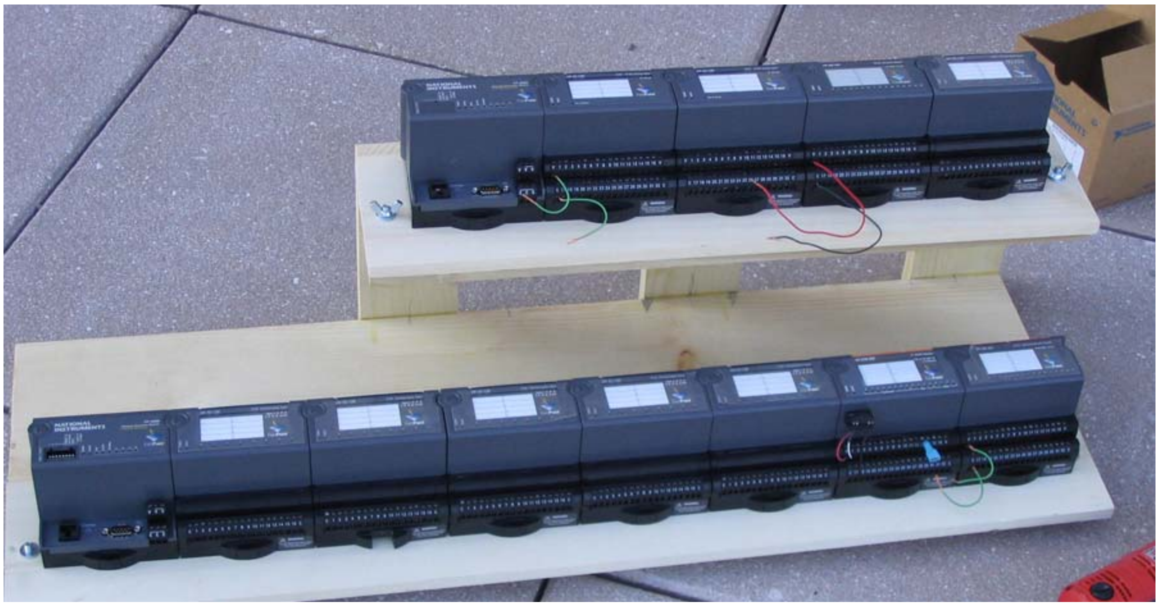

Figure 9. Fieldpoint Data Logging System

National Instruments uses a software program called LabView 8.0 to allow the user to write the programming language needed to operate the field instruments. The program takes the input from the instruments in volts and translates it to units that are more familiar to weather and temperature data. For example, the Relative Humidity Probes measure changes in relative humidity in volts, the Fieldpoint unit records the voltage and the Lab View program converts the voltage to degrees in Fahrenheit. The LabView software is also used to control how often the instruments take measurements.

All sensors were set to take and record measurements every 5 minutes as is similar practice ("Green Roof Test Plot", 2004). Data was downloaded from the logger on a weekly basis, given the expected storage requirements and capacity of the logger. The datalogger was also programmed to control the data collection rate. For example, as the rain gauge is activated by rainfall, the datalogger will record the measurements. This can be used to increase the sampling rate on the ultrasonic sensors monitoring water levels in the flumes. (Bliss, 2007) Table 2 provides a summary of each piece of equipment, its purpose, the quantity of instruments at the Giant Eagle site, the location of each instrument on site, the frequency of measurements, and the corresponding authors from the literature review that used a similar setup. Each instrument is set to take readings every 5 minutes, with one exception, the wind anemometer, that takes a reading every 10 seconds to better capture the sustained wind speed. The data logger records the time, date, and appropriate reading for each instrument and stores the information in a file. A file is created for each sensor type, all the thermocouples, the temperature probes, the RH and temperature sensors, the net radiometer, the wind speed and the wind direction. The data in each file is saved periodically, in groups of 1-5 days. The length of the files is limited somewhat to the amount of data the data logger can store. The controlling file was the thermocouple file, which had over 40 data points to store every 5 minutes. The other files were segmented and saved at the same date and time as the thermocouple file for simplicity.

Table 2. Equipment Summary

Equipment	Purpose	Quantity	Location	Measurement Frequency	Author
Omega Type T Thermocouple Wire	Measures point temperature	By the foot	9 measurement points at each monitoring location A, B, C, and D	Every 5 minutes	"Green Roof Text Plot", Wong 2003a, Niachou et al., Liu et al., Theodosiou
Campbell Scientific 107 Temperature Probe	Measures point temperature	2	At the midpoint of the soil layer at Locations A and B	Every 5 minutes	"Green Roof Text Plot", Eumorfopoulou et al., Liu et al.
Campbell Scientific HMP45C Temperature and Relative Humidity Probe	Measures relative humidity and temperature	2	Roughly 4 inches above the surface at Locations A and C	Every 5 minutes	Del Barrio, "Green Roof Text Plot", Wong 2003a, Niachou et al., Eumorfopoulou et al., Liu et al., Theodosiou
Campbell Scientific Q7.1Net Radiometer	Measures in-coming and out-going radiation	2	1 ft above surface at Locations A and C	Every 5 minutes	Del Barrio, Wong 2003a, Eumorfopoulou et al., Liu et al.
Campbell Scientific R.M. Young Wind Sentry Anemometer	Measures wind speed and direction	1	6 ft above surface at Location C	Every 10 seconds	Del Barrio, "Green Roof Text Plot", Wong 2003a, Eumorfopoulou et al., Liu et al., Theodosiou
Omega Thin Film Heat Flux Sensor	Measures heat flux	2	Just above the insulation of the roof panel at Locations A and C	Every 5 minutes	Del Barrio, Liu et al., Theodosiou
National Instruments Fieldpoint Data Logging System	Collects and stores data	1	In weather-proof enclosure on roof	-	Del Barrio, "Green Roof Text Plot", Wong 2003a, Niachou et al, Eumorfopoulou et al., Liu et al., Theodosiou

5.0 THERMAL PREFORMANCE MONITORING RESULTS

The results from the Giant Eagle Green Roof study are discussed below. This section will describe all the data collected from the Giant Eagle Study Site including what worked and what failed, similarities and differences between the green and control roofs, and trends found in the data. This section focuses solely on the thermal performance of the green roof. For details about the Stormwater Management Performance of the Giant Eagle green roof site please refer to Bliss, 2007.

The performance of the green and control roof at the Giant Eagle site is being continuously monitored starting in late July 2006. Data was downloaded and separated into groups of roughly three to seven days. Each data group had at least three day and night cycles. In some cases up to one week of data was stored in one group. Some data groups depict a week of steady weather, while others show changes in weather, such as gradually increasing or decreasing temperatures, storm systems, etc. Data group cut offs usually occurred when the file size became too large or if the data collection server needed to be shut down and rebooted for maintenance. The goal was to try to monitor the roofs as continuously as possible. The pertinent data results can be found in Appendixes A, B, and C.

Data from the Giant Eagle site could be analyzed in a number of ways. For the purpose of this results section, data will be examined from a warm weather week, depicting roof performance in the summer season; a moderate temperature week, depicting roof performance in the fall season; and a cold weather week, depicting roof performance in the winter season. From these three season groups, the records will be managed in various ways. The thermocouple data will be displayed two ways. The first will show all the thermocouple data graphically at each monitoring location. This will create a temperature profile of the monitoring location below, at, and above the roof or soil surface. Temperature profiles are meant to display how the roof behaves throughout the cross section, most notably the roof membrane, roof surface, and ambient temperature. The next data style will isolate the temperature measurement at the same profile height (i.e. roof membrane, roof surface) and graphically show the temperature at all four monitoring location. The single layer temperature will show if roof type has an effect on the thermal stress endured by the material compared to material at other points on the roof. This data is also useful in determining if roof type influences the urban heat island effect. Finally, the other weather monitoring instrument results will be shown in relation to ambient, surface, and roof membrane temperature. This is to show in other factors in the climate have an effect on roof thermal performance.

5.1 TEMPERATURE DATA

5.1.1 Temperature Profiles

Thermocouples and temperature probes were used to observe the temperature profile at the four monitoring locations A, B, C, and D. Locations A and B are placed over the green roof, Locations C and D the control roof. The individual monitoring points used to create the temperature profiles are below the decking, above the roof decking, below the waterproofing (roof) membrane, soil midpoint temperature (green roof only), soil or roof surface, 7cm above surface, 15cm above surface, 30cm above surface, 60cm above surface, and 1m above surface. The temperature profiles are as complete as possible. Unfortunately, there were times where the thermocouples, temperature probes, or data logger malfunctioned. The profiles selected for this section have minimal interference from faulty equipment.

All temperature profiles show a single color coded line for the temperature of the monitoring point over time. Most temperatures points were taken using thermocouple wire. The soil temperature points on the green roof were taken using a temperature probe, so standing water in the soil would not damage the instrument. The ambient temperature is also shown on each temperature profile. The ambient temperature was recorded by the relative humidity and temperature probe protected in a radiation shield.

To reiterate the data from the temperature profiles, two weeks from each season were selected. In the other performance data only one week will be selected.

5.1.1.1 Summer Profiles

The first summer data group selected for the results section spans July 27, 2006 to August 1, 2006. This data set was one of the first collected at the Giant Eagle site. The temperature profile for each monitoring location A, B, C, and D are shown in Figures 10, 11, 12, and 13 respectively. In each profile, the temperature locations “Roof Membrane,” “Roof or Soil Surface,” and “Ambient” are highlighted. These are the most important data points that will be discussed throughout this thesis. The thermocouple points are color coded. The blue and purple colors represent points located at the waterproofing membrane or below. The green colors are used for the roof surface and soil temperature when applicable. The red, pink, and orange colors are used for temperature points above the surface, including the ambient temperature. Also, the axis scales on all the temperature profiles remain constant. This is for ease of comparing temperature from one monitoring location to another.

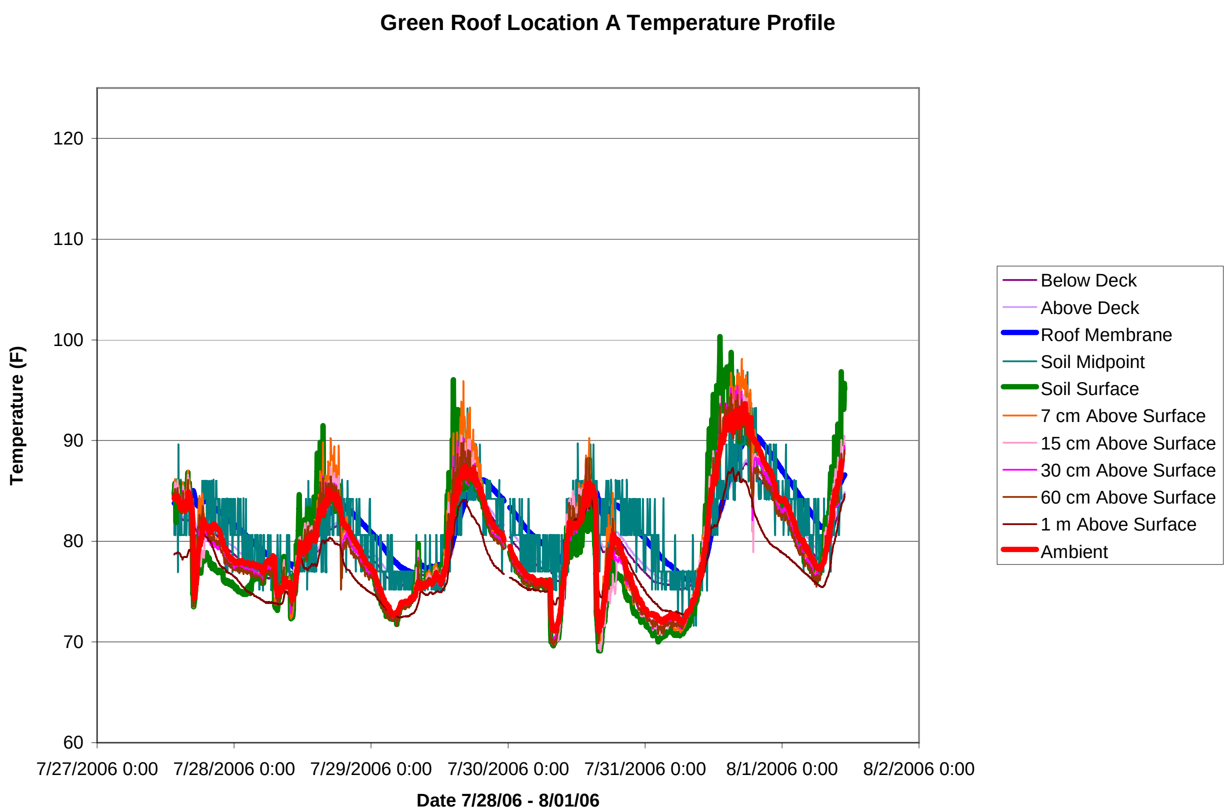

Figure 10. Green Roof Location A Temperature Profile for 7/28/06 through 8/1/06

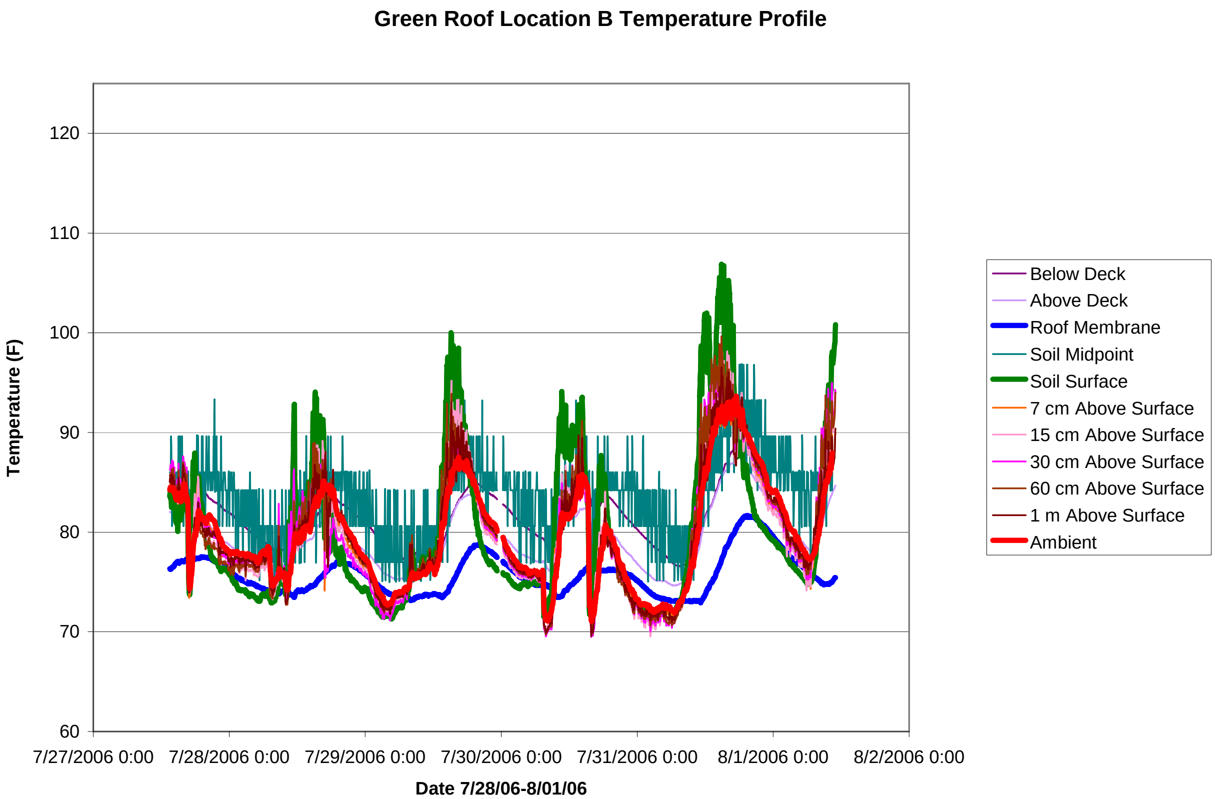

Figure 11. Green Roof Location B Temperature Profile for 7/28/06 through 8/1/06

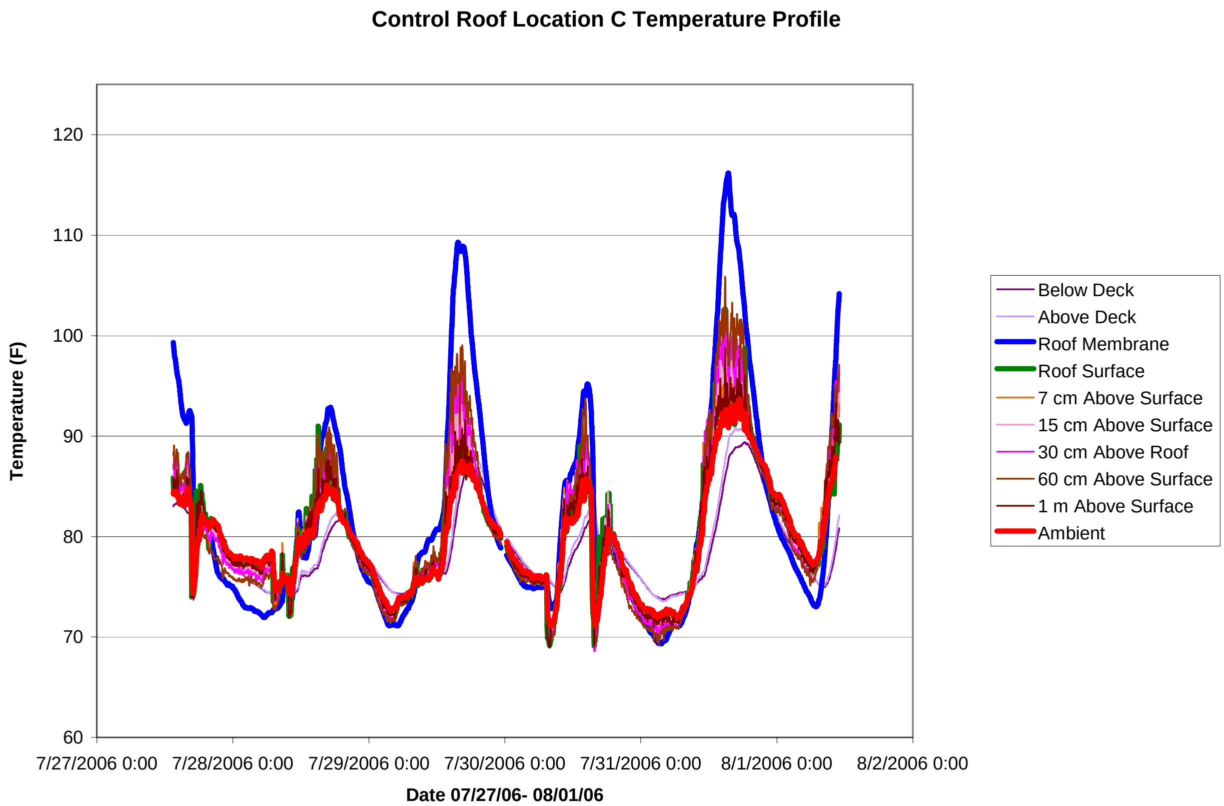

Figure 12. Control Roof Location C Temperature Profile for 7/28/06 through 8/1/06

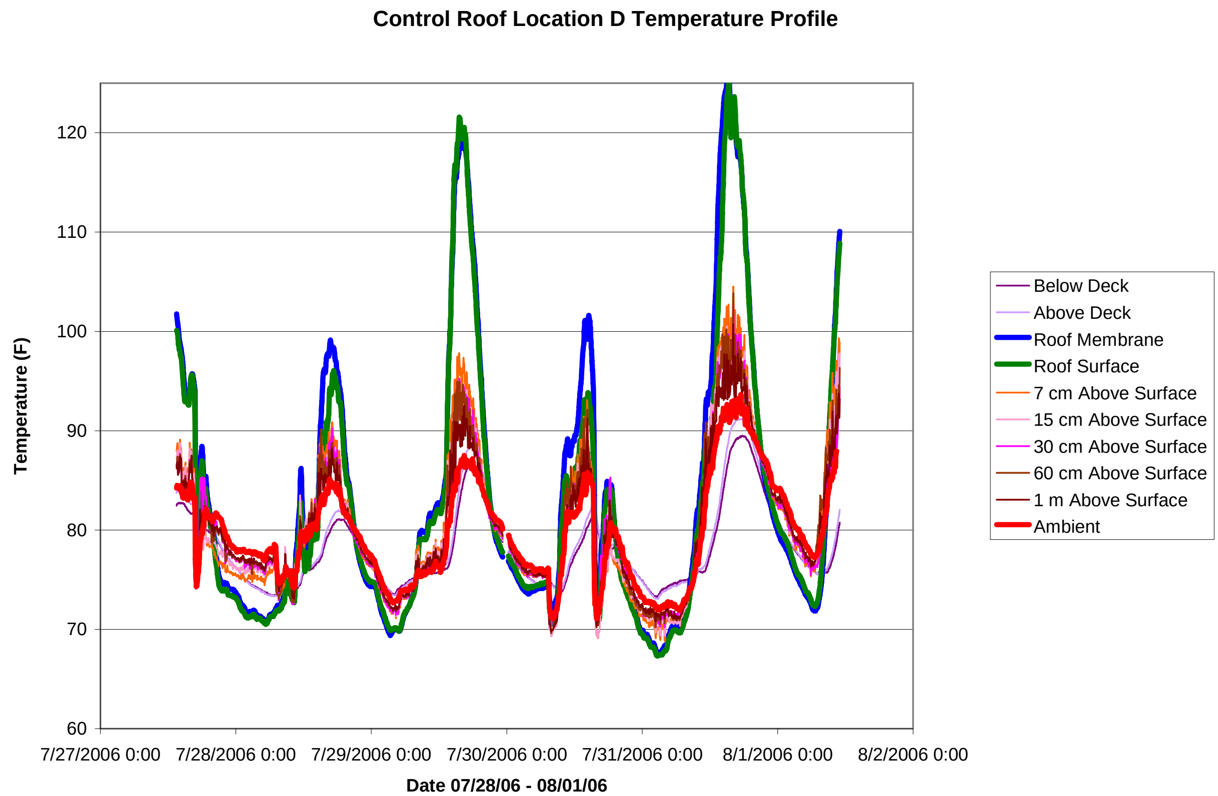

Figure 13. Control Roof Location D Temperature Profile for 7/28/06 through 8/1/06

The temperature profiles provide significant data about the performance of a roof type in warm summer weather. The ambient air temperature remains constant in all four figures. The nightly lows are around 70-75° Fahrenheit (F) and the daily highs are around 85-90° F. Storms early in the week tapered off into sun and warmer temperatures. (Wunderground.com, 2007) The ambient air temperature was warmer than the air on the interior of the building. The interior of the building is kept around 65-70° Fahrenheit at store level. The ambient air temperature is important to observe when comparing the other data points in the temperature profile.

Figures 10 and 11 depict the temperature profiles on the green roof, Locations A and B. Note all temperatures, above and below the roof surface hover close to one another. Tables 3 and 4 show the high and low temperatures experienced at each thermocouple point, as well as the average temperature and greatest temperature fluctuation for monitoring Locations A and B. Both profiles located on the green roof experience lows ranging from 69° to 76° Fahrenheit, and highs ranging from 87° to 106° Fahrenheit. Note the maximum temperature variation for the roofing membrane is 14.7° at Location A and 15.8° at Location B. This is significant because the temperature variations on the soil surfaces of the green roof are 31.2° and 35.6° respectively. This shows the shading benefit the green roof has on the roofing membrane, by reducing the thermal variation the membrane undergoes.

Table 3. Temperature Statistics for Monitoring Location A (7/28/06-8/01/06)

Temperature Statistics for Green Roof Monitoring Location A

	High	Low	Average	Fluctuation
Below Deck	87.8	75.2	81.5	12.6
Above Deck	88.1	75.5	81.8	12.6
Roofing Membrane	90.8	76.1	83.45	14.7
Soil Surface	100.3	69.1	84.7	31.2
7cm Above	98	69.5	83.75	28.5
15 cm Above	95.1	69.1	82.1	26
30 cm Above	95.4	69.7	82.55	25.7
60 cm Above	94.4	69.6	82	24.8
1 m Above	94.6	72.4	83.5	22.2

Table 4. Temperature Statistics for Monitoring Location B (7/28/06-8/01/06)

Temperature Statistics for Green Roof Monitoring Location B

	High	Low	Average	Fluctuation
Below Deck	88.5	76.6	82.55	11.9
Above Deck	87.5	74.6	81.05	12.9
Roofing Membrane	88.7	72.9	80.8	15.8
Soil Surface	106.8	71.2	89	35.6
7cm Above	94.7	69.9	82.3	24.8
15 cm Above	98.6	69.5	84.05	29.1
30 cm Above	97.4	69.4	83.4	28
60 cm Above	99.5	69.7	84.6	29.8
1 m Above	96.5	69.6	83.05	26.9

Next, the control roof statistics are examined. The control roof statistics are located in Tables 5 and 6. The average lows are similar to those found on the green roof, ranging from 67° to 73°. The high temperatures recorded on the control roof are warmer than those on the green roof. On the control roof the high temperatures in the temperature profile range from 89° to 125°. Again, the roofing membrane and roof surface must be brought in attention. At Location C the change in temperature over the week for the roof surface was 33.5°, at Location D it was 57.7°. The roofing membrane varied in temperature by 46.9° at Location C and 58.1° at Location D. While the maximum change in temperature occurred on the soil surface at the green roof locations, for the control roof locations the maximum variation occurred at the roofing membrane.

Table 5. Temperature Statistics for Monitoring Location C (7/28/06-8/01/06)

Temperature Statistics for Control Roof Monitoring Location C

	High	Low	Average	Fluctuation
Below Deck	89.4	73.8	81.6	15.6
Above Deck	90.9	73.5	82.2	17.4
Roofing Membrane	116.2	69.3	92.75	46.9
Roof Surface	102.6	69.1	85.85	33.5
7cm Above	100.3	69.2	84.75	31.1
15 cm Above	102.5	69.3	85.9	33.2
30 cm Above	104.6	68.6	86.6	36
60 cm Above	105.8	69.2	87.5	36.6
1 m Above	98.7	68.9	83.8	29.8

Table 6. Temperature Statistics for Monitoring Location D (7/28/06-8/01/06)

Temperature Statistics for Control Roof Monitoring Location D

	High	Low	Average	Fluctuation
Below Deck	89.5	73.3	81.4	16.2
Above Deck	91.2	73.1	82.15	18.1
Roofing Membrane	125.6	67.5	96.55	58.1
Roof Surface	125	67.3	96.15	57.7
7cm Above	104.4	68.8	86.6	35.6
15 cm Above	101.9	69.2	85.55	32.7
30 cm Above	102.8	70.2	86.5	32.6
60 cm Above	103.8	69.6	86.7	34.2
1 m Above	100.7	69.8	85.25	30.9

Next, another set of data from the summer season will be analyzed. This summer data group spans August 21, 2006 to August 28, 2006. The temperature profile for each monitoring Location A, B, C, and D are shown in Figures 14, 15, 16, and 17 respectively. In each profile, the temperature locations “Roof Membrane,” “Roof or Soil Surface,” and “Ambient” are highlighted. The same color coding is used in this data group. Again, the axis scales on all the temperature profiles remain constant for this data group. This is for ease of comparing temperature from one monitoring location to another.

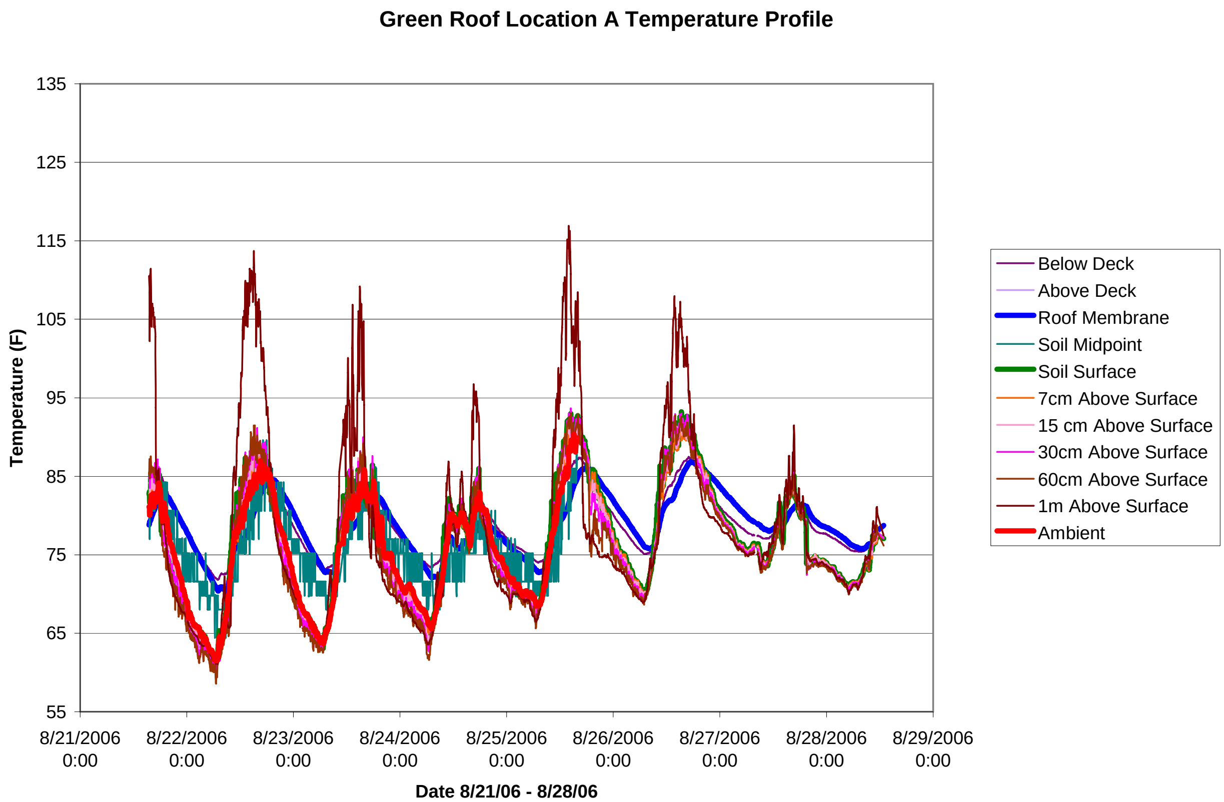

Figure 14. Green Roof Location A Temperature Profile for 8/21/06 through 8/28/06

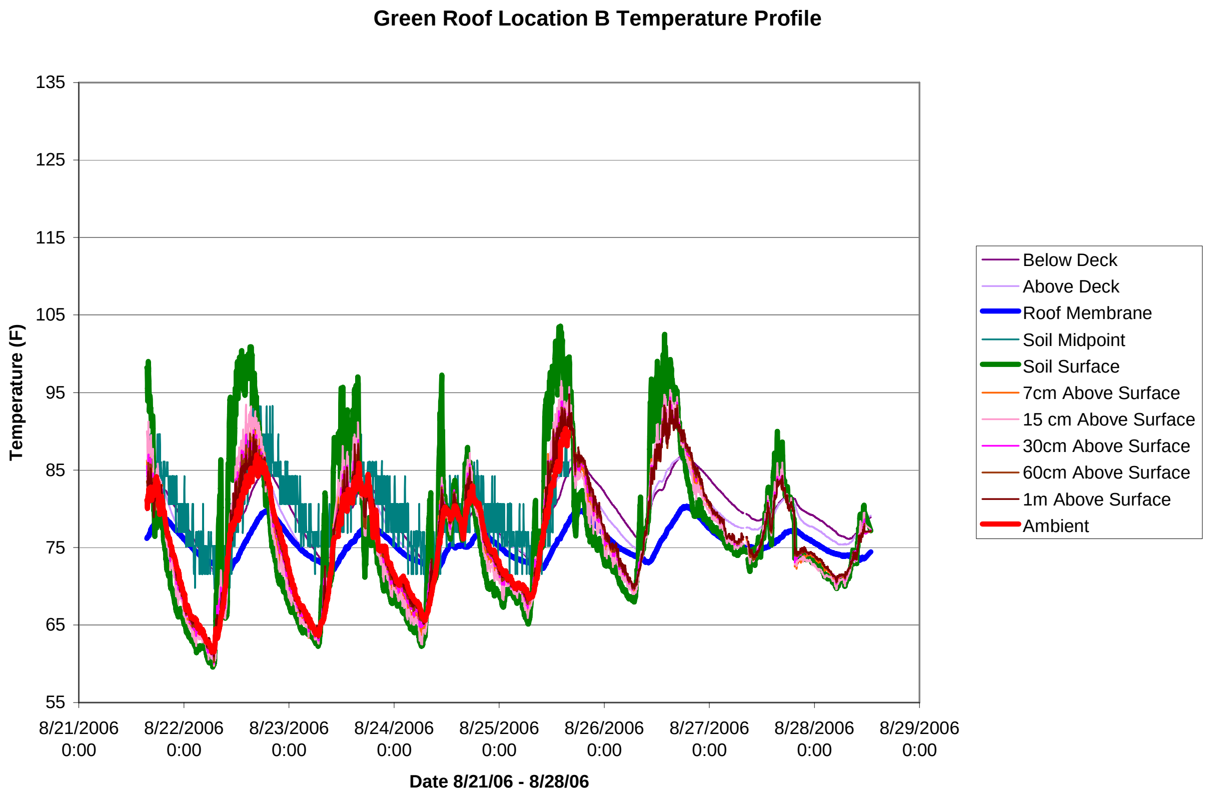

Figure 15. Green Roof Location B Temperature Profile for 8/21/06 through 8/28/06

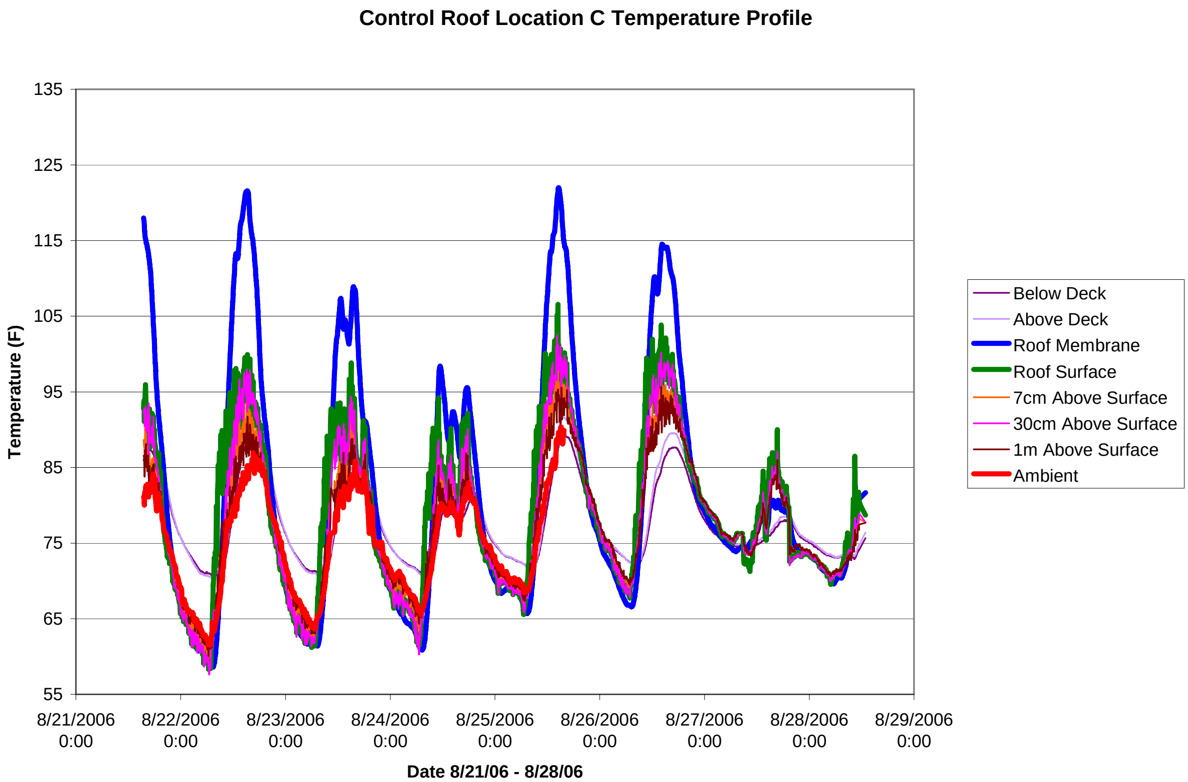

Figure 16. Control Roof Location C Temperature Profile for 8/21/06 through 8/28/06

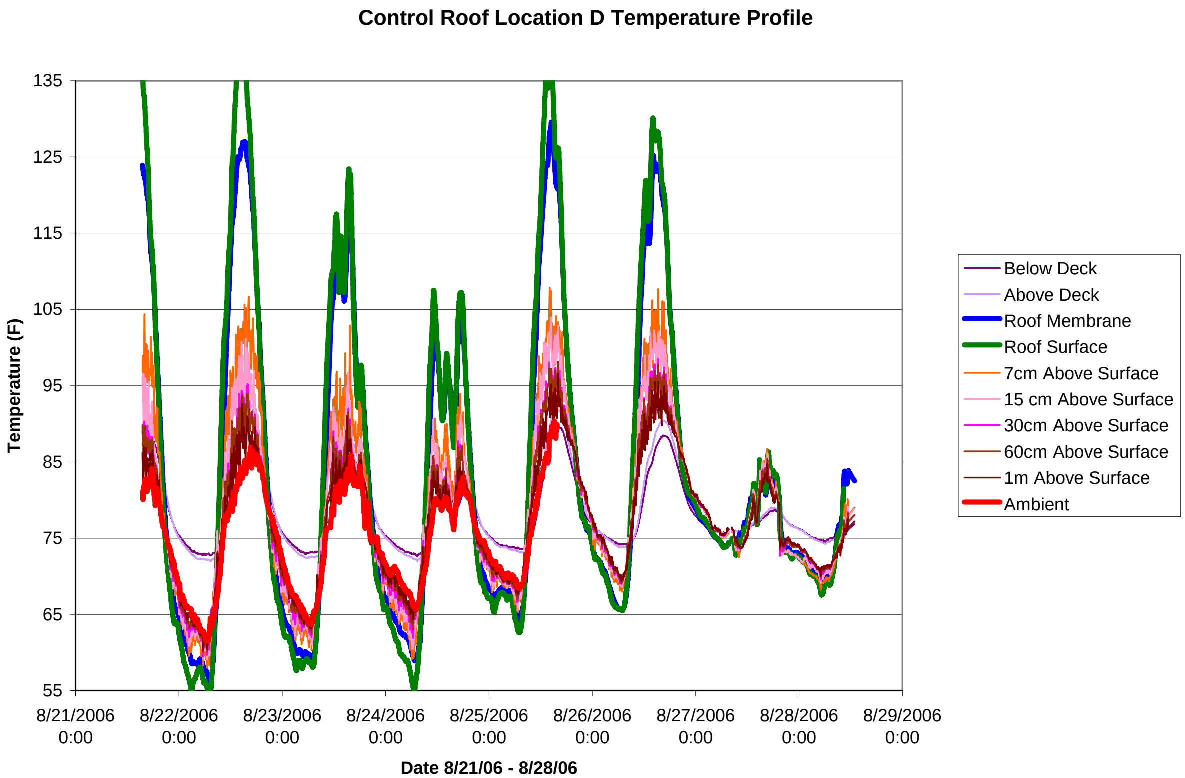

Figure 17. Control Roof Location D Temperature Profile for 8/21/06 through 8/28/06

These temperature profiles provide additional data about the performance of a roof type in warm summer weather. The ambient air temperature remains constant in all four figures. Unfortunately, a malfunction with the data logger lost the last three days of ambient temperature data. This data group was still utilized in this thesis since a majority of the other instrument readings were in order. Regrettably, the monitoring system was first installed in the summer months, and some data was lost due to malfunctions. The August 21-28, 2006 data set was significantly complete. The nightly lows are around 60-70° F and the daily highs are around 82-88° F. The beginning of the week was warm and calm, while the last three days brought some rain events. (Wunderground.com, 2007) The ambient air temperature was warmer than the air on the interior of the building. The ambient air temperature, while incomplete, is important to observe when comparing the other data points in the temperature profile.

Figures 14 and 15 depict the temperature profiles on the green roof, Locations A and B. Like with the earlier data group, all temperatures, above and below the roof surface hover close to one another. Tables 7 and 8 show the high and low temperatures experienced at each thermocouple point, as well as the average temperature and greatest temperature variation for monitoring Locations A and B. Both profiles located on the green roof experience lows ranging from 60° to 71° Fahrenheit, and highs ranging from 80° to 116° Fahrenheit. Note the maximum temperature variation for the roofing membrane is 16.6° at Location A and 8.6° at Location B. This is significant because the temperature variations on the soil surfaces of the green roof are 32.2° and 44.0° respectively. This shows the shading benefit the green roof has on the roofing membrane, by reducing the thermal variation the membrane undergoes.

Table 7. Temperature Statistics for Monitoring Location A (8/21/06-8/28/06)

Temperature Statistics for Green Roof Monitoring Location A

	High	Low	Average	Fluctuation
Below Deck	87.5	71.8	79.7	15.7
Above Deck	87.4	71.8	79.6	15.6
Roofing Membrane	86.9	70.3	78.6	16.6
Soil Surface	93.2	61.0	77.1	32.2
7cm Above	92.5	60.3	76.4	32.2
15 cm Above	92.9	59.9	76.4	33.0
30 cm Above	93.6	59.1	76.4	34.5
60 cm Above	93.0	58.6	75.8	34.4
1 m Above	116.9	61.1	89.0	55.8

Table 8. Temperature Statistics for Monitoring Location B (8/21/06-8/28/06)

Temperature Statistics for Green Roof Monitoring Location B	High	Low	Average	Fluctuation
Below Deck	86.8	71.6	79.2	15.2
Above Deck	86.5	71.8	79.2	14.7
Roofing Membrane	80.3	71.7	76.0	8.6
Soil Surface	103.6	59.6	81.6	44.0
7cm Above	94.8	59.7	77.3	35.1
15 cm Above	96.5	59.7	78.1	36.8
30 cm Above	94.8	60.1	77.5	34.7
60 cm Above	94.8	60.2	77.5	34.6
1 m Above	94.8	60.9	77.9	33.9

Next, the control roof statistics are examined. The control roof statistics are located in Tables 9 and 10. The average lows are similar to those found on the green roof, ranging from 57° to 72°. The high temperatures recorded on the control roof are appreciably warmer than those on the green roof. On the control roof, the high temperatures in the temperature profile range from 89° to 140°. Note the roofing membrane and roof surface. At Location C the change in temperature over the week for the roof surface was 48.2°, at Location D it was 86.1°. The roofing membrane varied in temperature by 63.4° at Location C and 73.3° at Location D. While the maximum change in temperature occurred on the soil surface at the green roof locations, for the control roof locations the maximum variation occurred at the roofing membrane and roof surface.

Table 9. Temperature Statistics for Monitoring Location C (8/22/06-8/29/06)

Temperature Statistics for Control Roof Monitoring Location C

	High	Low	Average	Fluctuation
Below Deck	89.4	70.5	80.0	18.9
Above Deck	91.9	69.9	80.9	22.0
Roofing Membrane	122.0	58.6	90.3	63.4
Roof Surface	106.5	58.3	82.4	48.2
7cm Above	98.5	59.6	79.1	38.9
15 cm Above	-	-		
30 cm Above	102.4	57.6	80.0	44.8
60 cm Above	-	-		
1 m Above	95.6	60.1	77.9	35.5

Table 10. Temperature Statistics for Monitoring Location D (8/22/06-8/29/06)

Temperature Statistics for Control Roof Monitoring Location D

	High	Low	Average	Fluctuation
Below Deck	90.2	72.6	81.4	17.6
Above Deck	92.5	72.0	82.3	20.5
Roofing Membrane	129.6	56.3	93.0	73.3
Roof Surface	140.8	54.7	97.8	86.1
7cm Above	107.8	58.0	82.9	49.8
15 cm Above	104.0	59.1	81.6	44.9
30 cm Above	98.5	59.5	79.0	39.0
60 cm Above	98.1	60.1	79.1	38.0
1 m Above	96.5	60.4	78.5	36.1

5.1.1.2 Autumn Profiles

This section will cover the roof performance in the autumn months. Unfortunately, the selection of autumn data sets is limited due to a combination of problems with the data logger and unusually warm temperatures from October until December. The first autumn data group that will be analyzed is from September 29, 2006 to October 6, 2006. The temperature profile for each monitoring Location A, B, C, and D are shown in Figures 18, 19, 20, and 21 respectively. In each profile, the key temperature locations "Roof Membrane," "Roof or Soil Surface," and "Ambient" are highlighted. The thermocouple points are color coded like the previous figures. Again, the axis scales on all the temperature profiles remain constant for this data group. This is for ease of comparing temperature from one monitoring location to another.

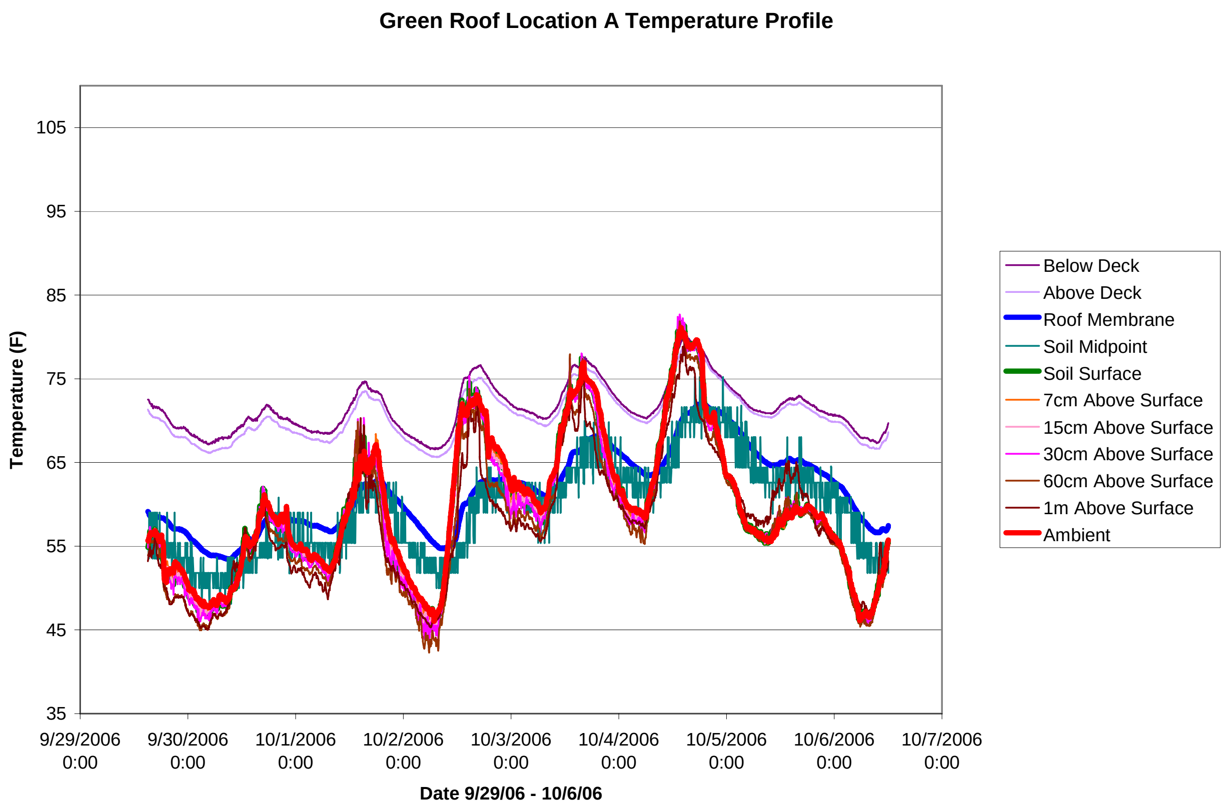

Figure 18. Green Roof Location A Temperature Profile for 9/29/06 – 10/6/06

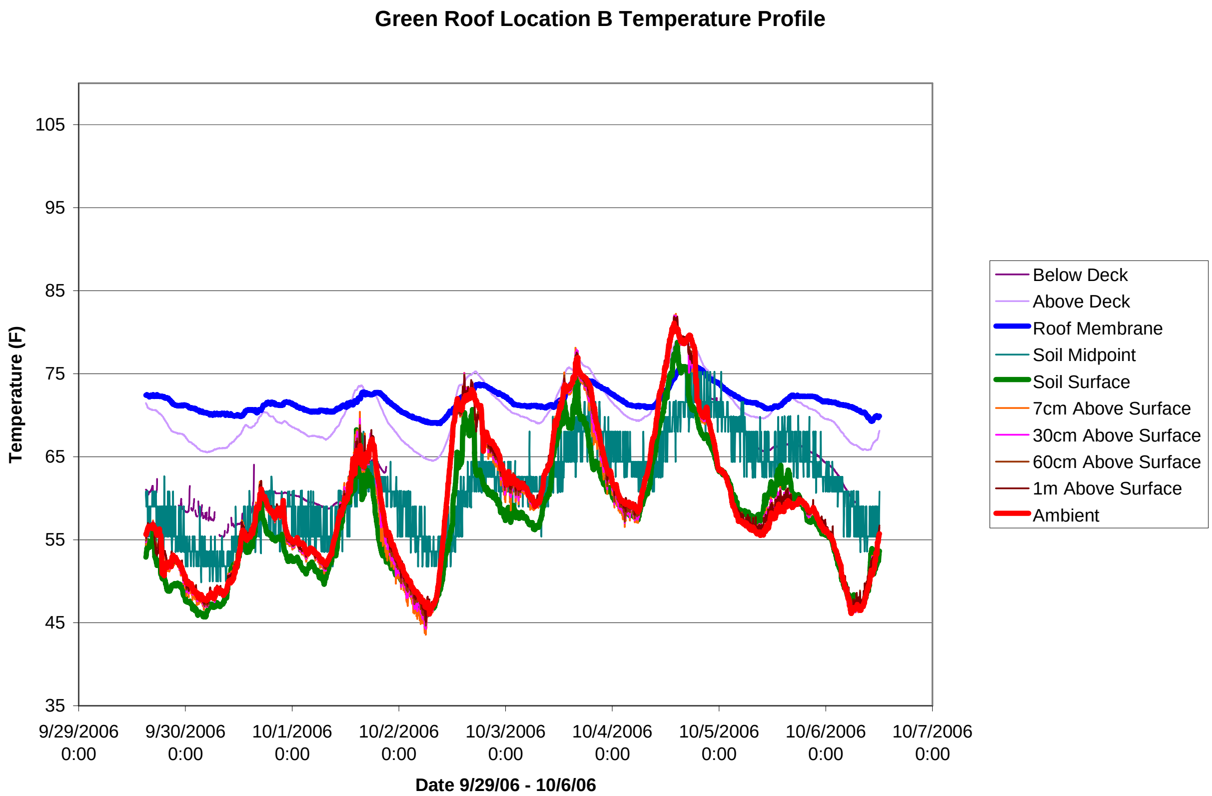

Figure 19. Green Roof Location B Temperature Profile for 9/29/06 – 10/6/06

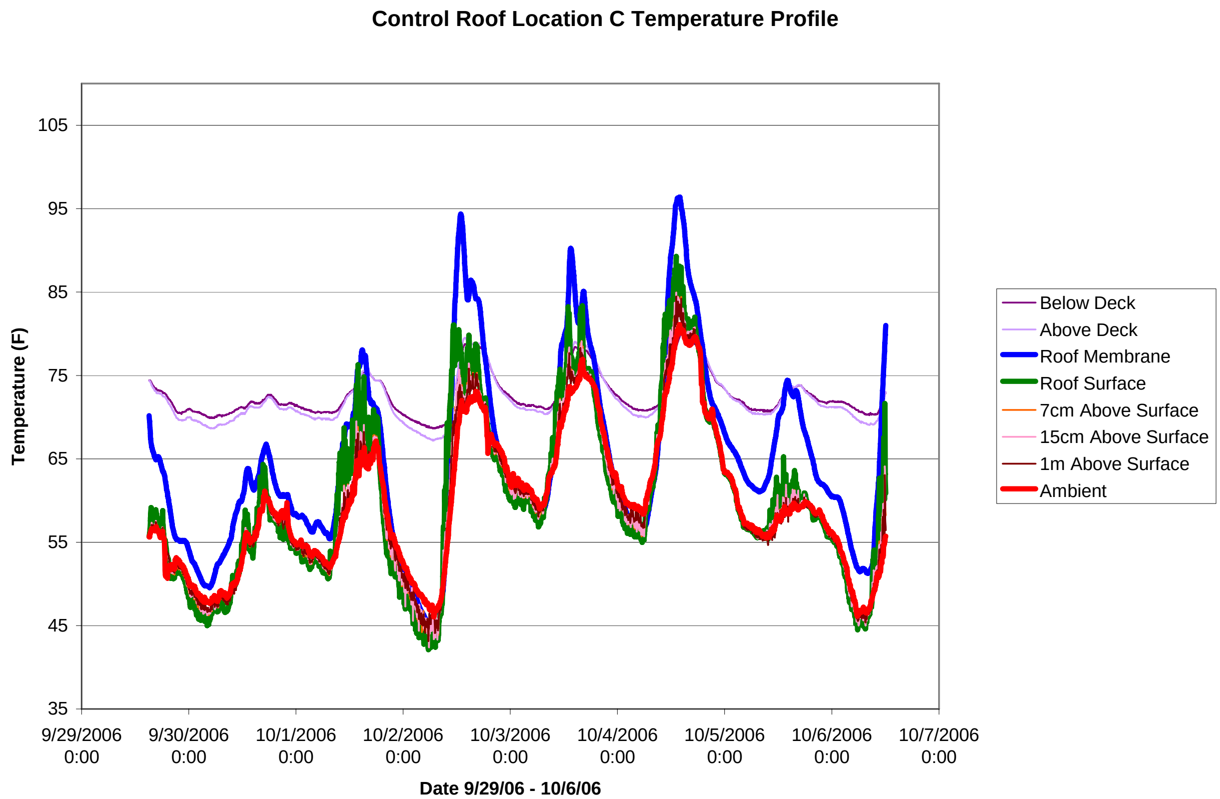

Figure 20. Control Roof Location C Temperature Profile for 9/29/06 – 10/6/06

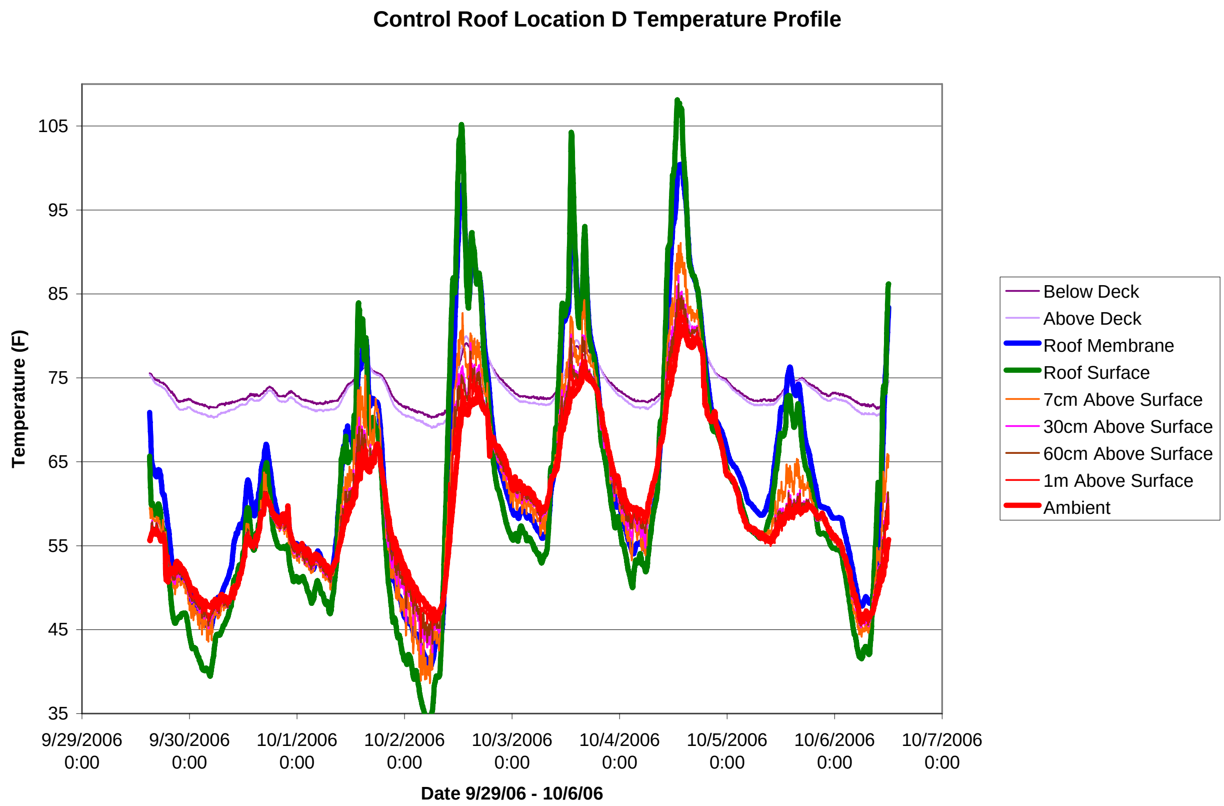

Figure 21. Control Roof Location D Temperature Profile for 9/29/06 – 10/6/06

The ambient temperature shows unseasonable warm weather for the region. The ambient air temperature remains constant in all four figures. The nightly lows are cooler, around 43-56° F and the daily highs are around 60-78° F. The mild days and cool evenings are typical for the Pittsburgh area in the fall, unfortunately both are somewhat warmer then expected. Only one day had rain this week, October 5th. (Wunderground.com, 2007) It is at this time of year when building and home owners might begin turning on their heating systems, especially at night, to maintain a comfortable climate inside. During the day the temperatures are warm and pleasant. The ambient air temperature is important to observe when comparing the other data points in the temperature profile.

Figures 18 and 19 depict the temperature profiles on the green roof, Locations A and B. Like with the summer data groups, all temperatures, above and below the roof surface hover close to one another. Both the above deck and below deck temperatures are now warmer then all other temperatures taken on the other side of the insulation. This is because these two readings are exposed to both the heating and the lighting systems on the interior of the building. The roof membrane, soil, and above surface measurements all seem to moderately follow the ambient temperature. These measurements do not quite reach the same extremes as ambient temperature. There is one exception. The roof membrane temperature at Location B is significantly warmer then would be expected. In following data groups this trend is continued. Unfortunately, there seems to be an anomaly at this temperature point, the thermocouple is malfunctioning. Due to its location in the roof structure, it can not be examined or replaced. From this point on, the Location B roof membrane temperature will be ignored.

Tables 11 and 12 show the high and low temperatures experienced at each thermocouple point, as well as the average temperature and greatest temperature variation for monitoring Locations A and B. Both profiles located on the green roof experience lows ranging from 42° to 66° F, and highs ranging from 72° to 82° F. Note the maximum temperature variation for the roofing membrane is 18.6° at Location A and 6.8° at Location B. This is significant because the temperature variations on the soil surfaces of the green roof are 36.2° and 36.0° respectively. This shows the shading benefit the green roof has on the roofing membrane, has continued into the fall months and still protects the roof membrane from temperature induced stress.

Table 11. Temperature Statistics for Monitoring Location A (9/29/06-10/6/06)

Temperature Statistics for Green Roof Monitoring Location A

	High	Low	Average	Fluctuation
Below Deck	80.1	66.6	71.5	13.5
Above Deck	79.1	65.6	70.6	13.5
Roofing Membrane	72.0	53.4	61.6	18.6
Soil Surface	81.8	45.6	59.4	36.2
7cm Above	82.0	45.4	59.4	36.6
15 cm Above	82.4	44.8	59.4	37.6
30 cm Above	82.7	43.8	58.9	38.9
60 cm Above	81.8	42.3	57.8	39.5
1 m Above	79.8	45.0	57.7	34.8

Table 12. Temperature Statistics for Monitoring Location B (9/29/06-10/6/06)

Temperature Statistics for Green Roof Monitoring Location B

	High	Low	Average	Fluctuation
Below Deck	72.2	55.4	62.7	16.8
Above Deck	79.3	64.5	70.4	14.8
Roofing Membrane	75.8	69.0	71.7	6.8
Soil Surface	78.7	45.7	57.6	33.0
7cm Above	82.2	73.6	59.3	8.6
15 cm Above	-	-		
30 cm Above	82.0	44.3	59.5	37.7
60 cm Above	81.8	44.7	59.7	37.1
1 m Above	81.9	45.1	59.8	36.8

Next, the control roof statistics are examined. The control roof statistics are located in Tables 13 and 14. The average lows are similar to those found on the green roof, ranging from 38° exterior to 70° in the interior of the building. The high temperatures recorded on the control roof are appreciably warmer than those on the green roof. On the control roof, the high temperatures in the temperature profile range from 80° to 108°. Again, the roofing membrane and roof surface must be brought in attention. At Location C the change in temperature over the week for the roof surface was 47.2°, at Location D it was 74.6°. The roofing membrane varied in temperature by 51.4° at Location C and 59.7° at Location D. While the maximum change in temperature occurred on the soil surface at the green roof locations, for the control roof locations the maximum variation occurred at the roofing membrane and roof surface.

Table 13. Temperature Statistics for Monitoring Location C (9/29/06-10/6/06)

Temperature Statistics for Control Roof Monitoring Location C

	High	Low	Average	Fluctuation
Below Deck	80.6	68.7	72.6	11.9
Above Deck	81.7	67.2	72.3	14.5
Roofing Membrane	96.4	45.0	64.8	51.4
Roof Surface	89.3	42.1	60.1	47.2
7cm Above	84.9	43.5	59.6	41.4
15 cm Above	84.9	42.4	59.7	42.5
30 cm Above	-	-		
60 cm Above	-	-		
1 m Above	84.5	43.2	59.6	41.3

Table 14. Temperature Statistics for Monitoring Location D (9/29/06-10/6/06)

Temperature Statistics for Control Roof Monitoring Location D

	High	Low	Average	Fluctuation
Below Deck	81.0	70.2	73.8	10.8
Above Deck	82.0	69.0	73.8	13.0
Roofing Membrane	100.5	40.8	63.2	59.7
Roof Surface	108.1	33.5	61.1	74.6
7cm Above	91.1	38.6	60.3	52.5
15 cm Above	-	-		
30 cm Above	87.2	42.1	59.9	45.1
60 cm Above	86.1	43.3	59.9	42.8
1 m Above	84.2	44.2	59.8	40.0

Later in the month of October, temperatures cooled a little more. The second data group that will be examined is October 20, 2006 to October 25, 2006. The temperature profile for each monitoring Location A, B, C, and D are shown in Figures 18, 19, 20, and 21 respectively.

Again, the graphs have a similar data scheme as the other temperature profiles. The ambient temperature, roof membrane, and roof surface are highlighted as well.

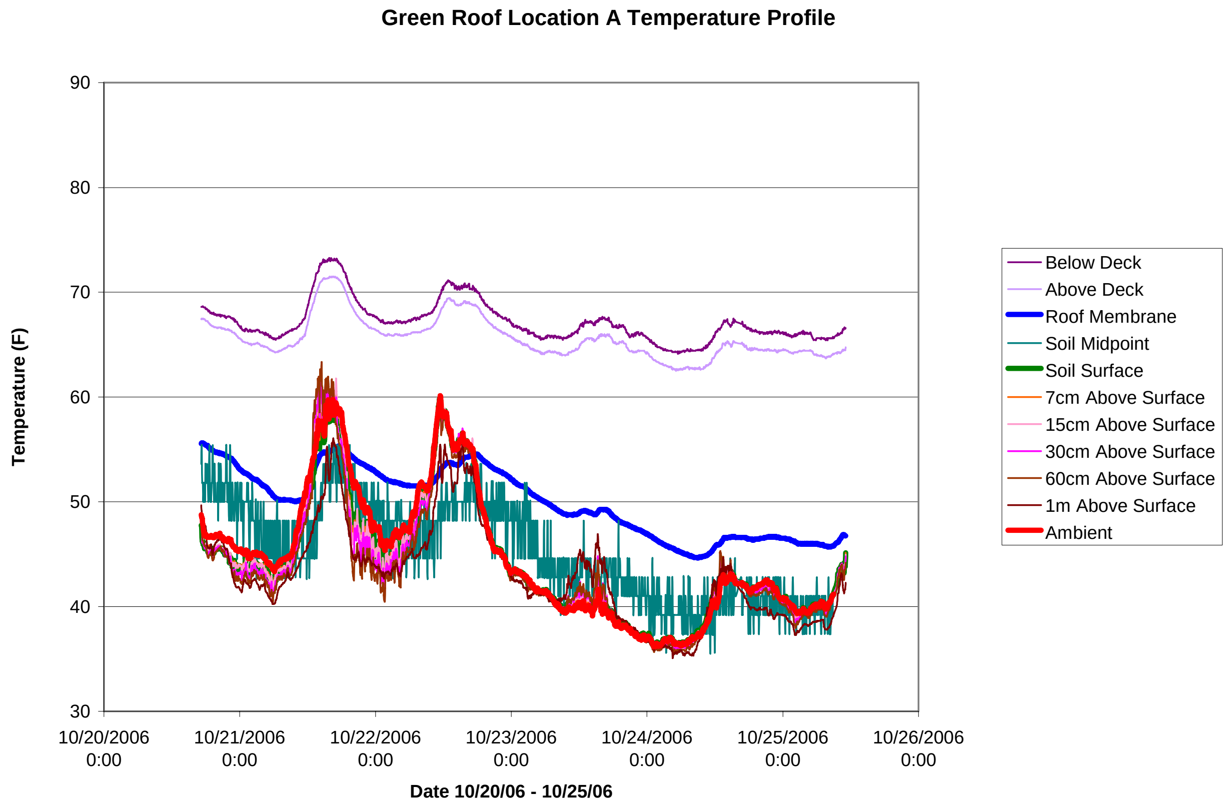

Figure 22. Green Roof Location A Temperature Profile for 10/20/06 – 10/25/06

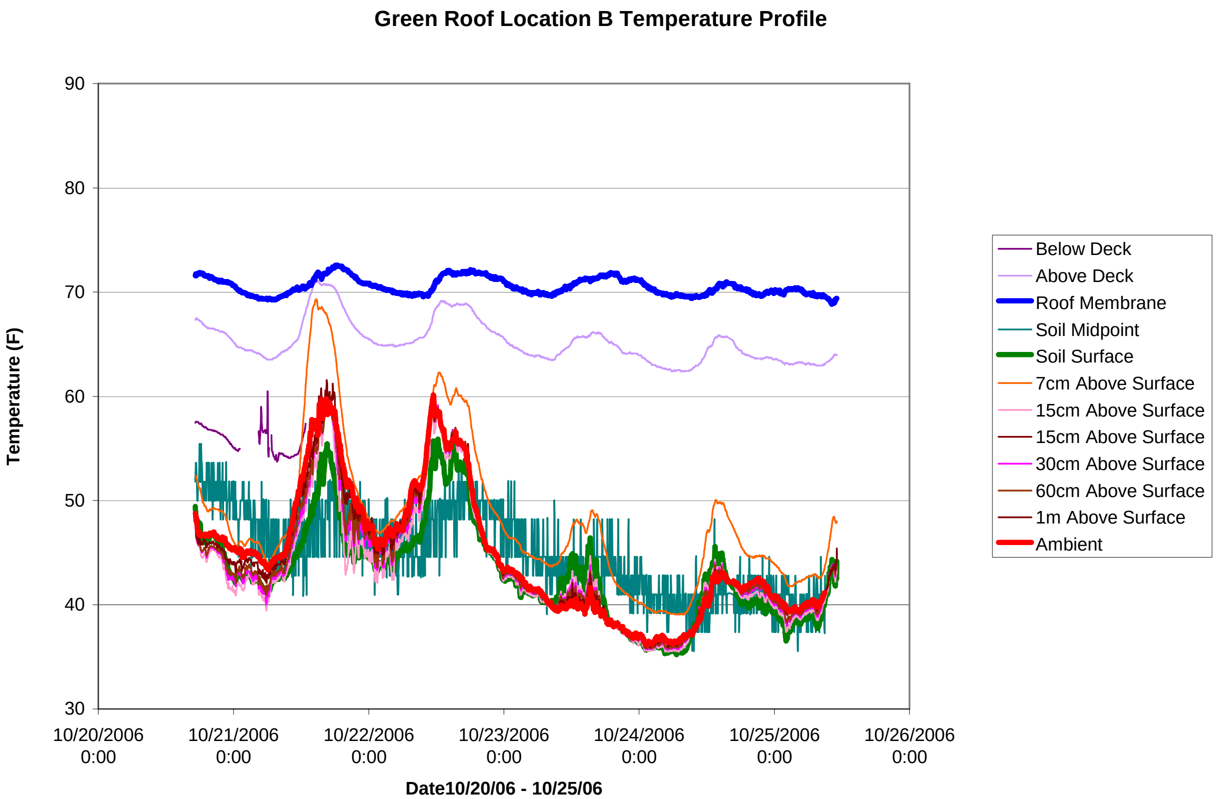

Figure 23. Green Roof Location B Temperature Profile for 10/20/06 – 10/25/06

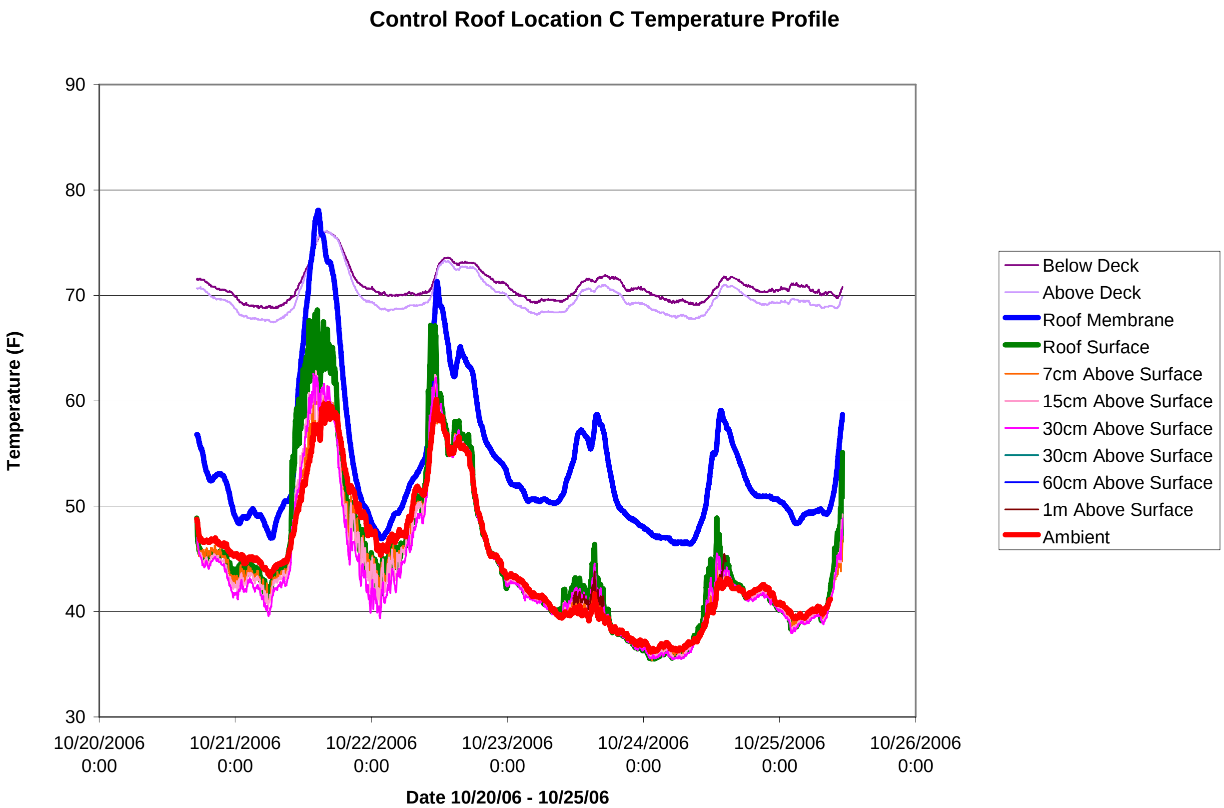

Figure 24. Control Roof Location C Temperature Profile for 10/20/06 – 10/25/06

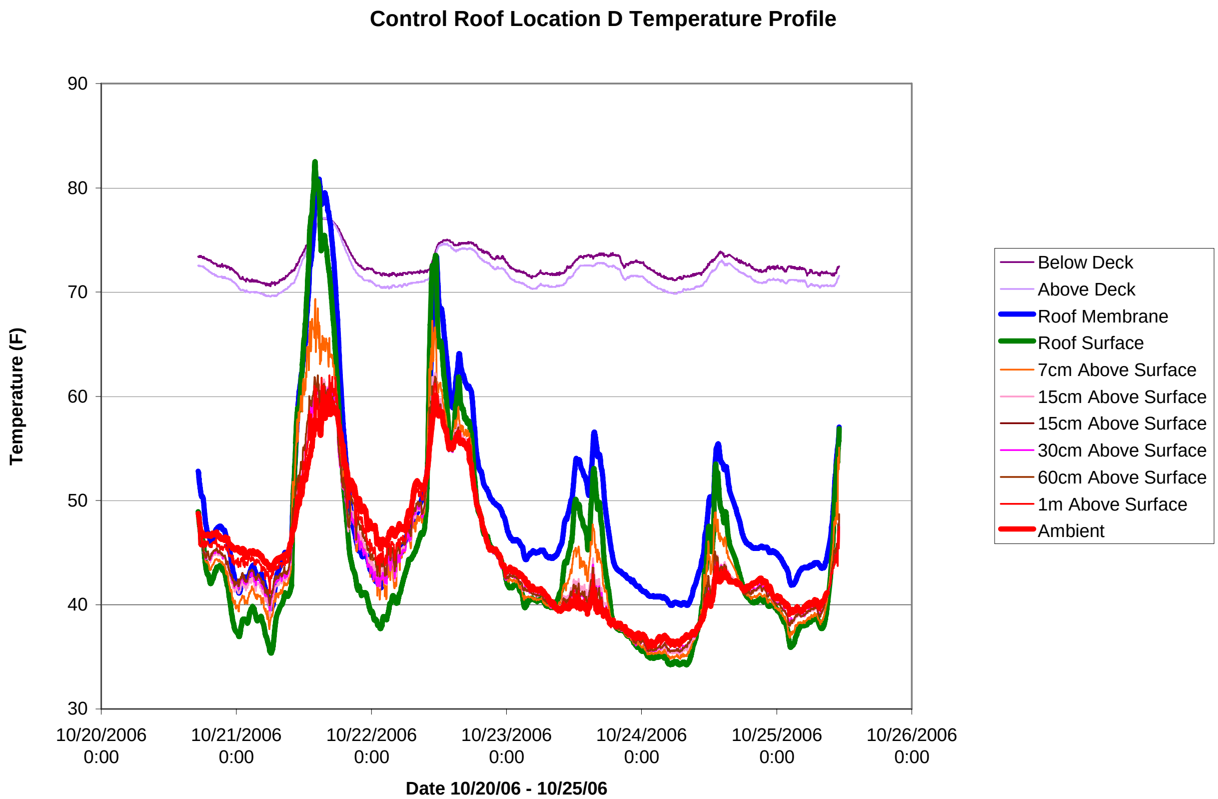

Figure 25. Control Roof Location D Temperature Profile for 10/20/06 – 10/25/06

These temperature profiles provide additional data about the performance of a roof type in mild autumn weather. The ambient air temperature remains constant in all four figures. Unfortunately, the malfunction with the thermocouple at the green roof Location B roof membrane has continued. This data group was still utilized in this thesis since a majority of the other instrument readings were in order. The nightly lows vary between 35-45° F and the daily highs range from 40-60° F. Much of the week was rainy, and on the 23^{rd} and 24^{th} the rain changed into snow. (Wunderground, 2007) Of course with the much colder temperatures and winter approaching, the grocery store continued to heat the interior of the building.

Figures 22 and 23 depict the temperature profiles on the green roof, Locations A and B. The data shows that while the exterior of the building was exposed to cold temperatures, the interior measurements (taken above and below the steel deck) remained warm. For the green roof locations these measurements varied between 65-70°F. Despite being exposed to the grocery store climate and protected from the outdoor climate by the insulation, the temperature at these locations still varied 5° between day and night. The majority of the other measurement locations closely follow the ambient air temperature. Unfortunately the malfunctioning Location B roof membrane thermocouple still shows temperatures near 70°F, 10-20 degrees warmer then Location A. Tables 15 and 16 show the high and low temperatures experienced at each thermocouple point, as well as the average temperature and largest change in temperature for monitoring Locations A and B. Both profiles located on the green roof experience lows ranging from 35° for thermocouples exposed outdoors to 65° F for those protected indoors, and highs ranging from 56-70° outdoors and near 71° F indoors. Note the maximum temperature variation for the roofing membrane is 11.0° at Location A (ignoring data from Location B). This is significant because the temperature variations on the soil surfaces of the green roof are 23.6° and 20.7° respectively. This shows the diurnal temperature stabilizing effect the green roof has on the roofing membrane, and the reduced range of temperature the membrane experiences.

Table 15. Temperature Statistics for Monitoring Location A (10/20/06-10/26/06)

Temperature Statistics for Green Roof Monitoring Location A

	High	Low	Average	Fluctuation
Below Deck	73.3	64.1	67.2	9.2
Above Deck	71.5	62.5	65.6	9.0
Roofing Membrane	55.6	44.6	50.0	11.0
Soil Surface	59.9	36.3	44.2	23.6
7cm Above	60.8	36.0	44.2	24.8
15 cm Above	61.8	35.9	44.3	25.9
30 cm Above	61.8	35.8	44.0	26.0
60 cm Above	63.3	35.7	43.7	27.6
1 m Above	56.1	35.1	43.0	21.0

Table 16. Temperature Statistics for Monitoring Location B (10/20/06-10/26/06)

Temperature Statistics for Green Roof Monitoring Location B

	High	Low	Average	Fluctuation
Below Deck	60.5	52.0	55.7	8.5
Above Deck	71.1	62.4	65.2	8.7
Roofing Membrane	72.6	68.8	70.5	3.8
Soil Surface	55.9	35.2	43.1	20.7
7cm Above	69.3	39.1	48.2	30.2
15 cm Above	61.4	35.5	43.4	25.9
30 cm Above	60.7	35.7	43.9	25.0
60 cm Above	61.0	35.8	44.0	25.2
1 m Above	61.5	35.9	44.4	25.6

Next, the control roof statistics are examined. The control roof statistics are located in Tables 17 and 18. The average lows are similar to those found on the green roof, ranging from 35° outdoors to 70° in the interior of the building. The difference in high temperatures between the control roof and green roof are not as obvious as before, but still relevant. On the control roof, the high temperatures in the temperature profile range from 62-80° outdoors and reach 76° indoors. Again, the roofing membrane and roof surface must be brought in attention. At

Location C the change in temperature over the week for the roof surface was 33.1°, at Location D it was 48.2°. The roofing membrane varied in temperature by 31.7° at Location C and 41.8° at Location D. The temperature variation in the roof membrane is two times the variation experienced by the roof membrane below the green roof. Even in a milder season, the green roof still provides thermal protection to the roof membrane.

Table 17. Temperature Statistics for Monitoring Location C (10/20/06-10/26/06)

Temperature Statistics for Control Roof Monitoring Location C

	High	Low	Average	Fluctuation
Below Deck	76.1	68.8	70.9	7.3
Above Deck	76.1	67.4	69.9	8.7
Roofing Membrane	78.1	46.4	53.7	31.7
Roof Surface	68.6	35.5	45.1	33.1
7cm Above	62.3	35.4	44.2	26.9
15 cm Above	62.8	35.5	44.2	27.3
30 cm Above	62.6	35.5	43.8	27.1
60 cm Above	-	-		
1 m Above	45.5	40.2	41.8	5.3

Table 18. Temperature Statistics for Monitoring Location D (10/20/06-10/26/06)

Temperature Statistics for Control Roof Monitoring Location D

	High	Low	Average	Fluctuation
Below Deck	77.1	70.6	72.7	6.5
Above Deck	77.1	69.6	71.7	7.5
Roofing Membrane	80.8	39.0	49.0	41.8
Roof Surface	82.5	34.3	44.9	48.2
7cm Above	69.3	34.8	44.5	34.5
15 cm Above	62.3	35.3	44.0	27.0
30 cm Above	61.7	35.5	43.9	26.2
60 cm Above	62.0	35.5	44.2	26.5
1 m Above	61.9	35.8	44.4	26.1

5.1.1.3 Winter Profiles

It was intended that the winter profiles display the thermal performance of the green and control roof in the cold snowy Pittsburgh winter. As it turned out, the year 2006 ended with abnormally mild temperatures. It was not until late January 2007 until the first significant snow of the season occurred. While the snow was highly anticipated for green roof evaluation, the thermocouples did not perform well when snow and ice fell on the region. Many thermocouples exposed to the elements, despite being covered with radiation shields, froze, giving a constant reading of 31°F. The data logger did not perform well either. Banks for thermocouples were shut down periodically, or would show readings of -454°. The cold weather resulted in many incomplete data sets. The two with the most complete results are shown in this section. Unfortunately, many temperature points were lost during this season.

The first winter data group spans November 29, 2006 to December 4, 2006. The temperature profile for each monitoring Location A, B, C, and D are shown in Figures 26, 27, 28, and 29 respectively. In each profile, the temperature locations “Roof Membrane,” “Roof or Soil Surface,” and “Ambient” are highlighted. The same color coding is used in this data group. Again, the axis scales on all the temperature profiles remain constant for this data group. This is for ease of comparing temperature from one monitoring location to another.

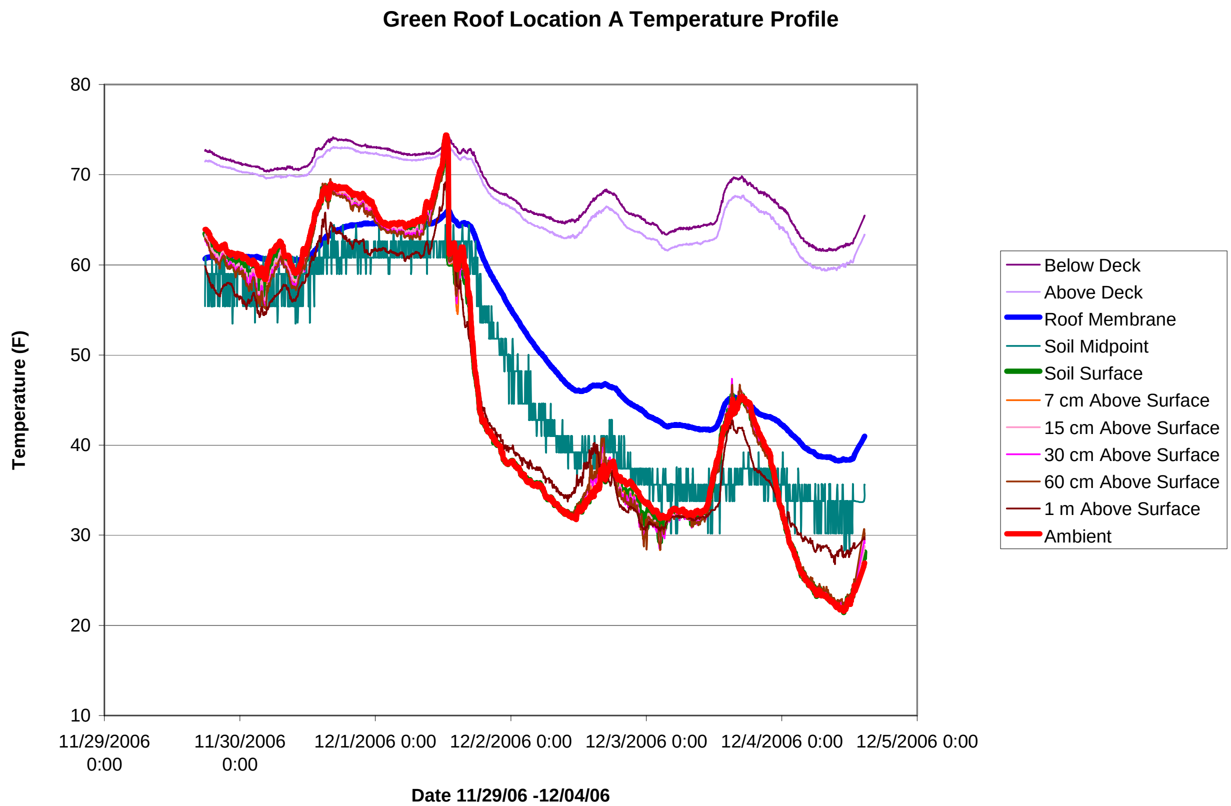

Figure 26. Green Roof Location A Temperature Profile for 11/29/06 – 12/04/06

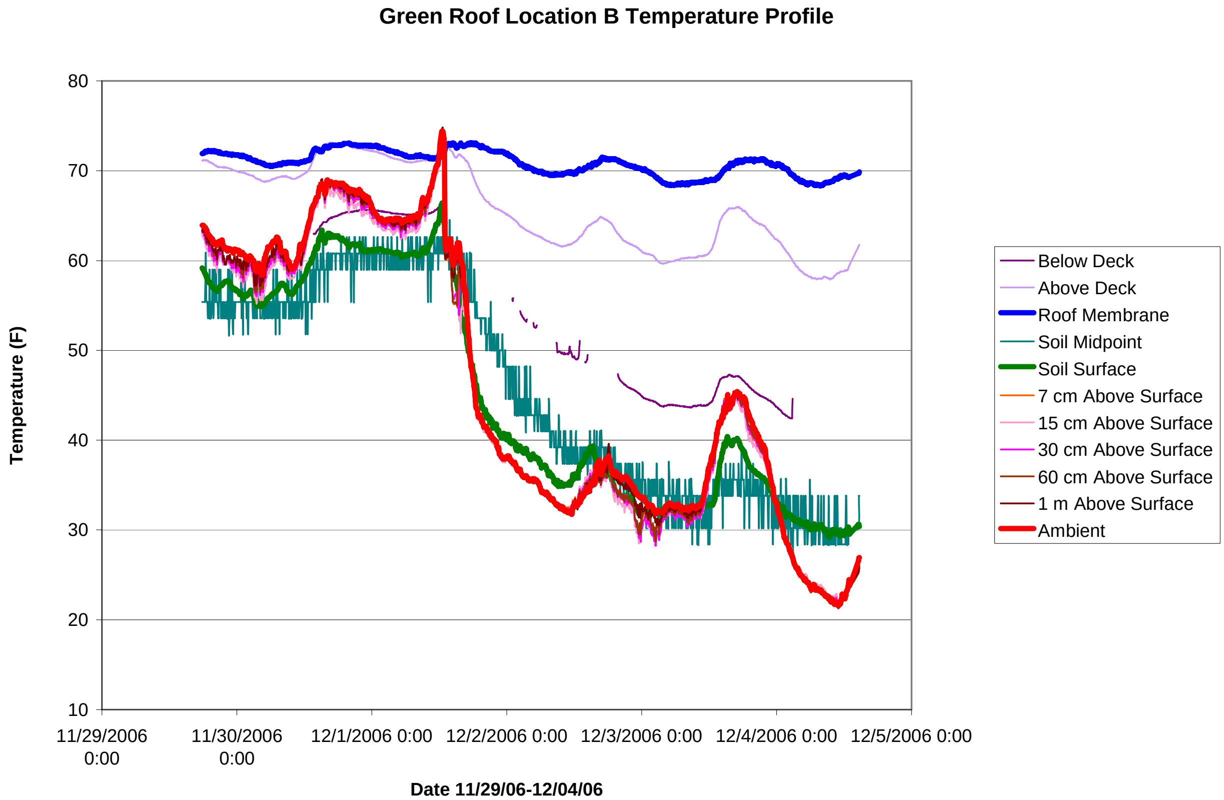

Figure 27. Green Roof Location B Temperature Profile for 11/29/06 – 12/04/06

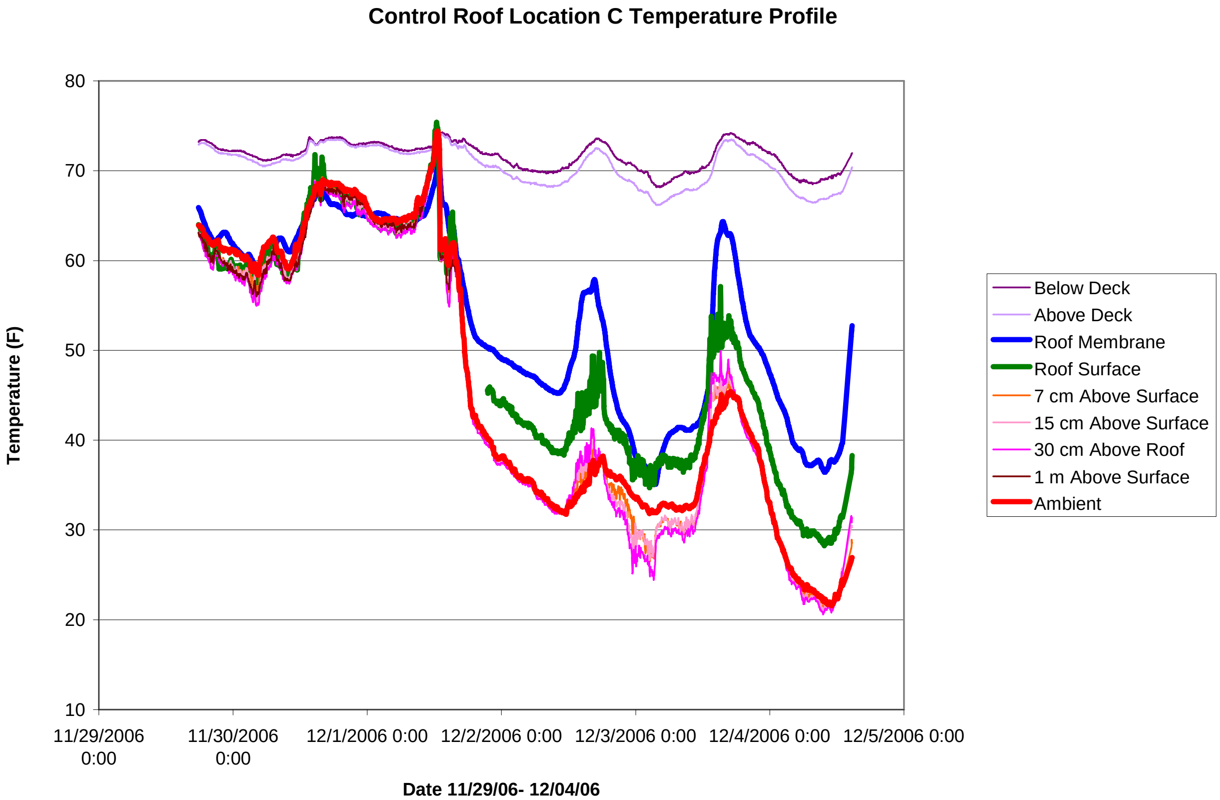

Figure 28. Control Roof Location C Temperature Profile for 11/29/06 – 12/04/06

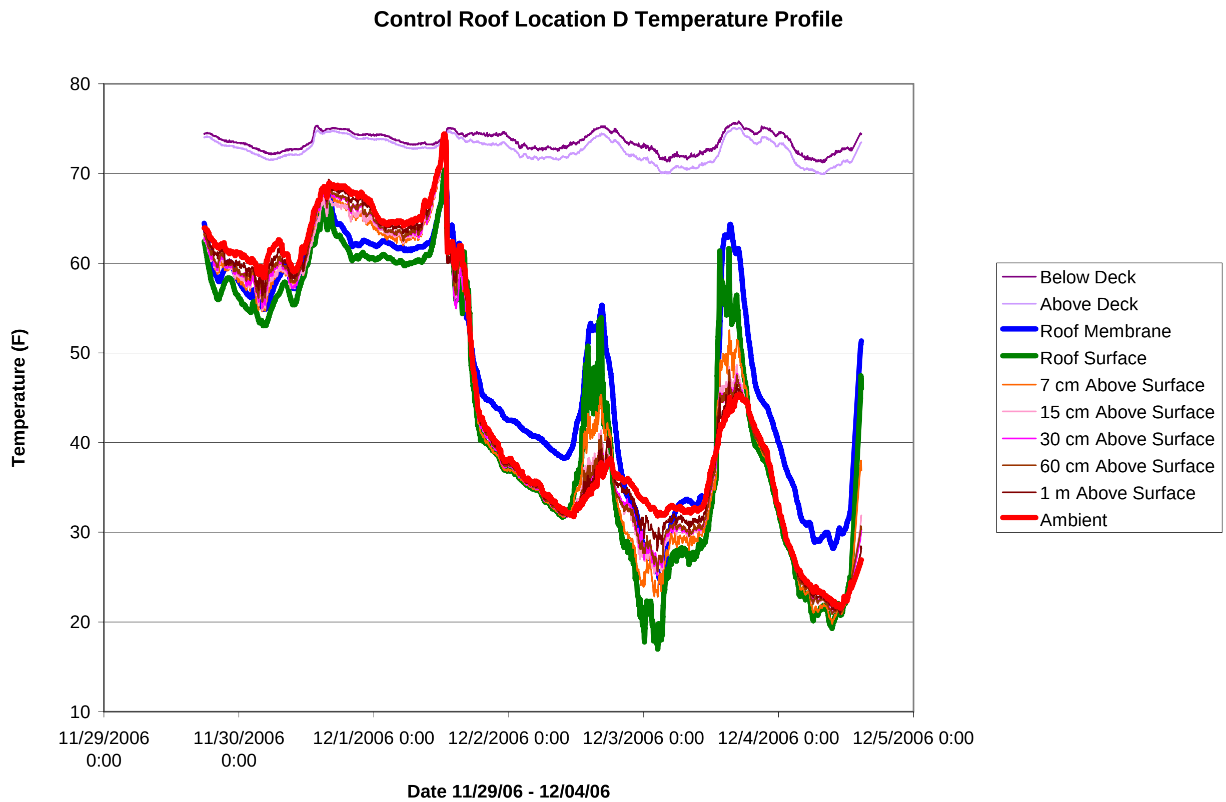

Figure 29. Control Roof Location D Temperature Profile for 11/29/06 – 12/04/06

These temperature profiles provide additional data about the performance of a roof type in mild winter weather. The ambient air temperature remains constant in all four figures. Unfortunately, the malfunction with the thermocouple at the green roof Location B roof membrane has continued. This data group was still utilized in this thesis since a majority of the other instrument readings were in order. During this week, a cold front moved into the area, so the first day and one half is very mild. The nightly low only dropped to 55° F and the daily high reached 71° F. On December 1st there was light rain, as a cold front brought cloudy, much cooler air for the remainder of the week. (Wunderground, 2007) Of course with the cold air, the grocery store continued to heat the interior of the building.

Figures 26 and 27 depict the temperature profiles on the green roof, Locations A and B. The data shows that while the exterior of the building was exposed to cold temperatures, the interior measurements (taken above and below the steel deck) remained warm. For the green roof locations these measurements varied between 65-70°F. Despite being exposed to the grocery store climate and protected from the outdoor climate by the insulation, the temperature at these locations still varied 5° between day and night. The majority of the other measurement locations closely follow the ambient air temperature. Unfortunately the malfunctioning Location B roof membrane thermocouple still shows temperatures near 70°F, 10-30 degrees warmer then Location A. Tables 19 and 20 show the high and low temperatures experienced at each thermocouple point, as well as the average temperature and largest change in temperature for monitoring Locations A and B. However, in this scenario the statistics are misleading. The drastic change in temperature from the beginning of the week to the end of the week skews the results. Note the low temperature of the roof membrane on the green roof is 38.2°F and the high is 66°F. The average temperature of the green roof membrane is 52.7°, about 10° warmer then the average temperature of the outdoor temperature points.

Table 19. Temperature Statistics for Monitoring Location A (11/29/06-12/04/06)

Temperature Statistics for Green Roof Monitoring Location A

	High	Low	Average	Fluctuation
Below Deck	74.3	61.5	68.4	12.8
Above Deck	73.3	59.9	67.0	13.4
Roofing Membrane	66.0	38.2	52.7	27.8
Soil Surface	74.1	21.4	46.1	52.7
7cm Above	73.9	21.4	45.9	52.5
15 cm Above	73.9	21.4	46.0	52.5
30 cm Above	73.5	21.5	45.8	52.0
60 cm Above	73.1	21.8	45.8	51.3
1 m Above	69.2	26.8	45.1	42.4

Table 20. Temperature Statistics for Monitoring Location B (11/29/06-12/04/06)

Temperature Statistics for Green Roof Monitoring Location B

	High	Low	Average	Fluctuation
Below Deck	66.8	42.4	53.2	24.4
Above Deck	71.3	57.9	65.9	13.4
Roofing Membrane	73.1	68.3	70.9	4.8
Soil Surface	66.4	29.2	45.2	37.2
7cm Above	74.4	21.8	45.8	52.6
15 cm Above	73.8	21.8	45.4	52.0
30 cm Above	74.7	21.4	45.7	53.3
60 cm Above	74.7	21.3	45.9	53.4
1 m Above	74.8	21.4	46.2	53.4

Next, the control roof statistics are examined. The control roof statistics are located in Tables 21 and 22. The highs and lows are similar to those found on the green roof. In the winter profiles, there is not the drastic change in temperature from the green roof membrane to the control roof membrane, as there was in the summer and fall profiles. The low temperature of the control roof membrane was 35.1° and 24.2° at Locations C and D respectively. This is slightly cooler than the green roof. The average temperature of the control roof membrane was 53.6° and 48.5°F. This is about the same as the green roof membrane. Locations A and C are very similar in temperature, and are exposed to the same amount of daylight and shadowing. It appears that the green roof and control roof have the same thermal performance for this data set. The green and control roof have similar results when there is a sudden change in the weather in which the roof is exposed.

Table 21. Temperature Statistics for Monitoring Location C (11/29/06-12/04/06)

Temperature Statistics for Control Roof Monitoring Location C	High	Low	Average	Fluctuation
Below Deck	74.3	68.2	71.6	6.1
Above Deck	74.1	66.2	70.6	7.9
Roofing Membrane	71.0	35.1	53.6	35.9
Roof Surface	75.4	28.3	49.8	47.1
7cm Above	74.4	21.1	45.7	53.3
15 cm Above	74.1	20.9	45.7	53.2
30 cm Above	74.0	20.6	45.3	53.4
60 cm Above	-	-	-	
1 m Above	74.1	56.0	62.9	18.1

Table 22. Temperature Statistics for Monitoring Location D (11/29/06-12/04/06)

Temperature Statistics for Control Roof Monitoring Location D	High	Low	Average	Fluctuation
Below Deck	75.8	71.2	73.6	4.6
Above Deck	75.1	69.9	72.7	5.2
Roofing Membrane	69.7	24.2	48.5	45.5
Roof Surface	70.4	17.0	44.2	53.4
7cm Above	73.7	19.8	45.2	53.9
15 cm Above	73.6	20.9	45.2	52.7
30 cm Above	74.1	20.9	45.3	53.2
60 cm Above	74.1	20.9	45.5	53.2
1 m Above	74.5	20.9	46.0	53.6

Finally, the last winter data group spans January 23, 2007 to January 29, 2007. This data set runs concurrently with the first significant snow fall of the season. Unfortunately, the data set is somewhat incomplete. The temperature profile for each monitoring Location A, B, C, and D are shown in Figures 30, 31, 32, and 33 respectively. In each profile, the temperature locations “Roof Membrane,” “Roof or Soil Surface,” and “Ambient” are highlighted. The same color coding is used in this data group. Again, the axis scales on all the temperature profiles remain constant for this data group. This is for ease of comparing temperature from one monitoring location to another.

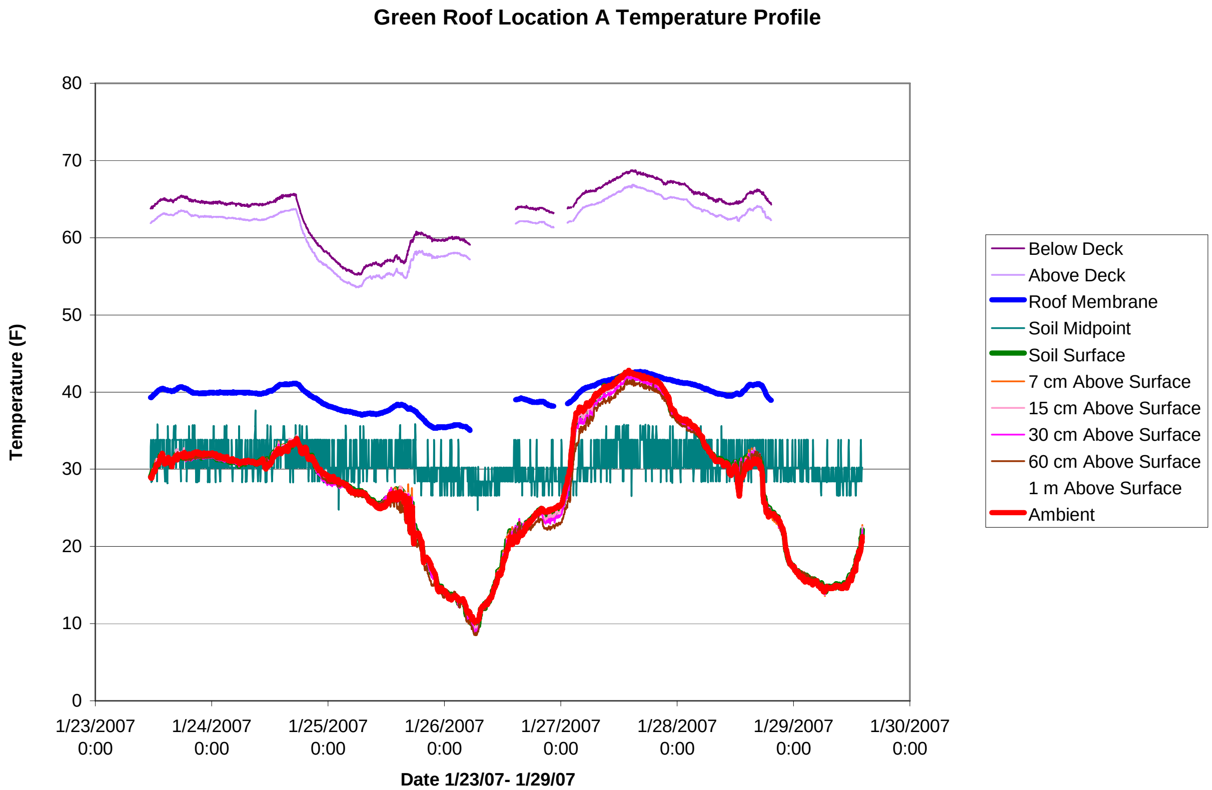

Figure 30. Green Roof Location A Temperature Profile for 01/23/07 – 01/29/07

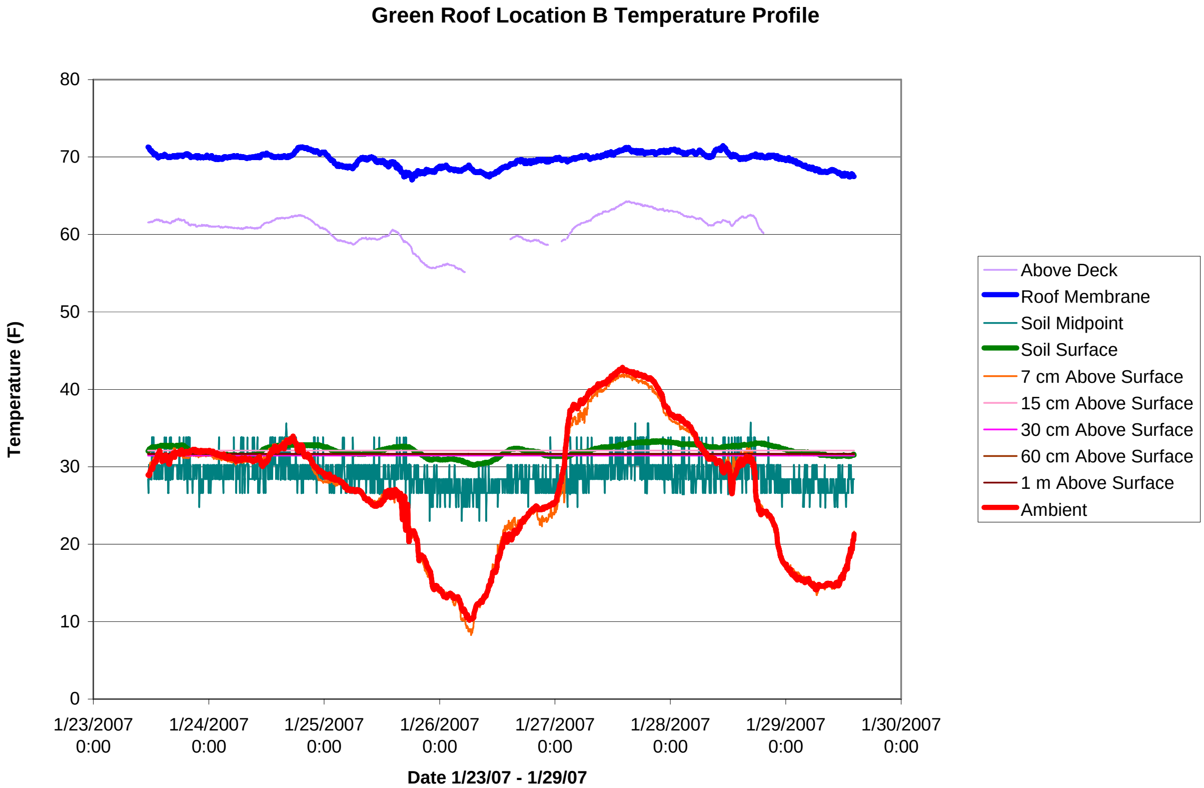

Figure 31. Green Roof Location B Temperature Profile for 01/23/07 – 01/29/07

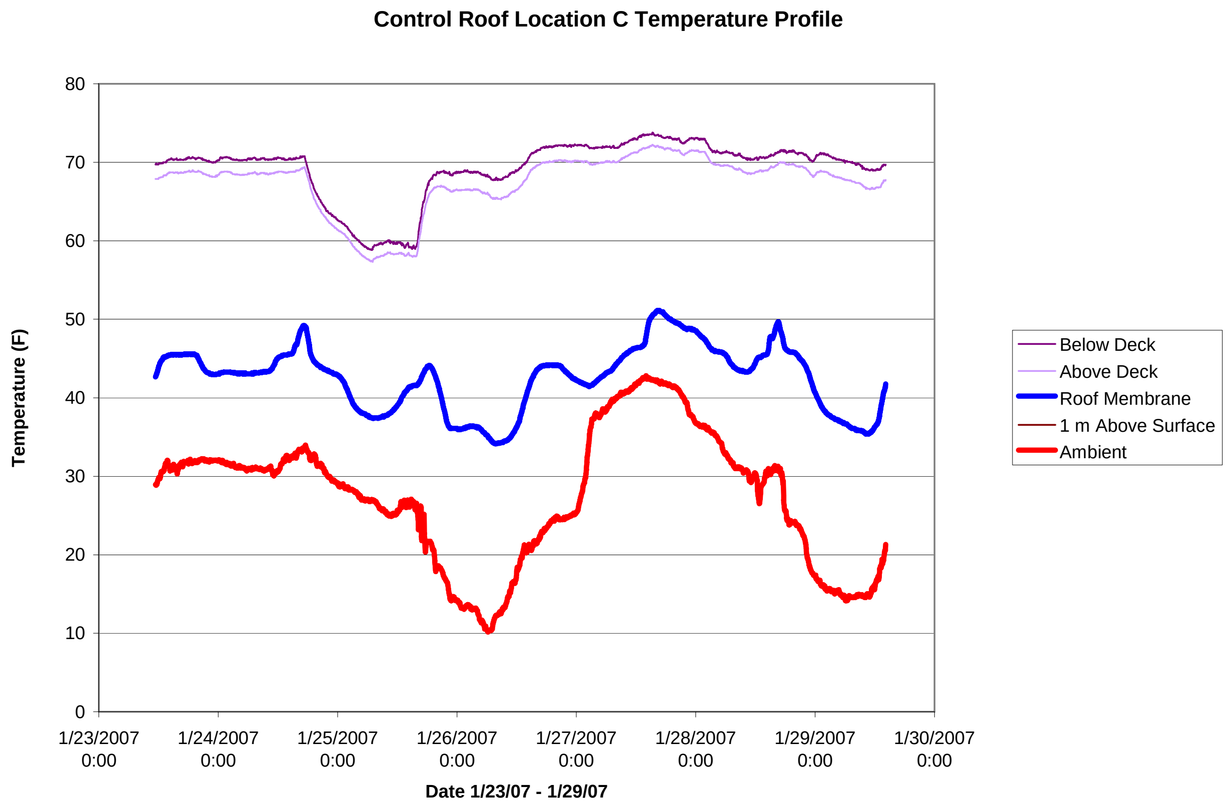

Figure 32. Control Roof Location C Temperature Profile for 01/23/07 – 01/29/07

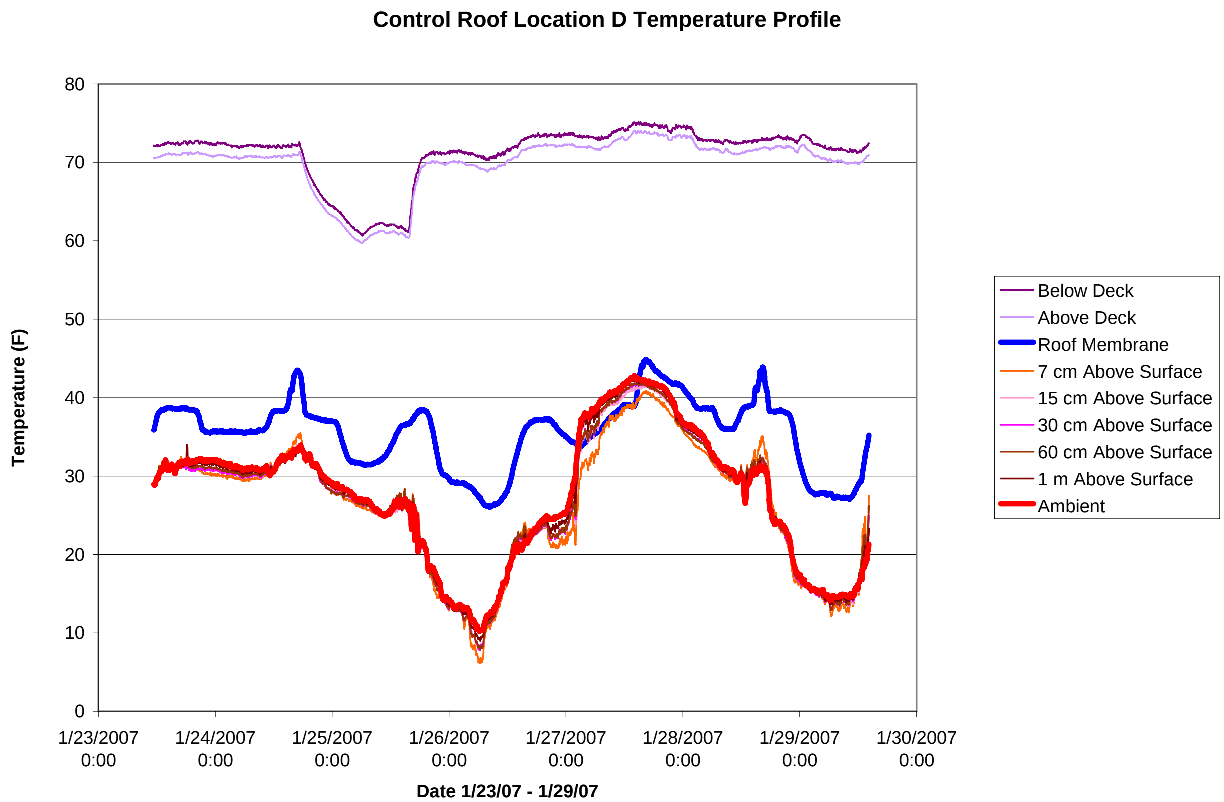

Figure 33. Control Roof Location D Temperature Profile for 01/23/07 – 01/29/07

These temperature profiles provide additional data about the performance of a roof type in typical winter weather. The ambient air temperature remains constant in all four figures. Unfortunately, the malfunction with the thermocouple at the green roof Location B roof membrane has continued. Regrettably, this is the most complete data set during a week with snow and freezing rain. During this week, the ambient temperature was consistent, cold throughout the day and night. The coldest night dropped to 9° F and the warmest day reached 41° F. There was light snow every day of the week. (Wunderground, 2007) It was the first week of "typical" winter weather for Pittsburgh for the 2006-2007 seasons.

Figures 30 and 31 depict the temperature profiles on the green roof, Locations A and B. The data shows that while the exterior of the building was exposed to cold temperatures, the interior measurements (taken above and below the steel deck) remained warm. For the green roof locations these measurements varied between 55-70°F. Despite being exposed to the grocery store climate and protected from the outdoor climate by the insulation, the temperature at these locations still varied 10° between day to day. Unfortunately a variety of the thermocouples malfunctioned in this data set. Most of the above surface temperatures followed the ambient air temperature. However, some of the thermocouples froze, and showed a constant temperature of 31.7°F. There is a gap in the data when the green roof below surface data logger module had a glitch briefly. Some of the thermocouples shut off completely. While the errors, glitches, and malfunctions were temporary, they did occur every time there was a significant snow fall.

Tables 23 and 24 show the high and low temperatures experienced at each thermocouple point, as well as the average temperature and largest change in temperature for monitoring Locations A and B. The outdoor measuring points average below the freezing point. The two indoor points are influenced by the grocery store heating system. Under the green roof, the roof membrane reaches a minimum temperature of 35°F. This is 25° warmer then the lowest evening temperature during the week. The above surface temperatures at Location A follow the ambient temperature closely. The above surface temperatures at Location B hold steady around 31°-32°. It can be assumed that the thermocouples at this location were covered in ice.

Table 23. Temperature Statistics for Monitoring Location A (01/23/07-01/29/07)

Temperature Statistics for Green Roof Monitoring Location A

	High	Low	Average	Fluctuation
Below Deck	68.7	55.2	63.3	13.5
Above Deck	66.9	53.6	61.4	13.3
Roofing Membrane	42.7	35.0	39.5	7.7
Soil Surface	42.5	9.4	27.5	33.1
7cm Above	42.5	8.8	27.4	33.7
15 cm Above	42.4	9.0	27.5	33.4
30 cm Above	42.2	8.8	27.2	33.4
60 cm Above	41.7	8.5	27.0	33.2
1 m Above	33.9	29.2	31.8	4.7

Table 24. Temperature Statistics for Monitoring Location B (01/23/07-01/29/07)

Temperature Statistics for Green Roof Monitoring Location B

	High	Low	Average	Fluctuation
Below Deck	-	-	-	
Above Deck	64.3	55.2	60.8	9.1
Roofing Membrane	71.5	67.0	69.6	4.5
Soil Surface	33.3	30.2	32.1	3.1
7cm Above	41.9	8.3	27.2	33.6
15 cm Above	32.1	32.1	32.1	0.0
30 cm Above	32.5	31.5	31.5	1.0
60 cm Above	31.6	31.6	31.6	0.0
1 m Above	31.7	31.7	31.7	0.0

Next, the control roof statistics are examined. The control roof statistics are located in Tables 25 and 26. The highs and lows are similar to those found on the green roof. In the winter profiles, there is not the drastic change in temperature from the green roof membrane to the control roof membrane, as there was in the summer and fall profiles. The low temperature of the control roof membrane was 34.1° and 26° at Locations C and D respectively. This is slightly cooler than the green roof. The average temperature of the control roof membrane was 42.6° and 35.5°F. This is about the same as the green roof membrane. Locations A and C are very similar in temperature, and are exposed to the same amount of daylight and shadowing. In this data set, all the above surface measuring points for Location C were lost. The above surface temperatures at Location D are similar to the green roof temperatures, and follow the ambient temperature as well. It seems that in cold weather, the two roof types have similar thermal performance.

Table 25. Temperature Statistics for Monitoring Location C (01/23/07-01/29/07)

Temperature Statistics for Control Roof Monitoring Location C

	High	Low	Average	Fluctuation
Below Deck	73.8	58.9	69.2	14.9
Above Deck	72.2	57.3	67.5	14.9
Roofing Membrane	51.1	34.1	42.6	17.0
Roof Surface	-	-	-	
7cm Above	-	-	-	
15 cm Above	-	-	-	
30 cm Above	-	-	-	
60 cm Above	-	-	-	
1 m Above	-	-	-	

Table 26. Temperature Statistics for Monitoring Location D (01/23/07-01/29/07)

Temperature Statistics for Control Roof Monitoring Location D

	High	Low	Average	Fluctuation
Below Deck	75.2	60.6	71.2	14.6
Above Deck	74.0	59.7	69.9	14.3
Roofing Membrane	44.9	26.0	35.5	18.9
Roof Surface	-	-	-	
7cm Above	40.9	6.1	26.4	34.8
15 cm Above	41.5	7.8	26.8	33.7
30 cm Above	41.8	7.8	26.8	34.0
60 cm Above	41.8	8.0	27.0	33.8
1 m Above	42.2	9.0	27.2	33.2

5.1.2 Single Layer Temperatures

While the temperature profiles provide significant data about the climate near the green and control roofs, these temperature layers can be singled out and examined individually. In this section, the same temperature point at all four monitoring locations (i.e. the roof membrane temperature at Location A-D) will be plotted against the ambient temperature. The results show the difference in temperature between the four monitoring locations. It is the goal of this section to examine the performance of a single layer within the temperature profile when compared to the other monitoring locations.

For the purpose of this thesis, four temperature points will be considered; roof membrane temperature, roof surface temperature, 7cm above roof surface temperature, and 30cm above surface temperature. The figures depict the similarities and differences between the four monitoring locations at a single layer. This allows for comparison between the green roof and control roof performance in summer, fall and winter conditions. While three data groups will be discussed in this section, additional figures can be found in the Appendix.

5.1.2.1 Roof Membrane Temperature

First the roof membrane will be assessed. Figures 26, 27, and 28 depict the temperature of the roof membrane in the summer, fall, and winter seasons. In each scenario, green roof Locations A and B are defined by a green and blue line, respectively, and control roof Locations C and D are defined by a pink and orange line, respectively. The ambient air temperature for the data group is shown with a bold red line. The summer data group selected is July 28 to August 1, 2006. The fall data group is October 20 to October 25, 2006. The winter group is January 23 to January 29, 2007. The same data sets will be utilized for all the single layer temperature comparisons.

The roof membrane temperatures clearly show the difference between the green and control roof. During the summer week when temperatures are hot, the ambient temperature reached a maximum temperature of 93.6°F on July 31st. Meanwhile the control roof Locations C and D reach maximum temperatures of 116.2°F and 125.6°F respectively at roughly the same time of day. For Location D, the difference in temperature between the roof membrane and ambient air temperature is 32°. On the same day, the membrane underneath the green roof also reached it maximum temperature. At Location A the temperature reached 90.8°F and at Location B it reached 81.7°F. At both green roof locations the maximum membrane temperature is slightly less then the maximum air temperature. It is also important to note the temperature of the roof membrane at night. After reaching very high temperatures during the day, the roof membrane on the control roof side actually drops lower then the ambient air temperature at night. The low ambient air temperature the morning of August 1st was 77.6°F. The roof membrane temperature for Locations C and D were 73.3° and 72.2°. While not as drastic as the afternoon difference, nightly, the control roof membrane does drop 5° cooler then the ambient air temperature. This phenomenon shows the ability of the roof membrane to absorb a great deal of energy during the day and release that energy at night. At the green roof locations the nightly low temperature for the same day is 81.8° and 74.8°F respectively. At Location A the minimum temperature does not exceed the ambient air low temperature; at Location B it does exceed the ambient air temperature by 2.8°. This shows that the green roof is protecting the waterproof membrane from absorbing a large amount of heat during the day and does not have to release much heat in the evening. The green roof is a reasonable method of protecting the waterproofing membrane from extreme temperature fluctuations in the summer months.

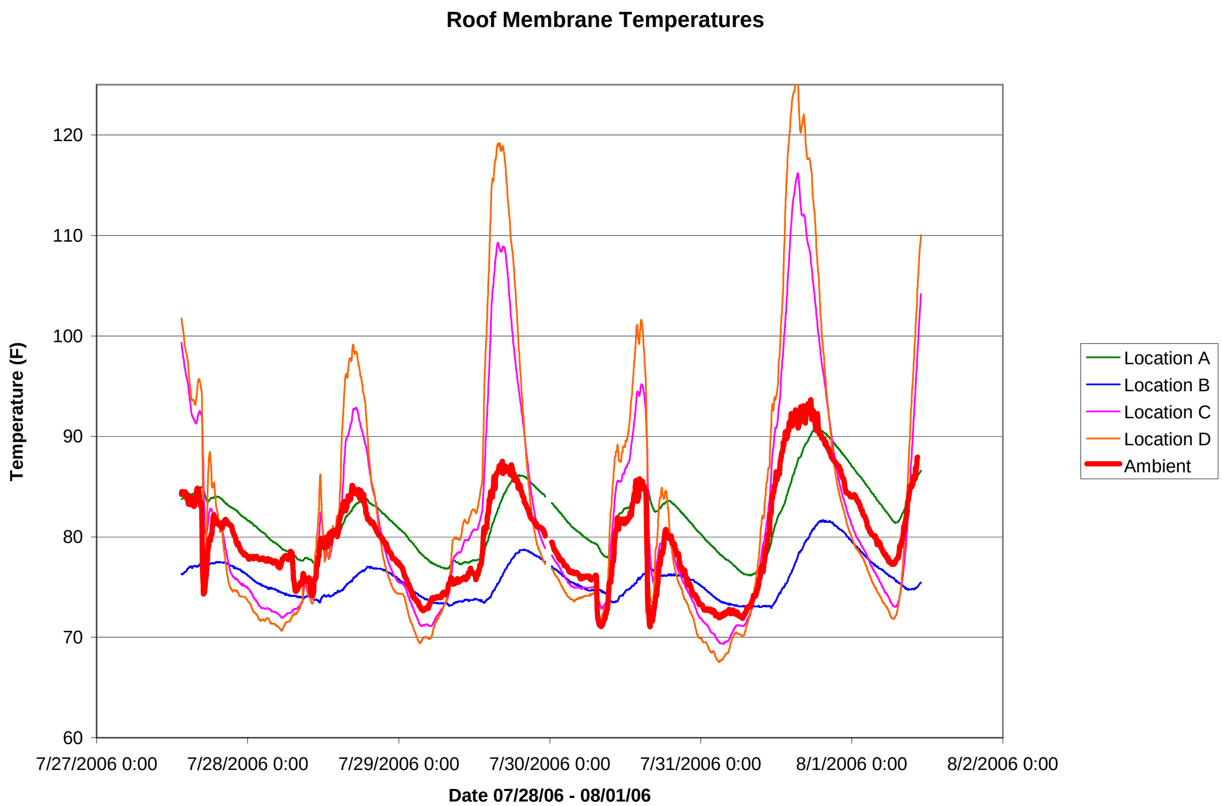

Figure 34. Roof Membrane Temperatures for 7/28/06 – 8/1/06

In the fall months, the ability of the waterproofing membrane to absorb energy during the day and release that energy at night persists, but is not as extreme. In this case the data set from October 20th to October 25th 2006 is examined. Figure 27 shows the roof membrane temperature at the four monitoring locations. Unfortunately, the thermocouple is corrupt and the results from Green Roof Location B monitoring point are not dependable. In this analysis, the results are shown, but appear very unusual, and thus will not be discussed.

The week of October 20th shows a week of transitional weather. The first two days are mild, with ambient air temperature reaching highs near 60°F and lows in the 40's. The second two days were much cooler; the high only reaching the mid 40's and the low dipping into the mid 30's. However, the temperature of the roof membrane tells a different story. On the first two days, the control roof temperatures are in the 70's, roughly 15° higher then the ambient temperature. Even as the cold front moved into the area, the control roof still rose in temperature 15-20° warmer then the ambient temperature. During these few days, the roof membrane temperature rarely dropped below the ambient air temperature. Only Location D fell below the ambient air by 5° the first evening. Also note that during the last two days, when the air temperature drops to highs in the 40's, the control roof membrane remains warmer than the air temperature during the day by as much as 15°. In the evening the roof membrane cools, but remains warmer than the air temperature. The results beneath the green roof are very interesting as well. During the first two days of warm temperatures, the membrane below the green roof only varied by 3-5° throughout the day and night. The temperature remained in the low to mid 50's, not nearly as extreme as the ambient air temperature itself. When the cooler air moves into the region the second half of the data set, Location A shows lower, but still steady, temperatures. The roof membrane is kept warmer then the air temperature by about 5°. The average temperature of the membrane beneath the green roof is cooler then the average temperature of the control roof membrane, but does not fluctuate as much. The diurnal fluctuation of the roof membrane is limited under the green roof, but very pronounced on the control roof.

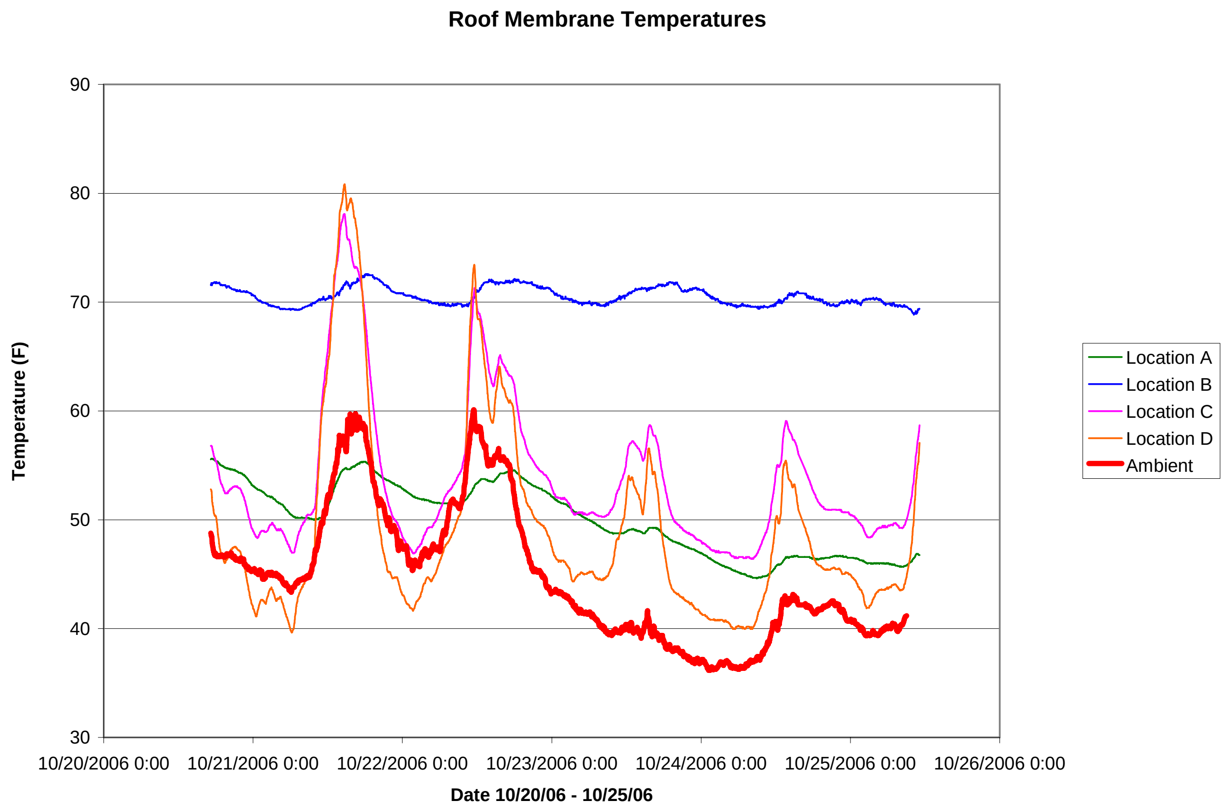

Figure 35. Roof Membrane Temperatures for 10/20/06 – 10/25/06

The winter data set selected is January 23rd to January 29th 2007. Figure 36 shows the roof membrane temperatures for Locations A, B, C, and D. Like in the previous data set, the Location B temperature is shown, but the results do not appear to be accurate. The temperature at Locations A, C, and D rise and fall with the ambient temperature, although somewhat muted. All the roof membrane temperatures keep 5-10° warmer then the ambient air. The two control roof temperatures seem to sandwich the green roof temperature. Unfortunately, with Location B malfunctioning, it cannot be definitively determined if the membrane temperature is affect by location, although it appears that the western side of the roof does stay warmer than the east side. The diurnal fluctuations of the green roof are minimal, while the diurnal fluctuations on the control average 5° or more. While the green roof does not seem to keep the roof membrane warm or better insulated during the winter months, it does keep the diurnal fluctuations minimal.

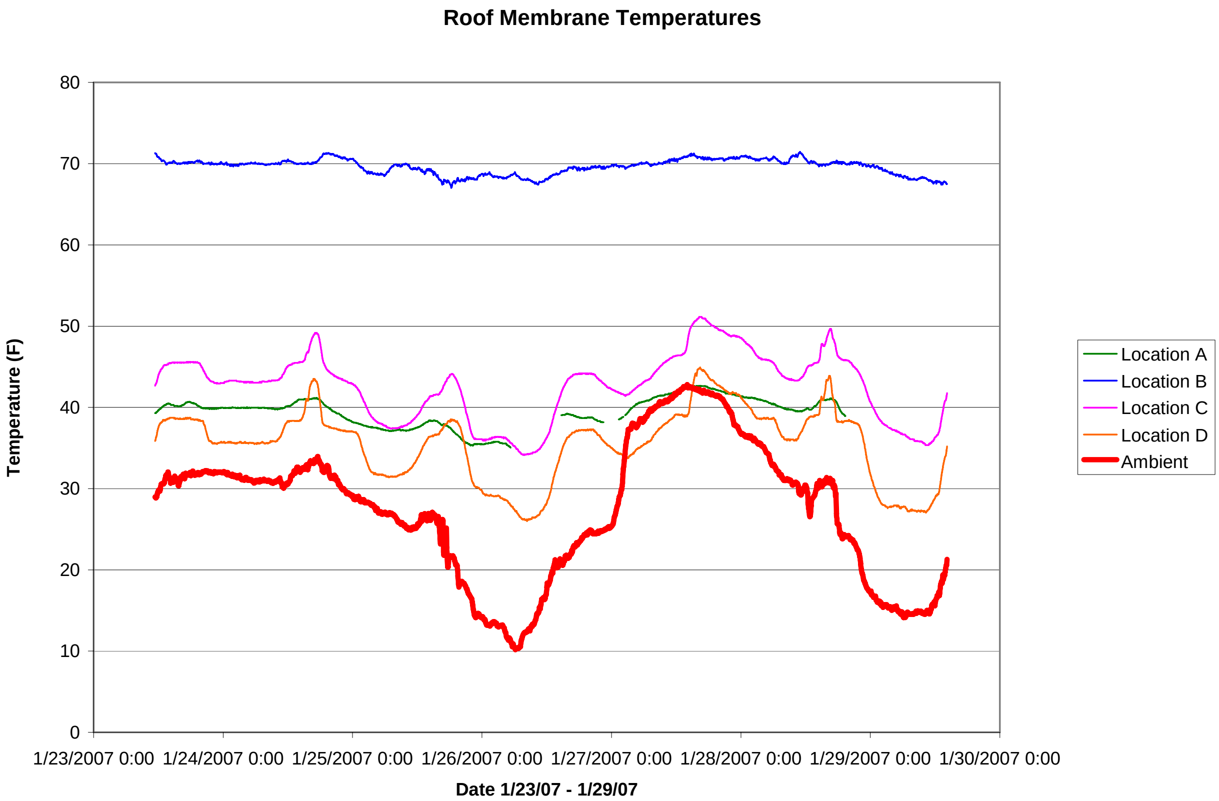

Figure 36. Roof Membrane Temperatures for 1/23/07– 1/29/07

5.1.2.2 Roof Surface Temperature

The roof surface temperature was taken on top of the roof membrane on the control roof, and on top of the soil on the green roof. The control roof temperature was taken with a thermocouple wire placed on top of the roof membrane. The thermocouple was sheltered slightly by aluminum foil and some of the gravel ballast covering the control roof. On the green roof the thermocouple was placed directly on the soil. It was weighed down by a few large stones to keep it from moving. The thermocouple was not placed underneath any vegetation.

The surface temperatures vary from the membrane temperatures. Generally the surface temperatures follow the ambient air temperature closer then the membrane temperature. During the summer week, the surface temperatures at Locations A and C mimic the ambient air temperature. Neither varies from the air temperature by more than 5°F at any point during the week. In contrast, Locations B and D rise in temperature greatly during the day and drop in temperature throughout the night. Location D reaches temperatures nearly 30° greater then the ambient temperature on two separate days. It seems that the surface temperature measurements are influenced more by location on the roof, rather than roof type. Locations B and D are on the eastern side of the building. They are exposed to more direct sunlight throughout the day. There are no surrounding buildings that cast a shadow or shade this half of the roof. On the western side of the building, the apartment complex to the south of the grocery store shades half of the roof throughout some of the day. This could be why the western half of the building (Locations A and C) do not reach the temperature extremes that the eastern side of the building does.

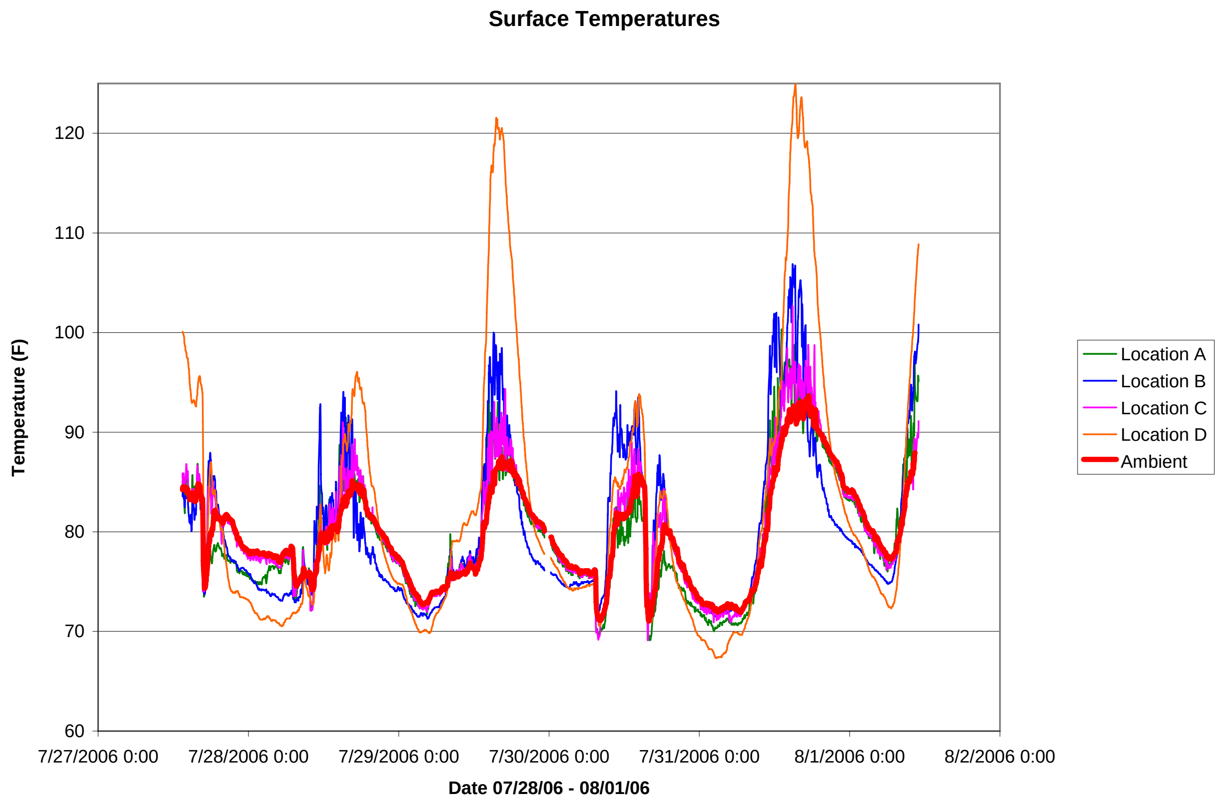

Figure 37. Surface Temperatures for 7/28/06 – 8/1/06

During the fall week, there is a switch in which locations reach the greatest daytime temperatures. In this case Locations C and D are the warmest locations. During the fall months when the days are shorter, the entire roof is exposed to less daylight throughout the course of the week. It appears that roof type influences surface temperature more than location in autumn. Control roof Locations C and D reach temperatures 7-20° greater than the ambient temperature. Conversely, the green roof locations vary only slightly from the ambient temperature. The temperature extremes on the roof are not as excessive during the fall as the summer data set. This is due to a combination of ambient temperature, exposure to solar radiation, and shading on the roof. The green roof seems to effectively keep surface temperatures cool during both the summer and fall months.

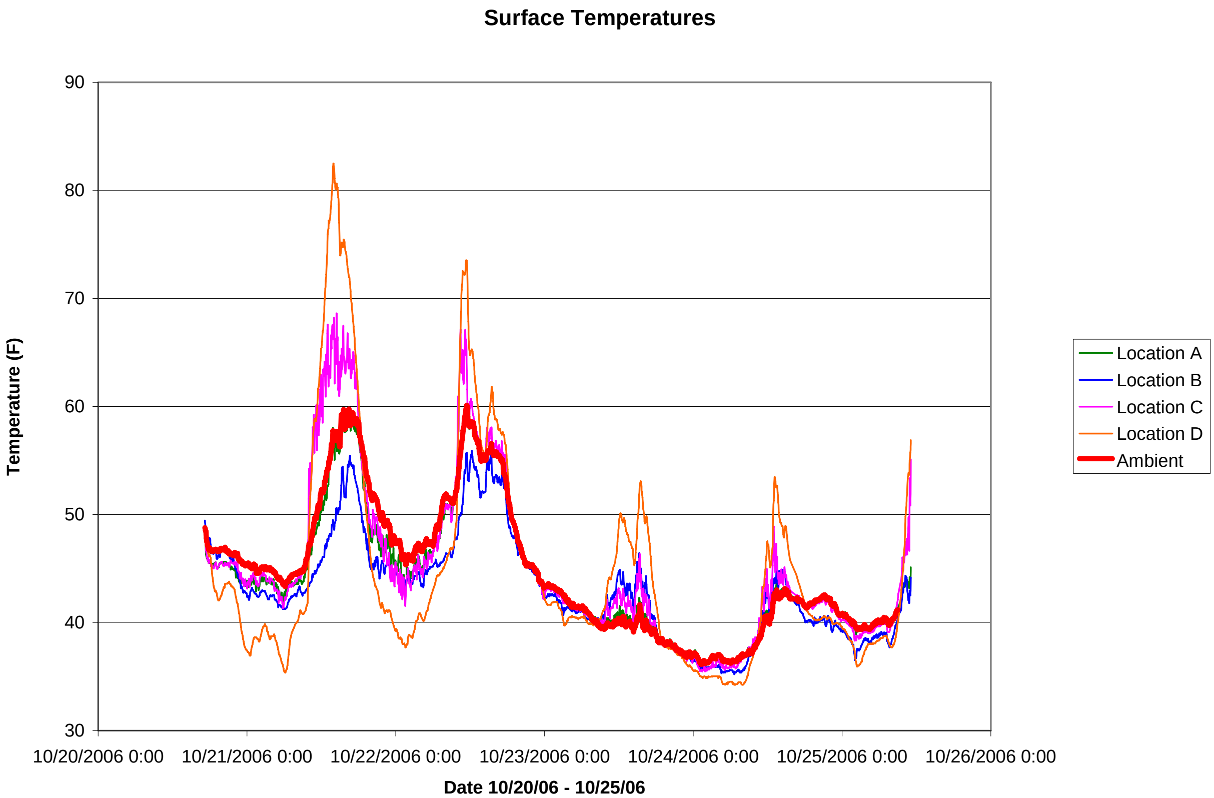

Figure 38. Surface Temperatures for 10/20/06 – 10/25/06

The results for the winter week do not provide much data. The thermocouples at the control roof malfunctioned and the thermocouple at Location B was covered in ice. Thus, only Location A remains. As shown in Figure 39, the surface temperature at Location A follows the ambient air temperature almost exactly. While the green roof surface tended to be cooler than the control roof surface during the summer and fall, it still reached temperatures warmer than the ambient air. In the winter, the surface does not differ from the ambient air. It is not warmer, but it is not cooler either. The green roof does not seem to provide the thermal benefit in the winter as it does in the summer and fall.

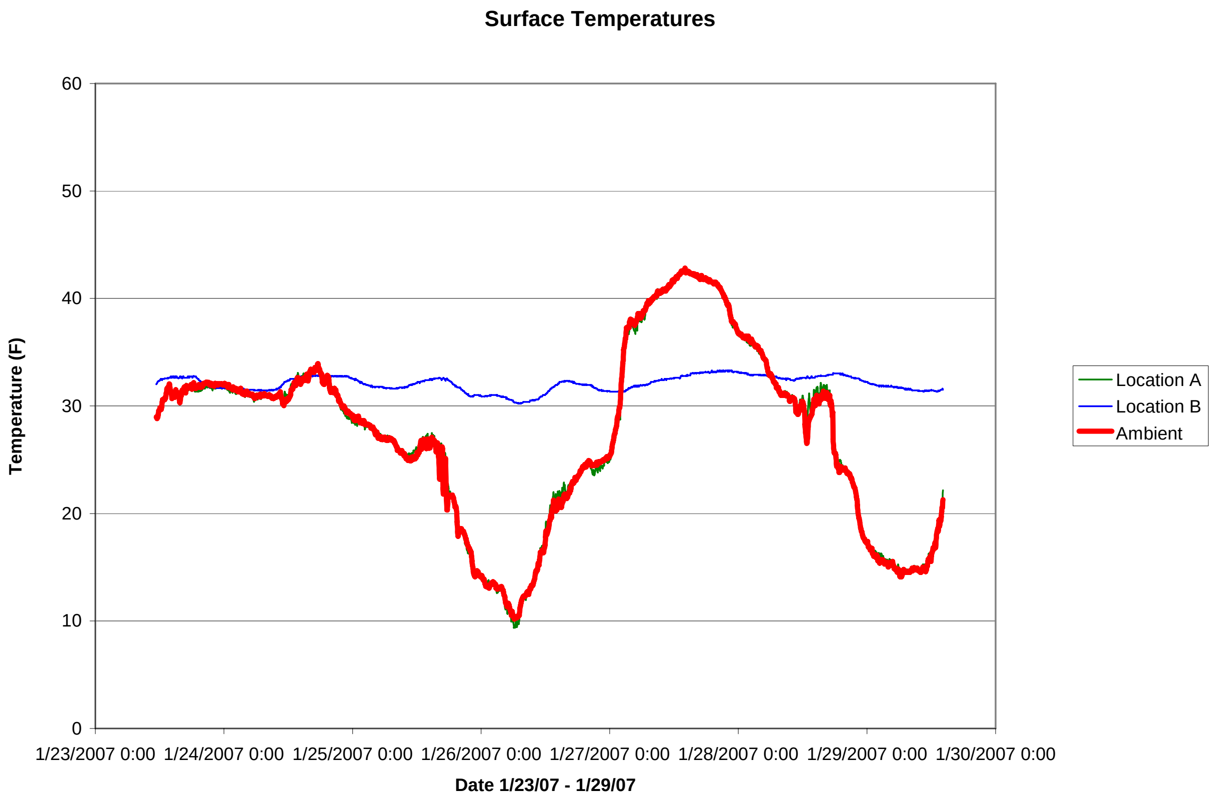

Figure 39. Surface Temperatures for 01/23/07 – 01/29/07

5.1.2.3 7 cm and 30 cm Above Surface Temperature

The Above Surface Temperature points were installed hoping to capture roof type effect on the Urban Heat Island. Unfortunately, a number of factors made recording this effect very hard. Wind current, eddies, reflection, radiation, and exposure could all influence the thermocouple results with varying effect. The radiation shields were used to reduce this influence, but could not completely eliminate it. The 7cm above surface temperatures are examined in this thesis since they are the open air temperature points that are most likely influenced by roof type, with minimal exposure to other deterrents. The 30 cm above surface temperatures are used to confirm the observations made at the 7cm locations.

The summer data set seemed to show the desired result at first. All temperatures rise and fall with the ambient temperature. The pink and orange peaks over the red ambient results seem to show that the control roof does in fact warm the air around it, with enough intensity to measure the effect. However, the green roof temperatures also rise above the ambient temperature, sometimes just as high as the corresponding control roof point. It does appear that the air is consistently warmer at the control roof Location D, which, out of all the locations, is exposed to the most sunlight through the course of a day. At the 7cm level, the control roof seems to stay slightly warmer than the ambient air temperature during a typical summer week.

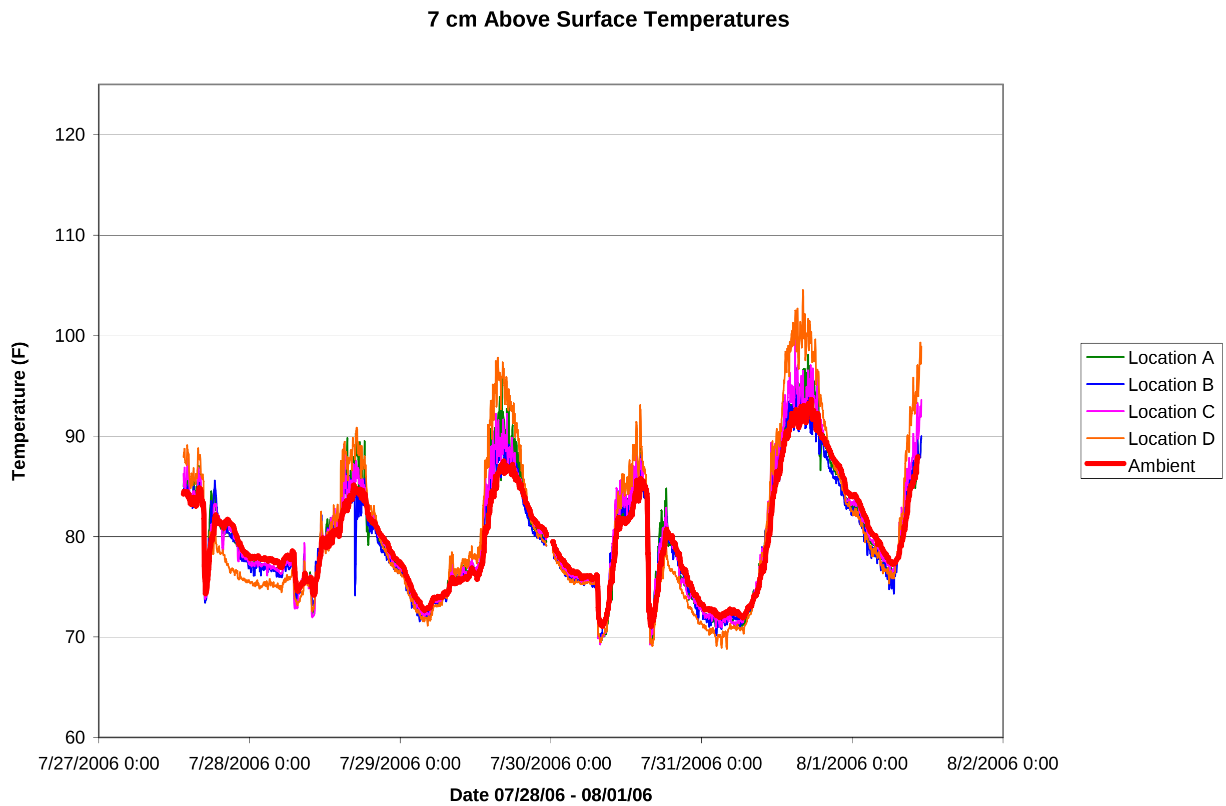

Figure 40. 7 cm Above Surface Temperatures for 7/28/06 – 8/1/06

To confirm the 7cm results, the 30cm Above Surface results will be examined next. It appears that the warming trend of the control roof continues at this distance above the roof surface. It seems even more promising since the green roof measuring points are consistently lower than the control roof points. However, the increase in air temperature above the roof surface only occurs when the ambient air temperature reaches it maximum in the afternoon hours. The transitional period between night and day and day and night do not have the same warming trends. In fact, in the evening, night, and early morning, all the temperatures are virtually the same.

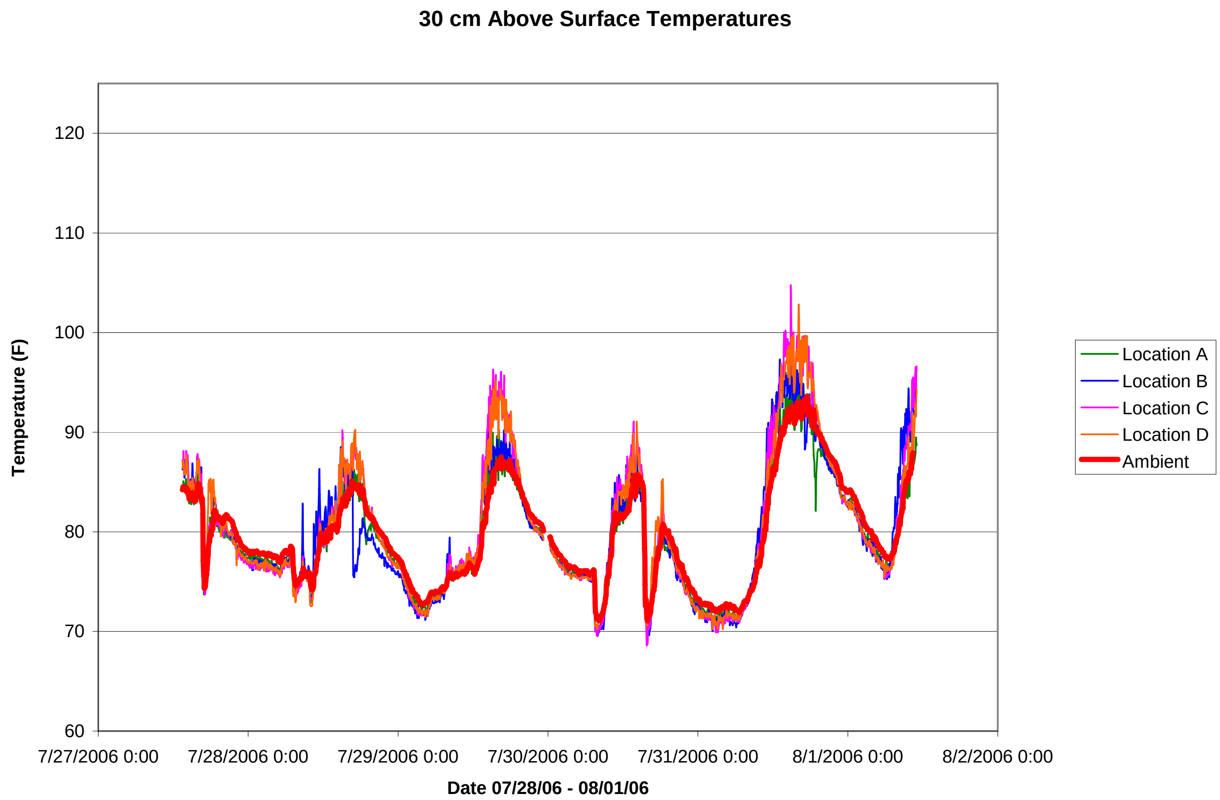

Figure 41. 30 cm Above Surface Temperatures for 7/28/06 – 8/1/06

The autumn results do not concur with the summer results. At the 7cm level, Locations B and D are warmer than the ambient air, while Locations A and C steadily follow the ambient air. With the malfunction at the Location B roof membrane point, the results at the 7cm level imply that the membrane is kept warmer by a source outside of the field of study. There may be a vent or heating conduit near this location that is altering the results. Since access to the interior of the store, above the merchandise, is restricted, this theory cannot be confirmed. The fact that the east side of the building seems warmer than the west might also be due to the sunlight exposure that is had on that side of the building. The cooler temperatures at Locations A and C may be from the shading provided by the apartment building to the south. The angle of the sun during the shorter fall days may make the warming trend of the control roof less pronounced, especially when one point is shaded throughout the morning.

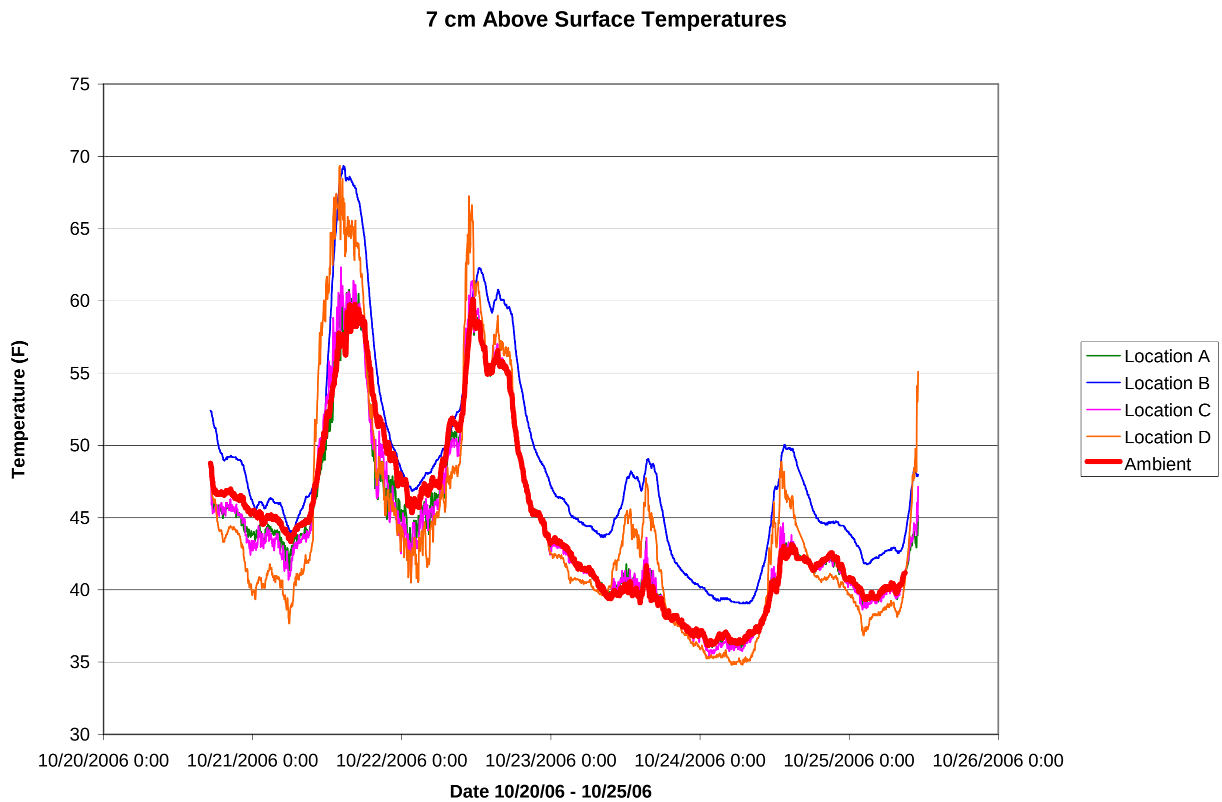

Figure 42. 7 cm Above Surface Temperatures for 10/20/06 – 10/25/06

The 30 cm Above Surface Temperatures have the opposite effect as seen in the previous data. In this case, the control roof results occasionally peek above the ambient air temperature, but it is the evening temperatures that stand out. The temperature at all locations dips below the ambient temperature, especially the first two evenings. The green roof temperatures do not drop as low as the control roof temperatures, but do vary from the ambient temperature unlike any of the previous data sets. The results at this elevation may be an abnormality, or the roof might behave differently in the fall as opposed to the summer. Since the roof is not exposed to as much solar radiation during the day it may fall to a lower temperature in the evening. The results at this location are inconclusive.

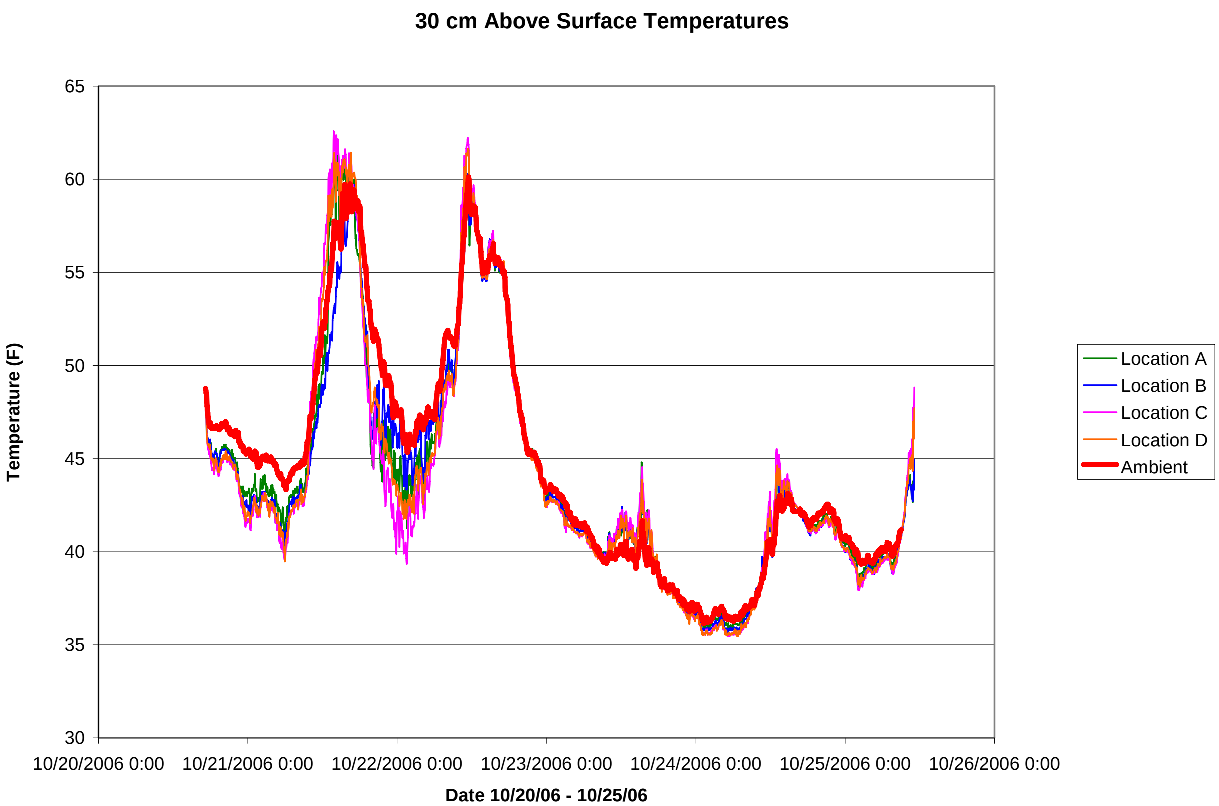

Figure 43. 30 cm Above Surface Temperatures for 10/20/06 – 10/25/06

Last to be examined is the winter data set. Figures 44 and 45 show the 7cm and 30cm Above Surface Temperature results. In both cases, the above surface temperatures do not vary significantly from the ambient temperature. The only exception is Location B at the 30cm height, it was covered in ice and had a constant temperature of 32°F. Since the winter results show no evidence of roof type influencing the air temperature around it, it emphases the results shown in the summer and fall data. If the temperatures are consistent in the winter, it would appear that the outside influences of eddies and reflectance are minimal. If this is true, that would mean that the air temperature above the roof is influenced by the roof itself during the warmer months. While the results do not show a benefit of one roof type over another during the winter months, it appears that roof type does have an effect in contributing to the Urban Heat Island during the warmer months.

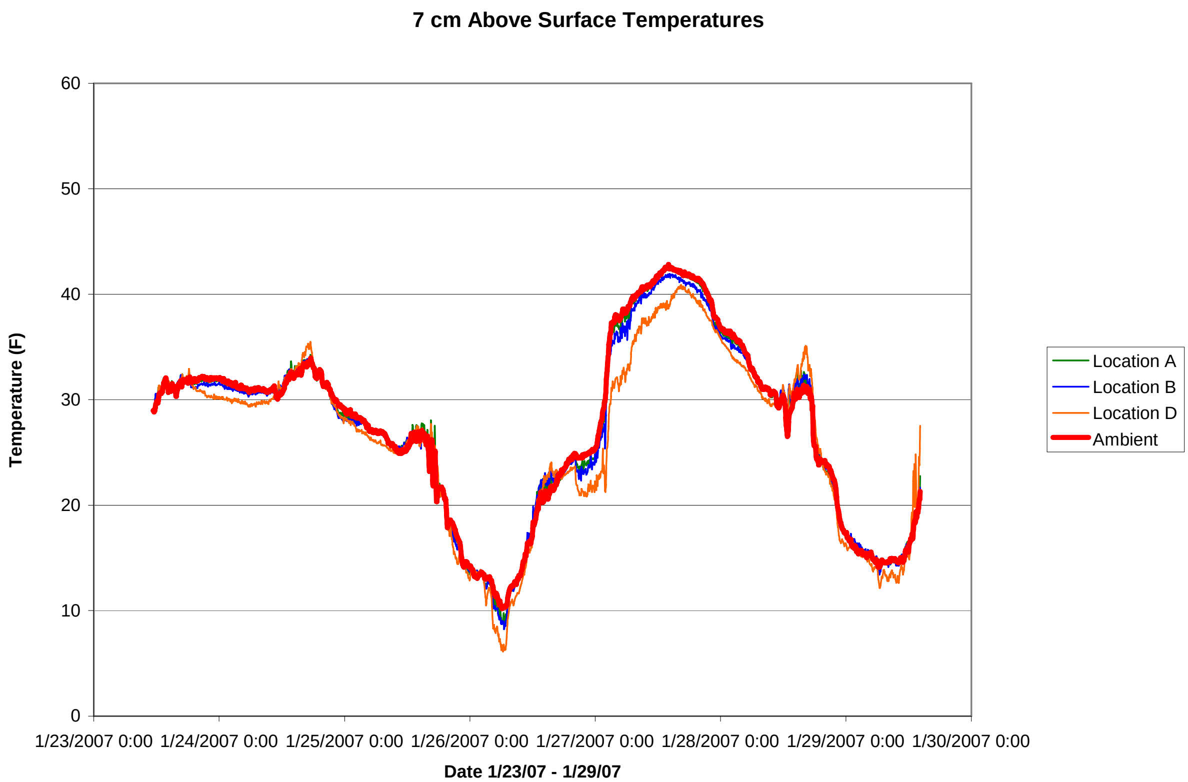

Figure 44. 7cm Above Surface Temperatures for 01/23/07 – 01/29/07

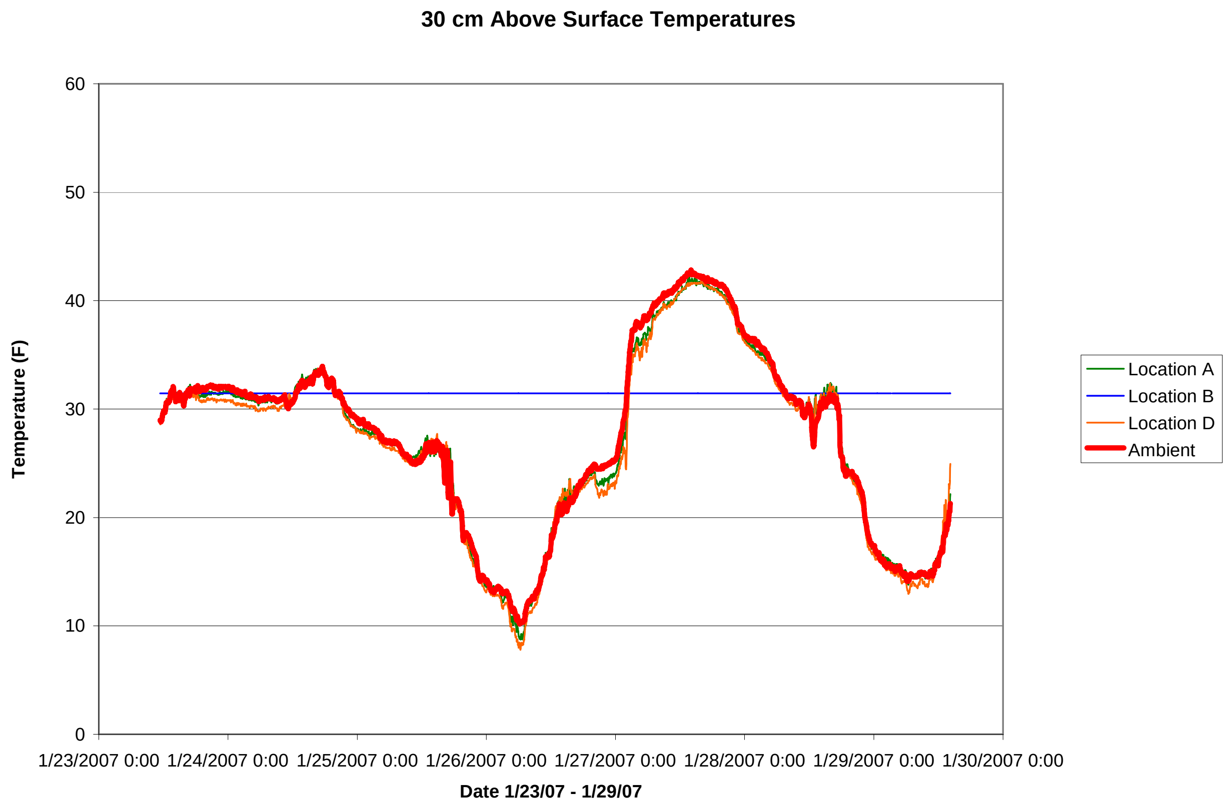

Figure 45. 30cm Above Surface Temperatures for 01/23/07 – 01/29/07

5.1.3 Thermal Camera Images

To confirm the surface temperature results of the thermocouples during the summer, a FLIR® Thermal Imaging Camera was used to take pictures of the roof on two separate occasions. The thermal camera was borrowed from the U.S. Office of Surface Mining, a local agency that uses the camera to investigate the effect of mine fires on ground temperatures. The camera was used to determine if the green roof surface really was significantly cooler than the control roof surface during the summer. The camera was used twice; once the morning of September 1st around 8:45AM and once the afternoon of September 8th around 2:00PM. Use of the camera was beneficial in that the camera takes a thermal picture of an entire area, while the thermocouples only supply the temperature at a single point.

Each thermal image must be examined closely. A function of the camera is that the range of temperatures defined in the scale adjusts to the temperatures seen by the lens automatically. This means that a green color might mean 70°F for one image, but means 85°F for another. When examining an image it is always important to confirm the color with the key shown on the right hand side. In the center of each picture, there is two white brackets that outline a rectangle. Each image displays the average temperature of the area enclosed by the rectangle in the upper right hand corner.

To demonstrate the capability of the thermal camera, the first image is actually a picture taken of the buildings surrounding the Giant Eagle site. In the image trees, houses, and a parking garage can clearly be seen "thermally" with the camera The small peak above the parking garage on the left side is actually the Cathedral of Learning on the University of Pittsburgh campus, over one mile away from the grocery store. The thermal camera is a great tool to use to check the temperature of a wide area of space.

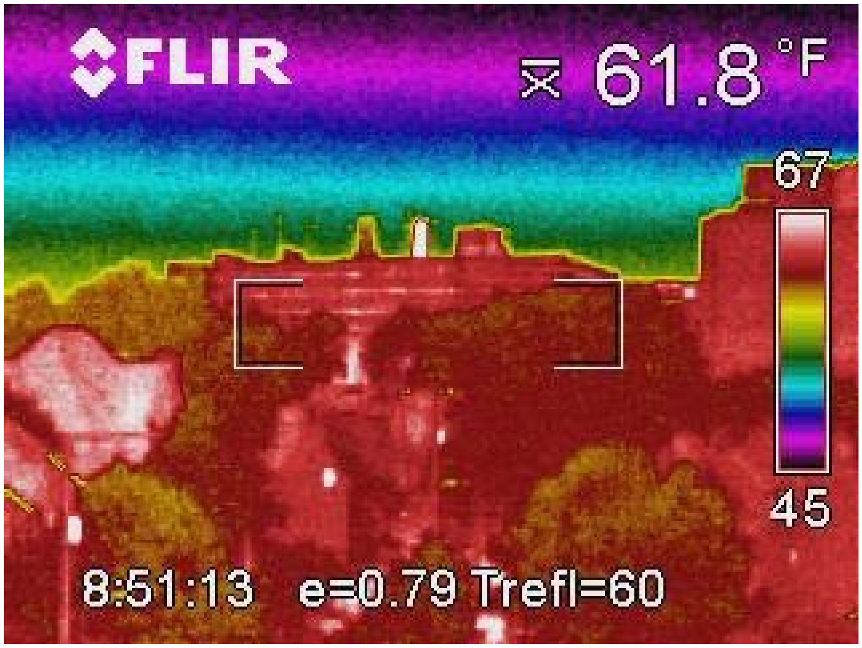

Figure 46. Thermal Image of Surroundings near the Giant Eagle Site

Selecting the proper area to image is important. Temperature can vary greatly throughout an area on a roof due to moisture, shading, or proximity to mechanical or HVAC equipment. In the case of the Shadyside Giant Eagle two major factors that affected the thermal image was water collecting on the control roof and vegetation size on the green roof. The following images were taken in locations that reduced these factors. Areas furthest from the roof drains and corners of the sky lights were the driest and thus warmest areas on the control roof. On the other hand, vegetation cover seemed to affect roof surface temperature on the green roof. Larger and well spread vegetation is cooler on the camera, while areas where the vegetation did not grow are warmer. While pockets of temperature change seem drastic in the camera images, it is important to examine the color coded scale on each picture. When the range of temperature the camera sees is small, like on the green roof, the midpoint colors of yellow and green represent temperatures of 80°F. Meanwhile, when the range of temperature is large, like on the control roof, yellow and green colors identify areas where temperature is 90°F. The thermal images present substantial amounts of information with a single picture, and every point on that picture should be examined.

Figure 47 shows a thermal image of the control roof the morning of September 1st, 2006. This morning was very cool, it was cloudy and the roof and surrounding air did not have a chance to warm from the sun. The image ranges in temperature from 52°F, shown in dark purple, to 70°F, shown in white. The gravel ballast can be seen in the image, each stone seems to vary in temperature. The skylights can also be seen in the upper left corner. The average temperature in the center of the image is 61.8°F. The ambient temperature that morning was about 60°F as well.

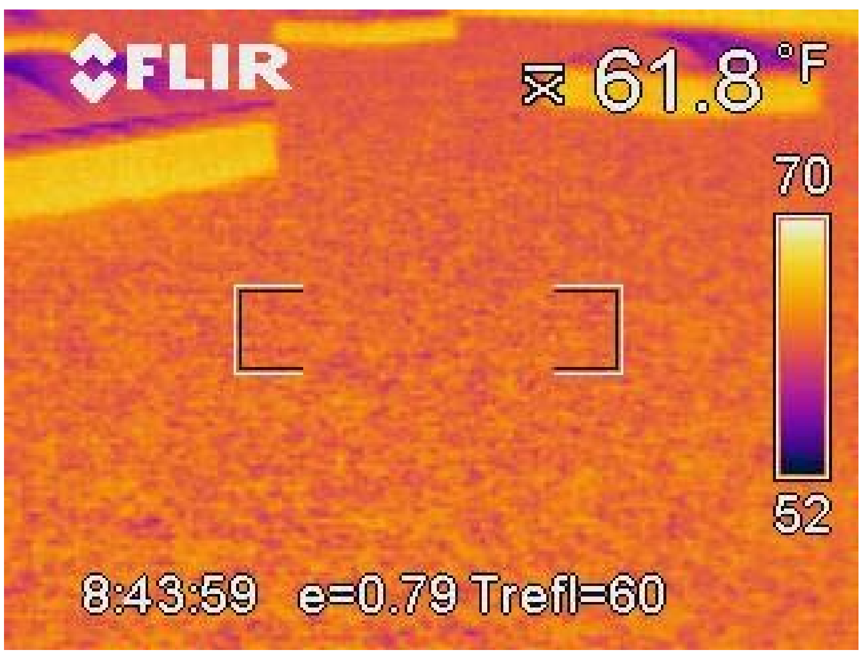

Figure 47. Thermal Image of the Control Roof September 1st, 2006

Figure 48 shows a thermal image on the green roof the same morning. Note that the color key has changed slightly; 56°F is now defined by the dark purple color, 73°F defined by white. The soil surface appears more constant in temperature, averaging 62.2°F. The yellow-orange streaks on the roof on the bottom half of the image are the irrigation hoses that were installed on the green roof. It is not possible to distinguish the vegetation from the soil in this image. The plants and soil have cooled uniformly. The difference in temperature between the green roof and control is negligible. Both surfaces are very close to the ambient air temperature. The thermal camera images show that on a cool morning, the surface of both roof types match the ambient air temperature.

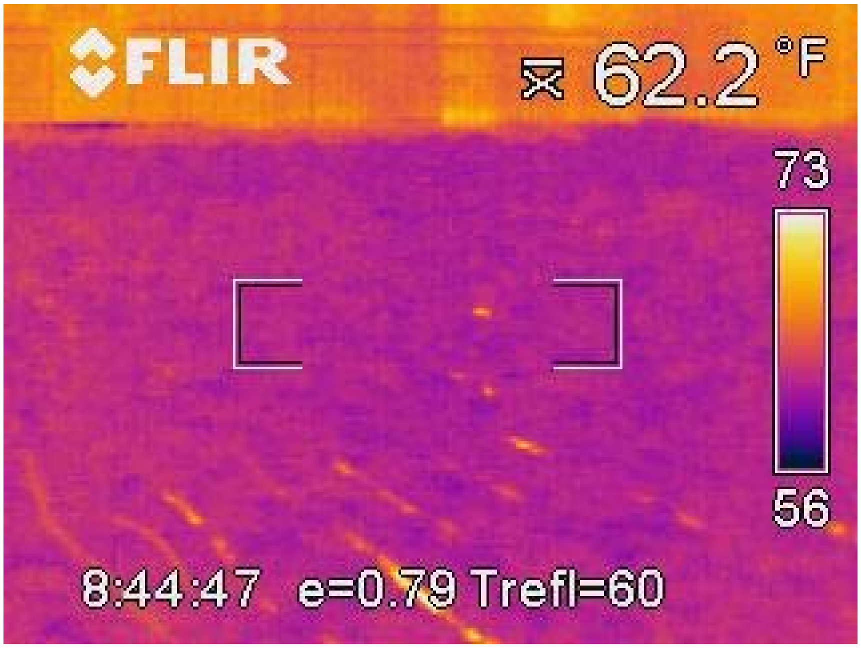

Figure 48. Thermal Image of the Green Roof September 1st, 2006

The following images were taken on the afternoon of September 8th, 2006. On this day, the ambient temperature was about 77°F. The control roof images show how exposure to solar radiation and increasing air temperatures affect the roof surface. Figure 49 shows the control roof, the Location C monitoring station can be seen in the center of the image. Note the color scale ranges from 68°F defined by purple, to 112°F defined by white. The gravel ballast on the roof appears in the warmer colors of the temperature scale. The average temperature of the center rectangle is 98.7°F. That is 20° warmer than the ambient air temperature. The screens on the skylights are the coolest objects in the image, while the roof and building materials in the image are the warmest objects. Figure 50 is another image of the control roof surface. Again, the average temperature at the center of the image is 102°F, significantly warmer than the ambient temperature. There were spots were the gravel ballast was retaining water from a previous precipitation event. In Figure 50, the dry gravel can be distinguished from the wet gravel by color. The dry gravel appears in shades of red and yellow (about 100°F in temperature), while the wet gravel appears in shades of green and yellow (about 90°F in temperature).

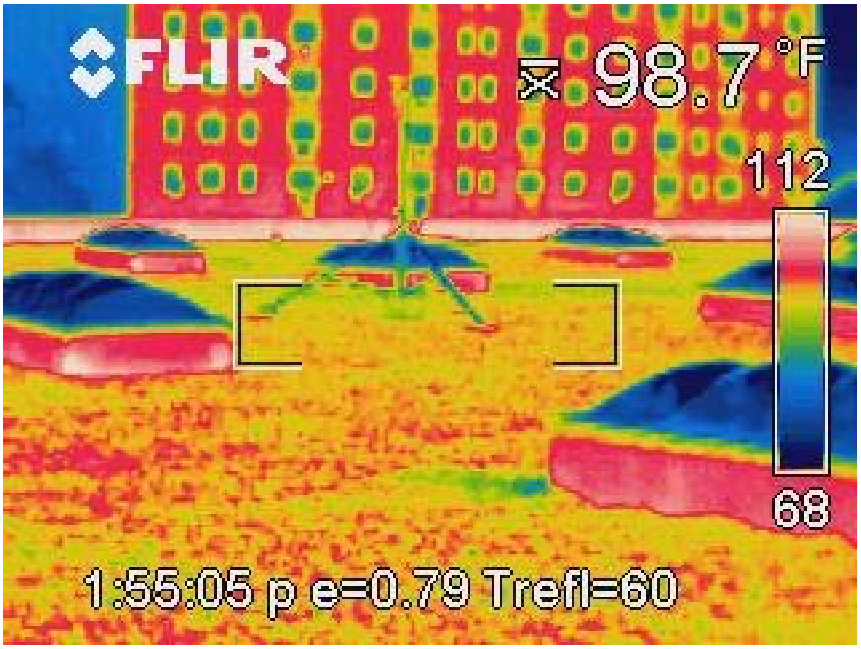

Figure 49. Thermal Image of the Control Roof September 8th, 2006

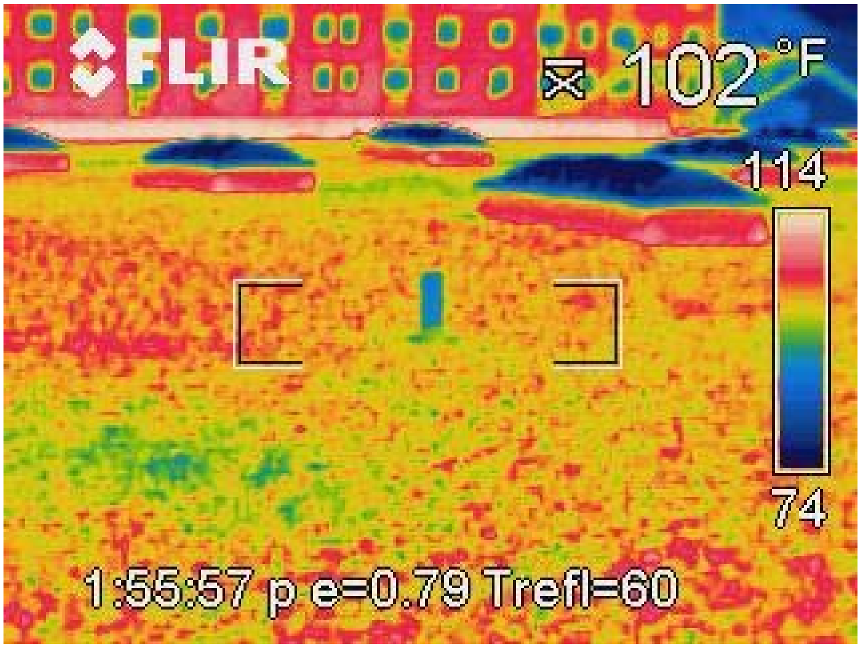

Figure 50. Thermal Image of the Control Roof September 8th, 2006

Figures 51 and 52 show images of the green roof surface. Note that the color key on these images differs greatly from the color key on the control roof images. The dark purple colors defines a temperature of 70-71°F and white defines a temperature of 88-89°F. The average temperature of the center rectangle of Figure 51 is 77.3°F. The average temperature for Figure 52 is 74.9°F. For both images, the average surface temperature reading is close to the ambient air temperature. The green roof is actually a few degrees cooler on the surface. It is also possible to distinguish the vegetation from the soil on these images of the green roof. The soil can be seen in green and yellow, while the sedums appear in blue. The vegetation is cooler in temperature than the soil substrate. The red streak in both images is the irrigation system, the water and equipment is warmer than the roof surface.

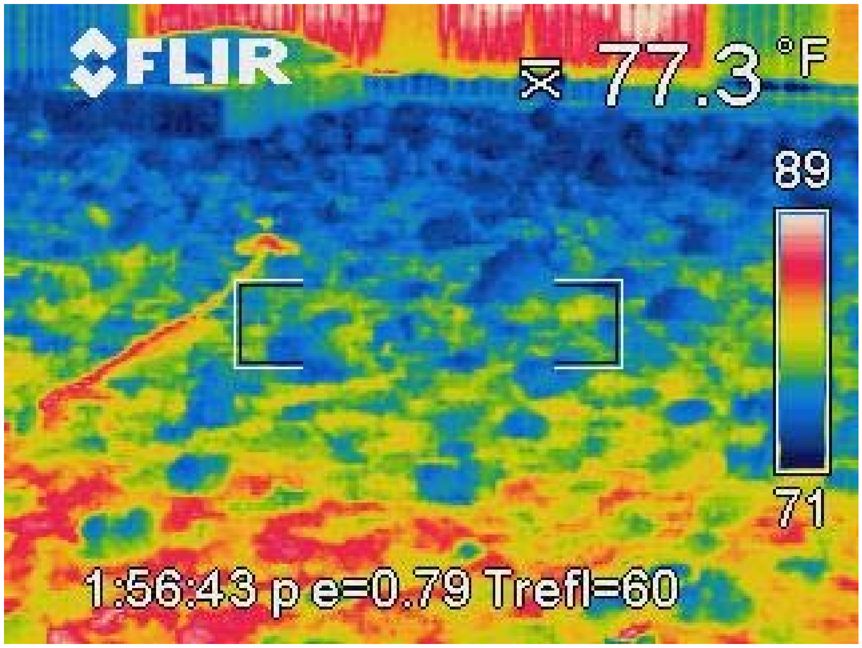

Figure 51. Thermal Image of the Green Roof September 8th, 2006

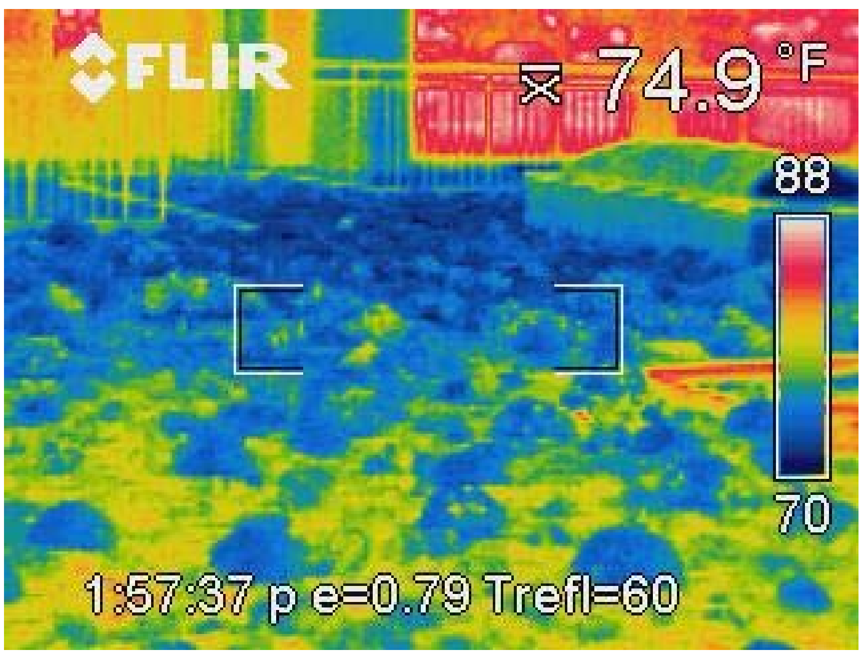

Figure 52. Thermal Image of the Green Roof September 8th, 2006

The temperature monitoring data corresponding to these dates was lost when the system crashed. So the findings of these images cannot be compared to the thermocouple data. Still, the images do provide significant information about the performance of the green roof compared to that of the control roof. The images show that in the evening, the roof surfaces cool evenly and that the next morning, every surface starts at approximately the same temperature. As the day progresses and the roof surfaces are exposed to sunlight, solar radiation, and warmer air, the difference in roof type can readily be seen. While the green roof surface matches the ambient temperature, the control roof surface becomes very hot. The vegetation on the green roof remains cool, while the gravel ballast on the control roof increases in temperature. The thermal images show how the temperature of the roof surfaces change with the climate throughout the day. The thermal images show that the green roof moderates its temperature in the summer heat while the control roof gains temperature in the summer heat. The thermal images help to show that green roofs do reduce the impact of the built environment on the Urban Heat Island.

5.2 SOLAR RADIATION DATA

This section describes the net solar radiation data collected at the Giant Eagle Site. Net radiometers were placed at monitoring locations A and C. The net radiometer output is the algebraic sum of the incoming short wave solar radiation and reflective long wave radiation. When the data is positive, the incoming radiation exceeds the outgoing radiation. When the data is negative, the outgoing radiation exceeds the incoming radiation. Net radiation describes the amount of solar energy the roof material is exposed to day and night. During the day, building materials absorb solar radiation and store the energy. At night, the energy is released back into the atmosphere. The purpose of the net radiometers is to capture the amount of energy that passes in and out of the roof microclimate. This data will be used to determine the efficiency of the green roof vegetation to use this energy, versus the control roof's ability to store and release the energy.

First, the net radiometer data will be discussed. The net radiation from a summer, fall, and winter data set is discussed. The change in seasons is important when discussing the effect of incoming solar radiation on objects on the earth's surface. For the northern half of the world, seasons change with the solstices and equinoxes. Spring begins with the vernal, or spring, equinox, that falls on March 20th or 21st. The equinox is when day and night are of equal length. The length of daytime increases until June 21st or 22nd, the summer solstice and the longest day of the year. This begins the summer season. From this point, daytime decreases until the fall equinox, when day and night are equal again, and the start of the fall season. This occurs on September 22nd or 23rd. Finally, the days continue to grow shorter during the fall until the winter solstice, the shortest day of the year, and the beginning of winter. This occurs on December 21st or 22nd. (NASA, 2007) Generally, January, February, and March make up the winter season; April, May, and June the spring; July, August, and September the summer; and October, November, and December the fall. Figure 53 shows the data from the summer data set, Figure 54 the fall data set, and Figure 55 the winter data set. In each figure the y-axis remains constant, from -200 W*m^{-2} to 1000 W*m^{-2}. This is to easily compare the amount of net radiation gained in each season. The net radiometer data over the green roof is shown in light blue, the net radiometer data over the control roof is black.

Examining the summer data, the net radiation peaks above 600 W*m^{-2} each day. This means the incoming radiation exceeds the reflected radiation on the roof by that amount. Note that the green roof radiometer peaks slightly above the control roof radiometer. This means the green roof surface is absorbing more and reflecting less energy than the control roof. In the evening, the net radiation at both locations drops below zero. Here, the reflective radiation exceeds the incoming radiation. Note that in the evening, the control roof radiation drops slightly below the green roof radiation. This means that the control roof is releasing more radiation into the atmosphere than the green roof. The green roof benefits from three factors that affect its ability to absorb and use energy; its higher thermal mass, the use of solar energy for photosynthesis by the vegetation, and the use of solar energy to evaporate water trapped in the substrate. These factors allow the green roof to absorb more energy, reflect less energy, and release less energy at night. Meanwhile, the control roof has a significantly lower mass and darker color. During the day the control roof surface absorbs some energy, which makes the membrane material very hot, but also reflects more energy than the green roof. Then at night, the heat that the control roof has collected during the day is released. This cools the roof membrane, but releases additional energy into the microclimate around the building. The difference is minimal, but enough to be measured. The difference between the two roofs is around 1-5 $W*m^{-2}$. The summer data does suggest that the control roof does mildly contribute to the Urban Heat Island Effect by reflecting more energy during the day and releasing more energy in the evening.

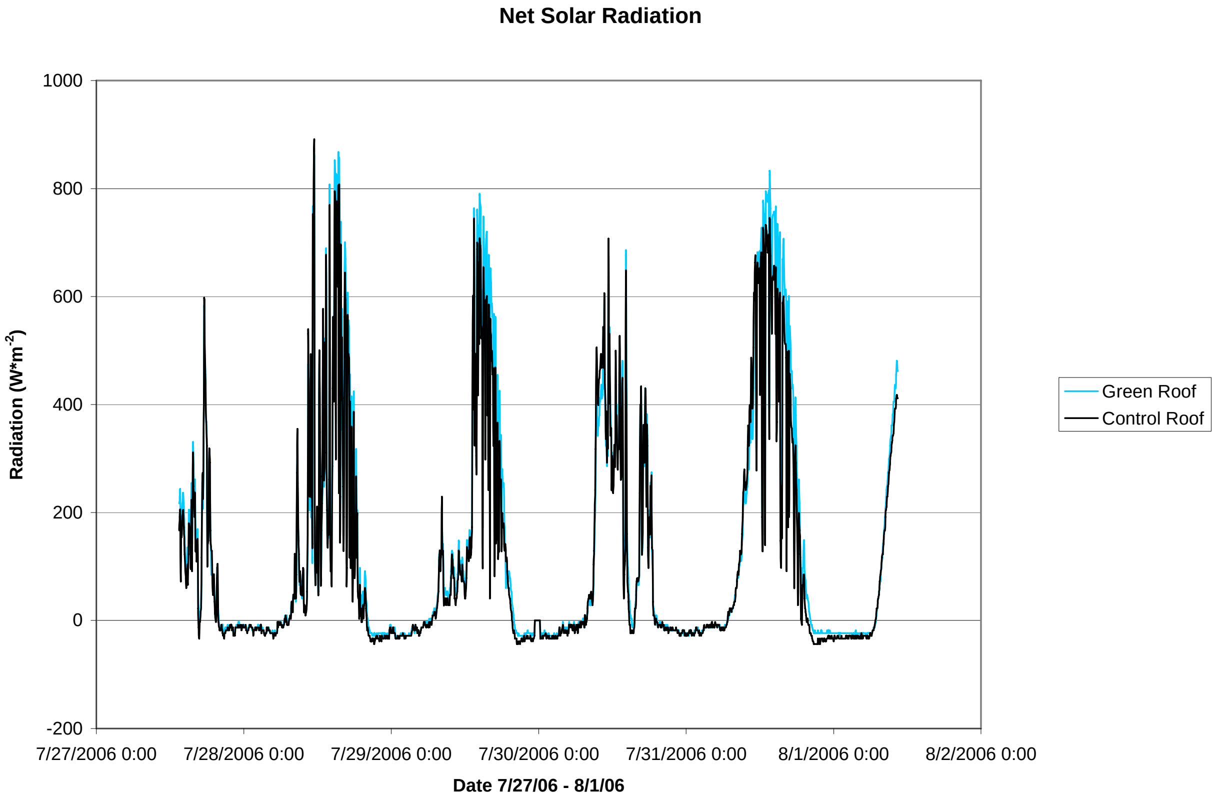

Figure 53. Summer Net Radiometer Data for 7/27/06 – 8/1/06

Figure 54 contains the fall data information. Examining the fall data, the net radiation only peaks above 200-400 W*m^{-2} each day. This means the incoming radiation exceeds the reflected radiation on the roof by that amount. On the first day with the largest gain in solar radiation, the green roof continues to exceed the control roof. However, on the remaining days when the net radiation was not a much as before, the control roof equals or exceeds the green roof net radiation. The difference between the green and control roof data is only 1-2 Wm^{-2} at most. In the evening, the net radiation at both locations drops below zero. The evening control roof radiation is roughly equal to the evening green roof radiation. This means both roof surfaces are releasing the same amount of energy. The fall data suggests that any reduction in the UHI effect green roofs have during the summer is quickly lost when the incoming solar radiation is reduced. In terms of the Urban Heat Island, both roofs perform equally in autumn.

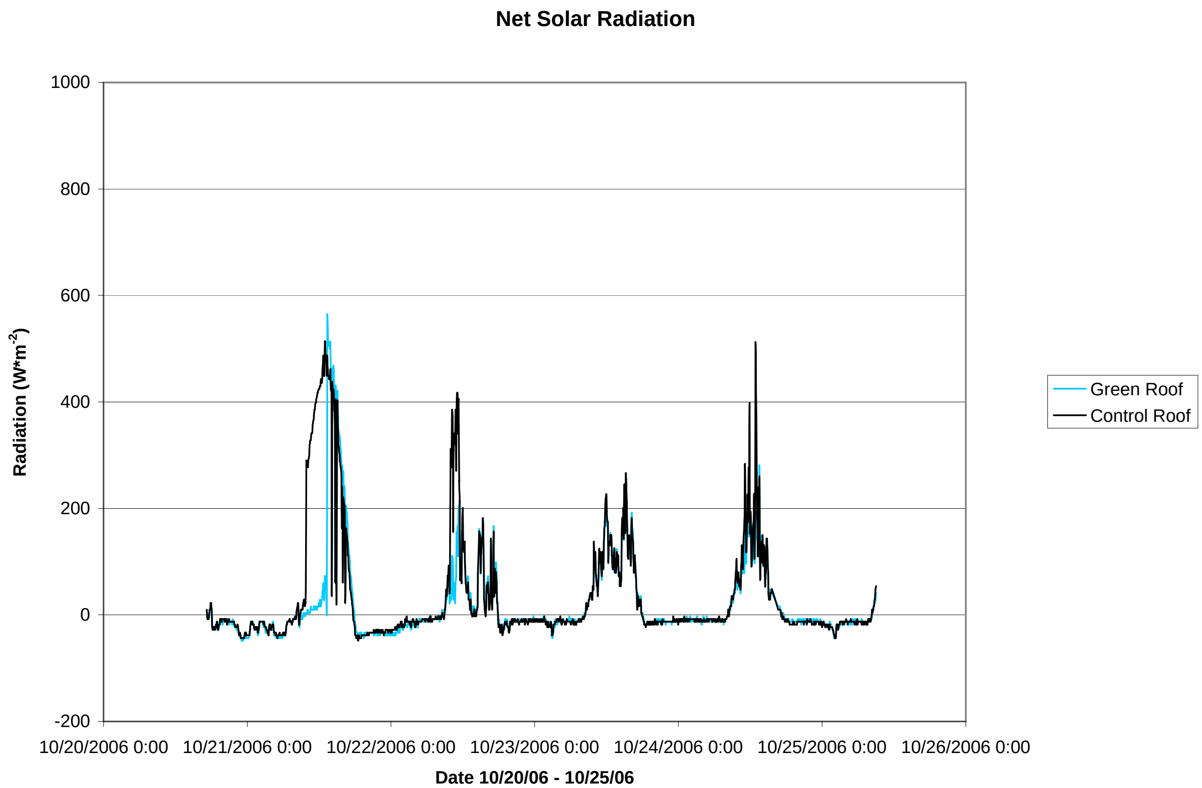

Figure 54. Fall Net Radiometer Data for 10/20/06 – 10/25/06

Figure 55 contains the winter data information. Examining the winter data, the net radiation struggles to reach 200 W*m^{-2} each day. The short daylight hours and the angle of the northern hemisphere from the sun greatly reduces the incoming solar radiation. The apartment building also casts a shadow over the roof though parts of the day, also reducing the net radiation. Like the fall data set, the winter data shows that the net radiation over both roof surfaces is roughly equal. Both the day and evening radiation totals are equivalent for both roof types. It is interesting to note that when the net radiation gain is minimal during the day, the same amount of radiation is released at night for both roof types in all three seasons. This implies that both roof types transfer energy from the interior of the store into the atmosphere. However, it is possible that the green roof could release slightly more energy than the control membrane during the winter because it has a higher thermal mass. The data collected at the Giant Eagle site suggests that different thermal behavior between the green and control roof are negligible in terms of affect on the Urban Heat Island. The winter data suggests that any benefit green roofs pose towards the Urban Heat Island during the summer is quickly lost when the incoming solar radiation is reduced. As with the fall data, the winter net radiation data shows that both the control roof and the green roof perform similarly in cold weather.

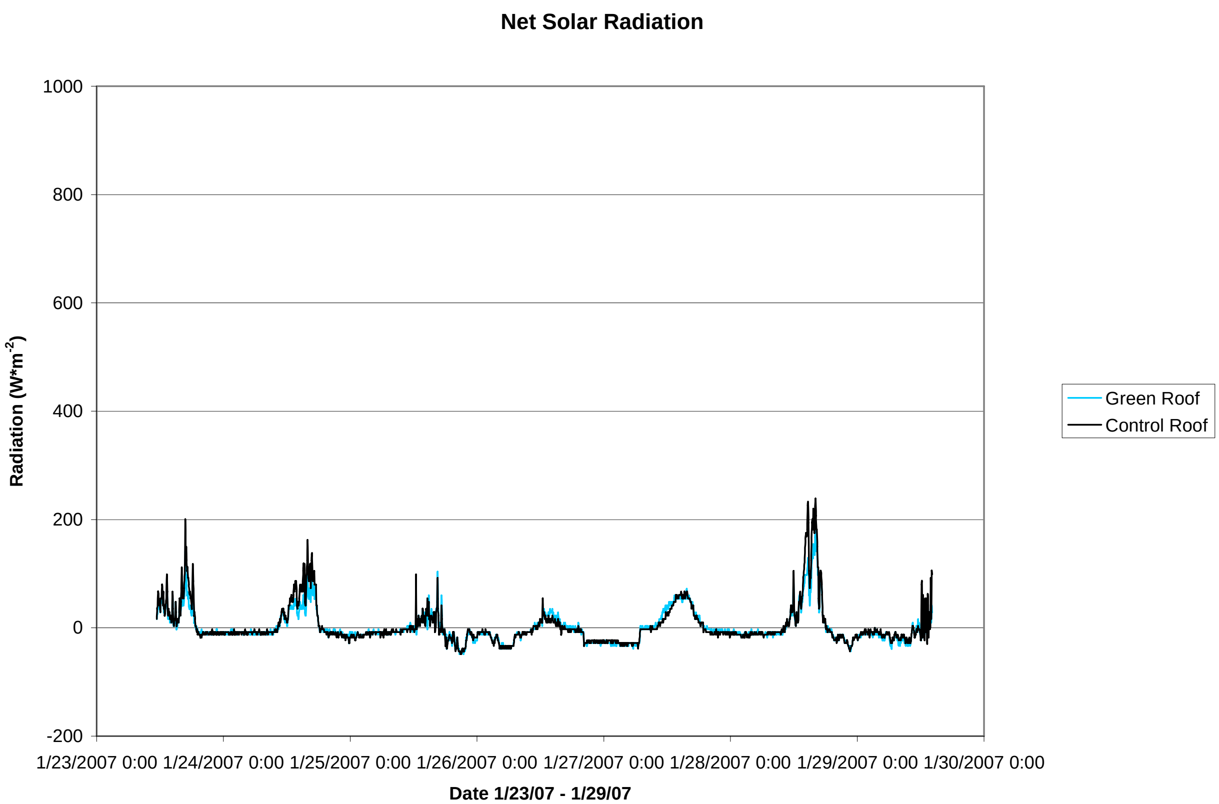

Figure 55. Winter Net Radiometer Data for 1/23/07 – 1/29/07

Next, the net radiometer data will be compared to the ambient and roof membrane temperature data. The same summer, fall, and winter data sets will be utilized. Each figure has a primary and secondary y-axis. The primary y-axis is the temperature axis, the roof membrane temperature and ambient air temperature uses this axis. The secondary y-axis is the net radiation axis; the net radiation is plotted against this axis. This allows for the solar radiation data to be compared to the temperature data easily. Note that the scales of each axis are not constant figure to figure.

In Figures 56, 57, and 58 it is easily seen that as incoming solar radiation increases, so does the temperature of the ambient air and of the roof membrane. In each scenario, the net radiation drops much faster than the temperature of the air or roof membrane. The control roof membrane points react faster than the green roof membrane points to increases in net radiation. The control roof points also warm more than the corresponding green roof point as net radiation increases. The following figures demonstrate the correlation between incoming solar radiation and roof and climate temperature.

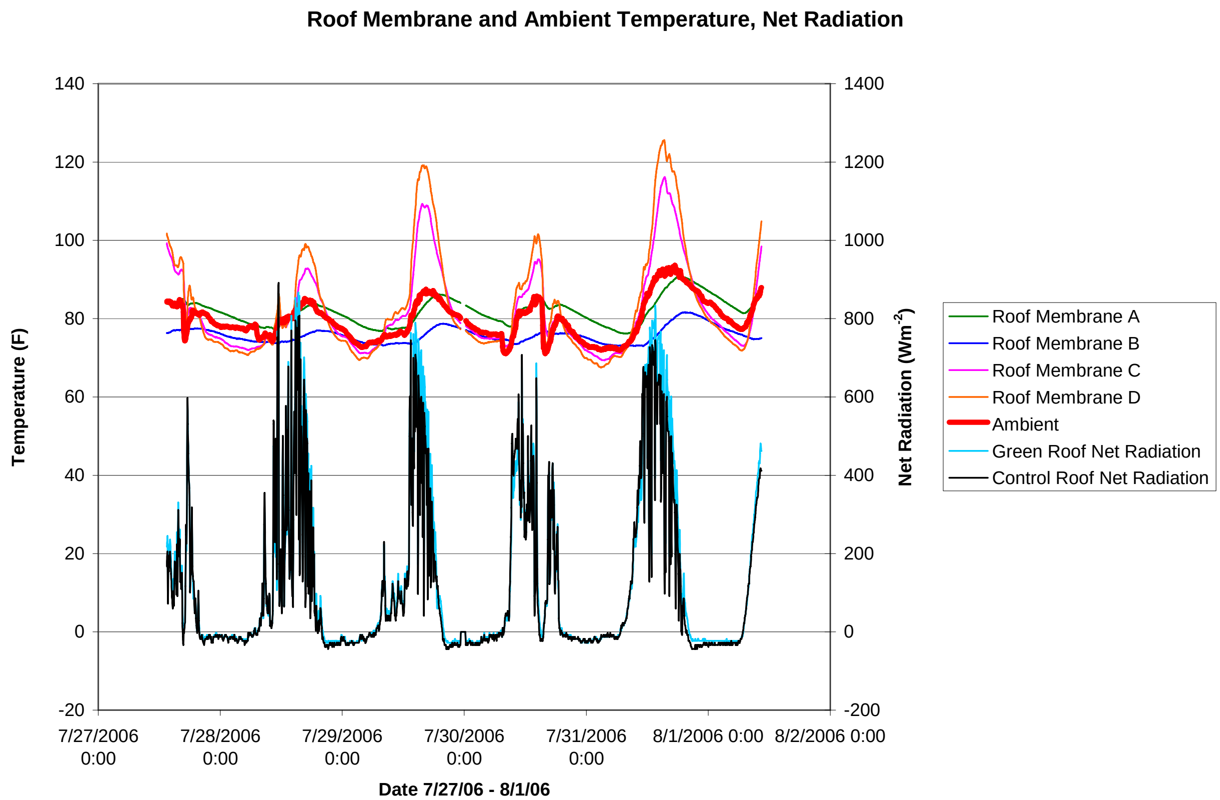

Figure 56. Summer Comparison Data for 7/27/06 – 8/1/06

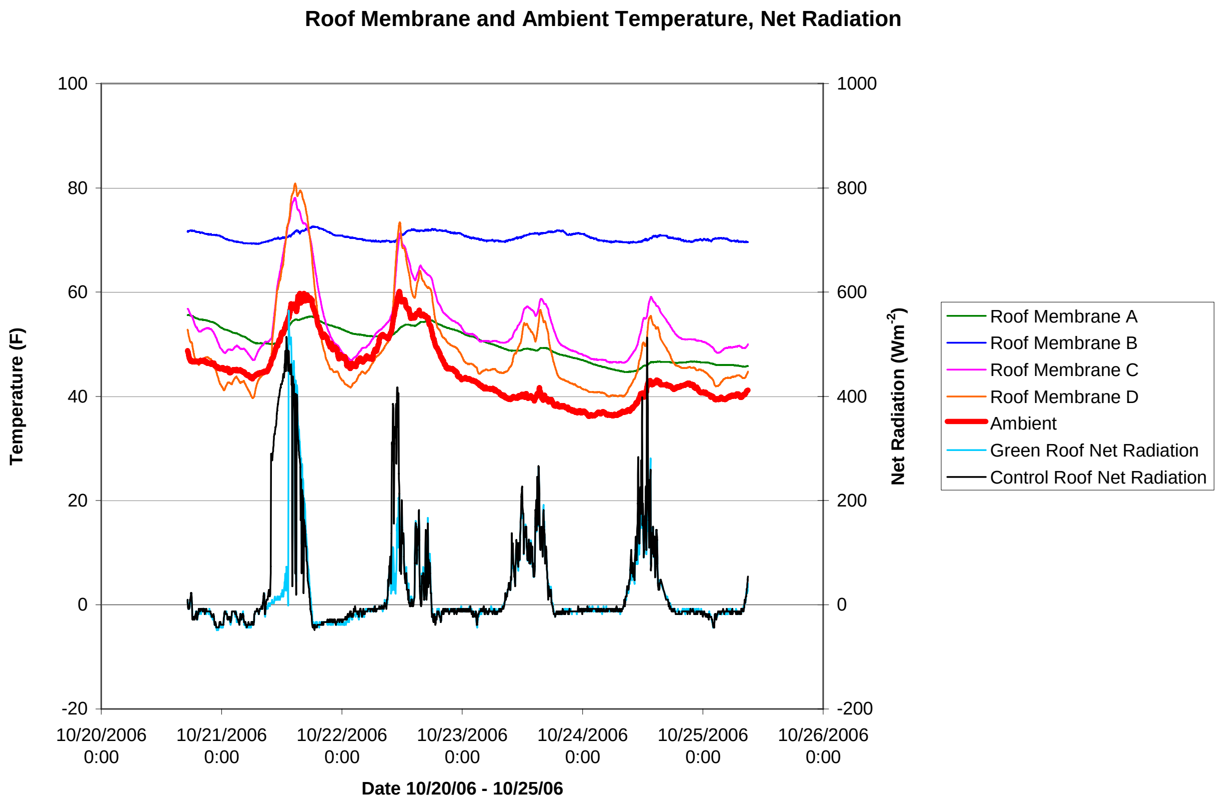

Figure 57. Fall Comparison Data for 10/20/06 – 10/25/06

Roof Membrane and Ambient Temperature, Net Radiation

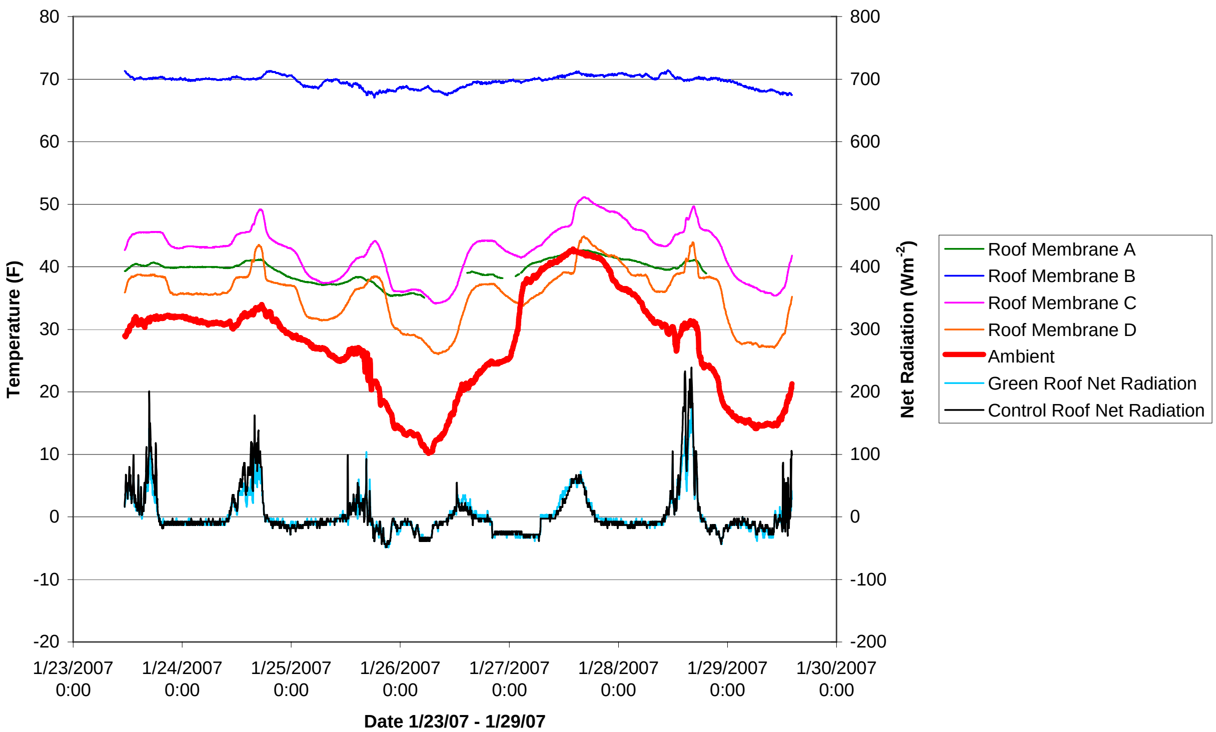

Figure 58. Winter Comparison Data for 1/23/07 – 1/29/07

5.3 WEATHER DATA

The Giant Eagle site was also equipped to monitor the relative humidity and wind speed and direction. These factors contribute to the performance of the vegetation of the green roof. Humidity affects the plants' ability to transpire. When the local air is significantly humid, it makes it harder for the plants biologic function to release water into the atmosphere. Lower levels of humidity encourage the evapotranspiration process. Wind speed has a similar effect on plant function. Moving air encourages evapotranspiration while still air hinders the process.

(Del Barrio,1998) While the biologic process of the roof vegetation will not be analyzed as part of this thesis, the relative humidity and wind speed has been included for the typical summer, fall and winter season.

5.3.1 Relative Humidity

Relative humidity is defined as “a ratio, expressed in percent, of the amount of atmospheric moisture present relative to the amount that would be present if the air were saturated. Since the latter amount is dependent on temperature, relative humidity is a function of both moisture content and temperature. Relative humidity is derived from the associated temperature and dew point for the indicated hour.” (Weather, 2007) The temperature at which air is 100% saturated, given the amount of water vapor, is commonly referred to as the dew point. The amount of moisture the air can hold is dependent on temperature. The volume of 1 kg of air increases with temperature, thus warmer air can store more moisture. Assuming dew point stays constant for a given period of time, as the air temperatures rises throughout the day, the relative humidity decreases. In the following graphs it can easily be seen how relative humidity changes in relation to temperature.

The RH sensor produces voltages that are easily converted to temperature and percent. Here, the relative humidity during the summer, fall, and winter sample periods are compared to ambient temperature. Since the ambient temperature is needed for the instrument to calculate the relative humidity, each instrument measures both. Figures 59, 60, and 61 show the relative humidity results for a summer, fall and winter time period. The left y-axis shows the relative humidity in percent and the right y-axis shows the ambient temperature in degrees Fahrenheit. The graphs show how relative humidity changes with ambient temperature, increasing as temperature decreases and decreasing as temperature increases. Sudden changes in relative humidity, like the events on July 30th in Figure 59 and January 25th in Figure 61 could signal a precipitation event. There was a significant thunderstorm on July 30th and a snow storm on January 25th. Relative humidity varies greatly throughout the course of a day.

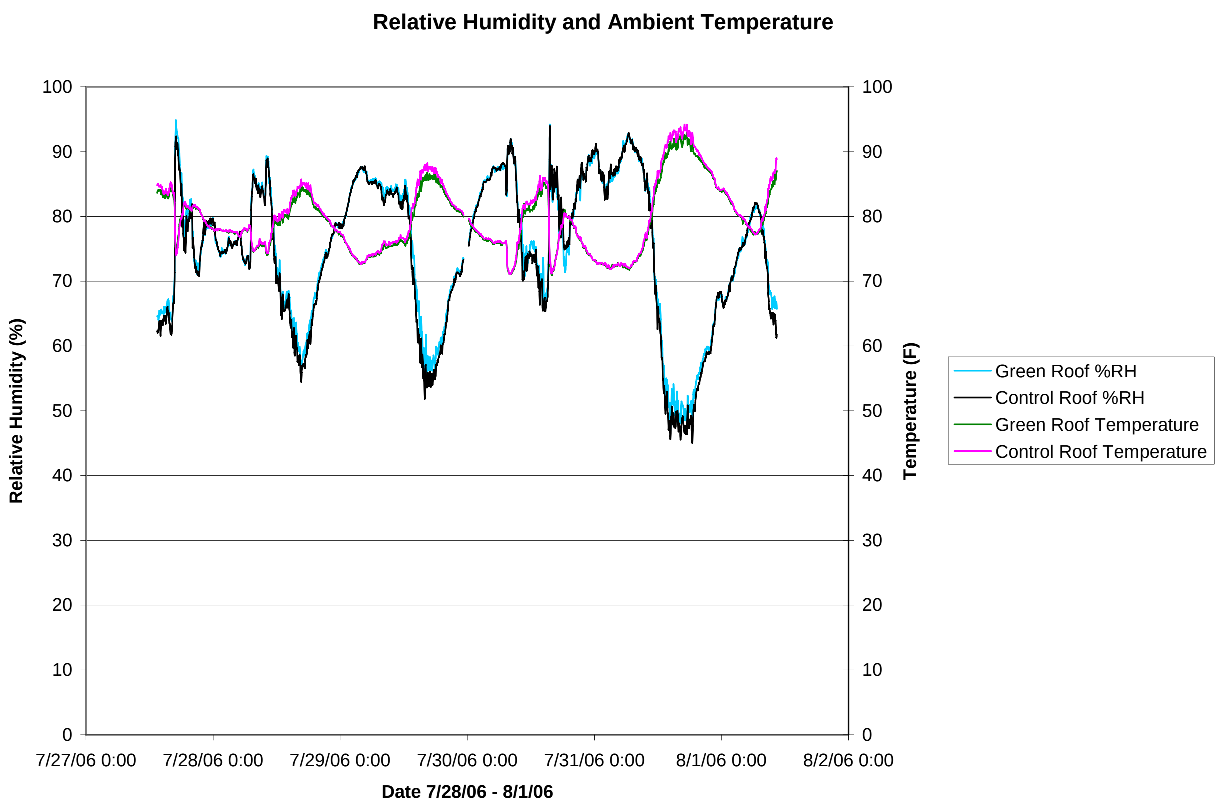

Figure 59. Relative Humidity and Ambient Temperature for 7/27/06 – 8/1/06

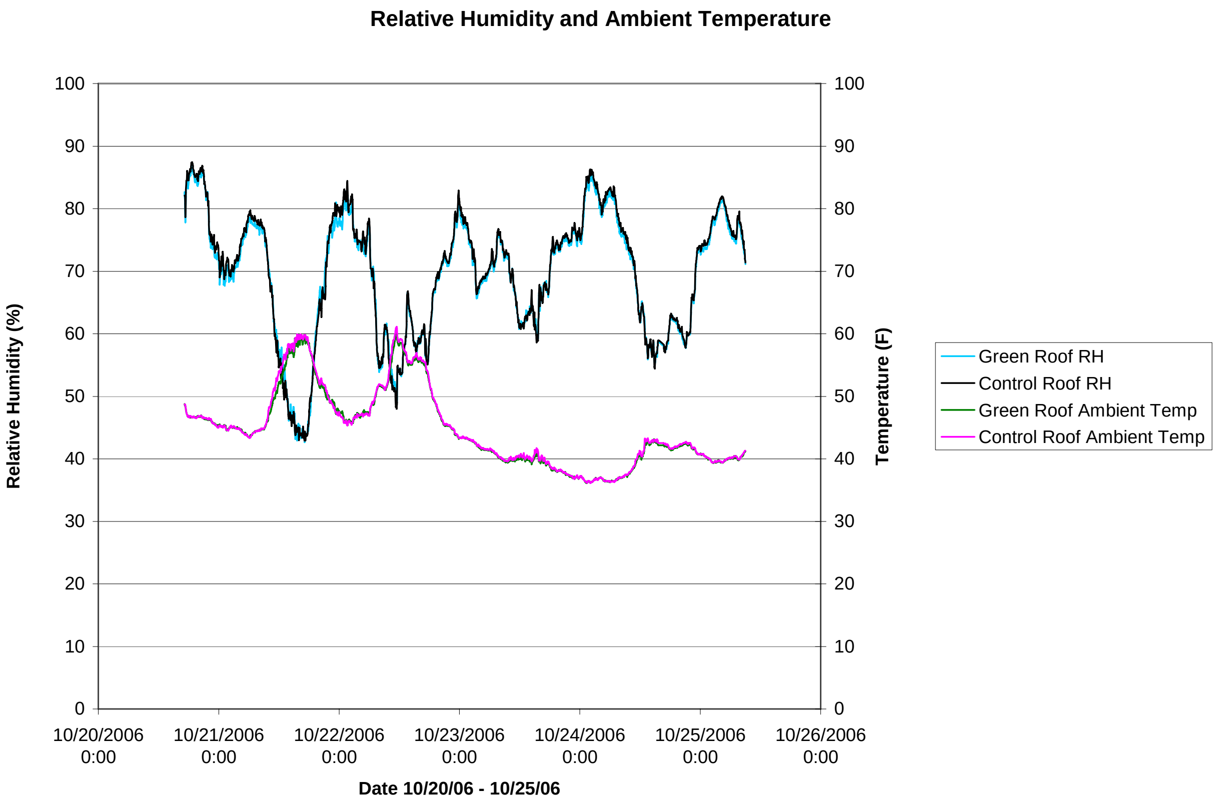

Figure 60. Relative Humidity and Ambient Temperature for 10/20/06 – 10/25/06

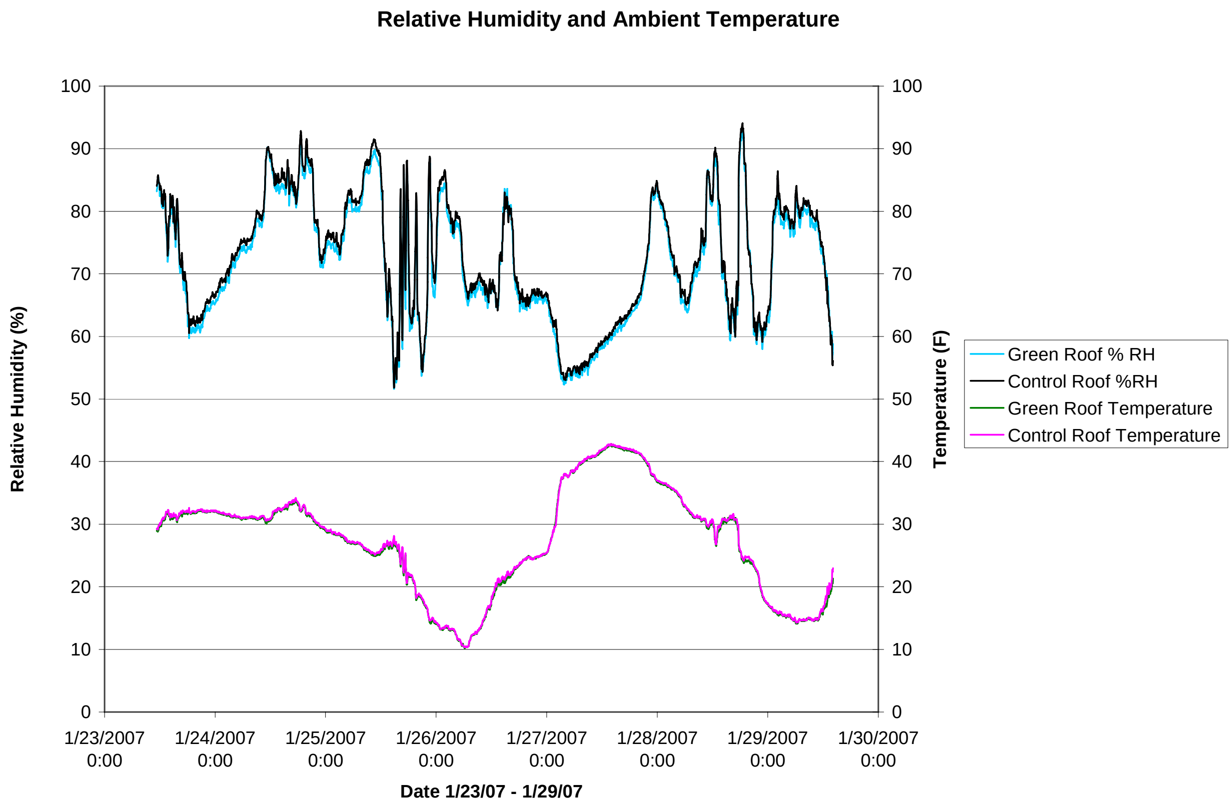

Figure 61. Relative Humidity and Ambient Temperature for 1/23/07 – 1/29/07

5.3.2 Wind Speed and Direction

A wind sentry set was used to monitor the wind conditions at the Giant Eagle site. The sentry set was placed at Location C on the control roof side of the building. The sentry set was placed here to minimize the influence of the surrounding buildings on the wind data collected. As air moves between and around buildings, it can increase in speed as eddys form. At Location C the sentry set is more than 100 feet away from the apartment complex, the closest building to that point. The summer data was collected every 5 minutes, while the fall and winter data was collected every 10 seconds. Due to the nature of wind data, the results were scattered. Unlike the temperature and solar radiation data, there was no building up during the day or decrease at night. The National Oceanic and Atmospheric Administration (NOAA) defines sustained wind speed as the 2 minute average of wind speed measurements taken every 5 seconds. (Weather, 2007) If the same method was used at the Giant Eagle site, a 5 day period would require roughly 86,400 measurement points, creating a file too large for the data logger to export. Instead, a measurement was taken every 10 seconds, in the fall and winter periods, every 5 minutes with the summer data. In order to normalize this data, a 20 minute average was taken and plotted against time for the summer data set, a 4 minute average for the fall and winter data sets. This method of averaging keeps the data points taken at the Giant Eagle site proportional to the process adhered to by NOAA. The average wind speed was typically around 15 mph and came from the west. Figures 62, 63, and 64 depict the wind speed data for the typical summer, fall, and winter week. In each case the average wind speed in miles per and hour is plotted against time. A linear trend line was added to better depict the average wind speed at the site. Figures 65, 66, and 67 depict the wind direction data for the corresponding weeks. Wind direction was averaged for each hour, similar to NOAA practice. (Weather, 2007) In this case the direction is measured in degrees, 0-360. Zero or 360 degrees is east, 90 degrees north, 180 degrees west, and 270 degrees south. Again the data is plotted against time.

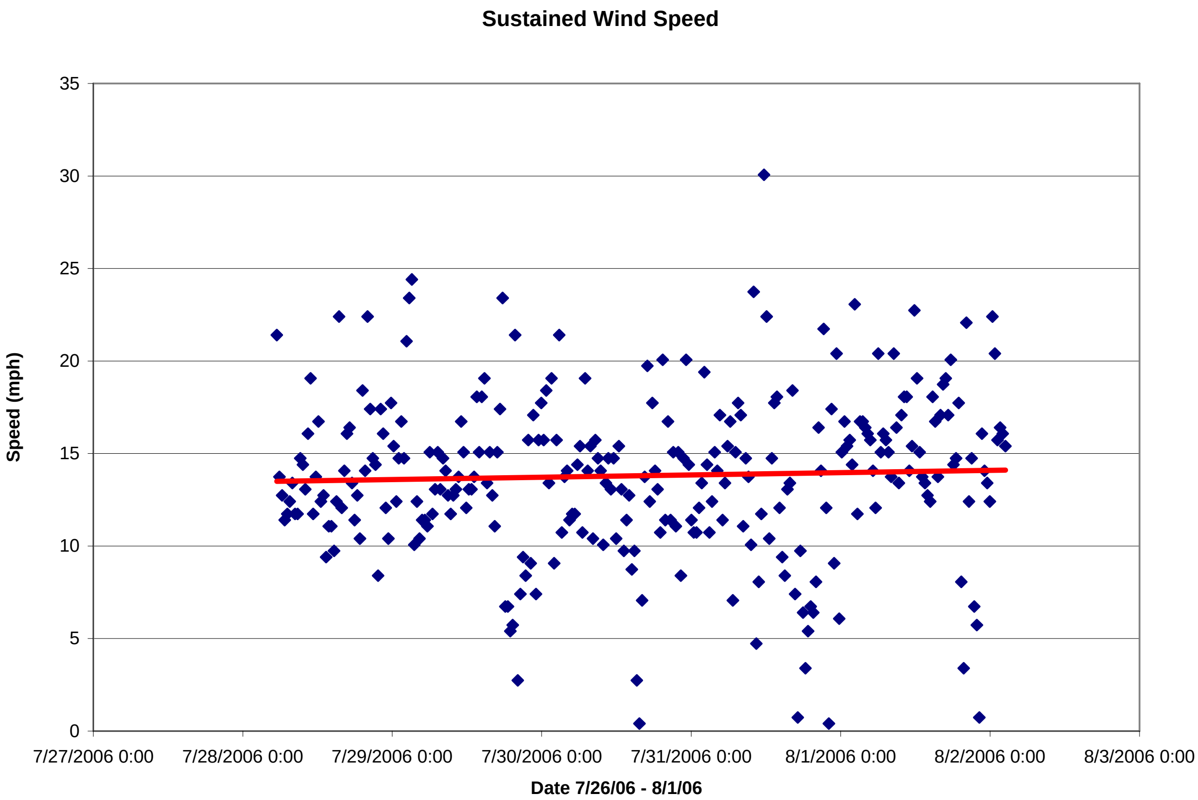

Figure 62. Average Wind Speed for 7/28/06 – 8/1/06

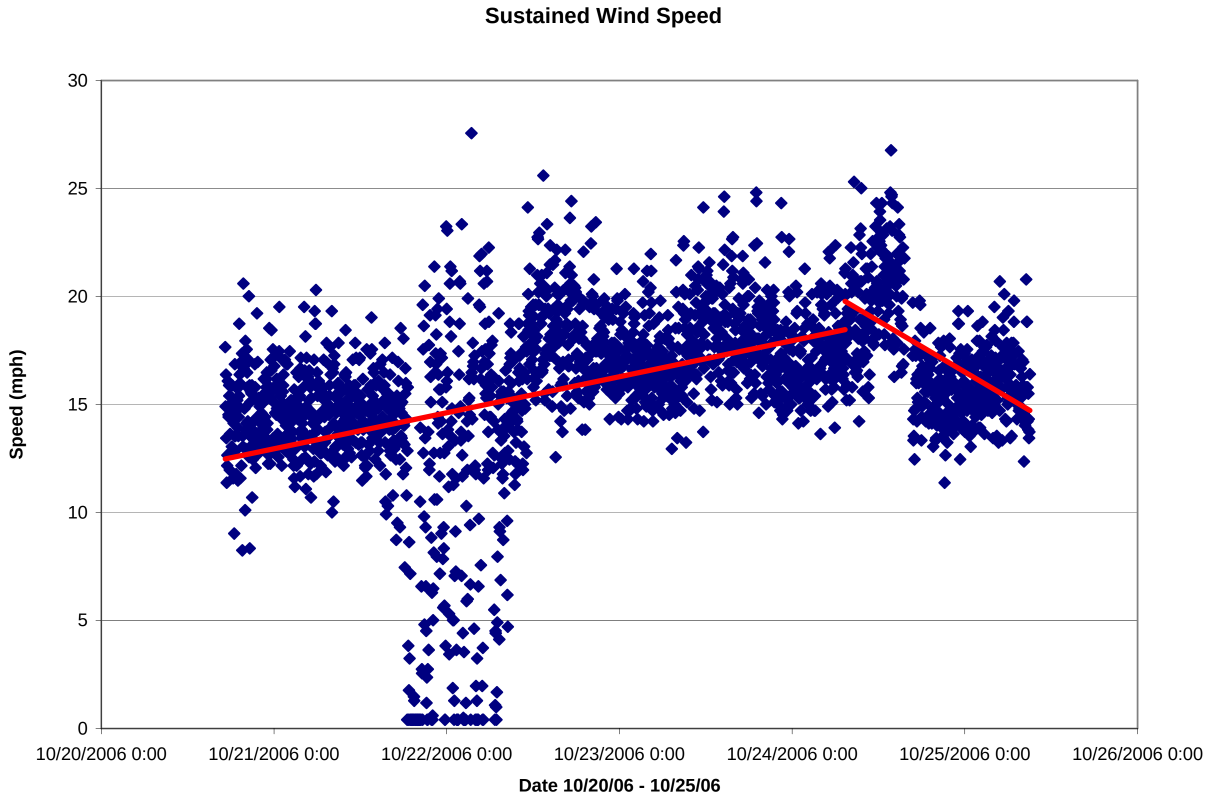

Figure 63. Average Wind Speed for 10/20/06 – 10/25/06

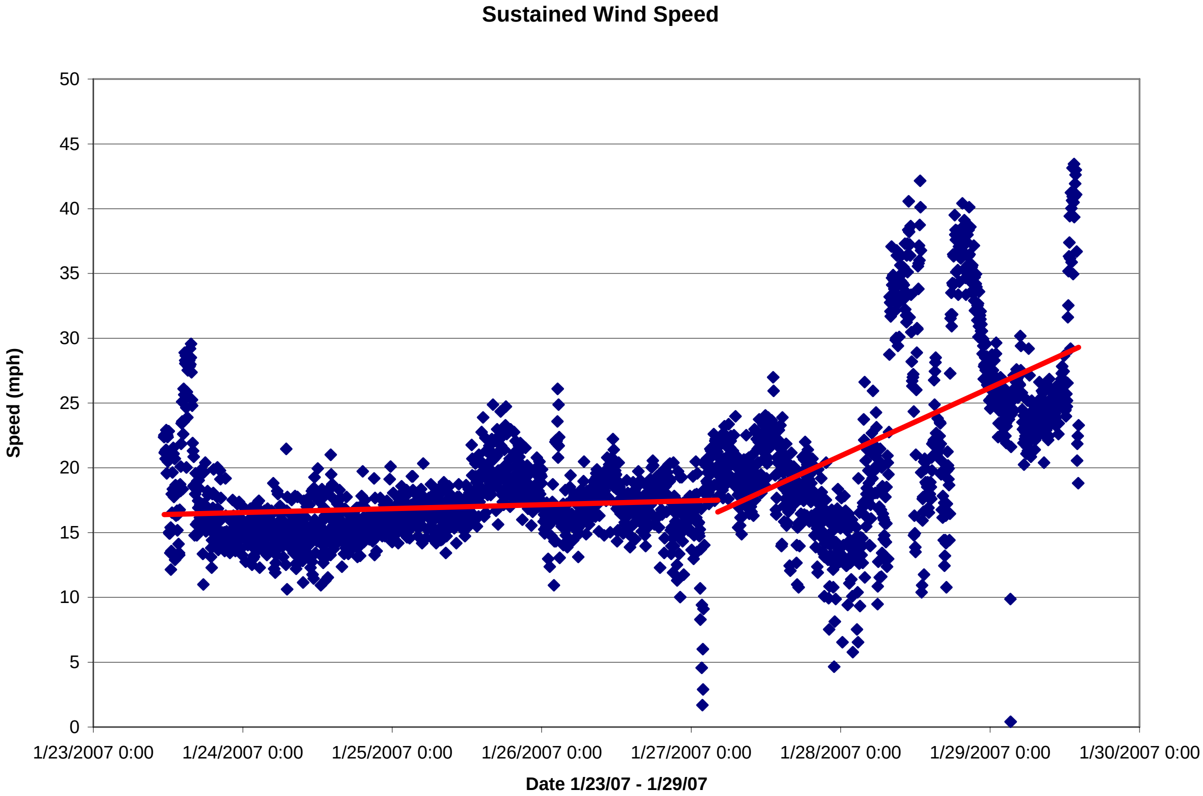

Figure 64. Average Wind Speed for 1/23/07 – 1/29/07

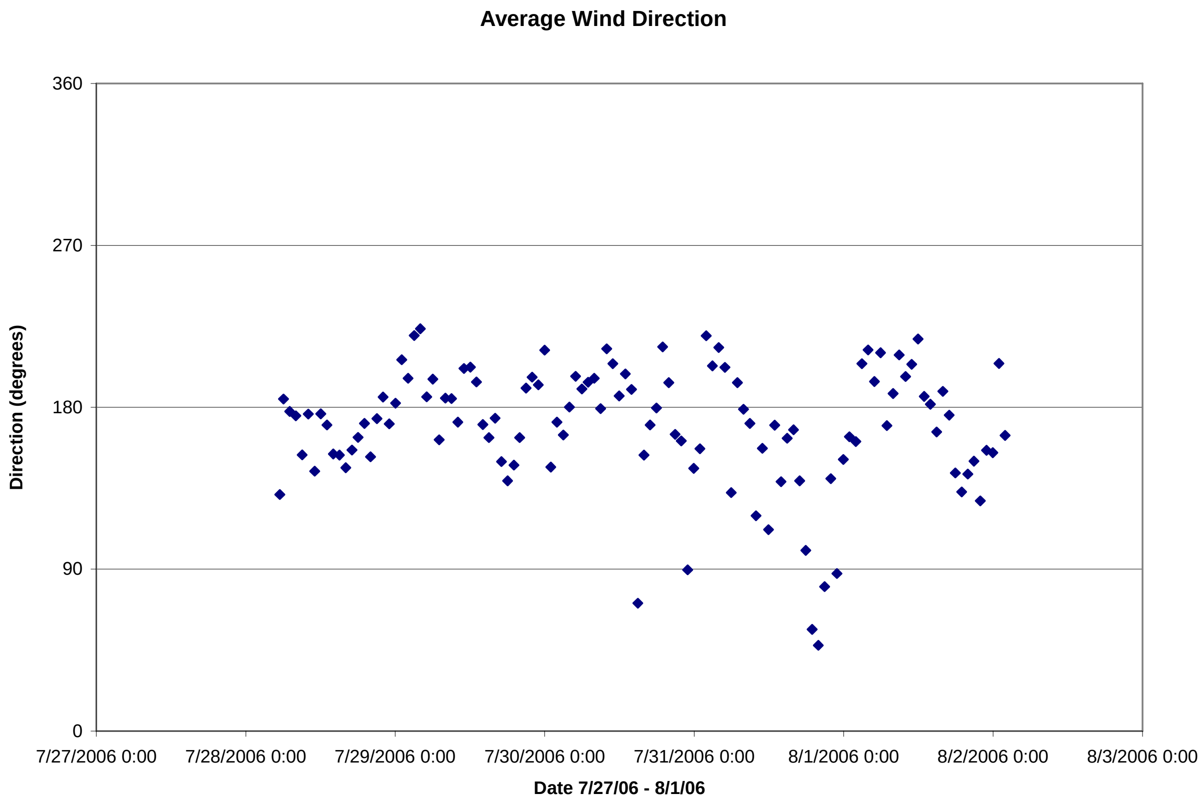

Figure 65. Average Wind Direction for 7/27/06 – 8/2/06

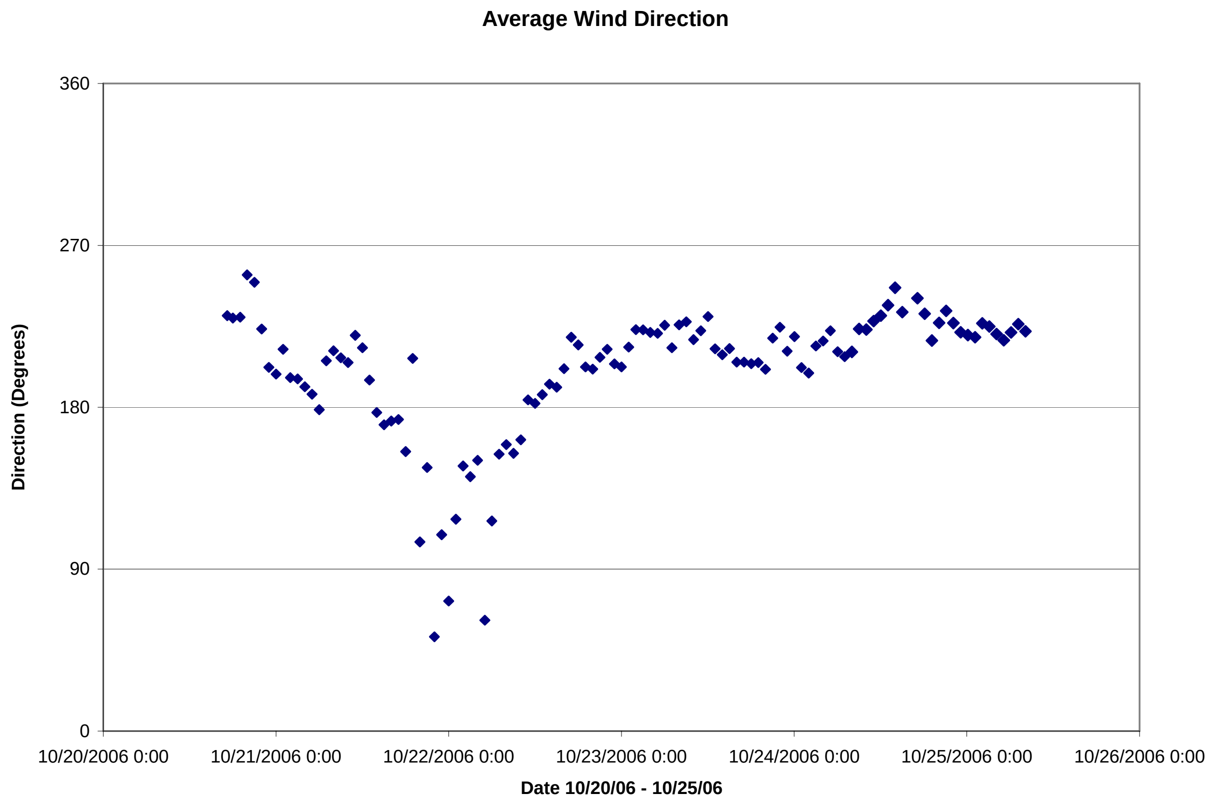

Figure 66. Average Wind Direction for 10/20/06 – 10/25/06

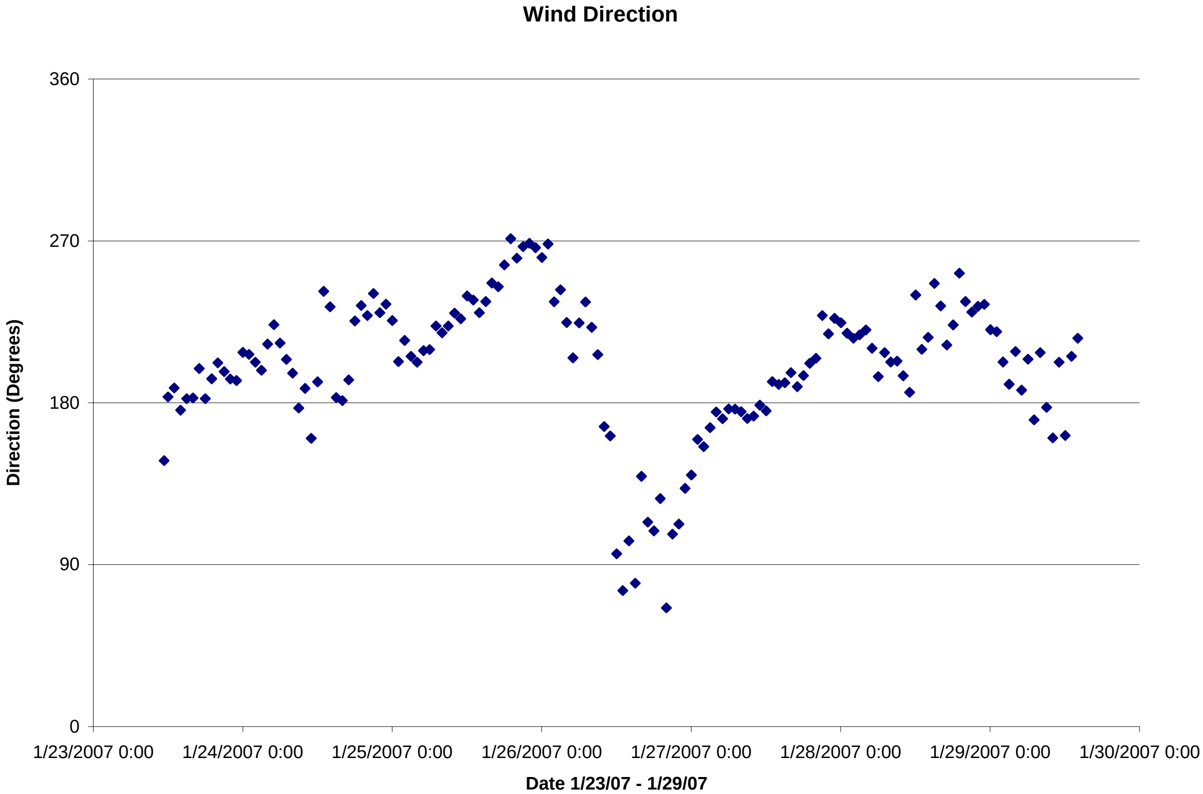

Figure 67. Average Wind Direction for 1/23/07 – 1/29/07

5.4 INSTRUMENT PERFORMANCE

Overall, the monitoring scheme at the Giant Eagle site was a success. The instruments and green roof predominantly performed as expected. The thermocouples provided insight into the thermal stress the roof membrane experienced given the conditions during the monitoring cycle. The thermocouples also demonstrated how the temperature below, at, and above the roof surface varied relative to one another. The short-wave solar radiation absorbed and released on a diurnal cycle shows the difference between conventional and green roof behavior. The thermal imaging reinforced the findings of the thermocouple monitoring system, and showed a clear thermal difference between the two roof types. The thermal performance monitoring system provides needed perceptivity into the thermal behavior of conventional and extensive green roofs.

Unfortunately, one instrument did not work in the monitoring scheme, the heat flux sensor. The sensor was placed between the roof membrane and insulation during the construction stage of the building. It was later connected to the data logger once construction was complete. However, the long length the sensor signal needed to travel to reach the data logger weakened the signal. As a result, the data logger never registered a voltage from the heat flux sensor. Due to the sensor's location in the roof structure, it could not be removed or replaced. The site conditions ultimately inhibit the use of a heat flux sensor. The distances from the Giant Eagle roof monitoring points to the data logger exclude the use of economical equipment that can monitor heat flux because the equipment does not generate a strong enough signal to reach the data logger.

The reliance of the data logger modules and instruments were also tested that the Giant Eagle site. All instruments are exposed to sun, heat, rain, wind, and snow. Overall, the instruments were fairly rugged. Extreme cold and snowy conditions did cause the data logger to miss measurements on occasion. However, when conditions improved, the data logger and impacted instruments were able to function again. Some thermocouple wire exposed to standing water and puddles malfunctioned almost immediately. When accessible, this wire was replaced or repaired and protected from the water if necessary. Fortunately, the functionality of the monitoring setup was consistent throughout a variety of weather conditions.

5.5 CONCLUSIONS

The data collected during the study period depicted the roof thermal characteristics. It described how the roof membrane absorbed, transferred and radiated heat when exposed to a variety of climate conditions. It showed that the conventional roof membrane, when exposed to direct solar radiation and warm ambient temperatures, absorbs energy and increases temperature. The data also shows that the roof releases that stored energy at night. However, the roof membrane underneath the extensive green roof is shielded from that energy. It stays relatively constant in temperature. For example, the variation in temperature of the roof membrane on July 31, 2006 was 15° and 16° on the green roof, and 47° and 58° on the control roof. The temperature data taken at four points across the roof (single layer measurements) show that the roof membrane exposed directly to the environment (i.e. the control roof) was greatly influenced by the air temperature and incident solar radiation. It reached very warm temperatures, especially when ambient temperatures and incident solar radiation were high, and decreased in temperature greatly at night. While the above surface measurement points were easily influenced by other factors, near the points closest to the roof membrane did warm slightly with the roof membrane. Measurements at the 7 cm and 15 cm above surface locations showed increases in temperature of 1-10° over the ambient temperature on the control roof, with increases of 0-2° over the green roof. It appears that the conventional roof membrane does have some adverse effect on the urban heat island effect. It can be assumed that the larger thermal stresses the control roof membrane undergoes, relative to the green roof membrane, could reduce the expected life of the membrane.

The membrane underneath the green roof has a much different experience. It is protected from the temperature extremes seen on the control roof. It appears that the green roof assembly did effectively absorb the incoming solar radiation and used that energy, as opposed to transferring it to lower layers of the roof. However, it should be noted that during the July to October monitoring period the green roof was regularly irrigated. The additional water would increase the evaporative capabilities of the green roof, and therefore reduce the roof membrane temperature. A combination of shading and evaporative cooling protected the membrane beneath the green roof from extreme thermal stress. This could mean increasing the membrane life cycle in the long term. However, during the winter months, the two roofs performed similarly. It appears that periods of warm temperatures and extended exposure to solar radiation demonstrate the green roof's benefits. However, this trend continues into the fall months as well. It can be assumed that roof performance would be similar in the fall and spring months. Ultimately, the green roof could provide thermal benefits for the building for roughly 9 months each year. During the winter, the green roof provides no added benefits, but it does not reduce the thermal integrity of the roof either. Overall, the green roof provides significant thermal benefits for the roof membrane.

The energy benefits of the green roof are harder to measure due to the building type on which the study was situated. A grocery store is a high energy user due to food storage requirements such as refrigerated display cases and freezers. The floor to roof distance also hinders the energy benefits of the green roof. A drop ceiling limits the effect that the green roof has on comfort and energy use in the occupied zone of the building. Lack of access to the building plans and interior store front for measurements inhibited the study to examine the green roof effect on interior temperature. Due to the building situation, the energy benefits of the green roof were compromised.

6.0 GREEN ROOF ENVIRONMENTAL LIFE CYCLE ASSESSMENT

6.1 INTRODUCTION

As discussed throughout this thesis, a green roof is one passive technique that can be used to address environmental issues in an urban setting. Research has shown that green roofs can be used to mitigate problems associated with storm water runoff, the Urban Heat Island Effect, wildlife habitat, and air and water quality (Liu and Baskaran, 2003, Wong et al., 2003a). Building owners are hesitant in considering the use of a green roof due to its increased initial costs, as compared with the initial costs of a conventional roof. In one of the few studies that consider the life cycle of green roofs, it was found that the life cycle cost of extensive, i.e., shallow soil roofs, are less than conventional roofs but that intensive, or deep soil roof systems have a higher life cycle cost (LCC) than conventional practice (Wong et al., 2003b). However, initial costs are not the only deciding factor in choosing a roof system for a building. Throughout the life of a building, many environmental costs will be incurred as well. A careful examination of all of the environmental aspects of building and maintaining either a green or conventional roof will create a Life Cycle Assessment (LCA). The goal of the LCA is to determine the option with the fewest environmental consequences. Building owners actually have many alternatives in choosing the best roof system for their structure.

Green roofs come in two forms, extensive and intensive. Both types of green roofs offer different advantages and disadvantages. An extensive green roof has between two to six inches of soil medium to support the plant life. This limits the size of plants that can be used on the roof, thus limiting the weight of the green roof on the rest of the structure. Generally foot traffic is not allowed on extensive green roofs because of the shallow and fragile root system. Often this type of green roof is retro-fitted to existing buildings, so that existing roof supports will not have to be replaced (Dunnett and Kingsbury, 2004). Intensive green roofs have six to forty-eight inches of soil to support larger plant life. These “roof top gardens” are advantageous to tenants who can walk on and enjoy the aesthetic benefits of the roof. Larger bushes and even trees can be planted on intensive green roofs. However, this imposes a large weight load on the roof of the building that requires additional structural support. Figure 68 gives a typical cross-section of a green roof. The layers of material generally remain the same for both extensive and intensive roofs.

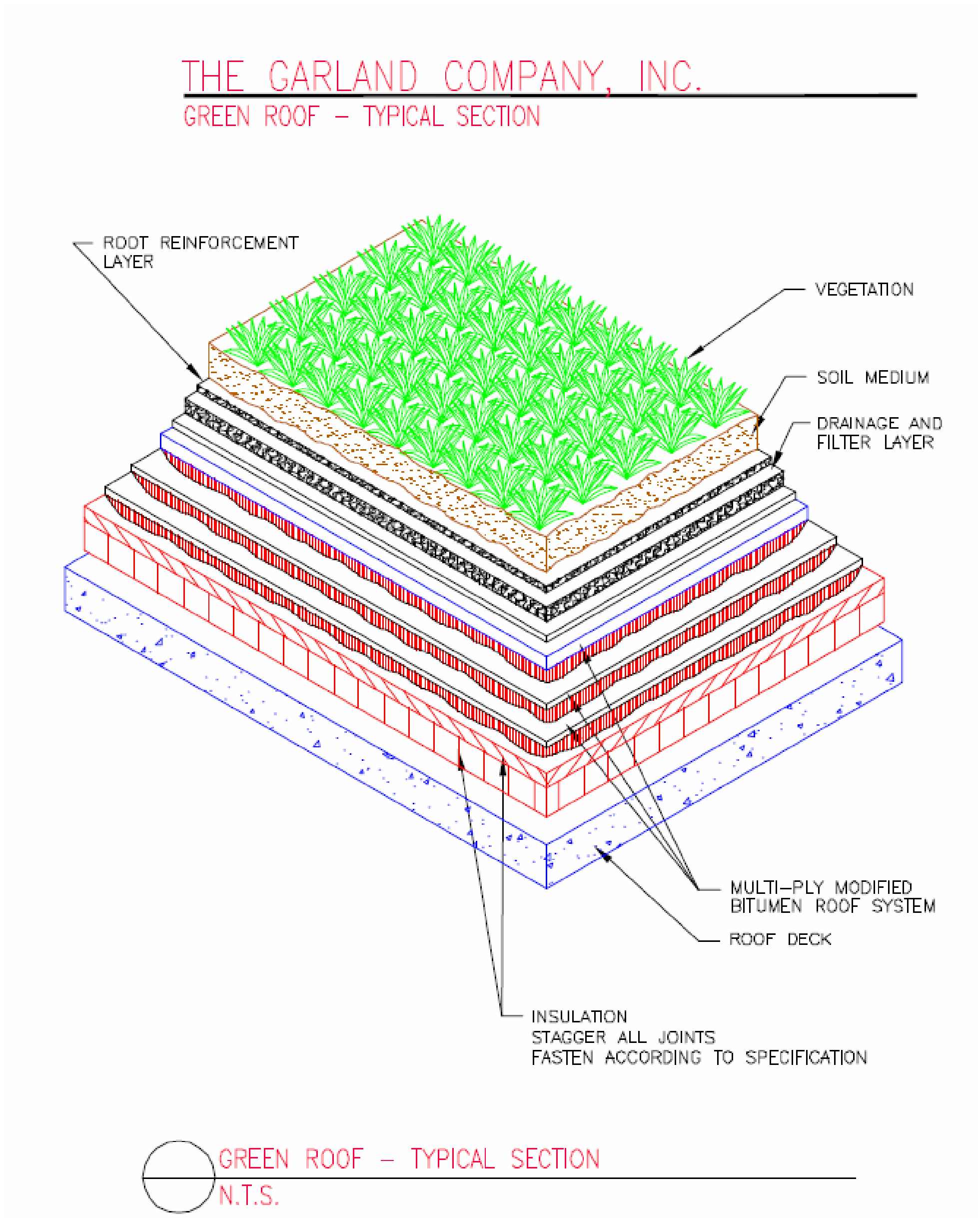

Figure 68. Typical Green Roof Cross-section (Source: The Garland Company)

6.2 GOAL AND SCOPE

6.2.1 Objective and Scope

The goal of this Life Cycle Assessment (LCA) project is to compare the environmental aspects and potential impacts associated with constructing a 12,000 square foot roof and determining the option with the smallest negative impact. That is, to find the environmentally preferable choice between an extensive green roof, an intensive green roof, and a conventional gravel ballasted roof. Much of the details and specifications of the roof models will be adapted from the Giant Eagle Grocery Store case study. Twelve thousand square feet of the addition will support an extensive green roof, with some of the apartments facing the roof. Figure 69 shows the green roof at the Giant Eagle site. A similar 12,000 square foot area of conventional rock-ballasted roof is also being monitored over another part of the new addition to the store front, this is shown in Figure 70. These two roof areas will serve as the model for the life cycle assessment. A fictitious intensive roof option with similar dimensions will also be considered in this assessment. The roofing option with the smallest negative impact will be determined.

Figure 69. Extensive Green Roof Site at Giant Eagle

Figure 70. Conventional Roof Site

A number of factors will be considered in the creation, operation, and demolition of the roof area. The life cycle inventory consists of compiling the different construction materials and transportation distances needed to manufacture and build the three different roofing systems. Some of the benefits of green roof technology will also be captured in this life cycle assessment. Process models will be developed to represent the water run-off benefit and the energy savings benefit. One process will address the change in storm water quantity and quality by applying run-off factors for pollutants to the different roof types to calculate the potential reduction of pollutants released to water due to the reduction in the run-off. Another process will be developed to model the energy consumption of the building depending on the type of roof. This will model the reduction in the use of electrical energy and natural gas for heating and cooling the building. The LCI will be used as the basis for an LCIA. The goal of the LCIA is to study the environmental aspects and potential impacts throughout the roof’s life, from raw material acquisition and product manufacturing to installation, operation, maintenance, and disposal.

6.2.2 System Description

This section describes the details of a built up roof system. In general a roof is the top covering of a building that prevents the ingress of weather into the building interior. Roofing comes in sloped or 'flat' form; however, roofs should never be truly flat. Flat roofs are often covered with tar and gravel and provided with drains to run off rain and snow. Typical roofing membranes are composed of built-up layers of tar and gravel, or single-layer membranes made of materials such as ethylene propylene diene terpolymer (EPDM) or polyvinyl chloride (PVC). The base or conventional roof in this LCA project is a rock-ballasted flat roof or one where the exterior sheathing of the roof is protected by a layer of gravel. Protecting the sheathing of a roof is important because this is the layer exposed to the weather, and can withstand much damage from storms, snow, and sun. It requires maintenance and replacement over the life of the building. The average life span of roof sheathing is 10-15 years before it requires replacement. In this LCA a life cycle of 10 years before the complete replacement of the roof membrane was used. The roof requires some access for its maintenance and replacement, so it must support some live load. However, to simplify the design and minimize the structural materials needed, access is restricted. The conventional roof provides suitable insulation and protection of the building interior from the weather, at a minimal structural weight.

An extensive green roof is thought to have a number of benefits over a conventional roof. An extensive green roof adds a drainage layer, filter fabric, soil layer and vegetation to the roof.

In this case 2-6 inches of soil, or soil substitute called substrate, is used to grow small sedum and other low rising vegetation with minimal root systems. It increases the life span of the sheathing by protecting it from weather elements, such as rain, snow, sleet, and sun. For most extensive green roofs the expected life span is 25 years, double that for a conventional roof. However, this is only an estimate from North American companies, where green roofs are a relatively new concept. In Europe, where the development of green roofs has gone on for decades, some research shows that green roofs can protect the roof membrane upward of 50 years (Roofscapes 2006). The added layers and soil also increase the building's insulation properties, improving the energy efficiency of the building. In some cases it may reduce the size of the drainage system needed for the building. Finally, the sedum and plants are selected so that maintenance and foot traffic on the roof will be minimal, or no more than a conventional roof. This means that no major structural changes need to be made to the frame of the building. In many cases, an extensive green roof can be retro-fitted to an existing building. Extensive roofs have a number of environmental benefits over conventional roofs at minimal structural changes.

The final option is an intensive green roof, or old-style roof top garden. This system requires the same additional layers as an extensive roof, however the soil layer is six inches in depth or greater and can support more substantial vegetation. Intensive roofs also improve the roof life span and provide additional insulation for the building. However, intensive roofs require more intensive maintenance and can withstand foot traffic from public use. This results in greater dead and live loads and a need for a stronger building structure. In the case of intensive roofs, the decision to include them in the design of a project needs to be made early so that the proper structural members can be selected to support the additional weight.

In Table 27, a review of the different roof layers in the three options is provided. All three roofs start with the basic roofing layers; structural steel joists, metal decking, insulation, and an underlayment layer, in this case fiberboard. The major differences come in the weatherproofing membrane, drainage, and soil layers of the roofs. For the control and extensive green roofs, all material amounts were obtained from the actual construction documents. The only differences in the material quantities between the conventional and green roofs are the layers needed to create the drainage plane and the growing medium of the green roof. It was assumed that since extensive green roofs are often retro-fitted to existing buildings and put minimal additional loads on the roof, the structural steel needed to support both the ballasted and the green roofs would be the same. In the case of the intensive green roof however, additional structural steel was used to support the considerable load placed by the thicker soil layer, larger vegetation, and increased live load.

Table 27. Roof layers

Roof Type **Roof Element**	**Conventional Roof**	**Extensive Green Roof**	**Intensive Green Roof**
Structural Support Member	Steel Joist	Steel Joist	Steel Joist
Decking	Metal Roof Deck	Metal Roof Deck	Metal Roof Deck
Insulation	85 mm Polystyrene	85 mm Polystyrene	85 mm Polystyrene
Underlayment	125 mm Fiber board	125 mm Fiber board	125 mm Fiber board
Waterproofing Membrane	3-Ply Polyurethane	Stress Ply EUV® The Garland Company Product	Stress Ply EUV® The Garland Company Product
Drainage Layer	None	HDPE Filter drain	HDPE Filter drain
Filter Fabric	None	HDPE Filter drain	HDPE Filter drain
Soil Medium	None	150 mm Growing Medium	1200 mm Growing Medium
Membrane Protection	Stone	Vegetation	Vegetation

Table 28 provides a summary of the annual energy demand of the building for each of the three roof options. A DOE2 eQuest energy simulation model (EQUEST 1998) was created by CTG Energetics Inc. for the grocery store to study the potential energy savings benefits of the extensive green roof over the conventional roof. The Department of Energy created this modeling software package with the expressed purpose of modeling the energy consumption of a building with an extensive refrigeration system, such as a grocery store. This program examines the building envelope, heating, ventilating, and air conditioning (HVAC) system, lighting loads, and refrigeration system loads to come up with the simulated annual energy consumption of the store. To develop the energy use processes, the annual difference in energy use between the alternative roofing systems was used, not the total annual energy demand as predicted by the model. In this case, the intensive green roof became the base case, because it was estimated to have the least energy use. The base case energy use was therefore set to 0. The extensive green roof has additional energy use relative to the intensive roof base case, and therefore is modeled to have positive energy use. The energy use of the extensive roof is greater than the intensive roof but less than the conventional roof. The energy model for the conventional roof indicates that it would use the most energy for operating building HVAC systems.

Table 28. Annual Energy Consumption

Roof Option	Annual Natural Gas Use (therm)	Change in Natural Gas Use	Annual Electricity Use (kWh)	Change in Electricity Use
Control Roof*1	9,211	21	2,122,699	16043
Extensive Green Roof Option*1	9,202	12	2,115,407	8751
Intensive Green Roof Option*2	9,190	Base case	2,106,656	Base case

*1 Numbers obtained from CTG Energetics Inc. DOE2 analysis

*2 Extrapolated from Extensive Roof Data

Table 29 summarizes the assumptions made for the water quality and quantity for each roof option. The runoff quantity factors were based on run-off coefficients for different types of land use (Dunnet and Kingsbury, 2004). The control roof runoff quality concentrations were obtained from a study on the quality of storm water run-off in Canada (Pitt and Lalor, 2000). Pollution reduction amounts were applied to the extensive roof and interpolated by growing medium thickness for the intensive roof (Kohler et al, 2002). The table shows the quantities per each storm event. However, the model multiplies these quantities by the average number of storm events per year in Pittsburgh.

Table 29. Storm Water Quality and Quantity

Quality*	Control Roof	Extensive Green Roof	Intensive Green Roof
Run-off Reduction	33%	60%	85%
Lead	75 µg/l	0.7 mg	0.4 mg
Zinc	8 µg/l	24.8 mg	12.4 mg
Cadmium	100 µg/l	0.04 mg	0.022 mg

*Per Storm Event

6.2.3 Functional Units

This section will discuss the functional units of this project. First, the project will compare the environmental impact of the 3 different roofing systems in the urban setting of Pittsburgh, Pennsylvania. All three provide basic insulation and protection from the elements to the respective building. However, the green roofs provide additional insulation as well as energy consumption, water run-off quantity and quality benefits. Within the environmental impact, the project will compare energy and resource use in the manufacturing, installation, operation, maintenance, and disposal of the three roof systems over a period of 45 years. The control roof has been given a life cycle of 15 years, while the green roofs will be examined for a period of both 45 years. While the systems will also be monitored for water run-off quantity and quality improvement and energy consumption improvements, initial assumptions will be made in this report as a starting point. Therefore the energy consumption and resource use of all the roof systems will be studied.

6.2.4 Environmental Stressor Categories

The software tool used to develop the process models for this analysis is Simapro 5.0 (Godhood and Ole, 2001). Simapro is a software database and process flow modeling program designed to help the user perform LCA under the guidelines provided in the International Organization for Standardization, or ISO 14040 series (ANSI/ISO, 1997). Simapro includes a number of LCIA methods by which to evaluate the LCI data. The main technique used in any LCA model is to caputre all relevent inflows and outflows of the process of producing, transporting, using, and disposing of a system. The life cycle inventory will capture the inflows and outflows of each process, while the Life Cycle Assessment will analyze the results. For example the emission of sulfur dioxide (SO_2) could increase acidity, which causes changes in soil chemistry, that could result in loss of trees. By using many environmental mechanisms the LCI results can be translated into a number of impact categories, such as acidification or climate change. (Goedkoop and Oele, 2001) For the LCI Simapro uses the data library Ecoinvent, that encompases 2500 processes updates for the year 2003. This library developed by Swiss institutes updates and integrates many popular life cycle inventory process databases ETH-ESU 96 and BUWAL250 which cover agriculture, energy supply, basic chemicals, transportation, construction materials, and material goods, like papers and plastics. The Ecoinvent database is well documented, consistant in specification of uncertain data, emissions are compartmentalized, includes standard capital goods, and is constantly updated by the Swiss ecoinvent center. (Goedkoop and Oele, 2001)

Simapro also encompasses impact assessment databases. These databases translate the results from the LCI into usable and relatable damage categories. These assessment databases categorized every emission and resource extraction indcated in the LCI, and place them in an impact classification. For example, sulfur dioxide and ammonia (SO_2 and NH_3) are both assigned to the acidification category. However, it is possbile to assign certain emissions to multiple damage categories, SO_2 can also be applied to the human health category due to its effect on respirtory diseases. Once the impact categories are assigned and LCI results are assigned to these impact categories, the characterization factors are defined. These factors reflect the relative contribution of an LCI result to the impact category. For example, over a 100 year time period, the contribution of 1 kg of methane (CH_4) to global warming is 23 times greater than the emission of 1 kg of carbond dioxide (CO_2). This means the characterization factor of CO_2 is 1, while the characterization factor of CH_4 is 23. Therefore, the impact category indicator result for global warming can be calculated by maultiplying the LCI result with the characterization factor. (Goedkoop and Oele, 2001) LCA analysis allows for a numerical comparison of a wide variety of environmental stressors to one another.

This LCA will use Eco-indicator 99 characterization factors and Impact 2002+ characterization factors for the assessment of environmental impacts. "The Eco-indicator 99 is both a science based impact assessment method for LCA and a pragmatic ecodesign method. It offers a way to measure various environmental impacts, and shows a final result in a single score" ("Eco-indicator", 2007). The Eco-indicator 99 results are dimensionless values that express the environmental load of a material or process over the life cycle. The Eco-indicator 99 impact assessment method includes impacts in the damage to mineral and fossil resources, ecosystem quality, and human health categories. Figure 71 shows the factors that Eco-indicator 99 examines in its analysis.

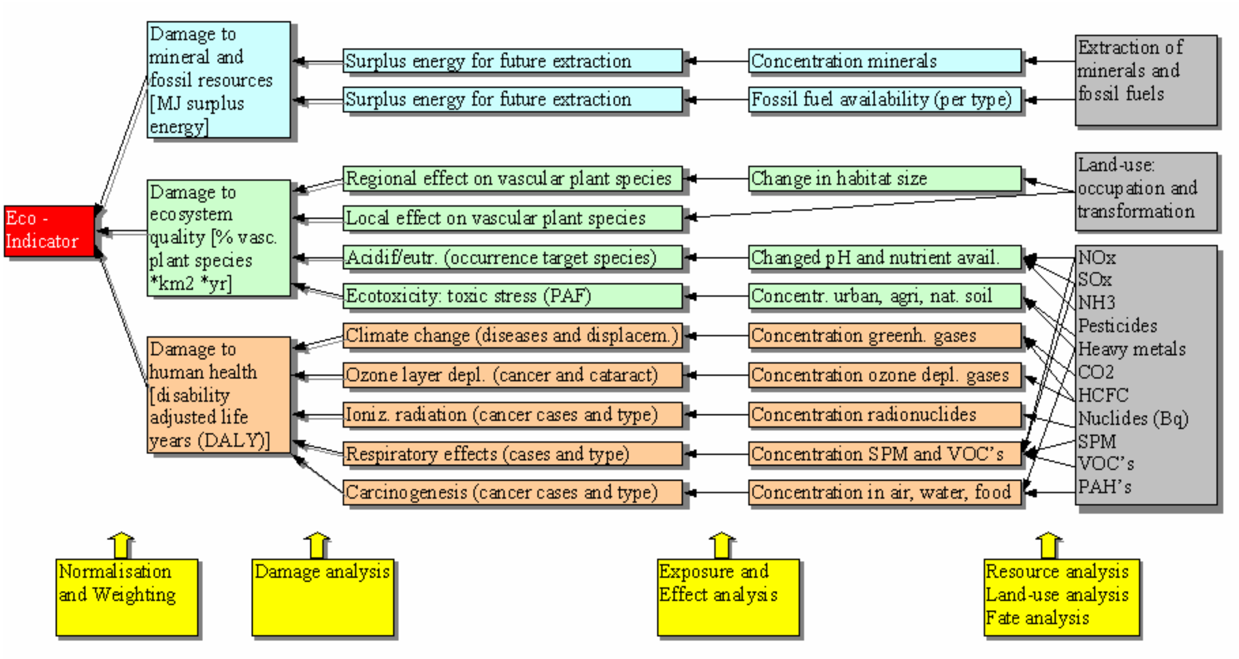

Figure 71. Eco-Indicator Categories (Source: Simapro 5.0 User Manual)

The IMPACT 2002+ life cycle impact assessment method proposes an implementation of a combined midpoint/damage approach, linking all types of life cycle inventory results to 14 midpoint categories to four damage categories. For IMPACT 2002+, new concepts and methods have been developed, especially for the comparative assessment of human toxicity and ecotoxicity. (GECOS, 2007) The four damage categories in the Impact 2002+ method are human health, ecosystem quality, climate change, and resources. The fourteen midpoint categories are divided into these four damage categories, but can sometimes overlap. Human toxicity, respiratory effects, ionizing radiation, ozone layer depletion, and photochemical oxidation make up the human health damage category. Ozone layer depletion, photochemical oxidation, aquatic ecotoxicity, terrestrial ecotoxicity, aquatic acidification, aquatic eutrophication, terrestrial acid/nutr, and land occupation make up the ecosystem quality. Global warming makes up the climate change category. Finally, non-renewable energy and mineral extraction make up the resources damage category.

All midpoint scores are expressed in units of a reference substance and related to the four damage categories human health, ecosystem quality, climate change, and resources. This is depicted in Figure 72. Normalization can be performed either at midpoint or at damage level. The IMPACT 2002+ method provides characterization factors for almost 1500 different LCI-result.

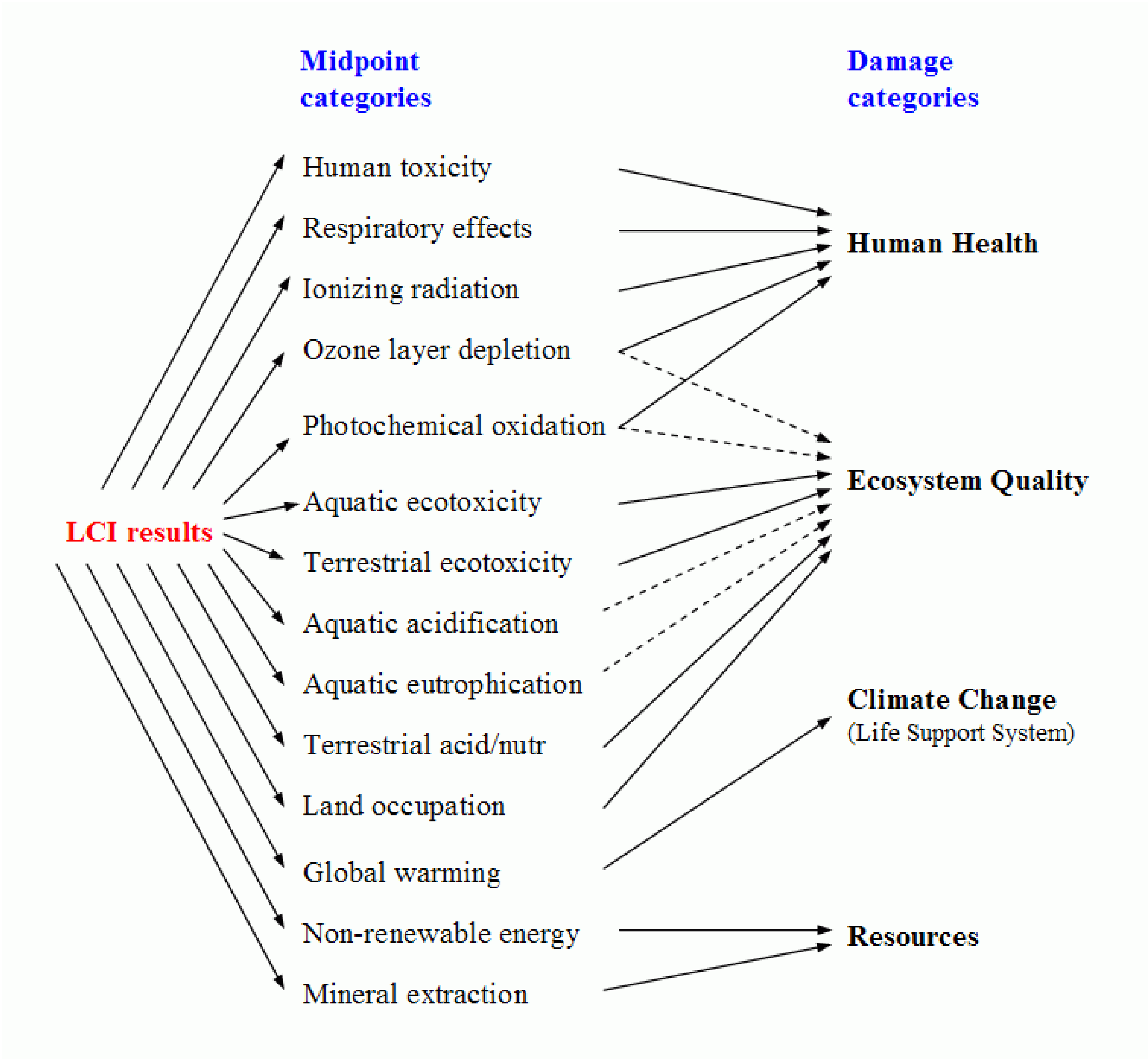

Figure 72. Impact 2002 Categories (Source: GECOS, 2007)

6.3 LIFE CYCLE INVENTORY

6.3.1 Study Boundaries

The LCI includes the energy consumption and waste production associated with acquiring the raw materials, producing the roofing materials, transporting the materials to the construction site, constructing the roof, maintaining the roof, and disposing the materials at the end of the life span. For this LCA, only the parts of the building structure and roof that are affected by the change in materials across the roof types will be examined. For all roofs these components are the load bearing structure, roof deck, insulation, fiberboard, and waterproof membrane. This will also serve as the basic roof layout for all three roof types, with additional layers defining specific roof types. Land use and the remainder of the building envelope, i.e. walls, will not be considered in this inventory. Figure 73 outlines the basic flow of energy, emissions, and materials.

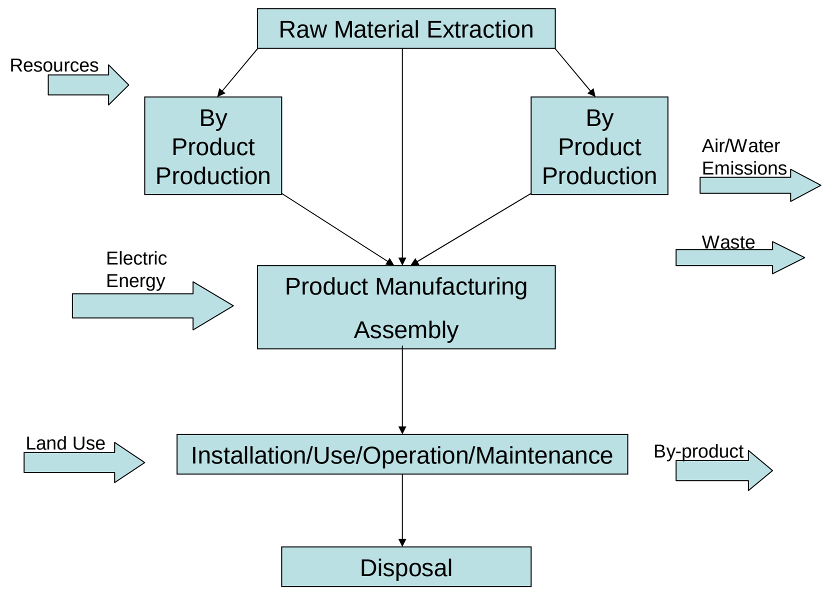

Figure 73. Basic Life Cycle Inventory Flow Diagram (Source: Battisti 2004)

6.3.2 Conventional Roof

The materials used in the conventional roof are structural steel, steel deck, insulation, underlayment, and the roof membrane. In the conventional roof, stone is used as ballast. The product materials analyzed under the conventional roof type are shown in Table 30. The material quantities for conventional roof are are from construction documents provided by Giant Eagle.

Table 30. Conventional Roof Material Mass and Transportation Distances

Element	Material	Mass [mtons]	Transportation [km]
Structural Support Member	Steel	6	320
Decking	Steel	2.5	40
Insulation	Polystyrene	0.6	40
Underlayment	Fiber board	34	25
Membrane	3-Ply Polyurethane	2	25
Asphalt	Adhesive	2	25
Ballast	Stone	53	25

6.3.3 Extensive Green Roof

The extensive green roof has the same basic materials as the conventional roof. The main difference is in the layers needed to support the vegetation. This includes the waterproofing system, drainage layer, filter layer, soil mixture, and plants. A 6 inch soil layer was used in the extensive roof. Table 31 depicts the materials that make up the extensive roof system. The material quantities for extensive green roof are are from construction documents provided by Giant Eagle.

Table 31. Extensive Green Roof Material Mass and Transportation Distances

Element	Material	Mass [mtons]	Transportation [km]
Structural Support Member	Steel	6	320
Decking	Steel	2.5	40
Insulation	Polystyrene	0.6	40
Underlayment	Fiber board	34	25
Membrane	Stress Ply EUV	55	780
Asphalt	Adhesive	2	25
Drainage Layer	HDPE Filter drain	0.2	780
Filter Fabric	HDPE	0.2	780
Growing Medium	-	40	425
Vegetation	-	-	25

6.3.4 Intensive Green Roof

Unlike the extensive and conventional roofs, the material quantities for the intensive roof are not from construction documents but are calculated for this analysis. The materials are identical to the extensive roof, with the exception of the thickness of the soil layer. A 4 foot soil layer was used for the intensive roof. Table 32 shows the materials needed to create the intensive roof.

Table 32. Intensive Green Roof Material Mass and Transportation Distances

Element	Material	Mass [mtons]	Transportation [km]
Structural Support Member	Steel	8	320
Decking	Steel	15	40
Insulation	Polystyrene	84	40
Underlayment	Fiber board	45	25
Membrane	Stress Ply EUV	55	780
Asphalt	Adhesive	2	25
Drainage Layer	HDPE Filter drain	0.2	780
Filter Fabric	HDPE	0.2	780
Growing Medium	-	270	425
Vegetation	-	-	25

6.3.5 Location

The transportation distances used are all to and from the city of Pittsburgh. For the conventional roof, the majority of the materials are local; the contractor obtained their materials from local manufacturers relatively close to the project site. For the additional green roof materials the Garland Company ships the materials from Dayton, Ohio and outside Charlotte, North Carolina. The company has four distribution centers in the U.S. Chicago, IL, Dayton, OH, Shreveport, LA, and Atlanta GA to minimize shipping costs.

Figure 74 shows the project location relative to the University of Pittsburgh.

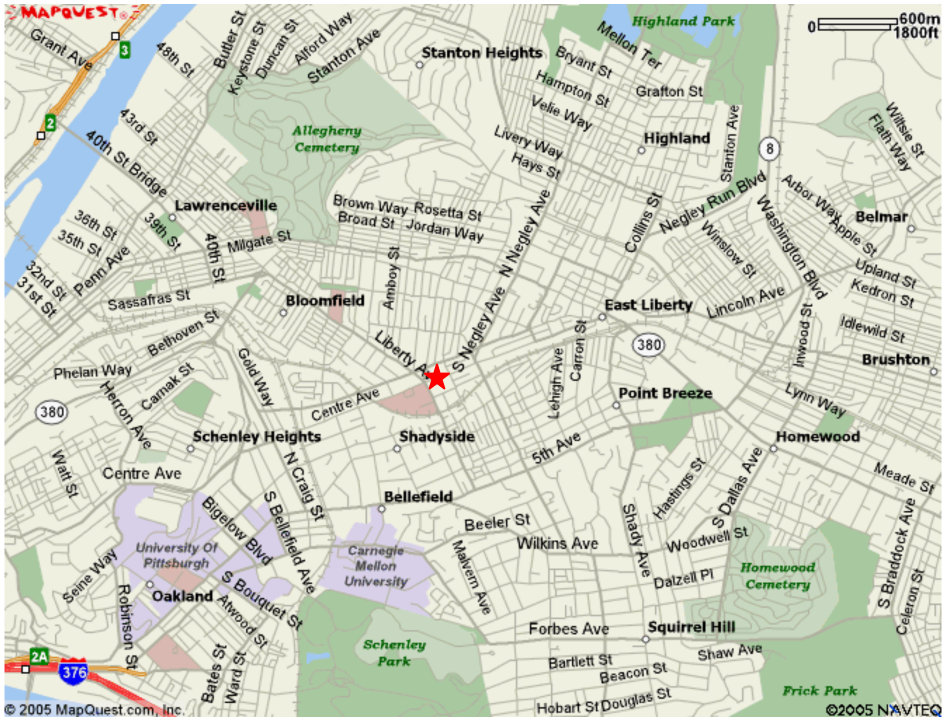

Figure 74. Project Location in Pittsburgh Mapquest.com

6.4 LIFE CYCLE IMPACT ASSESSMENT

6.4.1 Analysis

A Life Cycle Impact Assessment, or LCIA, was calculated for the entire life cycle inventory of each roof alternative. When using many of Simapro's evaluation methods, a dimensionless single score is calculated for each roof representing the environmental loading created by the products and processes in the model. The y-axis is marked with the unit kPt. This stands for a percentage. The percentage represents the relation of the characterization factors to one another. While the unit is dimensionless, meaning is does not give the exact amount of pollution or environmental stress created by the emissions in a damage category, it does give the change in characterization factor, meaning it shows the relationship between emissions in a damage category compared to other damage categories or other modelled systems. For example if one system or roof option scores 50 in a damage category, and another roof option scores 25 in the same damage category, this can be interpretated to mean that first system puts 25% more stress on the environment than the second. In order to maximize the potential of using Simapro Software, two different evaluation methods were used in the Life Cycle Impact Assessment. The Eco-indicator 99 and Impact 2002+ were used when analyzing the life cycle of all three roof options independently and when comparing the life cycles of the three roof types jointly. These methods provide the environmental endpoints that will most likely be affected by conventional roof and green roof construction.

When using Eco-indicator 99, a dimensionless single score is calculated for each roof representing the environmental loading created by the products and processes in the model. Figure 75 shows the single score results for each roof option. The control roof scores 38.4, extensive green roof 28, and the instensive green roof 4. The figure compares each roof to one another using 11 environmental loading categories, e.g., climate change, acidification, and eutrophication, aggregated into three impact areas, namely human health, ecosystem quality, and resources. This shows an percent increase in overall environmental stress from the intensive green roof to the extensive green roof of 24, from the extensive green roof to the control roof, a change of 11. Recall the difference in system models between the roof options. The intensive roof uses the most material, but this material is not replaced over the life cycle, the extensive roof uses less material a single time, however also requires 8751 kWh and 12 therm of energy annually, and the control roof requires material replacement 2 times and requires the most energy, 16043 kWh and 21 therm annually. Therefore comparing the two green roof options, it can be interpreted that the 23 change in stress from the intensive to extensive option is a result of the increase energy usage. The change between the extensive green roof option and the control roof option of 11 show the relative increase in environmental stress due to multiple material replacements and higher energy use.

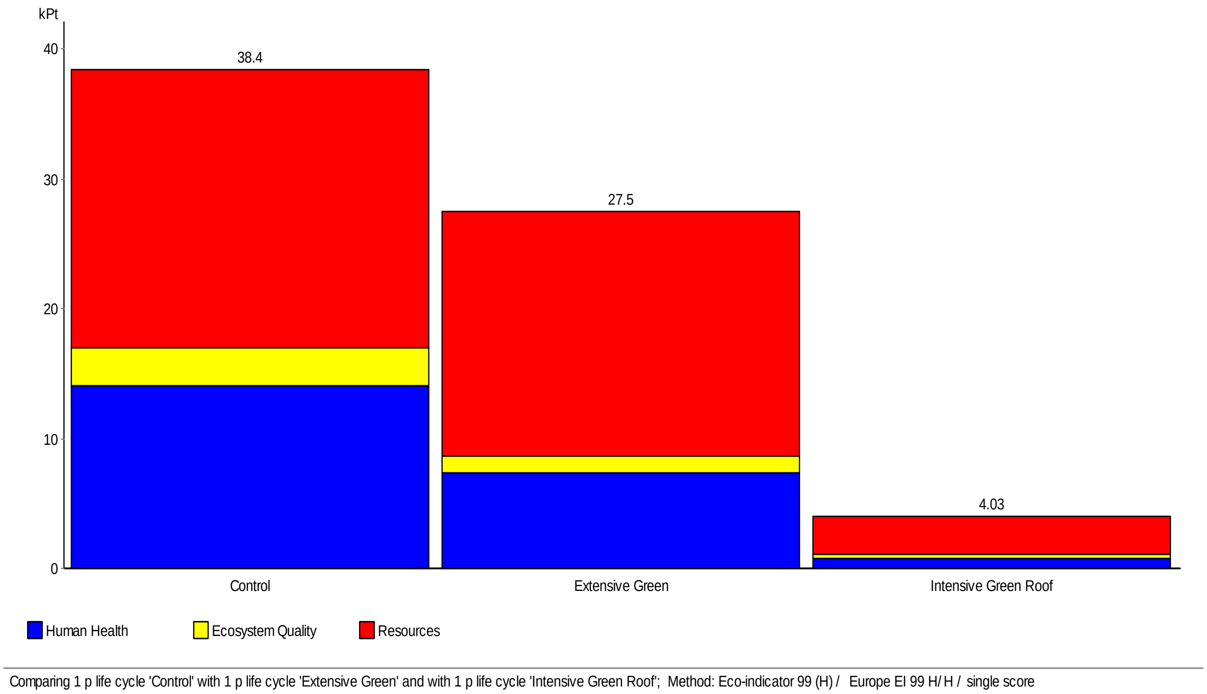

Figure 75. Eco-indicator 99 single score results for the three roof alternatives

One key outcomes in the LCIA should be noted, the effect building energy use has on the environmental impact score. It is important to remember that the intensive roof model did not include any building-related electrical or natural gas energy use and was the base case. The extensive and conventional roof alternatives had their respective additional energy uses included in the model. Using just a small additional amount of energy greatly affects the environmental loading of the building over the 45 year life cycle. The relative impact energy use has on the LCIA is easily seen in the process contribution of each roof option.

6.4.2 Control Roof

Figures 76 shows the Eco-indicator 99 process contribution of the control roof assembly. This method assigns a score that demonstrates the impact each process has in relationship to the other processes that make up the control roof life cycle. The assembly input that plays the largest role is natural gas usage. Natural gas in the LCIA model is used to heat the building. The second largest impact is made by coal used by electricity boilers. Again, this is another energy source needed to control the climate in the building. Impact 2002+ was also used to determine the environmental impacts of the control roof on specific environmental stressors. Figure 77 shows that the energy needs dominate impacts. In both LCA characterization methods, the process for natural gas need and coal for electricity boilers score the highest. Using Eco-indicator 99 these two processes combine for a score of 19280 Pt, while all remaining processes combine for a score of 14492 Pt, a 4788 Pt difference. Likewise, using Impact 2002+ characterizations these two processes score a combined 55 Pt, while all remaining processes combine to score 21 Pt.

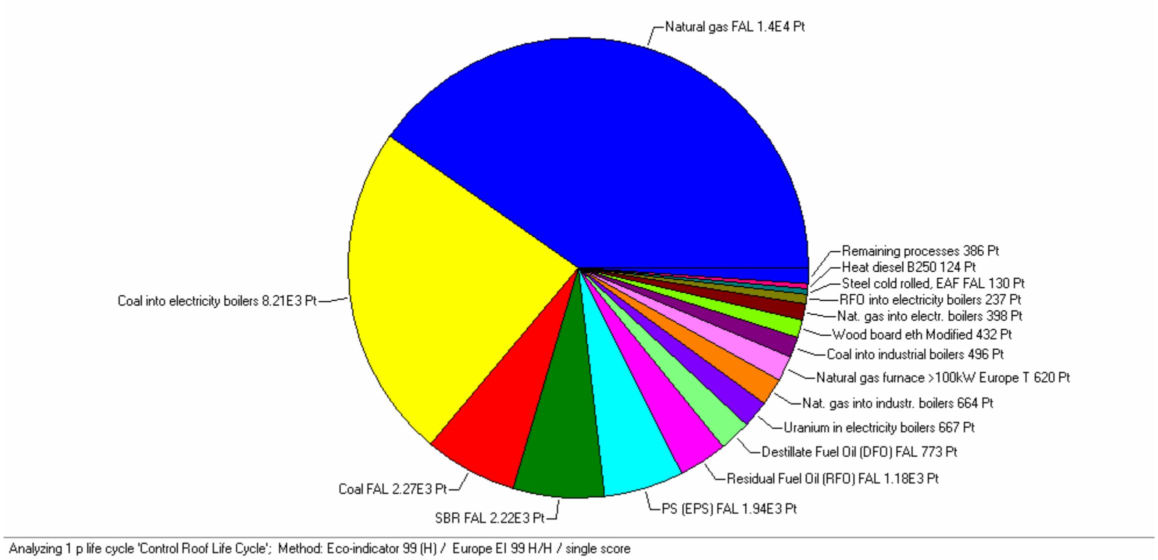

Figure 76. Eco-indicator 99 Control Roof Process Contribution Results

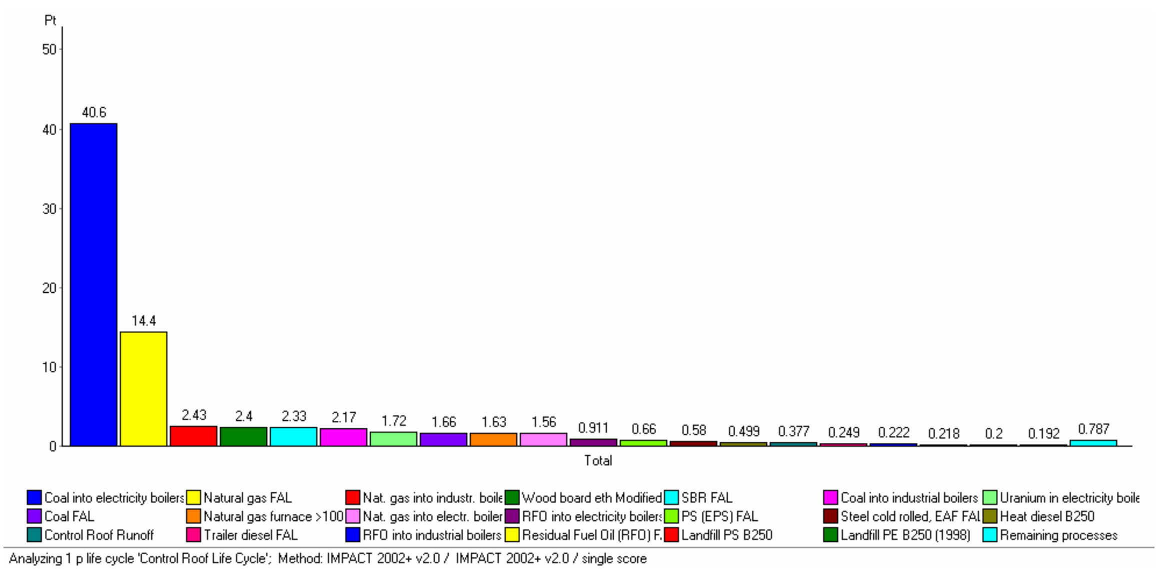

Figure 77. Impact 2002+ Control Roof Process Contribution Results

6.4.3 Extensive Green Roof

Next, the extensive green roof is examined. Figure 78 shows the Eco-indicator 99 process contribution results of the extensive green roof assembly. This method assigns a score that demonstrates the impact each process has in relationship to the other processes that make up the extensive green roof life cycle. The process that contributes the largest role is the energy consumption. Natural gas usage and coal usage for electricity boilers dominate half of the assembly contribution. This is because a moderate amount of energy needed to heat and cool the building was applied to the extensive green roof life cycle. It is also important to note that the numerical score given to the process contribution for the extensive green roof should not be compared directly to the score given the control and intensive green roofs. The score given in the process contribution is meant only to compare processes within the assembly, not to processes within a separate assembly. Impact 2002+ was also used to determine the environmental impacts of the extensive green roof on specific environmental stressors. Figure 79 shows that the energy needs dominate impacts. In both LCA characterization methods, the process for natural gas need and coal for electricity boilers score the highest. Using Eco-indicator 99 these two processes combine for a score of 11640 Pt, 7640 Pt less than the control roof. Meanwhile all remaining processes in the extensive green roof option combine for a score of 6063 Pt, a 5577 Pt difference. Likewise, using Impact 2002+ characterizations these two processes score a combined 30 Pt, while all remaining processes combine to score 10 Pt. These two processes alone account for 75% of the extensive green roof score.

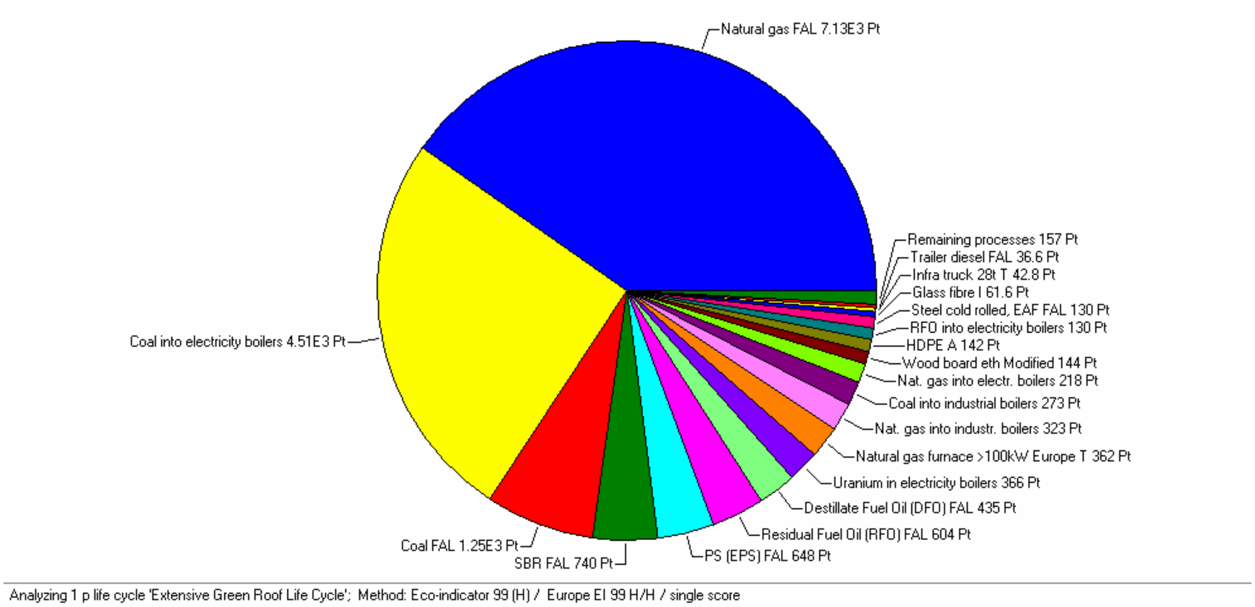

Figure 78. Eco-indicator 99 Extensive Green Roof Process Contribution Results

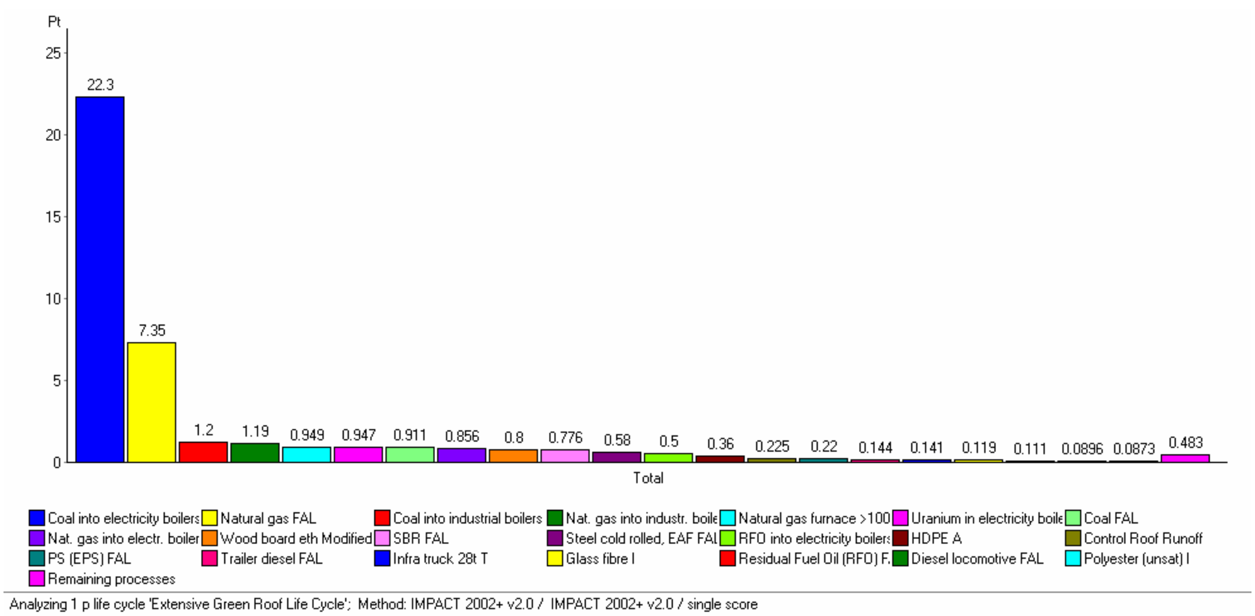

Figure 79. Impact 2002+ Extensive Green Roof Process Contribution Results

6.4.4 Intensive Green Roof

Finally, the intensive green roof is examined. Figure 80 shows the Eco-indicator 99 process contribution results of the intensive green roof assembly. This method assigns a score that demonstrates the impact each process has in relationship to the other processes that make up the intensive green roof life cycle. It is noted that the process contribution for the intensive green roof differs greatly from the prior roof assemblies. This is due to the fact that energy needs for the building were not modeled into this assembly. The intensive green roof was the base case, meaning it required the least amount of energy to heat and cool the building. Since the energy inputs were diminished, the intensive green roof assembly shows the effect individual materials have on the environmental stressors. Again, natural gas is the largest process contributor, but coal for electricity boilers was reduced to fourth largest contributor. Materials and transportation impacts are highlighted in the smaller contributing factors, such as truck transportation, steel, wood, and High Density Polyethelene (HDPE). Impact 2002+ was also used to determine the environmental impacts of the intensive green roof on specific environmental stressors. Figure 81 shows that the natural gas needs, fiberboard, steel, and truck transportation requirements dominate the impacts. The intensive roof case models the environmental stress of the building materials only; no additional energy needs were included. Thus this model scores much lower than the other options. Using Impact 2002+ characterizations gas usage and coal for electricity score the highest again, a combined 4 Pt, while all remaining processes combine to score 5 Pt. In this case the two energy processes account for only 40% of the intensive green roof score. Please note that the complete process contribution results can be found in the appendix.

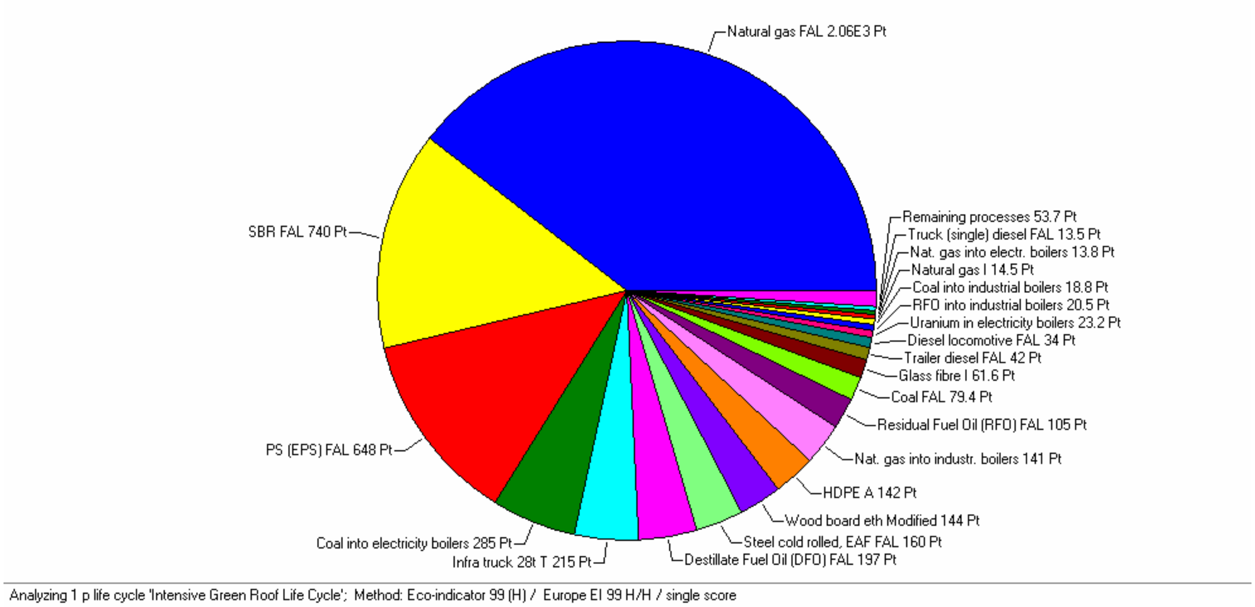

Figure 80. Eco-indicator 99 Intensive Green Roof Process Contribution Results

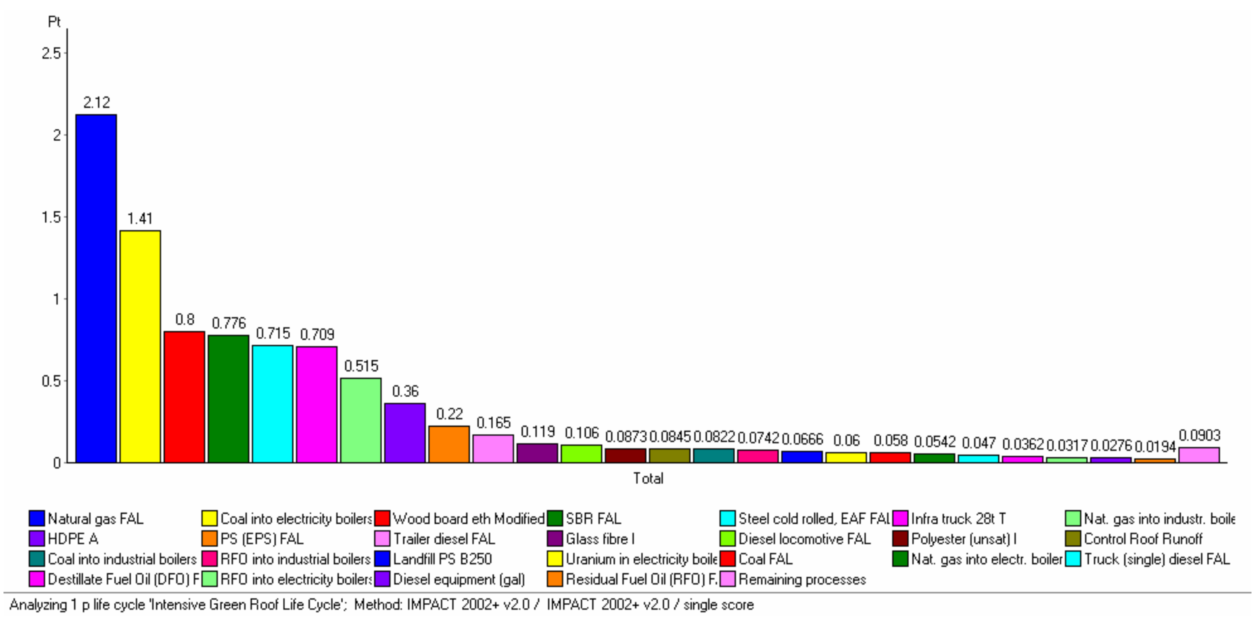

Figure 81. Impact 2002+ Intensive Green Roof Process Contribution Result

6.5 DISCUSSION OF RESULTS AND CONCLUSIONS

6.5.1 Comparison and Discussion

The same two environmental impact methods were used to not only compare processes within an assembly, but to compare the three roof assemblies to one another. The Eco-indicator 99 single scores results were discussed earlier in this report. For the Impact 2002+ method the single score, characterization, damage assessment, and normalization analysis options were used. Figure 82 shows the single score results. The control roof creates the greatest negative impact, with the extensive roof creating the second highest impact, and the intensive roof with the least negative impact. Note that the damage impact of the roofs is divided into four damage categories, human health, ecosystem quality, climate change, and resources. For all three roof assemblies, the majority of the impact created is in the human health category. The midpoints within this category are human toxicity, respiratory effects, ionizing radiation, and photochemical oxidation. Energy use again, creates the largest impact between the roof assemblies.

Each damage category must be analyzed separately. For instance, it would appear that the intensive green roof, with the lowest energy loads, eliminates the impact on ecosystem quality, it scored only 0.3 Pt. The control roof and extensive green roof scored 2 and 1 Pt respectively. While the ecosystem quality is largely impacted by gas and electricity energy usage, land occupation is not considered. In this model, it was assumed that a building would be built, and of course would need a roof. To isolate the impact of roof type, the building footprint was not considered in the model. If it were, the impact on the ecosystem quality, and in particular, land occupation, would alter.

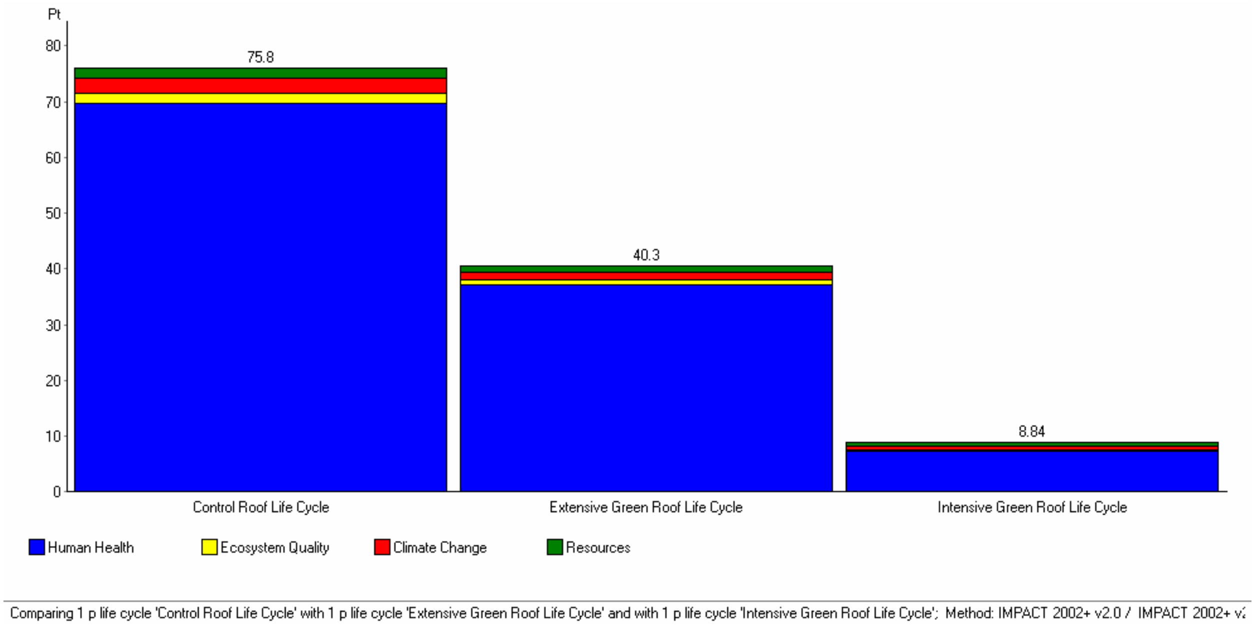

Figure 82. Imapct 2002+ Single Score Comparison of All Three Roof Assemblies

The normalization and damage assessment allows one to evaluate the impact of the roofs assemblies compared to one another. The normalization assessment shows that the largest impact is made on the human health category, with the ecosystem quality, climate change, and resource categories relatively small compared to human health. In each category, the control roof is the greatest stressor again, with the extensive green roof and intensive green roof following respectively.

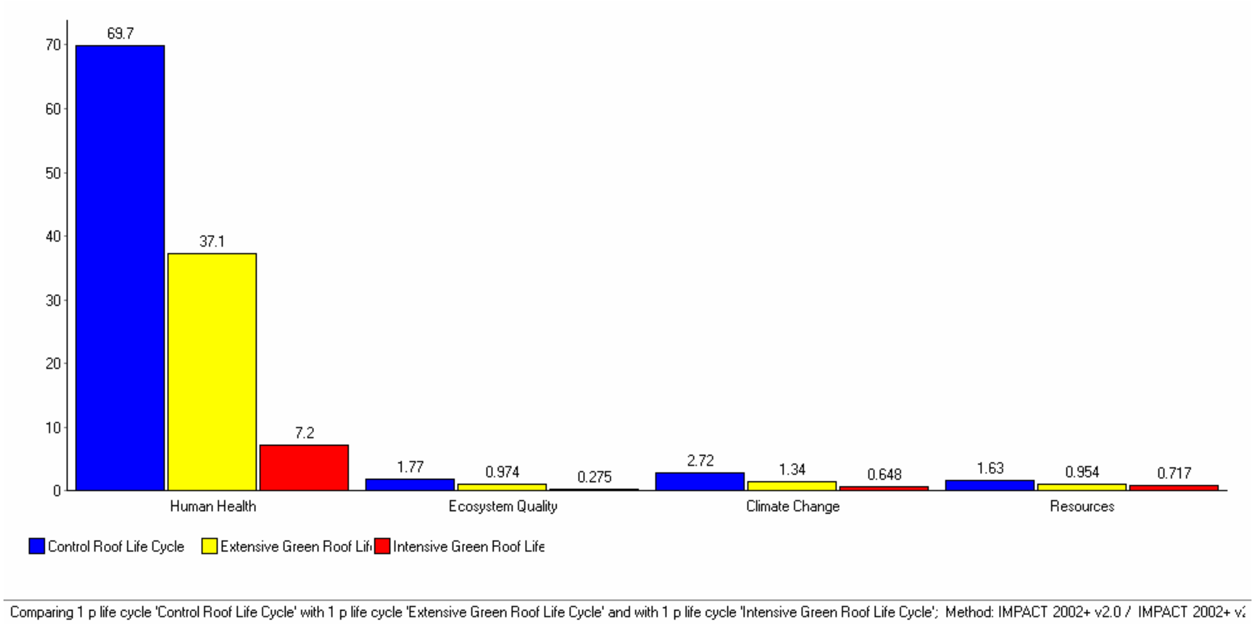

Figure 83. Imapct 2002+ Normalization Comparison of All Three Roof Assemblies

Finally, the damage assessment analysis designates each damage category as a percentage of damage. In each case, the control roof has the largest impact on the category, so the possible damage made is 100%. The extensive and intensive green roof results are shown as a percentage as compared to the control roof results. The extensive green roof impact is roughly 50% for each damage category, meaning the impact made by the extensive green roof is roughly half that for the control roof. The intensive green roof actually increases with each damage category, growing from 10% to 44% impact. Again, this is due to the way the three roofs were modeled. In the control and extensive green roof assemblies, both roof materials and energy needs create environmental impact. However, the intensive green roof models only the materials needed to create the roof. So as expected, the resources needed to manufacture the roof materials create the largest impact for the intensive green roof. This also shows how much energy demand can negatively impact the environment in terms of human health and ecosystem quality.

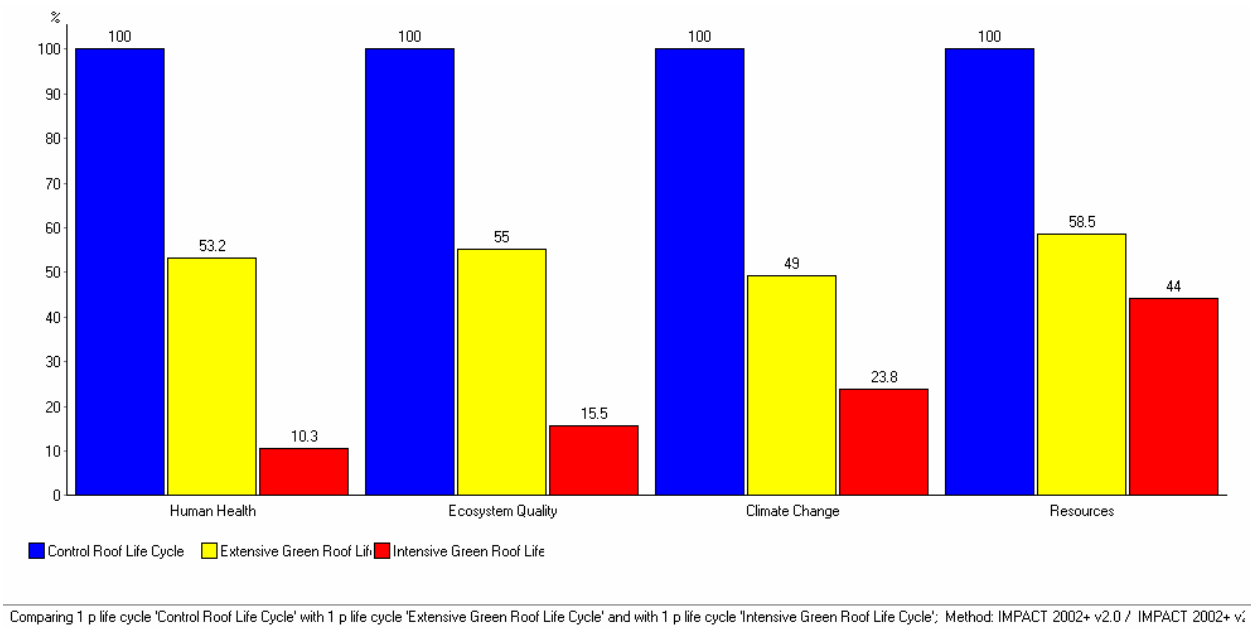

Figure 84. Imapct 2002+ Damage Assessment Comparison of All Three Roof Assemblies

6.5.2 Life Cycle Assessment Conclusions

The results from the LCA model provide insight in the environmental impact of different types of available roofs. The energy benefits provided by the green roof options make a noteworthy impact in the life cycle assessment. With the energy needs reduced, the materials needed to construct the roof then dictate the results of the LCA. Despite the need for additional resources, green roofs are the environmentally preferable choice when constructing a building due to the small reduction in energy demand and the increased life of the roofing membrane. However, it should be noted that this case study is limited to the building type, climate, and location of the study. Also, further research, case studies, and sensitivity analysis are needed to confirm or refute the conclusions made from this model.

7.0 CONCLUSIONS

This study presented the use of an extensive green roof compared to a conventional roof using modern construction methods. A green roof has many benefits over a conventional roof, environmental, economic, and aesthetic. This study examined the environmental benefits of green roofs, particularly thermal and energy benefits. This study evolved through a number of different phases. The first phase developed a monitoring system to capture the environmental benefits of green roofs. This monitoring system captured both the thermal and water quantity and quality characteristics of two different roof types, convention and extensive green. For this research, only the thermal characteristics were examined. The system was implemented and environmental data was collected continuously over a seven month period. This phase overlapped periods of summer, fall, and winter climate conditions. The data collected described roof behavior during the seven month period. The monitoring plan was successful and the data collected over that time was generally good quality. There were some gaps in data, where the computer system crashed or the data logger malfunctioned. However, the majority of the time the system worked to its full potential. The thermocouples, temperature probes, net radiometers, RH sensors, and wind sentry set captured the thermal performance of the two roof types over time.

The data results clearly show the effect the respective roof coverings have on the roof membranes. The stone ballast covering the membrane on the control roof cannot protect the membrane from the ambient conditions and incoming radiation. Despite the light color of the ballast, the roof surface reached extreme temperatures on a hot summer day. For example, on August 25, 2006 at Location D the roof membrane reached an afternoon high temperature of 130°F and the surface reached 140°F. That night, the surface and membrane cooled to low temperatures of 65°F, while the ambient temperature low was 70° that night. Meanwhile, on that same day at the green roof Location A the membrane high temperature was 86°F and the surface temperature high was 91°F. At night both the soil and surface and membrane low temperatures were 73°F and 76°F respectively. Both were slightly warmer than the evening low that night. This shows the absorption and release of energy of the roof materials exposed to the climate through a day. The green roof provides protection to the roof membrane and reduces the thermal stress of membrane during days with high ambient temperature, greater than 75°F and high incident solar radiation, greater than 500 $W*m^{-2}$ net.

The green roof also provides moderate protection in the fall. October 23, 2006 was a day of transition. The previous day had an afternoon high of 60°F and dropped to 40°F at night. The net radiation reached 400 $W*m^{-2}$. However, on the 23rd the afternoon high barely reached 42°F and held steady at 38°F at night. The net radiation this day only reached 250 $W*m^{-2}$. Yet the temperature profile at Locations A and D are very different. At the green roof location the soil surface followed the ambient temperature closely. The membrane was kept warm, and only varied 10° ranging from 45-55°F throughout the 23rd. Meanwhile, at Location D the surface temperature varied greatly from the ambient temperature. The surface rose in temperature to a high near 50°F. The membrane was even warmer, reaching 55°F. At night, the surface reached a low of 35°F and the membrane 40°F. While not as potent, the green roof continues to protect the membrane during mild and transitional autumn weather.

The green roof did not perform any better or worse than the control roof during the winter. Unfortunately, the cold weather caused a number of sensors to malfunction, making direct comparison hard. Still, on January 24, 2006 the ambient temperature was 30°F throughout the day and night. In net radiation at the site was only 200 W*m^{-2}. The soil midpoint at Location A was steady at 30°F as well, varying little even as colder air moved in later in the week. The membrane was warmer than the surrounding air, steady at 40°F. The membrane did not fluctuate in temperature more 2-3°. Meanwhile at Location D, the membrane fluctuated 10°, and even more as the week progressed (the surface data is not available). While the roof membrane is influenced by air temperature and the heat of the building, there is still some difference between the effects of the two roof coverings on the membrane. Both membranes are warmed by the building and are warmer than the ambient air. However, the membrane underneath green roof fluctuates little between day and night, while the membrane at the control roof fluctuates by 10° or more. The green roof still protects the membrane from the stress of temperature fluctuation, even during the colder winter ambient temperatures.

The net radiation at the site also influences roof performance. In the summer and fall when the roof is exposed to 400-800 W*m^{-2} net of incoming radiation throughout the day, the control roof easily stores this energy, while the soil and plants store and use that energy. Looking at the data from the summer and fall, the green roof shows slightly higher positive radiation during the day, meaning the green roof is reflecting less energy during the day, and slightly higher negative radiation at night, meaning the green roof is releasing less energy at night. During the winter the two roofs perform nearly the same, the short days, lower sun, and shading by the apartment building, greatly limits the energy transfer during the day. Exposure to solar radiation determines if the thermal benefits of the green roof will be great or small that day.

The results from the LCA model provide insight in the environmental impact of different types of available roofs. The LCA model shows that the energy benefits provided by the green roof options, while limited to a small perentage of the overall building energy use and with negligible economic impact, make a noteworthy impact in the life cycle assessment. The DOE2 model predicted only $100 electrical savings and $10 of gas savings with the extensive green roof option compared to the conrol roof each year. Yet using the respective 7292 kWh annual electricity and 9 therm annual gas energy reduction, the LCA model predicted impressive environmental benefits. Comparing the control and extensive green roofs, there is a 35.5 Pt difference. Looking closer at the need for natural gas and coal for electricity process for each roof option, the control roof scored a combined 55 Pt for these two processes, 29.65 Pt for the extensive green roof. With the energy needs reduced, the materials needed to construct the roof then dictate the results of the LCA. The intensive roof, the base case in energy needs, reflects the impact of only building materials. Gas and electricity are still needed for material production, but in much smaller amounts. The score of these processes drops to 3.53 Pt, 51.47 Pt less than the control roof with multiple material replacements and the highest energy demand, and 26.12 Pt less then the extensive green roof with moderate energy requirements. Despite the need for additional resources, green roofs are the environmentally preferable choice when constructing a building due to the small reduction in energy demand and the increased life of the roofing membrane. The Life Cycle Environmental Assessment shows that green roofs are the environmentally preferable choice for rooftops.

Overall, the proposed benefits of green roofs seem to be supported by this research. The green roof makes a significant impact on the thermal stress experience by the waterproofing membrane. This could translate to a longer life span of the membrane and reduce the need for new roofing materials. However, only extended experience with roof membranes under vegetated roofs will determine this conclusively, although evidence from other countries and climates support extended roof membrane life. The green roof provides environmental benefits over the building life cycle, as seen in the LCA model. Therefore, from thermal protection and energy savings perspectives, green roofs are a passive tool that can be used to improve the urban environment.

APPENDIX A

TEMPERATURE RESULTS

Temperature Measurements from July 28, 2006 to August 2, 2006.

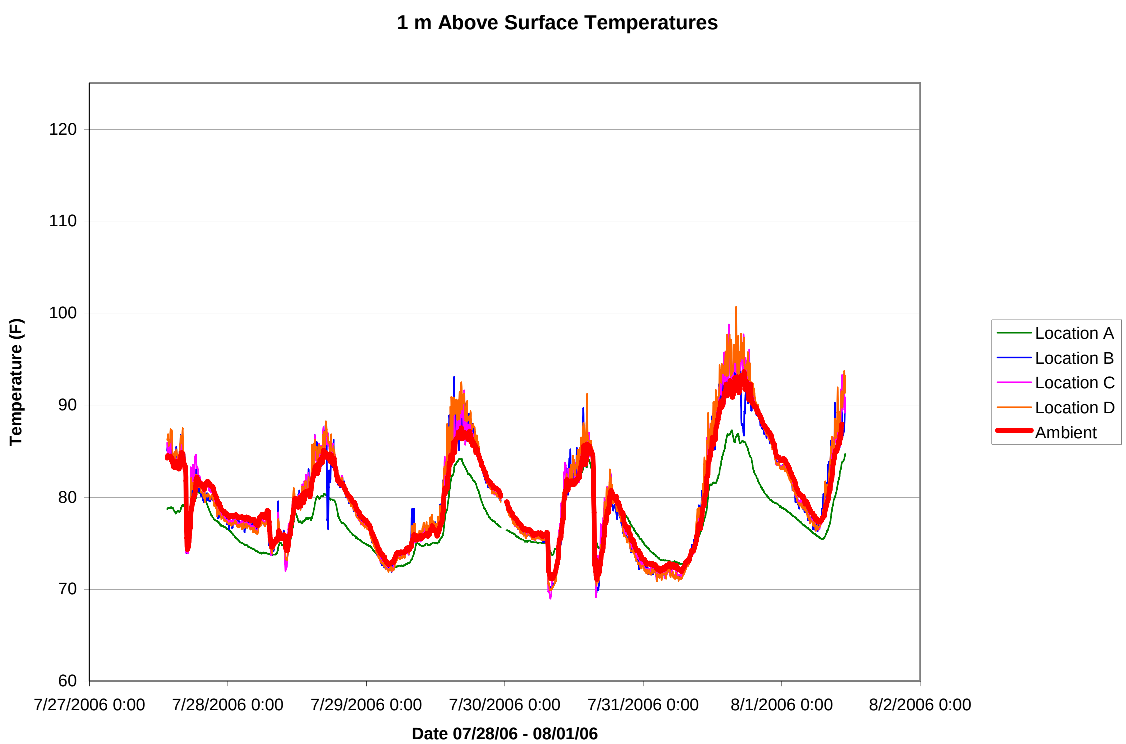

Figure 85. 1m Temperatures 7/28 – 8/1/06

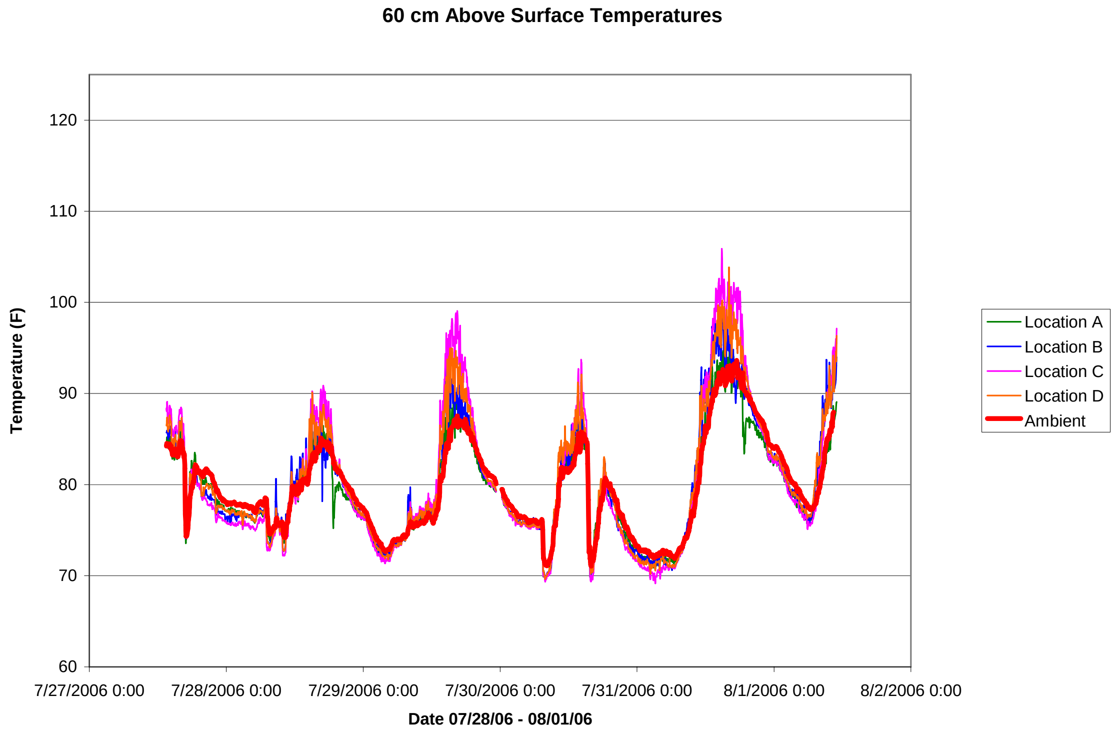

Figure 86. 60cm Temperatures 7/28 – 8/1/06

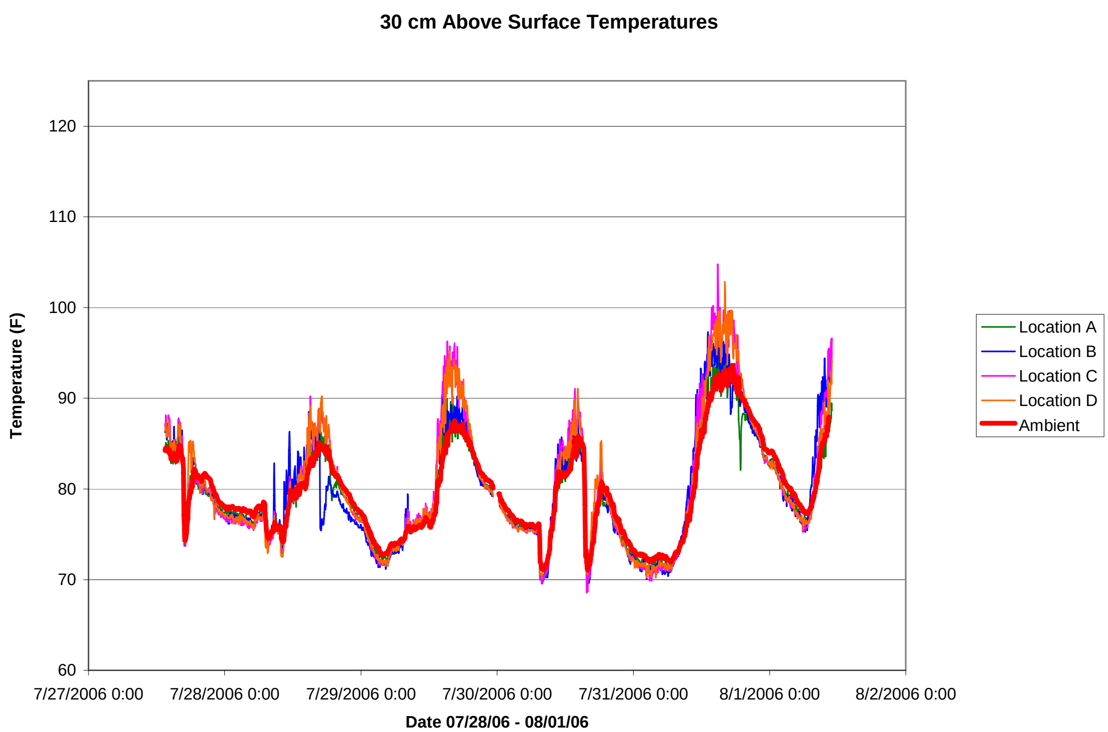

Figure 87. 30cm Temperatures 7/28 – 8/1/06

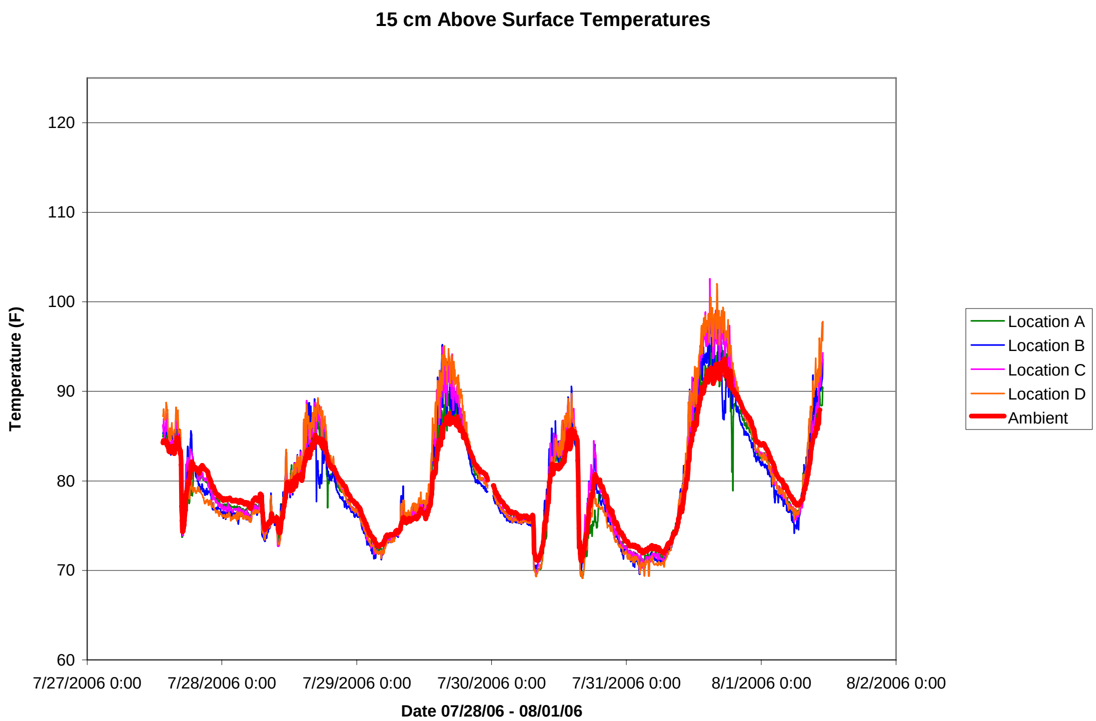

Figure 88. 15cm Temperatures 7/28 – 8/1/06

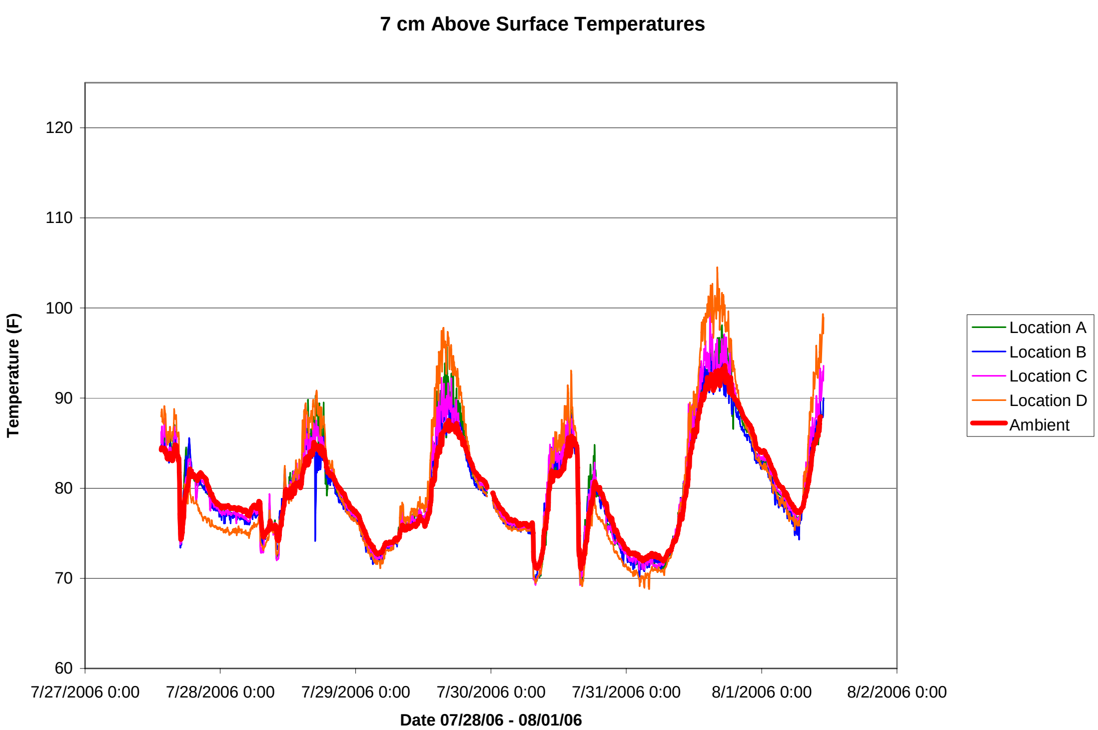

Figure 89. 7cm Temperatures 7/28 – 8/1/06

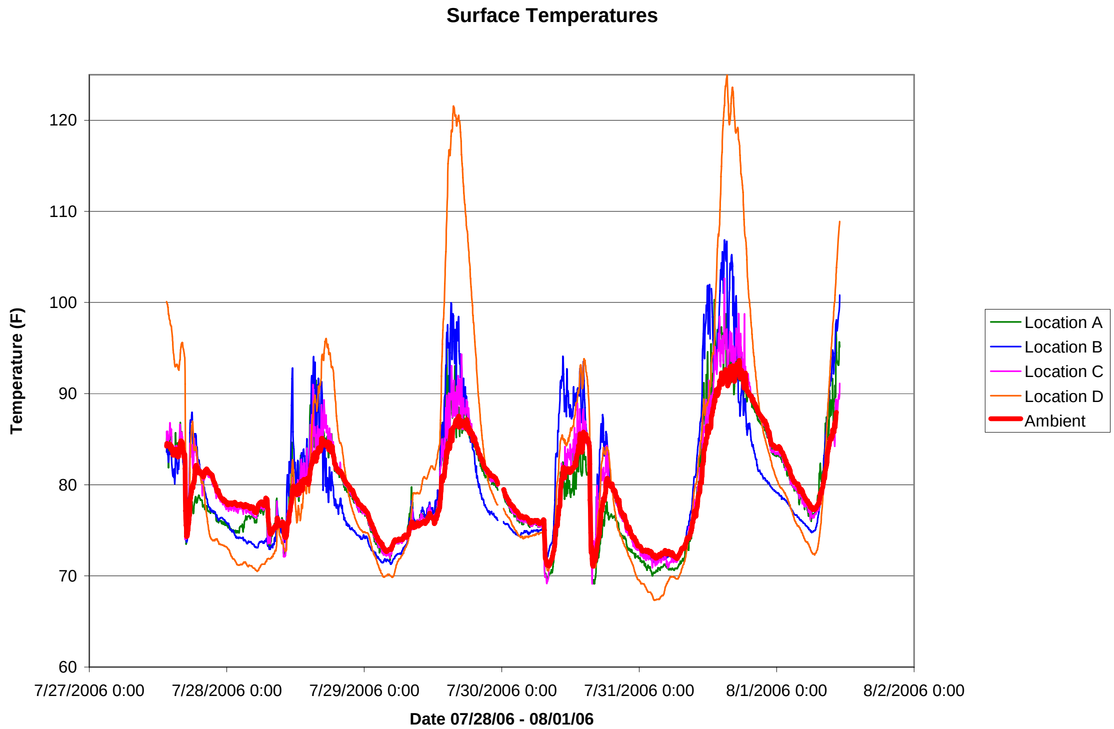

Figure 90. Surface Temperatures 7/28 – 8/1/06

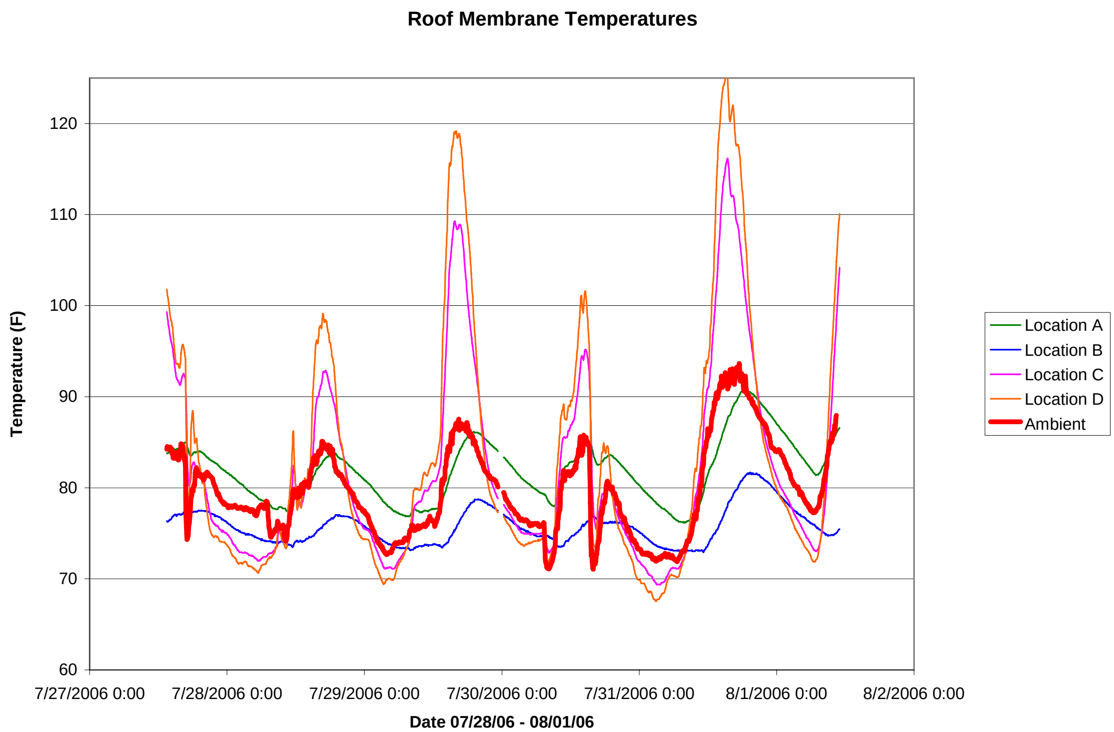

Figure 91. Roof Membrane Temperatures 7/28 – 8/1/06

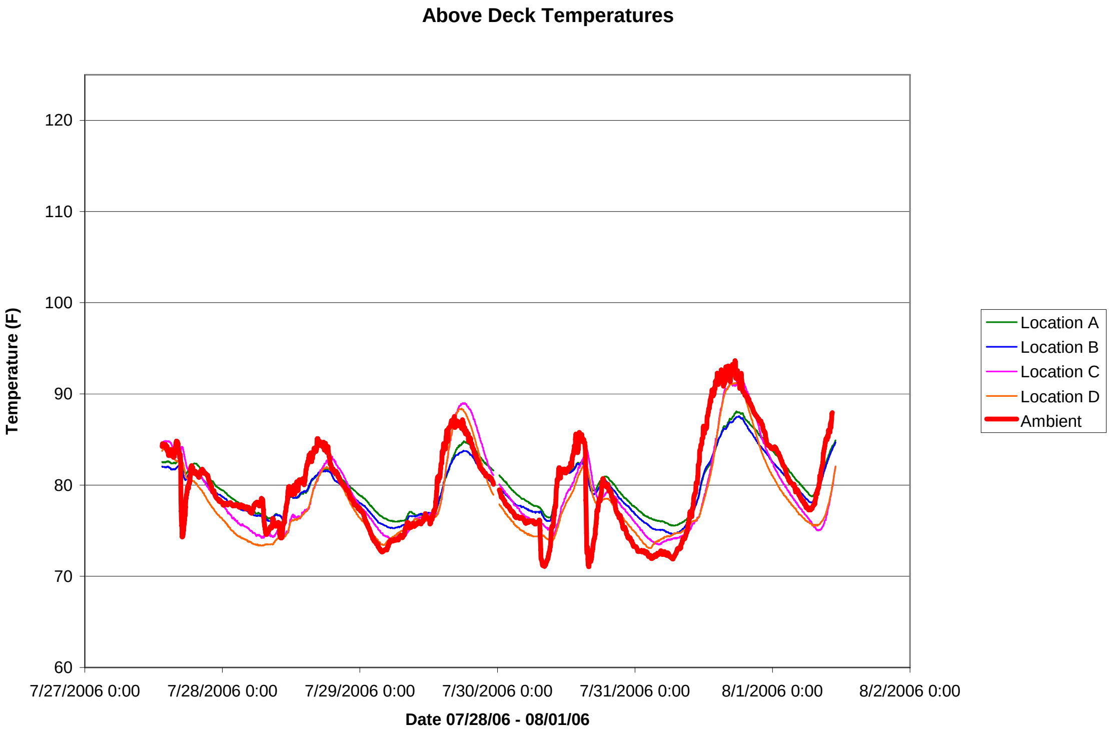

Figure 92. Above Deck Temperatures 7/28 – 8/1/06

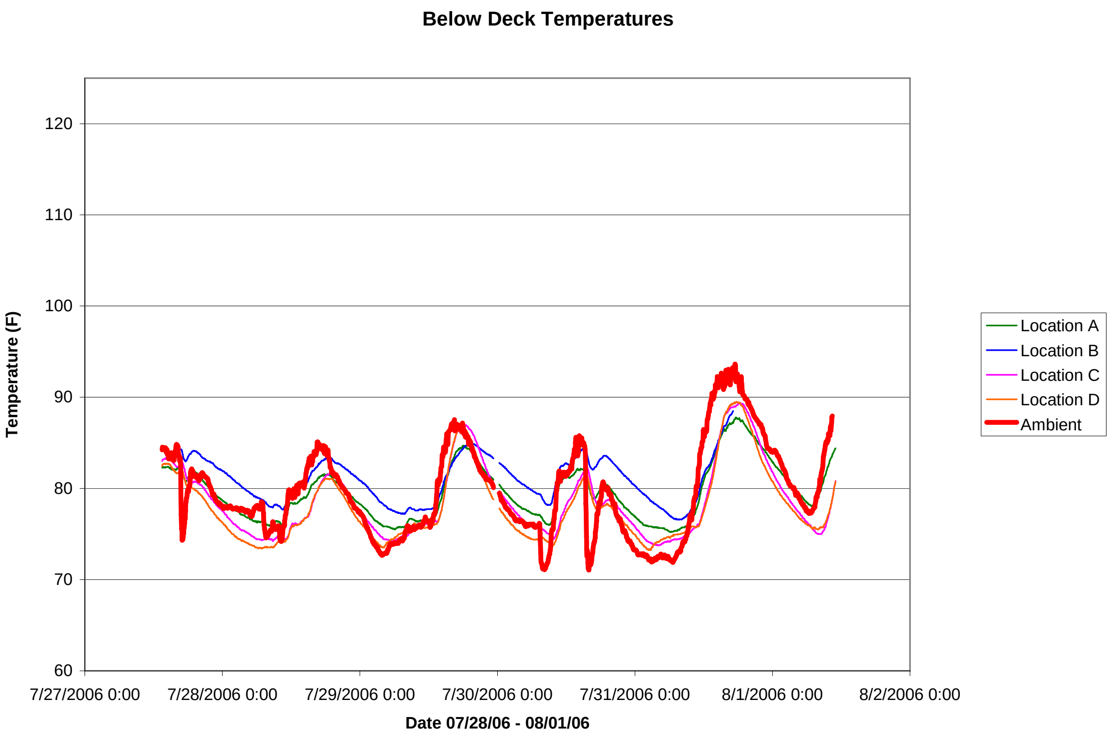

Figure 93. Below Deck Temperatures 7/28 – 8/1/06

Temperature Measurements from August 22, 2006 to August 29, 2006.

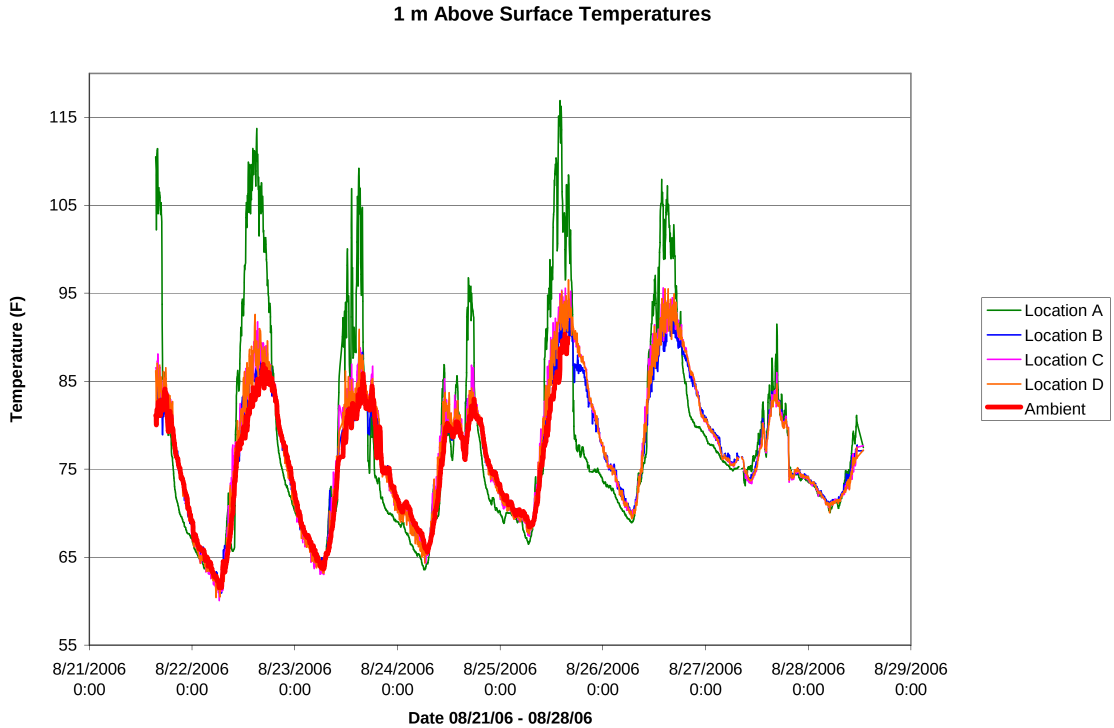

Figure 94. 1m Temperatures 8/21 – 8/28/06

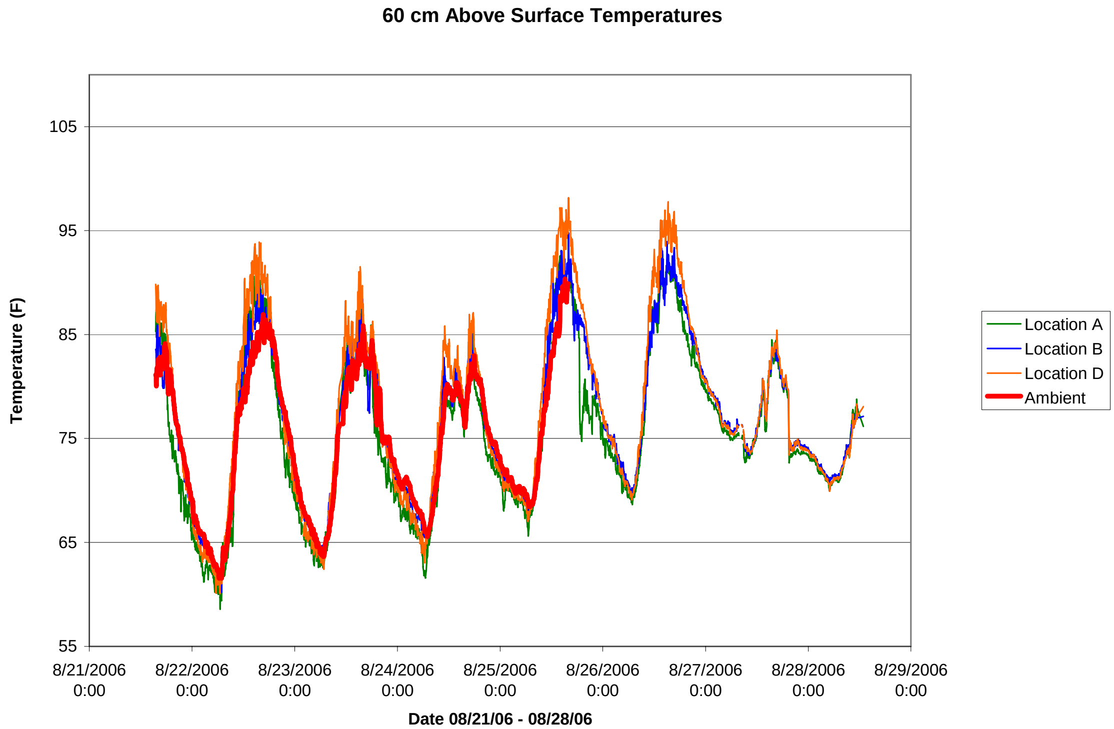

Figure 95. 60cm Temperatures for 8/21 – 8/28/06

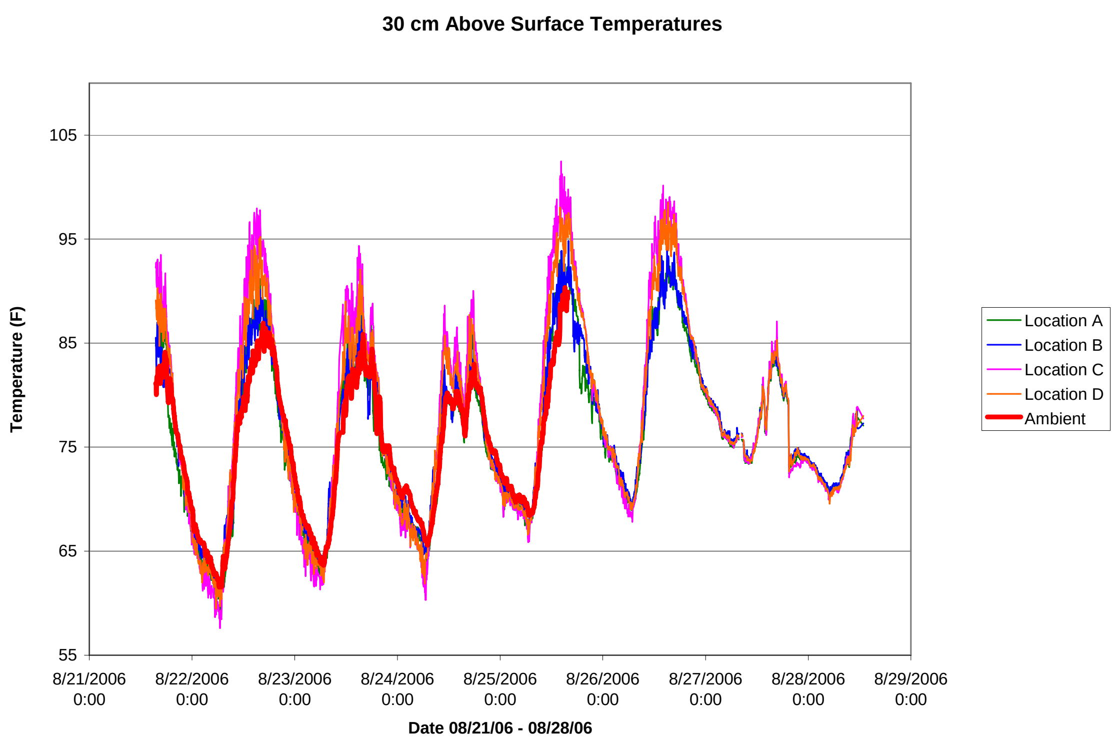

Figure 96. 30cm Temperatures for 8/21 – 8/28/06

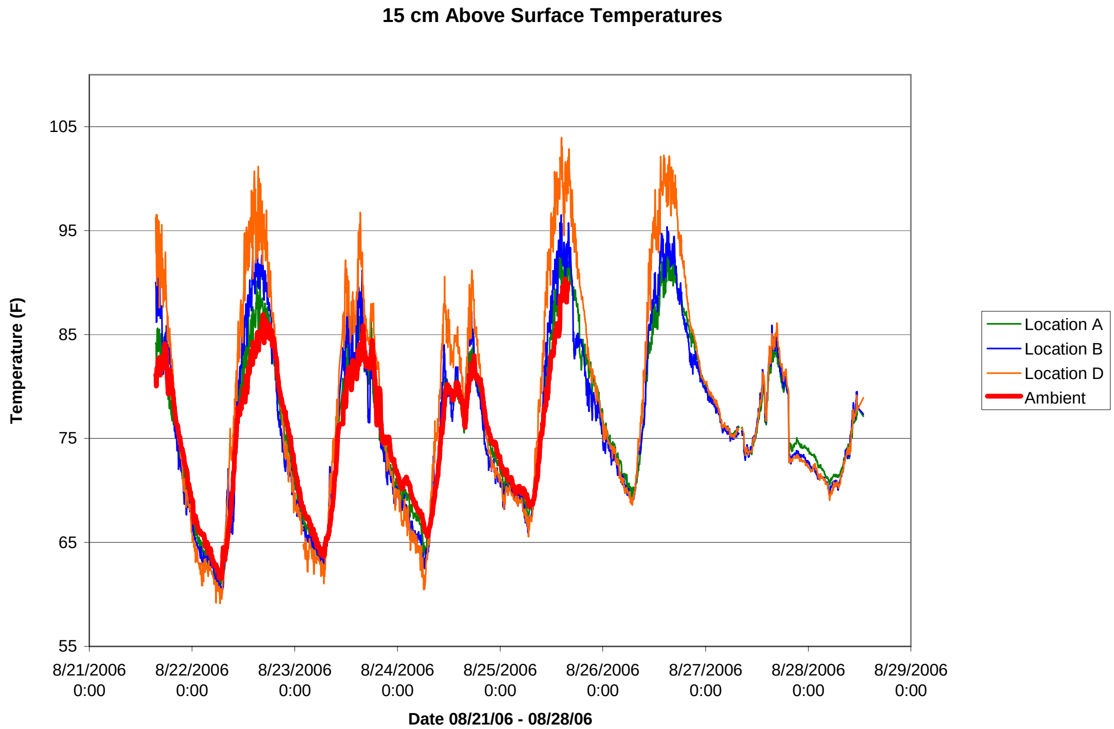

Figure 97. 15cm Temperatures for 8/21 – 8/28/06

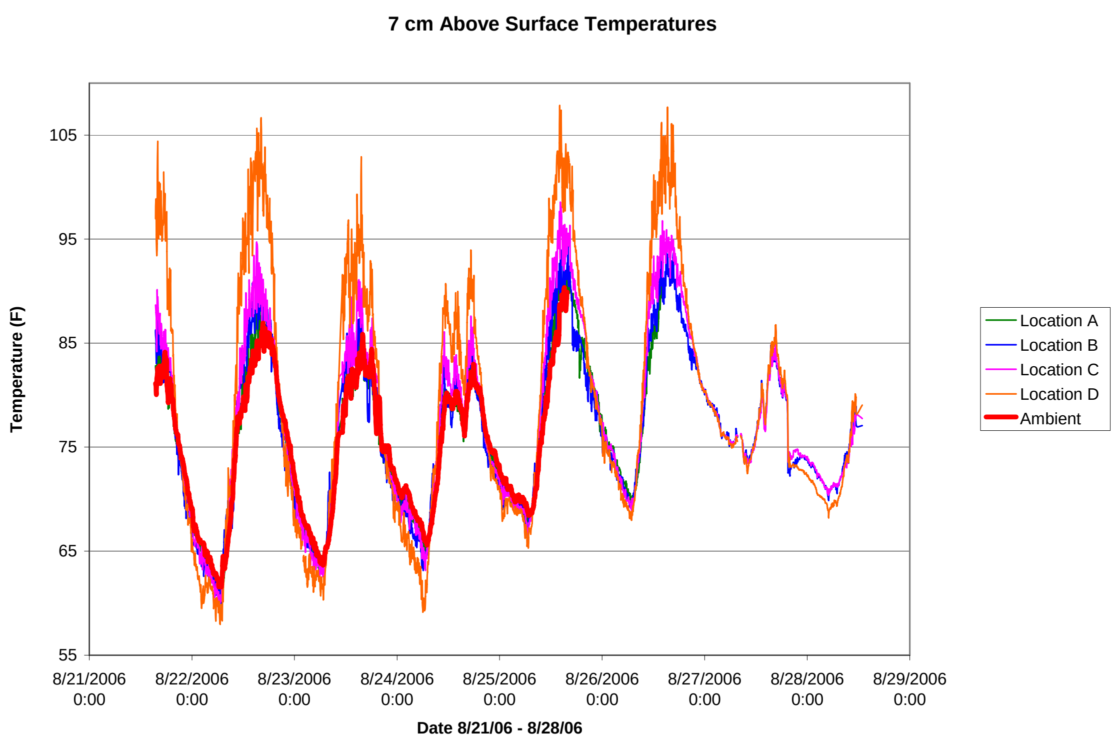

Figure 98. 7cm Temperatures for 8/21 – 8/28/06

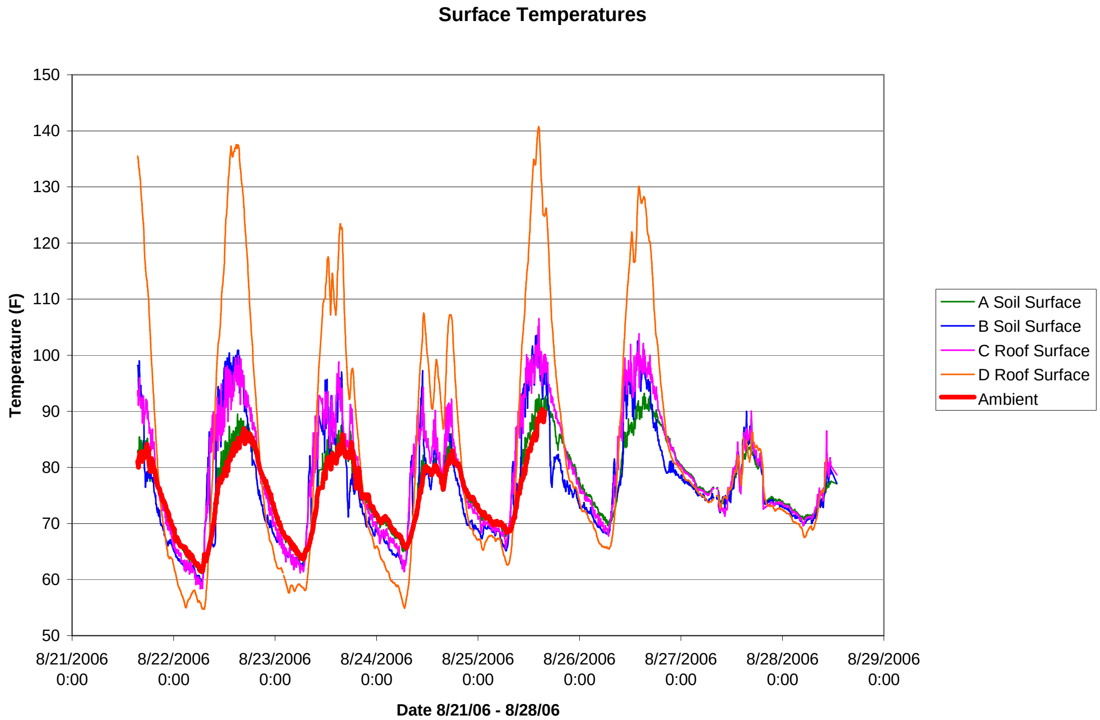

Figure 99. Surface Temperatures 8/21 – 8/28/06

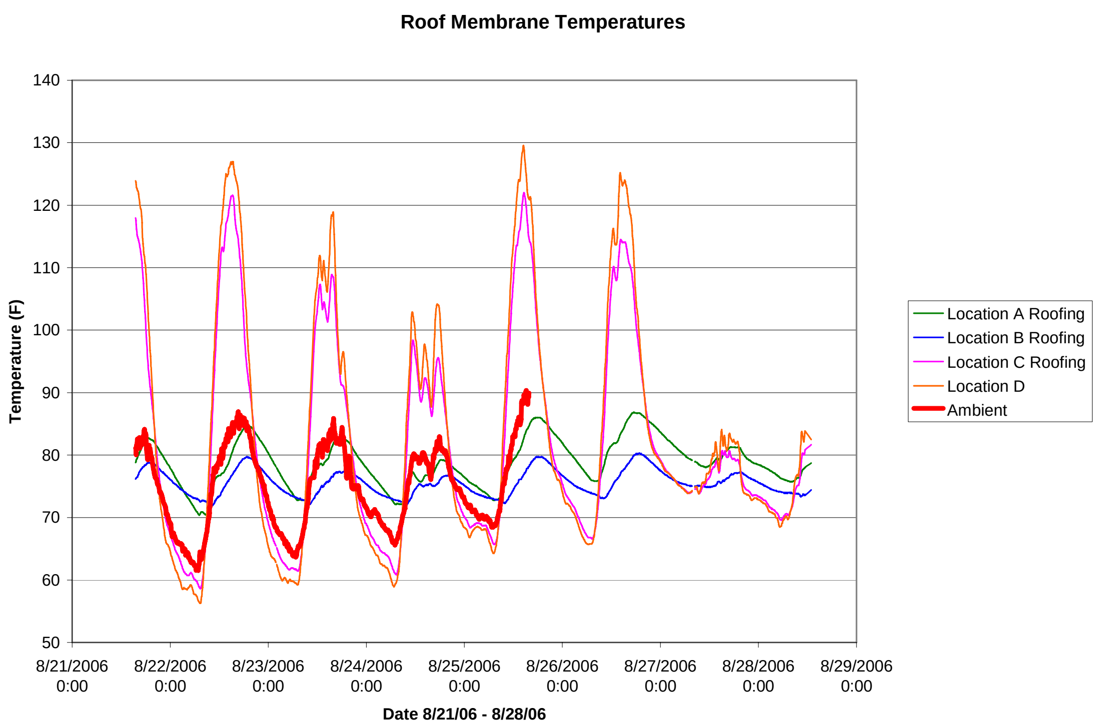

Figure 100. Roof Membrane Temperatures for 8/21 – 8/28/06

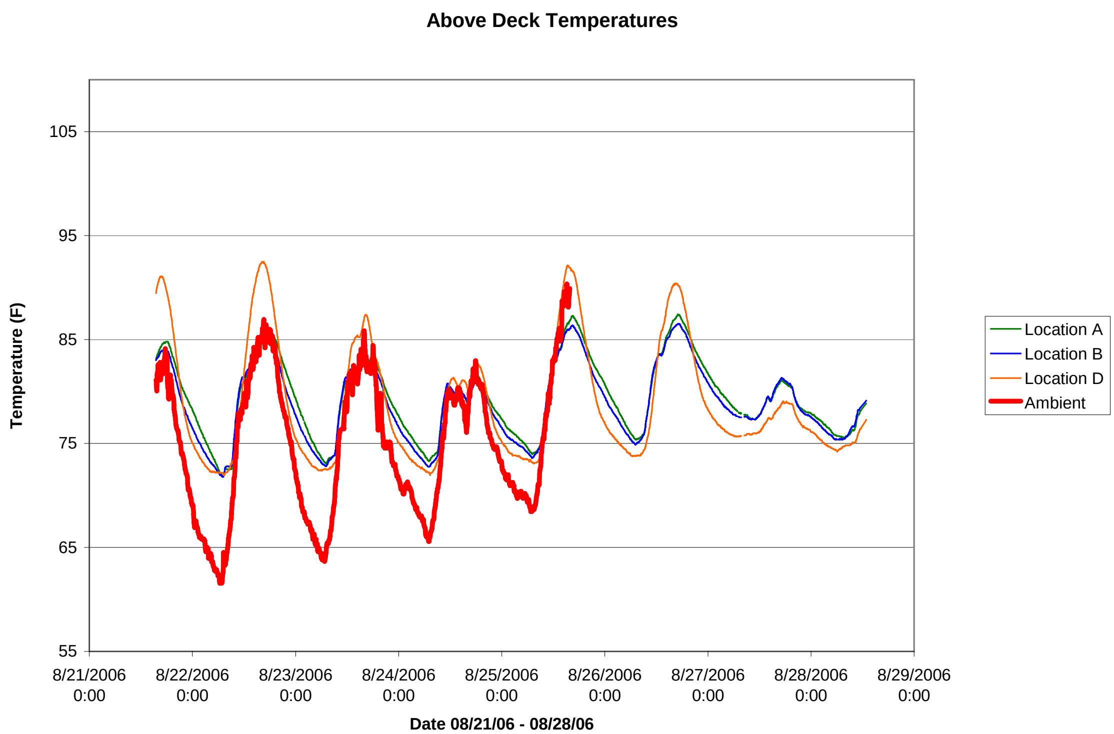

Figure 101. Above Deck Temperatures for 8/21 – 8/28/06

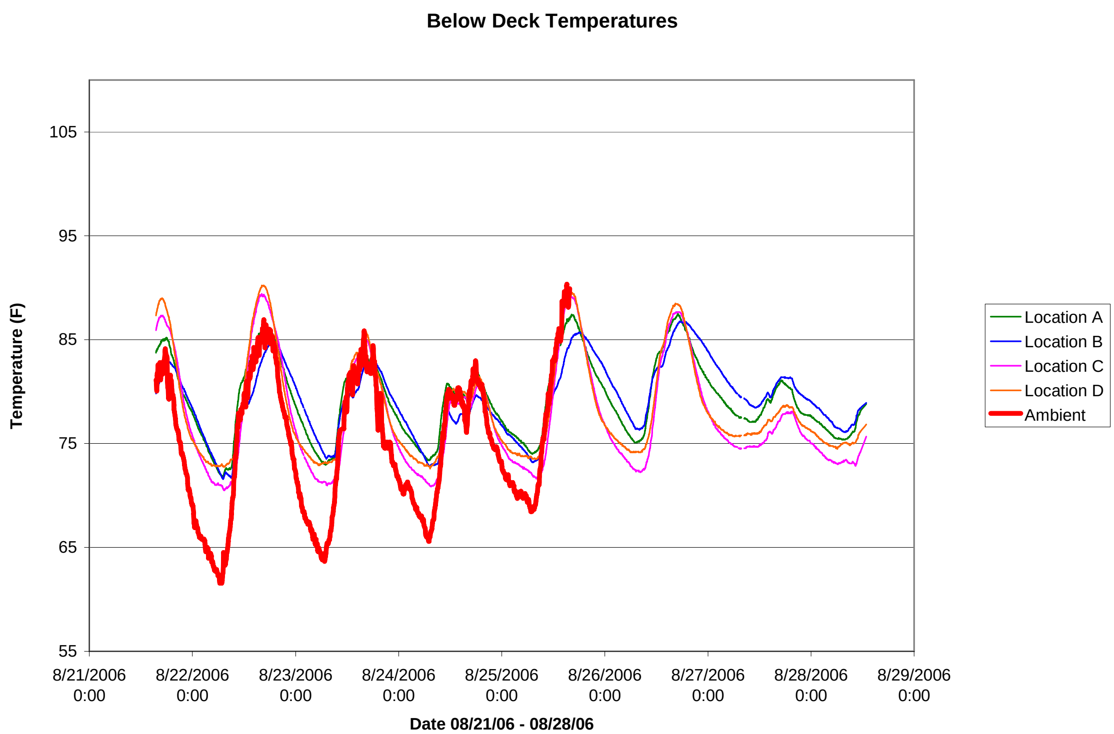

Figure 102. Below Deck Temperatures for 8/21 – 8/28/06

Temperature Measurements from September 1, 2006 to September 7, 2006.

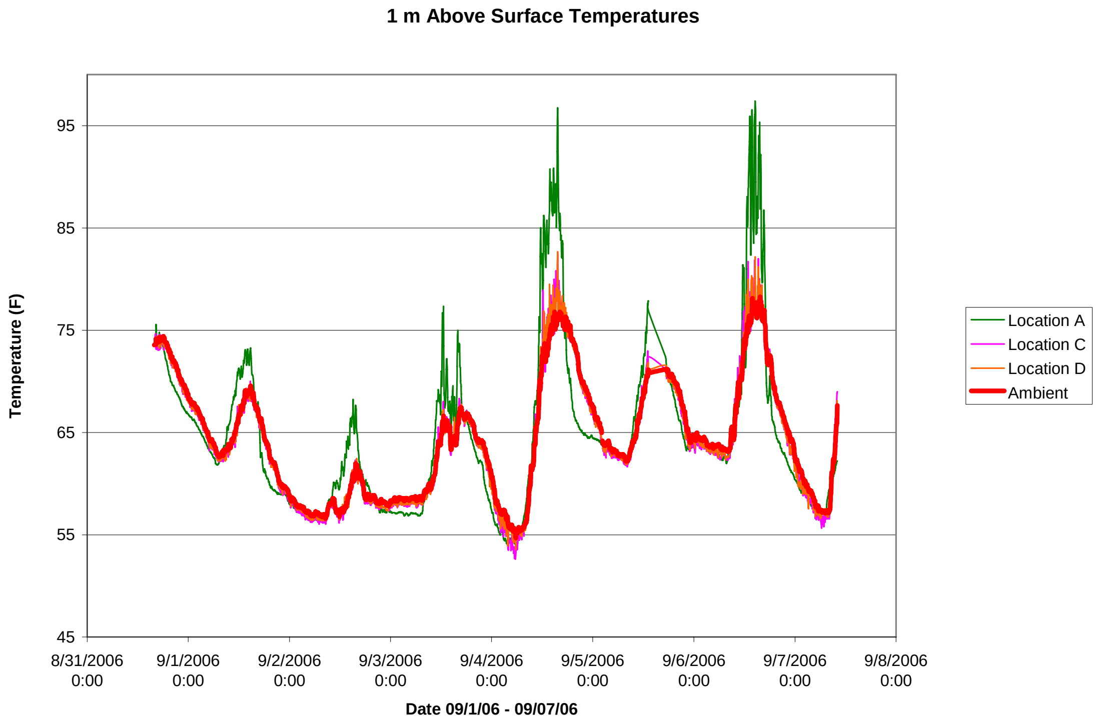

Figure 103. 1m Above Surface Temperatures for 9/1-7/06

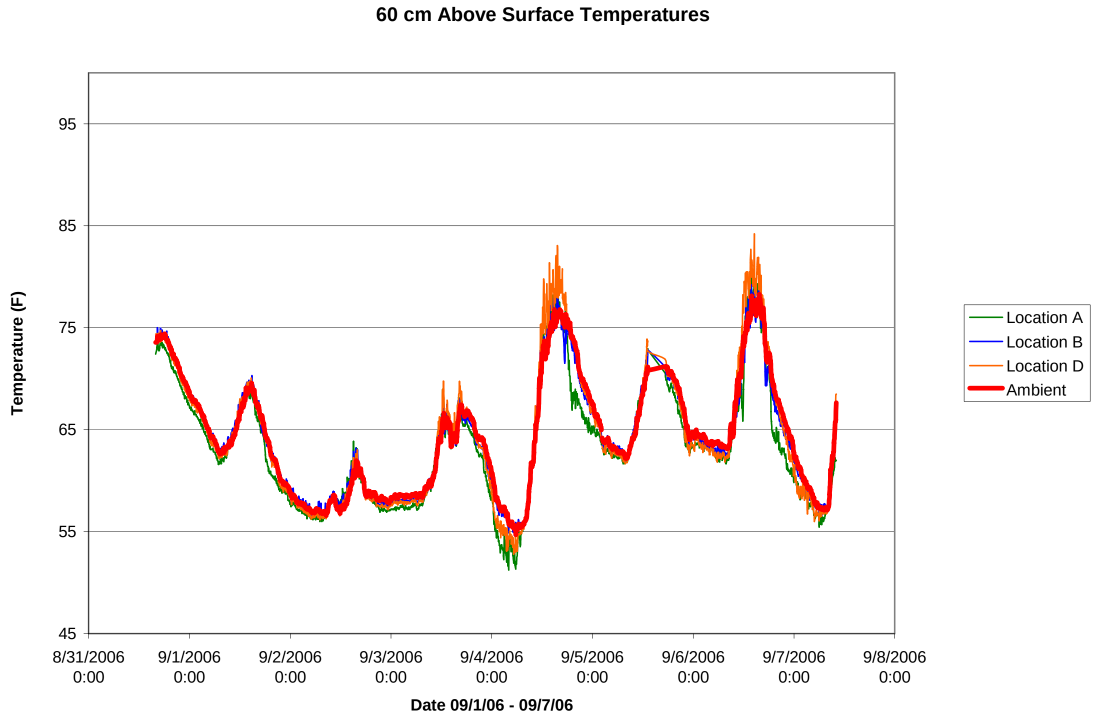

Figure 104. 60cm Above Surface Temperatures for 9/1-7/06

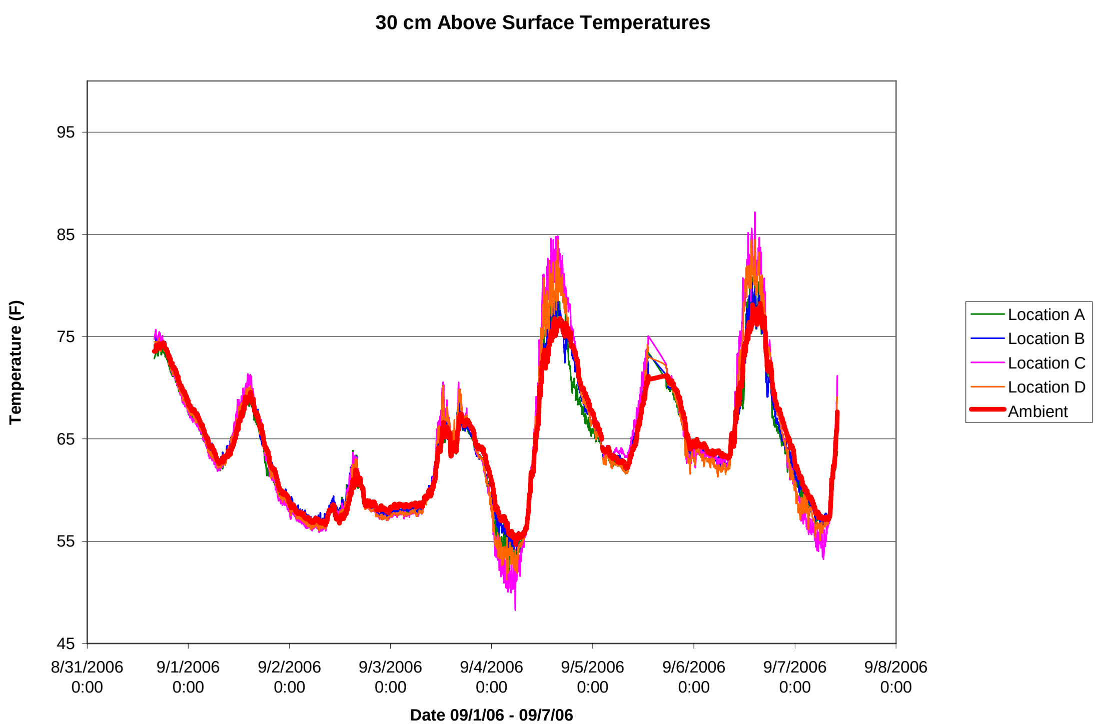

Figure 105. 30cm Above Surface Temperatures for 9/1-7/06

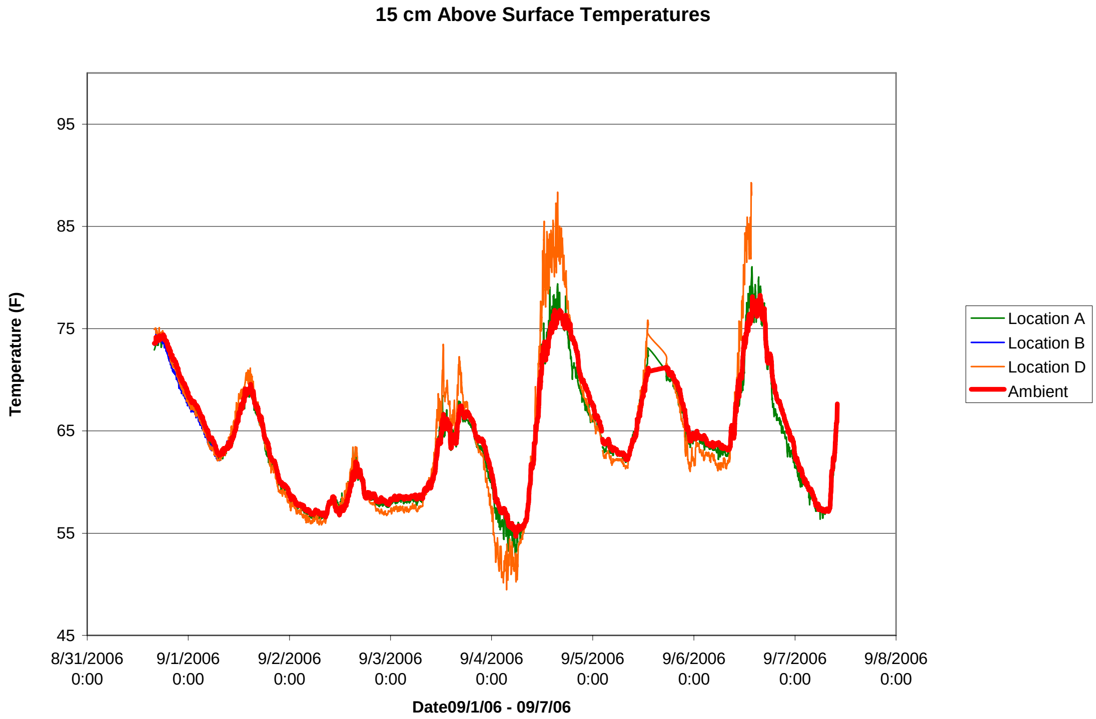

Figure 106. 15cm Above Surface Temperatures for 9/1-7/06

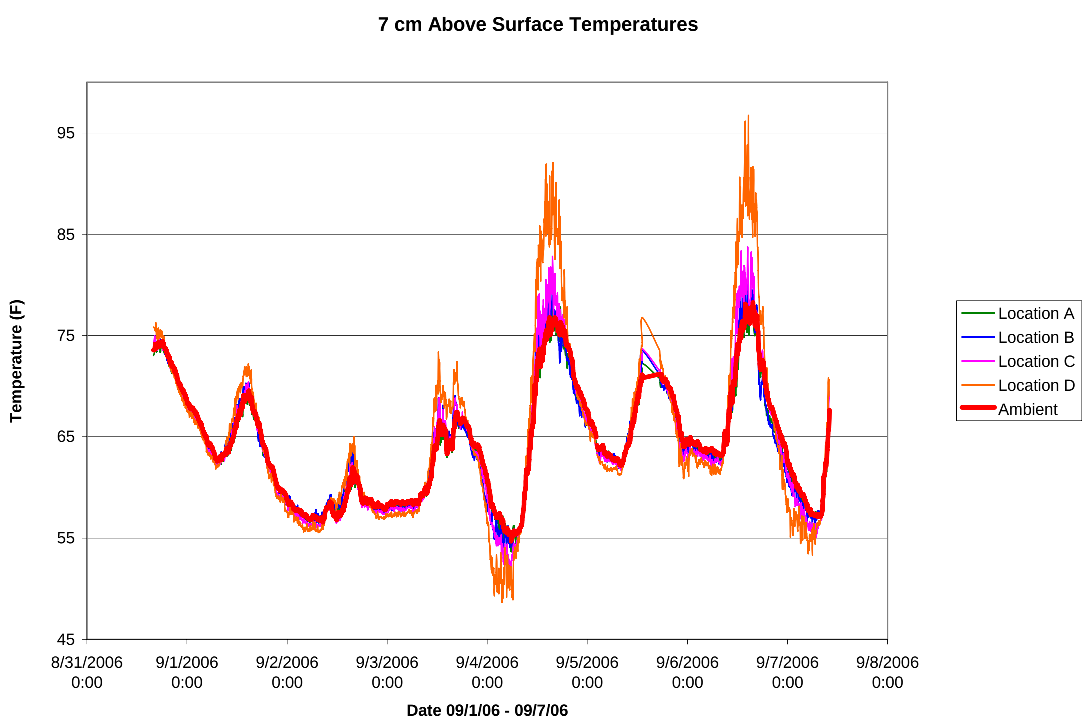

Figure 107. 7cm Above Surface Temperatures for 9/1-7/06

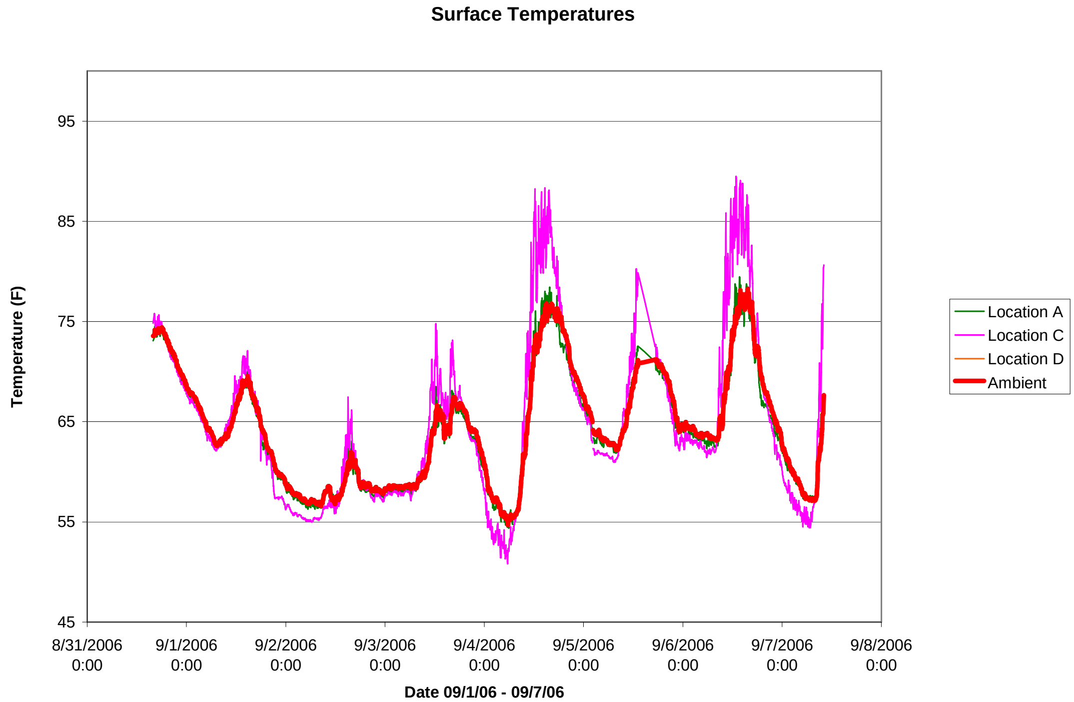

Figure 108. Surface Temperatures for 9/1-7/06

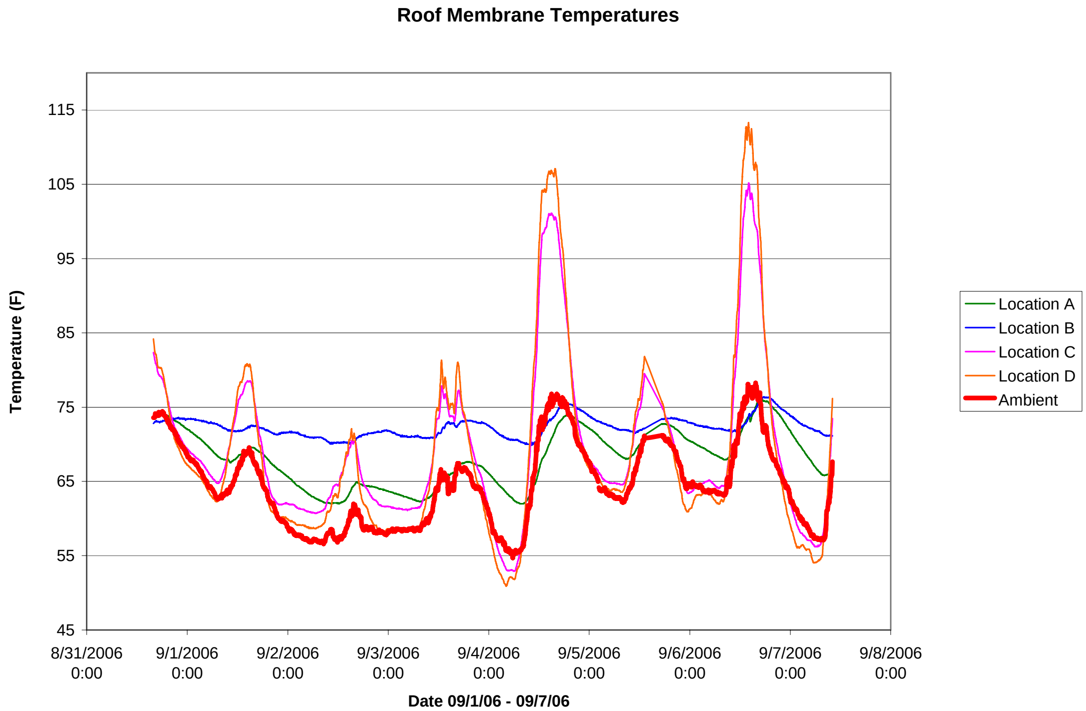

Figure 109. Roof Membrane Temperatures for 9/1-7/06

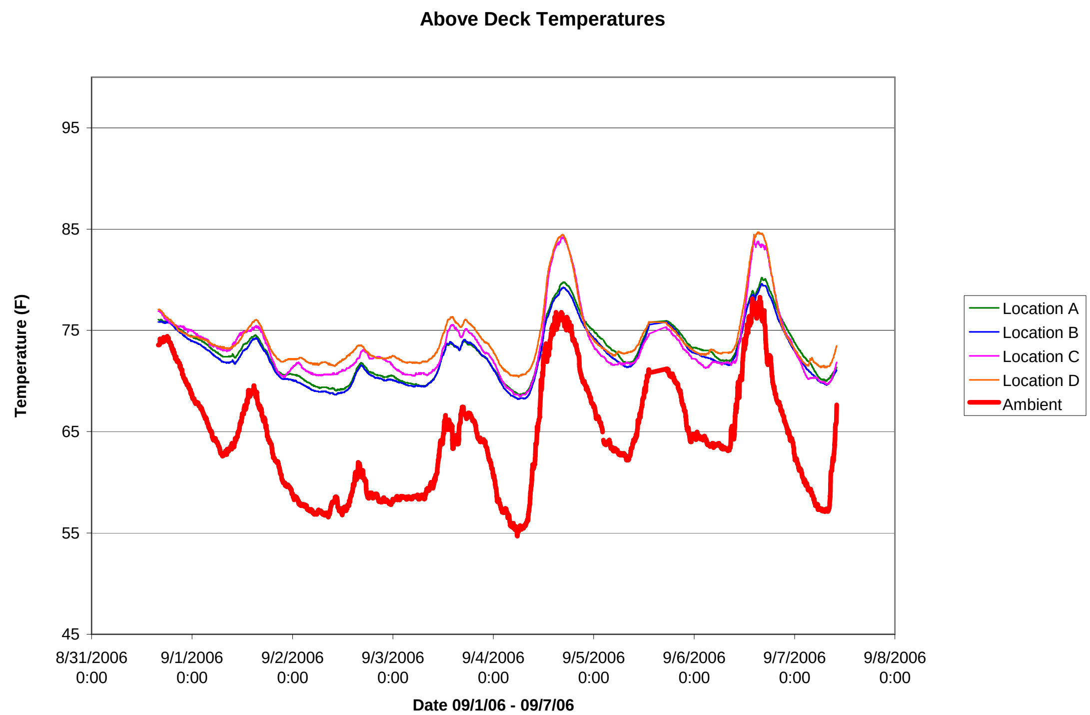

Figure 110. Above Deck Temperatures for 9/1-7/06

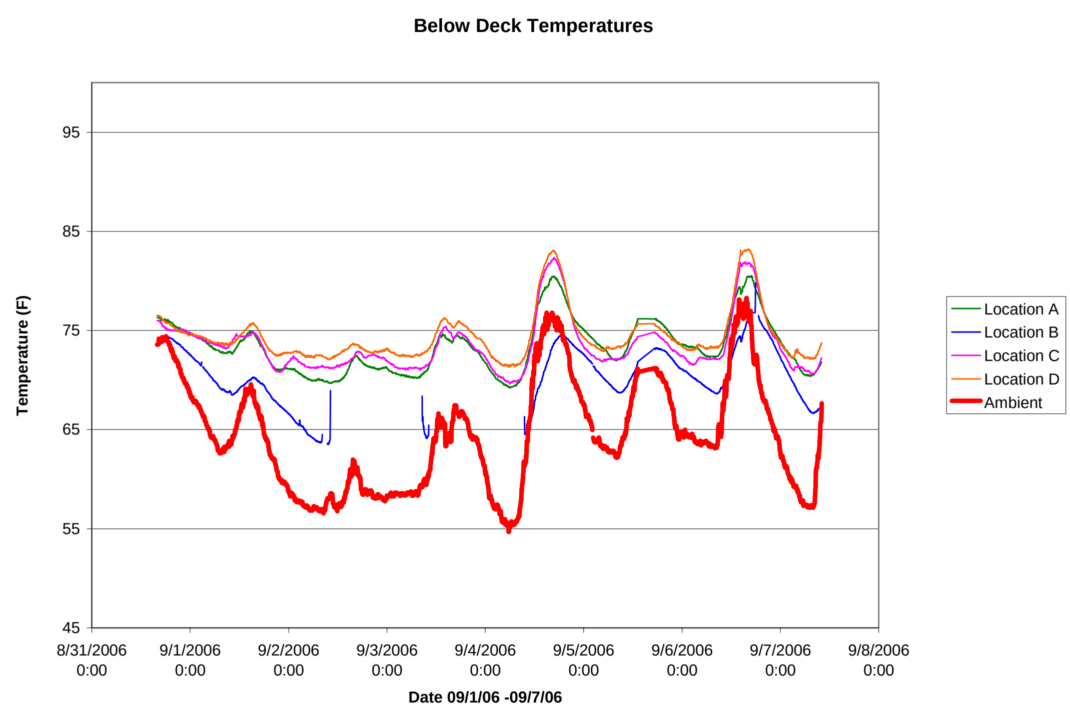

Figure 111. Below deck Temperatures for 9/1-7/06

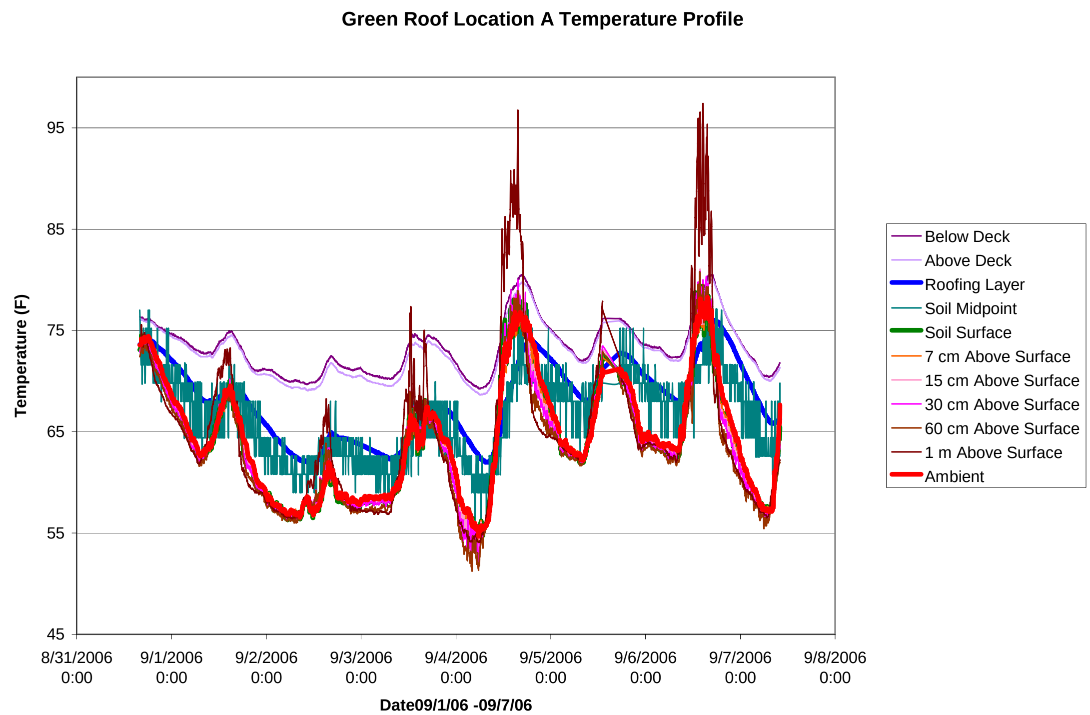

Figure 112. Green Roof Location A Temperature Profile for 9/1-7/06

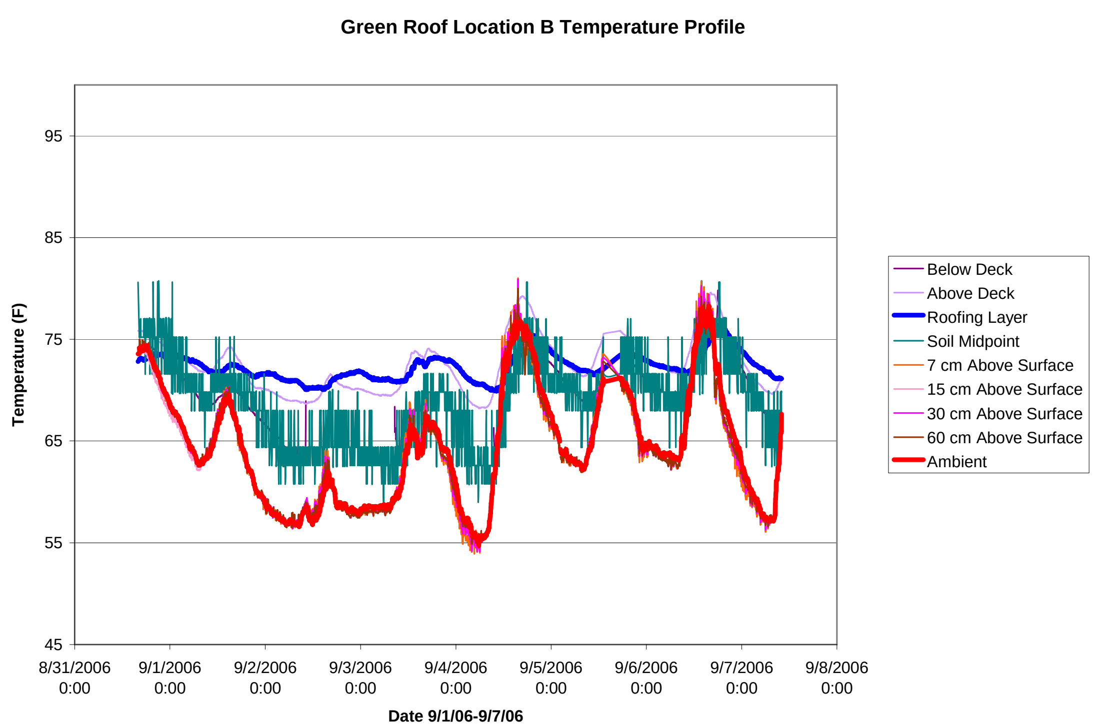

Figure 113. Green Roof Location B Temperature Profile for 9/1-7/06

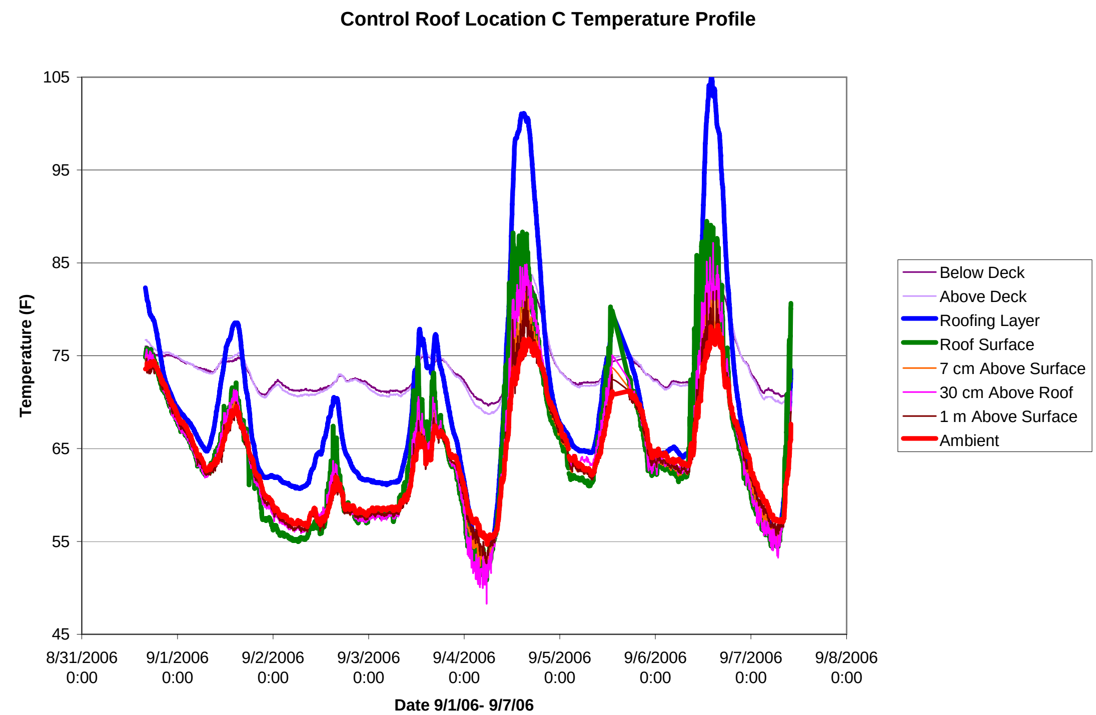

Figure 114. Control Roof Location C Temperature Profile for 9/1-7/06

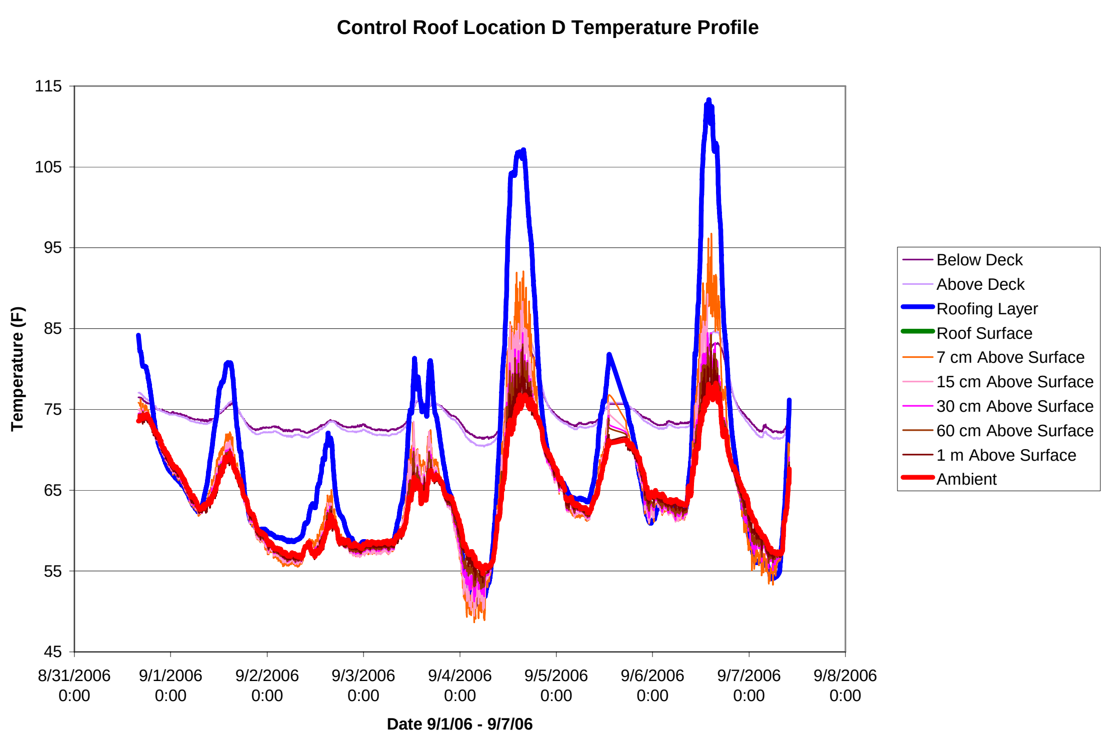

Figure 115. Control Roof Location D Temperature Profile for 9/1-7/06

Temperature Measurements from September 15, 2006 to September 19, 2006

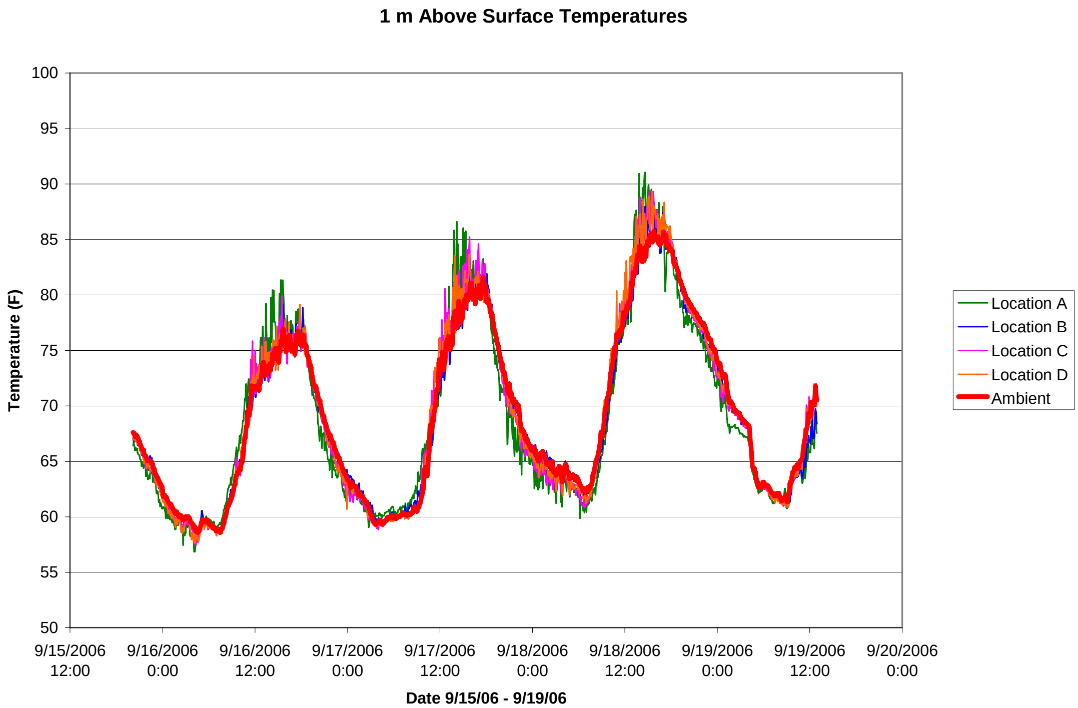

Figure 116. 1m Above Surface Temperatures for 9/15-19/06

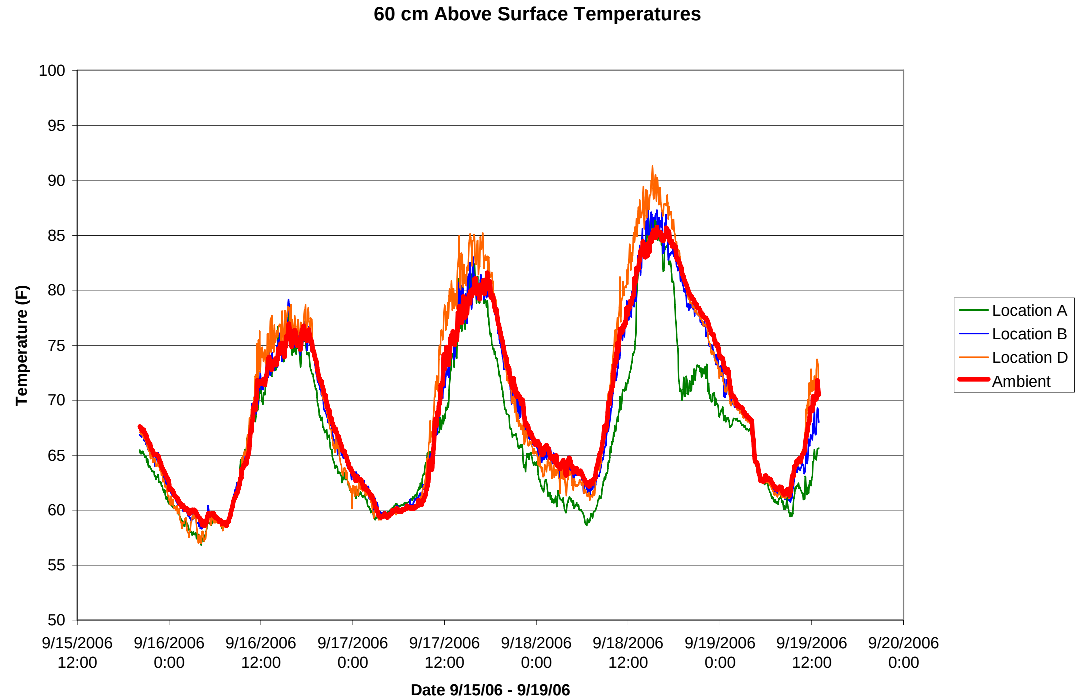

Figure 117. 60cm Above Surface Temperatures for 9/15-19/06

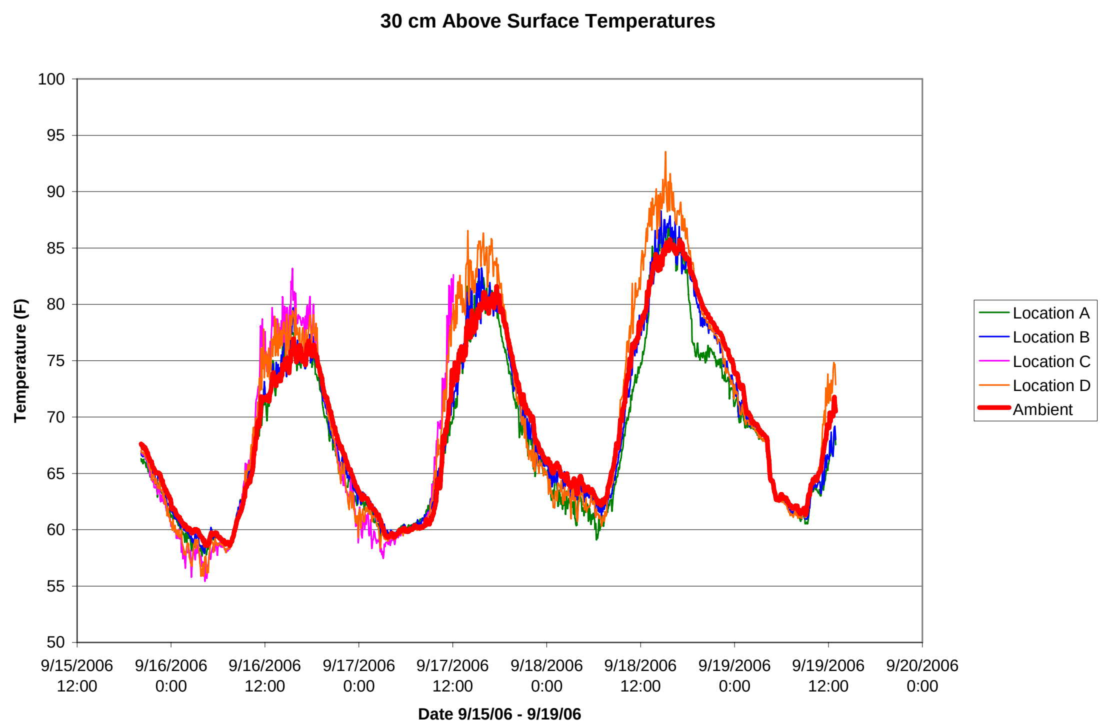

Figure 118. 30cm Above Surface Temperatures for 9/15-19/06

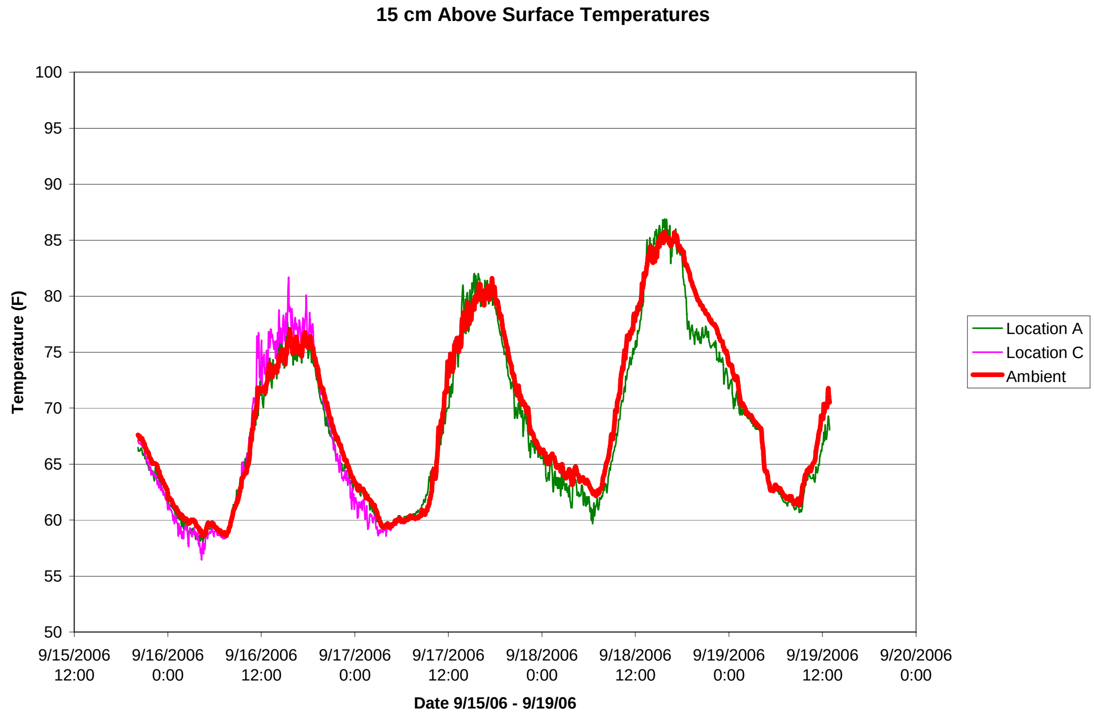

Figure 119. 15cm Above Surface Temperatures for 9/15-19/06

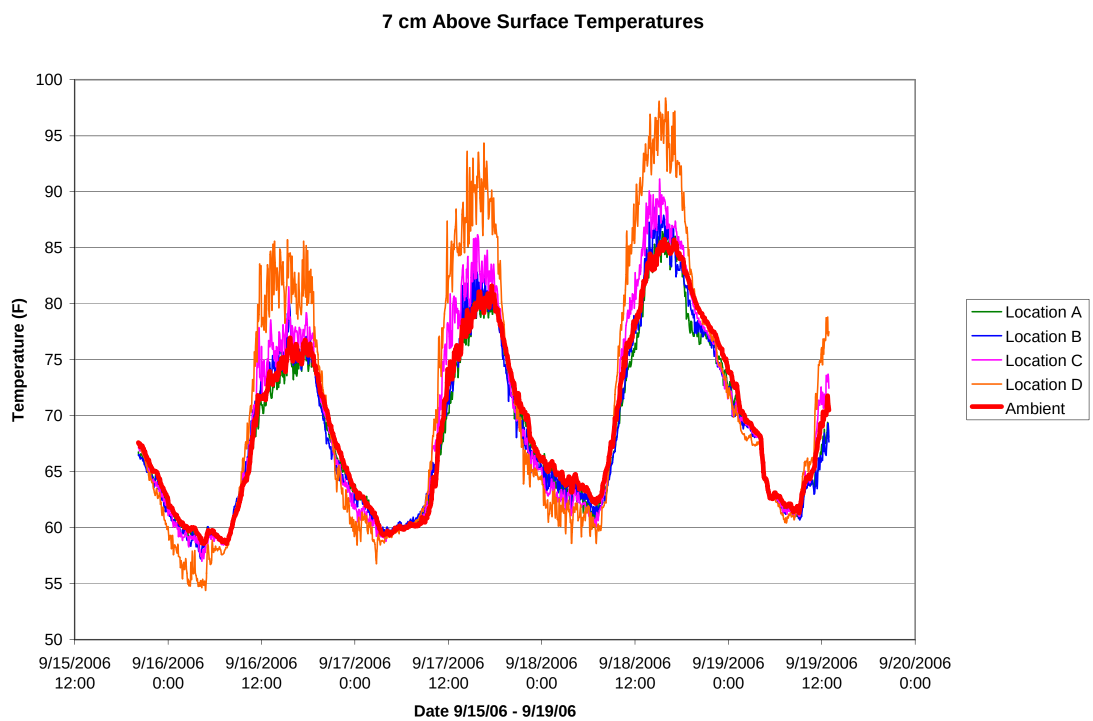

Figure 120. 7cm Above Surface Temperatures for 9/15-19/06

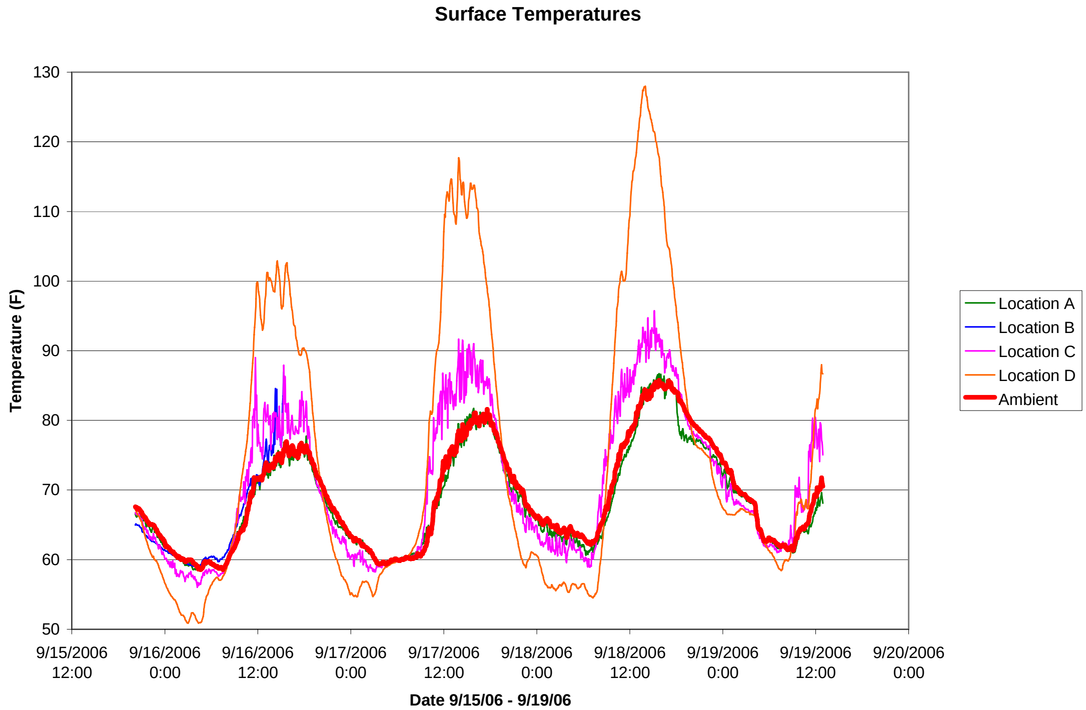

Figure 121. Surface Temperatures for 9/15-19/06

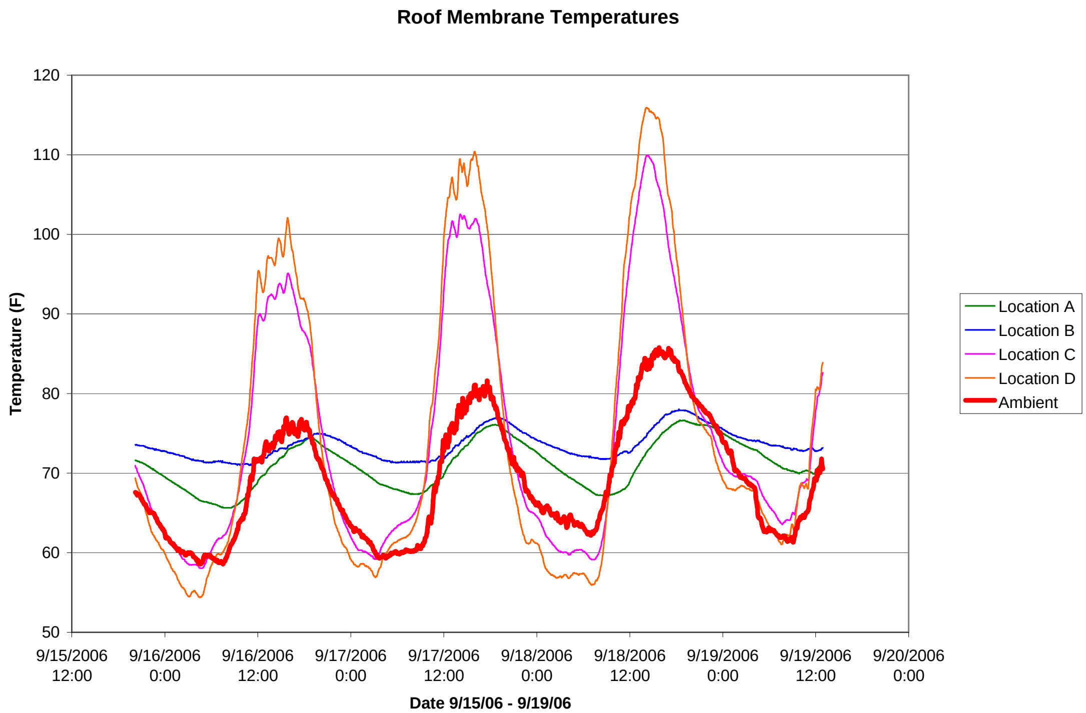

Figure 122. Roof Membrane Temperatures for 9/15-19/06

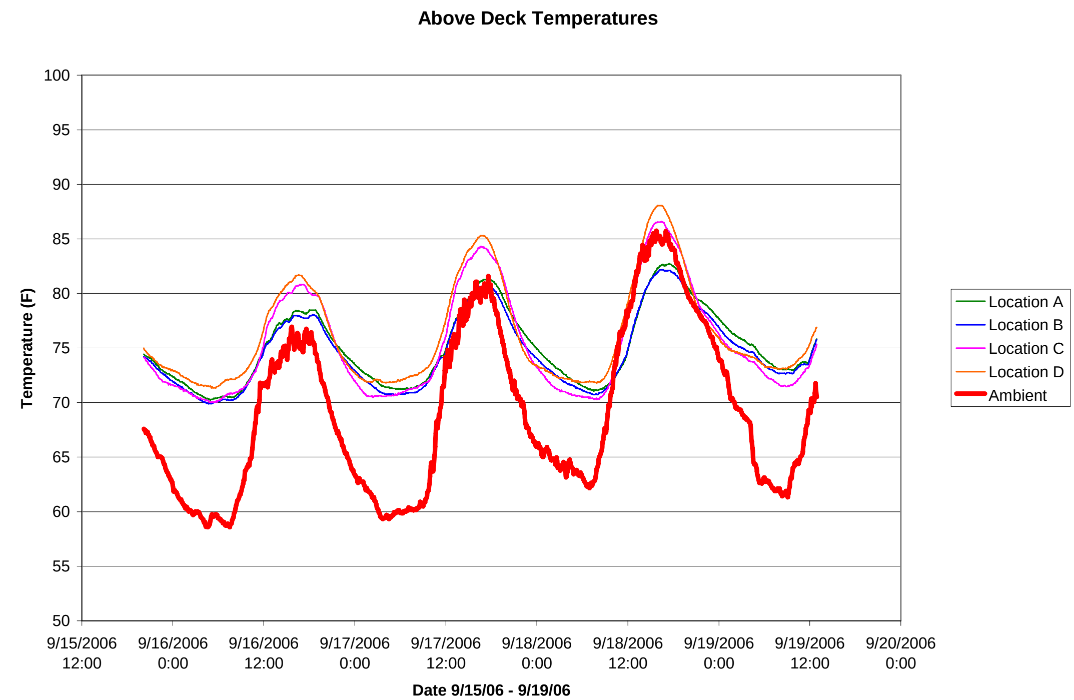

Figure 123. Above Deck Temperatures for 9/15-19/06

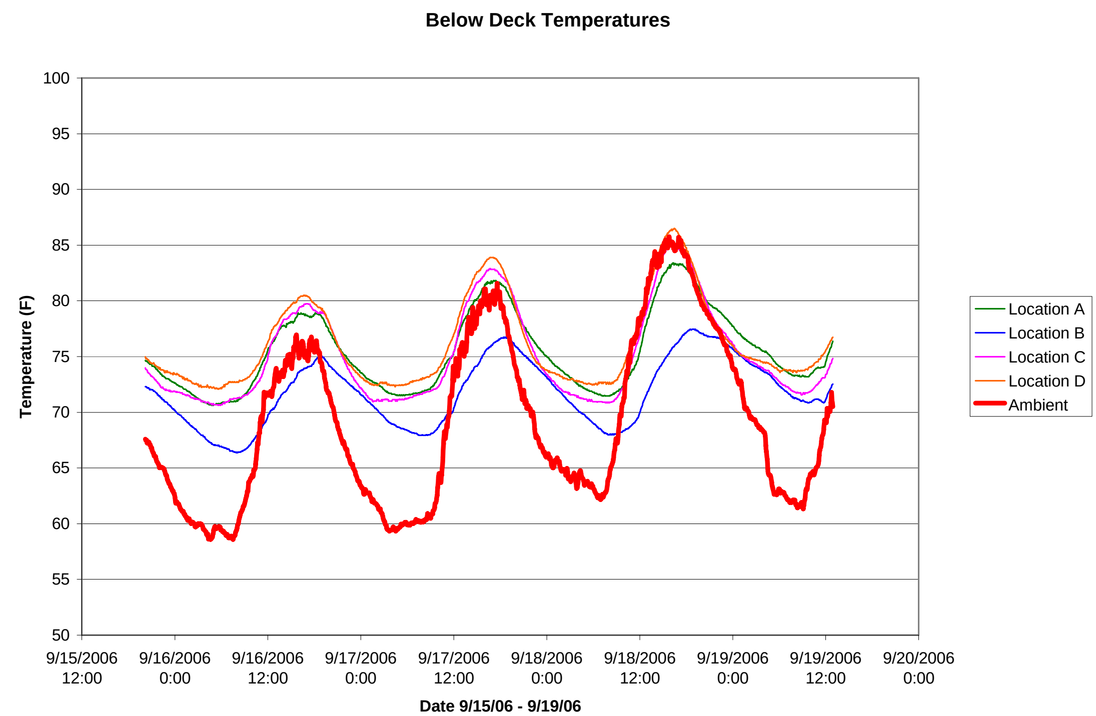

Figure 124. Below Deck Temperatures for 9/15-19/06

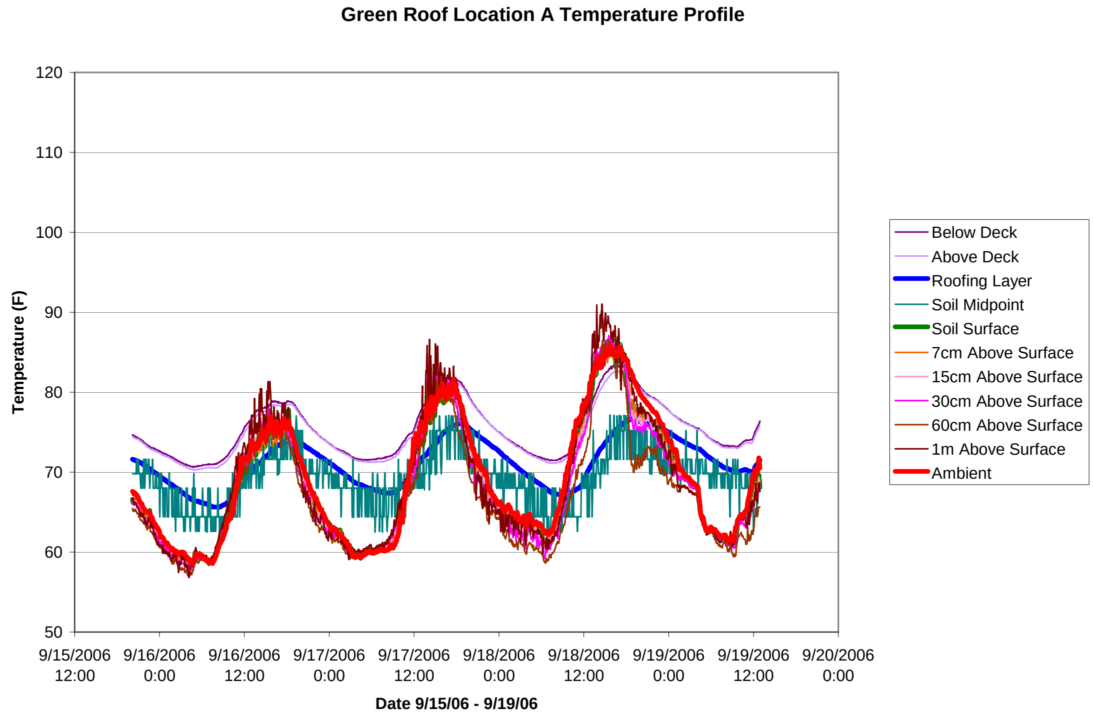

Figure 125. Green Roof Location A Temperature Profile for 9/15-19/06

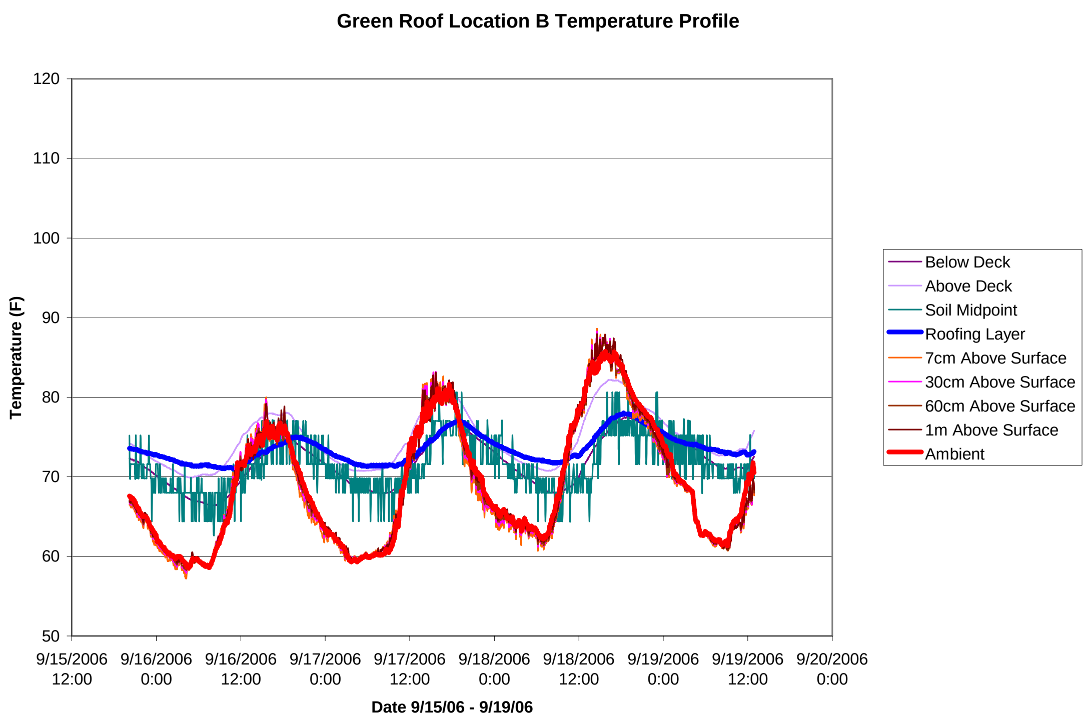

Figure 126. Green Roof Location B Temperature Profile for 9/15-19/06

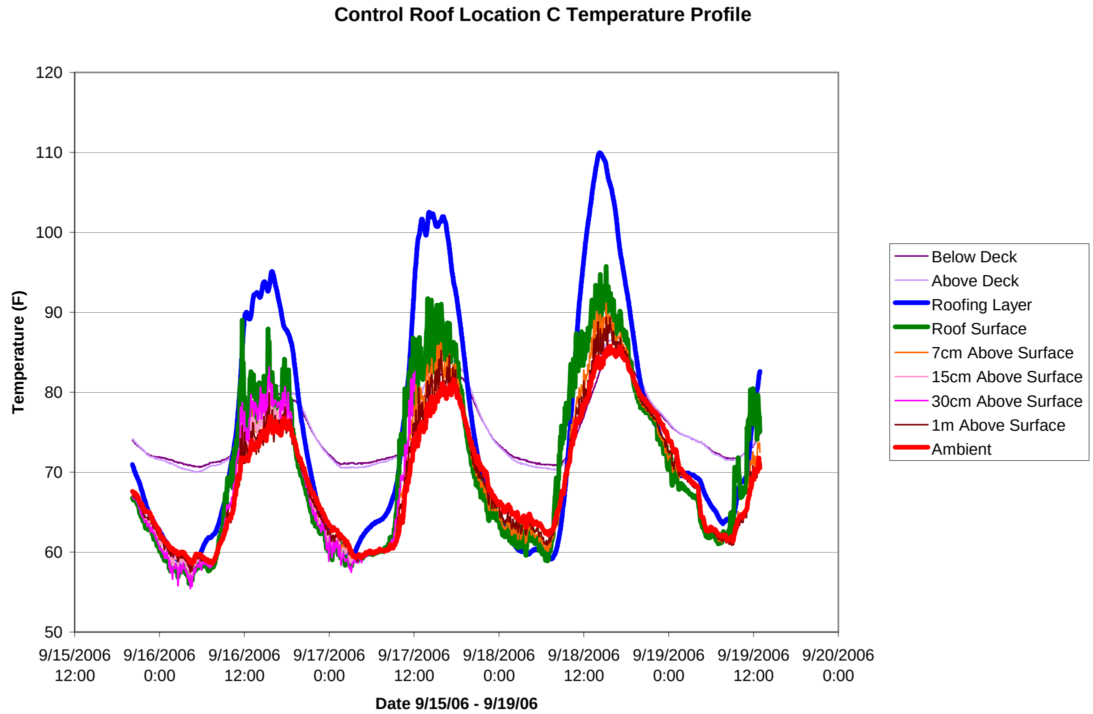

Figure 127. Control Roof Location C Temperature Profile for 9/15-19/06

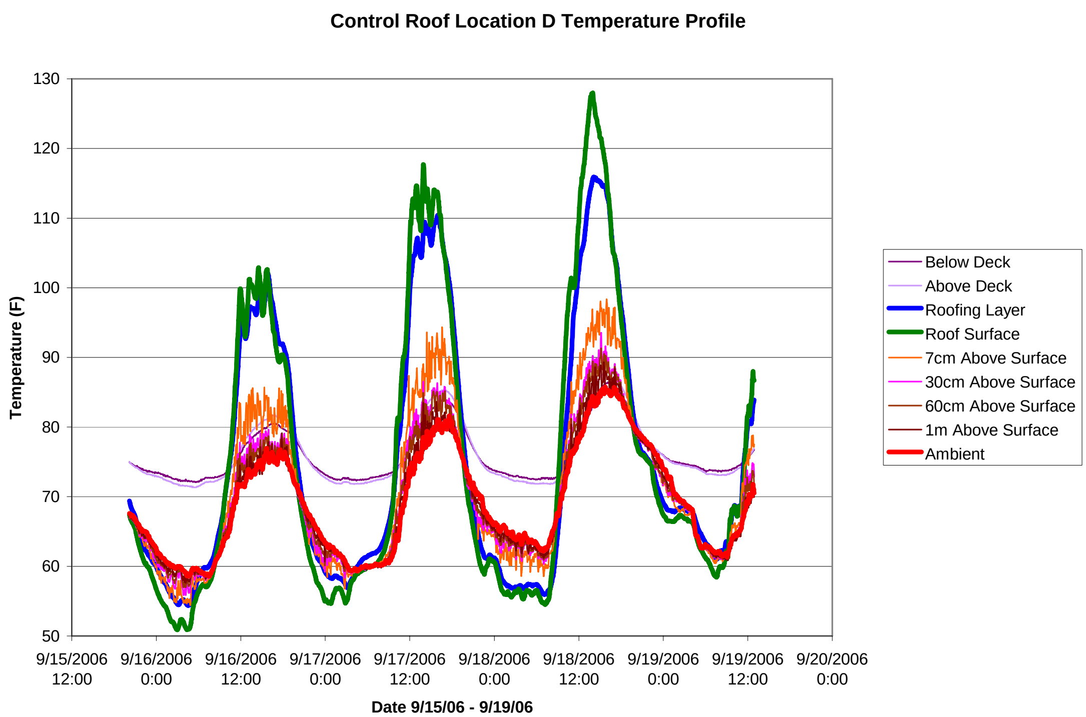

Figure 128. Control Roof Location D Temperature Profile for 9/15-19/06

Temperature Measurements from September 19, 2006 to September 25, 2006

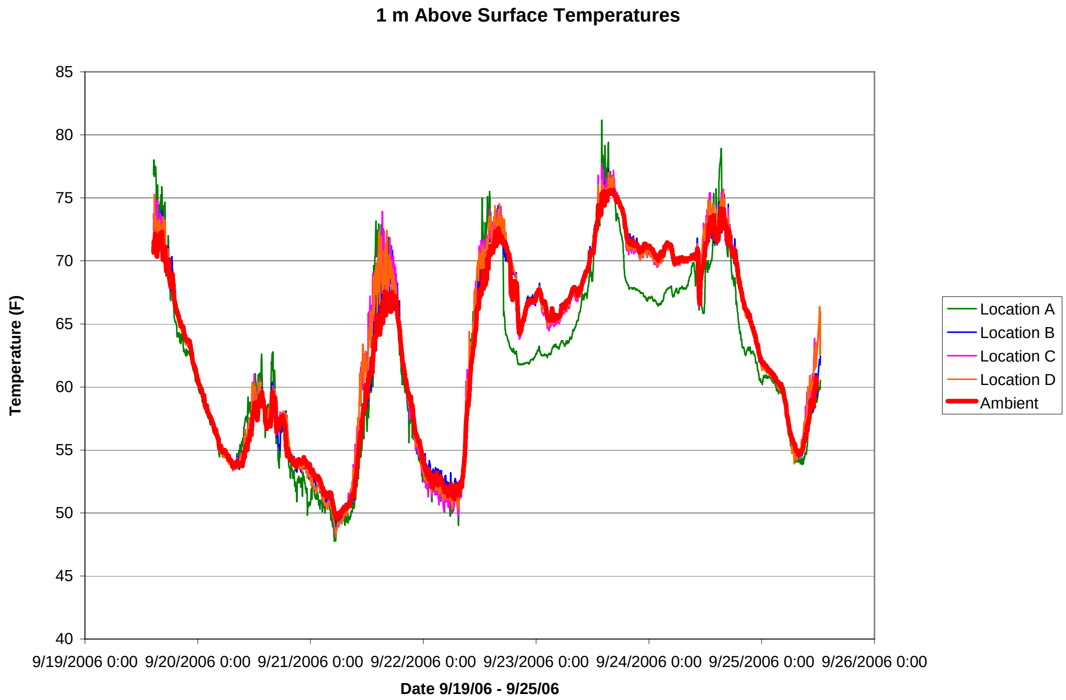

Figure 129. 1m Above Surface Temperatures for 9/19/06 – 9/25/06

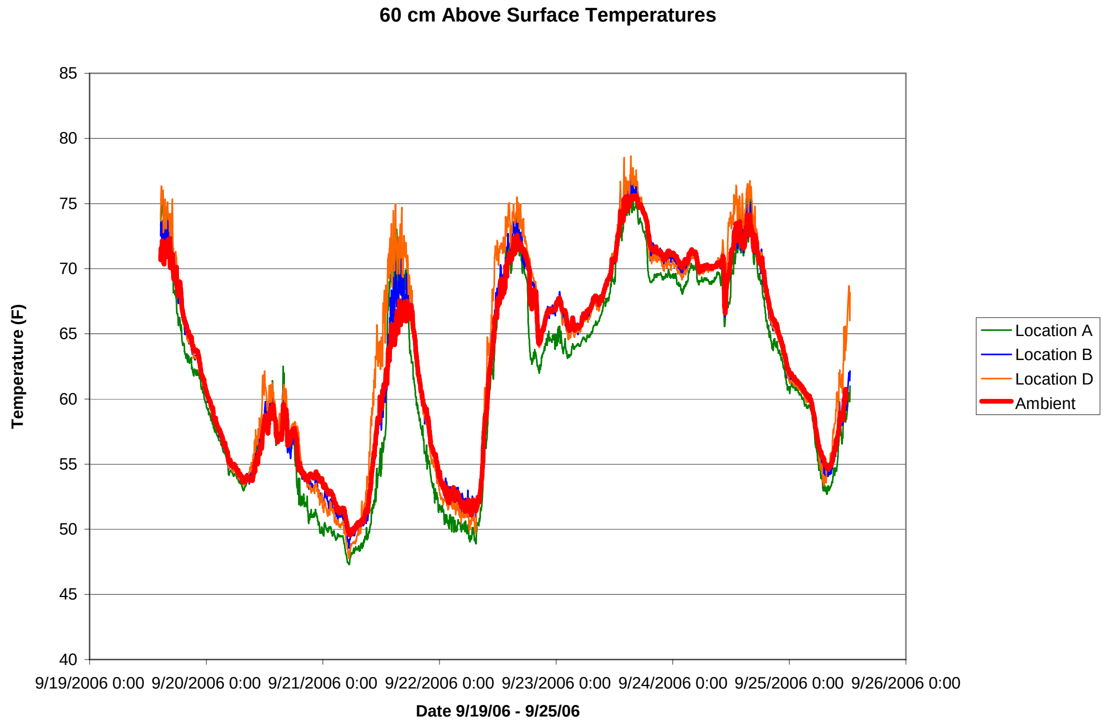

Figure 130. 60cm Above Surface Temperatures for 9/19/06 – 9/25/06

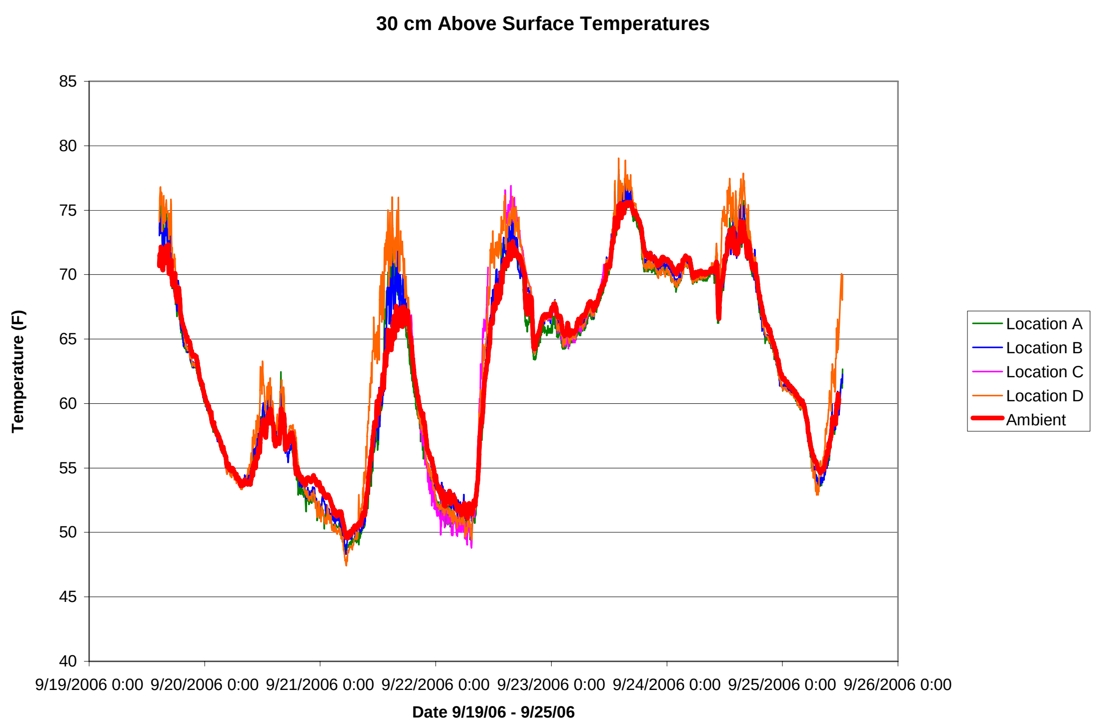

Figure 131. 30 cm Above Surface Temperatures for 9/19/06 – 9/25/06

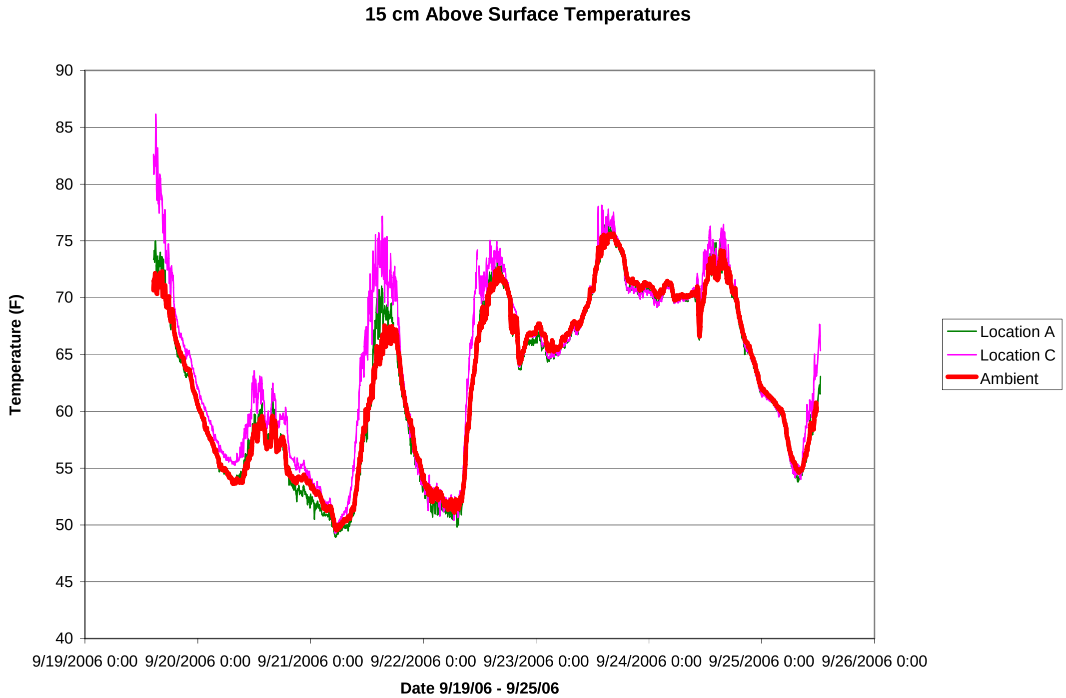

Figure 132. 15 cm Above Surface Temperatures for 9/19/06 – 9/25/06

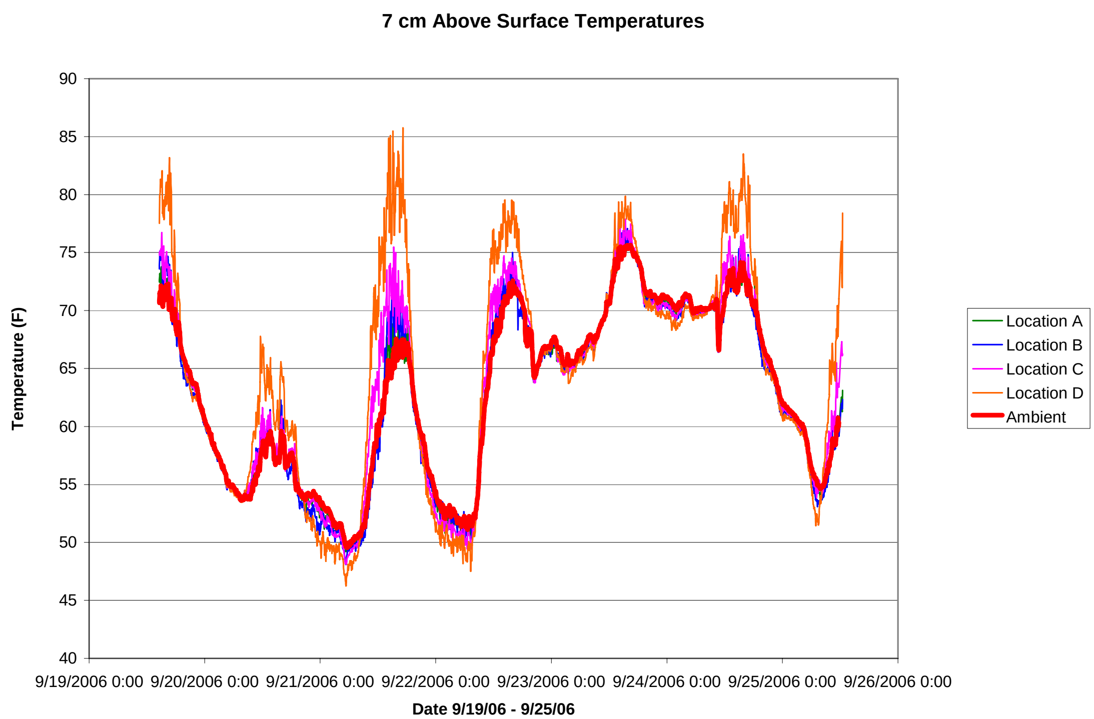

Figure 133. 7 cm Above Surface Temperatures for 9/19/06 – 9/25/06

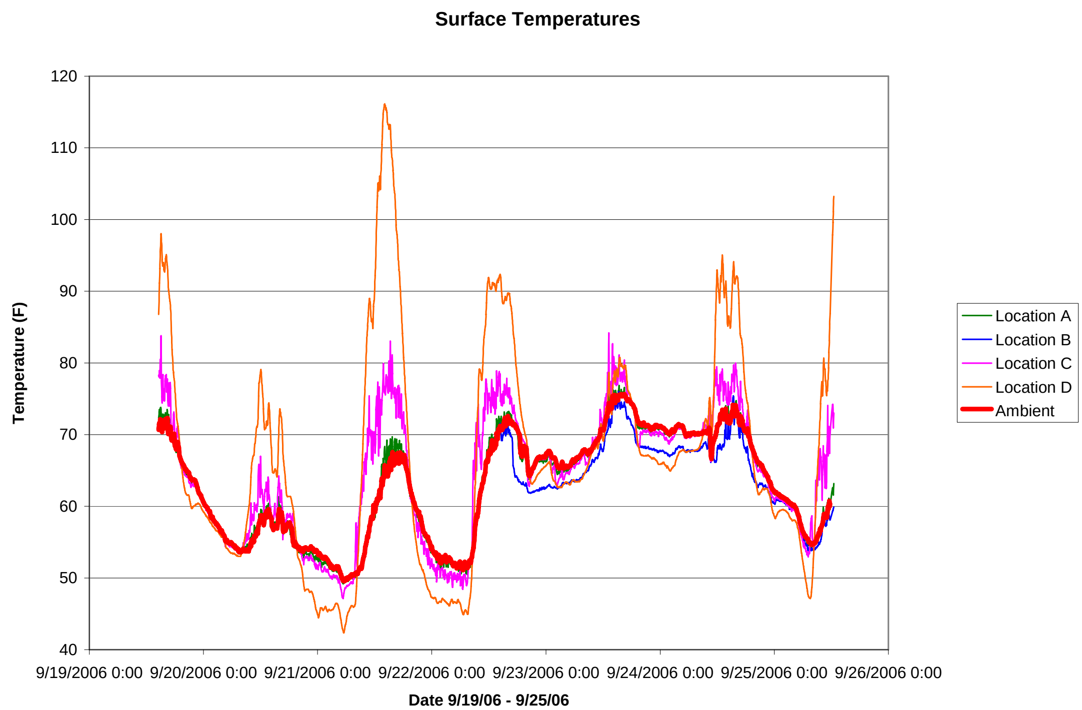

Figure 134. Surface Temperatures for 9/19/06 – 9/25/06

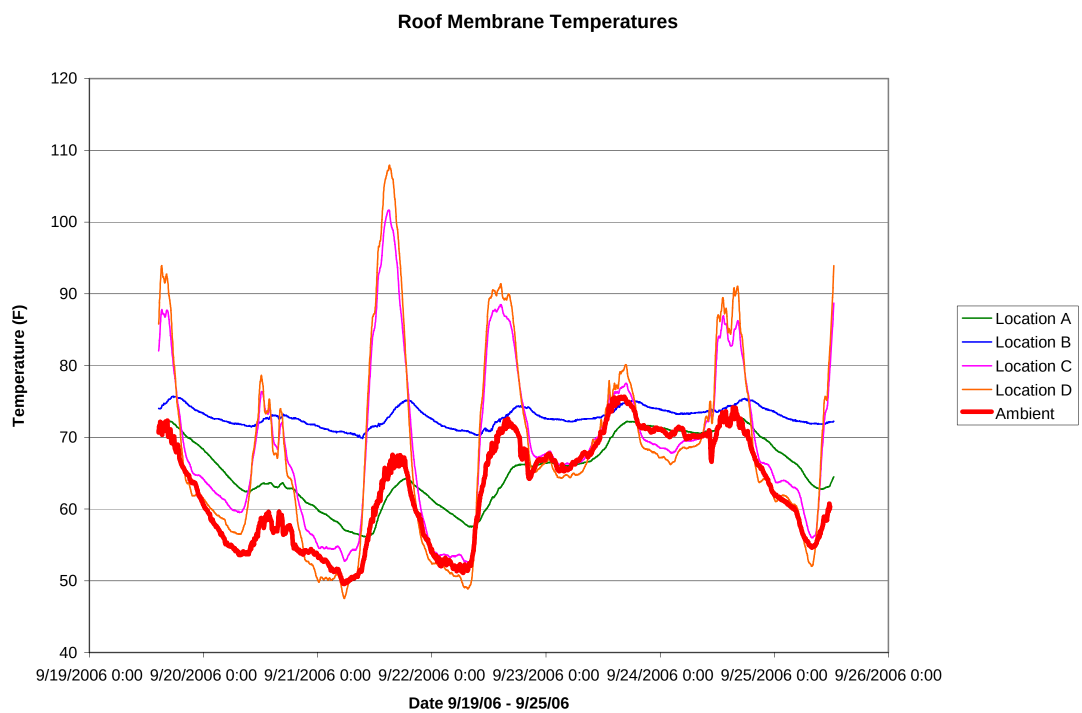

Figure 135. Roof Membrane Temperatures for 9/19/06 – 9/25/06

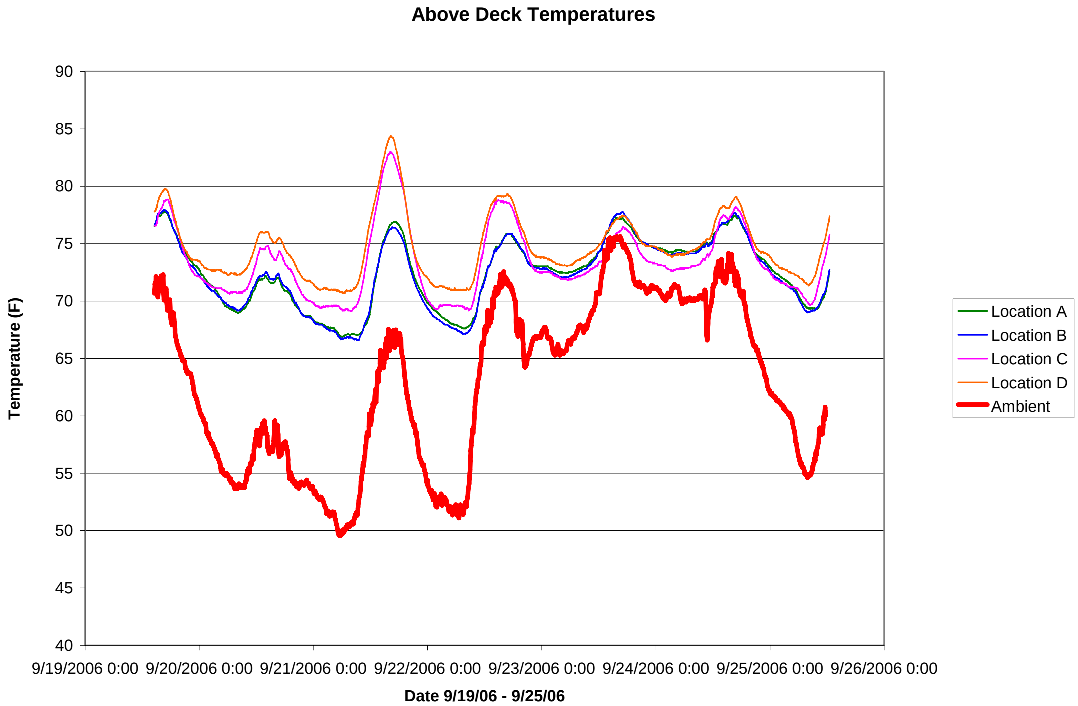

Figure 136. Above Deck Temperatures for 9/19/06 – 9/25/06

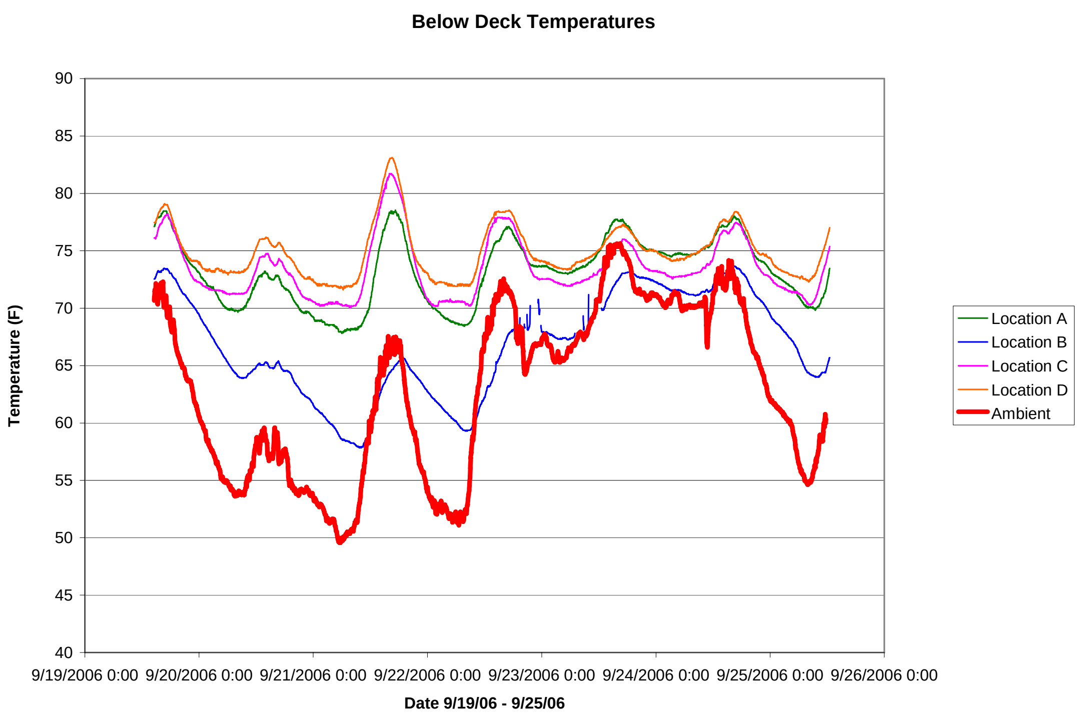

Figure 137. Below Deck Temperatures for 9/19/06 – 9/25/06

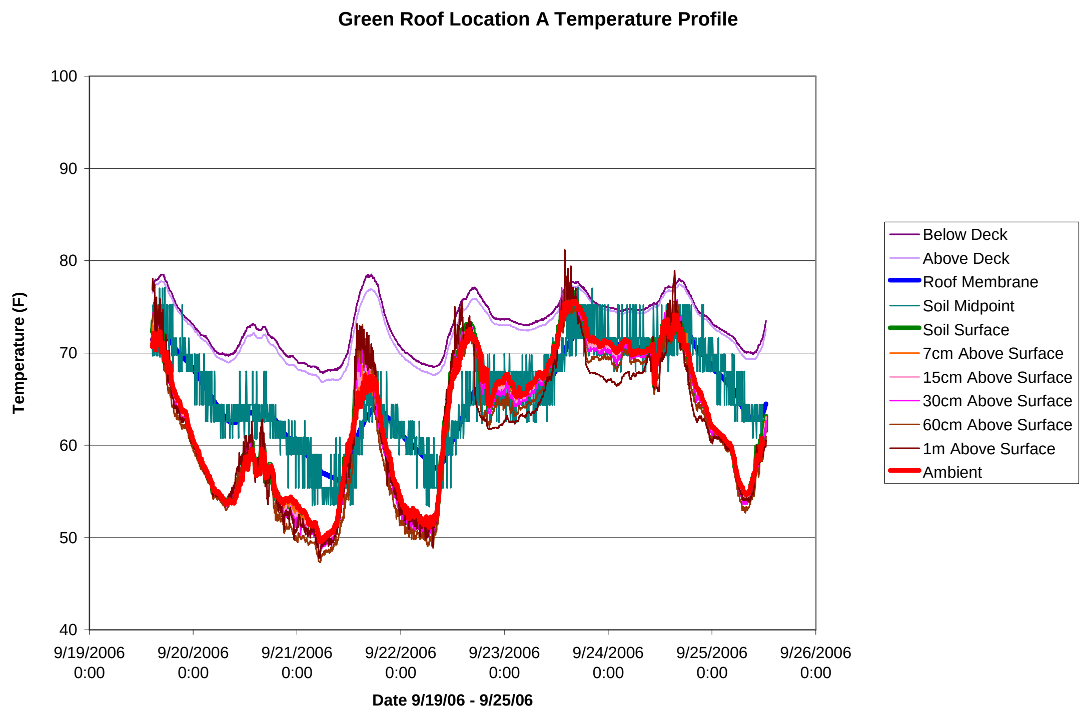

Figure 138. Green Roof Location A Temperature Profile for 9/19/06 – 9/25/06

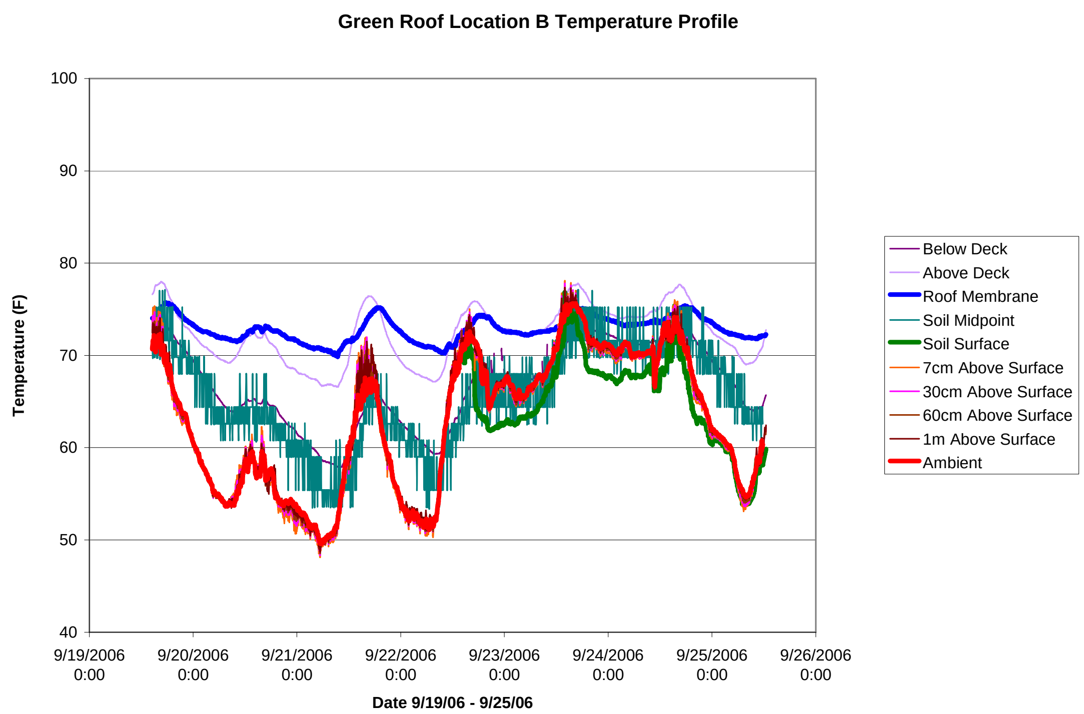

Figure 139. Green Roof Location B Temperature Profile for 9/19/06 – 9/25/06

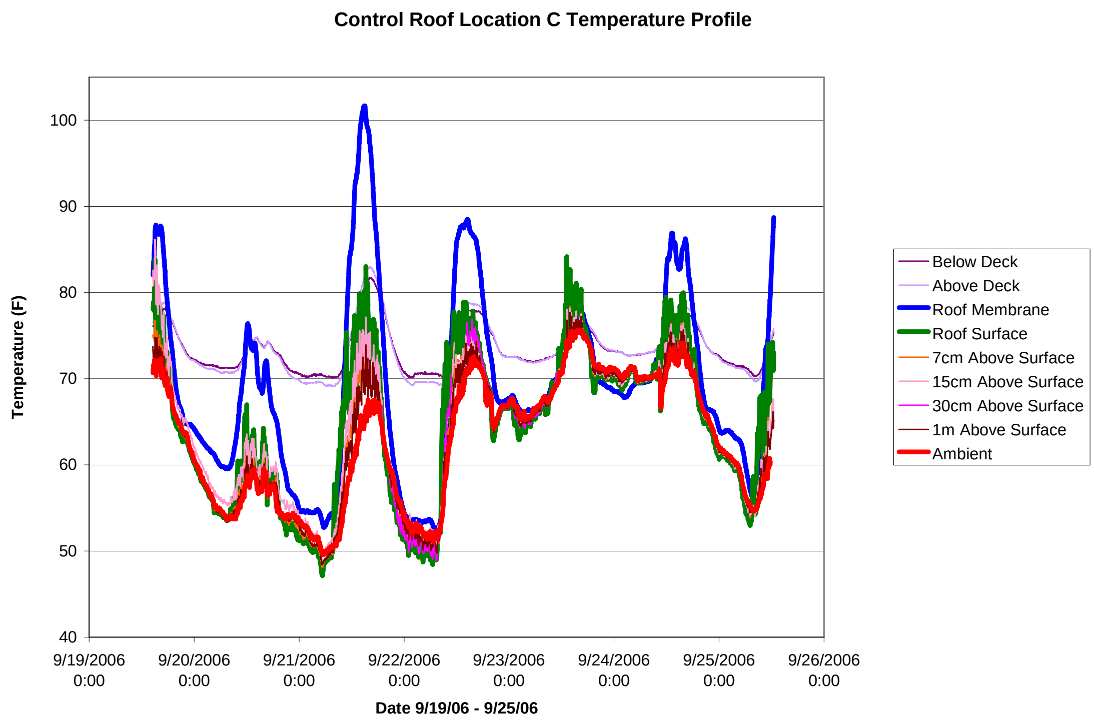

Figure 140. Control Roof Location C Temperature Profile for 9/19/06 – 9/25/06

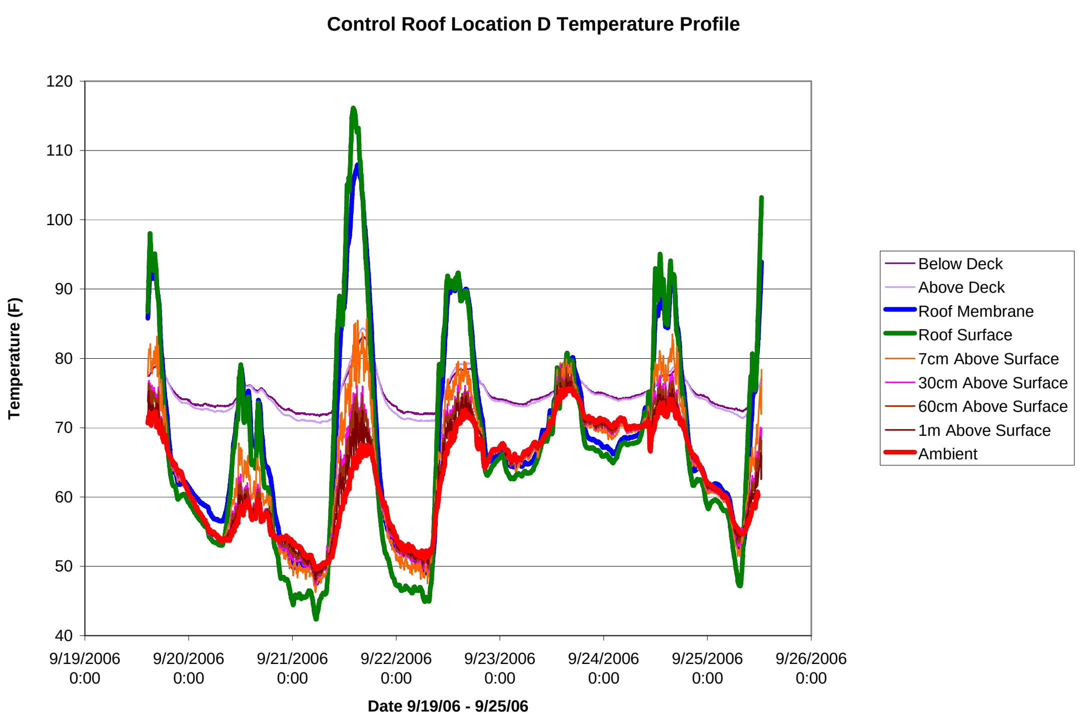

Figure 141. Control Roof Location D Temperature Profile for 9/19/06 – 9/25/06

Temperature Measurements for September 26, 2006 to September 29, 2006

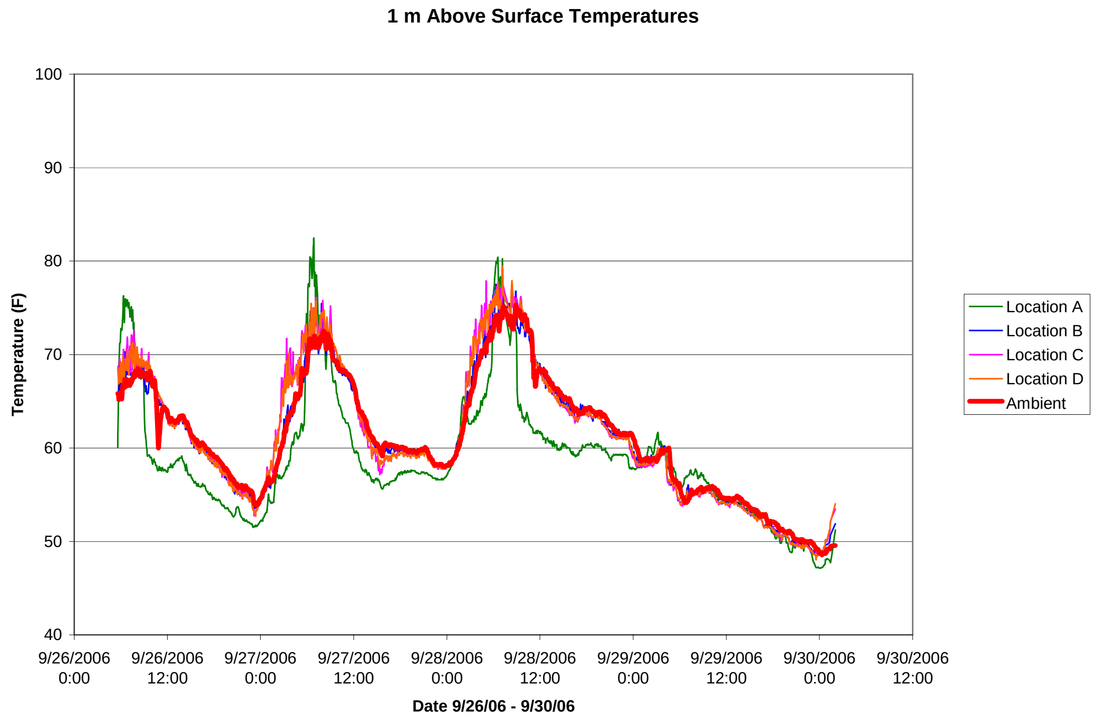

Figure 142. 1m Above Surface Temperatures for 9/26/06 – 9/30/06

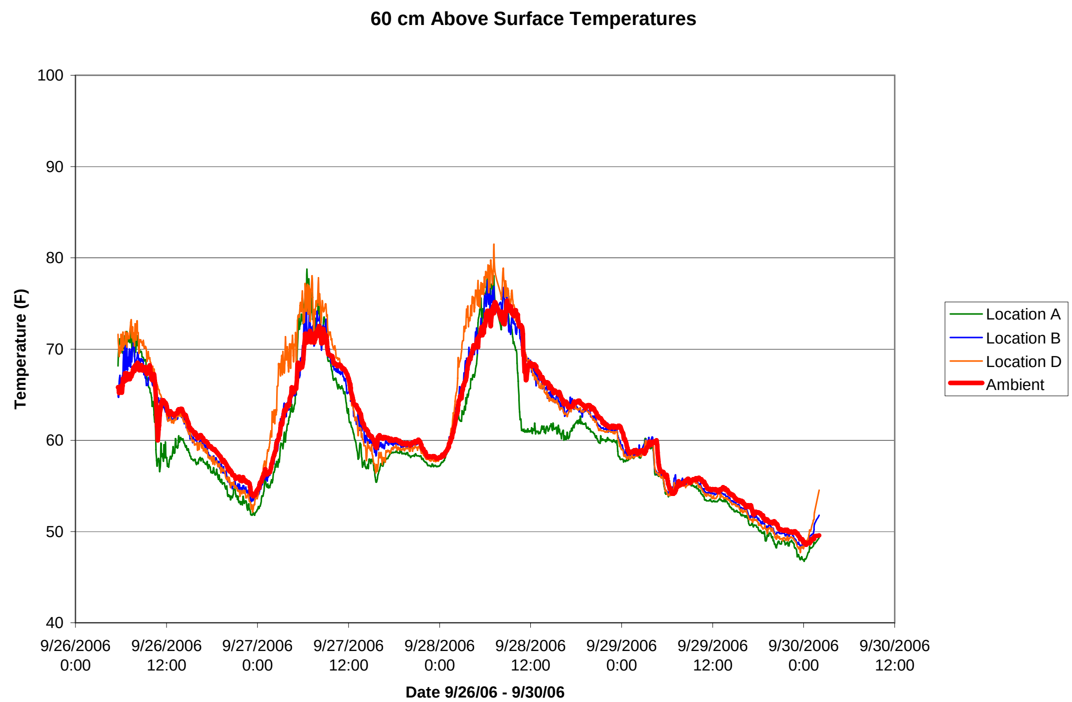

Figure 143. 60 cm Above Surface Temperatures for 9/26/06 – 9/30/06

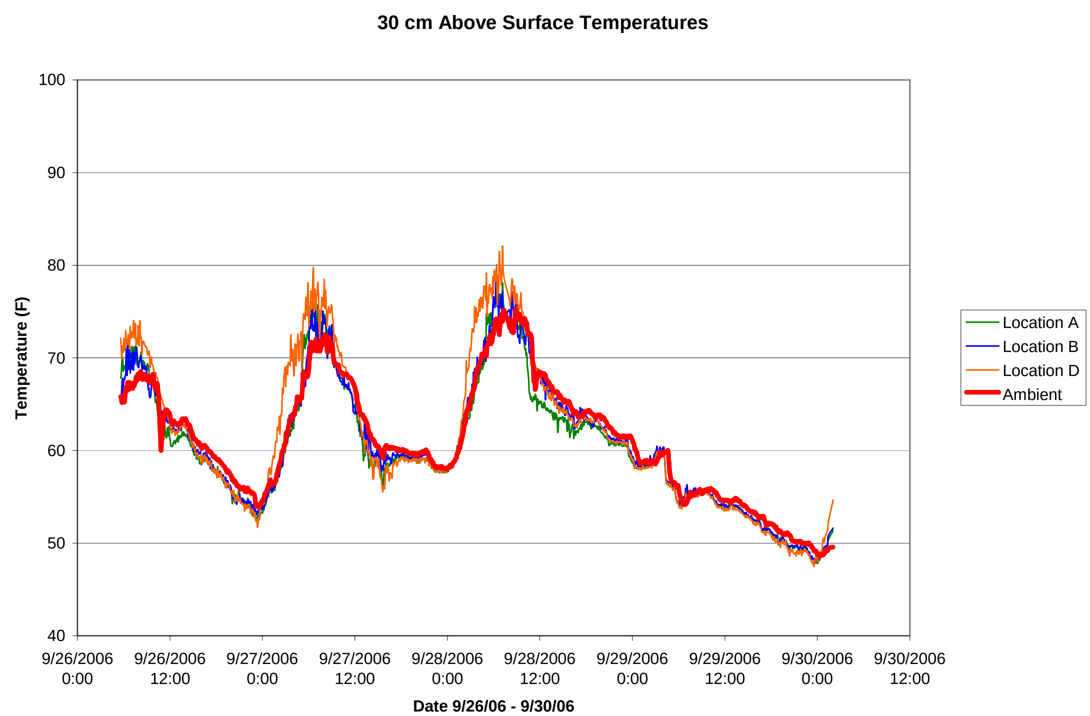

Figure 144. 30 cm Above Surface Temperatures for 9/26/06 – 9/30/06

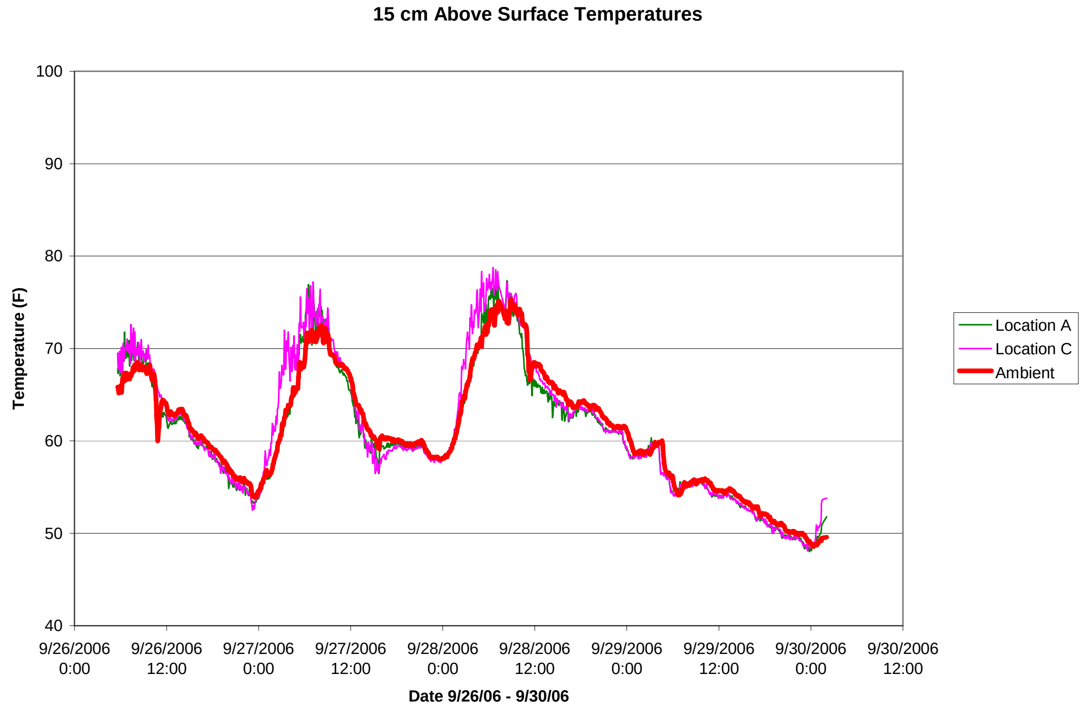

Figure 145. 15 cm Above Surface Temperatures for 9/26/06 – 9/30/06

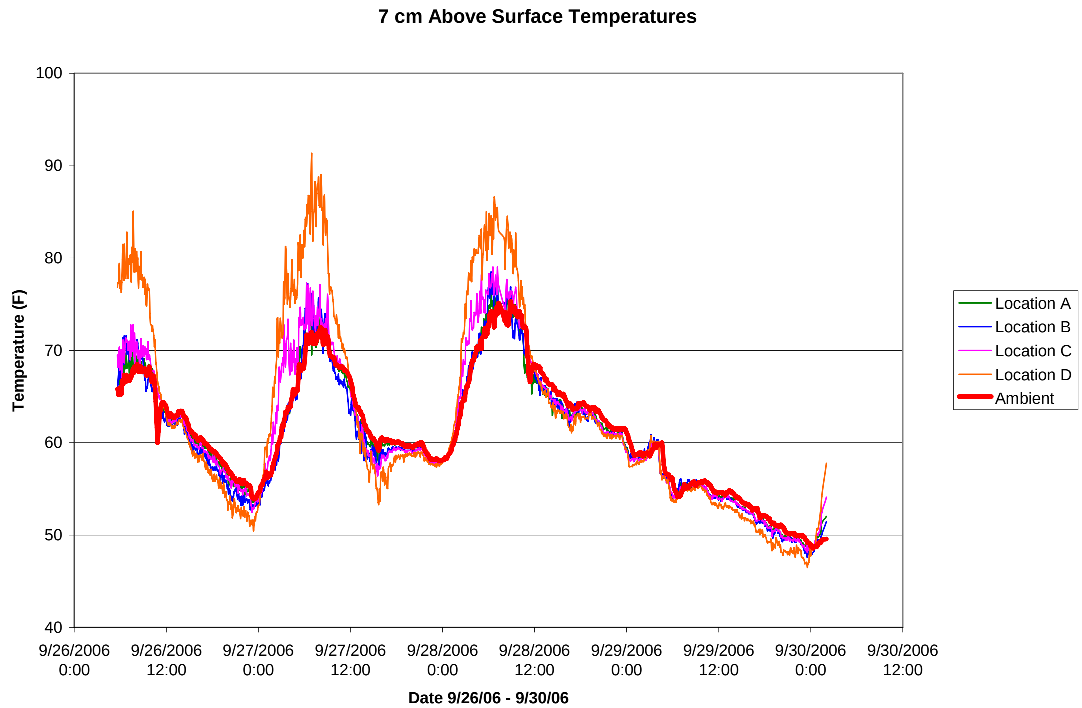

Figure 146. 7 cm Above Surface Temperatures for 9/26/06 – 9/30/06

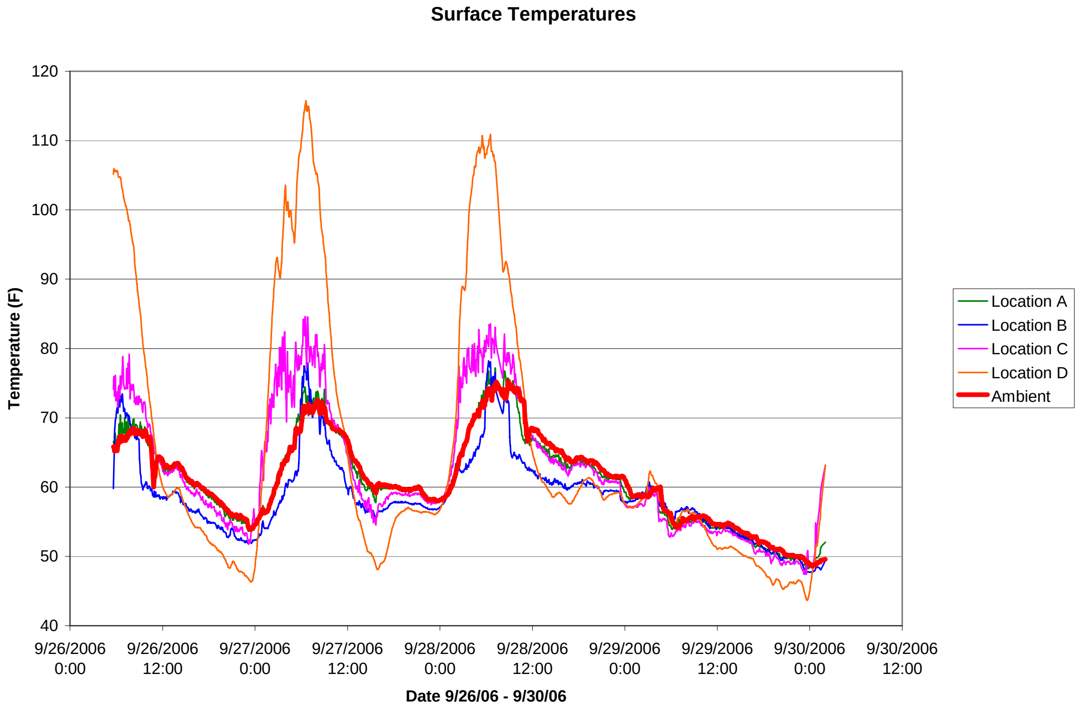

Figure 147. Surface Temperatures for 9/26/06 – 9/30/06

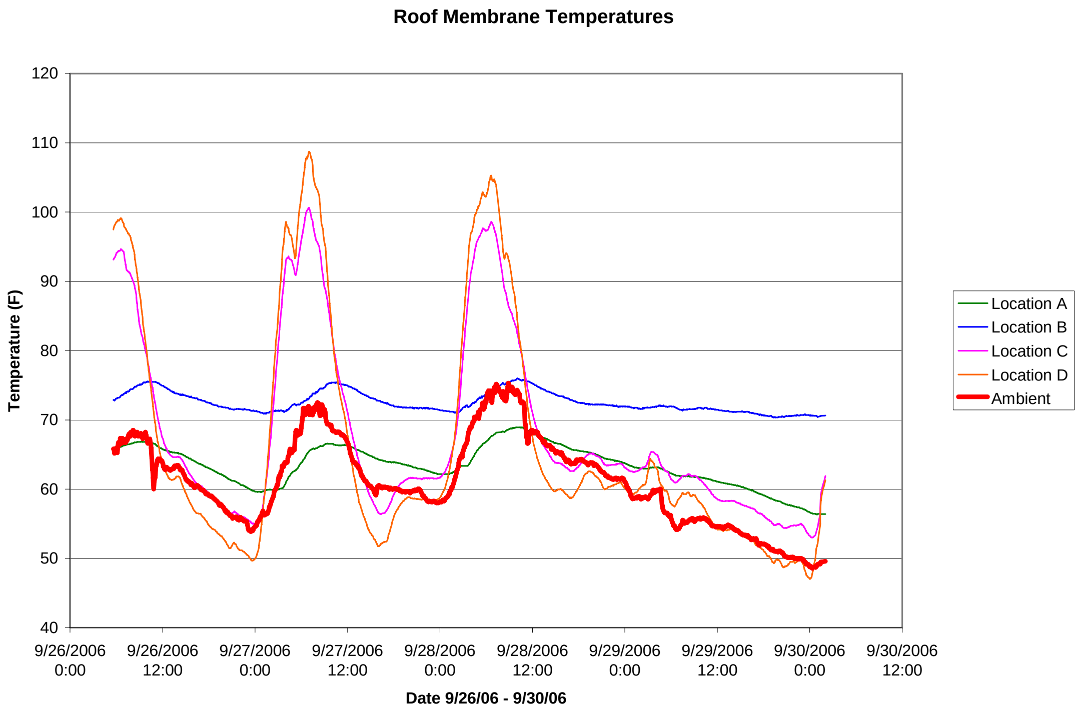

Figure 148. Roof Membrane Temperatures for 9/26/06 – 9/30/06

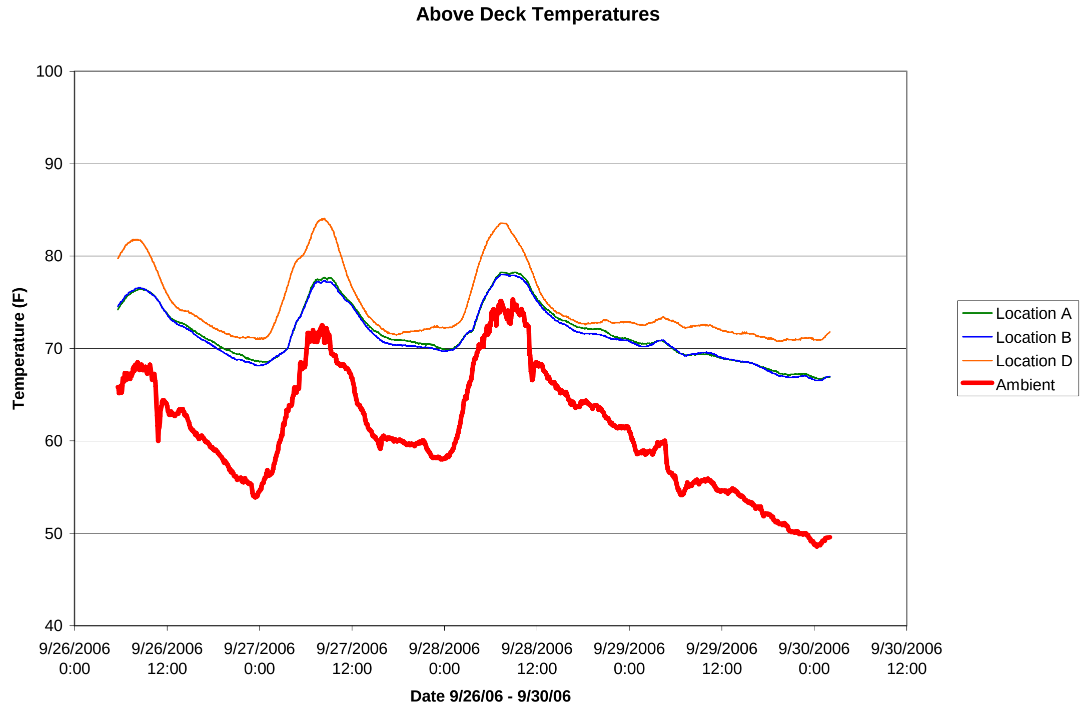

Figure 149. Above Deck Temperatures for 9/26/06 – 9/30/06

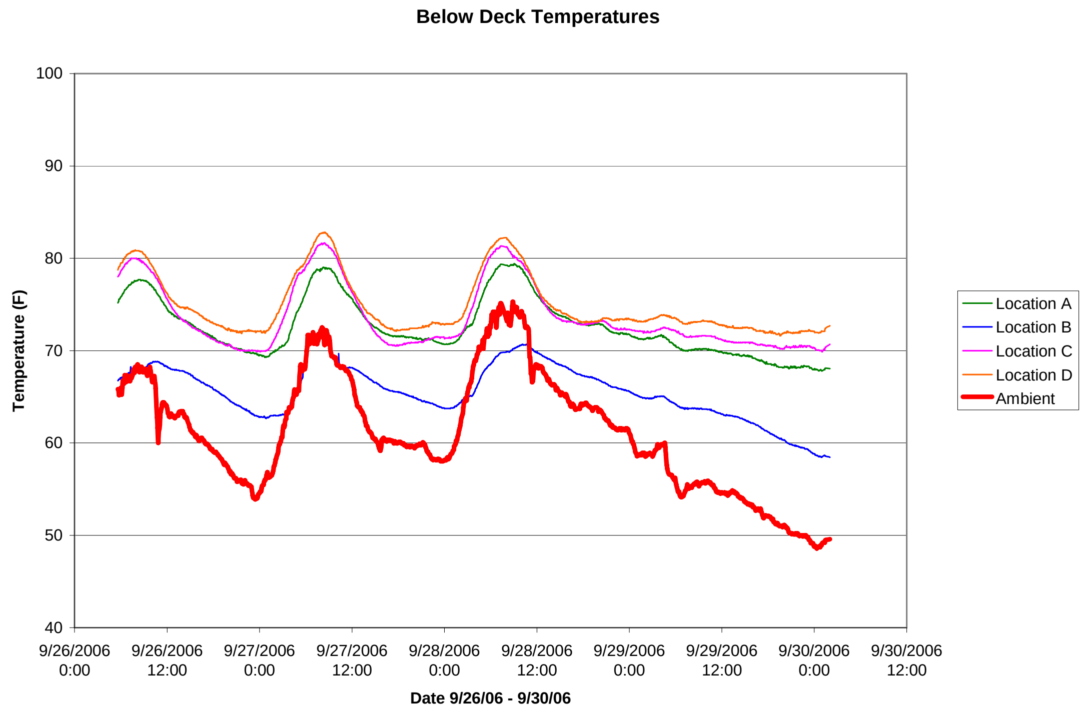

Figure 150. Below Deck Temperatures for 9/26/06 – 9/30/06

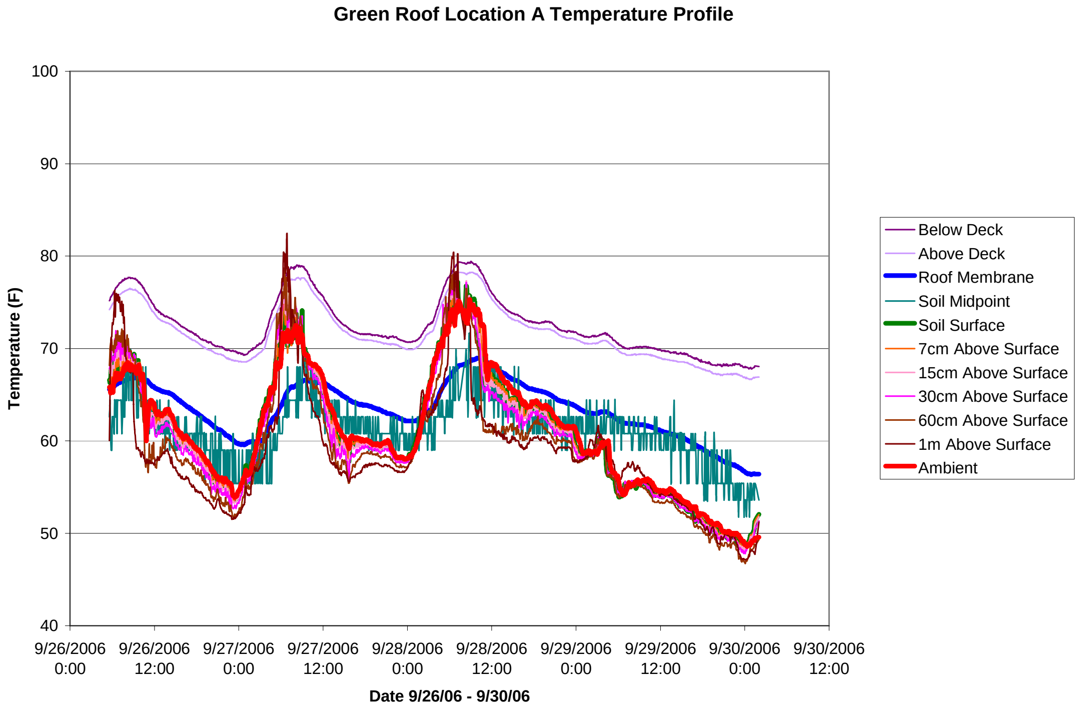

Figure 151. Green Roof Location A Temperature Profile for 9/26/06 – 9/30/06

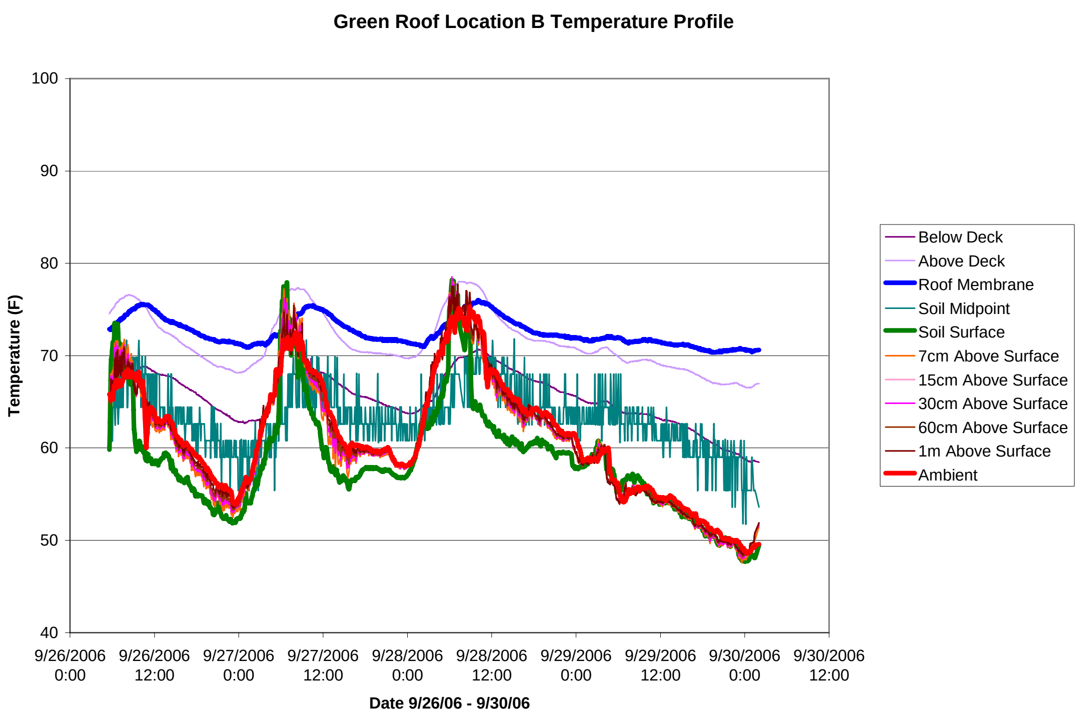

Figure 152. Green Roof Location B Temperature Profile for 9/26/06 – 9/30/06

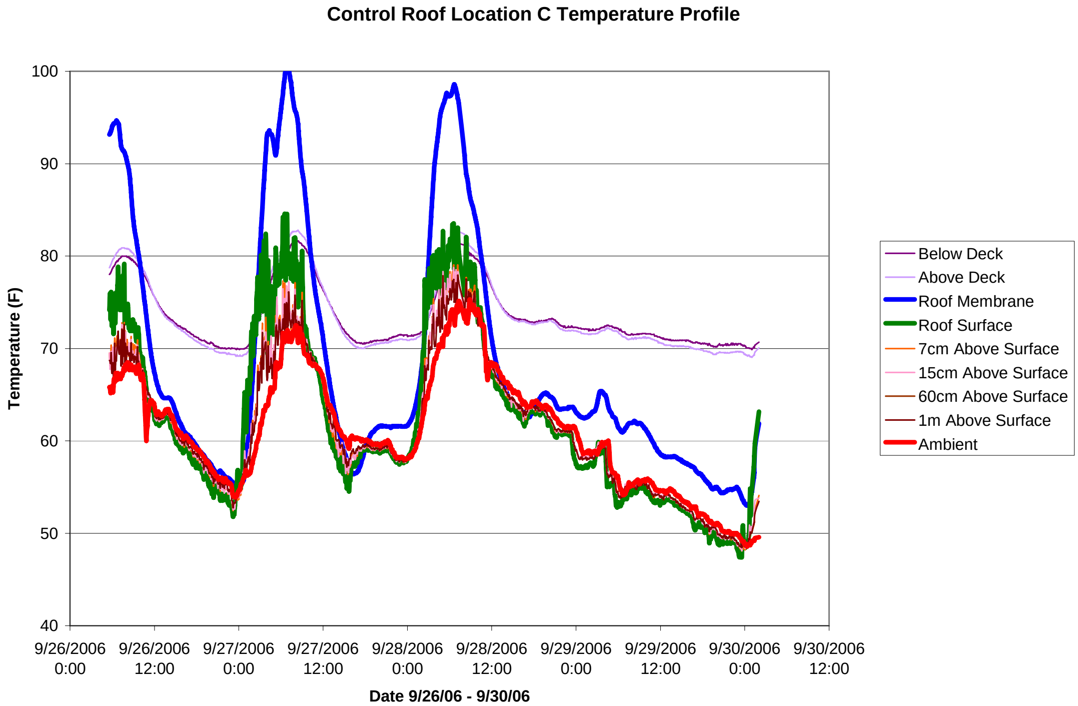

Figure 153. Control Roof Location C Temperature Profile for 9/26/06 – 9/30/06

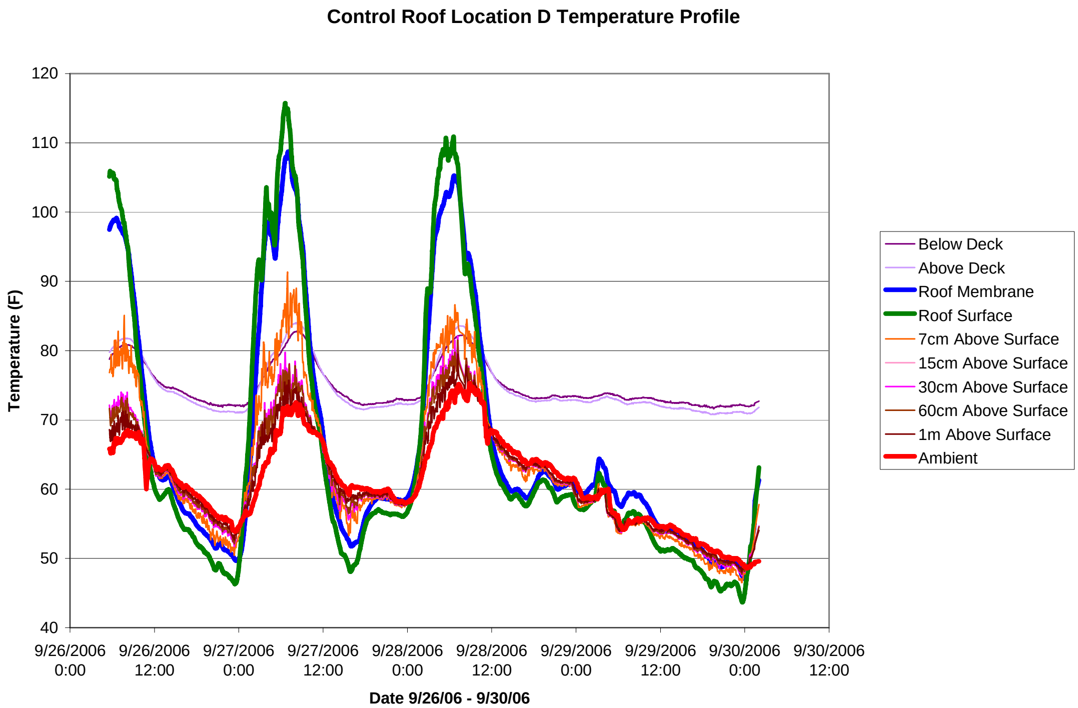

Figure 154. Control Roof Location D Temperature Profile for 9/26/06 – 9/30/06

Single Layer Temperature Measurements for 9/30/06 – 10/6/06

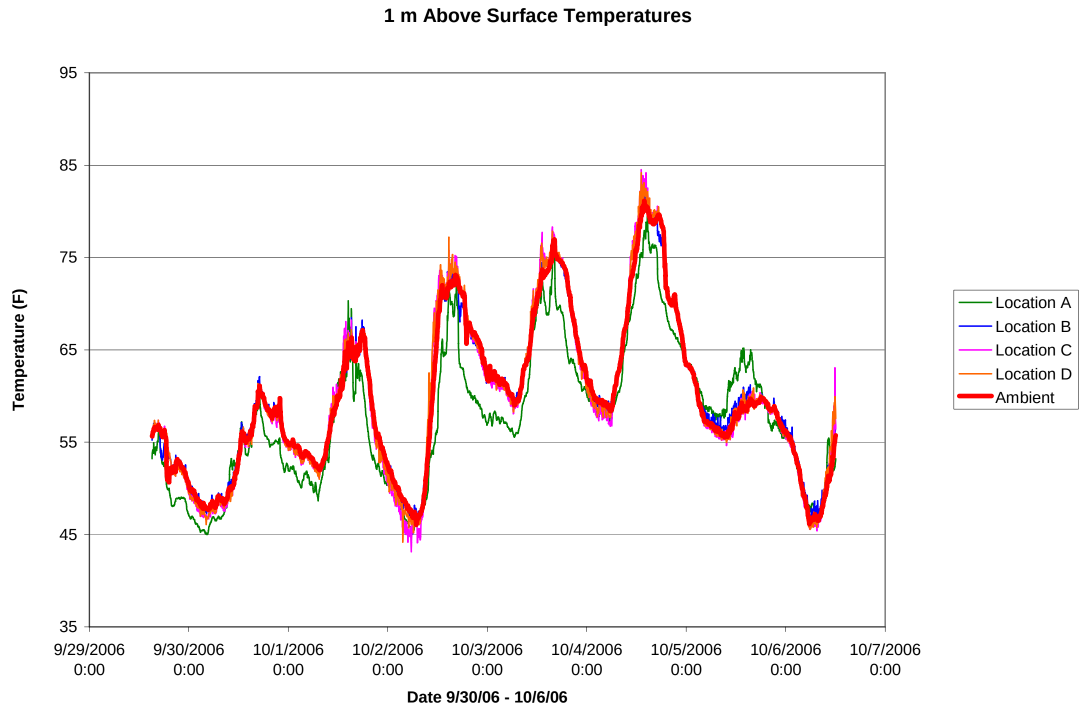

Figure 155. 1m Above Surface Temperatures for 9/30/06 – 10/6/06

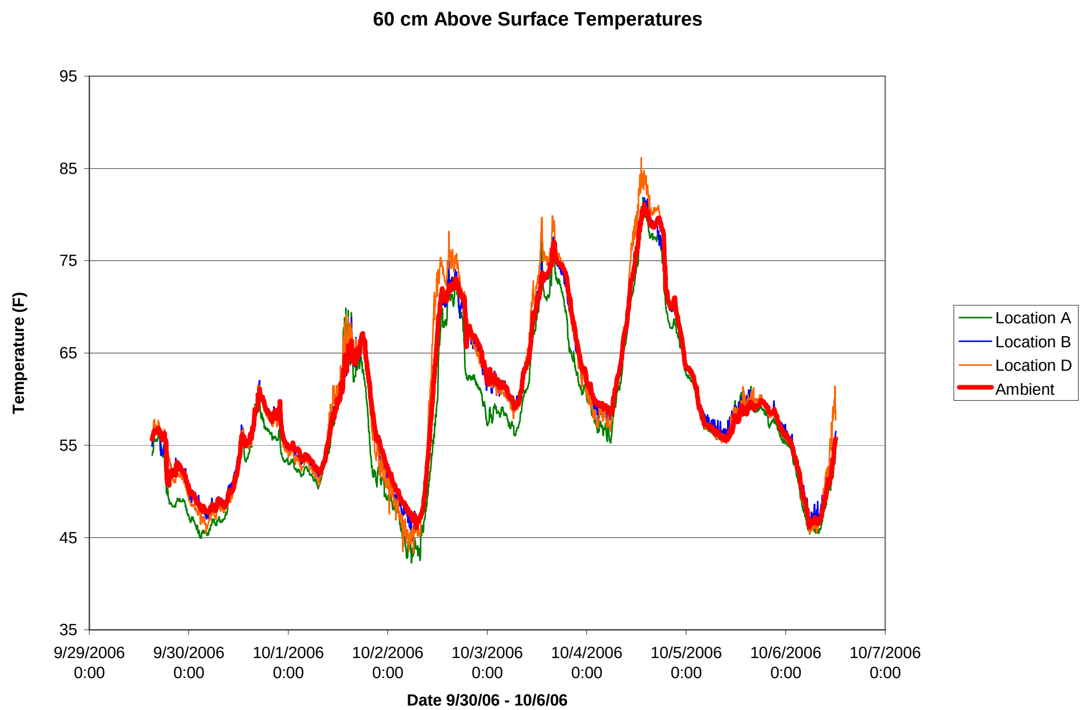

Figure 156. 60cm Above Surface Temperatures for 9/30/06 – 10/6/06

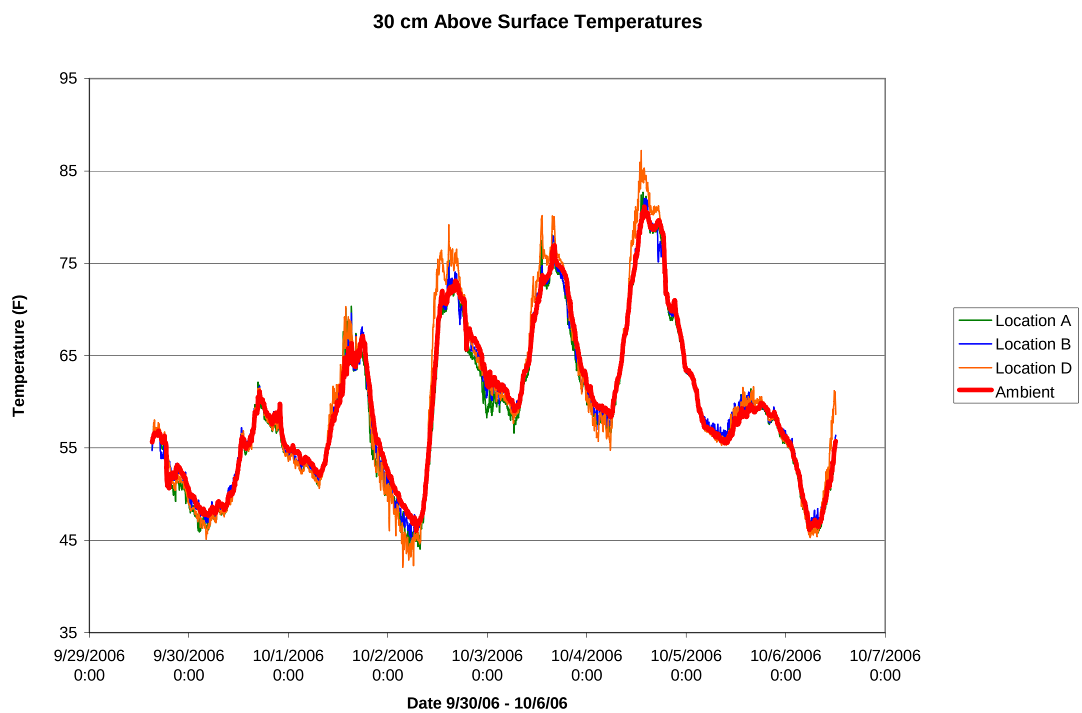

Figure 157. 30cm Above Surface Temperatures for 9/30/06 – 10/6/06

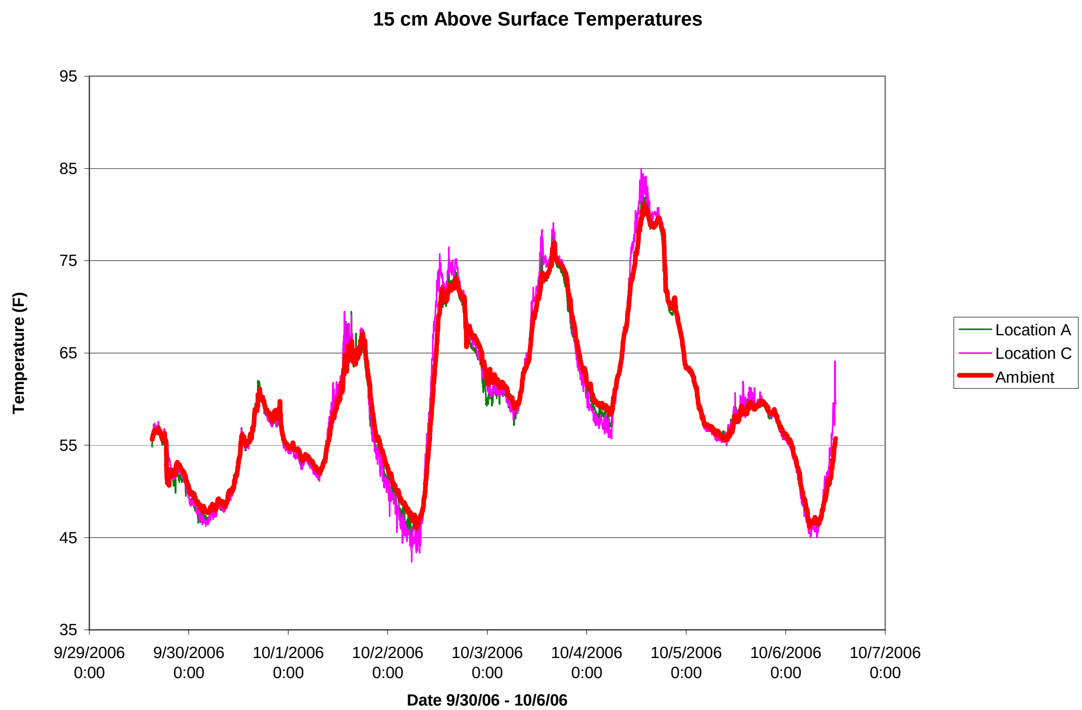

Figure 158. 15cm Above Surface Temperatures for 9/30/06 – 10/6/06

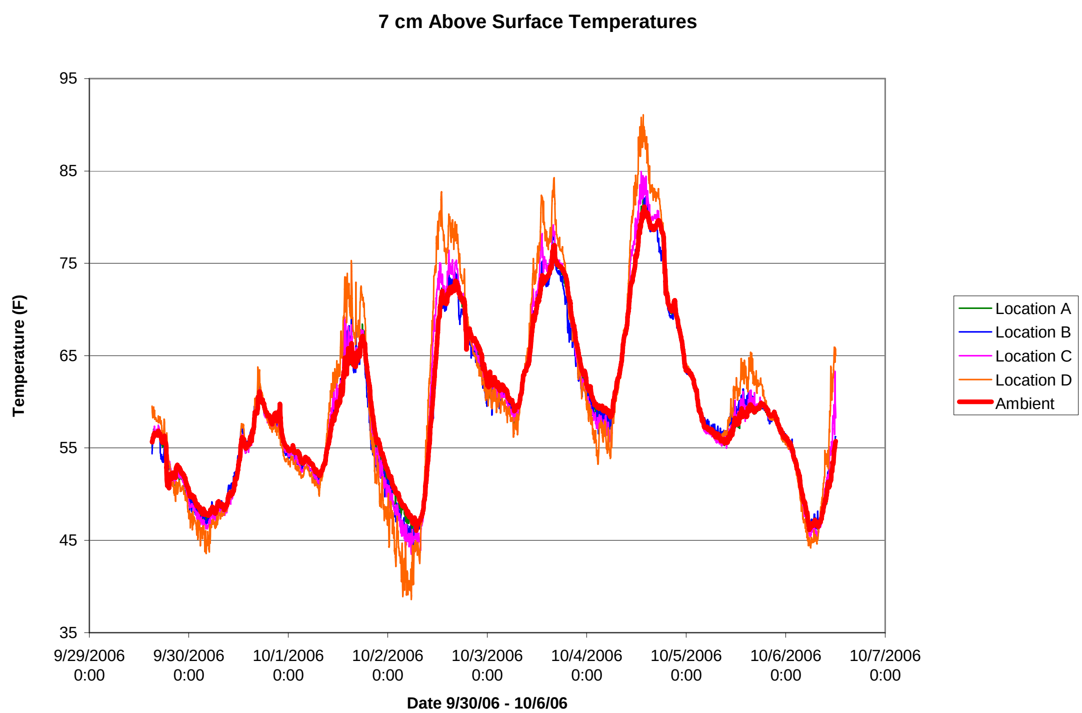

Figure 159. 7cm Above Surface Temperatures for 9/30/06 – 10/6/06

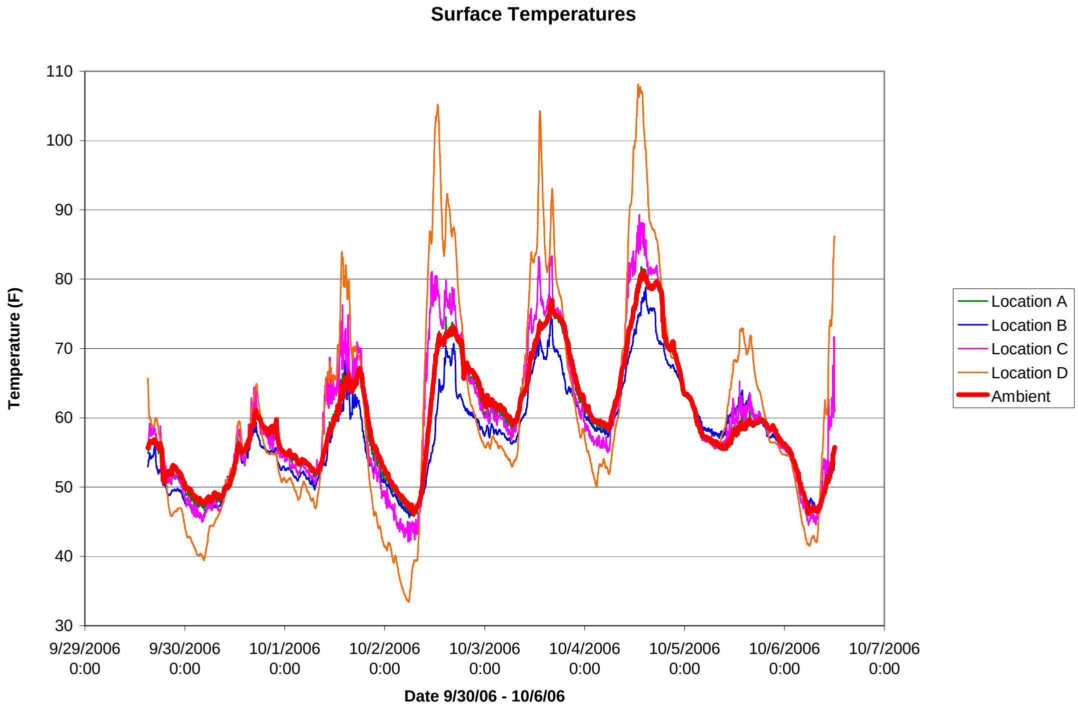

Figure 160. Surface Temperatures for 9/30/06 – 10/6/06

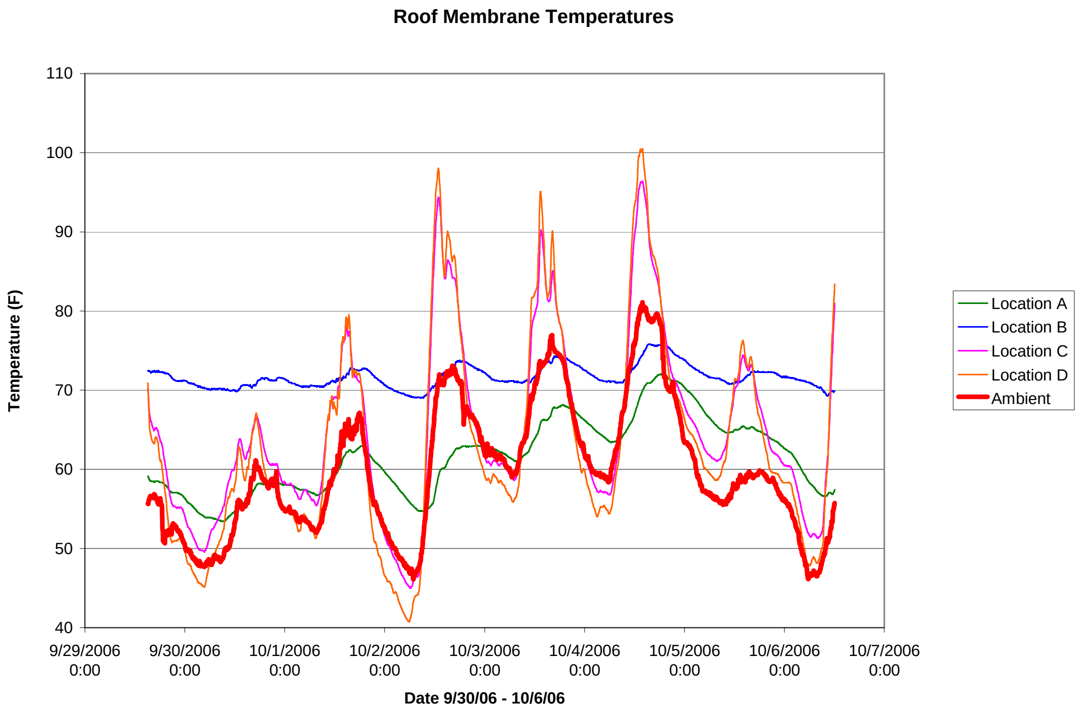

Figure 161. Roof Membrane Temperatures for 9/30/06 – 10/6/06

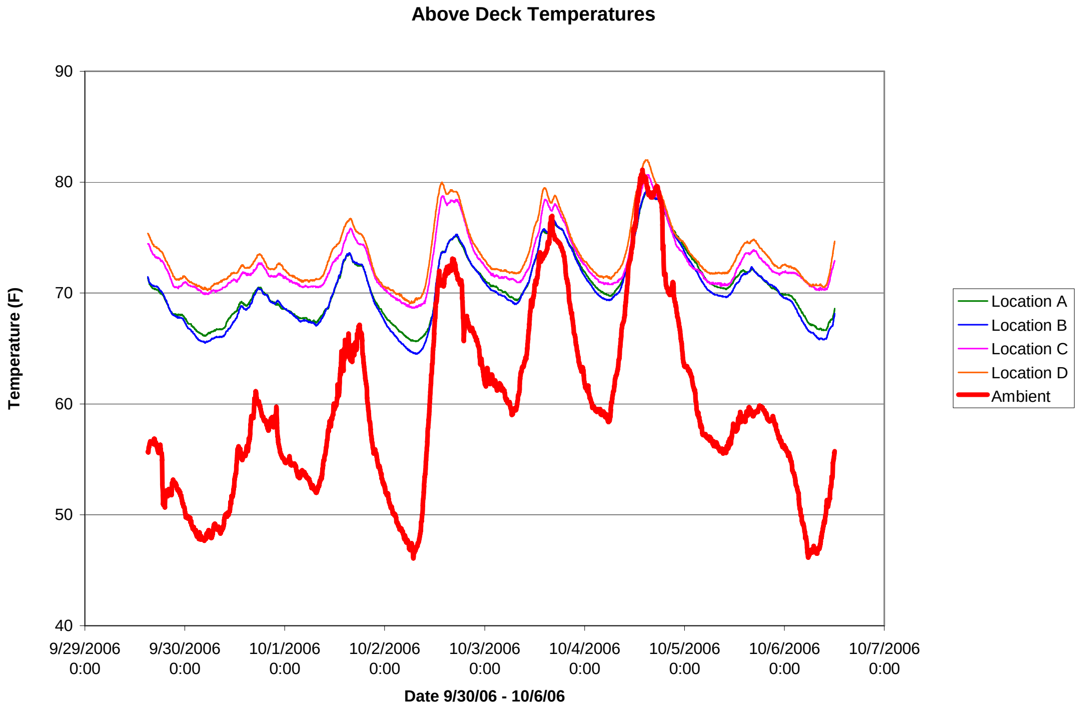

Figure 162. Above Deck Temperatures for 9/30/06 – 10/6/06

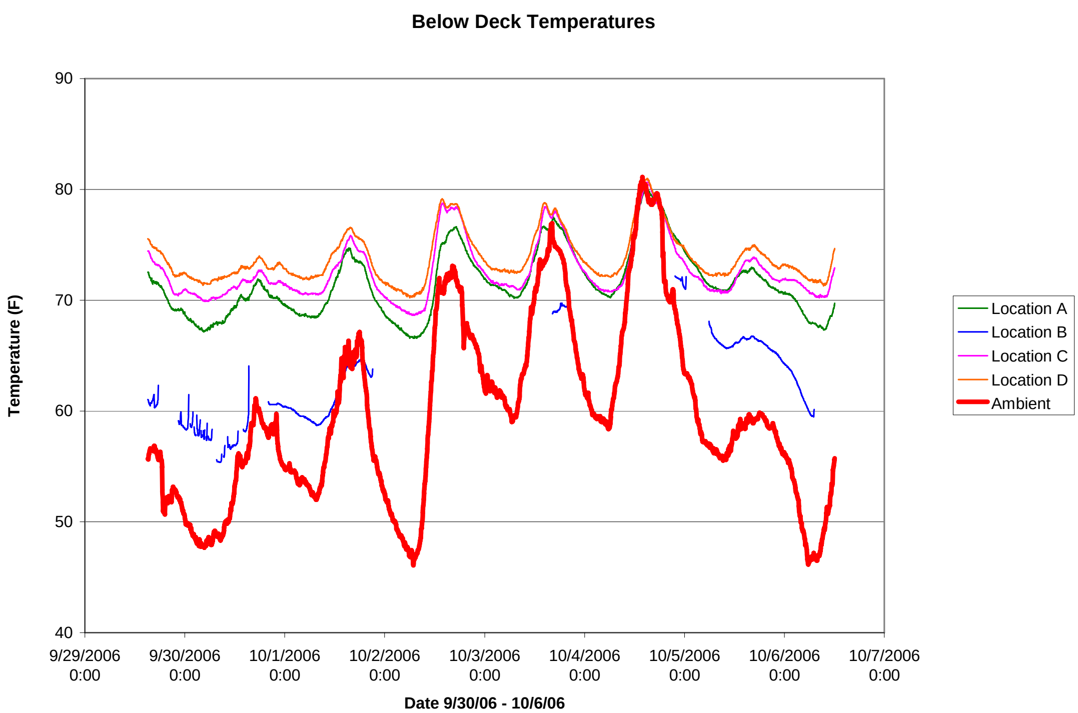

Figure 163. Below Deck Temperatures for 9/30/06 – 10/6/06

Single Layer Temperatures for October 20, 2006 to October 25, 2006

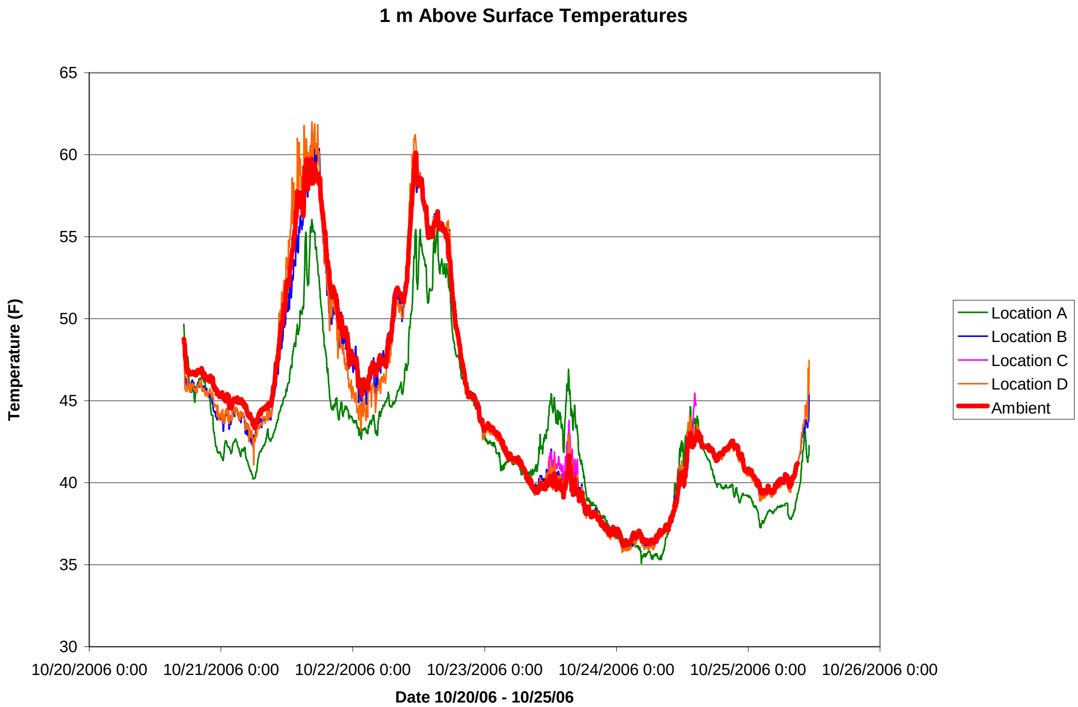

Figure 164. 1m Above Surface Temperatures for 10/20/06 – 10/25/06

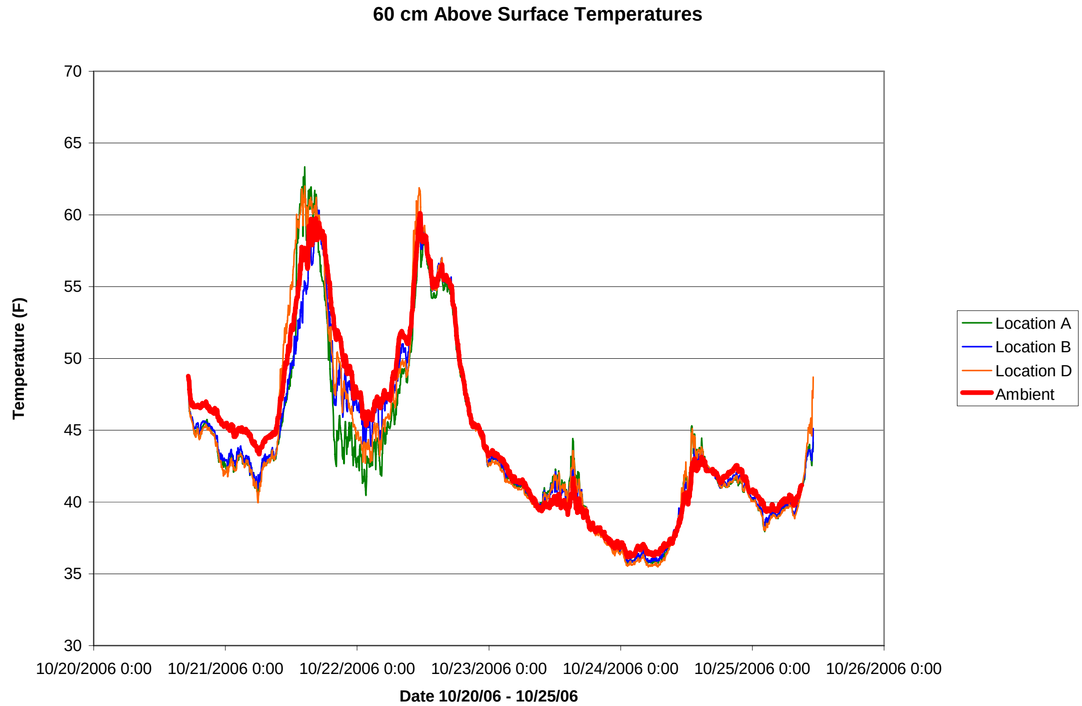

Figure 165. 60cm Above Surface Temperatures for 10/20/06 – 10/25/06

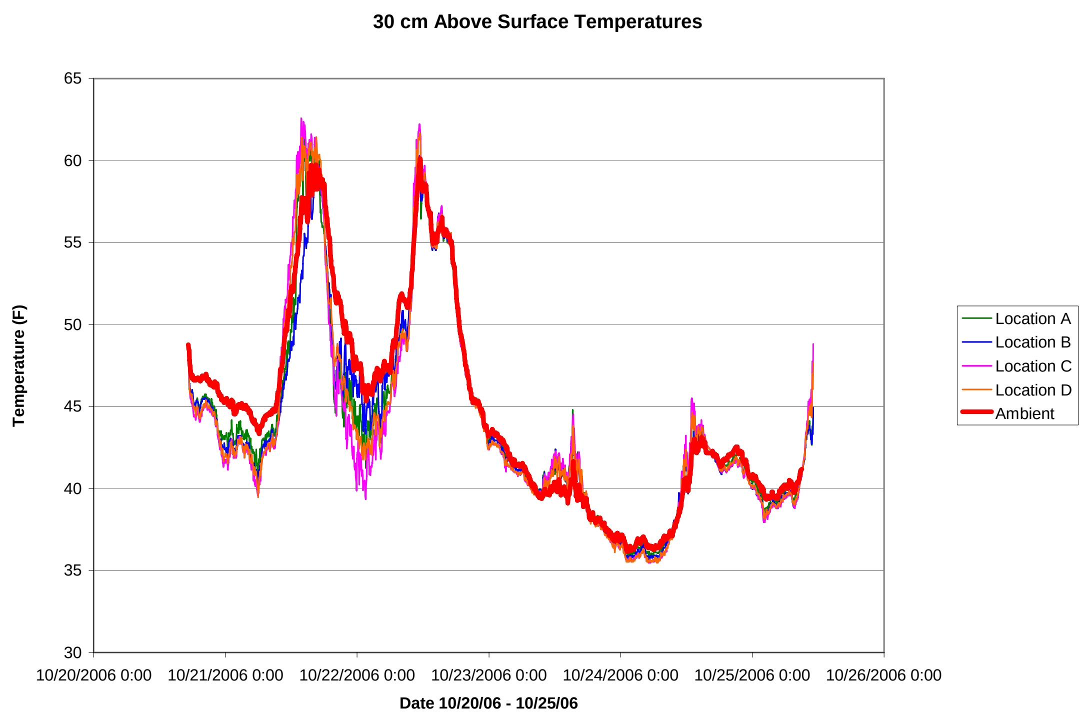

Figure 166. 30 cm Above Surface Temperatures for 10/20/06 – 10/25/06

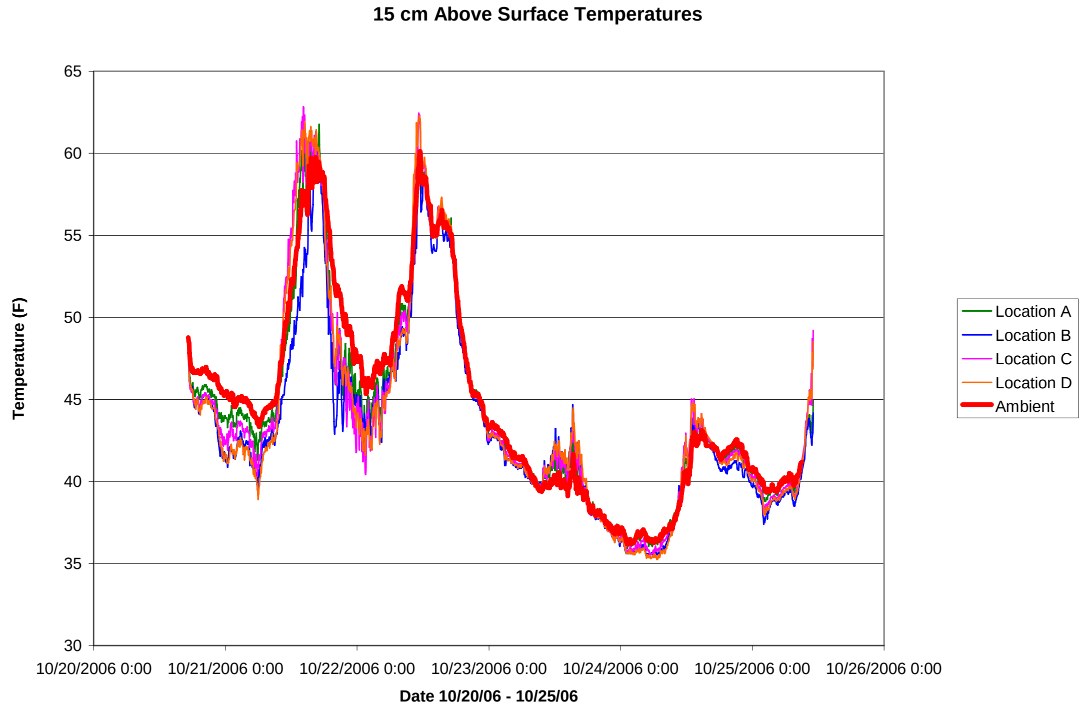

Figure 167. 15cm Above Surface Temperatures for 10/20/06 – 10/25/06

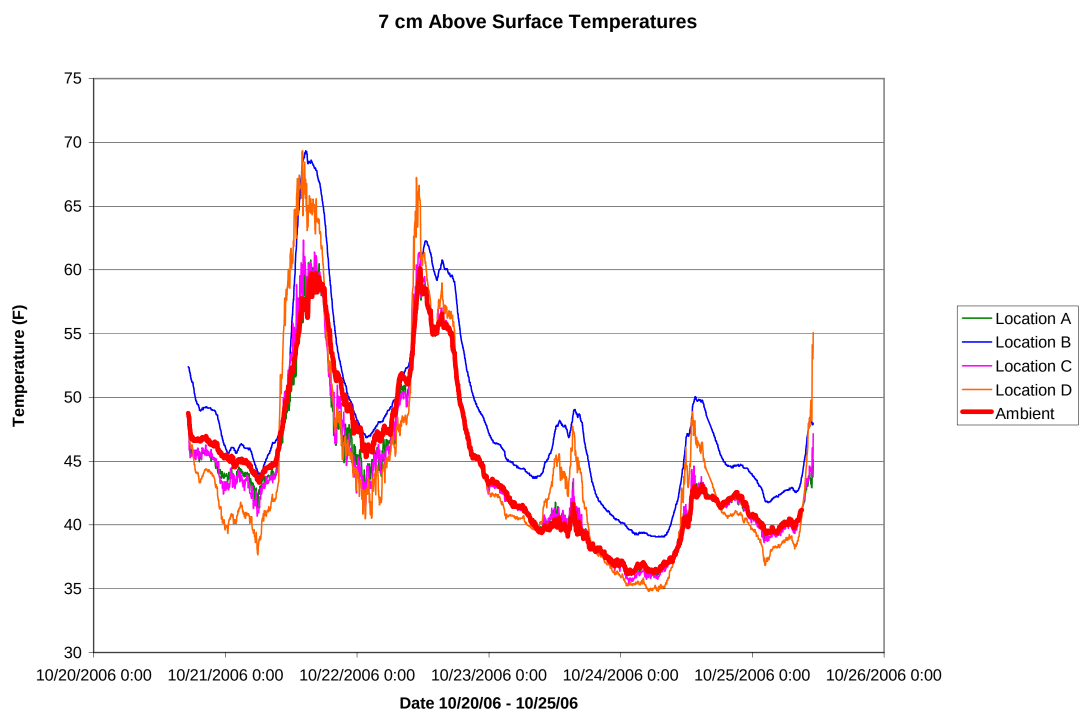

Figure 168. 7cm Above Surface Temperatures for 10/20/06 – 10/25/06

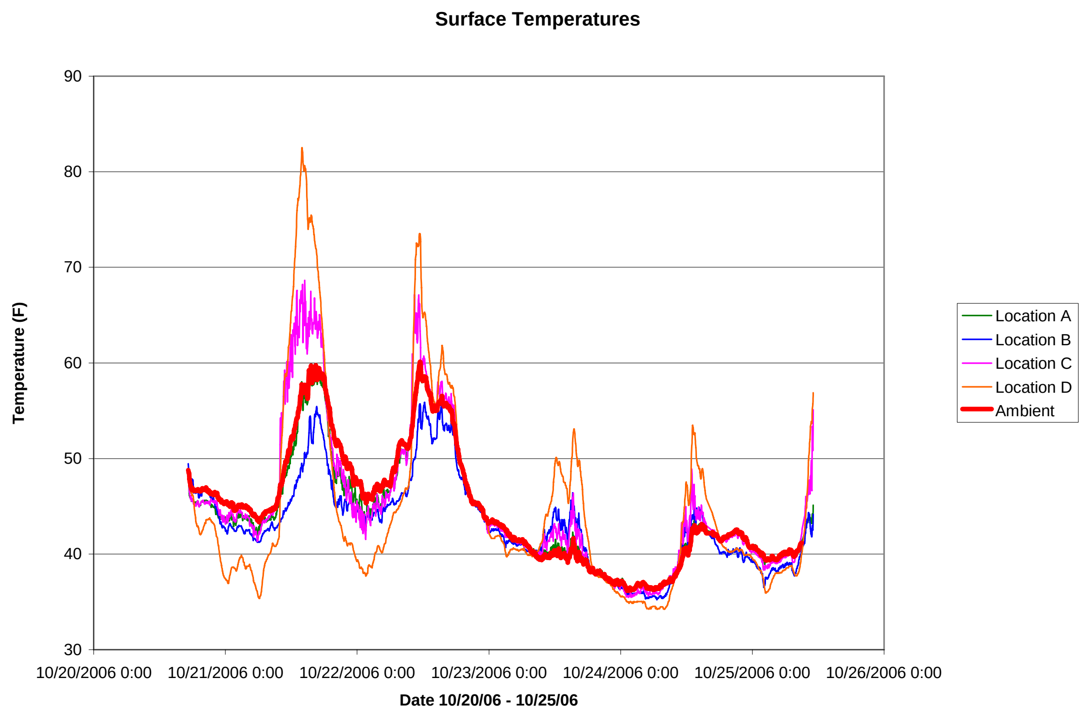

Figure 169. Surface Temperatures for 10/20/06 – 10/25/06

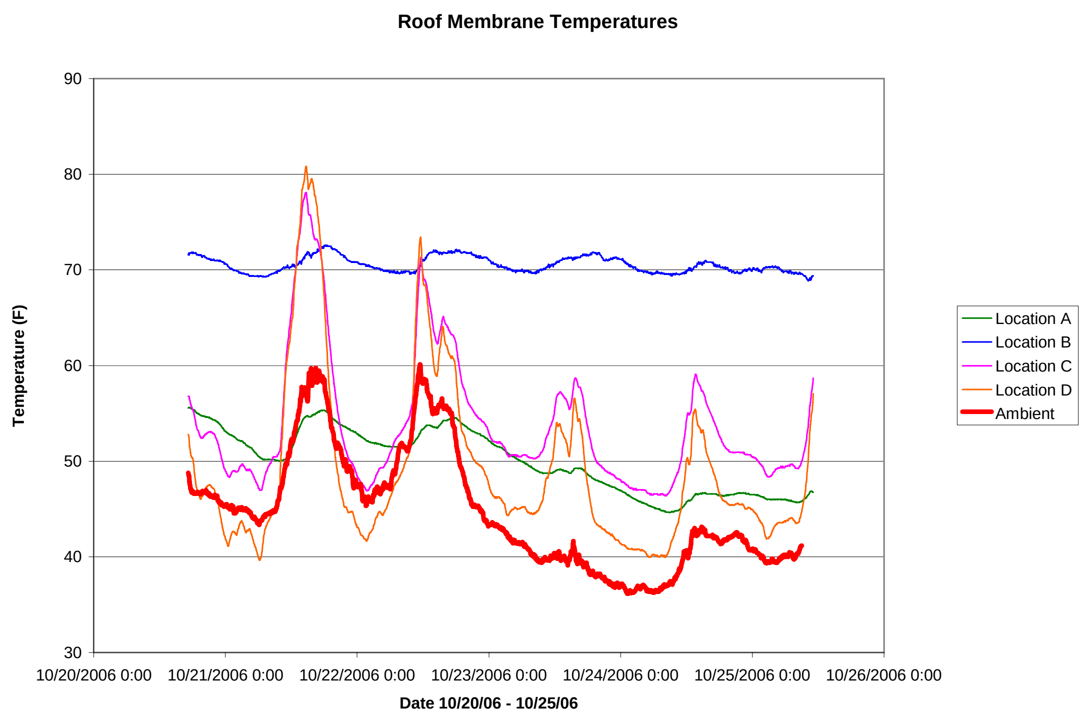

Figure 170. Roof Membrane Temperatures for 10/20/06 – 10/25/06

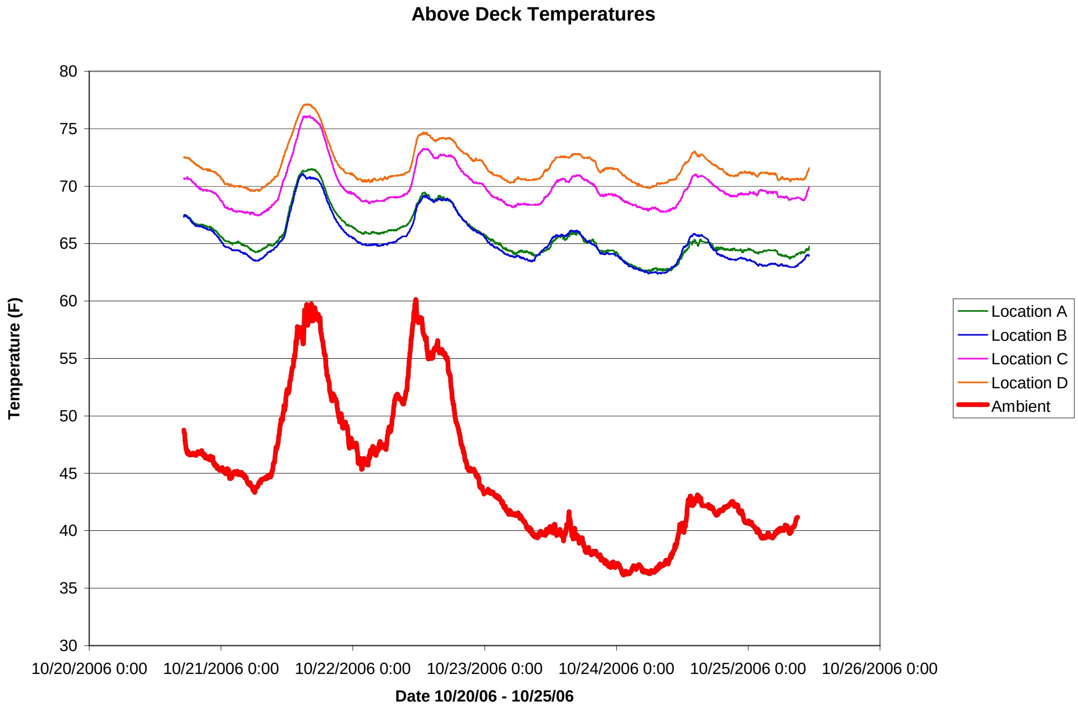

Figure 171. Above Deck Temperatures for 10/20/06 – 10/25/06

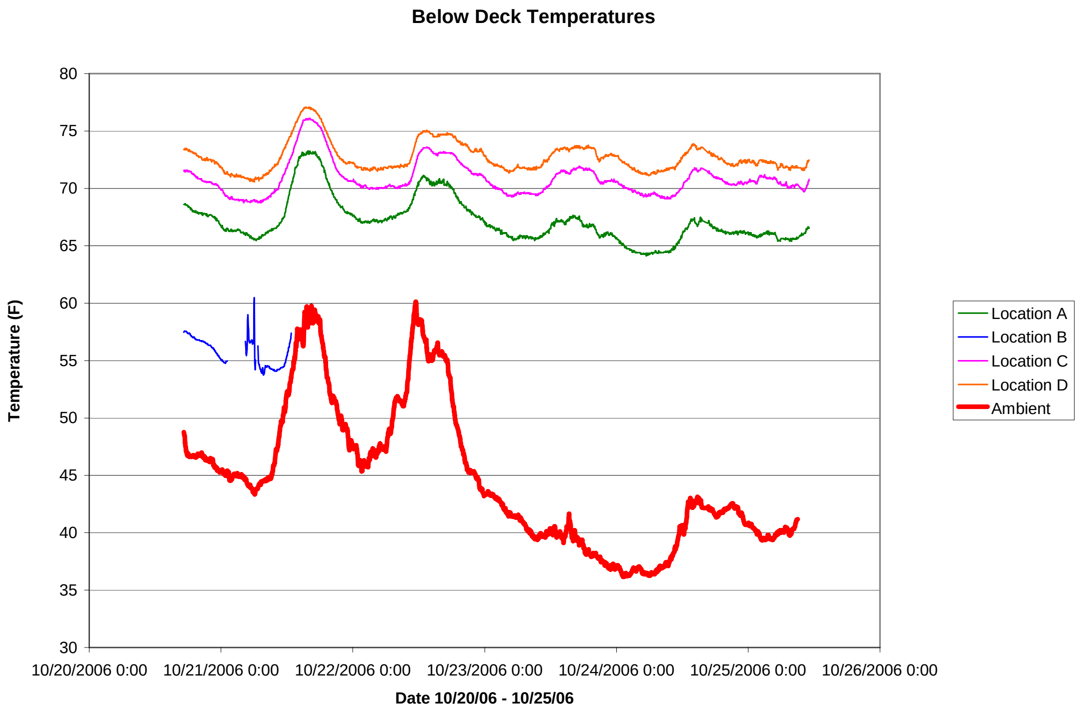

Figure 172. Below Deck Temperatures for 10/20/06 – 10/25/06

Temperature Measurements for November 1, 2006 to November 3, 2006

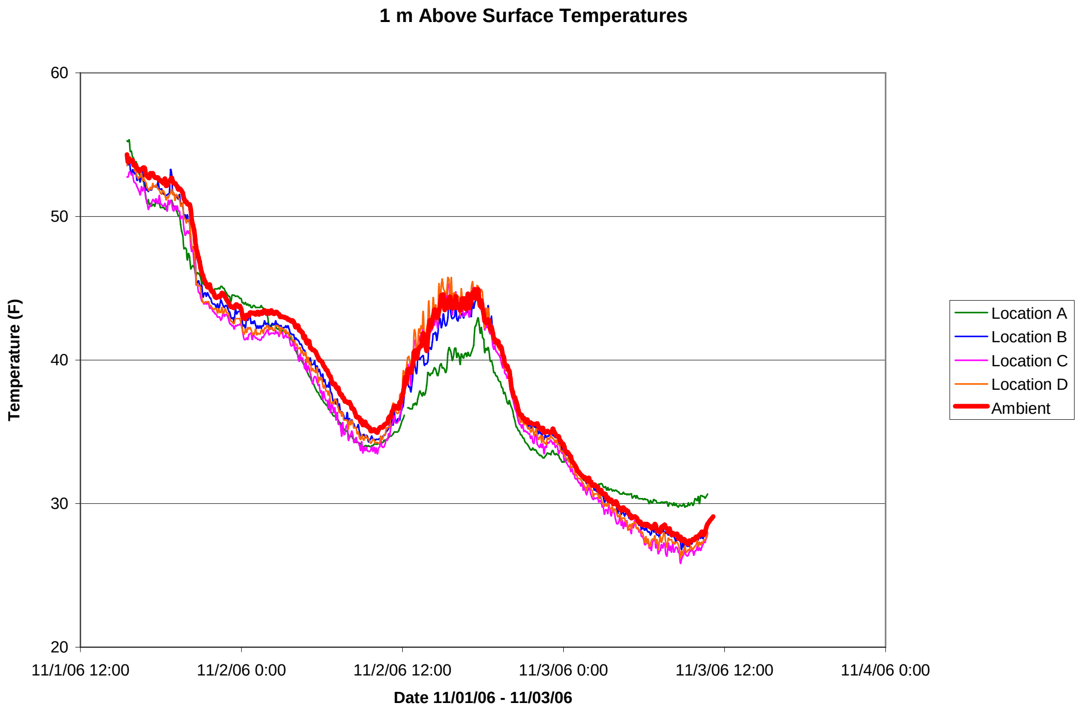

Figure 173. 1m Above Surface Temperatures for 11/1/06 – 11/3/06

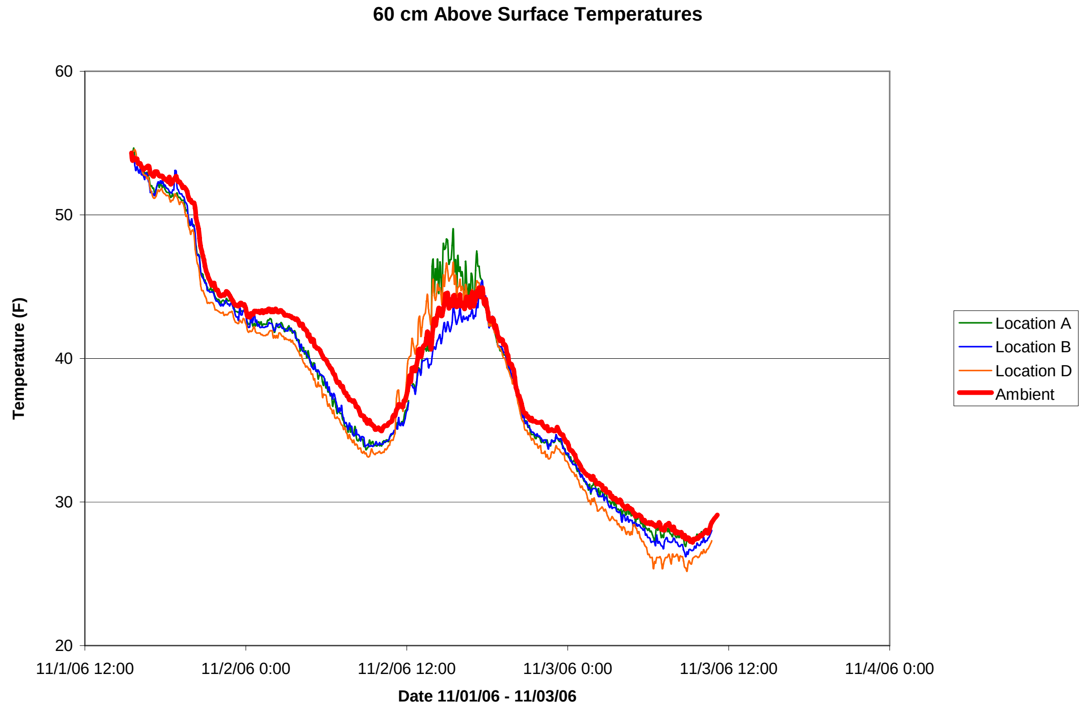

Figure 174. 60cm Above Surface Temperatures for 11/1/06 – 11/3/06

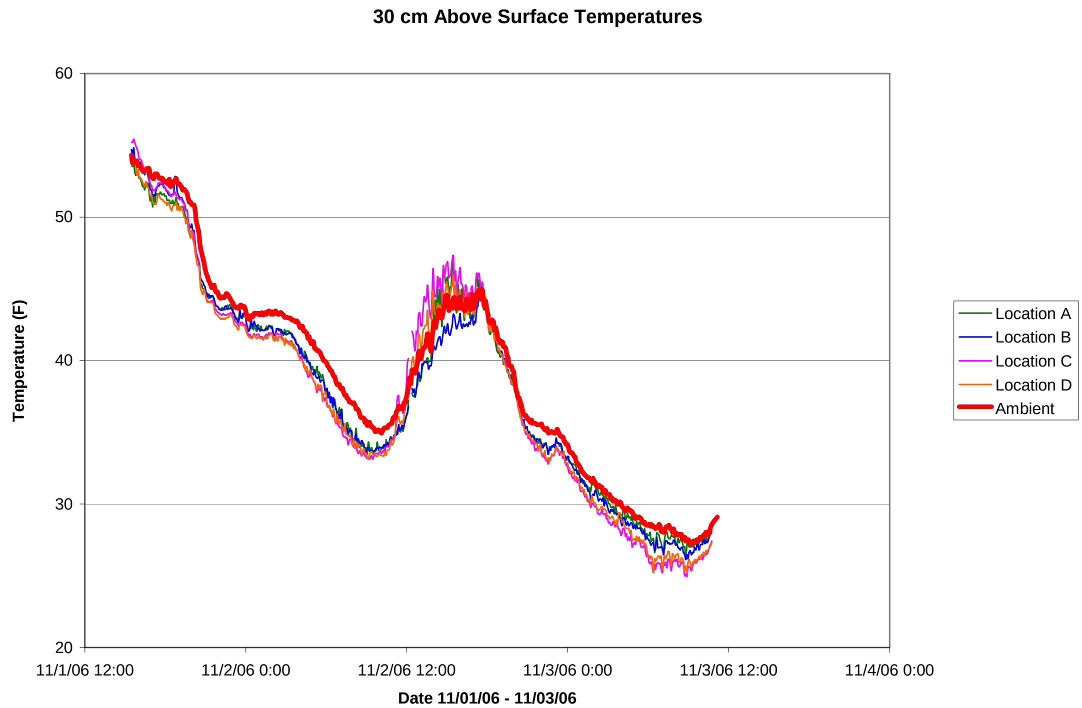

Figure 175. 30cm Above Surface Temperatures for 11/1/06 – 11/3/06

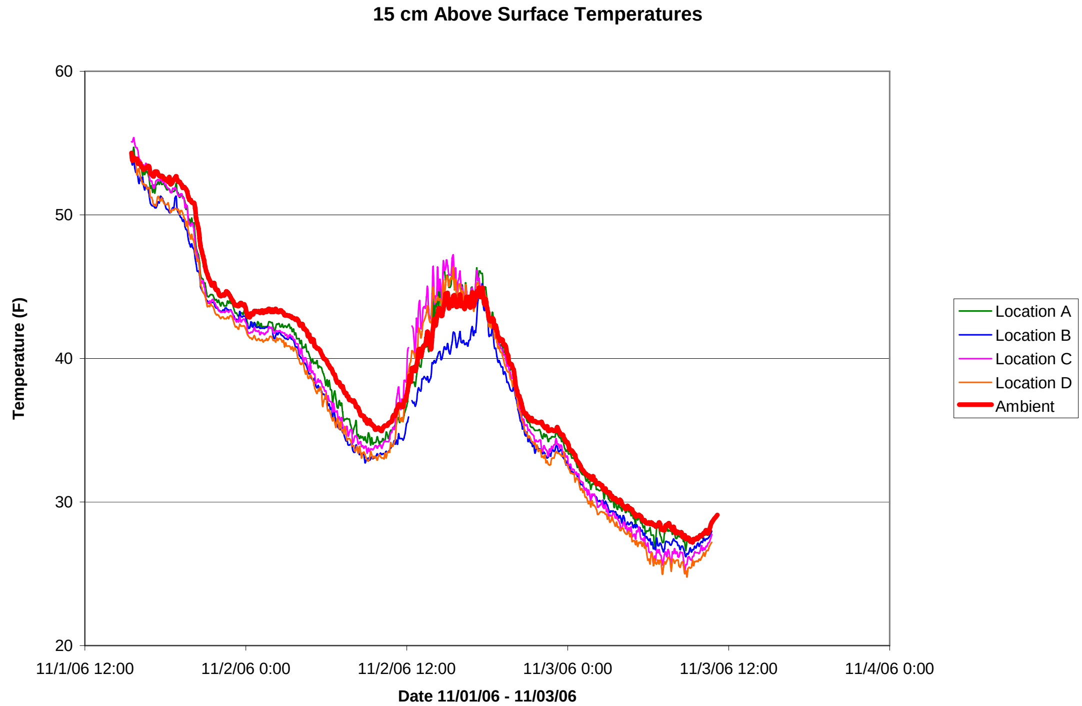

Figure 176. 15cm Above Surface Temperatures for 11/1/06 – 11/3/06

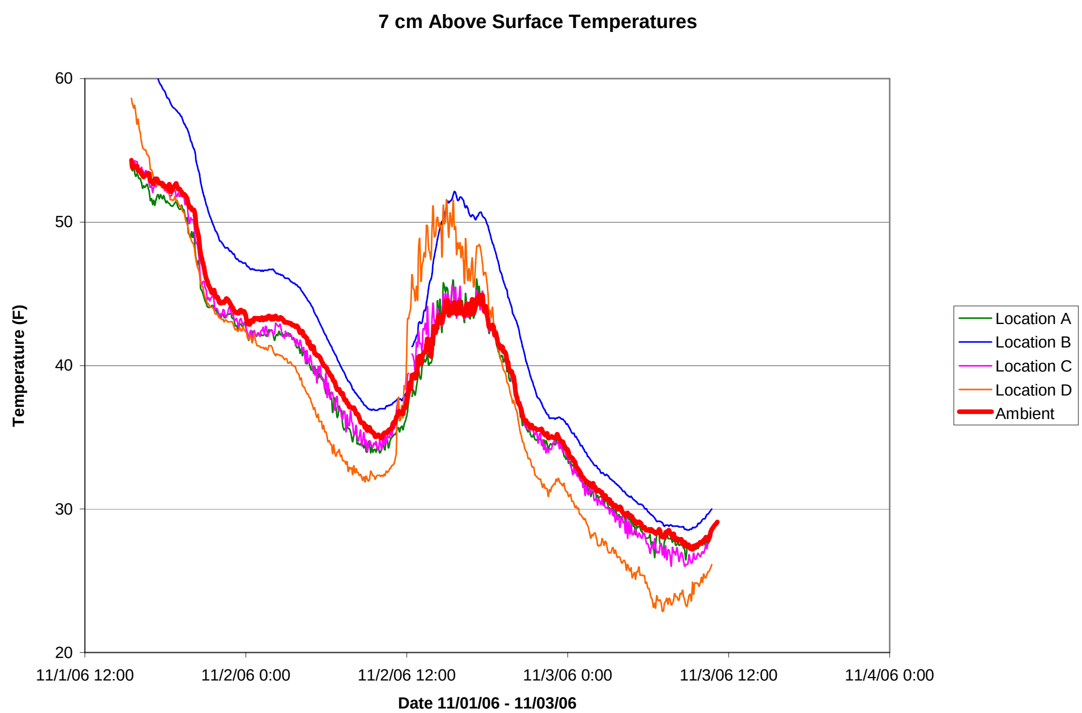

Figure 177. 7cm Above Surface Temperatures for 11/1/06 – 11/3/06

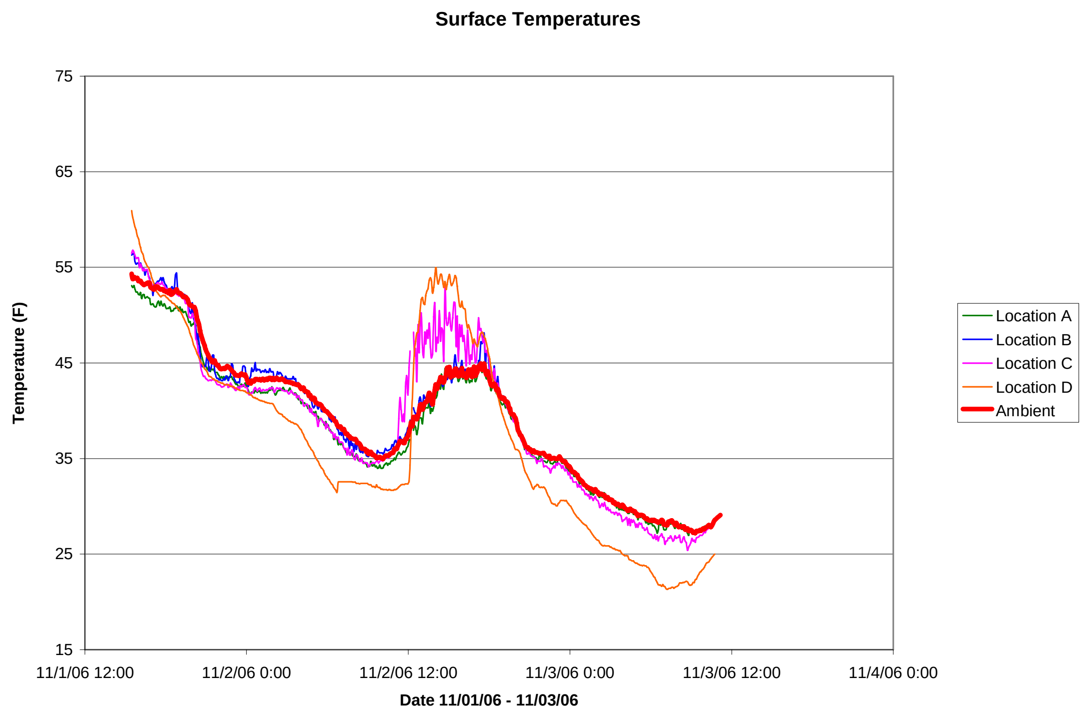

Figure 178. Surface Temperatures for 11/1/06 – 11/3/06

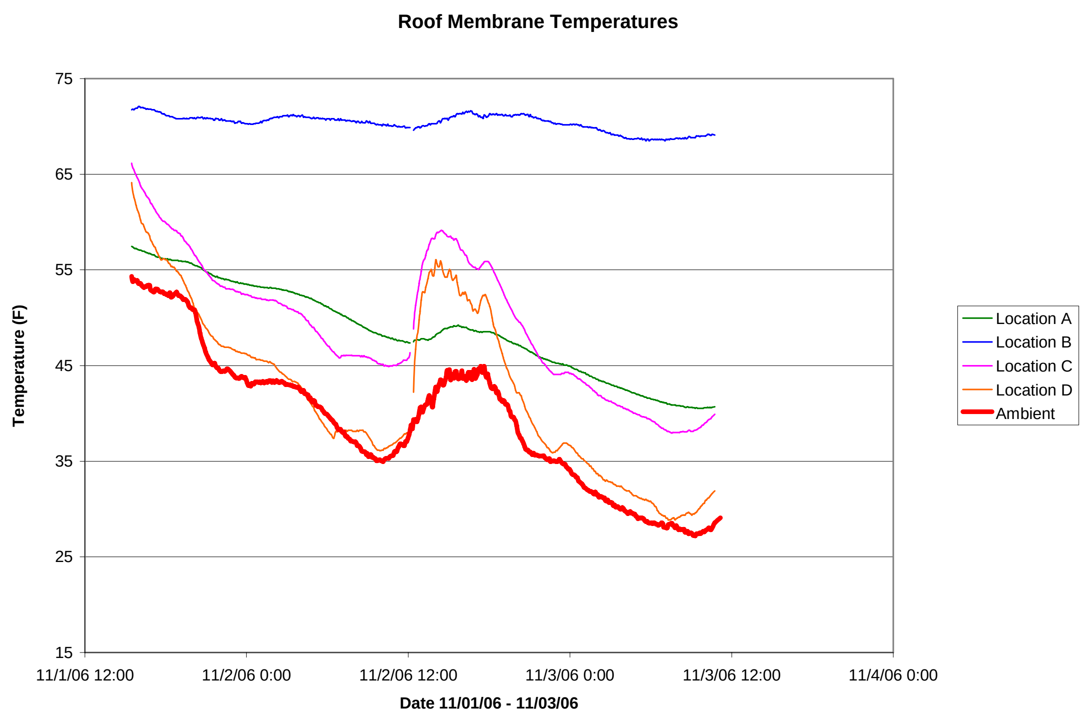

Figure 179. Roof Membrane Temperatures for 11/1/06 – 11/3/06

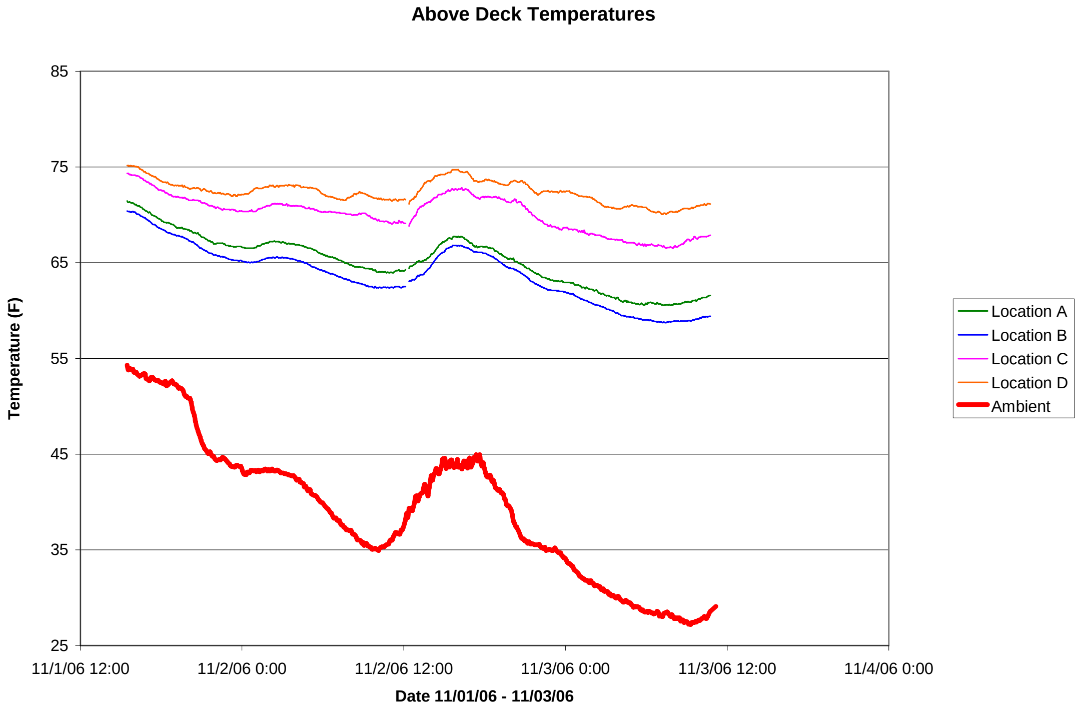

Figure 180. Above Deck Temperatures for 11/1/06 – 11/3/06

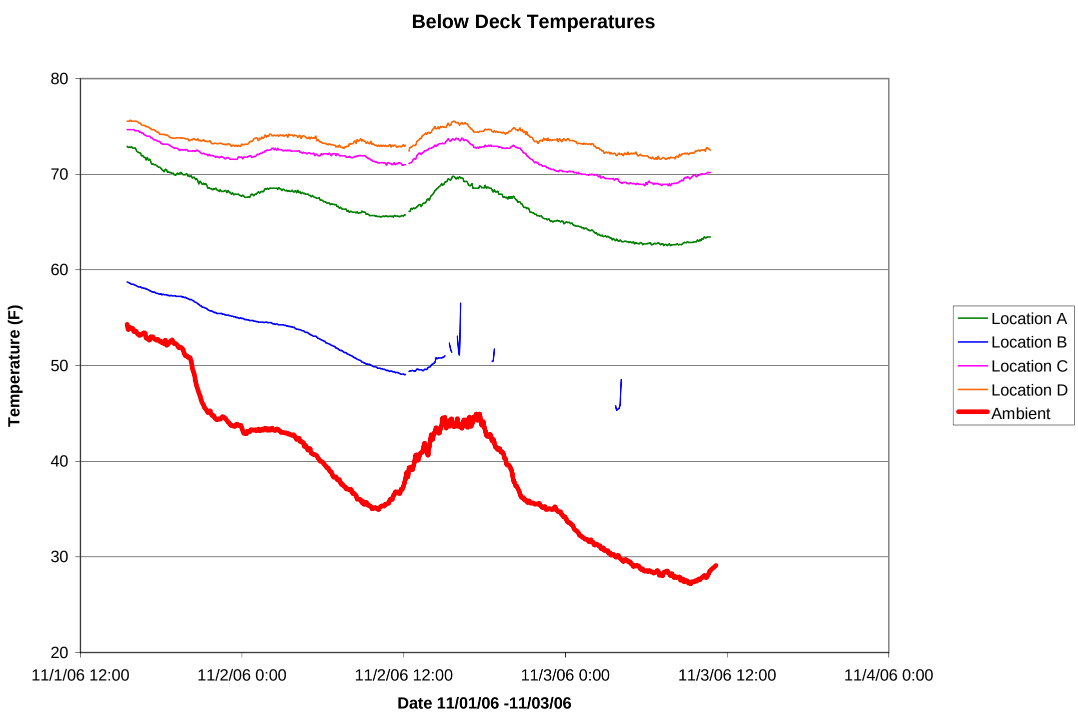

Figure 181. Below Deck Temperatures for 11/1/06 – 11/3/06

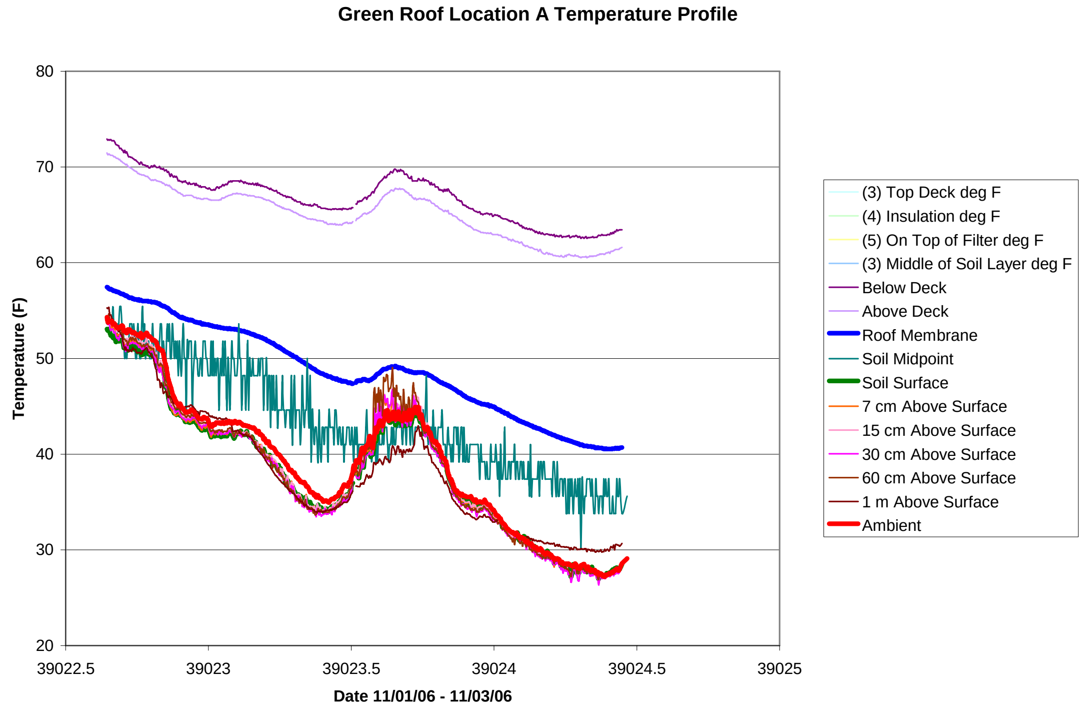

Figure 182. Green Roof Location A Temperature Profile for 11/1/06 -11/3/06

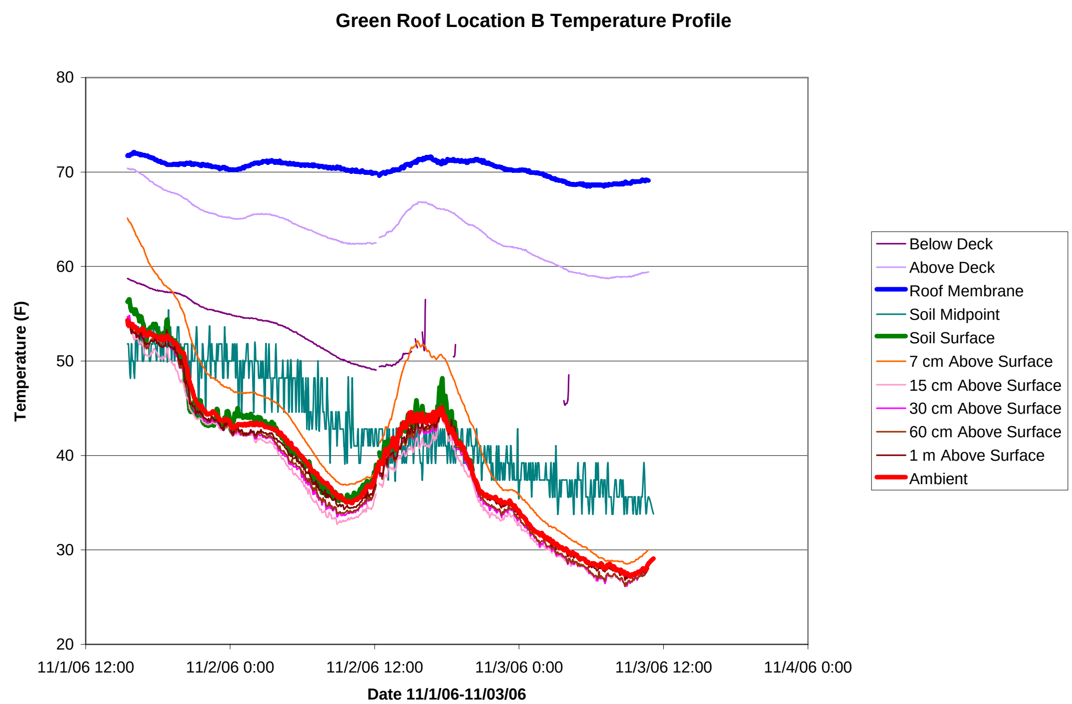

Figure 183. Green Roof Location B Temperature Profile for 11/1/06 -11/3/06

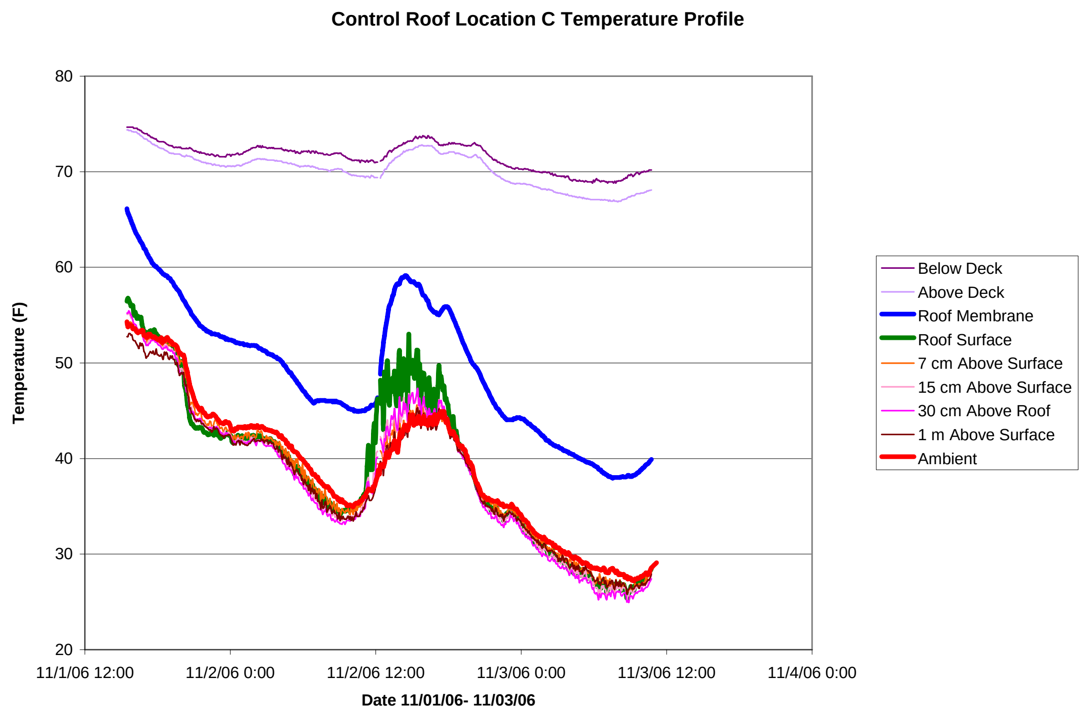

Figure 184. Control Roof Location C Temperature Profile for 11/1/06 -11/3/06

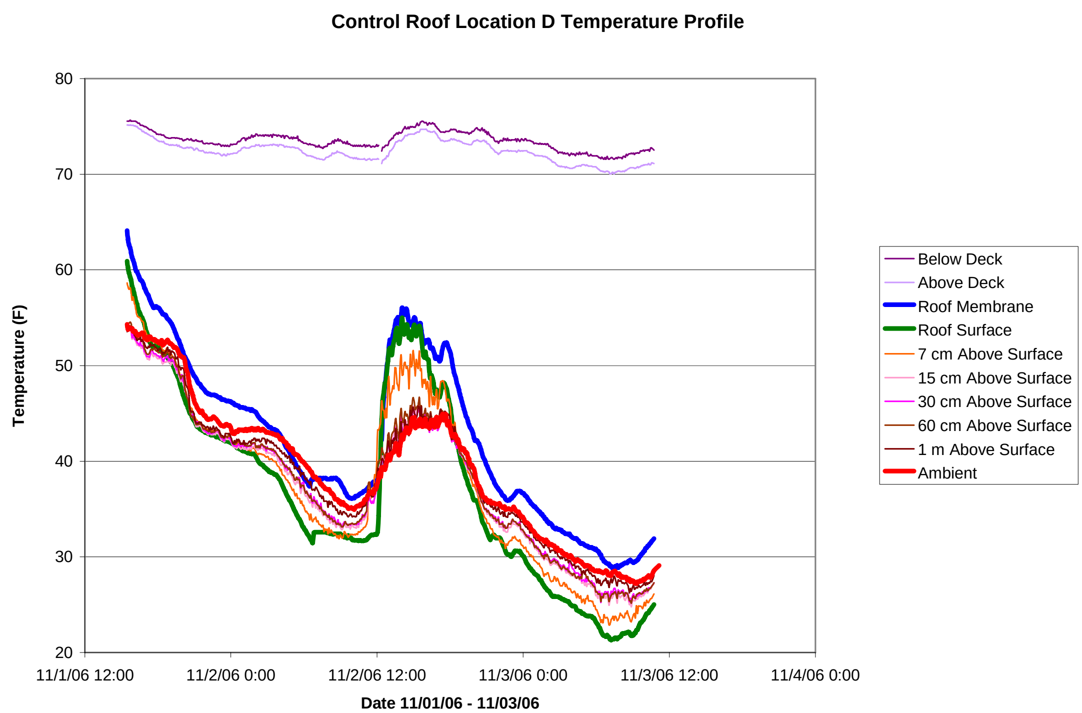

Figure 185. Control Roof Location D Temperature Profile for 11/1/06 -11/3/06

Temperature Measurements for November 27, 2006 to November 29, 2006

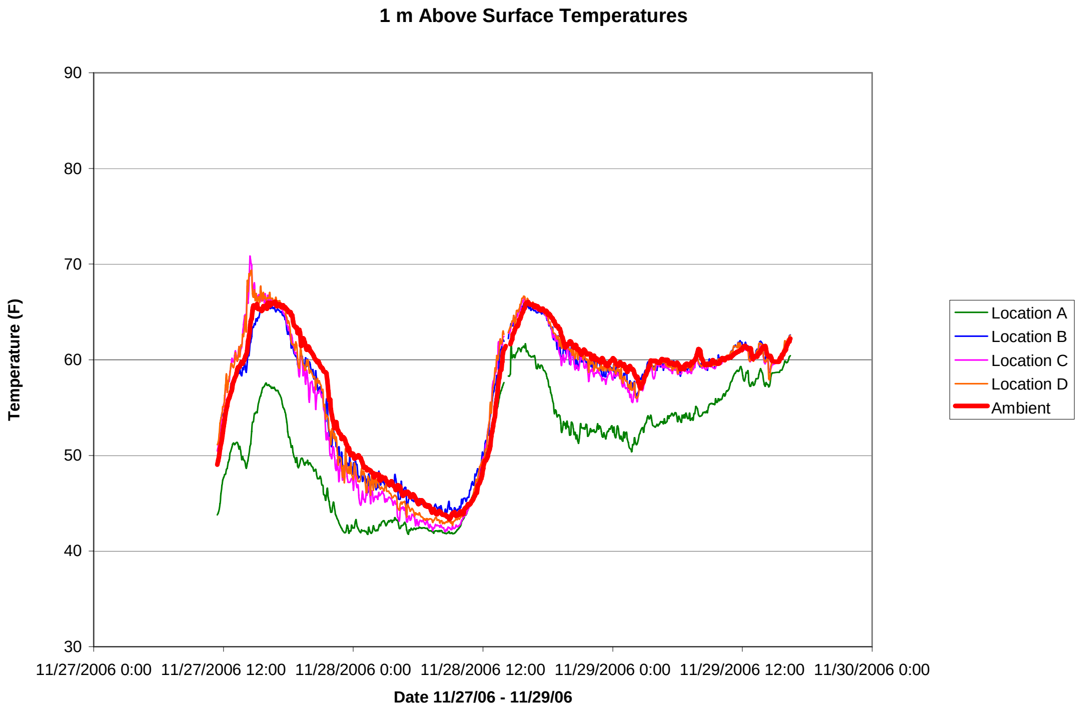

Figure 186. 1m Above Surface Temperatures for 11/27/06 – 11/29/06

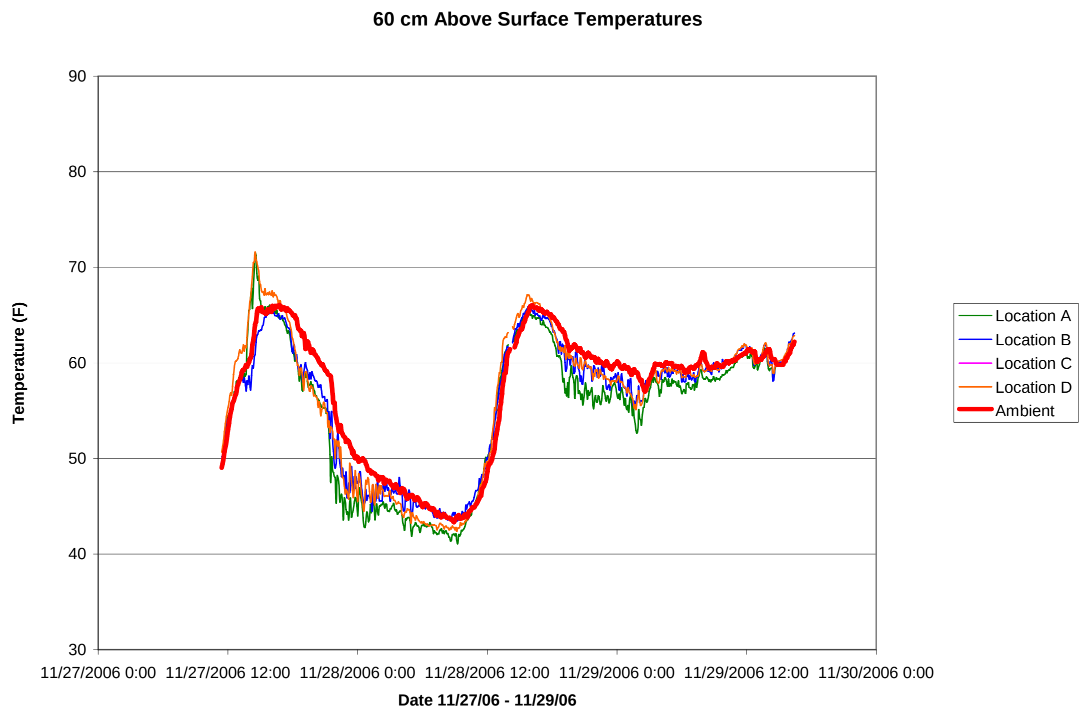

Figure 187. 60cm Above Surface Temperatures for 11/27/06 – 11/29/06

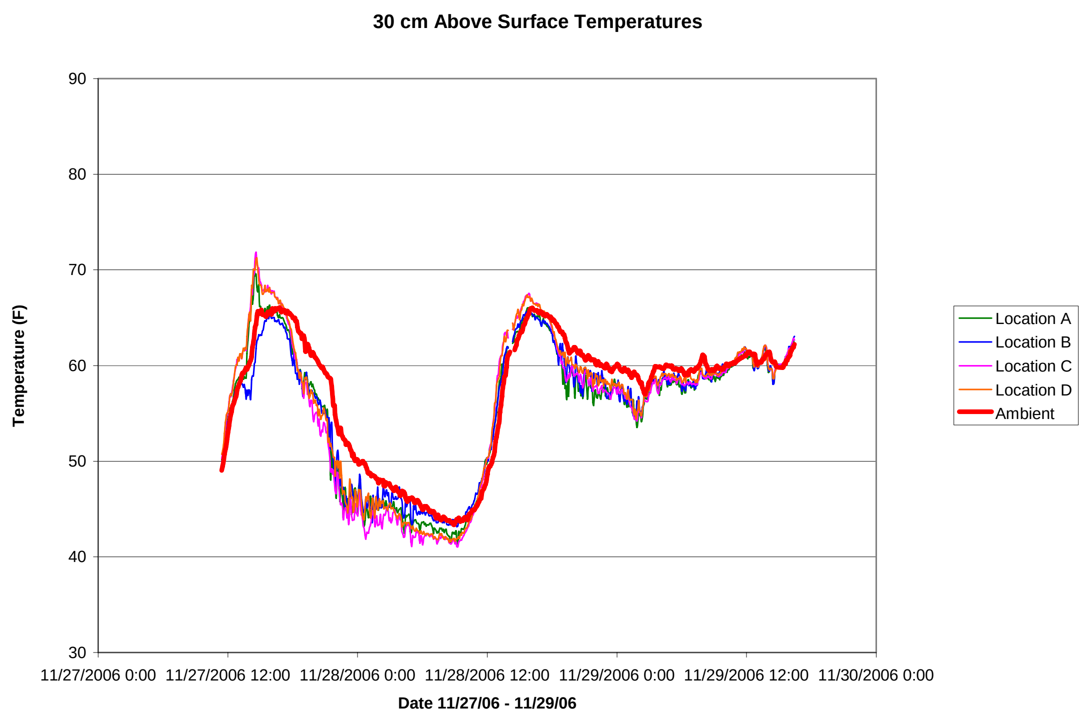

Figure 188. 30cm Above Surface Temperatures for 11/27/06 – 11/29/06

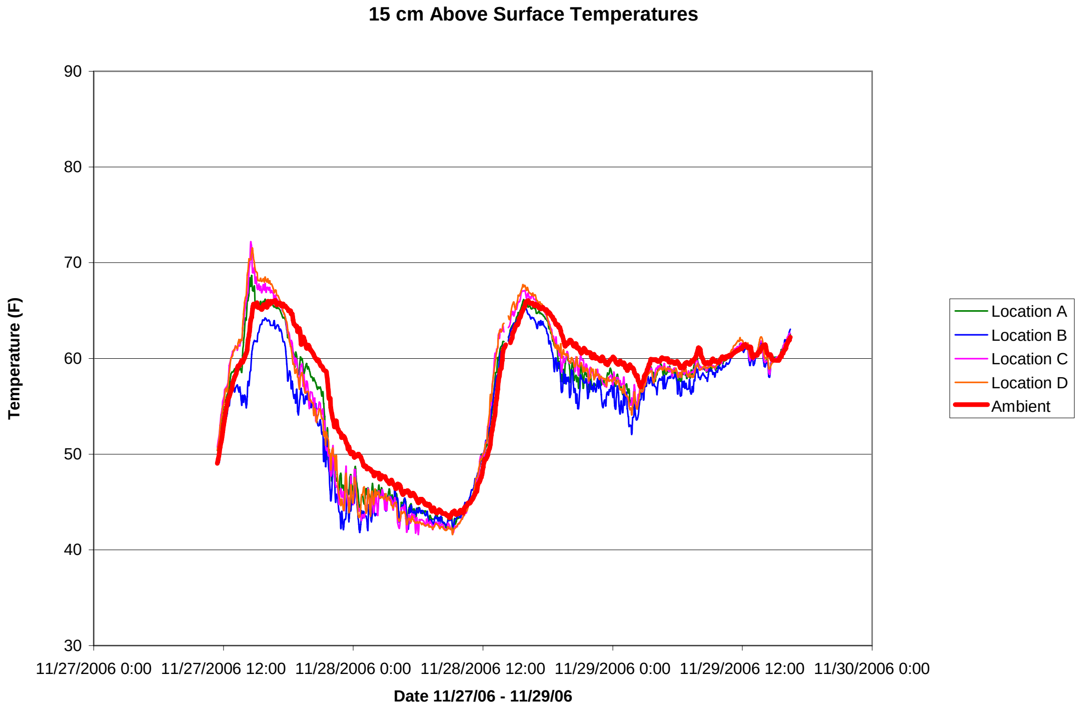

Figure 189. 15cm Above Surface Temperatures for 11/27/06 – 11/29/06

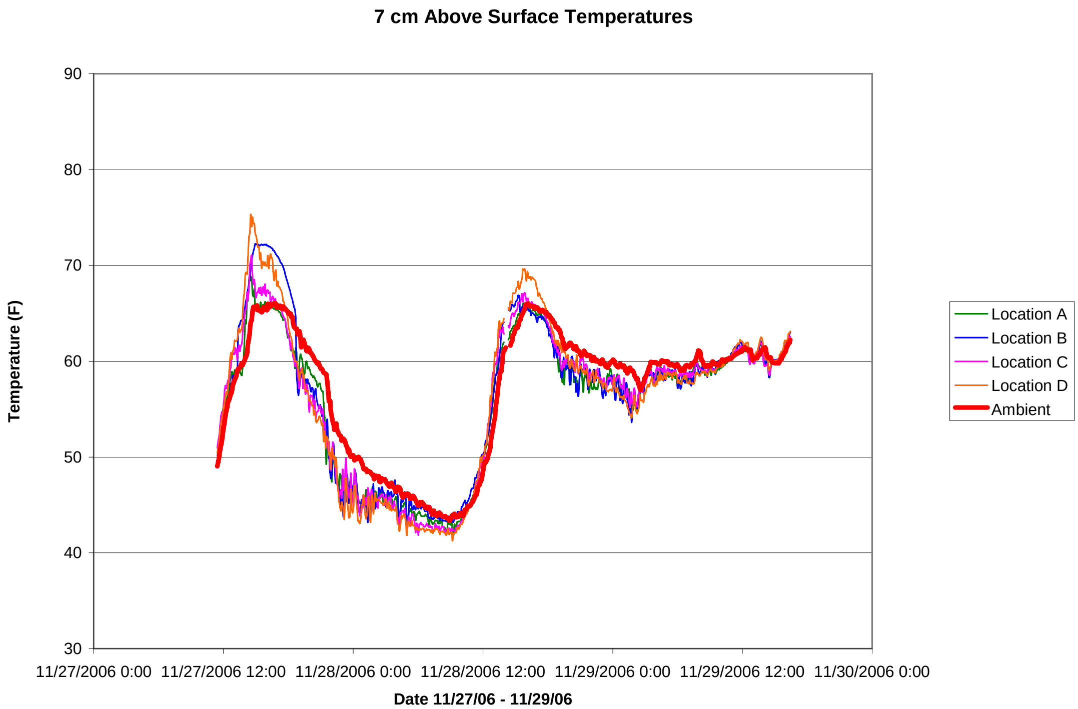

Figure 190. 7cm Above Surface Temperatures for 11/27/06 – 11/29/06

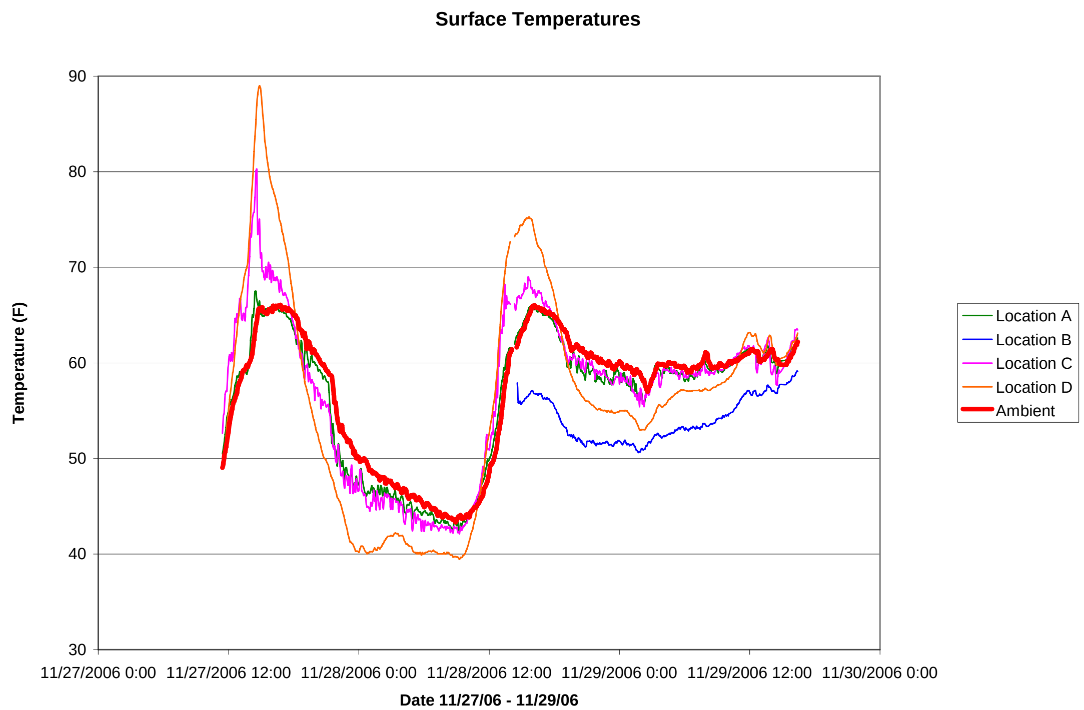

Figure 191. Surface Temperatures for 11/27/06 – 11/29/06

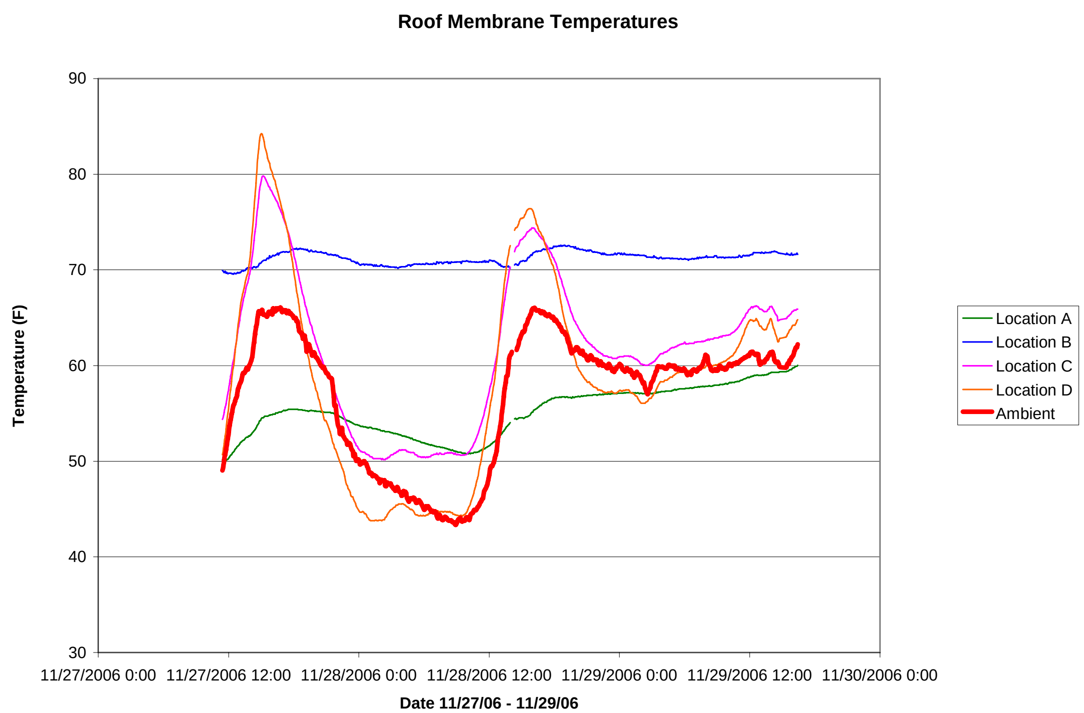

Figure 192. Roof Membrane Temperatures for 11/27/06 – 11/29/06

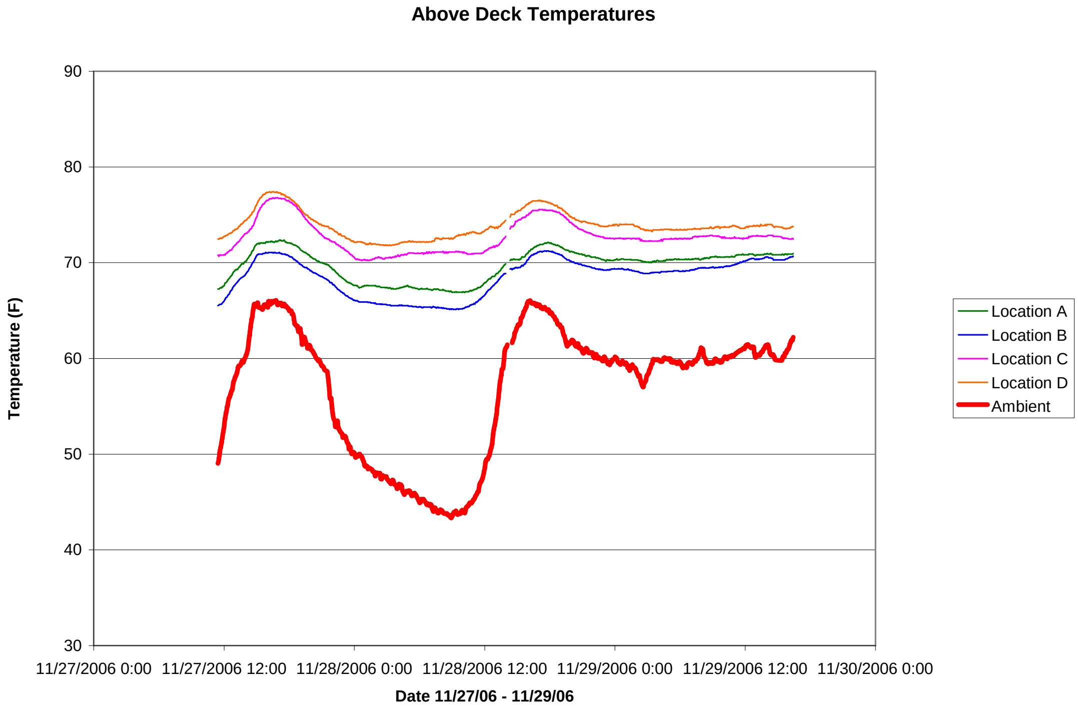

Figure 193. Above Deck Temperatures for 11/27/06 – 11/29/06

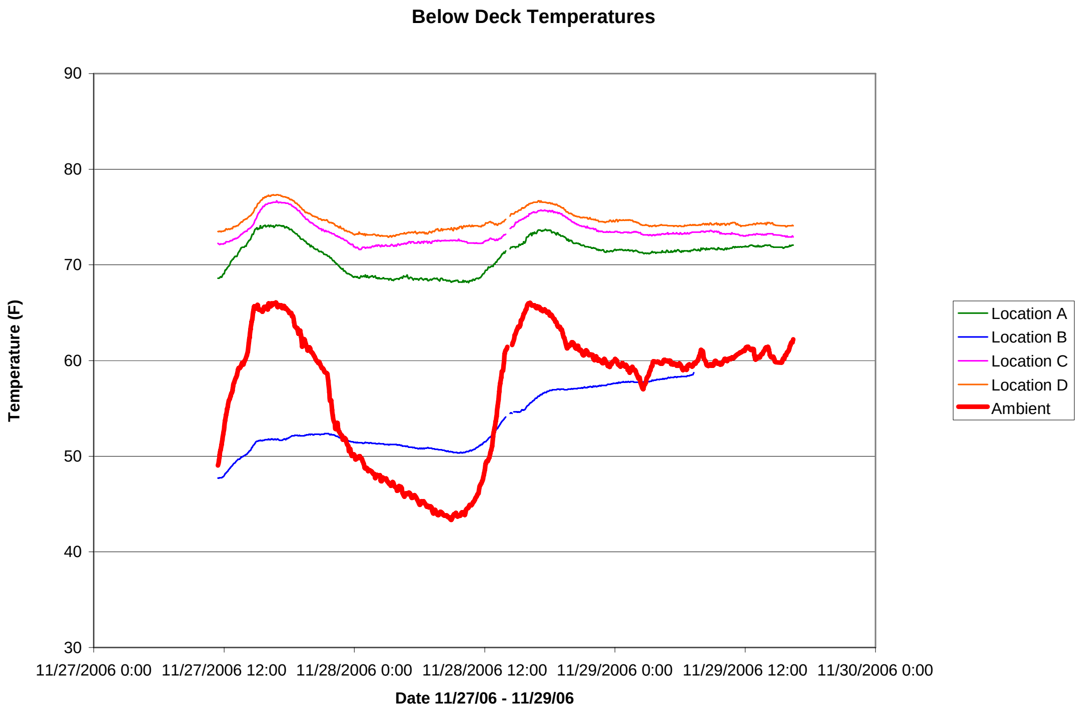

Figure 194. Below Deck Temperatures for 11/27/06 – 11/29/06

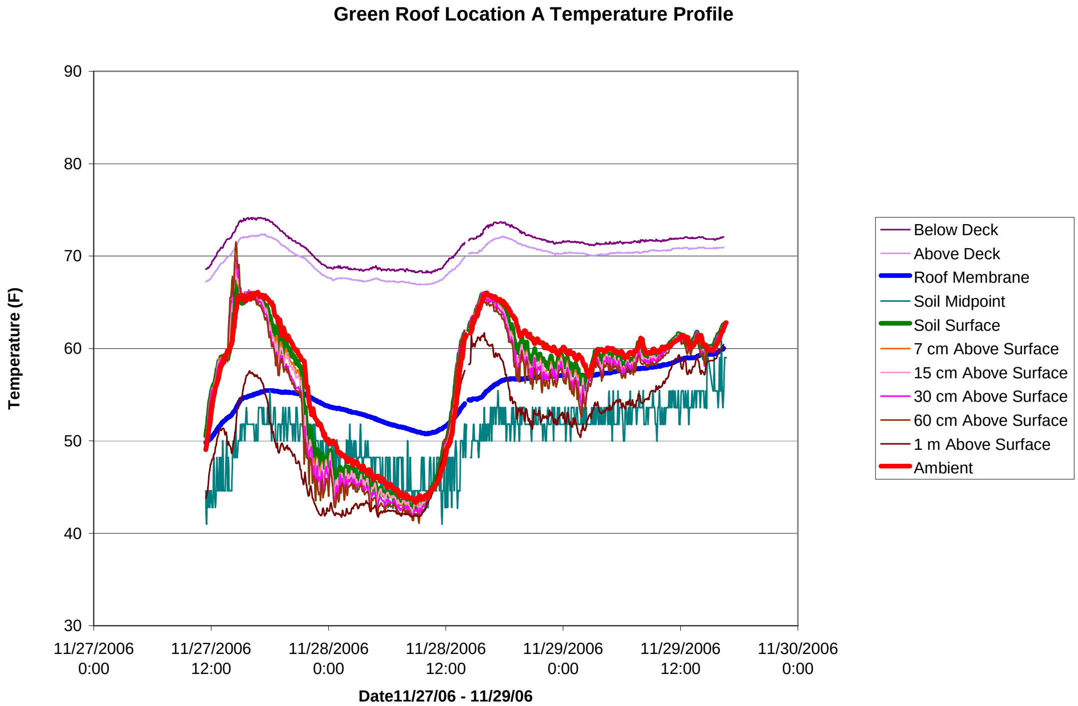

Figure 195. Green Roof Location A Temperature Profile for 11/27/06 – 11/29/06

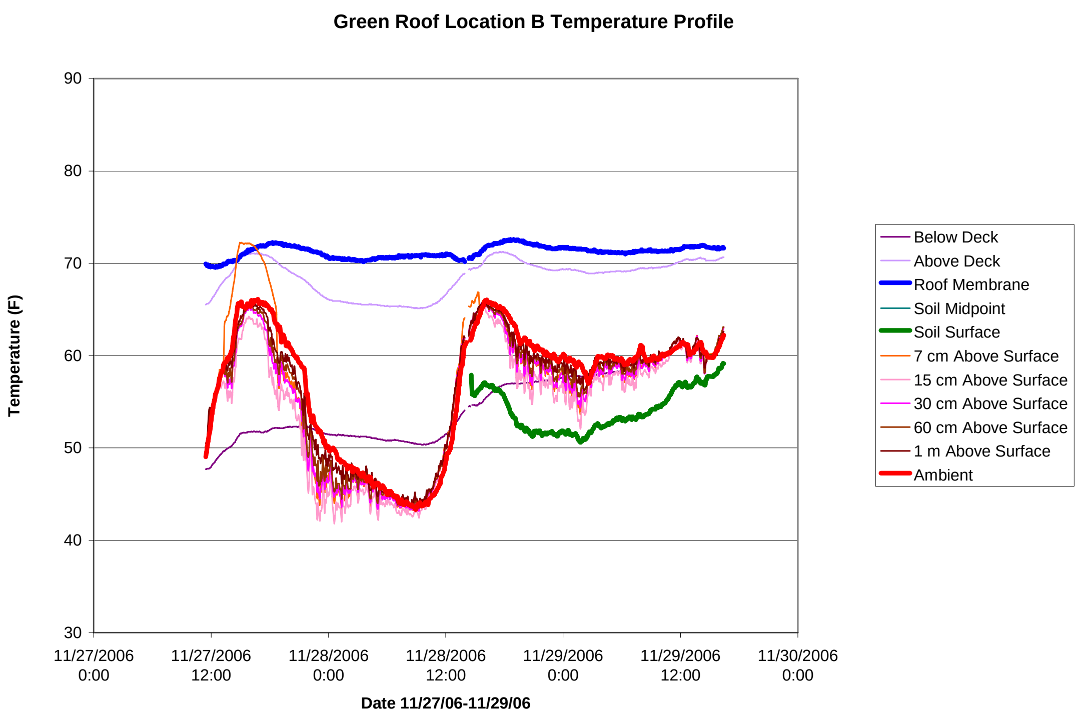

Figure 196. Green Roof Location B Temperature Profile for 11/27/06 – 11/29/06

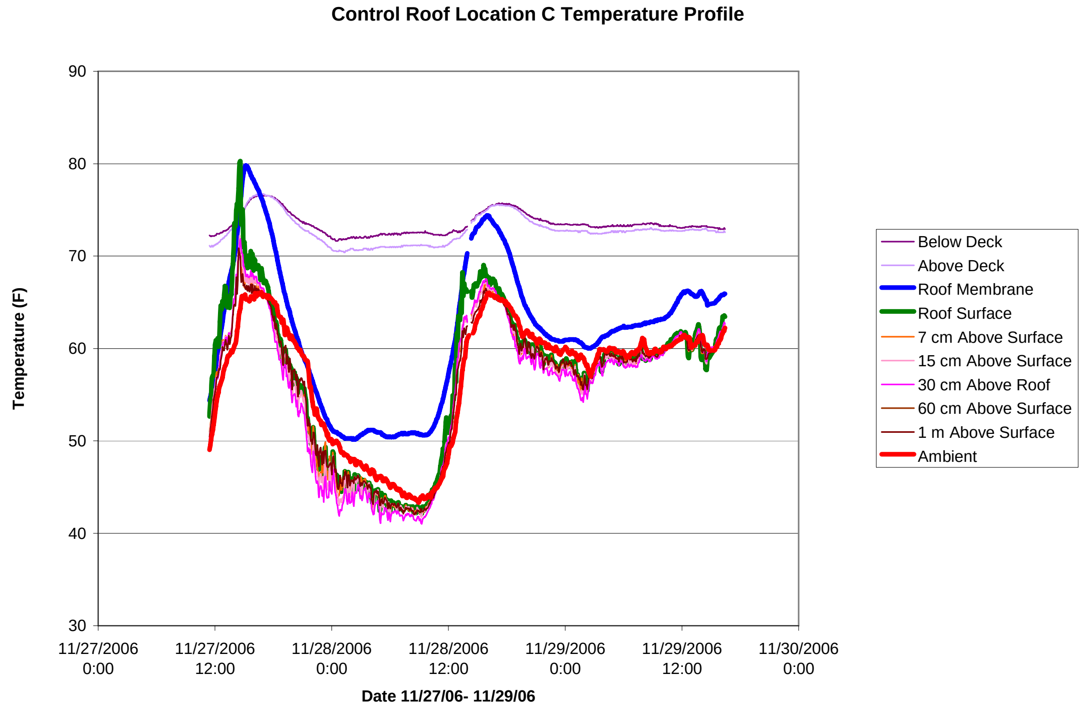

Figure 197. Control Roof Location C Temperature Profile for 11/27/06 – 11/29/06

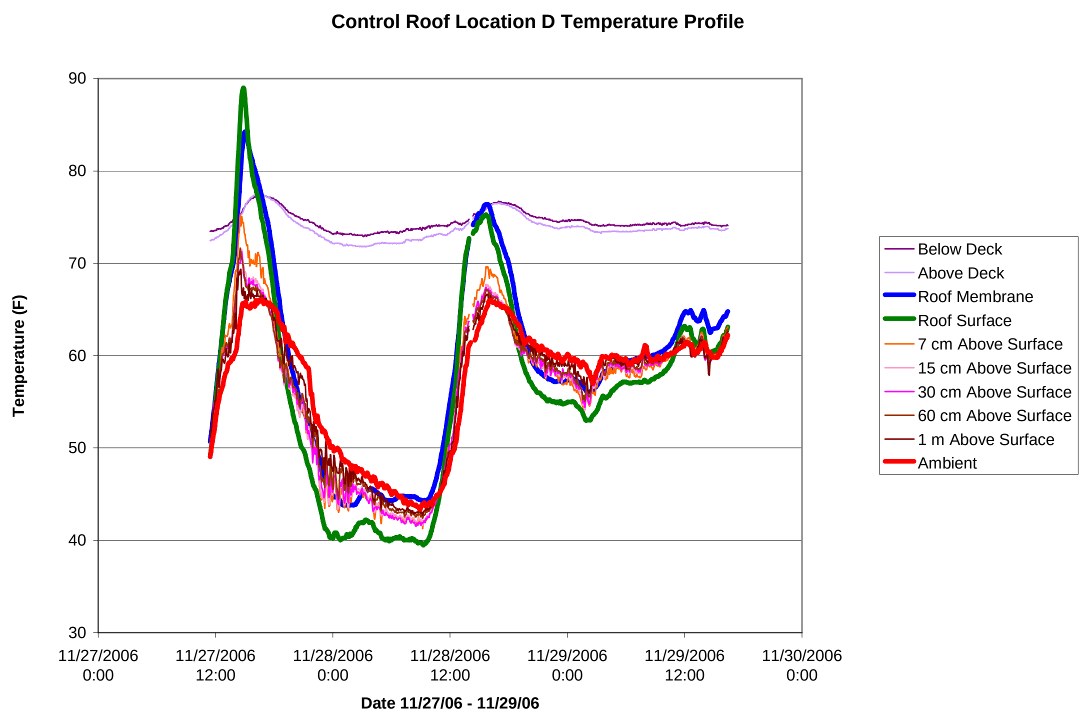

Figure 198. Control Roof Location D Temperature Profile for 11/27/06 – 11/29/06

Temperature Measurements for November 29, 2006 to December 4, 2006

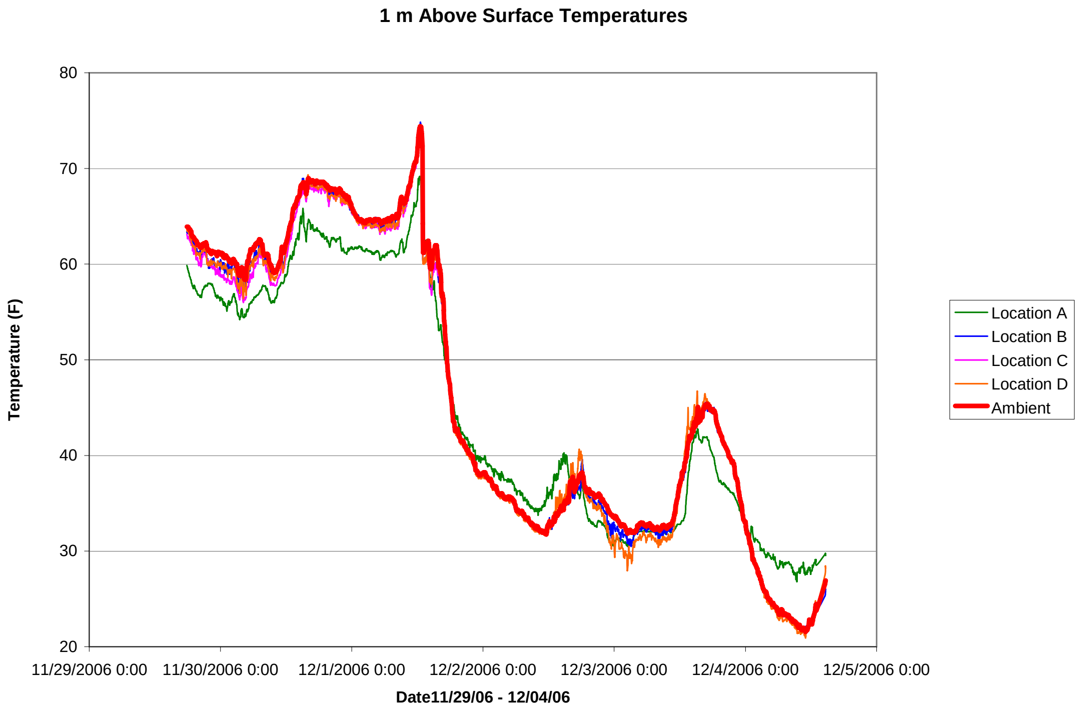

Figure 199. 1m Above Surface Temperatures for 11/29/06 – 12/4/06

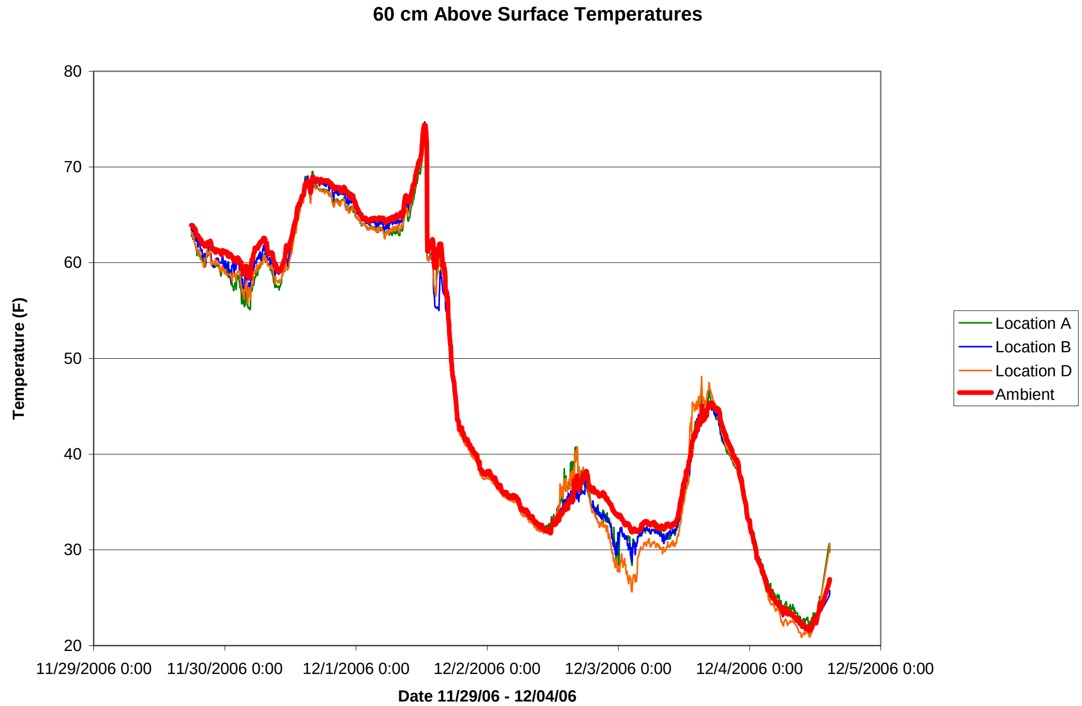

Figure 200. 60cm Above Surface Temperatures for 11/29/06 – 12/4/06

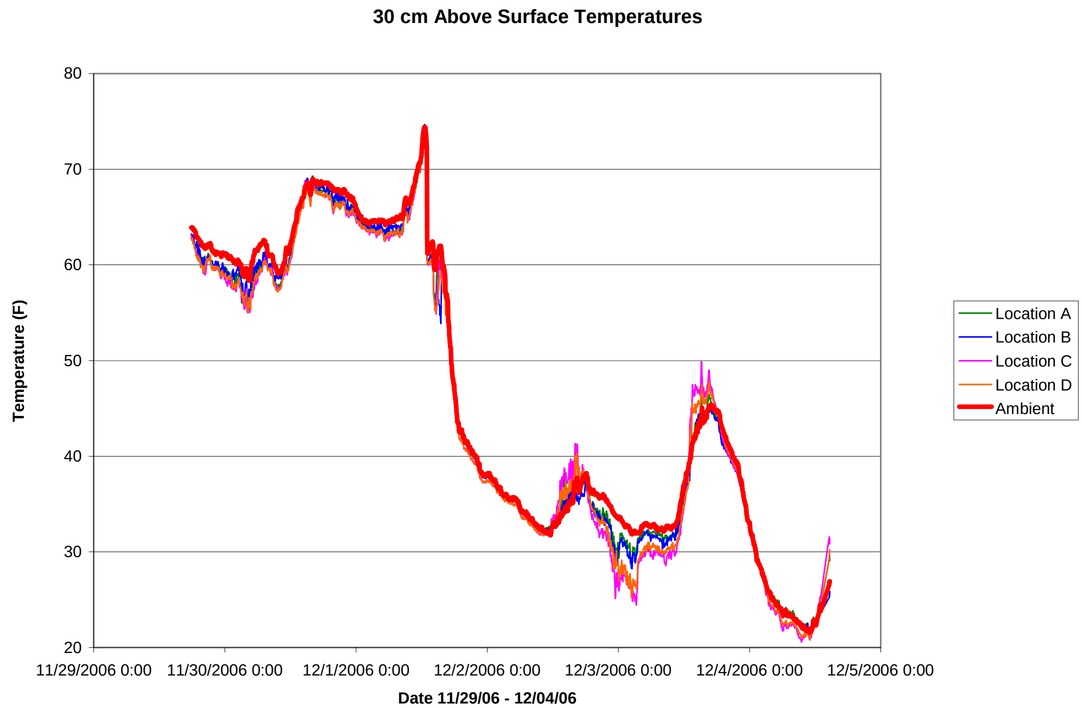

Figure 201. 30cm Above Surface Temperatures for 11/29/06 – 12/4/06

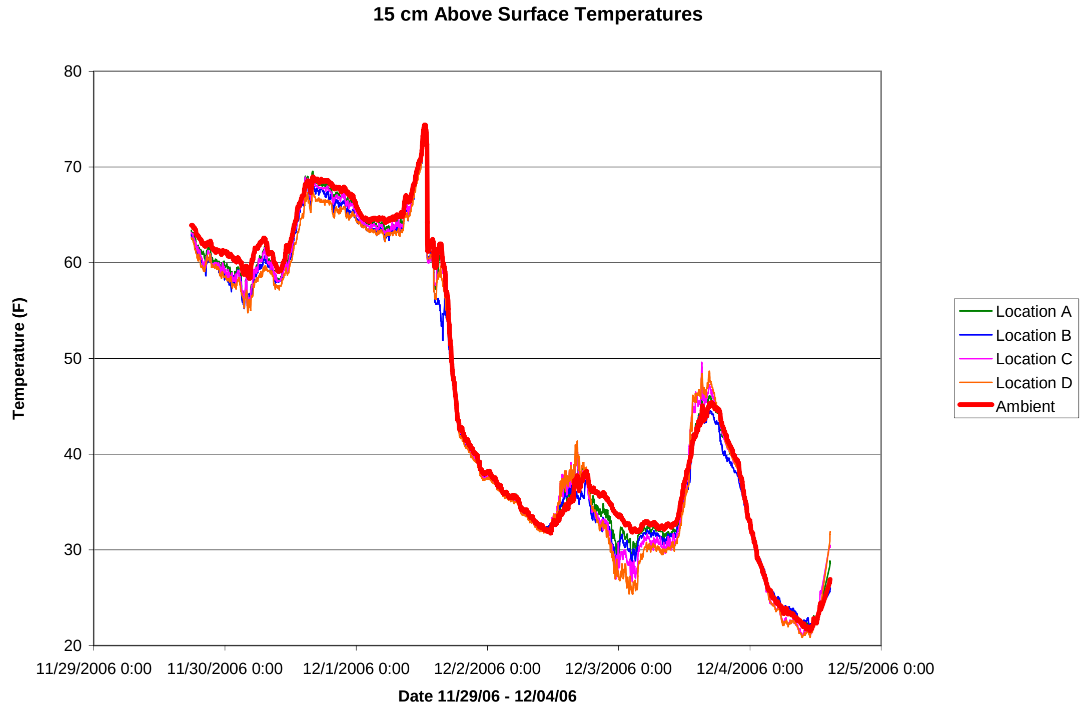

Figure 202. 15cm Above Surface Temperatures for 11/29/06 – 12/4/06

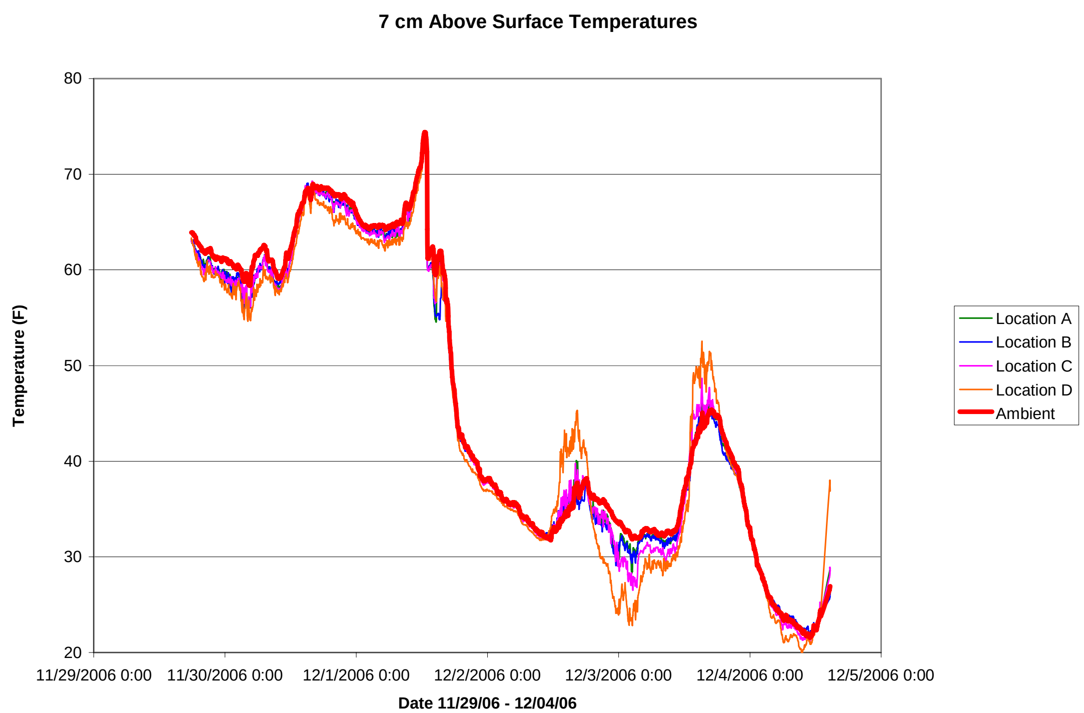

Figure 203. 7cm Above Surface Temperatures for 11/29/06 – 12/4/06

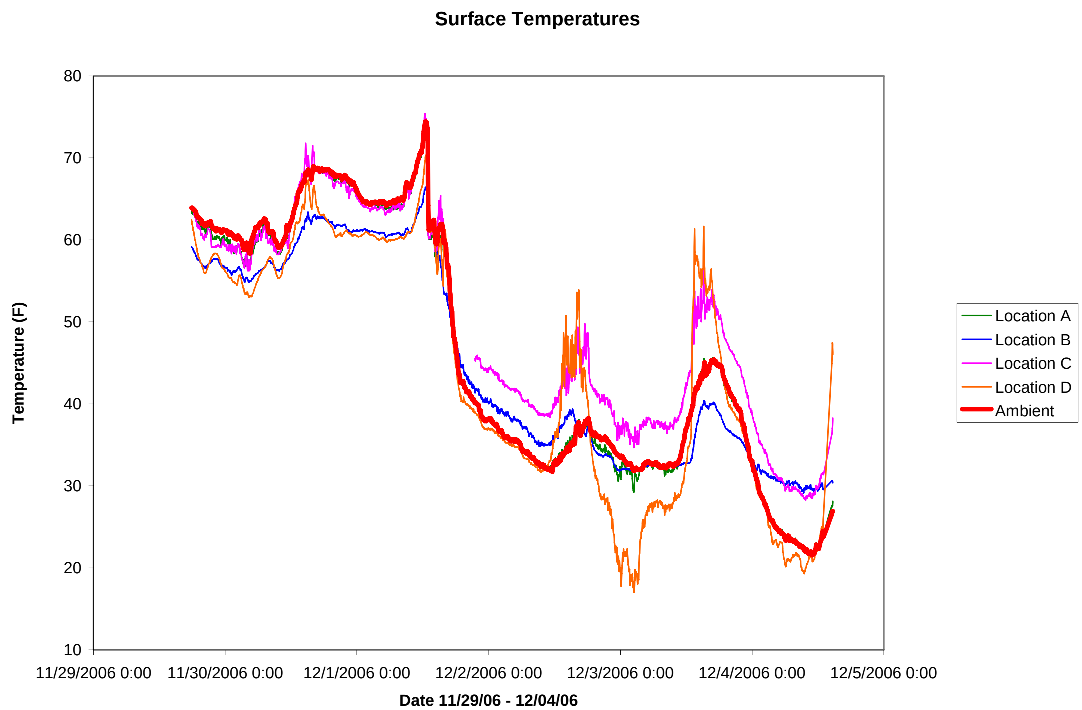

Figure 204. Surface Temperatures for 11/29/06 – 12/4/06

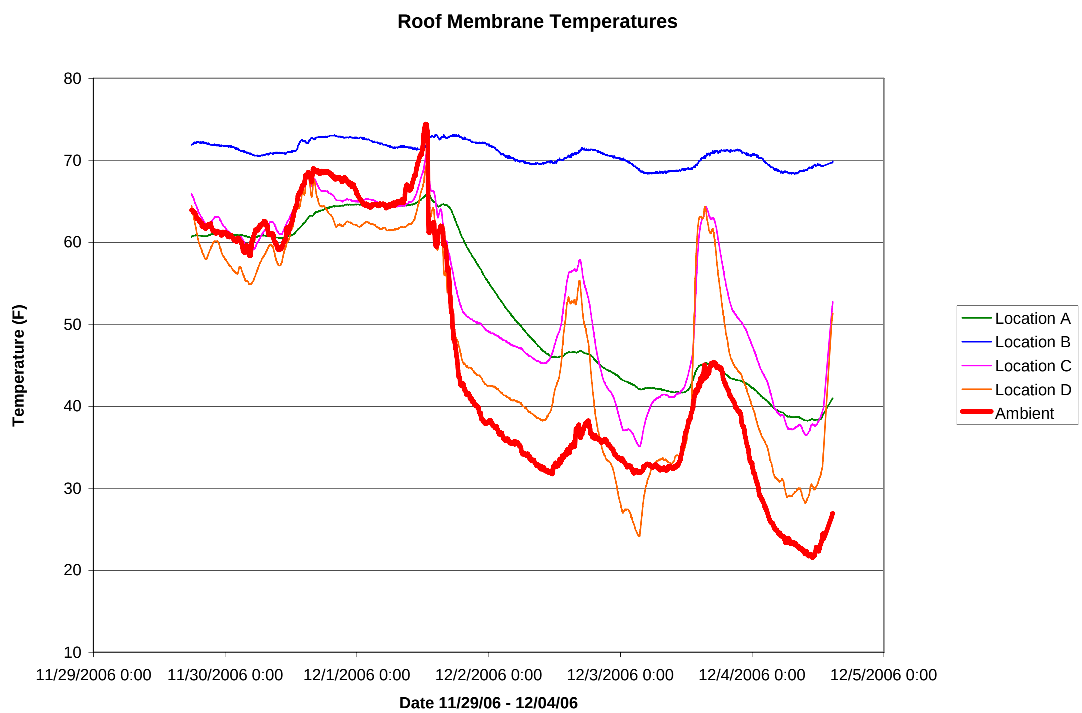

Figure 205. Roof Membrane Temperatures for 11/29/06 – 12/4/06

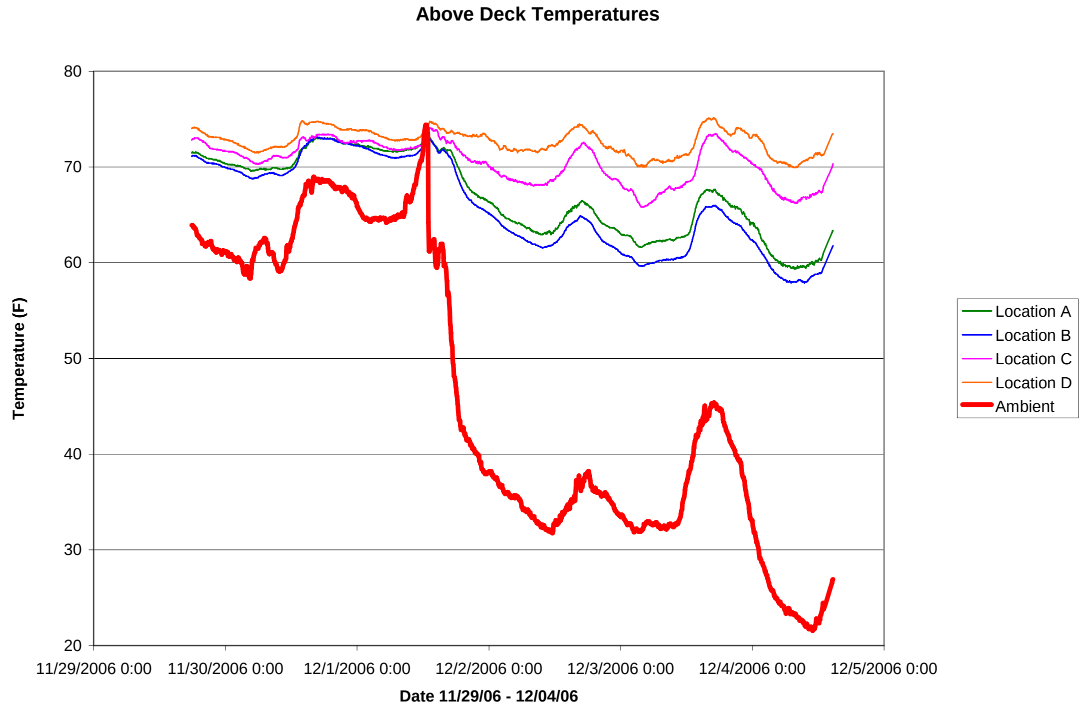

Figure 206. Above Deck Temperatures for 11/29/06 – 12/4/06

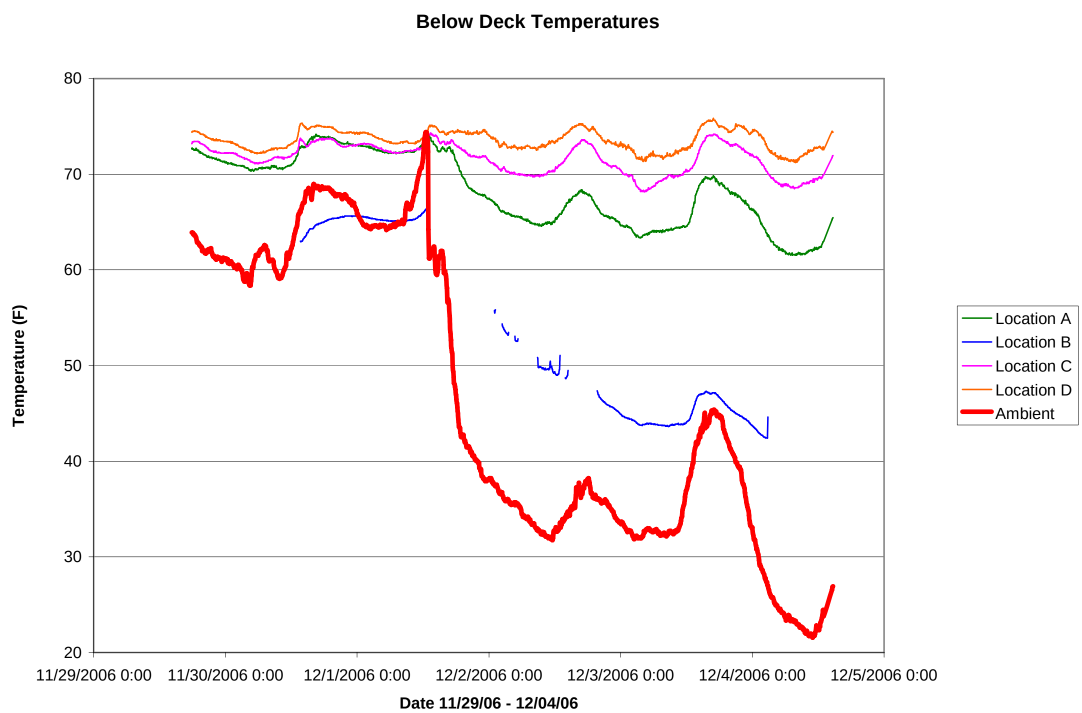

Figure 207. Below Deck Temperatures for 11/29/06 – 12/4/06

Temperature Measurements for December 7, 2006 to December 8, 2006

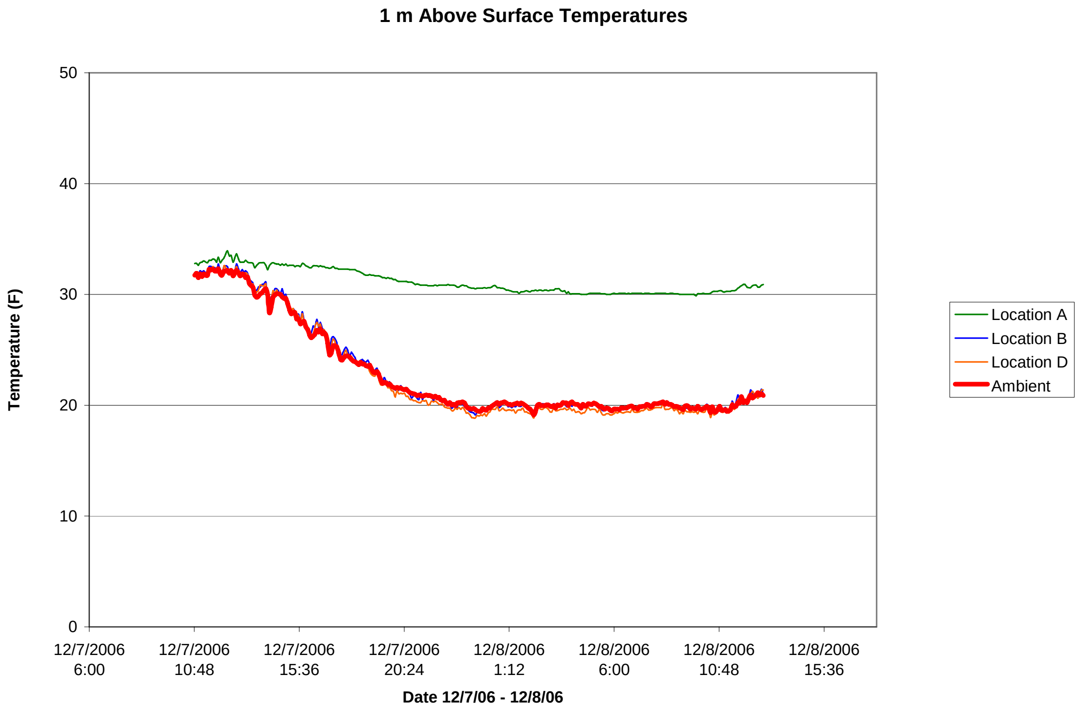

Figure 208. 1m Above Surface Temperatures for 12/7/06 – 12/8/06

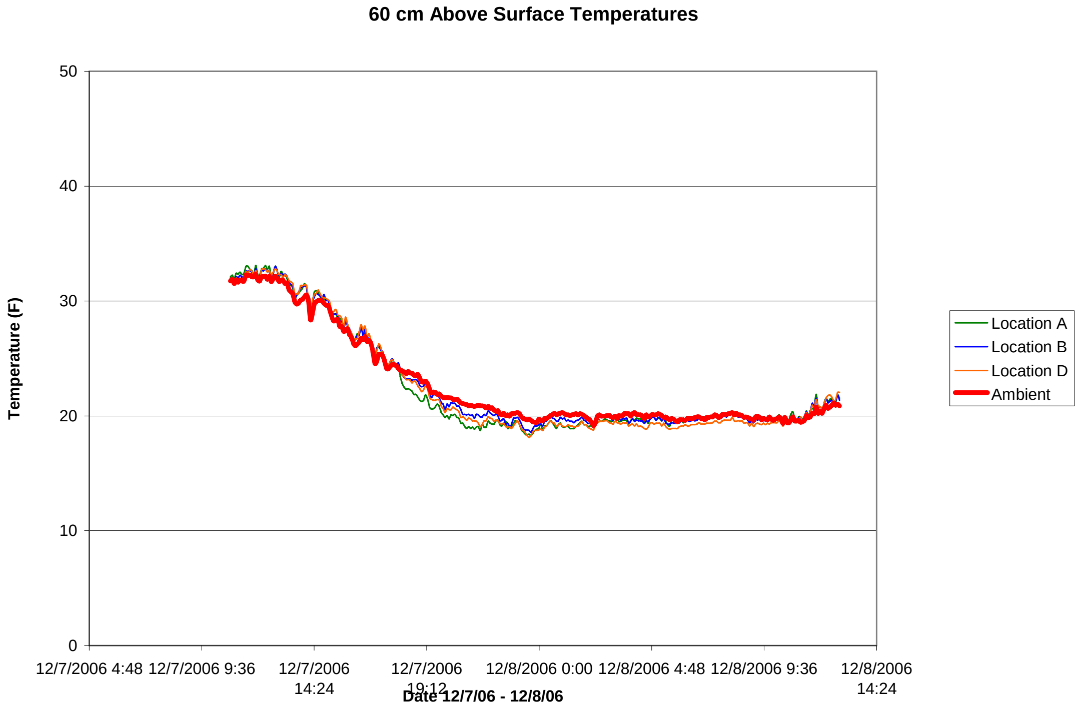

Figure 209. 60cm Above Surface Temperatures for 12/7/06 – 12/8/06

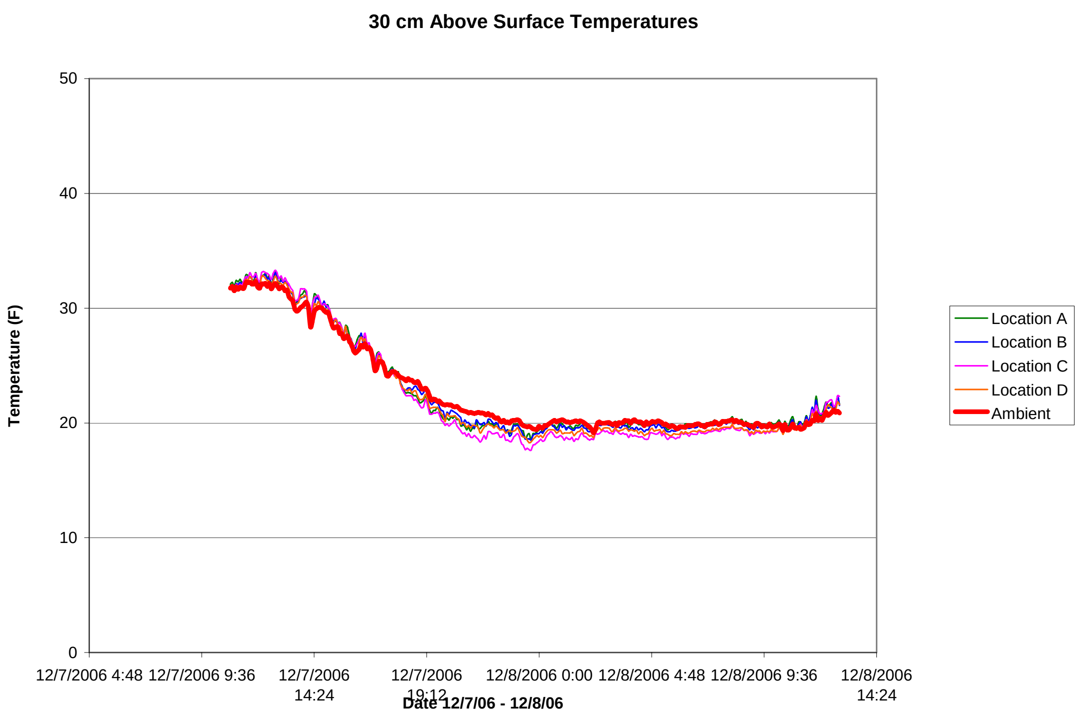

Figure 210. 30cm Above Surface Temperatures for 12/7/06 – 12/8/06

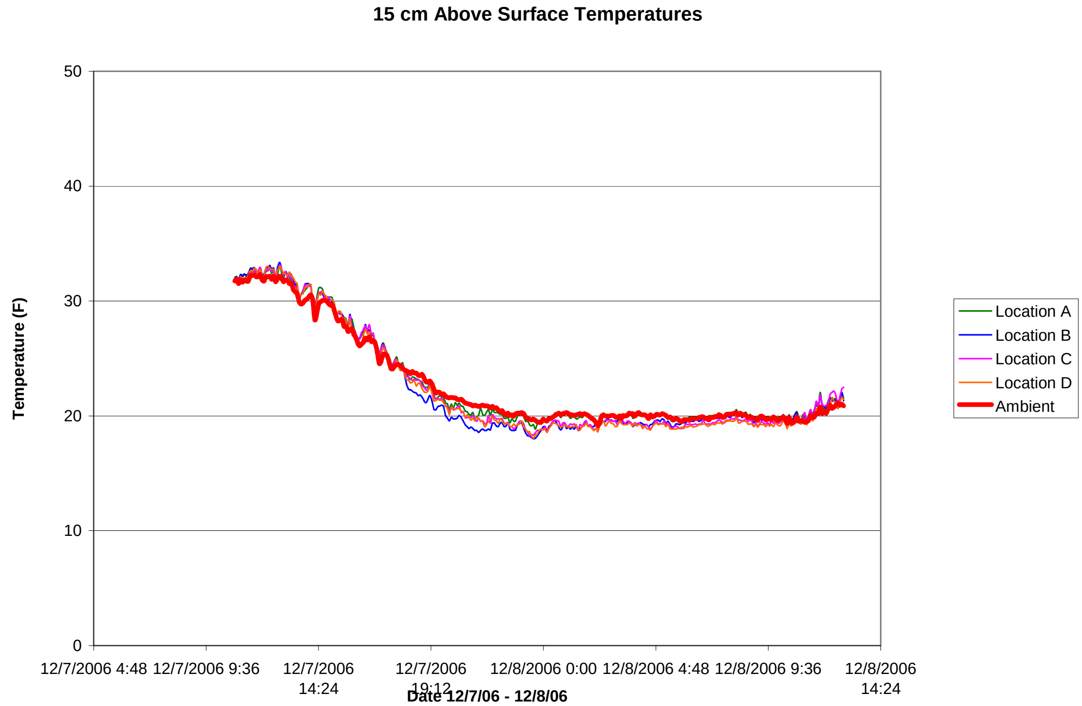

Figure 211. 15cm Above Surface Temperatures for 12/7/06 – 12/8/06

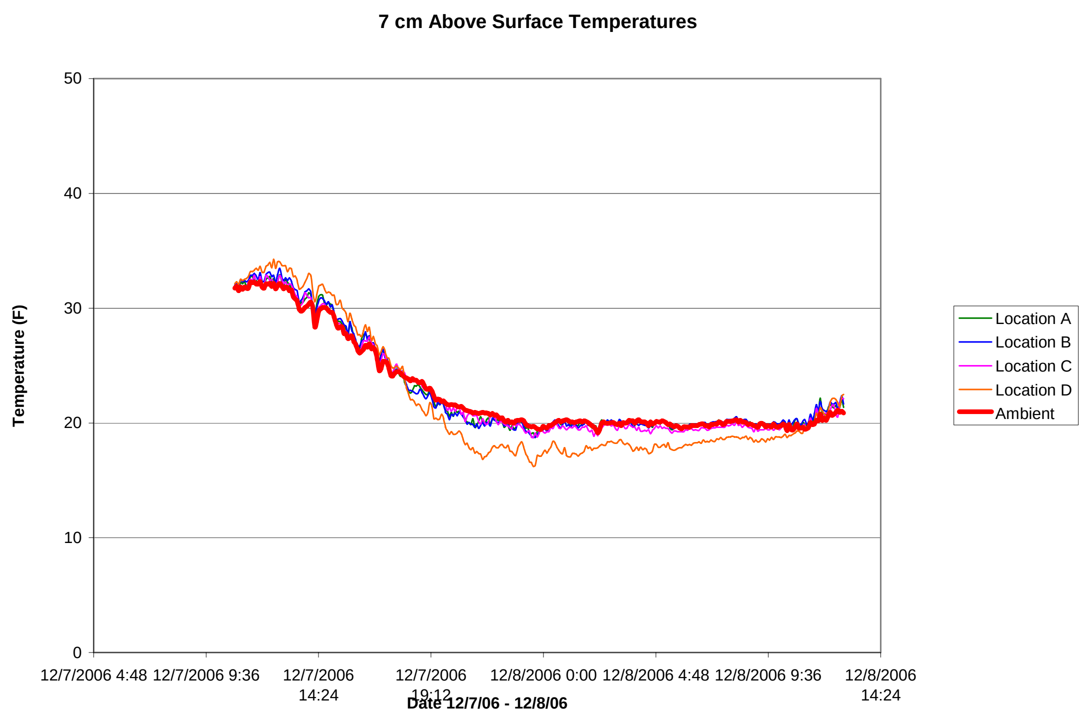

Figure 212. 7cm Above Surface Temperatures for 12/7/06 – 12/8/06

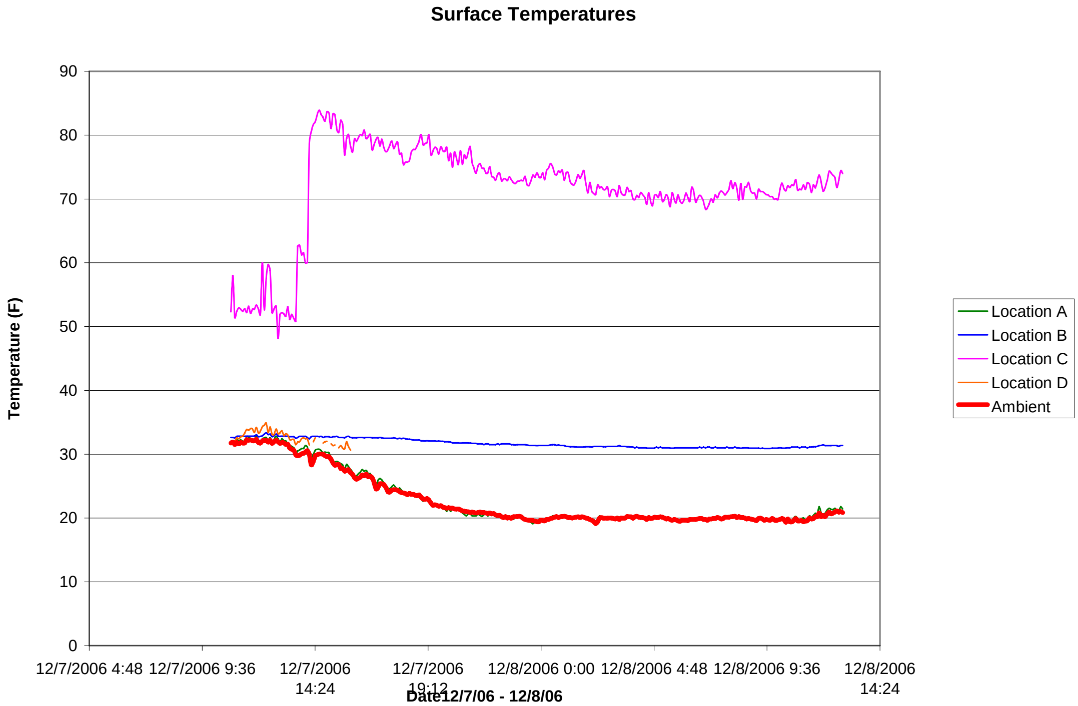

Figure 213. Surface Temperatures for 12/7/06 – 12/8/06

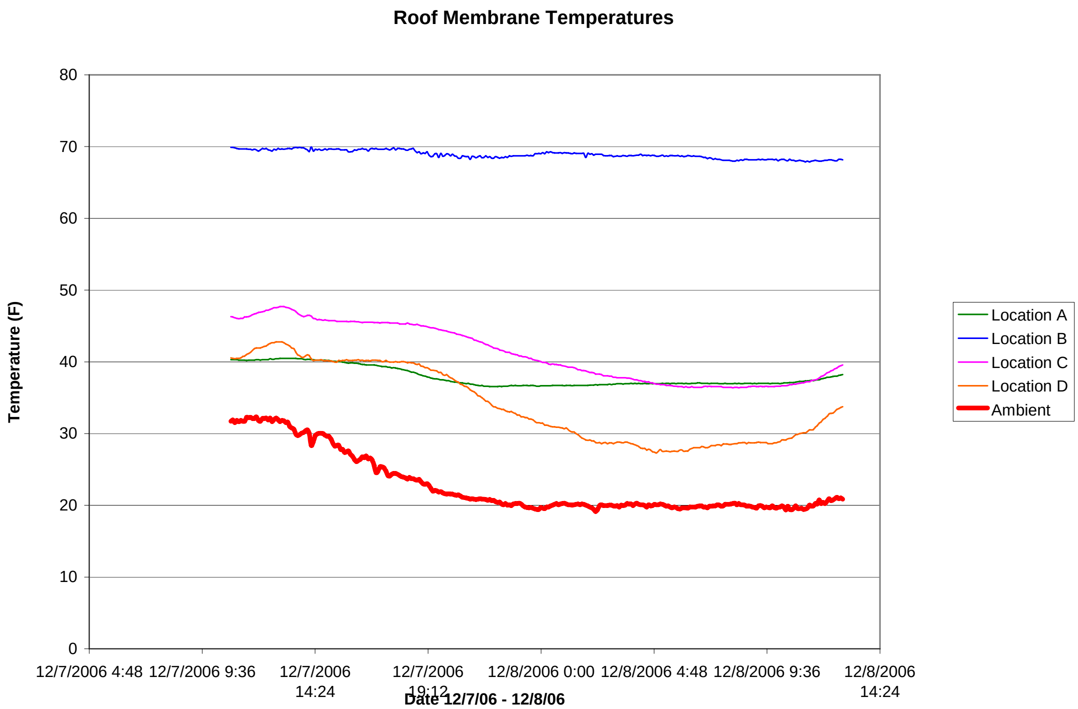

Figure 214. Roof Membrane Temperatures for 12/7/06 – 12/8/06

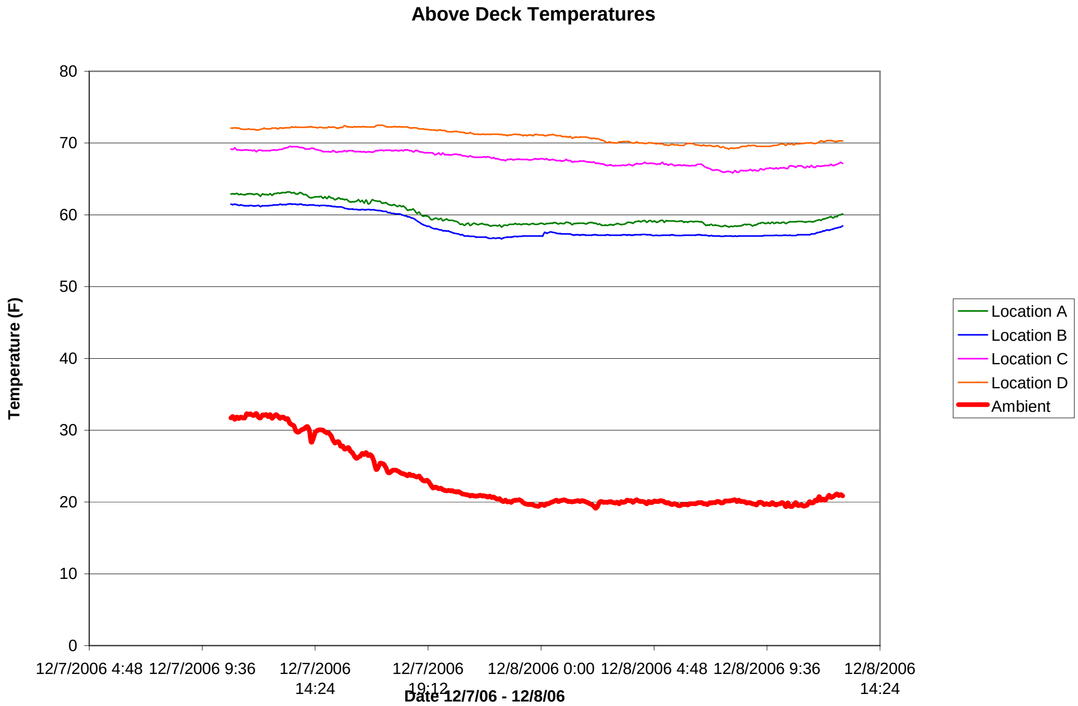

Figure 215. Above Deck Temperatures for 12/7/06 – 12/8/06

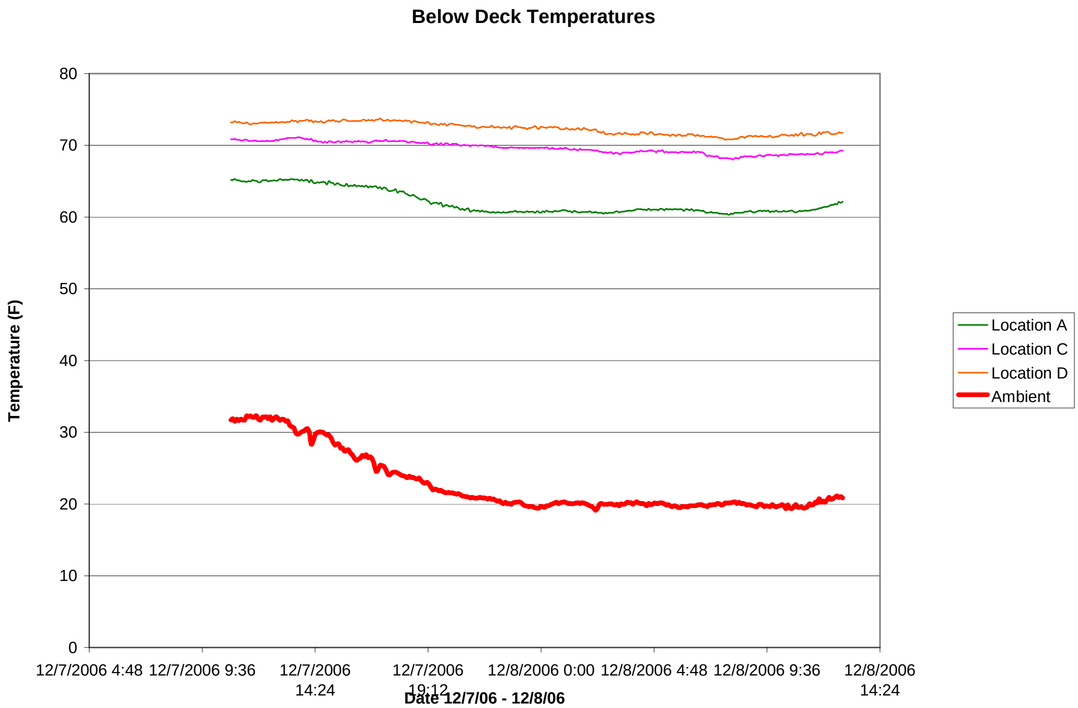

Figure 216. Below Deck Temperatures for 12/7/06 – 12/8/06

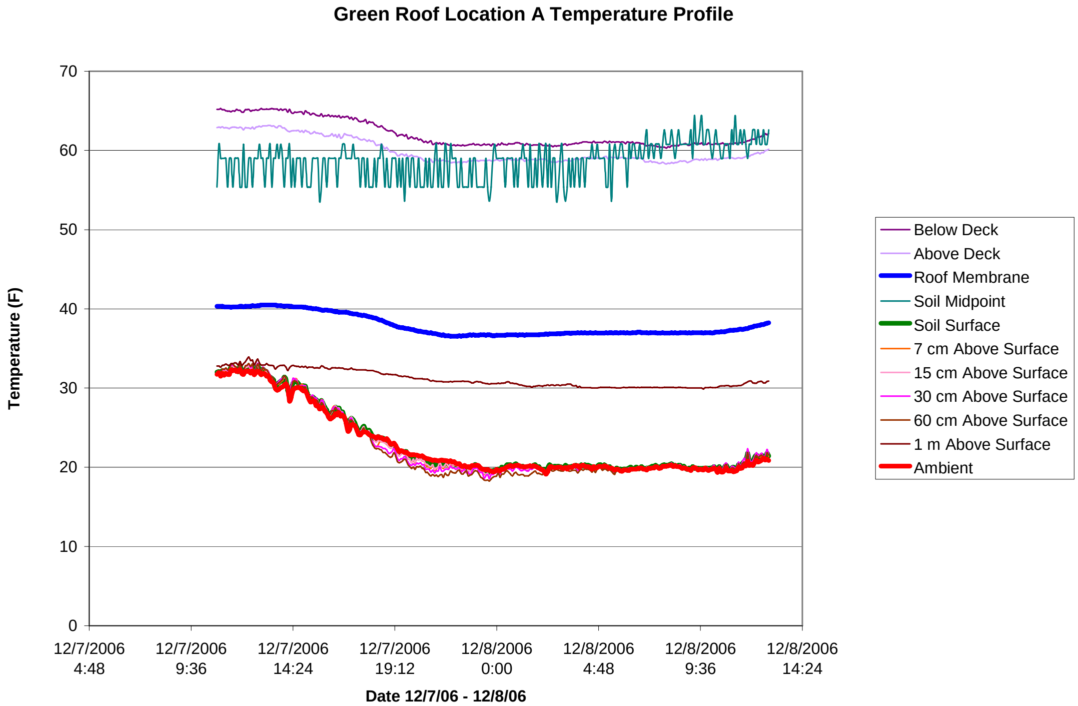

Figure 217. Green Roof Location A Temperature Profile for 12/7/06 – 12/8/06

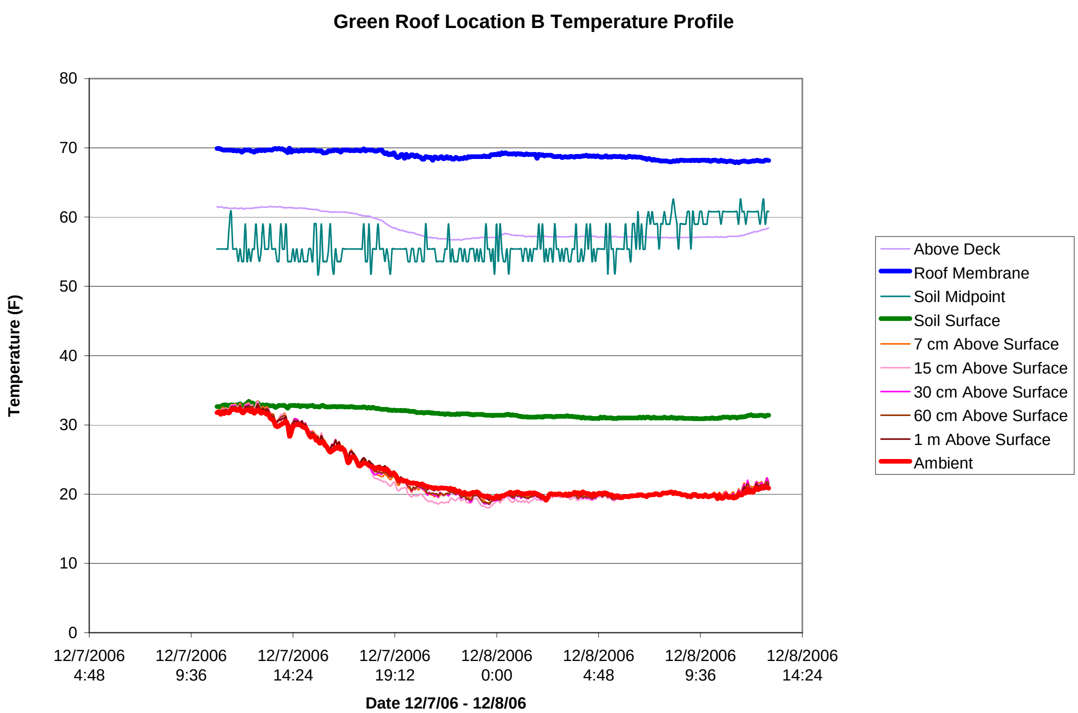

Figure 218. Green Roof Location B Temperature Profile for 12/7/06 – 12/8/06

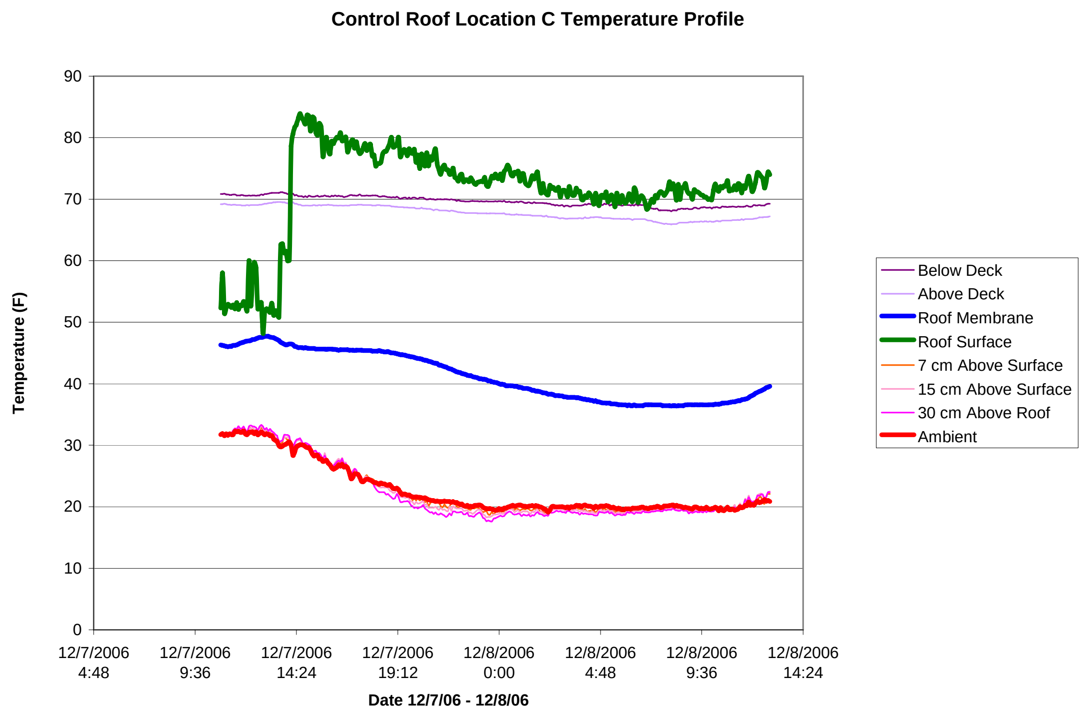

Figure 219. Control Roof Location C Temperature Profile for 12/7/06 – 12/8/06

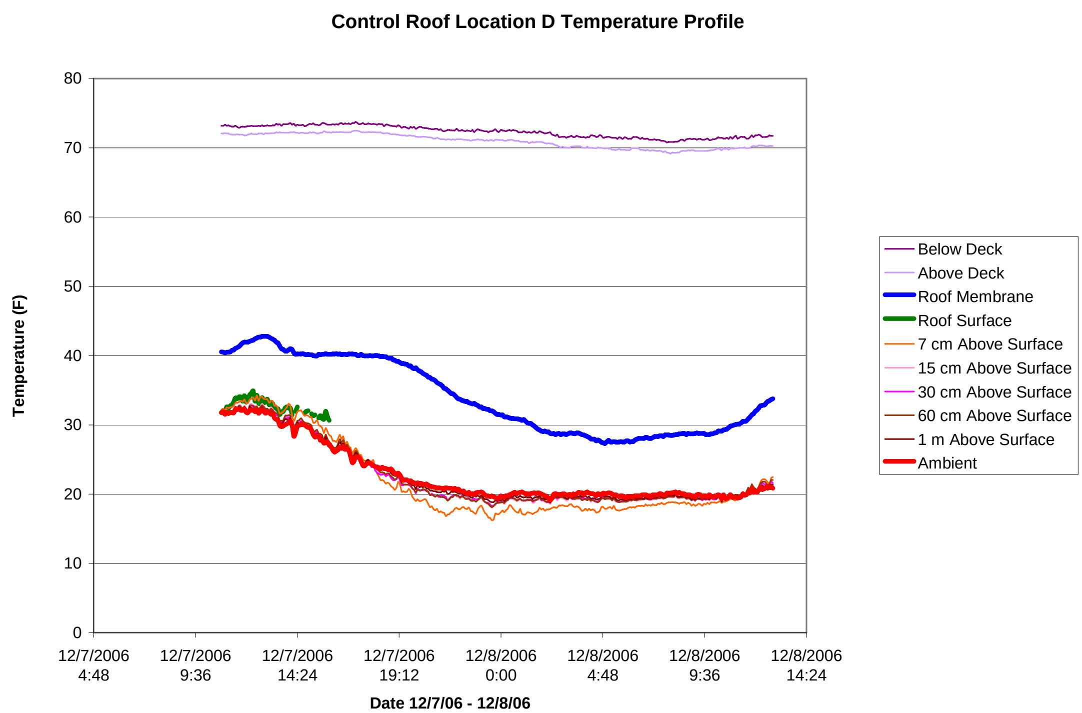

Figure 220. Control Roof Location D Temperature Profile for 12/7/06 – 12/8/06

Temperature Measurements for January 23, 2007 to January 29, 2007

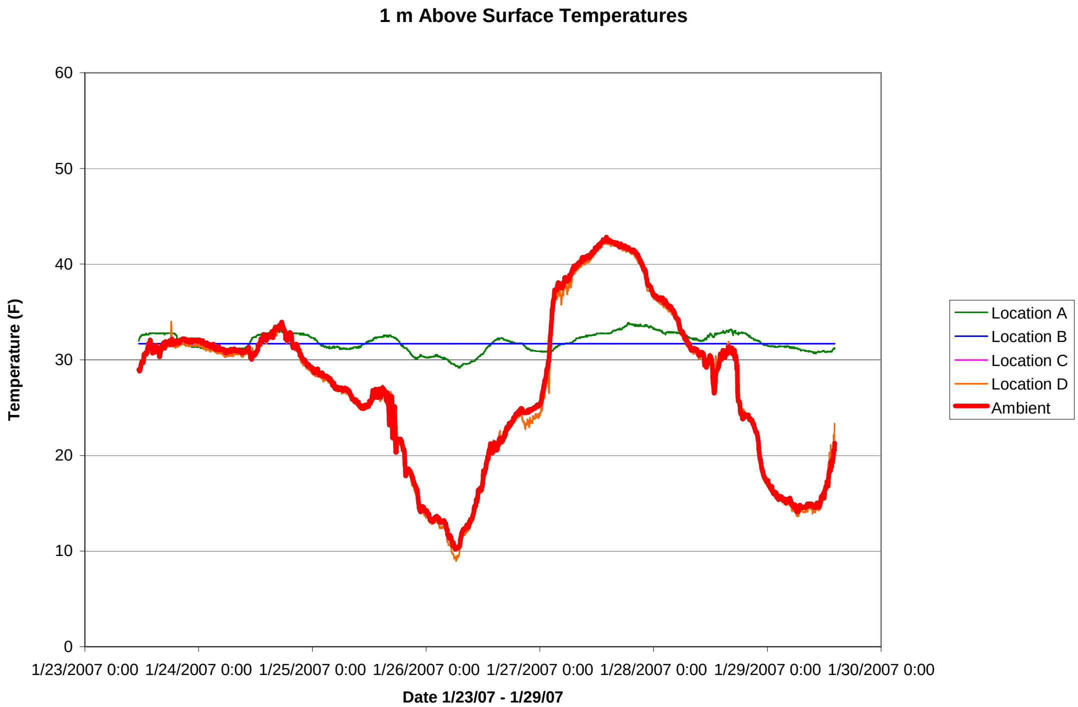

Figure 221. 1m Above Surface Temperatures for 1/23/07 – 1/29/07

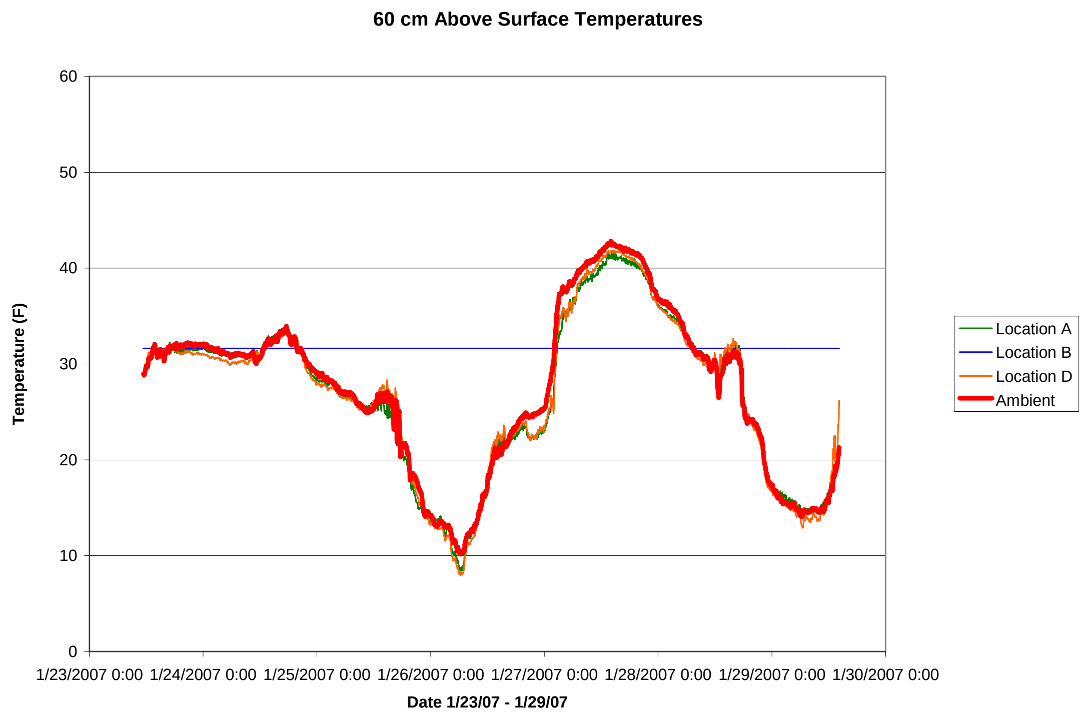

Figure 222. 60cm Above Surface Temperatures for 1/23/07 – 1/29/07

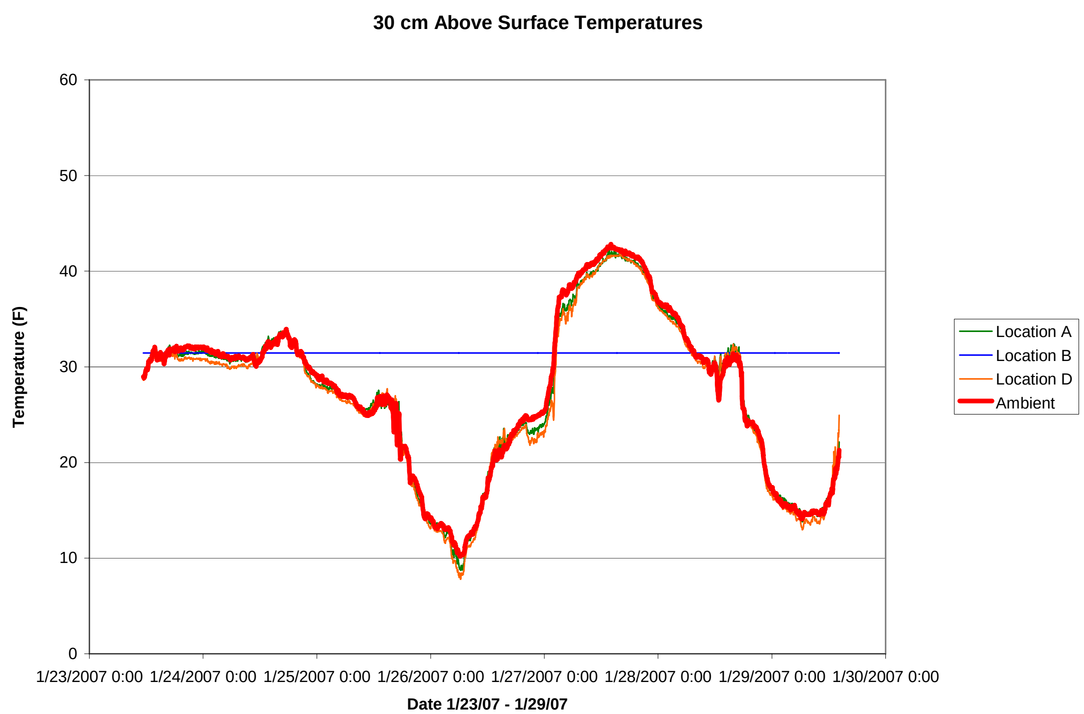

Figure 223. 30cm Above Surface Temperatures for 1/23/07 – 1/29/07

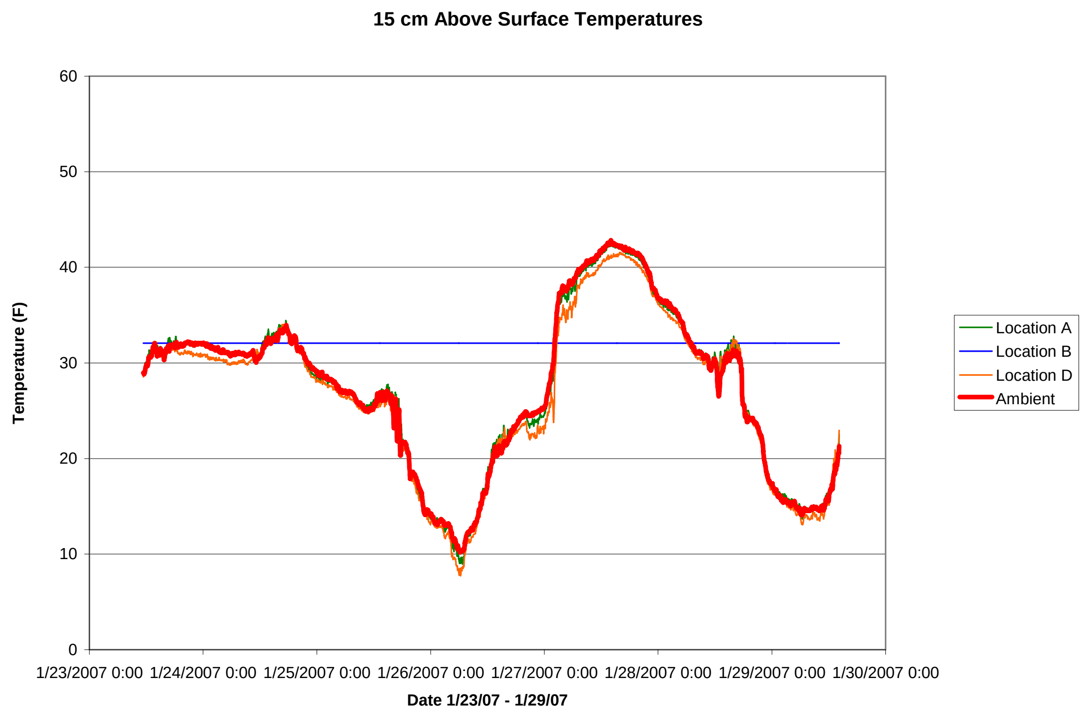

Figure 224. 15cm Above Surface Temperatures for 1/23/07 – 1/29/07

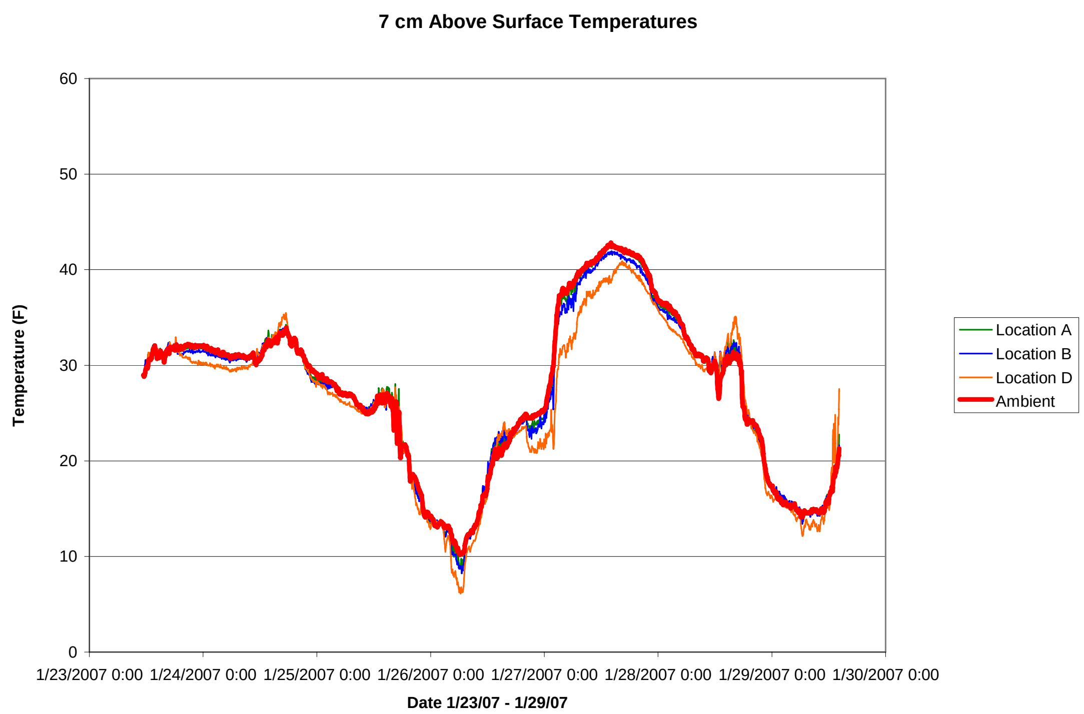

Figure 225. 7cm Above Surface Temperatures for 1/23/07 – 1/29/07

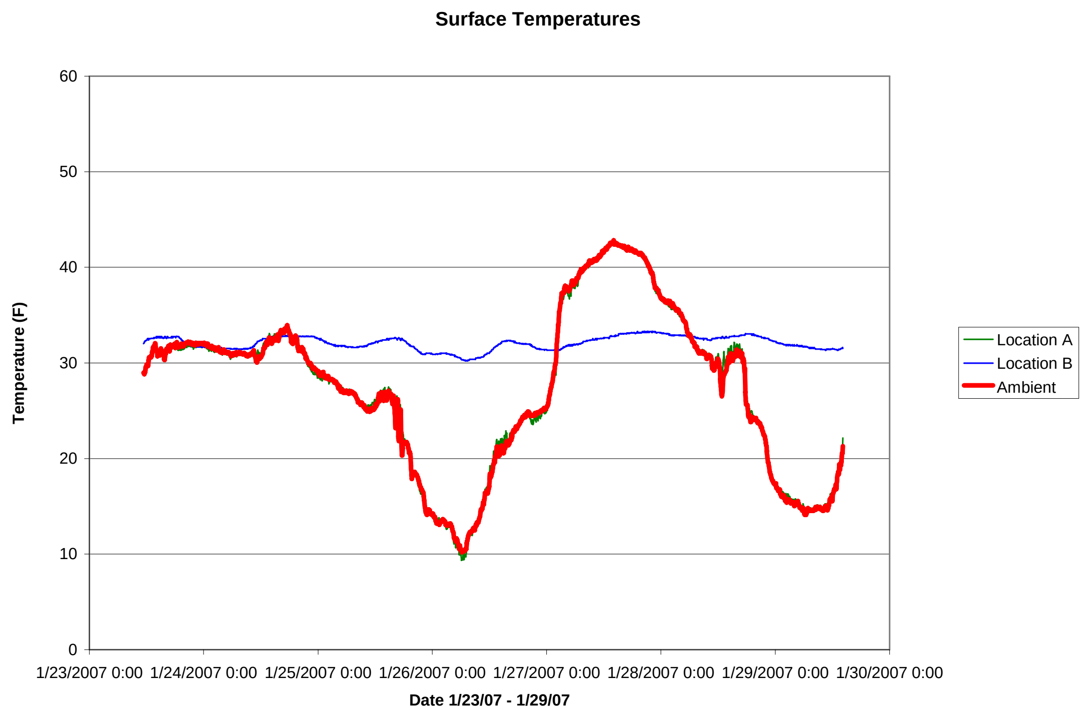

Figure 226. Surface Temperatures for 1/23/07 – 1/29/07

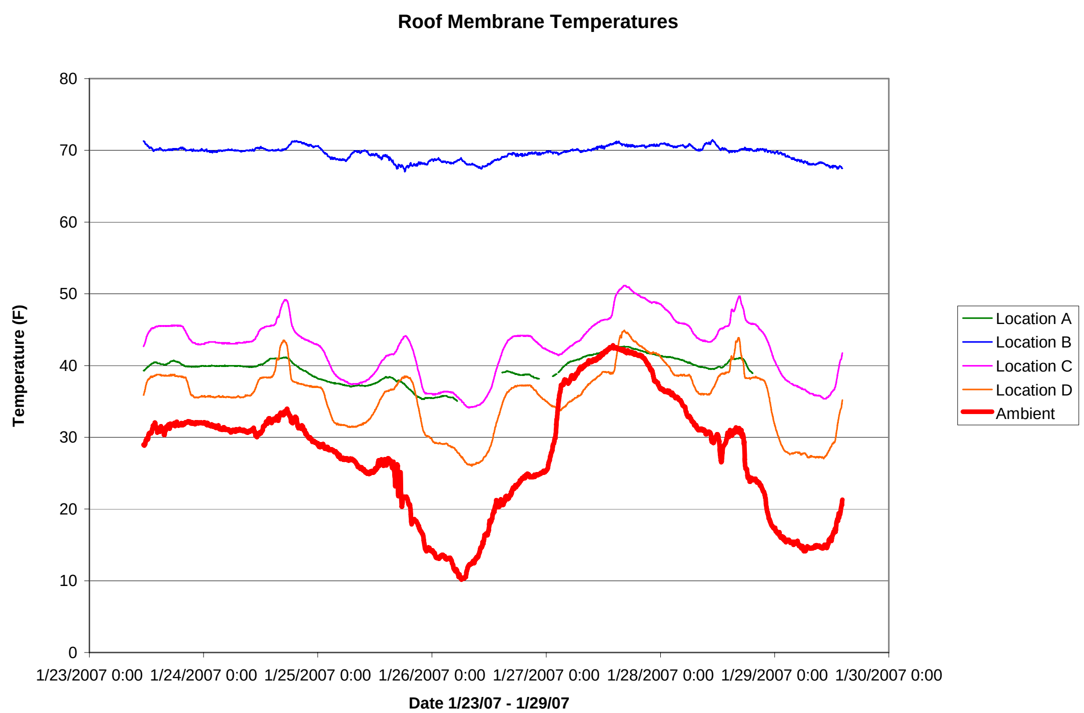

Figure 227. Roof Membrane Temperatures for 1/23/07 – 1/29/07

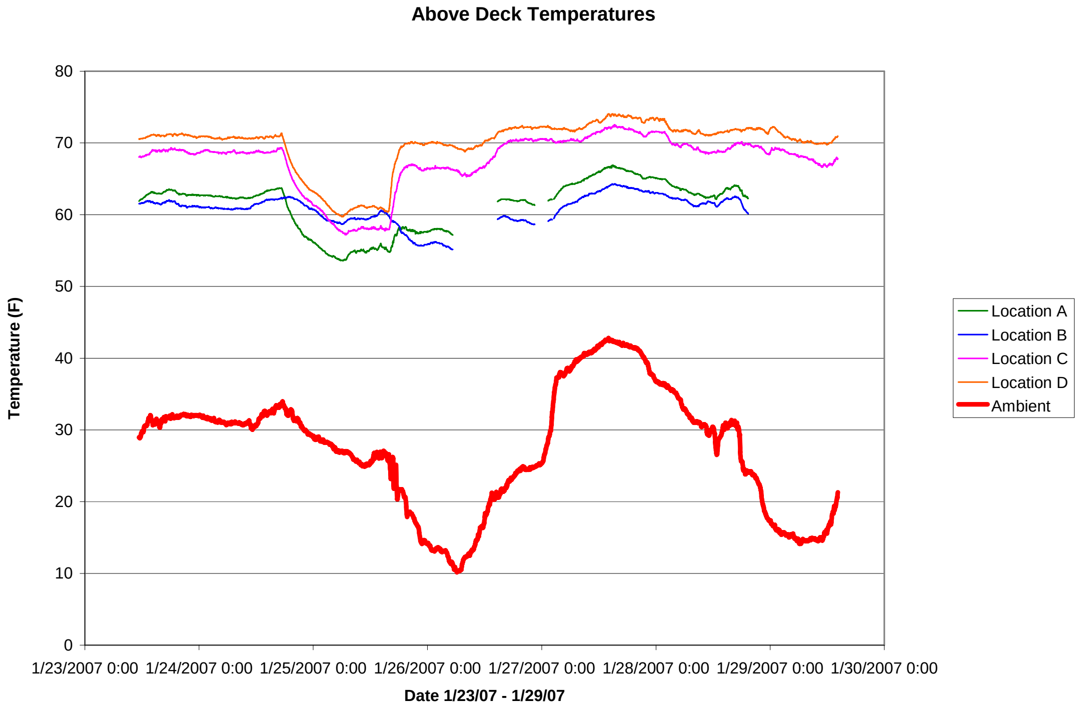

Figure 228. Above Deck Temperatures for 1/23/07 – 1/29/07

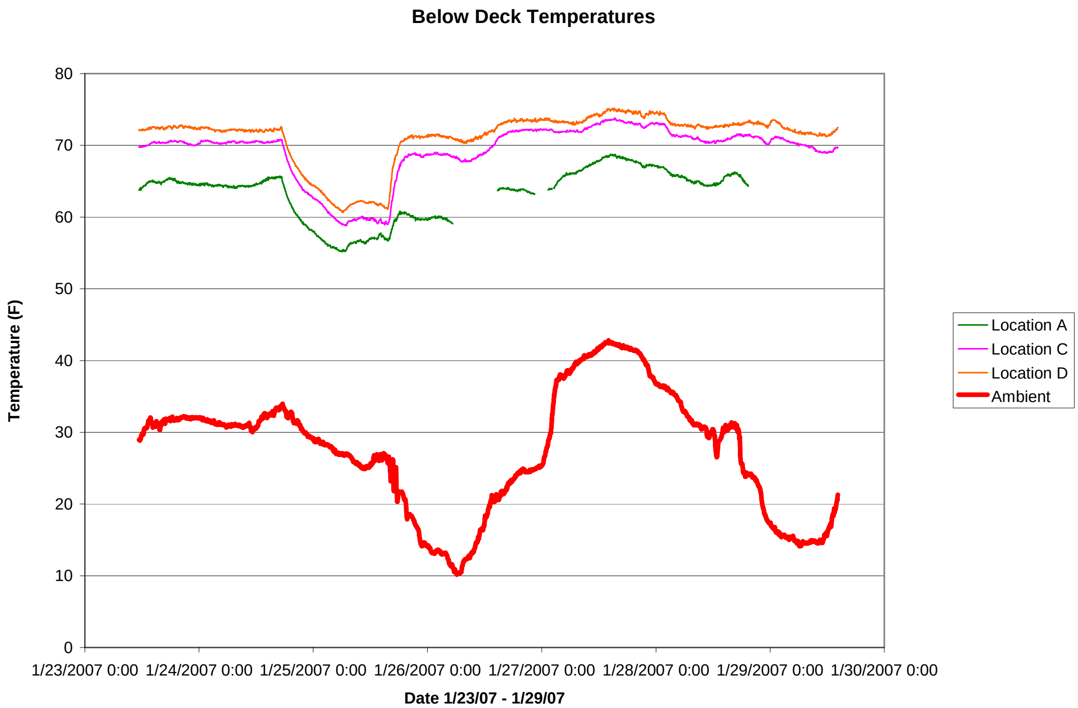

Figure 229. Below Deck Temperatures for 1/23/07 – 1/29/07

APPENDIX B

SOLAR RADIATION DATA

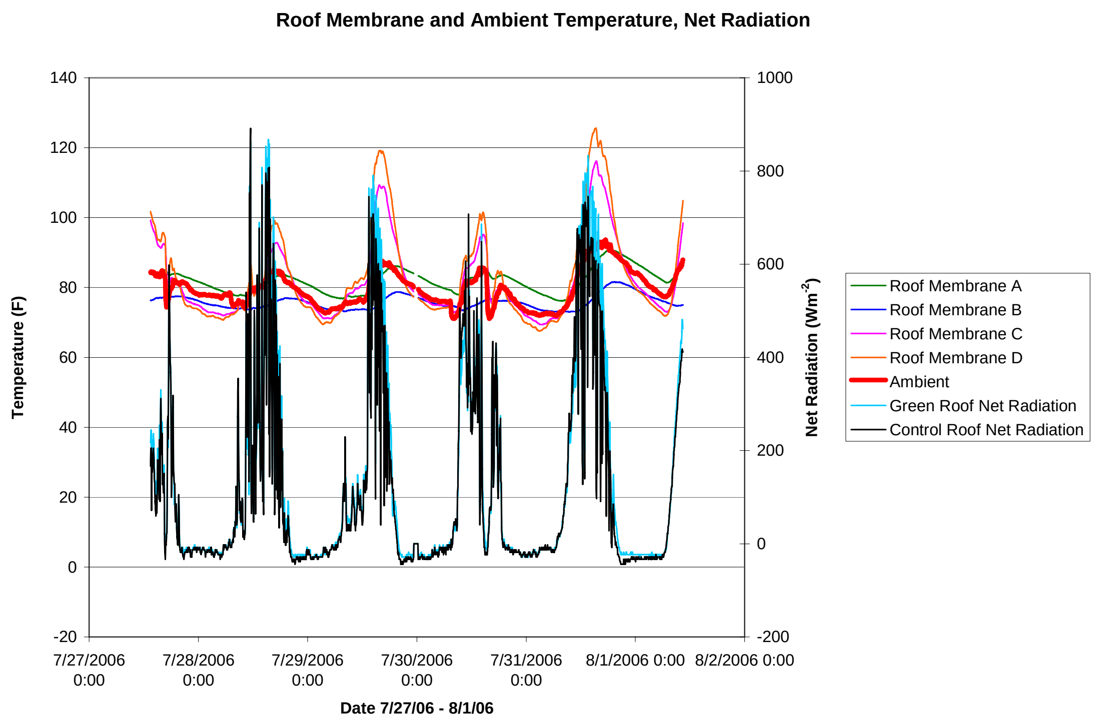

Figure 230. Roof Membrane, Ambient Temperature, Net Radiation for 7/27/06 – 8/1/06

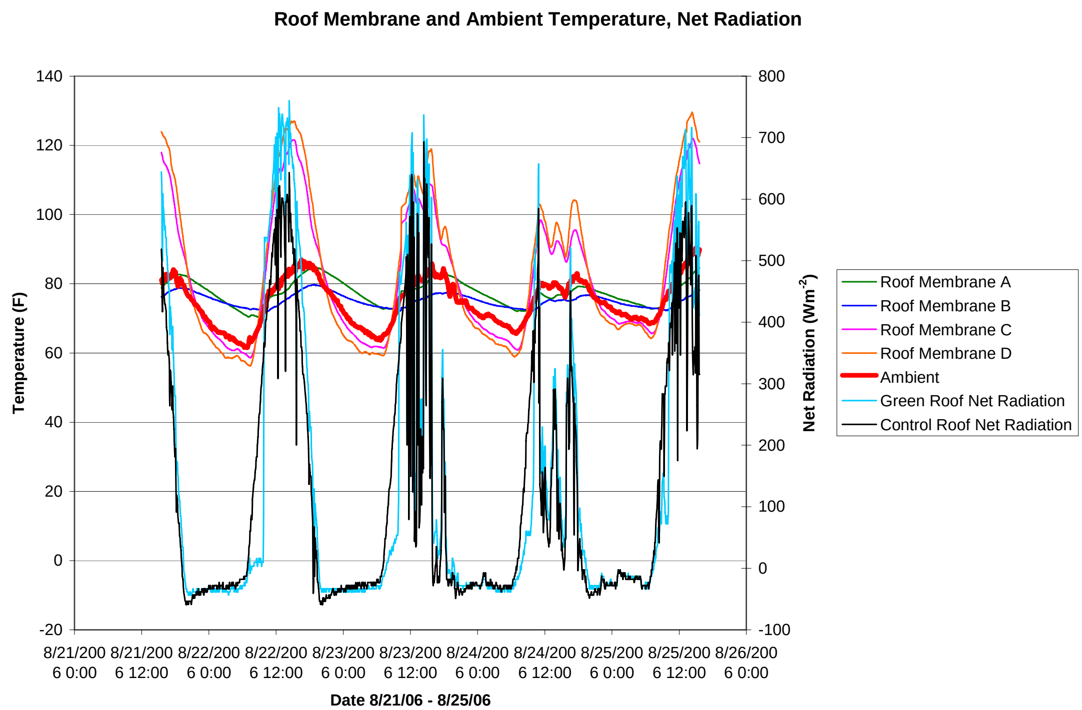

Figure 231. Roof Membrane, Ambient Temperature, Net Radiation for 8/21/06 – 8/25/06

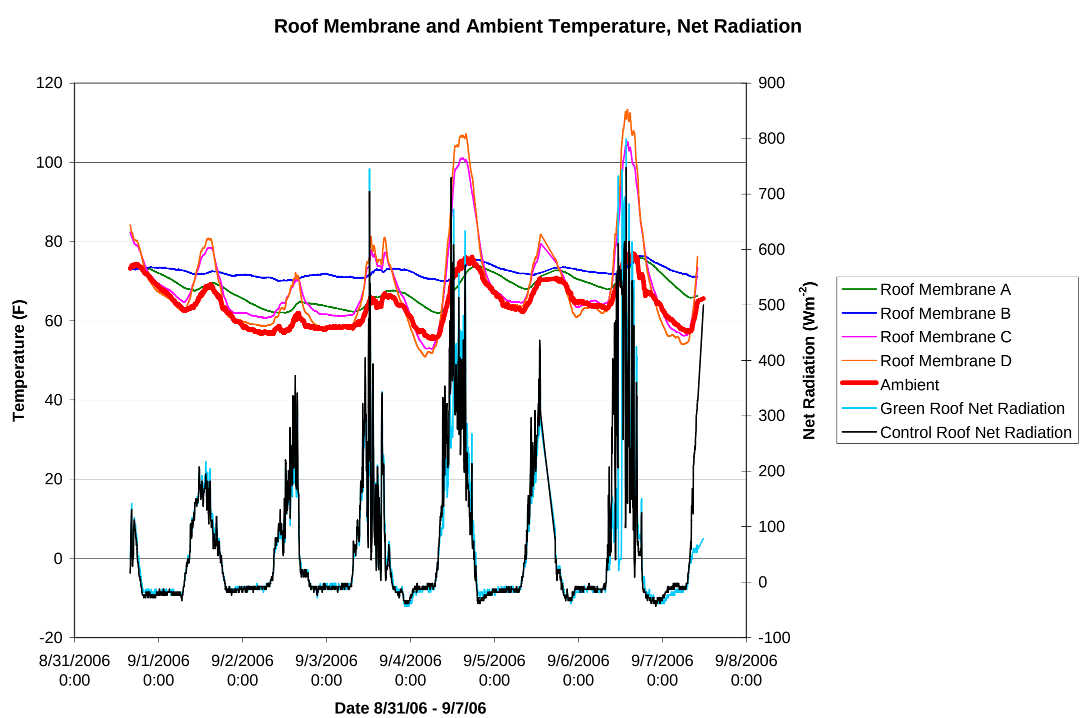

Figure 232. Roof Membrane, Ambient Temperature, Net Radiation for 8/31/06 – 9/7/06

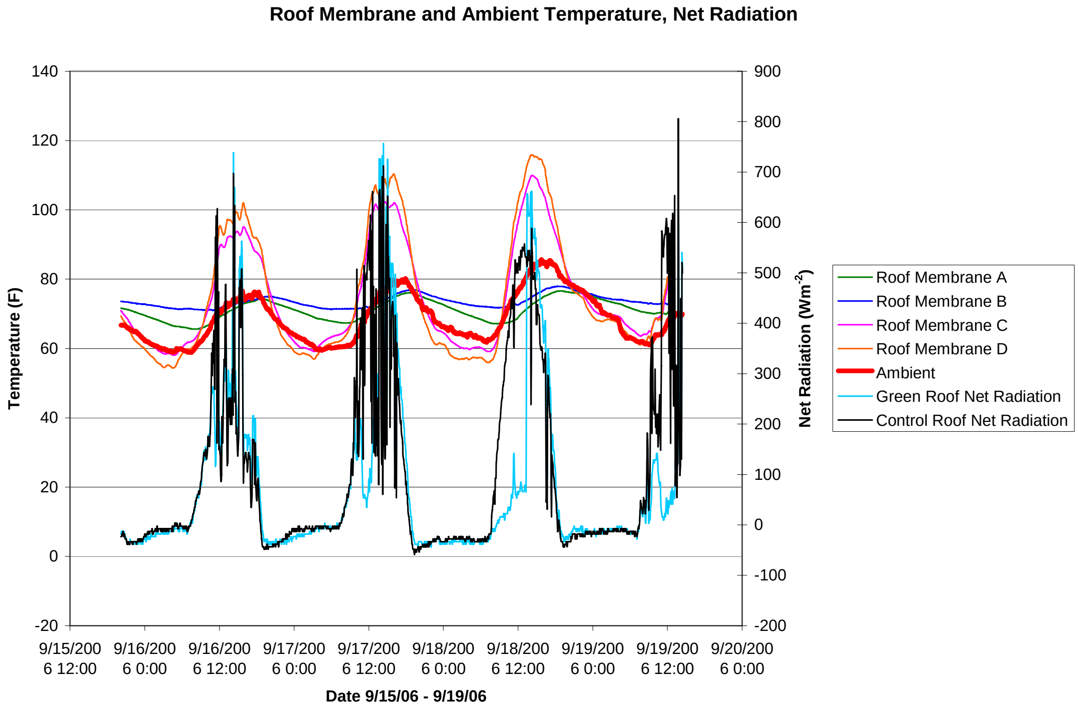

Figure 233. Roof Membrane, Ambient Temperature, Net Radiation for 9/15/06 – 9/19/06

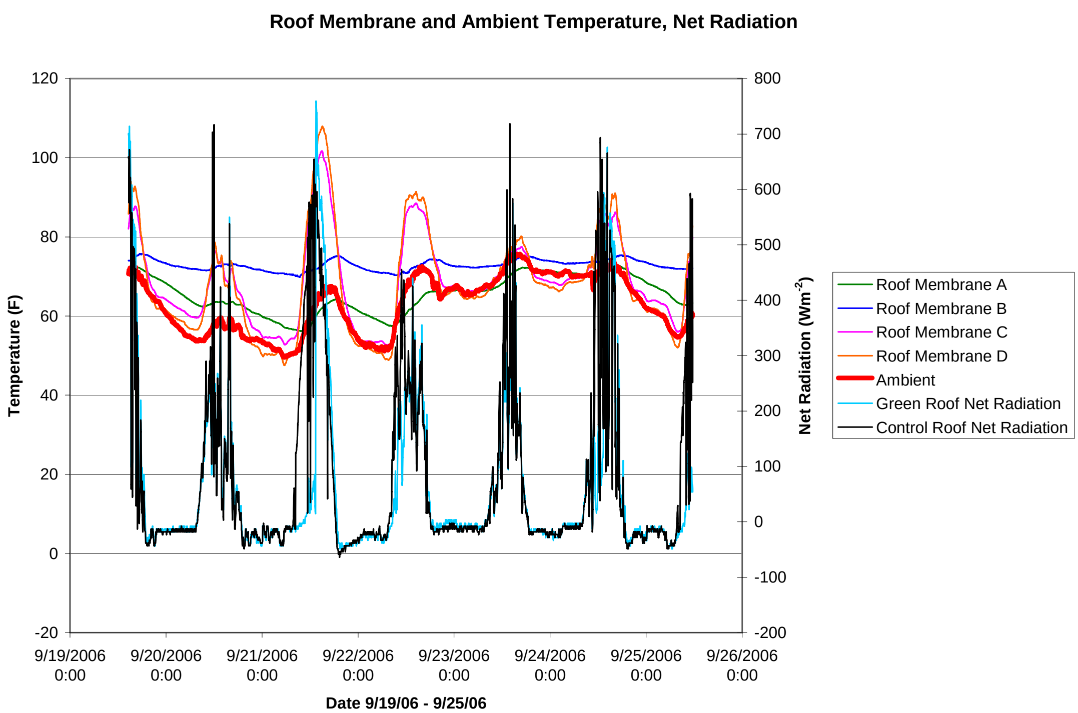

Figure 234. Roof Membrane, Ambient Temperature, Net Radiation for 9/19/06 – 9/25/06

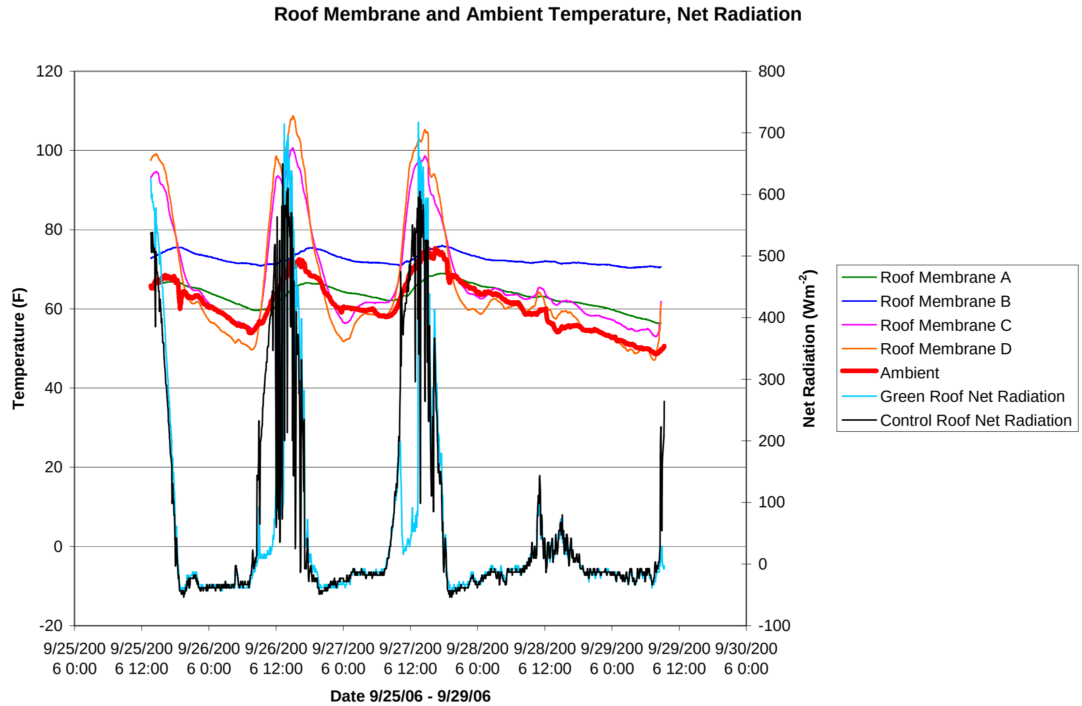

Figure 235. Roof Membrane, Ambient Temperature, Net Radiation for 9/25/06 – 9/29/06

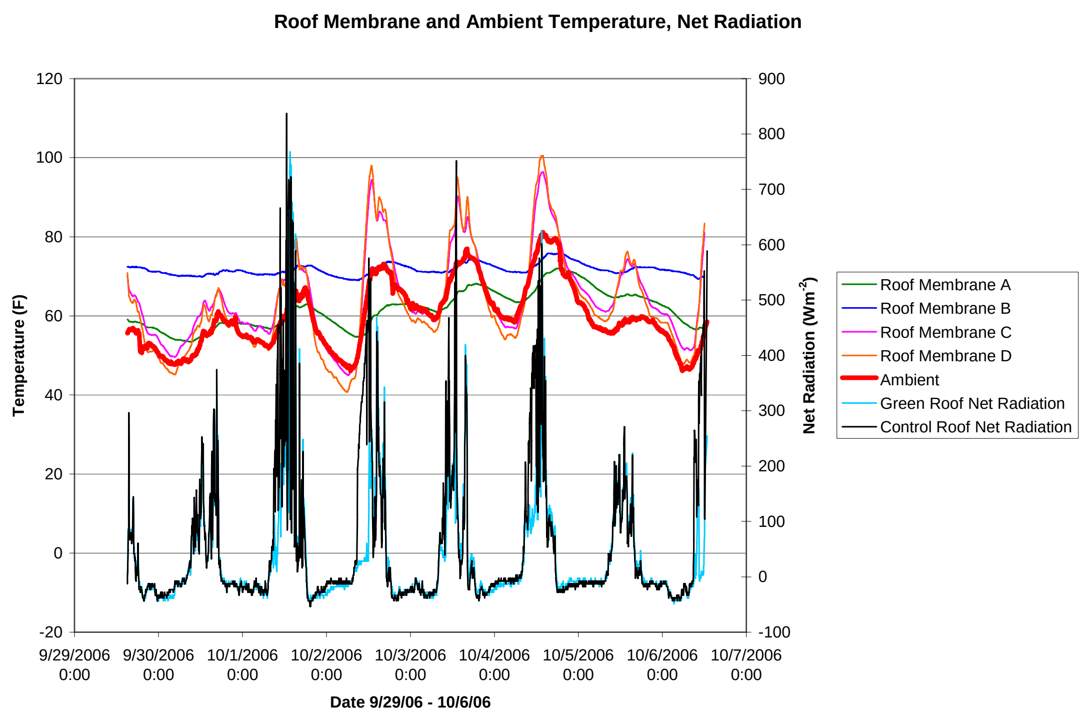

Figure 236. Roof Membrane, Ambient Temperature, Net Radiation for 9/29/06 – 10/6/06

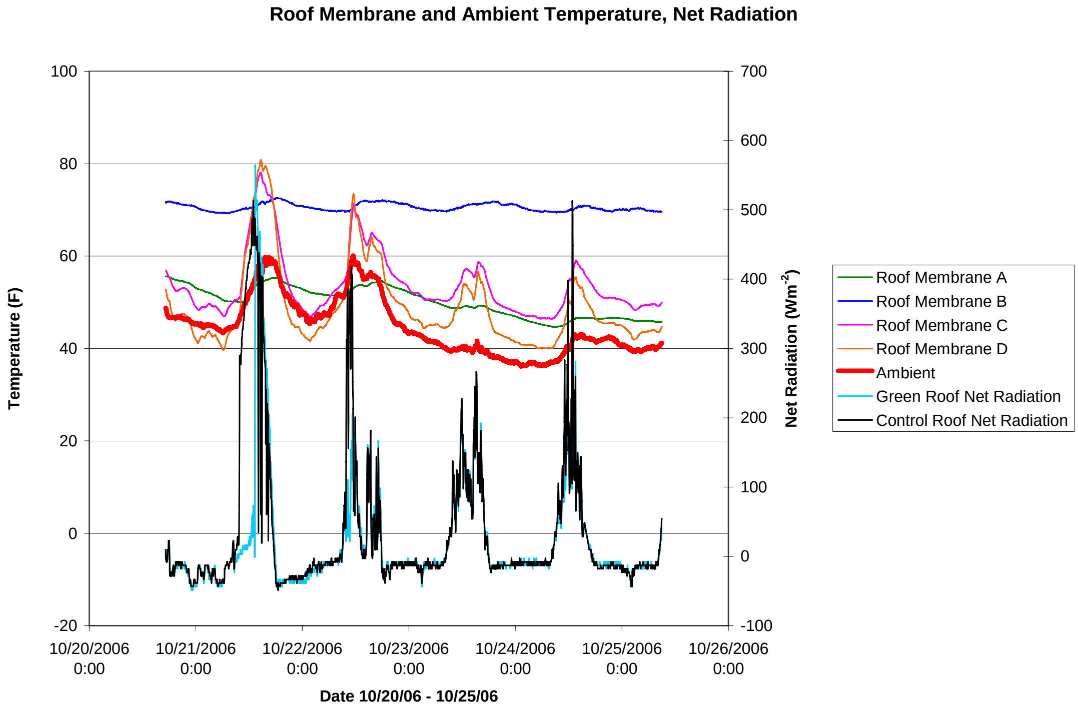

Figure 237. Roof Membrane, Ambient Temperature, Net Radiation for 10/20/06 – 10/25/06

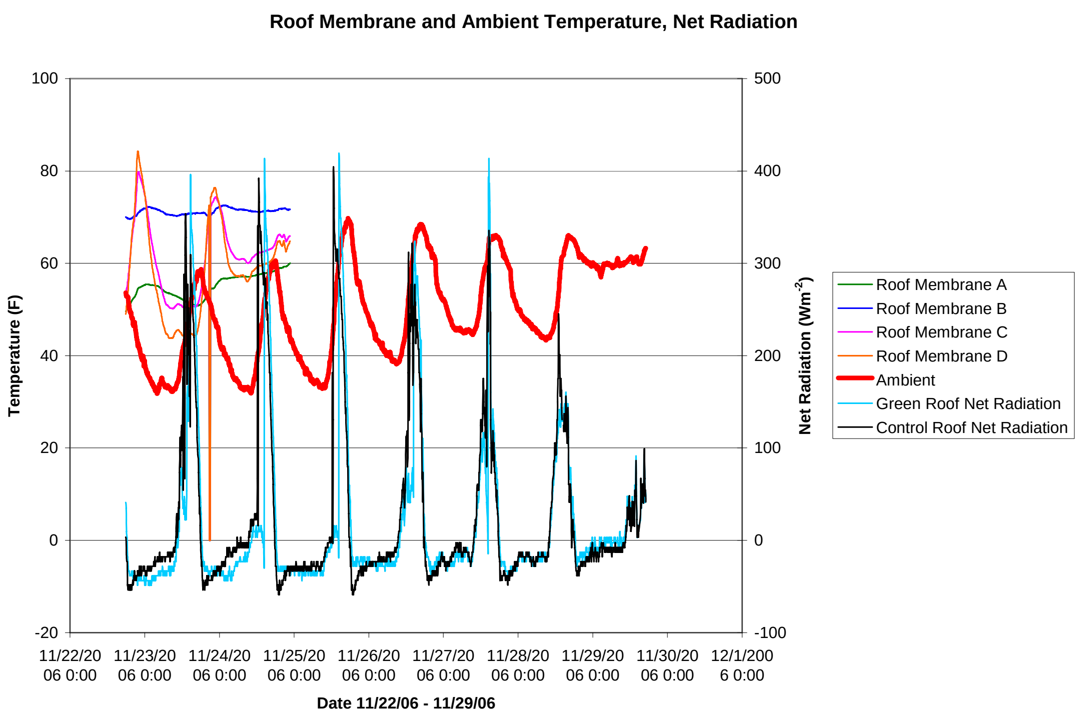

Figure 238. Roof Membrane, Ambient Temperature, Net Radiation for 11/22/06 – 11/29/06

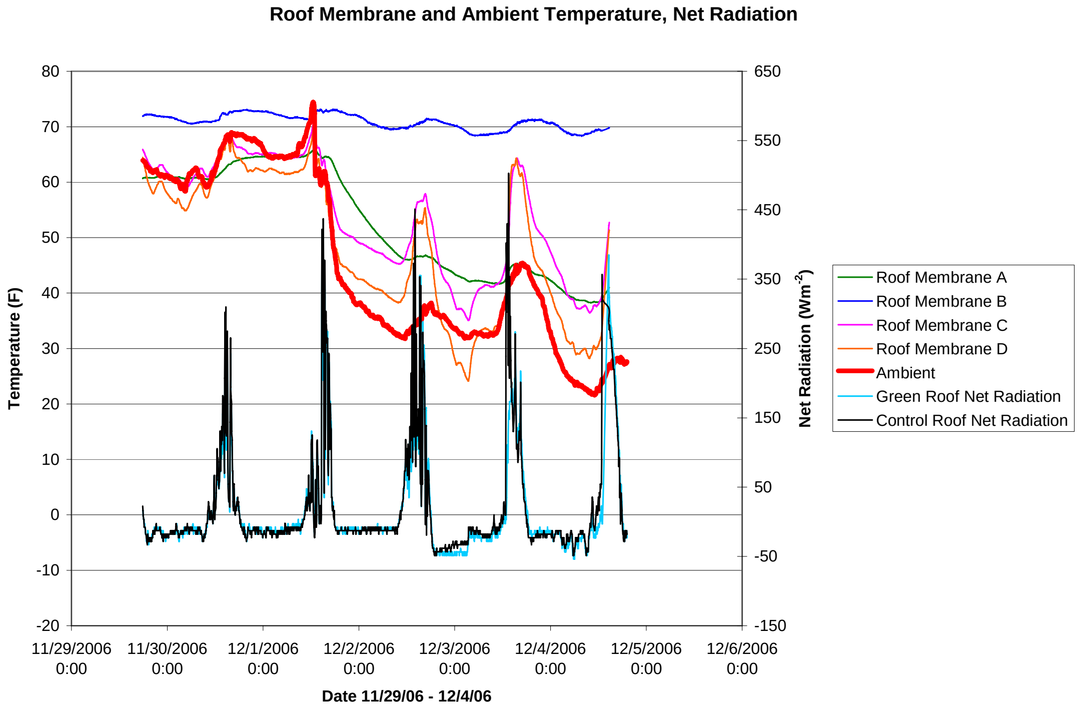

Figure 239. Roof Membrane, Ambient Temperature, Net Radiation for 11/29/06 – 12/4/06

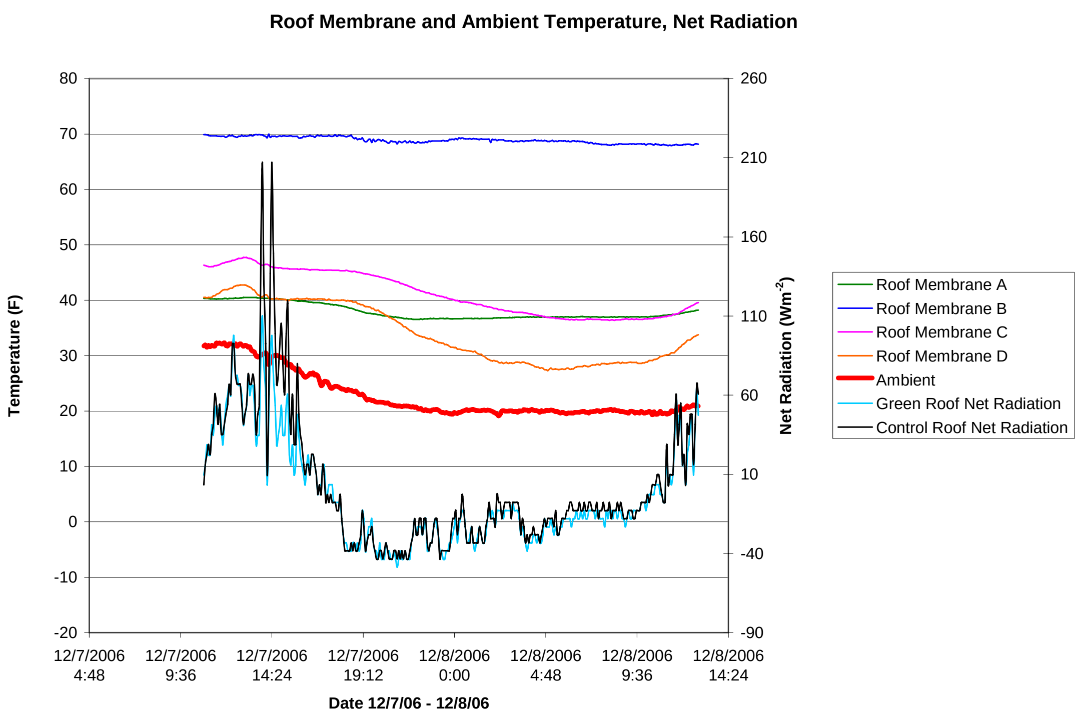

Figure 240. Roof Membrane, Ambient Temperature, Net Radiation for 12/7/06 – 12/8/06

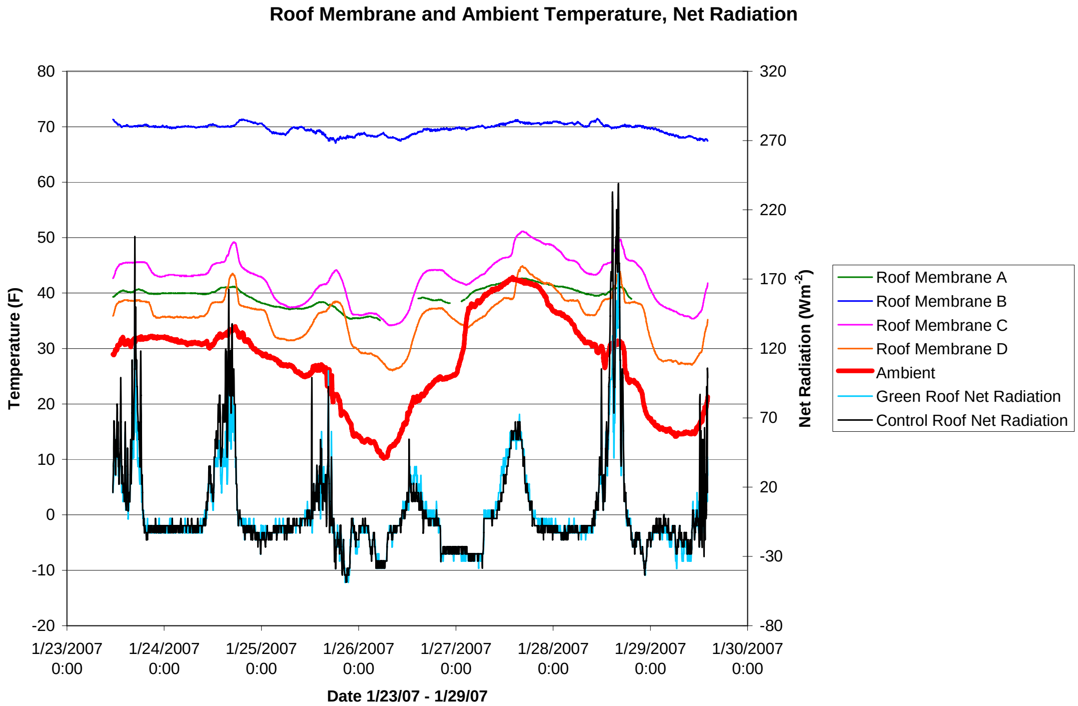

Figure 241. Roof Membrane, Ambient Temperature, Net Radiation for 1/23/07 – 1/29/07

APPENDIX C

RELATIVE HUMIDITY RESULTS

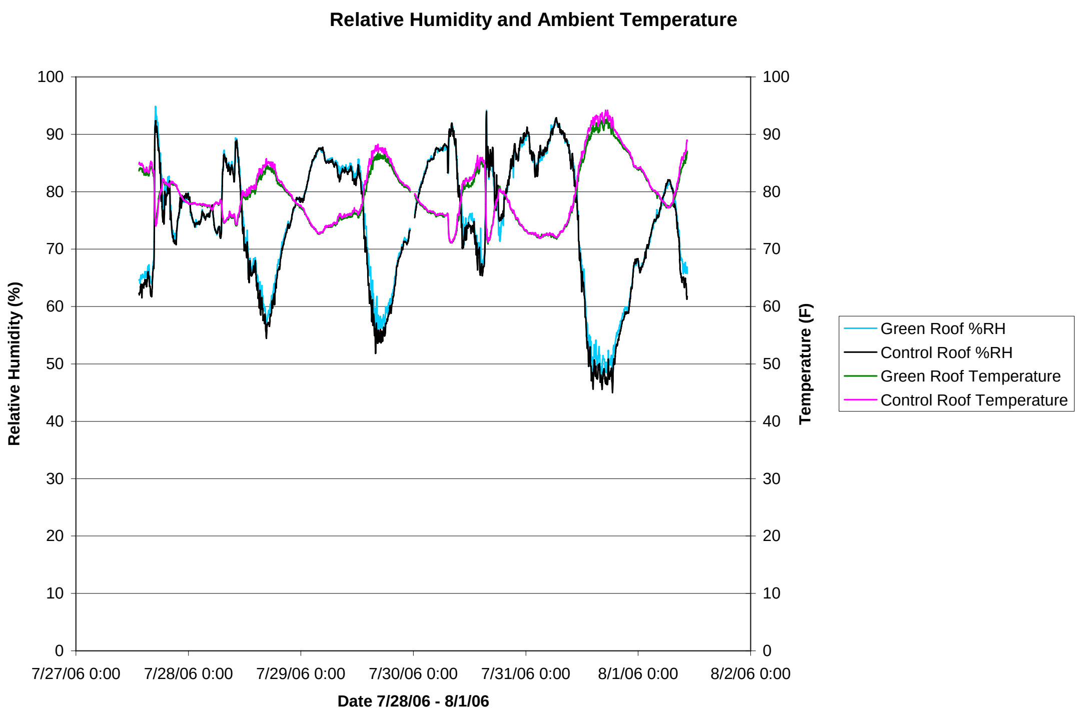

Figure 242. Relative Humidity and Ambient Temperature for 7/27/06 – 8/1/06

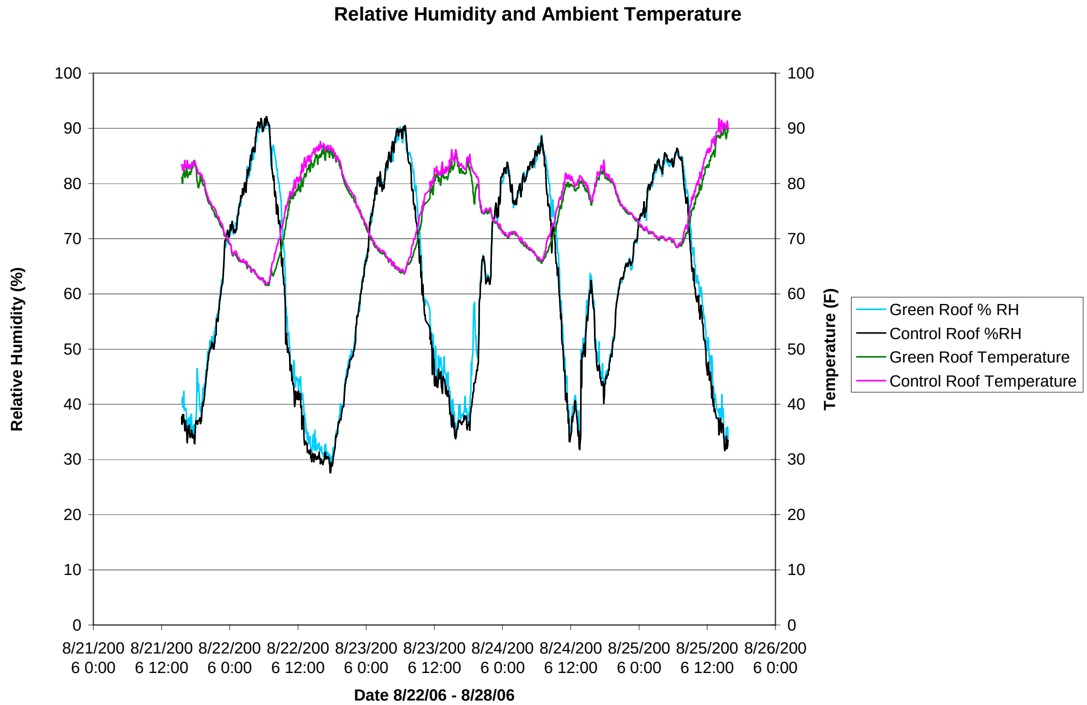

Figure 243. Relative Humidity and Ambient Temperature for 8/22/06 – 8/28/06

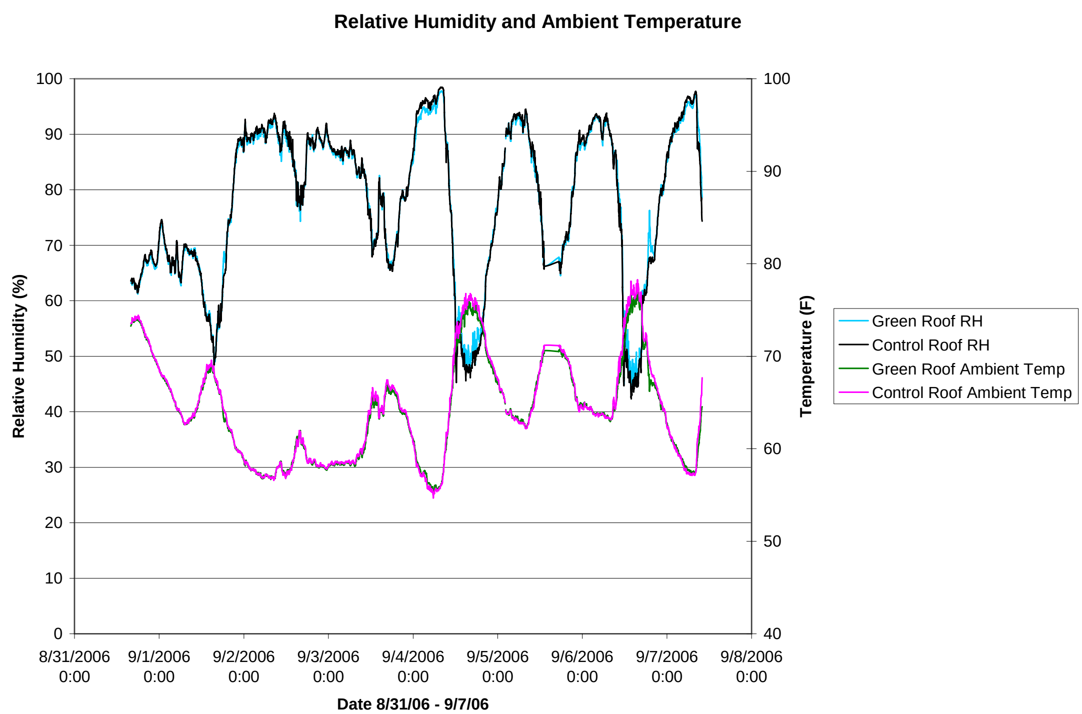

Figure 244. Relative Humidity and Ambient Temperature for 8/31/06 – 9/7/06

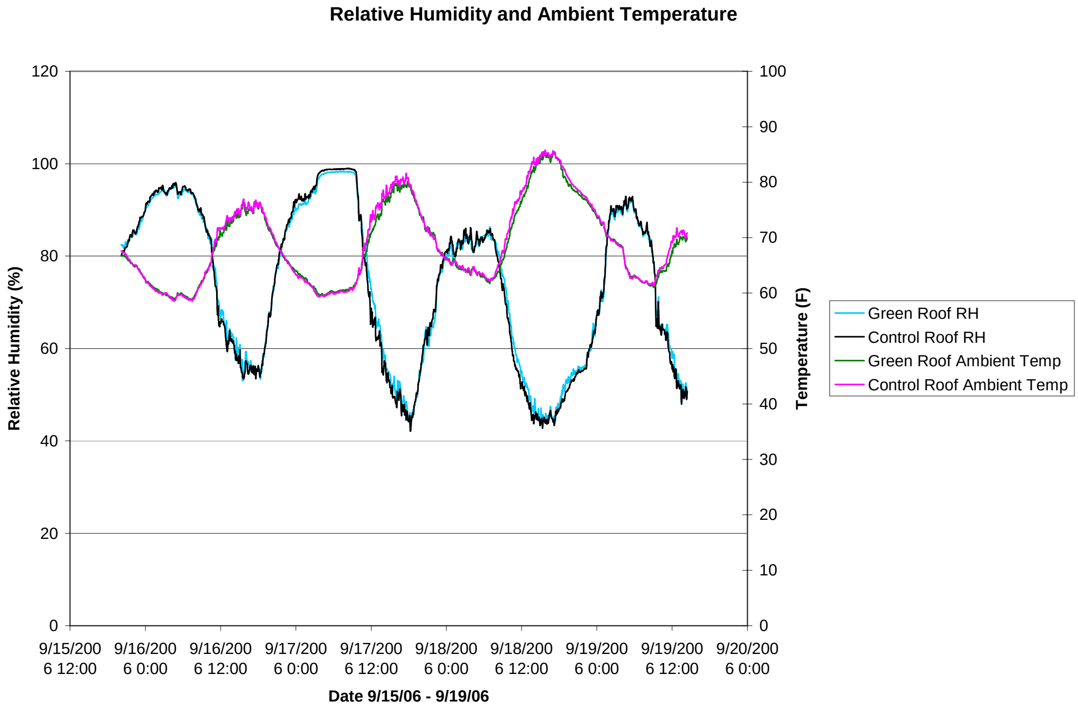

Figure 245. Relative Humidity and Ambient Temperature for 9/15/06 – 9/19/06

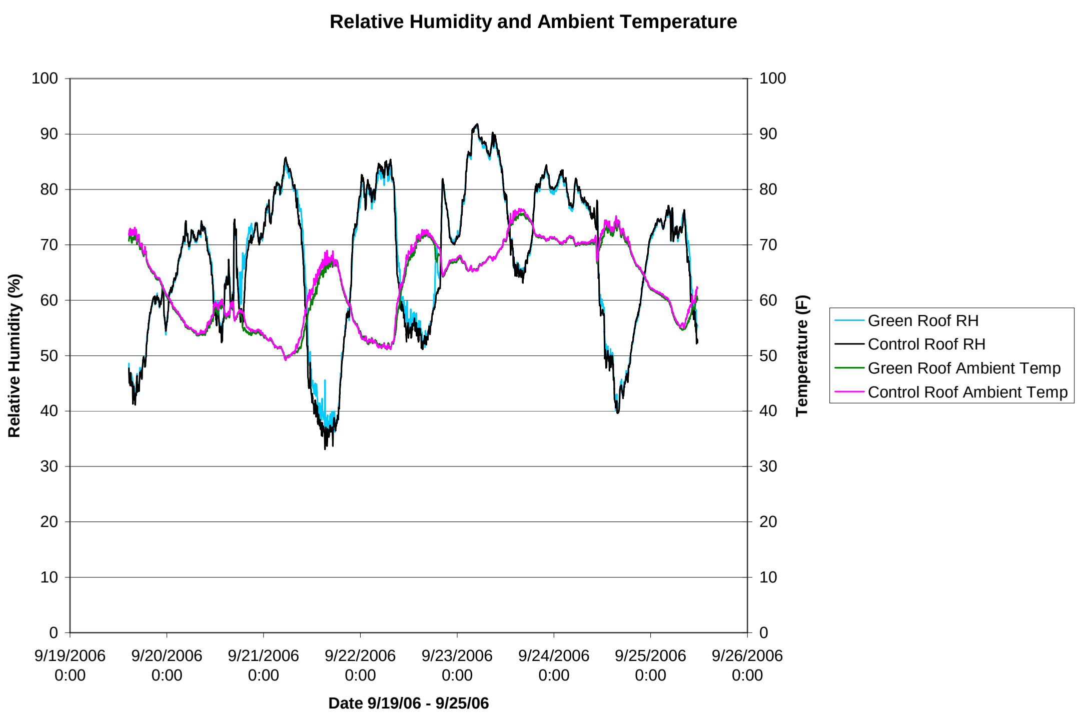

Figure 246. Relative Humidity and Ambient Temperature for 9/19/06 – 9/25/06

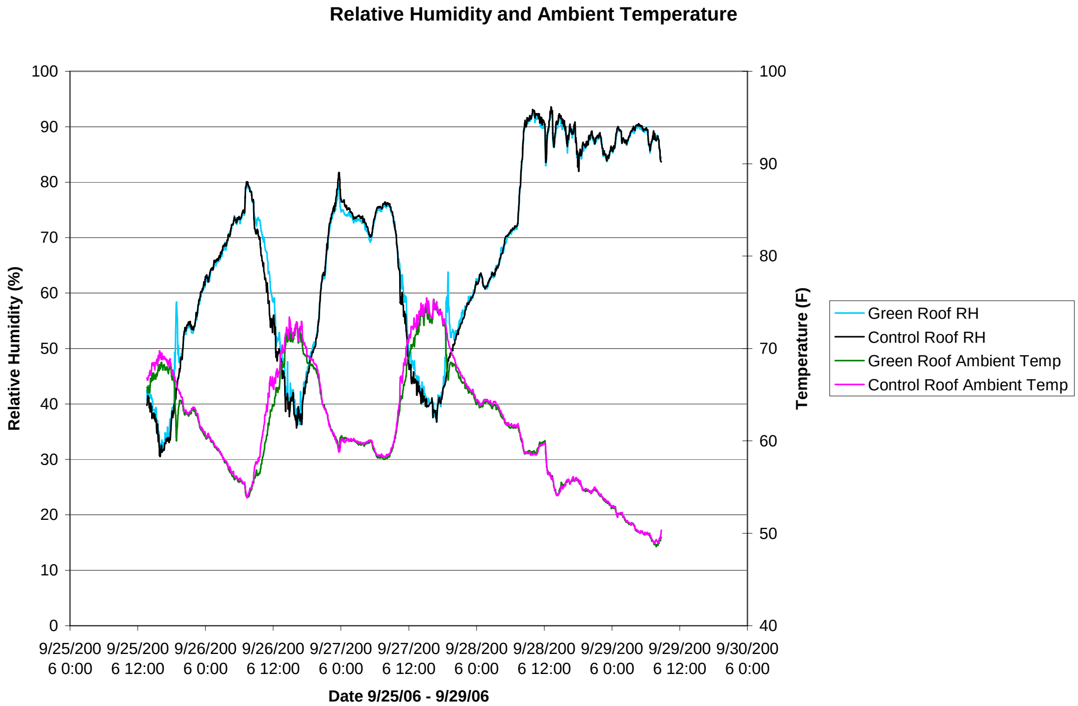

Figure 247. Relative Humidity and Ambient Temperature for 9/25/06 – 9/29/06

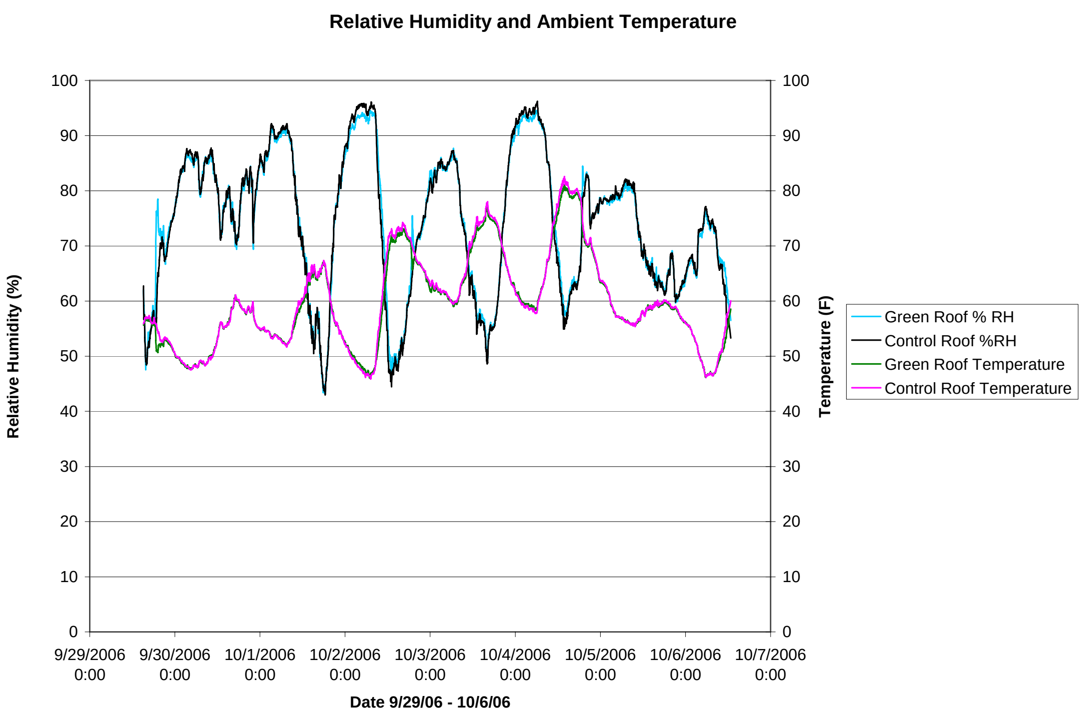

Figure 248. Relative Humidity and Ambient Temperature for 9/29/06 – 10/6/06

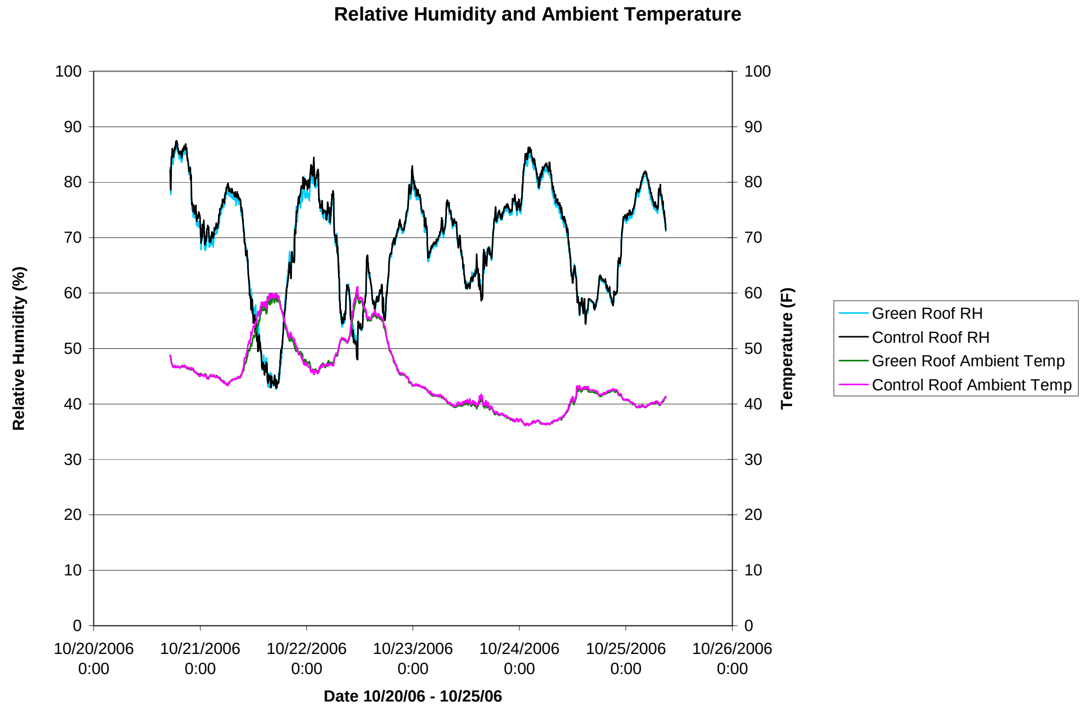

Figure 249. Relative Humidity and Ambient Temperature for 10/20/06 – 10/25/06

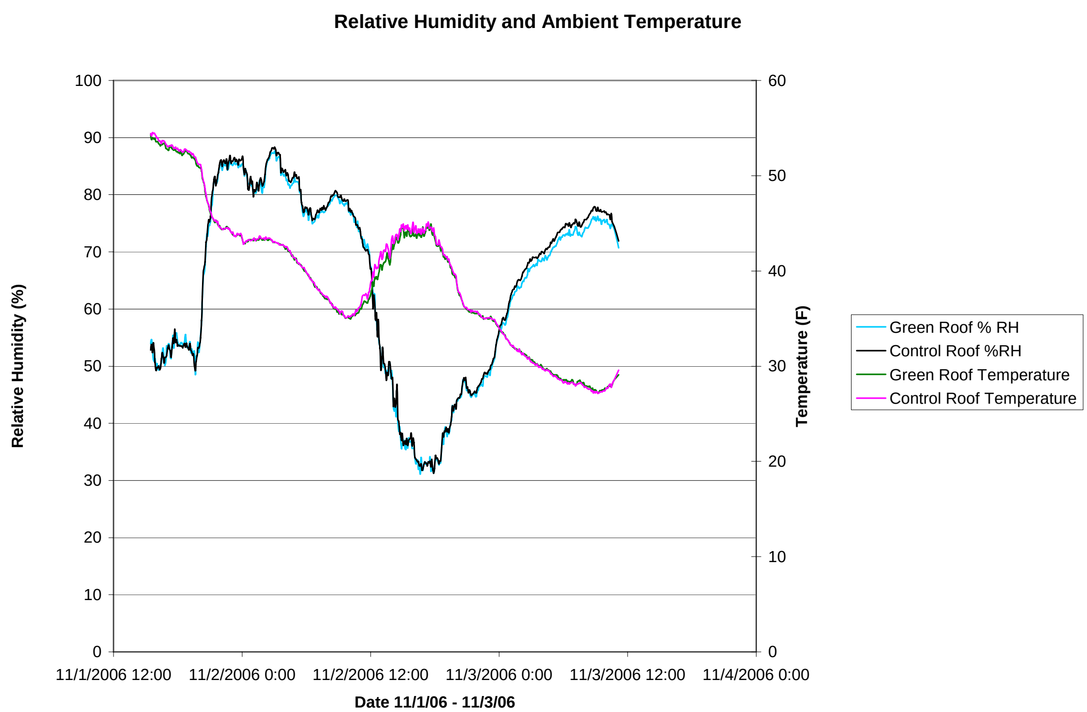

Figure 250. Relative Humidity and Ambient Temperature for 11/1/06 – 11/3/06

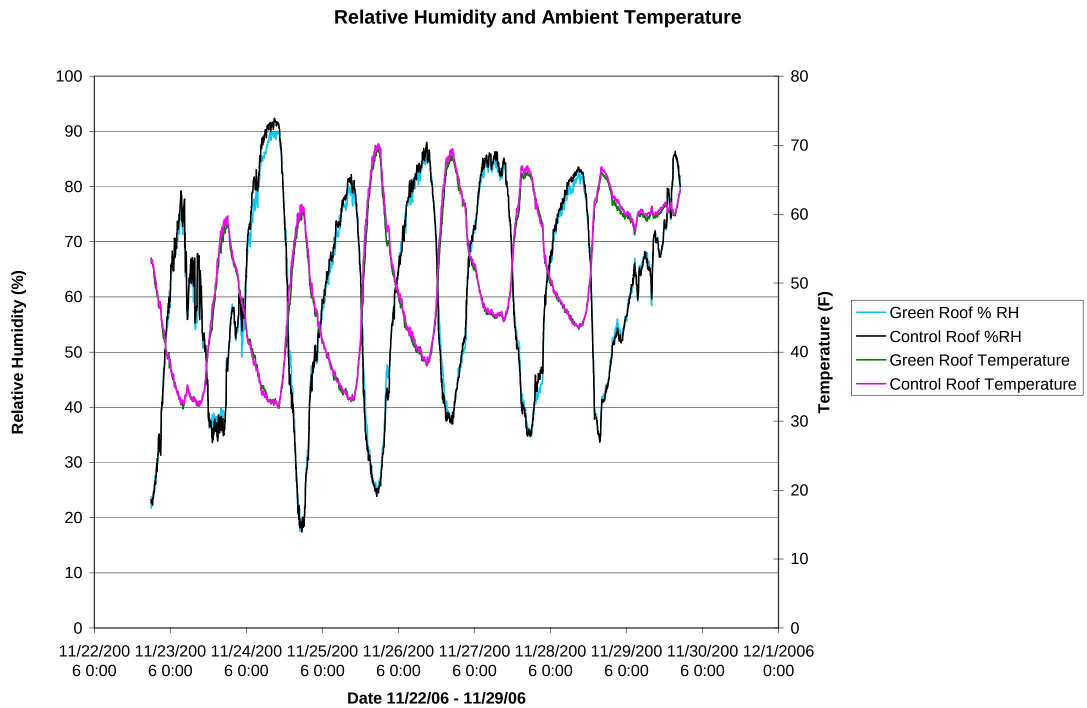

Figure 251. Relative Humidity and Ambient Temperature for 11/22/06 – 11/29/06

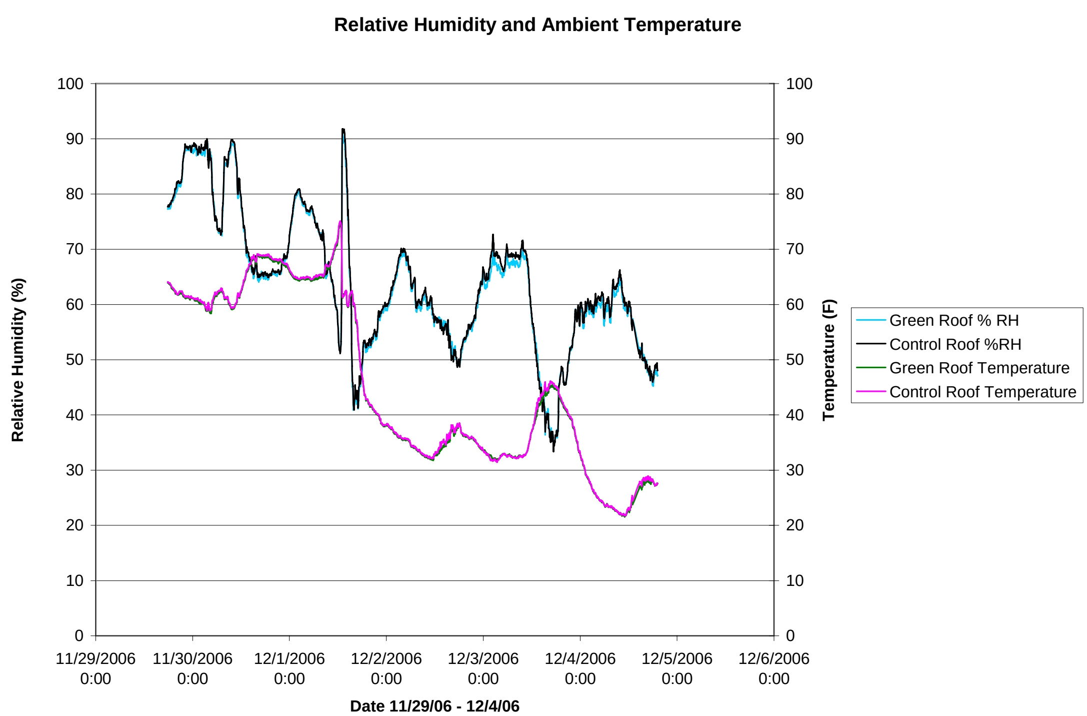

Figure 252. Relative Humidity and Ambient Temperature for 11/29/06 –12/4/06

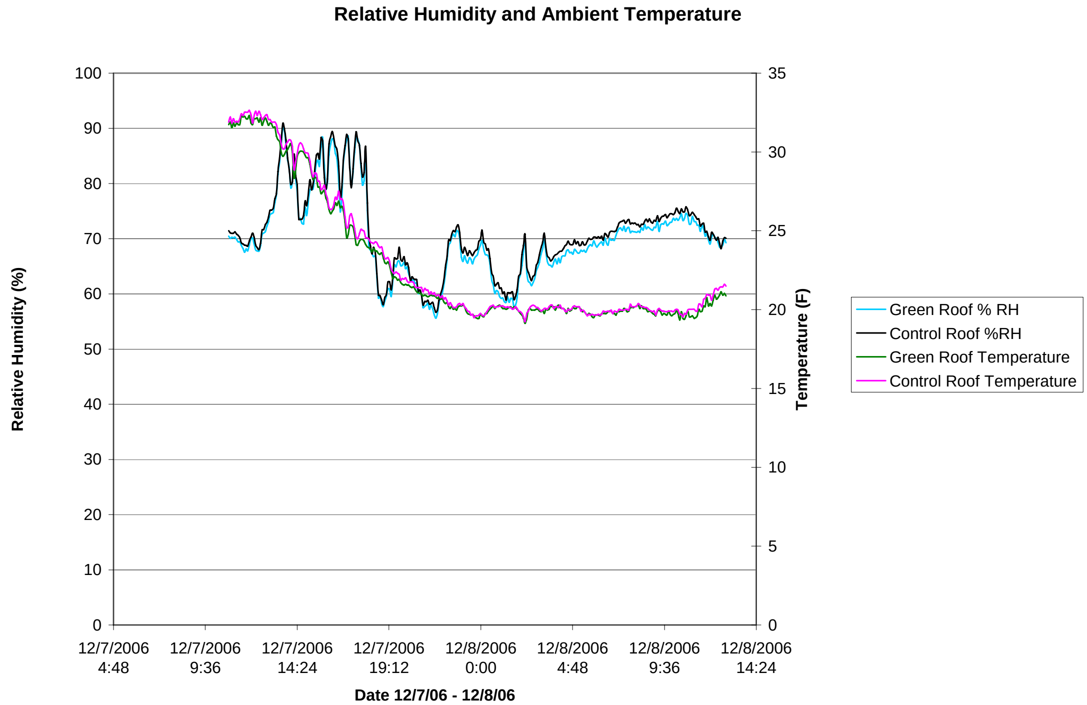

Figure 253. Relative Humidity and Ambient Temperature for 12/7/06 – 12/8/06

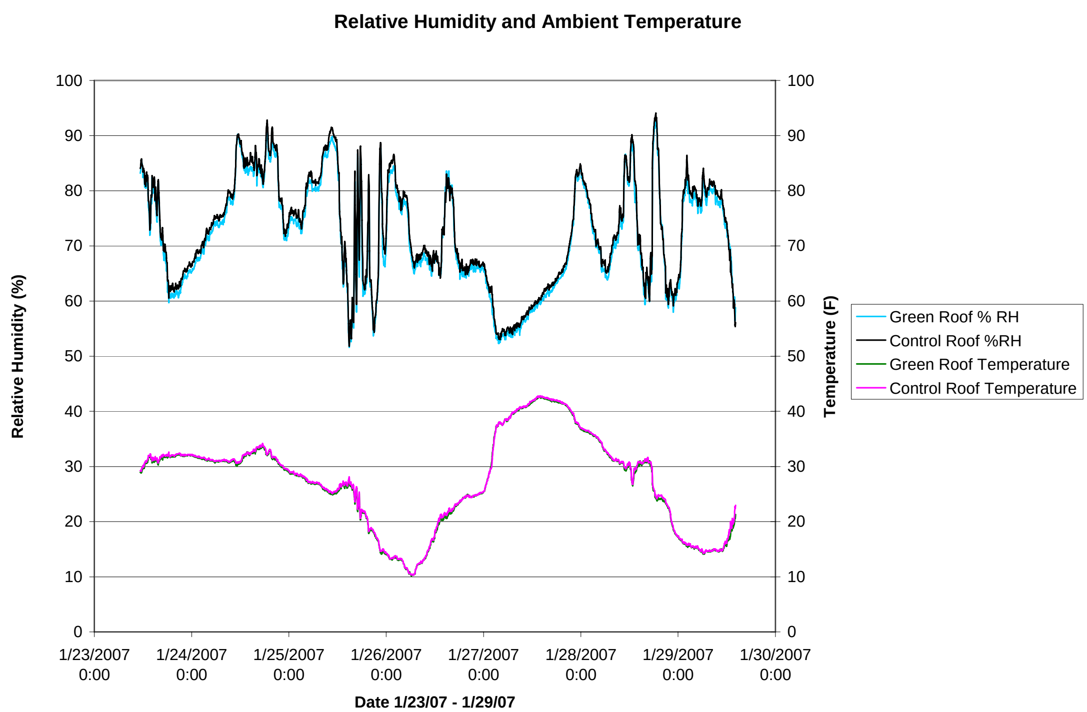

Figure 254. Relative Humidity and Ambient Temperature for 1/23/07 – 1/29/07

APPENDIX D

LIFE CYCLE ASSESSMENT SIMAPRO RESULTS

D.1 CONTROL ROOF ECO-INDICATOR 99 RESULTS

SimaPro 5.0 LCI Results Date: 2/9/2007 Time: 4:11:54 PM
Project: Green Roof

Title:
Method: Eco-indicator 99 (H) / Europe EI 99 H/H
Emission compartment: All compartments
Value: Amount
Category:
Skip unused: No
Relative mode: Non

No	Substance	Compartment	Unit	Total	Control Roof 45 years	Landfill B250 (98)
1	Asphalt	Raw	tn.lg	12.4	12.4	x
2	baryte	Raw	kg	7.98	7.98	x
3	bauxite	Raw	kg	3.49	3.49	x
4	bentonite	Raw	kg	1.98	1.98	x
5	chromium (in ore)	Raw	g	151	151	x
6	clay	Raw	kg	8.55	8.55	x
7	coal	Raw	g	117	117	x
8	coal ETH	Raw	kg	790	789	0.898
9	coal FAL	Raw	tn.lg	198	198	x
10	cobalt (in ore)	Raw	µg	403	403	x
11	copper (in ore)	Raw	kg	1.45	1.45	x
12	crude oil (feedstock) FAL	Raw	tn.lg	6.63	6.63	x
13	crude oil ETH	Raw	kg	997	940	57.4
14	crude oil FAL	Raw	tn.lg	10.1	10.1	x

15	crude oil IDEMAT	Raw	kg	23.6	23.6	x
16	energy from hydro power	Raw	MWh	80.2	80.2	x
17	gas from oil production	Raw	l	65.2	65.2	x
18	gravel	Raw	tn.lg	17.3	17.3	x
19	iron (in ore)	Raw	kg	67.9	67.9	x
20	iron (ore)	Raw	g	3.21	3.21	x
21	lead (in ore)	Raw	g	604	604	x
22	lignite ETH	Raw	kg	901	900	0.937
23	limestone	Raw	tn.lg	12.3	12.3	x
24	manganese (in ore)	Raw	g	46.7	46.7	x
25	marl	Raw	kg	57.2	57.2	x
26	methane (kg)	Raw	g	123	123	x
27	methane (kg) ETH	Raw	kg	5.27	5.27	x
28	molybdene (in ore)	Raw	µg	721	721	x
29	natural gas	Raw	kg	1.42	1.42	x
30	natural gas (feedstock) FAL	Raw	tn.lg	8.88	8.88	x
31	natural gas (vol)	Raw	m3	4.32	x	4.32
32	natural gas ETH	Raw	m3	3.43E3	3.43E3	x
33	natural gas FAL	Raw	tn.lg	46.9	46.9	x
34	nickel (in ore)	Raw	g	93	93	x
35	oxygen	Raw	kg	256	256	x
36	palladium (in ore)	Raw	mg	2.03	2.03	x
37	petroleum gas ETH	Raw	m3	42.1	42.1	x
38	platinum (in ore)	Raw	mg	2.29	2.29	x
39	pot. energy hydropower	Raw	MJ	44.1	15	29.1
40	potential energy water ETH	Raw	MWh	1.51	1.51	x
41	process water	Raw	cu.in	847	x	847
42	reservoir content ETH	Raw	m3y	121	121	x
43	rhenium (in ore)	Raw	mg	1.75	1.75	x
44	rhodium (in ore)	Raw	mg	2.16	2.16	x
45	rock salt	Raw	kg	3.92	3.92	x
46	sand	Raw	kg	89.8	89.8	x
47	scrap, external	Raw	tn.lg	8.73	8.73	x
48	silver	Raw	mg	3.98	3.98	x
49	silver (in ore)	Raw	g	1.92	1.92	x
50	tin (in ore)	Raw	g	1.07	1.07	x
51	turbine water ETH	Raw	m3	2.71E4	2.71E4	x
52	uranium (in ore)	Raw	mg	596	346	250
53	uranium (in ore) ETH	Raw	g	66.6	66.6	x
54	uranium FAL	Raw	g	794	794	x
55	water	Raw	tn.lg	166	166	x
56	Water1	Raw	m3	3.15E4	3.15E4	x
57	wood	Raw	g	218	209	8.79
58	wood (dry matter) ETH	Raw	tn.lg	21.1	21.1	x
59	wood/wood wastes FAL	Raw	kg	137	137	x
60	zeolite	Raw	mg	75	75	x

61	zinc (in ore)	Raw	g	8.42	8.42	x
62	1,2-dichloroethane	Air	µg	185	185	x
63	acetaldehyde	Air	g	6.52	6.52	x
64	acetic acid	Air	g	20.9	20.9	x
65	acetone	Air	g	1.38	1.38	x
66	acrolein	Air	g	6.87	6.87	x
67	Al	Air	g	46.7	46.7	x
68	aldehydes	Air	kg	2.65	2.65	x
69	alkanes	Air	g	96.1	96.1	x
70	alkenes	Air	g	243	243	x
71	ammonia	Air	oz	557	557	0.205
72	As	Air	g	24.8	24.8	x
73	B	Air	g	34.4	34.4	x
74	Ba	Air	mg	754	754	x
75	Be	Air	g	2.85	2.85	x
76	benzaldehyde	Air	µg	165	165	x
77	benzene	Air	g	222	221	0.717
78	benzo(a)pyrene	Air	mg	48.9	48.9	x
79	Br	Air	g	3.57	3.57	x
80	butane	Air	g	162	162	x
81	butene	Air	g	5.94	5.94	x
82	Ca	Air	g	55.9	55.9	x
83	Cd	Air	g	6.08	6.06	0.0133
84	CFC-11	Air	mg	20.8	20.8	x
85	CFC-114	Air	mg	556	556	x
86	CFC-116	Air	mg	38	38	x
87	CFC-12	Air	mg	4.47	4.47	x
88	CFC-13	Air	mg	2.81	2.81	x
89	CFC-14	Air	mg	342	342	x
90	Cl2	Air	g	3.99	3.99	x
91	CO	Air	kg	489	488	1.12
92	CO2	Air	tn.lg	15.1	13.4	1.73
93	CO2 (fossil)	Air	tn.lg	562	562	x
94	CO2 (non-fossil)	Air	kg	189	189	x
95	cobalt	Air	g	9.74	9.74	x
96	Cr	Air	g	52.2	52.2	x
97	Cu	Air	g	3.66	3.66	x
98	CxHy	Air	g	194	194	x
99	CxHy aromatic	Air	g	8.22	7.02	1.2
100	CxHy chloro	Air	µg	6.09	6.09	x
101	CxHy halogenated	Air	µg	66.8	x	66.8
102	cyanides	Air	mg	25.7	25.7	x
103	dichloroethane	Air	mg	358	358	x
104	dichloromethane	Air	g	29.1	29.1	x
105	dioxin (TEQ)	Air	µg	45.5	45.1	0.362
106	dust	Air	g	628	438	190

107	dust (coarse)	Air	g	62.3	62.3	x
108	dust (coarse) process	Air	kg	1.84	1.84	x
109	dust (PM10) mobile	Air	g	97.5	97.5	x
110	dust (PM10) stationary	Air	kg	10.3	10.3	x
111	dust (SPM)	Air	g	7.79	7.79	x
112	ethane	Air	g	688	688	x
113	ethanol	Air	g	2.78	2.78	x
114	ethene	Air	g	176	176	x
115	ethylbenzene	Air	g	7.28	7.28	x
116	ethyne	Air	mg	87.8	87.8	x
117	Fe	Air	g	35.5	35.5	x
118	formaldehyde	Air	g	159	159	x
119	H2S	Air	g	58.5	58.5	x
120	HALON-1301	Air	mg	330	317	13.7
121	HCFC-21	Air	g	1.36	1.36	x
122	HCFC-22	Air	mg	5.07	5.07	x
123	HCl	Air	lb	77.8	77.8	0.0112
124	He	Air	g	42.5	42.5	x
125	heptane	Air	g	11	11	x
126	hexachlorobenzene	Air	µg	17.2	17.2	x
127	hexane	Air	g	23.6	23.6	x
128	HF	Air	oz	172	171	0.213
129	HFC-134a	Air	pg	-0.188	-0.188	x
130	Hg	Air	g	13.5	13.4	0.113
131	I	Air	g	1.61	1.61	x
132	K	Air	g	17.7	17.7	x
133	kerosene	Air	g	175	175	x
134	La	Air	mg	21.8	21.8	x
135	metals	Air	g	80.3	79.6	0.715
136	methane	Air	kg	1.54E3	1.35E3	198
137	methanol	Air	g	2.86	2.86	x
138	Mg	Air	g	16.7	16.7	x
139	Mn	Air	g	93.6	93.6	0.000299
140	Mo	Air	mg	173	173	x
141	MTBE	Air	mg	132	132	x
142	n-nitrodimethylamine	Air	g	1.45	1.45	x
143	N2	Air	g	958	958	x
144	N2O	Air	oz	160	160	0.192
145	Na	Air	g	10.7	10.7	x
146	naphthalene	Air	mg	379	379	x
147	Ni	Air	g	103	103	0.0927
148	non methane VOC	Air	kg	843	842	1.22
149	NOx	Air	tn.lg	2.07	2.07	x
150	NOx (as NO2)	Air	kg	47.3	44.6	2.69
151	organic substances	Air	kg	14.5	14.5	x
152	P	Air	mg	9.96	9.96	x

153	P-tot	Air	mg	745	745	x
154	PAH's	Air	g	1.3	1.29	0.00196
155	particulates (PM10)	Air	kg	113	113	x
156	particulates (unspecified)	Air	kg	534	534	x
157	Pb	Air	g	28.8	28.7	0.0138
158	pentachlorobenzene	Air	µg	46	46	x
159	pentachlorophenol	Air	µg	7.42	7.42	x
160	pentane	Air	g	185	185	x
161	phenol	Air	g	20.1	20.1	x
162	propane	Air	g	241	241	x
163	propene	Air	g	8.35	8.35	x
164	propionic acid	Air	g	2.04	2.04	x
165	Pt	Air	µg	616	616	x
166	Sb	Air	g	3.32	3.32	x
167	Sc	Air	mg	7.33	7.33	x
168	Se	Air	g	49.5	49.5	x
169	silicates	Air	g	168	168	x
170	Sn	Air	mg	16.6	16.6	x
171	SO2	Air	g	332	332	x
172	soot	Air	g	6.37	6.37	x
173	SOx	Air	tn.lg	4.9	4.9	x
174	SOx (as SO2)	Air	oz	948	927	20.6
175	Sr	Air	mg	748	748	x
176	tetrachloroethene	Air	g	6.54	6.54	x
177	tetrachloromethane	Air	g	10.8	10.8	x
178	Th	Air	mg	14.5	14.5	x
179	Ti	Air	g	2.09	2.09	x
180	Tl	Air	mg	5.28	5.28	x
181	toluene	Air	g	84.9	84.9	x
182	trichloroethene	Air	g	6.49	6.49	x
183	trichloromethane	Air	mg	9.45	9.45	x
184	U	Air	mg	15.7	15.7	x
185	V	Air	g	17.3	17.3	x
186	vinyl chloride	Air	mg	58.5	58.5	x
187	xylene	Air	g	73.5	73.5	x
188	Zn	Air	g	25.5	23.1	2.38
189	Zr	Air	mg	1.56	1.56	x
190	1,1,1-trichloroethane	Water	µg	596	596	x
191	acenaphthylene	Water	g	1.34	1.34	x
192	Acid as H+	Water	mg	24.5	24.5	x
193	acids (unspecified)	Water	kg	42.5	42.5	x
194	Ag	Water	mg	23.1	23.1	x
195	Al	Water	oz	46.1	46.1	0.054
196	alkanes	Water	g	4.58	4.58	x
197	alkenes	Water	mg	422	422	x
198	anorg. dissolved subst.	Water	kg	7.37	6.24	1.13

199	AOX	Water	mg	194	182	11.2
200	As	Water	g	2.61	2.6	0.00521
201	B	Water	kg	18.6	18.6	x
202	Ba	Water	g	228	221	7.32
203	baryte	Water	kg	1.62	1.62	x
204	Be	Water	mg	2.27	2.27	x
205	benzene	Water	g	4.87	4.87	x
206	BOD	Water	oz	289	289	0.00907
207	calcium compounds	Water	g	25.9	25.9	x
208	calcium ions	Water	kg	4.05	4.05	x
209	Cd	Water	g	142	141	0.595
210	chlorinated solvents (unspec.)	Water	mg	7.75	7.75	x
211	chlorobenzenes	Water	µg	7.16	7.16	x
212	chromate	Water	g	5.16	5.16	x
213	Cl-	Water	kg	175	173	1.84
214	Co	Water	g	2.51	2.51	x
215	COD	Water	lb	105	105	0.0185
216	Copper	Water	kg	4.41	4.41	x
217	Cr	Water	g	205	205	0.0391
218	Cr (VI)	Water	mg	2.41	2.41	x
219	crude oil	Water	mg	10.7	10.7	x
220	Cs	Water	mg	31.1	31.1	x
221	Cu	Water	g	8.38	6.71	1.67
222	CxHy	Water	g	2.86	2.86	x
223	CxHy aromatic	Water	g	39.7	37.3	2.45
224	CxHy chloro	Water	mg	16.8	14.2	2.54
225	cyanide	Water	g	17.8	17.8	0.0113
226	di(2-ethylhexyl)phthalate	Water	µg	20.8	20.8	x
227	dibutyl p-phthalate	Water	µg	136	136	x
228	dichloroethane	Water	mg	184	184	x
229	dichloromethane	Water	mg	718	718	x
230	dimethyl p-phthalate	Water	µg	856	856	x
231	dissolved organics	Water	mg	137	137	x
232	dissolved solids	Water	tn.lg	3.04	3.04	x
233	dissolved substances	Water	g	532	532	x
234	DOC	Water	g	50.2	50.2	0.0224
235	ethyl benzene	Water	mg	754	754	x
236	fats/oils	Water	g	974	897	76.5
237	fatty acids as C	Water	g	167	167	x
238	Fe	Water	lb	64.2	64.2	0.00527
239	fluoride ions	Water	g	722	722	x
240	formaldehyde	Water	g	12.1	12.1	x
241	glutaraldehyde	Water	mg	200	200	x
242	H2	Water	mg	688	688	x
243	H2S	Water	mg	120	120	x
244	H2SO4	Water	kg	4.64	4.64	x

245	hexachloroethane	Water	µg	4.09	4.09	x
246	Hg	Water	mg	94.3	27.5	66.8
247	HOCL	Water	g	10	10	x
248	I	Water	g	3.09	3.09	x
249	K	Water	g	541	541	x
250	Kjeldahl-N	Water	g	7.06	6	1.06
251	Lead	Water	g	693	693	x
252	metallic ions	Water	g	498	480	17.7
253	Mg	Water	kg	1.1	1.1	x
254	Mn	Water	kg	15.8	15.8	x
255	Mo	Water	g	4.67	4.67	x
256	MTBE	Water	mg	15.7	15.7	x
257	N-tot	Water	g	95.2	89.1	6.11
258	N organically bound	Water	g	7.44	7.44	x
259	Na	Water	kg	13	13	x
260	NH3	Water	g	337	337	x
261	NH3 (as N)	Water	g	104	104	x
262	NH4+	Water	g	476	35.5	440
263	Ni	Water	g	50.2	50.2	0.0154
264	nitrate	Water	oz	55	5.47	49.6
265	nitrite	Water	g	2.64	2.64	x
266	non methane VOC	Water	g	674	674	x
267	OCl-	Water	g	9.91	9.91	x
268	oil	Water	kg	56.5	56.5	x
269	organic carbon	Water	kg	1.29	1.29	x
270	other organics	Water	kg	10.8	10.8	x
271	P-compounds	Water	mg	44.8	44.8	x
272	P-tot	Water	µg	7.44	7.44	x
273	PAH's	Water	mg	676	639	37.5
274	Pb	Water	g	26.1	26	0.0239
275	phenol	Water	g	1.25	1.25	x
276	phenols	Water	g	7.42	7.04	0.38
277	phosphate	Water	oz	85.2	85.2	0.00411
278	Ru	Water	mg	310	310	x
279	S	Water	mg	2.06	2.06	x
280	salt	Water	g	1.91	1.91	x
281	salts	Water	kg	3.17	3.17	x
282	Sb	Water	mg	21.7	21.7	x
283	Se	Water	g	6.51	6.51	x
284	Si	Water	g	1.16	1.16	x
285	Sn	Water	mg	12.2	12.2	x
286	SO3	Water	g	11.9	11.9	x
287	Sr	Water	g	203	203	x
288	sulphate	Water	lb	617	615	1.89
289	sulphates	Water	g	135	135	x
290	sulphide	Water	g	178	178	0.0898

291	suspended solids	Water	kg	364	364	x
292	suspended substances	Water	g	1.1E3	936	166
293	tetrachloroethene	Water	µg	485	485	x
294	tetrachloromethane	Water	µg	740	740	x
295	Ti	Water	g	75.8	75.8	x
296	TOC	Water	kg	6.37	2.89	3.48
297	toluene	Water	g	6.3	5.96	0.341
298	tributyltin	Water	mg	56.2	56.2	x
299	trichloroethene	Water	mg	30.7	30.7	x
300	trichloromethane	Water	mg	114	114	x
301	triethylene glycol	Water	g	50.2	50.2	x
302	undissolved substances	Water	kg	5.18	5.18	x
303	V	Water	g	6.83	6.83	x
304	vinyl chloride	Water	µg	138	138	x
305	VOC as C	Water	g	10.8	10.8	x
306	W	Water	mg	54.5	54.5	x
307	xylene	Water	g	3.48	3.48	x
308	Zinc	Water	kg	1.13	1.13	x
309	Zn	Water	g	239	97.6	141
310	final waste (inert)	Solid	kg	6.68	6.68	x
311	high active nuclear waste	Solid	mm3	19.3	19.3	x
312	low,med. act. nucl. waste	Solid	cm3	4.34	4.34	x
313	mineral waste	Solid	g	535	535	x
314	produc. waste (not inert)	Solid	g	386	386	x
315	slag	Solid	g	57.3	57.3	x
316	solid waste	Solid	tn.lg	94.3	94.3	x
317	Al (ind.)	Soil	g	103	103	x
318	As (ind.)	Soil	mg	41	41	x
319	C (ind.)	Soil	g	311	311	x
320	Ca (ind.)	Soil	g	410	410	x
321	carbon	Soil	kg	2.35	x	2.35
322	Cd	Soil	mg	258	x	258
323	Cd (ind.)	Soil	mg	1.3	1.3	x
324	Co (ind.)	Soil	µg	831	831	x
325	Cr (ind.)	Soil	mg	513	513	x
326	Cu (ind.)	Soil	mg	4.15	4.15	x
327	Fe (ind.)	Soil	g	206	206	x
328	Hg	Soil	mg	64.1	x	64.1
329	Hg (ind.)	Soil	µg	119	119	x
330	Mn (ind.)	Soil	g	4.1	4.1	x
331	N	Soil	mg	36.4	36.4	x
332	N-tot	Soil	g	35.2	x	35.2
333	Ni (ind.)	Soil	mg	6.23	6.23	x
334	oil (ind.)	Soil	g	475	475	x
335	oil biodegradable	Soil	g	280	280	x
336	P-tot	Soil	g	5.2	5.2	x

337	Pb	Soil	mg	28.4	x	28.4
338	Pb (ind.)	Soil	mg	19	19	x
339	S (ind.)	Soil	g	61.7	61.7	x
340	Zn	Soil	mg	4.96	x	4.96
341	Zn (ind.)	Soil	g	1.58	1.58	x
342	Ag110m to air	Non mat.	mBq	25.4	25.4	x
343	Ag110m to water	Non mat.	Bq	174	174	x
344	alpha radiation (unspecified) to water	Non mat.	mBq	20.4	20.4	x
345	Am241 to air	Non mat.	mBq	514	514	x
346	Am241 to water	Non mat.	Bq	67.7	67.7	x
347	Ar41 to air	Non mat.	kBq	54.8	54.8	x
348	Ba140 to air	Non mat.	mBq	143	143	x
349	Ba140 to water	Non mat.	Bq	1.06	1.06	x
350	beta radiation (unspecified) to air	Non mat.	mBq	8.94	8.94	x
351	C14 to air	Non mat.	kBq	43.2	43.2	x
352	C14 to water	Non mat.	kBq	3.43	3.43	x
353	Cd109 to water	Non mat.	mBq	6.16	6.16	x
354	Ce141 to air	Non mat.	mBq	2.41	2.41	x
355	Ce141 to water	Non mat.	mBq	159	159	x
356	Ce144 to air	Non mat.	Bq	5.47	5.47	x
357	Ce144 to water	Non mat.	kBq	1.55	1.55	x
358	Cm (alpha) to air	Non mat.	mBq	815	815	x
359	Cm (alpha) to water	Non mat.	Bq	89.7	89.7	x
360	Cm242 to air	Non mat.	µBq	2.48	2.48	x
361	Cm244 to air	Non mat.	µBq	22.5	22.5	x
362	Co57 to air	Non mat.	µBq	43.2	43.2	x
363	Co57 to water	Non mat.	Bq	1.09	1.09	x
364	Co58 to air	Non mat.	mBq	718	718	x
365	Co58 to water	Non mat.	Bq	544	544	x
366	Co60 to air	Non mat.	Bq	1.12	1.12	x
367	Co60 to water	Non mat.	kBq	15.4	15.4	x
368	Conv. to industrial area	Non mat.	mm2	478	478	x
369	Cr51 to air	Non mat.	mBq	94.7	94.7	x
370	Cr51 to water	Non mat.	Bq	23.4	23.4	x
371	Cs134 to air	Non mat.	Bq	19.5	19.5	x
372	Cs134 to water	Non mat.	kBq	3.47	3.47	x
373	Cs136 to water	Non mat.	mBq	5.72	5.72	x
374	Cs137 to air	Non mat.	Bq	37.6	37.6	x
375	Cs137 to water	Non mat.	kBq	32	32	x
376	Fe59 to air	Non mat.	µBq	979	979	x
377	Fe59 to water	Non mat.	mBq	18.8	18.8	x
378	Fission and activation products (RA) to water	Non mat.	Bq	185	185	x
379	H3 to air	Non mat.	kBq	403	403	x
380	H3 to water	Non mat.	kBq	1.01E5	1.01E5	x
381	heat losses to air	Non mat.	MJ	518	518	x

382	heat losses to soil	Non mat.	kJ	203	203	x
383	heat losses to water	Non mat.	MJ	39.8	39.8	x
384	I129 to air	Non mat.	Bq	147	147	x
385	I129 to water	Non mat.	kBq	9.78	9.78	x
386	I131 to air	Non mat.	Bq	28.2	28.2	x
387	I131 to water	Non mat.	Bq	9.08	9.08	x
388	I133 to air	Non mat.	Bq	8.49	8.49	x
389	I133 to water	Non mat.	Bq	4.87	4.87	x
390	I135 to air	Non mat.	Bq	12.5	12.5	x
391	K40 to air	Non mat.	Bq	70.8	70.8	x
392	K40 to water	Non mat.	Bq	225	225	x
393	Kr85 to air	Non mat.	kBq	2.53E6	2.53E6	x
394	Kr85m to air	Non mat.	kBq	6.93	6.93	x
395	Kr87 to air	Non mat.	kBq	2.48	2.48	x
396	Kr88 to air	Non mat.	kBq	111	111	x
397	Kr89 to air	Non mat.	kBq	2.2	2.2	x
398	La140 to air	Non mat.	mBq	69.9	69.9	x
399	La140 to water	Non mat.	mBq	221	221	x
400	land use (sea floor) II-III	Non mat.	m2a	130	130	x
401	land use (sea floor) II-IV	Non mat.	m2a	13.4	13.4	x
402	land use II-III	Non mat.	m2a	260	260	x
403	land use II-IV	Non mat.	m2a	336	336	x
404	land use III-IV	Non mat.	m2a	26.7	26.7	x
405	land use IV-IV	Non mat.	cm2a	413	413	x
406	Mn54 to air	Non mat.	mBq	26.3	26.3	x
407	Mn54 to water	Non mat.	kBq	2.31	2.31	x
408	Mo99 to water	Non mat.	mBq	74.4	74.4	x
409	Na24 to water	Non mat.	Bq	32.8	32.8	x
410	Nb95 to air	Non mat.	mBq	4.72	4.72	x
411	Nb95 to water	Non mat.	mBq	604	604	x
412	Np237 to air	Non mat.	µBq	26.9	26.9	x
413	Np237 to water	Non mat.	Bq	4.32	4.32	x
414	Occup. as contin. urban land	Non mat.	cm2a	687	687	x
415	Occup. as convent. arable land	Non mat.	m2a	0.839	0.839	x
416	Occup. as forest land	Non mat.	mm2a	96.9	96.9	x
417	Occup. as industrial area	Non mat.	m2a	18.9	18.9	x
418	Pa234m to air	Non mat.	Bq	16.3	16.3	x
419	Pa234m to water	Non mat.	Bq	301	301	x
420	Pb210 to air	Non mat.	Bq	430	430	x
421	Pb210 to water	Non mat.	Bq	179	179	x
422	Pm147 to air	Non mat.	Bq	13.9	13.9	x
423	Po210 to air	Non mat.	Bq	635	635	x
424	Po210 to water	Non mat.	Bq	179	179	x
425	Pu alpha to air	Non mat.	Bq	1.64	1.64	x
426	Pu alpha to water	Non mat.	Bq	269	269	x
427	Pu238 to air	Non mat.	µBq	55.9	55.9	x

428	Pu241 beta	Non mat.	kBq	6.69	6.69	x
429	Pu241 Beta to air	Non mat.	Bq	44.8	44.8	x
430	Ra224 to water	Non mat.	kBq	1.55	1.55	x
431	Ra226 to air	Non mat.	Bq	575	575	x
432	Ra226 to water	Non mat.	kBq	1.25E3	1.25E3	x
433	Ra228 to air	Non mat.	Bq	34.7	34.7	x
434	Ra228 to water	Non mat.	kBq	3.08	3.08	x
435	radio active noble gases to air	Non mat.	kBq	11.2	11.2	x
436	radioactive substance to air	Non mat.	kBq	9.66E6	9.64E6	2.17E4
437	radioactive substance to water	Non mat.	kBq	486	285	201
438	radionuclides (mixed) to water	Non mat.	mBq	162	162	x
439	Rn220 to air	Non mat.	kBq	3.27	3.27	x
440	Rn222 (long term) to air	Non mat.	kBq	3.62E6	3.62E6	x
441	Rn222 to air	Non mat.	kBq	3.94E4	3.94E4	x
442	Ru103 to air	Non mat.	µBq	322	322	x
443	Ru103 to water	Non mat.	mBq	357	357	x
444	Ru106 to air	Non mat.	Bq	164	164	x
445	Ru106 to water	Non mat.	kBq	16.4	16.4	x
446	Sb122 to water	Non mat.	Bq	1.06	1.06	x
447	Sb124 to air	Non mat.	mBq	7.21	7.21	x
448	Sb124 to water	Non mat.	Bq	55.1	55.1	x
449	Sb125 to air	Non mat.	mBq	1.91	1.91	x
450	Sb125 to water	Non mat.	Bq	8.68	8.68	x
451	Sr89 to air	Non mat.	mBq	46.2	46.2	x
452	Sr89 to water	Non mat.	Bq	2.41	2.41	x
453	Sr90 to air	Non mat.	Bq	26.9	26.9	x
454	Sr90 to water	Non mat.	kBq	3.26	3.26	x
455	Tc99 to air	Non mat.	mBq	1.14	1.14	x
456	Tc99 to water	Non mat.	kBq	1.71	1.71	x
457	Tc99m to water	Non mat.	mBq	502	502	x
458	Te123m to air	Non mat.	mBq	112	112	x
459	Te123m to water	Non mat.	mBq	45	45	x
460	Te132 to water	Non mat.	mBq	18.4	18.4	x
461	Th228 to air	Non mat.	Bq	29.4	29.4	x
462	Th228 to water	Non mat.	kBq	6.18	6.18	x
463	Th230 to air	Non mat.	Bq	181	181	x
464	Th230 to water	Non mat.	kBq	47.2	47.2	x
465	Th232 to air	Non mat.	Bq	18.6	18.6	x
466	Th232 to water	Non mat.	Bq	42	42	x
467	Th234 to air	Non mat.	Bq	16.3	16.3	x
468	Th234 to water	Non mat.	Bq	304	304	x
469	U alpha to air	Non mat.	Bq	584	584	x
470	U alpha to water	Non mat.	kBq	19.7	19.7	x
471	U234 to air	Non mat.	Bq	195	195	x
472	U234 to water	Non mat.	Bq	403	403	x
473	U235 to air	Non mat.	Bq	9.46	9.46	x

474	U235 to water	Non mat.	Bq	601	601	x
475	U238 to air	Non mat.	Bq	246	246	x
476	U238 to water	Non mat.	kBq	1.01	1.01	x
477	waste heat to air	Non mat.	MWh	-35.8	-35.8	x
478	waste heat to soil	Non mat.	MJ	454	454	x
479	waste heat to water	Non mat.	GJ	1.04	1.04	x
480	Xe131m to air	Non mat.	kBq	11.4	11.4	x
481	Xe133 to air	Non mat.	kBq	1.78E3	1.78E3	x
482	Xe133m to air	Non mat.	Bq	833	833	x
483	Xe135 to air	Non mat.	kBq	369	369	x
484	Xe135m to air	Non mat.	kBq	67.2	67.2	x
485	Xe137 to air	Non mat.	kBq	1.49	1.49	x
486	Xe138 to air	Non mat.	kBq	18.5	18.5	x
487	Y90 to water	Non mat.	mBq	123	123	x
488	Zn65 to air	Non mat.	mBq	132	132	x
489	Zn65 to water	Non mat.	Bq	69.2	69.2	x
490	Zr95 to air	Non mat.	mBq	1.64	1.64	x
491	Zr95 to water	Non mat.	Bq	139	139	x

→

D.2 EXTENSIVE GREEN ROOF ECO-INDICATOR 99 RESULTS

SimaPro 5.0 LCI Results Date: 2/9/2007 Time: 4:13:35 PM
Project: Green Roof
Title:
Method: Eco-indicator 99 (H) / Europe EI 99 H/H
Emission compartment: All compartments
Value: Amount
Category:
Skip unused: No
Relative mode: Non

No	Substance	Compartment	Unit	Total	Extensive Roof 45 years	Landfill B250 (98)
1	air	Raw	kg	39	39	x
2	Asphalt	Raw	tn.lg	4.13	4.13	x
3	baryte	Raw	kg	4.39	4.39	x
4	bauxite	Raw	kg	19.8	19.8	x
5	bentonite	Raw	kg	1.22	1.22	x
6	calcium sulphate	Raw	mg	815	815	x
7	chalk	Raw	pg	1.04E-10	1.04E-10	x

8	chromium (in ore)	Raw	g	280	280	x
9	clay	Raw	kg	3.34	3.34	x
10	clay minerals	Raw	tn.lg	2.95	2.95	x
11	coal ETH	Raw	lb	829	829	0.381
12	coal FAL	Raw	tn.lg	109	109	x
13	cobalt (in ore)	Raw	µg	174	174	x
14	copper (in ore)	Raw	g	927	927	x
15	crude oil (feedstock) FAL	Raw	tn.lg	2.21	2.21	x
16	crude oil ETH	Raw	kg	344	333	10.9
17	crude oil FAL	Raw	tn.lg	5.35	5.35	x
18	crude oil IDEMAT	Raw	kg	76.7	76.7	x
19	dolomite	Raw	kg	45.4	45.4	x
20	energy (undef.)	Raw	MJ	18.3	18.3	x
21	energy from biomass	Raw	MJ	9.91	9.91	x
22	energy from coal	Raw	MJ	803	803	x
23	energy from hydro power	Raw	MWh	44.1	44.1	x
24	energy from hydrogen	Raw	MJ	49	49	x
25	energy from lignite	Raw	MJ	33.8	33.8	x
26	energy from natural gas	Raw	MWh	2.17	2.17	x
27	energy from oil	Raw	MWh	4.49	4.49	x
28	energy from peat	Raw	kJ	774	774	x
29	energy from sulphur	Raw	kJ	989	989	x
30	energy from uranium	Raw	GJ	1.09	1.09	x
31	energy from wood	Raw	kJ	4.36	4.36	x
32	energy recovered	Raw	MJ	-207	-207	x
33	feldspar	Raw	kg	45.4	45.4	x
34	ferromanganese	Raw	mg	38.4	38.4	x
35	fluorspar	Raw	g	211	211	x
36	gas from oil production	Raw	l	107	107	x
37	granite	Raw	g	201	201	x
38	gravel	Raw	tn.lg	7.5	7.5	x
39	iron (in ore)	Raw	kg	62.9	62.9	x
40	KCl	Raw	mg	336	336	x
41	lead (in ore)	Raw	kg	2.44	2.44	x
42	lignite ETH	Raw	lb	793	793	0.396
43	limestone	Raw	tn.lg	7.2	7.2	x
44	manganese (in ore)	Raw	g	86.3	86.3	x
45	marl	Raw	kg	34.5	34.5	x
46	methane (kg)	Raw	g	202	202	x
47	methane (kg) ETH	Raw	kg	2.44	2.44	x
48	molybdene (in ore)	Raw	µg	399	399	x
49	NaCl	Raw	kg	10.8	10.8	x
50	NaOH	Raw	kg	136	136	x
51	natural gas	Raw	kg	264	264	x
52	natural gas (feedstock) FAL	Raw	tn.lg	2.96	2.96	x
53	natural gas (vol)	Raw	l	824	x	824

54	natural gas ETH	Raw	m3	1.9E3	1.9E3	x	
55	natural gas FAL	Raw	tn.lg	23.9	23.9	x	
56	nickel (in ore)	Raw	g	171	171	x	
57	nitrogen	Raw	kg	21.4	21.4	x	
58	olivine	Raw	mg	396	396	x	
59	oxygen	Raw	kg	256	256	x	
60	palladium (in ore)	Raw	mg	1.21	1.21	x	
61	petroleum gas ETH	Raw	m3	22.7	22.7	x	
62	phosphate (as P2O5)	Raw	mg	127	127	x	
63	platinum (in ore)	Raw	mg	1.36	1.36	x	
64	pot. energy hydropower	Raw	MJ	5.66	x	5.66	
65	potential energy water ETH	Raw	GJ	2.14	2.14	x	
66	process water	Raw	cu.in	158	x	158	
67	reservoir content ETH	Raw	m3y	47.5	47.5	x	
68	rhenium (in ore)	Raw	mg	1.03	1.03	x	
69	rhodium (in ore)	Raw	mg	1.29	1.29	x	
70	rock salt	Raw	kg	1.65	1.65	x	
71	rutile	Raw	pg	1.49E-10	1.49E-10	x	
72	sand	Raw	tn.lg	5.1	5.1	x	
73	scrap, external	Raw	tn.lg	8.73	8.73	x	
74	shale	Raw	g	2.31	2.31	x	
75	silver	Raw	mg	6.56	6.56	x	
76	silver (in ore)	Raw	mg	947	947	x	
77	sulphur (bonded)	Raw	g	51.8	51.8	x	
78	sulphur (elemental)	Raw	g	107	107	x	
79	tin (in ore)	Raw	mg	530	530	x	
80	turbine water ETH	Raw	m3	1.08E4	1.08E4	x	
81	uranium (in ore)	Raw	mg	235	187	48.5	
82	uranium (in ore) ETH	Raw	g	26.4	26.4	x	
83	uranium FAL	Raw	g	436	436	x	
84	water	Raw	tn.lg	57.8	57.8	x	
85	water (cooling)	Raw	tn.lg	11	11	x	
86	water (drinking, for process.)	Raw	kg	948	948	x	
87	water (process)	Raw	kg	69.6	69.6	x	
88	water (sea, for cooling)	Raw	tn.lg	5.64	5.64	x	
89	water (sea, for processing)	Raw	kg	33.9	33.9	x	
90	water (surface, for cooling)	Raw	kg	55.4	55.4	x	
91	water (surface, for process.)	Raw	g	706	706	x	
92	water (well, for cooling)	Raw	g	877	877	x	
93	water (well, for processing)	Raw	g	16.9	16.9	x	
94	Water1	Raw	m3	1.88E4	1.88E4	x	
95	wood	Raw	g	305	303	1.69	
96	wood (dry matter) ETH	Raw	tn.lg	7.04	7.04	x	
97	wood/wood wastes FAL	Raw	kg	74.2	74.2	x	
98	zeolite	Raw	mg	124	124	x	
99	zinc (in ore)	Raw	g	30.8	30.8	x	

100	1,2-dichloroethane	Air	µg	305	305	x
101	acetaldehyde	Air	g	2.33	2.33	x
102	acetic acid	Air	g	11.3	11.3	x
103	acetone	Air	mg	585	585	x
104	acrolein	Air	g	3.77	3.77	x
105	Al	Air	g	20.8	20.8	x
106	aldehydes	Air	kg	1.4	1.4	x
107	alkanes	Air	g	35	35	x
108	alkenes	Air	g	81.5	81.5	x
109	ammonia	Air	oz	510	510	0.0529
110	As	Air	g	14.1	14.1	x
111	B	Air	g	14	14	x
112	Ba	Air	mg	327	327	x
113	Be	Air	g	1.56	1.56	x
114	benzaldehyde	Air	µg	60.9	60.9	x
115	benzene	Air	g	94.6	94.5	0.136
116	benzo(a)pyrene	Air	mg	20.5	20.5	x
117	Br	Air	g	1.52	1.52	x
118	butane	Air	g	89.5	89.5	x
119	butene	Air	g	18.6	18.6	x
120	Ca	Air	g	24.1	24.1	x
121	Cd	Air	g	3.22	3.21	0.004
122	CFC-11	Air	mg	8.25	8.25	x
123	CFC-114	Air	mg	220	220	x
124	CFC-116	Air	mg	87.3	87.3	x
125	CFC-12	Air	mg	1.77	1.77	x
126	CFC-13	Air	mg	1.11	1.11	x
127	CFC-14	Air	mg	785	785	x
128	CFC (soft)	Air	mg	16.4	16.4	x
129	Cl2	Air	g	88.2	88.2	x
130	CO	Air	lb	546	546	0.47
131	CO2	Air	kg	7.57E3	7.24E3	336
132	CO2 (fossil)	Air	tn.lg	304	304	x
133	CO2 (non-fossil)	Air	kg	103	103	x
134	cobalt	Air	g	5.17	5.17	x
135	Cr	Air	g	25.9	25.9	x
136	CS2	Air	µg	22.4	22.4	x
137	Cu	Air	g	1.6	1.6	x
138	CxHy	Air	kg	1.94	1.94	x
139	CxHy aromatic	Air	g	150	150	0.228
140	CxHy chloro	Air	g	12.5	12.5	x
141	CxHy halogenated	Air	µg	12.5	x	12.5
142	cyanides	Air	mg	20.8	20.8	x
143	dichloroethane	Air	mg	164	164	x
144	dichloromethane	Air	g	16	16	x
145	dioxin (TEQ)	Air	µg	23.4	23.3	0.0704

146	dust	Air	g	979	943	36.2
147	dust (coarse)	Air	g	103	103	x
148	dust (coarse) process	Air	kg	1.05	1.05	x
149	dust (PM10) mobile	Air	g	40.4	40.4	x
150	dust (PM10) stationary	Air	kg	3.6	3.6	x
151	dust (SPM)	Air	g	496	496	x
152	ethane	Air	g	383	383	x
153	ethanol	Air	g	1.18	1.18	x
154	ethene	Air	g	594	594	x
155	ethylbenzene	Air	g	2.95	2.95	x
156	ethyne	Air	mg	81.8	81.8	x
157	F2	Air	g	12.6	12.6	x
158	Fe	Air	g	17.3	17.3	x
159	formaldehyde	Air	g	80.8	80.8	x
160	H2	Air	g	32.6	32.6	x
161	H2S	Air	g	34.4	34.4	x
162	H2SO4	Air	ng	431	431	x
163	HALON-1301	Air	mg	133	130	2.6
164	HCFC-21	Air	g	5.07	5.07	x
165	HCFC-22	Air	mg	2.02	2.02	x
166	HCl	Air	oz	682	682	0.0561
167	HCN	Air	pg	5.1E-16	5.1E-16	x
168	He	Air	g	22.8	22.8	x
169	heptane	Air	g	5.48	5.48	x
170	hexachlorobenzene	Air	µg	9.14	9.14	x
171	hexane	Air	g	11.7	11.7	x
172	HF	Air	oz	94	93.9	0.0705
173	HFC-134a	Air	pg	-0.109	-0.109	x
174	Hg	Air	g	7.46	7.45	0.0162
175	I	Air	mg	667	667	x
176	K	Air	g	13.4	13.4	x
177	kerosene	Air	g	96.3	96.3	x
178	La	Air	mg	9.51	9.51	x
179	mercaptans	Air	mg	6.42	6.42	x
180	metals	Air	g	44.3	44.1	0.137
181	methane	Air	kg	752	714	38
182	methanol	Air	g	1.24	1.24	x
183	Mg	Air	g	7.45	7.45	x
184	Mn	Air	g	49.8	49.8	5.74E-5
185	Mo	Air	mg	79.7	79.7	x
186	MTBE	Air	mg	44.2	44.2	x
187	n-nitrodimethylamine	Air	mg	796	796	x
188	N2	Air	g	532	532	x
189	N2O	Air	oz	86.3	86.3	0.037
190	Na	Air	g	4.86	4.86	x
191	naphthalene	Air	mg	207	207	x

192	Ni	Air	g	53.8	53.8	0.0176
193	NO2	Air	g	62.1	62.1	x
194	non methane VOC	Air	lb	826	826	0.509
195	NOx	Air	tn.lg	1.14	1.14	x
196	NOx (as NO2)	Air	oz	403	385	18
197	organic substances	Air	kg	8.33	8.33	x
198	P	Air	mg	16.4	16.4	x
199	P-tot	Air	mg	312	312	x
200	PAH's	Air	mg	816	816	0.375
201	particulates (PM10)	Air	kg	61.8	61.8	x
202	particulates (unspecified)	Air	kg	304	304	x
203	Pb	Air	g	25.5	25.5	0.00264
204	pentachlorobenzene	Air	µg	24.5	24.5	x
205	pentachlorophenol	Air	µg	3.94	3.94	x
206	pentane	Air	g	102	102	x
207	phenol	Air	g	20.8	20.8	x
208	propane	Air	g	132	132	x
209	propene	Air	g	5.63	5.63	x
210	propionic acid	Air	g	1.19	1.19	x
211	Pt	Air	µg	217	217	x
212	Sb	Air	g	1.77	1.77	x
213	Sc	Air	mg	3.24	3.24	x
214	Se	Air	g	27.1	27.1	x
215	silicates	Air	g	70.4	70.4	x
216	Sn	Air	mg	9.68	9.68	x
217	SO2	Air	g	232	232	x
218	SOx	Air	tn.lg	2.56	2.56	x
219	SOx (as SO2)	Air	oz	402	398	4.15
220	Sr	Air	mg	333	333	x
221	tetrachloroethene	Air	g	3.59	3.59	x
222	tetrachloromethane	Air	g	5.9	5.9	x
223	Th	Air	mg	7.01	7.01	x
224	Ti	Air	mg	927	927	x
225	Tl	Air	mg	2.26	2.26	x
226	toluene	Air	g	34.7	34.7	x
227	trichloroethene	Air	g	3.56	3.56	x
228	trichloromethane	Air	mg	4.33	4.33	x
229	U	Air	mg	6.95	6.95	x
230	V	Air	g	8.52	8.52	x
231	vinyl chloride	Air	mg	26.9	26.9	x
232	xylene	Air	g	39.7	39.7	x
233	Zn	Air	g	18.6	18.1	0.475
234	Zr	Air	mg	1.15	1.15	x
235	1,1,1-trichloroethane	Water	mg	2.73	2.73	x
236	acenaphthylene	Water	mg	689	689	x
237	Acid as H+	Water	g	15.4	15.4	x

238	acids (unspecified)	Water	kg	42.3	42.3	x
239	Ag	Water	mg	14.1	14.1	x
240	Al	Water	g	621	621	0.294
241	alkanes	Water	g	2.48	2.48	x
242	alkenes	Water	mg	229	229	x
243	anorg. dissolved subst.	Water	g	216	x	216
244	AOX	Water	mg	61	58.9	2.13
245	As	Water	g	1.24	1.24	0.000996
246	B	Water	kg	10.2	10.2	x
247	Ba	Water	g	92.6	91.3	1.39
248	baryte	Water	g	892	892	x
249	Be	Water	µg	914	914	x
250	benzene	Water	g	2.69	2.69	x
251	BOD	Water	oz	114	114	0.00172
252	calcium compounds	Water	g	42.6	42.6	x
253	calcium ions	Water	kg	1.85	1.85	x
254	carbonate	Water	g	8.33	8.33	x
255	Cd	Water	g	70.7	70.5	0.195
256	chlorinated solvents (unspec.)	Water	mg	7.1	7.1	x
257	chlorobenzenes	Water	µg	7.14	7.14	x
258	chromate	Water	g	2.7	2.7	x
259	Cl-	Water	lb	180	179	0.864
260	Cl2	Water	µg	119	119	x
261	Co	Water	g	1.2	1.2	x
262	COD	Water	oz	789	789	0.0562
263	Copper	Water	kg	2.63	2.63	x
264	Cr	Water	g	126	126	0.00745
265	Cr (VI)	Water	mg	1.09	1.09	x
266	crude oil	Water	mg	17.7	17.7	x
267	Cs	Water	mg	16.8	16.8	x
268	Cu	Water	g	3.95	3.41	0.543
269	CxHy	Water	g	30.8	30.8	x
270	CxHy aromatic	Water	g	13.3	12.8	0.466
271	CxHy chloro	Water	µg	682	199	483
272	cyanide	Water	g	17.6	17.6	0.00214
273	detergent/oil	Water	g	22.2	22.2	x
274	di(2-ethylhexyl)phthalate	Water	µg	28.1	28.1	x
275	dibutyl p-phthalate	Water	µg	69.8	69.8	x
276	dichloroethane	Water	mg	84.5	84.5	x
277	dichloromethane	Water	mg	393	393	x
278	dimethyl p-phthalate	Water	µg	439	439	x
279	dissolved organics	Water	g	9.17	9.17	x
280	dissolved solids	Water	tn.lg	1.45	1.45	x
281	dissolved substances	Water	g	254	254	x
282	DOC	Water	g	27.7	27.7	0.0043
283	ethyl benzene	Water	mg	408	408	x

284	F2	Water	g	17.8	17.8	x
285	fats/oils	Water	g	461	447	14.5
286	fatty acids as C	Water	g	90.4	90.4	x
287	Fe	Water	oz	556	556	0.0162
288	fluoride ions	Water	g	407	407	x
289	formaldehyde	Water	g	4.05	4.05	x
290	glutaraldehyde	Water	mg	110	110	x
291	H2S	Water	mg	96	96	x
292	H2SO4	Water	kg	2.55	2.55	x
293	hexachloroethane	Water	µg	1.87	1.87	x
294	Hg	Water	mg	106	96.6	9.53
295	HOCL	Water	g	4.17	4.17	x
296	I	Water	g	1.67	1.67	x
297	K	Water	g	268	268	x
298	Kjeldahl-N	Water	mg	201	x	201
299	Lead	Water	g	414	414	x
300	metallic ions	Water	g	189	185	3.37
301	Mg	Water	g	529	529	x
302	Mn	Water	kg	8.67	8.67	x
303	Mo	Water	g	2.13	2.13	x
304	MTBE	Water	mg	5.25	5.25	x
305	N-tot	Water	g	31.2	30	1.16
306	N organically bound	Water	g	3.71	3.71	x
307	Na	Water	kg	6.82	6.82	x
308	NH3	Water	g	181	181	x
309	NH3 (as N)	Water	g	42.8	42.8	x
310	NH4+	Water	g	117	3.49	114
311	Ni	Water	g	46.8	46.8	0.00295
312	nitrate	Water	g	558	194	363
313	nitrite	Water	g	1.05	1.05	x
314	non methane VOC	Water	g	225	225	x
315	OCl-	Water	g	3.99	3.99	x
316	oil	Water	kg	27.5	27.5	x
317	organic carbon	Water	g	431	431	x
318	other organics	Water	kg	5.65	5.65	x
319	P-compounds	Water	mg	24.3	24.3	x
320	P-tot	Water	µg	12.2	12.2	x
321	P2O5	Water	mg	344	344	x
322	PAH's	Water	mg	271	264	7.12
323	Pb	Water	g	22.1	22.1	0.00586
324	phenol	Water	g	1.83	1.83	x
325	phenols	Water	g	2.84	2.76	0.0723
326	phosphate	Water	oz	46.4	46.4	0.000789
327	Ru	Water	mg	167	167	x
328	S	Water	mg	3.4	3.4	x
329	salt	Water	g	3.15	3.15	x

330	salts	Water	kg	1.28	1.28	x
331	Sb	Water	mg	11.3	11.3	x
332	Se	Water	g	3.1	3.1	x
333	Si	Water	mg	588	588	x
334	Sn	Water	mg	5.4	5.4	x
335	SO3	Water	g	7.27	7.27	x
336	Sr	Water	g	108	108	x
337	sulphate	Water	lb	385	384	0.4
338	sulphates	Water	g	403	403	x
339	sulphide	Water	g	59.3	59.2	0.0171
340	sulphur/sulphide	Water	g	1.49	1.49	x
341	suspended solids	Water	kg	202	202	x
342	suspended substances	Water	g	54	22.4	31.6
343	tetrachloroethene	Water	µg	222	222	x
344	tetrachloromethane	Water	µg	339	339	x
345	Ti	Water	g	36.9	36.9	x
346	TOC	Water	oz	270	246	23.5
347	toluene	Water	g	2.29	2.23	0.0648
348	tributyltin	Water	mg	32.4	32.4	x
349	trichloroethene	Water	mg	14.1	14.1	x
350	trichloromethane	Water	mg	51.9	51.9	x
351	triethylene glycol	Water	g	27.7	27.7	x
352	undissolved substances	Water	kg	2.83	2.83	x
353	V	Water	g	3.23	3.23	x
354	vinyl chloride	Water	µg	63	63	x
355	VOC as C	Water	g	5.81	5.81	x
356	W	Water	mg	23	23	x
357	xylene	Water	g	1.92	1.92	x
358	Zinc	Water	g	677	677	x
359	Zn	Water	g	109	62.4	46.9
360	chemical waste (inert)	Solid	g	175	175	x
361	chemical waste (regulated)	Solid	kg	2.54	2.54	x
362	construction waste	Solid	g	91.5	91.5	x
363	final waste (inert)	Solid	kg	10.9	10.9	x
364	high active nuclear waste	Solid	mm3	31.7	31.7	x
365	industrial waste	Solid	g	949	949	x
366	inorganic general	Solid	kg	24.9	24.9	x
367	low,med. act. nucl. waste	Solid	cm3	7.14	7.14	x
368	metal scrap	Solid	g	3.9	3.9	x
369	mineral waste	Solid	kg	24	24	x
370	paper/board packaging	Solid	pg	5.3E-10	5.3E-10	x
371	plastics packaging	Solid	g	3.46	3.46	x
372	produc. waste (not inert)	Solid	g	635	635	x
373	slags/ash	Solid	kg	1.91	1.91	x
374	solid waste	Solid	tn.lg	51.6	51.6	x
375	unspecified	Solid	g	384	384	x

376	waste in incineration	Solid	g	9.53	9.53	x
377	waste to recycling	Solid	g	3.62	3.62	x
378	wood packaging	Solid	mg	9.86	9.86	x
379	Al (ind.)	Soil	g	56.2	56.2	x
380	As (ind.)	Soil	mg	22.5	22.5	x
381	C (ind.)	Soil	g	170	170	x
382	Ca (ind.)	Soil	g	225	225	x
383	carbon	Soil	g	449	x	449
384	Cd	Soil	mg	84.7	x	84.7
385	Cd (ind.)	Soil	mg	3.15	3.15	x
386	Co (ind.)	Soil	µg	410	410	x
387	Cr (ind.)	Soil	mg	281	281	x
388	Cu (ind.)	Soil	mg	2.05	2.05	x
389	Fe (ind.)	Soil	g	113	113	x
390	Hg	Soil	mg	9.15	x	9.15
391	Hg (ind.)	Soil	µg	59.8	59.8	x
392	Mn (ind.)	Soil	g	2.25	2.25	x
393	N	Soil	mg	18.9	18.9	x
394	N-tot	Soil	g	9.11	x	9.11
395	Ni (ind.)	Soil	mg	3.08	3.08	x
396	oil (ind.)	Soil	g	163	163	x
397	oil biodegradable	Soil	g	93.3	93.3	x
398	P-tot	Soil	g	2.85	2.85	x
399	Pb	Soil	mg	9.41	x	9.41
400	Pb (ind.)	Soil	mg	9.68	9.68	x
401	S (ind.)	Soil	g	33.7	33.7	x
402	Zn	Soil	mg	1.65	x	1.65
403	Zn (ind.)	Soil	mg	863	863	x
404	Ag110m to air	Non mat.	mBq	10.2	10.2	x
405	Ag110m to water	Non mat.	Bq	69.8	69.8	x
406	alpha radiation (unspecified) to water	Non mat.	mBq	8.18	8.18	x
407	Am241 to air	Non mat.	mBq	204	204	x
408	Am241 to water	Non mat.	Bq	26.8	26.8	x
409	Ar41 to air	Non mat.	kBq	22	22	x
410	Ba140 to air	Non mat.	mBq	54.6	54.6	x
411	Ba140 to water	Non mat.	mBq	377	377	x
412	beta radiation (unspecified) to air	Non mat.	mBq	3.21	3.21	x
413	C14 to air	Non mat.	kBq	17	17	x
414	C14 to water	Non mat.	kBq	1.36	1.36	x
415	Cd109 to water	Non mat.	mBq	2.19	2.19	x
416	Ce141 to air	Non mat.	µBq	965	965	x
417	Ce141 to water	Non mat.	mBq	56.3	56.3	x
418	Ce144 to air	Non mat.	Bq	2.17	2.17	x
419	Ce144 to water	Non mat.	Bq	613	613	x
420	Cm (alpha) to air	Non mat.	mBq	323	323	x
421	Cm (alpha) to water	Non mat.	Bq	35.5	35.5	x

422	Cm242 to air	Non mat.	nBq	995	995	x
423	Cm244 to air	Non mat.	µBq	9.04	9.04	x
424	Co57 to air	Non mat.	µBq	17.4	17.4	x
425	Co57 to water	Non mat.	mBq	388	388	x
426	Co58 to air	Non mat.	mBq	288	288	x
427	Co58 to water	Non mat.	Bq	200	200	x
428	Co60 to air	Non mat.	mBq	448	448	x
429	Co60 to water	Non mat.	kBq	6.07	6.07	x
430	Conv. to industrial area	Non mat.	mm2	733	733	x
431	Cr51 to air	Non mat.	mBq	37.6	37.6	x
432	Cr51 to water	Non mat.	Bq	8.32	8.32	x
433	Cs134 to air	Non mat.	Bq	7.73	7.73	x
434	Cs134 to water	Non mat.	kBq	1.37	1.37	x
435	Cs136 to water	Non mat.	mBq	2.03	2.03	x
436	Cs137 to air	Non mat.	Bq	14.9	14.9	x
437	Cs137 to water	Non mat.	kBq	12.7	12.7	x
438	Fe59 to air	Non mat.	µBq	394	394	x
439	Fe59 to water	Non mat.	mBq	6.68	6.68	x
440	Fission and activation products (RA) to water	Non mat.	Bq	74.5	74.5	x
441	H3 to air	Non mat.	kBq	161	161	x
442	H3 to water	Non mat.	kBq	4.01E4	4.01E4	x
443	heat losses to air	Non mat.	MJ	852	852	x
444	heat losses to soil	Non mat.	kJ	334	334	x
445	heat losses to water	Non mat.	MJ	65.5	65.5	x
446	I129 to air	Non mat.	Bq	58.1	58.1	x
447	I129 to water	Non mat.	kBq	3.88	3.88	x
448	I131 to air	Non mat.	Bq	10.5	10.5	x
449	I131 to water	Non mat.	Bq	3.44	3.44	x
450	I133 to air	Non mat.	Bq	3.4	3.4	x
451	I133 to water	Non mat.	Bq	1.73	1.73	x
452	I135 to air	Non mat.	Bq	5.04	5.04	x
453	K40 to air	Non mat.	Bq	29.5	29.5	x
454	K40 to water	Non mat.	Bq	91.5	91.5	x
455	Kr85 to air	Non mat.	kBq	1E6	1E6	x
456	Kr85m to air	Non mat.	kBq	2.51	2.51	x
457	Kr87 to air	Non mat.	Bq	912	912	x
458	Kr88 to air	Non mat.	kBq	44.4	44.4	x
459	Kr89 to air	Non mat.	Bq	794	794	x
460	La140 to air	Non mat.	mBq	27.6	27.6	x
461	La140 to water	Non mat.	mBq	78.3	78.3	x
462	land use (sea floor) II-III	Non mat.	m2a	71.1	71.1	x
463	land use (sea floor) II-IV	Non mat.	m2a	7.33	7.33	x
464	land use II-III	Non mat.	m2a	105	105	x
465	land use II-IV	Non mat.	m2a	113	113	x
466	land use III-IV	Non mat.	m2a	11.6	11.6	x

467	land use IV-IV	Non mat.	cm2a	410	410	x
468	Mn54 to air	Non mat.	mBq	10.5	10.5	x
469	Mn54 to water	Non mat.	Bq	915	915	x
470	Mo99 to water	Non mat.	mBq	26.4	26.4	x
471	Na24 to water	Non mat.	Bq	11.6	11.6	x
472	Nb95 to air	Non mat.	mBq	1.88	1.88	x
473	Nb95 to water	Non mat.	mBq	214	214	x
474	Np237 to air	Non mat.	µBq	10.7	10.7	x
475	Np237 to water	Non mat.	Bq	1.71	1.71	x
476	Occup. as contin. urban land	Non mat.	m2a	0.113	0.113	x
477	Occup. as convent. arable land	Non mat.	m2a	1.38	1.38	x
478	Occup. as forest land	Non mat.	mm2a	160	160	x
479	Occup. as industrial area	Non mat.	m2a	11.3	11.3	x
480	Pa234m to air	Non mat.	Bq	6.44	6.44	x
481	Pa234m to water	Non mat.	Bq	119	119	x
482	Pb210 to air	Non mat.	Bq	175	175	x
483	Pb210 to water	Non mat.	Bq	72.7	72.7	x
484	Pm147 to air	Non mat.	Bq	5.5	5.5	x
485	Po210 to air	Non mat.	Bq	261	261	x
486	Po210 to water	Non mat.	Bq	72.7	72.7	x
487	Pu alpha to air	Non mat.	mBq	648	648	x
488	Pu alpha to water	Non mat.	Bq	107	107	x
489	Pu238 to air	Non mat.	µBq	22.5	22.5	x
490	Pu241 beta	Non mat.	kBq	2.65	2.65	x
491	Pu241 Beta to air	Non mat.	Bq	17.8	17.8	x
492	Ra224 to water	Non mat.	Bq	832	832	x
493	Ra226 to air	Non mat.	Bq	229	229	x
494	Ra226 to water	Non mat.	kBq	495	495	x
495	Ra228 to air	Non mat.	Bq	14.5	14.5	x
496	Ra228 to water	Non mat.	kBq	1.66	1.66	x
497	radio active noble gases to air	Non mat.	kBq	3.99	3.99	x
498	radioactive substance to air	Non mat.	kBq	5.3E6	5.3E6	4.21E3
499	radioactive substance to water	Non mat.	kBq	189	150	39.1
500	radionuclides (mixed) to water	Non mat.	mBq	63.3	63.3	x
501	Rn220 to air	Non mat.	kBq	1.34	1.34	x
502	Rn222 (long term) to air	Non mat.	kBq	1.43E6	1.43E6	x
503	Rn222 to air	Non mat.	kBq	1.56E4	1.56E4	x
504	Ru103 to air	Non mat.	µBq	125	125	x
505	Ru103 to water	Non mat.	mBq	127	127	x
506	Ru106 to air	Non mat.	Bq	64.8	64.8	x
507	Ru106 to water	Non mat.	kBq	6.48	6.48	x
508	Sb122 to water	Non mat.	mBq	377	377	x
509	Sb124 to air	Non mat.	mBq	2.88	2.88	x
510	Sb124 to water	Non mat.	Bq	21.5	21.5	x
511	Sb125 to air	Non mat.	µBq	701	701	x
512	Sb125 to water	Non mat.	Bq	3.08	3.08	x

513	Sr89 to air	Non mat.	mBq	18.5	18.5	x
514	Sr89 to water	Non mat.	mBq	854	854	x
515	Sr90 to air	Non mat.	Bq	10.7	10.7	x
516	Sr90 to water	Non mat.	kBq	1.29	1.29	x
517	Tc99 to air	Non mat.	µBq	453	453	x
518	Tc99 to water	Non mat.	Bq	679	679	x
519	Tc99m to water	Non mat.	mBq	178	178	x
520	Te123m to air	Non mat.	mBq	45.2	45.2	x
521	Te123m to water	Non mat.	mBq	16	16	x
522	Te132 to water	Non mat.	mBq	6.53	6.53	x
523	Th228 to air	Non mat.	Bq	12.2	12.2	x
524	Th228 to water	Non mat.	kBq	3.32	3.32	x
525	Th230 to air	Non mat.	Bq	71.9	71.9	x
526	Th230 to water	Non mat.	kBq	18.7	18.7	x
527	Th232 to air	Non mat.	Bq	7.76	7.76	x
528	Th232 to water	Non mat.	Bq	17.1	17.1	x
529	Th234 to air	Non mat.	Bq	6.44	6.44	x
530	Th234 to water	Non mat.	Bq	120	120	x
531	U alpha to air	Non mat.	Bq	231	231	x
532	U alpha to water	Non mat.	kBq	7.8	7.8	x
533	U234 to air	Non mat.	Bq	77.3	77.3	x
534	U234 to water	Non mat.	Bq	160	160	x
535	U235 to air	Non mat.	Bq	3.75	3.75	x
536	U235 to water	Non mat.	Bq	238	238	x
537	U238 to air	Non mat.	Bq	98.6	98.6	x
538	U238 to water	Non mat.	Bq	402	402	x
539	waste heat to air	Non mat.	MWh	-2.14	-2.14	x
540	waste heat to soil	Non mat.	MJ	201	201	x
541	waste heat to water	Non mat.	MJ	846	846	x
542	Xe131m to air	Non mat.	kBq	4.19	4.19	x
543	Xe133 to air	Non mat.	kBq	709	709	x
544	Xe133m to air	Non mat.	Bq	335	335	x
545	Xe135 to air	Non mat.	kBq	143	143	x
546	Xe135m to air	Non mat.	kBq	24.4	24.4	x
547	Xe137 to air	Non mat.	Bq	545	545	x
548	Xe138 to air	Non mat.	kBq	6.71	6.71	x
549	Y90 to water	Non mat.	mBq	43.6	43.6	x
550	Zn65 to air	Non mat.	mBq	51.6	51.6	x
551	Zn65 to water	Non mat.	Bq	24.6	24.6	x
552	Zr95 to air	Non mat.	µBq	659	659	x
553	Zr95 to water	Non mat.	Bq	55	55	x

→

D.3 INTENSIVE GREEN ROOF ECO-INDICATOR 99 RESULTS

SimaPro 5.0 LCI Results Date: 2/9/2007 Time: 4:14:30 PM
Project: Green Roof

Title:
Method: Eco-indicator 99 (H) / Europe EI 99 H/H
Emission compartment: All compartments
Value: Amount
Category:
Skip unused: No
Relative mode: Non

No (98)	Substance	Compartment	Unit	Total	Intensive Roof 45 years	Landfill B250
1	air	Raw	kg	39	39	x
2	Asphalt	Raw	tn.lg	4.13	4.13	x
3	baryte	Raw	kg	3.6	3.6	x
4	bauxite	Raw	kg	48.5	48.5	x
5	bentonite	Raw	kg	2.53	2.53	x
6	calcium sulphate	Raw	mg	815	815	x
7	chalk	Raw	pg	1.04E-10	1.04E-10	x
8	chromium (in ore)	Raw	kg	1.22	1.22	x
9	clay	Raw	kg	3.51	3.51	x
10	clay minerals	Raw	tn.lg	25.7	25.7	x
11	coal ETH	Raw	kg	624	624	0.173
12	coal FAL	Raw	tn.lg	6.99	6.99	x
13	cobalt (in ore)	Raw	µg	297	297	x
14	copper (in ore)	Raw	kg	2.21	2.21	x
15	crude oil (feedstock) FAL	Raw	tn.lg	2.21	2.21	x
16	crude oil ETH	Raw	kg	752	741	10.9
17	crude oil FAL	Raw	tn.lg	1.41	1.41	x
18	crude oil IDEMAT	Raw	kg	76.7	76.7	x
19	dolomite	Raw	kg	45.4	45.4	x
20	energy (undef.)	Raw	MJ	18.3	18.3	x
21	energy from biomass	Raw	MJ	9.91	9.91	x
22	energy from coal	Raw	MJ	803	803	x
23	energy from hydro power	Raw	MWh	2.88	2.88	x
24	energy from hydrogen	Raw	MJ	49	49	x
25	energy from lignite	Raw	MJ	33.8	33.8	x
26	energy from natural gas	Raw	MWh	2.17	2.17	x
27	energy from oil	Raw	MWh	4.49	4.49	x
28	energy from peat	Raw	kJ	774	774	x

29	energy from sulphur	Raw	kJ	989	989	x
30	energy from uranium	Raw	GJ	1.09	1.09	x
31	energy from wood	Raw	kJ	4.36	4.36	x
32	energy recovered	Raw	MJ	-207	-207	x
33	feldspar	Raw	kg	45.4	45.4	x
34	ferromanganese	Raw	mg	38.4	38.4	x
35	fluorspar	Raw	g	211	211	x
36	gas from oil production	Raw	l	107	107	x
37	granite	Raw	g	201	201	x
38	gravel	Raw	tn.lg	64.5	64.5	x
39	iron (in ore)	Raw	kg	196	196	x
40	KCl	Raw	mg	336	336	x
41	lead (in ore)	Raw	kg	11.9	11.9	x
42	lignite ETH	Raw	kg	484	484	0.18
43	limestone	Raw	tn.lg	1.53	1.53	x
44	manganese (in ore)	Raw	g	384	384	x
45	marl	Raw	kg	83.4	83.4	x
46	methane (kg)	Raw	g	202	202	x
47	methane (kg) ETH	Raw	kg	4.33	4.33	x
48	molybdene (in ore)	Raw	mg	1.05	1.05	x
49	NaCl	Raw	kg	10.8	10.8	x
50	NaOH	Raw	kg	136	136	x
51	natural gas	Raw	kg	264	264	x
52	natural gas (feedstock) FAL	Raw	tn.lg	2.96	2.96	x
53	natural gas (vol)	Raw	l	824	x	824
54	natural gas ETH	Raw	m3	237	237	x
55	natural gas FAL	Raw	tn.lg	6.82	6.82	x
56	nickel (in ore)	Raw	g	743	743	x
57	nitrogen	Raw	kg	21.4	21.4	x
58	olivine	Raw	mg	396	396	x
59	oxygen	Raw	kg	317	317	x
60	palladium (in ore)	Raw	mg	3.45	3.45	x
61	petroleum gas ETH	Raw	m3	50.6	50.6	x
62	phosphate (as P2O5)	Raw	mg	127	127	x
63	platinum (in ore)	Raw	mg	3.89	3.89	x
64	pot. energy hydropower	Raw	MJ	5.66	x	5.66
65	potential energy water ETH	Raw	GJ	2.98	2.98	x
66	process water	Raw	cu.in	158	x	158
67	reservoir content ETH	Raw	m3y	65.1	65.1	x
68	rhenium (in ore)	Raw	mg	2.93	2.93	x
69	rhodium (in ore)	Raw	mg	3.67	3.67	x
70	rock salt	Raw	kg	2.8	2.8	x
71	rutile	Raw	pg	1.49E-10	1.49E-10	x
72	sand	Raw	tn.lg	39.2	39.2	x
73	scrap, external	Raw	tn.lg	10.8	10.8	x
74	shale	Raw	g	2.31	2.31	x

75	silver	Raw	mg	6.56	6.56	x
76	silver (in ore)	Raw	g	1.86	1.86	x
77	sulphur (bonded)	Raw	g	51.8	51.8	x
78	sulphur (elemental)	Raw	g	107	107	x
79	tin (in ore)	Raw	g	1.04	1.04	x
80	turbine water ETH	Raw	m3	1.51E4	1.51E4	x
81	uranium (in ore)	Raw	mg	235	187	48.5
82	uranium (in ore) ETH	Raw	g	35.2	35.2	x
83	uranium FAL	Raw	g	27.9	27.9	x
84	water	Raw	tn.lg	86	86	x
85	water (cooling)	Raw	tn.lg	11	11	x
86	water (drinking, for process.)	Raw	kg	948	948	x
87	water (process)	Raw	kg	69.6	69.6	x
88	water (sea, for cooling)	Raw	tn.lg	5.64	5.64	x
89	water (sea, for processing)	Raw	kg	33.9	33.9	x
90	water (surface, for cooling)	Raw	kg	55.4	55.4	x
91	water (surface, for process.)	Raw	g	706	706	x
92	water (well, for cooling)	Raw	g	877	877	x
93	water (well, for processing)	Raw	g	16.9	16.9	x
94	Water1	Raw	m3	7.05E3	7.05E3	x
95	wood	Raw	g	305	303	1.69
96	wood (dry matter) ETH	Raw	tn.lg	7.06	7.06	x
97	wood/wood wastes FAL	Raw	kg	7.54	7.54	x
98	zeolite	Raw	mg	124	124	x
99	zinc (in ore)	Raw	g	150	150	x
100	1,2-dichloroethane	Air	µg	305	305	x
101	acetaldehyde	Air	g	2.56	2.56	x
102	acetic acid	Air	g	4.11	4.11	x
103	acetone	Air	mg	870	870	x
104	acrolein	Air	mg	241	241	x
105	Al	Air	g	31.3	31.3	x
106	aldehydes	Air	g	793	793	x
107	alkanes	Air	g	43.3	43.3	x
108	alkenes	Air	g	82.6	82.6	x
109	ammonia	Air	oz	586	586	0.0529
110	As	Air	g	4.82	4.82	x
111	B	Air	g	19.1	19.1	x
112	Ba	Air	mg	477	477	x
113	Be	Air	mg	118	118	x
114	benzaldehyde	Air	µg	67.8	67.8	x
115	benzene	Air	g	156	156	0.136
116	benzo(a)pyrene	Air	mg	32.4	32.4	x
117	Br	Air	g	2.21	2.21	x
118	butane	Air	g	57	57	x
119	butene	Air	g	89	89	x
120	Ca	Air	g	37.2	37.2	x

121	Cd	Air	g	1	1	0.004
122	CFC-11	Air	mg	11.1	11.1	x
123	CFC-114	Air	mg	295	295	x
124	CFC-116	Air	mg	400	400	x
125	CFC-12	Air	mg	2.38	2.38	x
126	CFC-13	Air	mg	1.49	1.49	x
127	CFC-14	Air	g	3.6	3.6	x
128	CFC (soft)	Air	mg	16.4	16.4	x
129	Cl2	Air	g	87.1	87.1	x
130	CO	Air	lb	265	264	0.47
131	CO2	Air	kg	5.18E3	4.84E3	336
132	CO2 (fossil)	Air	tn.lg	35.1	35.1	x
133	CO2 (non-fossil)	Air	kg	9.89	9.89	x
134	cobalt	Air	mg	937	937	x
135	Cr	Air	g	6.2	6.2	x
136	CS2	Air	µg	22.4	22.4	x
137	Cu	Air	g	2.96	2.96	x
138	CxHy	Air	kg	1.94	1.94	x
139	CxHy aromatic	Air	g	151	150	0.228
140	CxHy chloro	Air	g	12.5	12.5	x
141	CxHy halogenated	Air	µg	12.5	x	12.5
142	cyanides	Air	mg	59.1	59.1	x
143	dichloroethane	Air	mg	115	115	x
144	dichloromethane	Air	g	1.03	1.03	x
145	dioxin (TEQ)	Air	µg	4.79	4.72	0.0704
146	dust	Air	g	979	943	36.2
147	dust (coarse)	Air	g	103	103	x
148	dust (coarse) process	Air	kg	2.44	2.44	x
149	dust (PM10) mobile	Air	g	63.7	63.7	x
150	dust (PM10) stationary	Air	kg	4	4	x
151	dust (SPM)	Air	g	496	496	x
152	ethane	Air	g	56.3	56.3	x
153	ethanol	Air	g	1.75	1.75	x
154	ethene	Air	kg	2.86	2.86	x
155	ethylbenzene	Air	g	4.07	4.07	x
156	ethyne	Air	mg	265	265	x
157	F2	Air	g	12.6	12.6	x
158	Fe	Air	g	31.7	31.7	x
159	formaldehyde	Air	g	72.6	72.6	x
160	H2	Air	g	32.6	32.6	x
161	H2S	Air	g	14.8	14.8	x
162	H2SO4	Air	ng	431	431	x
163	HALON-1301	Air	mg	296	294	2.6
164	HCFC-21	Air	g	24.6	24.6	x
165	HCFC-22	Air	mg	2.66	2.66	x
166	HCl	Air	oz	57.2	57.1	0.0561

167	HCN	Air	pg	5.1E-16	5.1E-16	x
168	He	Air	g	51	51	x
169	heptane	Air	g	10.8	10.8	x
170	hexachlorobenzene	Air	µg	20.8	20.8	x
171	hexane	Air	g	23	23	x
172	HF	Air	g	219	217	2
173	Hg	Air	mg	785	768	16.2
174	I	Air	mg	916	916	x
175	K	Air	g	37.3	37.3	x
176	kerosene	Air	g	6.16	6.16	x
177	La	Air	mg	13.9	13.9	x
178	mercaptans	Air	mg	6.42	6.42	x
179	metals	Air	g	6.77	6.63	0.137
180	methane	Air	kg	150	112	38
181	methanol	Air	g	1.95	1.95	x
182	Mg	Air	g	11.4	11.4	x
183	Mn	Air	g	16.4	16.4	5.74E-5
184	Mo	Air	mg	147	147	x
185	MTBE	Air	mg	44.9	44.9	x
186	n-nitrodimethylamine	Air	mg	50.9	50.9	x
187	N2	Air	g	58.8	58.8	x
188	N2O	Air	g	257	256	1.05
189	Na	Air	g	8.55	8.55	x
190	naphthalene	Air	mg	17	17	x
191	Ni	Air	g	13	13	0.0176
192	NO2	Air	g	62.1	62.1	x
193	non methane VOC	Air	lb	416	415	0.509
194	NOx	Air	kg	181	181	x
195	NOx (as NO2)	Air	oz	360	342	18
196	organic substances	Air	kg	8.36	8.36	x
197	P	Air	mg	16.4	16.4	x
198	P-tot	Air	mg	467	467	x
199	PAH's	Air	mg	808	807	0.375
200	particulates (PM10)	Air	kg	9.53	9.53	x
201	particulates (unspecified)	Air	kg	47.1	47.1	x
202	Pb	Air	g	45.9	45.9	0.00264
203	pentachlorobenzene	Air	µg	55.6	55.6	x
204	pentachlorophenol	Air	µg	8.95	8.95	x
205	pentane	Air	g	65.5	65.5	x
206	phenol	Air	g	11.6	11.6	x
207	propane	Air	g	59.4	59.4	x
208	propene	Air	g	17.1	17.1	x
209	propionic acid	Air	mg	82.1	82.1	x
210	Pt	Air	µg	252	252	x
211	Sb	Air	mg	233	233	x
212	Sc	Air	mg	4.76	4.76	x

213	Se	Air	g	2.65	2.65	x
214	silicates	Air	g	99.5	99.5	x
215	Sn	Air	mg	23.2	23.2	x
216	SO2	Air	g	232	232	x
217	SOx	Air	kg	482	482	x
218	SOx (as SO2)	Air	oz	638	634	4.15
219	Sr	Air	mg	502	502	x
220	tetrachloroethene	Air	mg	230	230	x
221	tetrachloromethane	Air	mg	412	412	x
222	Th	Air	mg	9.8	9.8	x
223	Ti	Air	g	1.36	1.36	x
224	Tl	Air	mg	3.39	3.39	x
225	toluene	Air	g	27.4	27.4	x
226	trichloroethene	Air	mg	228	228	x
227	trichloromethane	Air	mg	3.04	3.04	x
228	U	Air	mg	9.94	9.94	x
229	V	Air	g	17.7	17.7	x
230	vinyl chloride	Air	mg	18.9	18.9	x
231	xylene	Air	g	99.4	99.4	x
232	Zn	Air	g	28.2	27.7	0.475
233	Zr	Air	mg	2.9	2.9	x
234	1,1,1-trichloroethane	Water	mg	13.5	13.5	x
235	acenaphthylene	Water	mg	245	245	x
236	Acid as H+	Water	g	15.4	15.4	x
237	acids (unspecified)	Water	kg	52.1	52.1	x
238	Ag	Water	mg	35.2	35.2	x
239	Al	Water	oz	36.2	36.1	0.0104
240	alkanes	Water	g	4.88	4.88	x
241	alkenes	Water	mg	451	451	x
242	anorg. dissolved subst.	Water	g	216	x	216
243	AOX	Water	mg	118	116	2.13
244	As	Water	g	2.06	2.06	0.000996
245	B	Water	g	691	691	x
246	Ba	Water	g	176	174	1.39
247	baryte	Water	g	718	718	x
248	Be	Water	mg	1.26	1.26	x
249	benzene	Water	g	5.52	5.52	x
250	BOD	Water	oz	82	82	0.00172
251	calcium compounds	Water	g	42.6	42.6	x
252	calcium ions	Water	kg	2.9	2.9	x
253	carbonate	Water	g	8.33	8.33	x
254	Cd	Water	g	32.3	32.1	0.195
255	chlorinated solvents (unspec.)	Water	mg	22.6	22.6	x
256	chlorobenzenes	Water	µg	27.3	27.3	x
257	chromate	Water	mg	386	386	x
258	Cl-	Water	lb	119	118	0.864

259	Cl2	Water	µg	119	119	x
260	Co	Water	g	2	2	x
261	COD	Water	oz	334	334	0.0562
262	Copper	Water	g	988	988	x
263	Cr	Water	g	100	100	0.00745
264	Cr (VI)	Water	mg	1.56	1.56	x
265	crude oil	Water	mg	17.7	17.7	x
266	Cs	Water	mg	37.4	37.4	x
267	Cu	Water	g	6.98	6.44	0.543
268	CxHy	Water	g	30.9	30.9	x
269	CxHy aromatic	Water	g	23.1	22.6	0.466
270	CxHy chloro	Water	µg	682	199	483
271	cyanide	Water	g	22.2	22.2	0.00214
272	detergent/oil	Water	g	22.2	22.2	x
273	di(2-ethylhexyl)phthalate	Water	µg	107	107	x
274	dibutyl p-phthalate	Water	µg	24.8	24.8	x
275	dichloroethane	Water	mg	59.4	59.4	x
276	dichloromethane	Water	mg	326	326	x
277	dimethyl p-phthalate	Water	µg	156	156	x
278	dissolved organics	Water	g	9.17	9.17	x
279	dissolved solids	Water	kg	552	552	x
280	dissolved substances	Water	g	418	418	x
281	DOC	Water	g	3.28	3.27	0.0043
282	ethyl benzene	Water	mg	912	912	x
283	F2	Water	g	17.8	17.8	x
284	fats/oils	Water	g	812	797	14.5
285	fatty acids as C	Water	g	189	189	x
286	Fe	Water	oz	73.1	73.1	0.0162
287	fluoride ions	Water	g	70.6	70.6	x
288	formaldehyde	Water	g	4.06	4.06	x
289	glutaraldehyde	Water	mg	88.5	88.5	x
290	H2S	Water	mg	265	265	x
291	H2SO4	Water	g	172	172	x
292	hexachloroethane	Water	µg	1.31	1.31	x
293	Hg	Water	mg	105	95.8	9.53
294	HOCL	Water	g	5.65	5.65	x
295	I	Water	g	3.73	3.73	x
296	K	Water	g	480	480	x
297	Kjeldahl-N	Water	mg	201	x	201
298	Lead	Water	g	155	155	x
299	metallic ions	Water	g	106	103	3.37
300	Mg	Water	g	876	876	x
301	Mn	Water	g	580	580	x
302	Mo	Water	g	3.36	3.36	x
303	MTBE	Water	mg	5.32	5.32	x
304	N-tot	Water	g	62.1	60.9	1.16

305	N organically bound	Water	g	8.09	8.09	x
306	Na	Water	kg	13.6	13.6	x
307	NH3	Water	g	22.5	22.5	x
308	NH3 (as N)	Water	g	68.6	68.6	x
309	NH4+	Water	g	117	3.49	114
310	Ni	Water	g	59.3	59.3	0.00295
311	nitrate	Water	g	1.06E3	701	363
312	nitrite	Water	g	1.4	1.4	x
313	non methane VOC	Water	g	225	225	x
314	OCl-	Water	g	5.47	5.47	x
315	oil	Water	kg	11.5	11.5	x
316	organic carbon	Water	g	431	431	x
317	other organics	Water	kg	1.18	1.18	x
318	P-compounds	Water	mg	22.2	22.2	x
319	P-tot	Water	µg	12.2	12.2	x
320	P2O5	Water	mg	344	344	x
321	PAH's	Water	mg	697	690	7.12
322	Pb	Water	g	32.2	32.2	0.00586
323	phenol	Water	g	1.56	1.56	x
324	phenols	Water	g	5.89	5.82	0.0723
325	phosphate	Water	g	154	154	0.0224
326	Ru	Water	mg	372	372	x
327	S	Water	mg	3.4	3.4	x
328	salt	Water	g	3.15	3.15	x
329	salts	Water	kg	1.74	1.74	x
330	Sb	Water	mg	22	22	x
331	Se	Water	g	5.13	5.13	x
332	Si	Water	mg	592	592	x
333	Sn	Water	mg	7.39	7.39	x
334	SO3	Water	g	20.6	20.6	x
335	Sr	Water	g	237	237	x
336	sulphate	Water	lb	256	255	0.4
337	sulphates	Water	g	403	403	x
338	sulphide	Water	g	59.7	59.7	0.0171
339	sulphur/sulphide	Water	g	1.49	1.49	x
340	suspended solids	Water	kg	29	29	x
341	suspended substances	Water	g	54	22.4	31.6
342	tetrachloroethene	Water	µg	156	156	x
343	tetrachloromethane	Water	µg	238	238	x
344	Ti	Water	g	63.5	63.5	x
345	TOC	Water	lb	71	69.6	1.47
346	toluene	Water	g	4.56	4.49	0.0648
347	tributyltin	Water	mg	71.3	71.3	x
348	trichloroethene	Water	mg	9.89	9.89	x
349	trichloromethane	Water	mg	36.8	36.8	x
350	triethylene glycol	Water	g	3.27	3.27	x

351	undissolved substances	Water	kg	2.39	2.39	x
352	V	Water	g	5.3	5.3	x
353	vinyl chloride	Water	µg	44.2	44.2	x
354	VOC as C	Water	g	13	13	x
355	W	Water	mg	34.1	34.1	x
356	xylene	Water	g	3.94	3.94	x
357	Zinc	Water	g	254	254	x
358	Zn	Water	g	118	70.7	46.9
359	chemical waste (inert)	Solid	g	175	175	x
360	chemical waste (regulated)	Solid	kg	2.54	2.54	x
361	construction waste	Solid	g	91.5	91.5	x
362	final waste (inert)	Solid	kg	10.9	10.9	x
363	high active nuclear waste	Solid	mm3	31.7	31.7	x
364	industrial waste	Solid	g	949	949	x
365	inorganic general	Solid	kg	24.9	24.9	x
366	low,med. act. nucl. waste	Solid	cm3	7.14	7.14	x
367	metal scrap	Solid	g	3.9	3.9	x
368	mineral waste	Solid	kg	24	24	x
369	paper/board packaging	Solid	pg	5.3E-10	5.3E-10	x
370	plastics packaging	Solid	g	3.46	3.46	x
371	produc. waste (not inert)	Solid	g	635	635	x
372	slags/ash	Solid	kg	1.91	1.91	x
373	solid waste	Solid	tn.lg	4.8	4.8	x
374	unspecified	Solid	g	384	384	x
375	waste in incineration	Solid	g	9.53	9.53	x
376	waste to recycling	Solid	g	3.62	3.62	x
377	wood packaging	Solid	mg	9.86	9.86	x
378	Al (ind.)	Soil	g	46.6	46.6	x
379	As (ind.)	Soil	mg	18.7	18.7	x
380	C (ind.)	Soil	g	145	145	x
381	Ca (ind.)	Soil	g	187	187	x
382	carbon	Soil	g	449	x	449
383	Cd	Soil	mg	84.7	x	84.7
384	Cd (ind.)	Soil	mg	14.5	14.5	x
385	Co (ind.)	Soil	µg	802	802	x
386	Cr (ind.)	Soil	mg	233	233	x
387	Cu (ind.)	Soil	mg	4.01	4.01	x
388	Fe (ind.)	Soil	g	93.4	93.4	x
389	Hg	Soil	mg	9.15	x	9.15
390	Hg (ind.)	Soil	µg	120	120	x
391	Mn (ind.)	Soil	g	1.87	1.87	x
392	N	Soil	mg	39.1	39.1	x
393	N-tot	Soil	g	9.11	x	9.11
394	Ni (ind.)	Soil	mg	6.02	6.02	x
395	oil (ind.)	Soil	g	178	178	x
396	oil biodegradable	Soil	g	93.6	93.6	x

397	P-tot	Soil	g	2.41	2.41	x
398	Pb	Soil	mg	9.41	x	9.41
399	Pb (ind.)	Soil	mg	20	20	x
400	S (ind.)	Soil	g	28	28	x
401	Zn	Soil	mg	1.65	x	1.65
402	Zn (ind.)	Soil	mg	740	740	x
403	Ag110m to air	Non mat.	mBq	13.9	13.9	x
404	Ag110m to water	Non mat.	Bq	94.7	94.7	x
405	alpha radiation (unspecified) to water	Non mat.	mBq	11.1	11.1	x
406	Am241 to air	Non mat.	mBq	272	272	x
407	Am241 to water	Non mat.	Bq	35.8	35.8	x
408	Ar41 to air	Non mat.	kBq	30	30	x
409	Ba140 to air	Non mat.	mBq	69.3	69.3	x
410	Ba140 to water	Non mat.	mBq	430	430	x
411	beta radiation (unspecified) to air	Non mat.	mBq	3.73	3.73	x
412	C14 to air	Non mat.	kBq	22.5	22.5	x
413	C14 to water	Non mat.	kBq	1.81	1.81	x
414	Cd109 to water	Non mat.	mBq	2.49	2.49	x
415	Ce141 to air	Non mat.	mBq	1.3	1.3	x
416	Ce141 to water	Non mat.	mBq	64.2	64.2	x
417	Ce144 to air	Non mat.	Bq	2.9	2.9	x
418	Ce144 to water	Non mat.	Bq	819	819	x
419	Cm (alpha) to air	Non mat.	mBq	432	432	x
420	Cm (alpha) to water	Non mat.	Bq	47.5	47.5	x
421	Cm242 to air	Non mat.	µBq	1.35	1.35	x
422	Cm244 to air	Non mat.	µBq	12.3	12.3	x
423	Co57 to air	Non mat.	µBq	23.6	23.6	x
424	Co57 to water	Non mat.	mBq	442	442	x
425	Co58 to air	Non mat.	mBq	392	392	x
426	Co58 to water	Non mat.	Bq	242	242	x
427	Co60 to air	Non mat.	mBq	603	603	x
428	Co60 to water	Non mat.	kBq	8.07	8.07	x
429	Conv. to industrial area	Non mat.	mm2	733	733	x
430	Cr51 to air	Non mat.	mBq	50.5	50.5	x
431	Cr51 to water	Non mat.	Bq	9.48	9.48	x
432	Cs134 to air	Non mat.	Bq	10.3	10.3	x
433	Cs134 to water	Non mat.	kBq	1.84	1.84	x
434	Cs136 to water	Non mat.	mBq	2.31	2.31	x
435	Cs137 to air	Non mat.	Bq	19.9	19.9	x
436	Cs137 to water	Non mat.	kBq	16.9	16.9	x
437	Fe59 to air	Non mat.	µBq	536	536	x
438	Fe59 to water	Non mat.	mBq	7.61	7.61	x
439	Fission and activation products (RA) to water	Non mat.	Bq	101	101	x
440	H3 to air	Non mat.	kBq	218	218	x
441	H3 to water	Non mat.	kBq	5.37E4	5.37E4	x

442	heat losses to air	Non mat.	MJ	852	852	x
443	heat losses to soil	Non mat.	kJ	334	334	x
444	heat losses to water	Non mat.	MJ	65.5	65.5	x
445	I129 to air	Non mat.	Bq	77.7	77.7	x
446	I129 to water	Non mat.	kBq	5.18	5.18	x
447	I131 to air	Non mat.	Bq	12.8	12.8	x
448	I131 to water	Non mat.	Bq	4.33	4.33	x
449	I133 to air	Non mat.	Bq	4.61	4.61	x
450	I133 to water	Non mat.	Bq	1.97	1.97	x
451	I135 to air	Non mat.	Bq	6.85	6.85	x
452	K40 to air	Non mat.	Bq	44	44	x
453	K40 to water	Non mat.	Bq	129	129	x
454	Kr85 to air	Non mat.	kBq	1.34E6	1.34E6	x
455	Kr85m to air	Non mat.	kBq	2.95	2.95	x
456	Kr87 to air	Non mat.	kBq	1.1	1.1	x
457	Kr88 to air	Non mat.	kBq	60.2	60.2	x
458	Kr89 to air	Non mat.	Bq	932	932	x
459	La140 to air	Non mat.	mBq	36.7	36.7	x
460	La140 to water	Non mat.	mBq	89.2	89.2	x
461	land use (sea floor) II-III	Non mat.	m2a	57.1	57.1	x
462	land use (sea floor) II-IV	Non mat.	m2a	5.89	5.89	x
463	land use II-III	Non mat.	m2a	135	135	x
464	land use II-IV	Non mat.	m2a	114	114	x
465	land use III-IV	Non mat.	m2a	8.25	8.25	x
466	land use IV-IV	Non mat.	m2a	0.149	0.149	x
467	Mn54 to air	Non mat.	mBq	14.2	14.2	x
468	Mn54 to water	Non mat.	kBq	1.22	1.22	x
469	Mo99 to water	Non mat.	mBq	30.1	30.1	x
470	Na24 to water	Non mat.	Bq	13.3	13.3	x
471	Nb95 to air	Non mat.	mBq	2.54	2.54	x
472	Nb95 to water	Non mat.	mBq	244	244	x
473	Np237 to air	Non mat.	µBq	14.2	14.2	x
474	Np237 to water	Non mat.	Bq	2.29	2.29	x
475	Occup. as contin. urban land	Non mat.	m2a	0.113	0.113	x
476	Occup. as convent. arable land	Non mat.	m2a	1.38	1.38	x
477	Occup. as forest land	Non mat.	mm2a	160	160	x
478	Occup. as industrial area	Non mat.	m2a	11.3	11.3	x
479	Pa234m to air	Non mat.	Bq	8.62	8.62	x
480	Pa234m to water	Non mat.	Bq	160	160	x
481	Pb210 to air	Non mat.	Bq	251	251	x
482	Pb210 to water	Non mat.	Bq	102	102	x
483	Pm147 to air	Non mat.	Bq	7.35	7.35	x
484	Po210 to air	Non mat.	Bq	379	379	x
485	Po210 to water	Non mat.	Bq	102	102	x
486	Pu alpha to air	Non mat.	mBq	865	865	x
487	Pu alpha to water	Non mat.	Bq	142	142	x

488	Pu238 to air	Non mat.	µBq	30.5	30.5	x	
489	Pu241 beta	Non mat.	kBq	3.54	3.54	x	
490	Pu241 Beta to air	Non mat.	Bq	23.7	23.7	x	
491	Ra224 to water	Non mat.	kBq	1.86	1.86	x	
492	Ra226 to air	Non mat.	Bq	310	310	x	
493	Ra226 to water	Non mat.	kBq	662	662	x	
494	Ra228 to air	Non mat.	Bq	21.6	21.6	x	
495	Ra228 to water	Non mat.	kBq	3.71	3.71	x	
496	radio active noble gases to air	Non mat.	kBq	4.55	4.55	x	
497	radioactive substance to air	Non mat.	kBq	3.58E5	3.54E5	4.21E3	
498	radioactive substance to water	Non mat.	kBq	189	150	39.1	
499	radionuclides (mixed) to water	Non mat.	mBq	82.9	82.9	x	
500	Rn220 to air	Non mat.	kBq	1.91	1.91	x	
501	Rn222 (long term) to air	Non mat.	kBq	1.92E6	1.92E6	x	
502	Rn222 to air	Non mat.	kBq	2.09E4	2.09E4	x	
503	Ru103 to air	Non mat.	µBq	163	163	x	
504	Ru103 to water	Non mat.	mBq	145	145	x	
505	Ru106 to air	Non mat.	Bq	86.5	86.5	x	
506	Ru106 to water	Non mat.	kBq	8.65	8.65	x	
507	Sb122 to water	Non mat.	mBq	430	430	x	
508	Sb124 to air	Non mat.	mBq	3.88	3.88	x	
509	Sb124 to water	Non mat.	Bq	28	28	x	
510	Sb125 to air	Non mat.	µBq	839	839	x	
511	Sb125 to water	Non mat.	Bq	3.51	3.51	x	
512	Sr89 to air	Non mat.	mBq	24.9	24.9	x	
513	Sr89 to water	Non mat.	mBq	974	974	x	
514	Sr90 to air	Non mat.	Bq	14.2	14.2	x	
515	Sr90 to water	Non mat.	kBq	1.73	1.73	x	
516	Tc99 to air	Non mat.	µBq	605	605	x	
517	Tc99 to water	Non mat.	Bq	907	907	x	
518	Tc99m to water	Non mat.	mBq	203	203	x	
519	Te123m to air	Non mat.	mBq	61.5	61.5	x	
520	Te123m to water	Non mat.	mBq	18.2	18.2	x	
521	Te132 to water	Non mat.	mBq	7.44	7.44	x	
522	Th228 to air	Non mat.	Bq	18.3	18.3	x	
523	Th228 to water	Non mat.	kBq	7.43	7.43	x	
524	Th230 to air	Non mat.	Bq	96.1	96.1	x	
525	Th230 to water	Non mat.	kBq	25	25	x	
526	Th232 to air	Non mat.	Bq	11.6	11.6	x	
527	Th232 to water	Non mat.	Bq	24	24	x	
528	Th234 to air	Non mat.	Bq	8.62	8.62	x	
529	Th234 to water	Non mat.	Bq	161	161	x	
530	U alpha to air	Non mat.	Bq	309	309	x	
531	U alpha to water	Non mat.	kBq	10.4	10.4	x	
532	U234 to air	Non mat.	Bq	103	103	x	
533	U234 to water	Non mat.	Bq	214	214	x	

534	U235 to air	Non mat.	Bq	5.01	5.01	x
535	U235 to water	Non mat.	Bq	318	318	x
536	U238 to air	Non mat.	Bq	135	135	x
537	U238 to water	Non mat.	Bq	540	540	x
538	waste heat to air	Non mat.	MWh	-16.1	-16.1	x
539	waste heat to soil	Non mat.	MJ	173	173	x
540	waste heat to water	Non mat.	GJ	2.82	2.82	x
541	Xe131m to air	Non mat.	kBq	5.07	5.07	x
542	Xe133 to air	Non mat.	kBq	950	950	x
543	Xe133m to air	Non mat.	Bq	455	455	x
544	Xe135 to air	Non mat.	kBq	184	184	x
545	Xe135m to air	Non mat.	kBq	28.9	28.9	x
546	Xe137 to air	Non mat.	Bq	653	653	x
547	Xe138 to air	Non mat.	kBq	7.92	7.92	x
548	Y90 to water	Non mat.	mBq	49.7	49.7	x
549	Zn65 to air	Non mat.	mBq	67.8	67.8	x
550	Zn65 to water	Non mat.	Bq	28	28	x
551	Zr95 to air	Non mat.	µBq	896	896	x
552	Zr95 to water	Non mat.	Bq	73.5	73.5	x

→

BIBLIOGRAPHY

3 Rivers Wet Weather Demonstration Program. (2006). “Overview of the Problem.” http://www.3riverswetweather.com, 06/27/06.

ANSI/ISO. (2000). “Environmental management — Life cycle assessment — Principles and framework.” *14040-1997*, NSF International, Ann Arbor, MI.

Bass, B. and Baskaran, B. (2003). “Evaluating Rooftop and Vertical Gardens as an Adaptation Strategy for Urban Areas.” National Research Council Canada publication NRCC-46737.

Battisti, Riccardo. (2004). The methodology of Life Cycle Assessment and its application in the building sector. *Proc.*, *Summer Academy of Meditereanen Solar Architecture*, ISES, Rome, Italy, pp. 1-11.

Baumann, H. and Tillman, A. (2004). *The Hitch Hiker’s Guide to LCA.* Studentlitteratur, Lund, Sweden.

Bliss, D. (2007). “Stormwater Runoff Mitigation and Water Quality Improvements through the Use of a Green Roof in Pittsburgh, PA.” M.S. Thesis, University of Pittsburgh.

Del Barrio, E.P. (1998.) “Analysis of the green roofs cooling potential in buildings.” Energy and Building, 27, pp. 179-193.

Dunnett, N. and Kingsbury, N. (2004). *Planting Green Roofs and Living Walls*, Timber Press, Inc., Portland, OR.

EQUEST. (1998). eQuest - the quick energy simulation tool. http://www.doe2.com/download/equest/eQUESTv3-Overview.pdf

Eco-indicator. (2007). “Eco-indicator 99.” http://www.pre.nl, 2/11/07.

Eumorfopoulou, E. and Aravantinos, D. (1998). “The contribution of a planted roof to the thermal protection of buildings in Greece.” Energy and Building, 27, pp. 29-36.

GEOCOS. “IMPACT2002+.” http://gecos.epfl.ch/lcsystems/Fichiers_communs/Recherche/IMPACT2002+.html, 03/16/07.

Goedkoop, M., Effting, S., and Collignon, M. (2000). *The Eco-indicator 99: A damage oriented method for Life Cycle Impact Assessment.* PRé Consultants B.V., the Netherlands.

Goedkoop, M., and Oele, M. (2001). SimaPro User Manual. PRé Consultants B.V., the Netherlands.

Green Roof. (2007). "Green Roofs for Healthy Cities." http://www.greenroofs.org/, 04/16/07.

"Green Roof Test Plot: 2003 End of Year Project Summary Report" (2004). Prepared by MWH for the City of Chicago Department of Environment.

Gutteridge, B. (2003). "Toronto's Green Roof Demonstration Project." Proceedings to Greening Rooftops for Sustainable Communities: Chicago 2003.

Heerwagen, D. (2004). *Passive and Active Environmental Controls*. McGraw Hill Higher Education, Boston.

Humbert, S., Margni, M., Jolliet, O. (2005). *IMPACT 2002+: User Guide Draft for version 2.1.* Industrial Ecology & Life Cycle Systems Group, Swiss Federal Institute of Technology Lausanne (EPFL), Lausanne, Switzerland.

Köhler, M. and Schmidt, M. (2004). "Study of Extensive 'Green Roofs' in Berlin." http://www.roofscapes.com/water_quality, 09/22/04.

Kohler, M., Schmidt, M., Grimme, F. W., Laar, M., de Assunção Paiva, V. L., Tavares, S. (2002). "Green Roofs in Temperate Climates and in the Hot-Humid Tropics- Far Beyond the Aesthetics." *Environmental Management and Health*, 13(4).

Liu, K.K.Y. (2002). "Energy Efficiency and Environmental Benefits of Rooftop Gardens." Construction Canada, 44(2), pp. 17-23.

Lui, K. (2003). "Engineering Performance of Rooftop Gardens Through Field Evaluation." Proceedings to RCI 18th International Convention and Trade Show, Tampa Florida, March 13-18, 2003, pp. 1-15.

Lui, K. and Baskaran, B. (2003). "Thermal Performance of Green Roofs Through Field Evaluation." Proceedings to the First North American Green Roof Infrastructure Conference, Awards, and Trade Show, Chicago, Illinois, May 29-30, 2003, pp. 1-10.

Low Impact Development Center, Inc. (2004). "Green Roofs." http://www.lid-stormwater.net/greenroofs/greenroofs_home.htm, 01/07/04.

NASA. (2007). "A Change of Season." http://liftoff.msfc.nasa.gov/News/2001/News-AutumnalEquinox.asp, 06/29/07.

Niachou, A., Papakonstantinou, K., Santamouris, M., Tsangressoulis, A., and Mihalakakou, G. (2001). "Analysis of the green roof thermal properties and investigation of its energy performance." Energy and Building, 33, pp. 719-729.

Osmundson, T. (1999). *Roof Gardens: History, Design, and Construction*, W. W. Norton & Company, Inc., New York.

Pitt, R. and Lalor, M. (2000). "The Role of Pollution Prevention in Stormwater Management - Models and Applications to Urban Water Systems." Monograph 9. James, W., ed., CHI, Guelph, Ontario.

Roofscapes. (2006). "Green Roof Benefits." http://www.roofmeadow.com/PDF/Benefits.pdf, 07/09/06.

Saiz, S., Kennedy, C., Bass, B., and Pressnail, K. (2006). "Comparative Life Cycle Assessment of Standard and Green Roofs." Environmental Science and Technology, Vol. 40, No. 3, pp. 4312-4315.

Takahashi, K., Yoshida, H., Tanaka, Y., Aotake, N., and Wang, F. (2004). "Measurement of thermal environment in Kyoto city and its prediction by CFD simulation." Energy and Buildings, 36, pp. 771-779.

Theodosiou, T. (2003). "Summer period analysis of the performance of a planted roof as a passive cooling technique." Energy and Buildings, 35, pp. 909-917.

Toronto. (2007). "What is a Green Roof." http://www.toronto.ca/greenroofs, 05/15/07.

United States Environmental Protection Agency. (2006). "Heat Island Effect", http://www.epa.gov/cgi-bin/epaprintonly.cgi, 08/08/06.

United States Green Building Council. (2007). "What is Lead", http://www.usgbc.org/DisplayPage.aspx?CategoryID=19, 05/18/07.

Weather. (2007). "Sustained Wind Speed." http://www.weather.gov, 05/14/07.

Wikipedia. (2006). "Green Roof." http://en.wikipedia.org/wiki/Green_Roof, 08/04/06.

Wong, N. H., Chen, Y., Ong, C. L., Sia, A. (2003a). "Investigation of thermal benefits of rooftop garden in the tropical environment." *Building and Environment*, 38, pp. 261-270.

Wong, N. H., Yok, T.P., and Chen, Y. (2007). "Study of thermal performance of extensive rooftop greenery systems in the tropical climate." *Building and Environment*, 42, pp. 25-54.

Wong, N. H., Tay, S. F., Wong, R., Ong, C. L., Sia, A. (2003b). "Life cycle cost analysis of rooftop gardens in Singapore." *Building and Environment*, 38, pp. 499-509.